Role of Protein Disulphide Isomerase and its family members in Amyotrophic Lateral Sclerosis

Sonam Parakh

(Master of Biotechnology and Bioinformatics)

Submitted in total fulfillment of the requirements of the degree of Doctor of Philosophy

October 2015

Department of Biomedical Sciences

Faculty of Medicine & Health Sciences

Macquarie University

Sydney, Australia

Abstract

Superoxide dismutase (SOD1), Tar-DNA binding protein-43 (TDP-43) and Fused in Sarcoma (FUS) are major proteins linked to Amyotrophic Lateral Sclerosis (ALS) pathology. Whilst neurodegenerative mechanisms are not fully defined in ALS, dysfunction to the Endoplasmic Reticulum (ER) is increasingly implicated in the pathology of the disease. Protein disulphide isomerase (PDI) is an ER chaperone which also functions as an isomerase and aids in the formation and reduction of protein disulphide bonds. It is primarily located in the ER but it is also found in other cellular locations. Our laboratory previously demonstrated that over-expression of PDI is protective against mutant SOD1 in neuronal cultures. PDI has also been shown to co-localise with FUS and TDP-43 positive inclusions in ALS patients. Here we examined whether over-expression of PDI is protective against mutant TDP-43 and FUS induced ER stress and ER-Golgi transport defects and mislocalisation into cytoplasm in cellular models. Furthermore, we examined the mechanism by which PDI is protective and suggests that the disulphide interchange activity is important for its protective function. Also PDI in the cytoplasm further accentuates its protective ability. Importantly, PDI was examined in vivo and it was demonstrated that a small molecule mimic of the PDI active site -1,2 bis (mercaptoacetamido) cyclohexane BMC reduced the loss of motor neuron in $SOD1^{G93A}$ mice signifying the relevance of PDI in disease pathology. The results in this study demonstrate that PDI is protective against the major misfolded proteins linked to ALS; therefore the molecular mimic may be a novel therapeutic target in multiple forms of ALS.

Declaration

I declare that the work presented in this thesis titled "Role of Protein disulphide Isomerase and its family members in Amyotrophic Lateral Sclerosis" has not previously been submitted, in either whole or part, for the purposes of obtaining any other degree to any other university or institution other than Macquarie University. Unless otherwise acknowledged, this work was carried out by the author.

Signed: Sonam Parakh

Date: 13/10/15

Preface

All work described in this thesis was performed by the author, except where hereby stated. The author acknowledges the following people for assistance in performing the experiments reported in this thesis:

Chapter 4

Site-directed mutagenesis reactions for generation of PDI mutants was performed by Masters student Navya Billa in the laboratory, La Trobe University Melbourne, Australia. Dr Bradley Turner performed the in vivo experiments and administered BMC in $SOD1^{G93A}$ mice, Florey Institute of Neuroscience and Mental Health, The University of Melbourne, Australia). Experiments performed to investigate which activity of PDI is protective against mutant FUS induced ER stress and mislocalisation in neuronal cultures were performed by Jess Sultana, PhD student in the laboratory Macquarie University, Sydney, Australia.

Chapter 5

Experiments performed to investigate whether ERp57 is protective against mutant TDP-43 induced ER stress and mis-localisation in neuronal cultures were performed by Emma Perri, PhD student in the laboratory La Trobe University Melbourne, Australia.

Chapter 6

Harvesting of primary neurons from the cortex of C57BL/6 mouse embryos were performed by Dr Vinod Sundaramoorthy, Macquarie University, Sydney, Australia. Cytoplasmic PDI was constructed with the kind assistance of Dr Damian Spencer.

Acknowledgements

It's a pleasure to thank all those people who helped me during my PhD. First and foremost, I would like to express my sincere thanks and gratitude to my supervisor Julie Atkin. Your guidance, advice and endless support has been the most important throughout my PhD. I am extremely grateful for all your enthusiastic encouragement and useful critiques during my Masters and PhD. I would also like to thank Damian Spencer who encouraged and helped me establish my grounds in research. I owe my deepest gratitude to Kai Soo and Manal Farg, for sharing their valuable experience and advice throughout the years. A very special thanks to all my lab members Vinod Sundaramoorthy, Jess Sultana, Emma Perri and David Rayner. Thank you so much for making this journey smoother and lot happier. My sincere thanks to Roger Chung for his constant guidance and solving all non-science queries.

This thesis won't have been possible without the constant love and support of my wonderful friends who patiently comforted me and encouraged me during PhD. Neena Shankar, Arun Kumar, Jayant Sreekumar, Aravind, Raunak Dattani, Neha Agarwal, Umang Bhakta, Mayuri Tharani, Neha Narula, Aastha Gupta, Sneha Jain, Ritesh Parekh and Kunal Kalra. Thank you so much for your unfailing willingness to lend a hand or a sympathetic ear. I am deeply grateful to Pujyashree Deepak Bhai and Dimple bhai. Niruma and Dadji. To my cousin Dr Sagun Parakh for helping me decide me career path without your constant encouragement I would not be where I am today. Last but most importantly my deepest gratitude to my parents Santosh Parakh and Shobha Parakh and my younger brother Shreyans Parakh, for being my greatest support and lifeline. Thank you for all the inexplicable love and support. I am very lucky to have you guys, I truly appreciate everything you have done for me.

Dedicated to my brother - Shreyans Parakh

Table of contents

General Introduction

ALS	Amyotrophic lateral sclerosis
AMPA	α-amino-3-hydroxy-5-methyl-4-isoxazolepropionic acid
ANOVA	analysis of variance
ARJALS	autosomal recessive juvenile ALS
ASK1	apoptosis signal-regulating kinase 1
ATF4	activating transcription factor 4
ATF6	activating transcription factor 6
ATP	adenosine triphosphate
BCA	bicinchoninic acid
BMAA	β-methylamino-L-alanine
BIM BCL2	interacting mediator of cell death
BiP	immunoglobulin binding protein
BMAA	β-N-methlyamino-l-alanine
BMC	1,2 bis(mercaptoacetamido)cyclohexane
C9ORF72	Chromosome 9 open reading frame 72 gene
Ca2+	calcium ions
cDMEM	complete Dulbecco's modified Eagle's medium
cDNA	complementary D
CHMP2B	charged multivesicular body protein 2B
CHOP	enhancer binding protein (C/EBP) homologous protein
CMA	Chaperone-mediated autophagy
CMT	Charcot-Marie-Tooth disease
CNS	central nervous system
COP	coat protein complex
CSF	cerebrospinal fluid
DAPI	4',6 diamidino-2-phenylindole
DENN	differentially expressed in normal and neoplastic cells
DMEM	Dulbecco's modified Eagle's medium
DMSO	dimethyl sulphoxide
DNA	deoxyribonucleic acid

dNTPs	deoxynucleoside triphosphates
E. coli	Escherichia coli
EAAT2	excitatory amino acid transporter 2
EDTA	ethylenediaminetetraacetic acid
eIF2α	eukaryotic translation initiation factor 2 subunit α
ERAD	ER-associated degradation pathway
ER	endoplasmic reticulum
ERGIC	ER-Golgi intermediate compartment
ERo1	ER oxidoreductin 1
ERp57	Endoplasmic reticulum protein 57
ERp72	Endoplasmic reticulum protein 72
EWSR1	Ewing sarcoma breakpoint region 1
ESCRT	endosomal sorting complex required for transport
fALS	familial ALS
FAD	flavin adenine dinucleotide
FDA	Food and Drug Administration
FCS	fetal calf serum
FDA	food and drugs administration
FTD	frontotemporal dementia
FTLD	frontotemporal lobar degeneration
FUS	fused in sarcoma
GWAS	genome-wide association studies
HIV	human immunodeficiency virus
HuR	Hu Antigen R
IPSCs	Induced pluripotent stem cells
IRE1	inositol-requiring kinase 1
JNK	c-Jun N-terminal kinase
Kan	kanamycin
KAP3	kinesin associated protein 3
LMN	lower motor neuron

MAM	mitochondrial-associated ER membrane
MHC	major histocompatibility complex
mTOR	mammalian target of rapamycin
NES	nuclear export signal
NF-κB	nuclear factor kappa-light-chain-enhancer of activated B cells
NF-H	neurofilament heavy chain
NLS	nuclear localization sequence
NMDAR	N-methyl d-aspartate receptor
Nrf2	nuclear factor E2 related factor 2
PD	Parkinson Disease
PDI	Protein disulphide isomerase
PLC	peptide loading complex
PLS	primary lateral sclerosis
PMA	progressive muscular atrophy
PNA	peptide nucleic acids
RNase A	ribonuclease A
sALS	sporadic ALS
SGs	stress granules
SMA	spinal muscular atrophy
SOD1	superoxide dismutase 1
STAT3	signal transducer and activator of transcription 3
TAF15	TATA-binding protein associated factor 15
TAP	transporter associated with antigen processing
TBK1	TANK-binding kinase 1
TBS	tris buffered saline
TDP-43	transactive response DNA binding protein of 43 kDa
TIAR	TIA-1-related protein
TLS	translocated in sarcoma
TUBA4A	tubulin, alpha 4a

UAD	ubiquitin association domain
UBL	ubiquitin like domain
UMN	upper motor neurons
UPR	unfolded protein response
UPS	ubiquitin proteasome system
VAPB	vesicle associated membrane protein-associated protein B
VCP	valosin containing protein
VEGF	vascular endothelial growth factor
VSVG	vesicular stomatitis virus glycoprotein
XBP-1	X-Box binding protein-1

Units of magnitude and measure

C	Celsius
Da	Dalton/s
g	Acceleration due to gravity at Earth's surface
g	Gram/s
hr	Hour/s
k	Kilo
L	Litre/s
m	Metre/s
M	Molar
min	Minute/s
n	Number of distinct units in a dataset
pI	Isoelectric point
s	Second/s
U	Unit/s
V	Volt/s
Vol	Volume
µ	Micro

Publications

Experimental Paper

- Browne EC, Parakh S, Langford SJ, Atkin JD and Abbott BM (2016) *"**Efficacy of peptide nucleic acid and conjugates against specific cellular pathologies of amyotrophic lateral sclerosis".*** Bioorganic and Medical Chemistry 24(7): 1520-1527.

- Soo K, Halloran, Sudaramoorthy V, Parakh S, Toth R, Southam K, Mclean C, Lock P, King A Farg M, Atkin J (2015) "***ER-Golgi transport dysfunction is a common pathogenic mechanism in SOD1, TDP43 and FUS-associated ALS".*** *Acta neuropathologica*: 1-19.

- Walker AK, Soo KY, Sundaramoorthy V, Parakh S, Ma Y, Farg MA, Wallace RH, Crouch PJ, Turner BJ, Horne MK (2013) "***ALS-associated TDP-43 induces endoplasmic reticulum stress, which drives cytoplasmic TDP-43 accumulation and stress granule formation".*** *PloS one* **8**: 1-12

Review Papers

- Perri E, Parakh S, Thomas C, Spencer D and Atkin J (2015) "***The Unfolded Protein Response and the role of Protein Disulphide Isomerase in neurodegeneration***". Frontiers in Cell and Developmental Biology.3:80

- Parakh S and Atkin J (2015) ***"Novel roles for protein disulphide isomerase in disease states: a double edged sword".*** *Frontiers in Cell and Developmental Biology* **3:** 1-11

- Parakh S, Spencer DM, Halloran MA, Soo KY, Atkin JD (2012) ***Redox Regulation in Amyotrophic Lateral Sclerosis.*** *Oxidative Medicine and Cellular Longevity* **408681:**1-12

- Halloran MA, Parakh S, Atkin JD (2013) ***The Role of S-nitrosylation and S-glutathionylation of Protein Disulphide Isomerase (PDI) in Protein Misfolding and Neurodegeneration.*** *International Journal of Cell Biology* **797914**:1-15

Manuscripts in Preparation

- Parakh S, Spencer D and Atkin J ***"ERp57 is protective against pathology induced by mutant SOD1 in ALS cellular models".***

Chapter 1 General Introduction

1.1 Amyotrophic lateral Sclerosis (ALS)

Amyotrophic lateral sclerosis (ALS) also known as Lou Gehrig's disease in the USA, is a lethal neurodegenerative disease that affects the upper and lower motor neurons of the brain stem, cortex and spinal cord [1]. Due to the progressive denervation, ALS causes death within 3-5 years of diagnosis on average due to respiratory failure [2]. The symptoms generally include muscle weakness, paralysis and atrophy, with patients having disability in eating, drinking and slurred speech [3]. Since the aetiology of the disease is still under investigation, treatment of patients is primarily palliative [4]. Riluzole is the only Food and Drug Administration (FDA) approved drug used for the treatment of ALS but it may only increase survival by a few months [5, 6]. Therefore, there is an essential requirement for identification of new therapeutic targets.

ALS is classified into two types. The majority of the cases are sporadic (sALS) whereas approximately 15% of cases are genetic termed as familial ALS (fALS) [7, 8]. Nonetheless, there is a great clinical and pathological overlap between the two forms [9]. Therefore, insights gained from studying fALS are likely to be applicable to those with sALS as well. Additional genetic and environmental risk factors have also been identified such as viral infection, smoking and exercise (section 1.4). Understanding the molecular mechanisms of disease in ALS will allow the design of effective therapeutics in the future. Furthermore, potential therapies targeted at fALS may be applicable to all kinds of ALS. Current evidence identifies induction of endoplasmic reticulum (ER) stress as central mechanism in disease pathology. This thesis focuses on understanding the role of protein disulphide isomerase (PDI) a chaperone induced during ER stress and its family members in ALS, with the objective of using PDI and its protective ability as therapeutic target in disease pathology.

1.2 Clinical Features of ALS

Classical ALS affects both primary and lower motor neurons and patients have clear dysfunction in these regions affecting the arm, leg and facial muscles [10]. If only upper motor neurons (UMN) are affected the disease is known as primary lateral sclerosis (PLS) [11]. In contrast if only the lower motor neuron (LMN) in the spinal cord are affected the disease is termed progressive muscular atrophy (PMA) [12]. However, if the lowest motor neurons in the brainstem are affected the resulting condition is known as progressive bulbar plasy, causing slurred speech [13]. ALS also shares clinical and neuropathological similarities with frontotemporal dementia (FTD) which is characterised by behavioural and language dysfunction [14]. There is a great clinical and pathological overlap between ALS and FTD; around 15% of patients with pathologically confirmed FTD have ALS [15] while another 25% may have slight motor system dysfunction [16]. Recent identification of common genetic causes of both ALS and FTD involving mutations in *FUS*, *TARDBP* and hexanucleotide expansions in *C9ORF72* [17, 18], represents a spectrum of overlapping clinical symptoms.

In ALS, 75-80% of patients, symptoms begin with limb involvement, while around 20-25% of patients have bulbar symptoms during disease onset [19].Women have a greater frequency of bulbar onset than men [20]. Patients generally are hyper-reflexic and stiff; symptoms may include spasms and sudden, uncontrolled straightening movements of the lower limbs [21]. Muscle fasciculations occur, early during the disease state, particularly in the tongue and limb regions [12]. As ALS progresses, muscle atrophy and cramps become common, and spasticity causes gait abnormalities [22]. Patients with bulbar involvement may also develop swallowing difficulties (dysphagia). A mixture of spastic and flaccid components may characterize the patients speech, resulting in dysarthria with severe disintegration and slowness of articulation [23]. Since, the disease primarily involves motor neurons, extraocular movements, bowel and bladder control are preserved in most cases [24].

1.3 Epidemiology of ALS

ALS occurs throughout the world with no racial, ethnic or socioeconomic boundaries. It has a worldwide incidence of 2–3 individuals per 100,000 population per year [25] and a prevalence of 4–6 per 100,000 population [26]. The incidence of ALS is higher in men than in women, with an overall male-to-female ratio of 1.5-2:1 [27]. In European population the incidence rate is high with Finland reporting the highest rate of ALS [28]. Meanwhile, incidence rate of ALS outside populations of European descent is less well-characterized and comparatively lower among Africans, Asians [29] and Alaska natives [30]. More whites are affected than nonwhites in the United States with white-to-nonwhite ratio of 1.6:1 however, it could be due to limited case findings in nonwhites [31]. In 2011 the US National registry analysed a total of 12,187 people with ALS. For the 10,971 patients for whom race was known 79.1% white people developed ALS whereas only 6.5% of non-white population had ALS [32]. Peak age of onset is 58–63 years for sporadic disease and 47-52 years for familial disease also, incidence decreases rapidly after 80 years of age [33].

1.4 Environmental considerations for ALS

Many environmental factors have been associated with the development of ALS, including smoking, viral infection, cyanotoxins and Gulf war service [34]. ALS prevalence is also observed in people with a history of brain trauma [35] and involvement in extensive athlete's exercise [36] or professional soccer players [37]. Some studies suggest exposure to heavy metal such as lead, mercury or pesticides and organic solvents may have an indirect impact on ALS. However, no direct relation has been established with ALS [38].

Smoking has been considered as an established risk since 2009 after assessment of many thorough case studies [39, 40]. The number of years of smoking increases the risk of ALS, while the number of years since stopping smoking decreases risk [41]. Additionally a different study with over 10,000 ALS patients and 11,000 matched controls identified an increased risk of ALS in women who smoked, but not men,

compared to non-smokers [42]. However, various contradicting studies have also come into light leaving the question unanswered [43]. ALS-like syndrome can also occur in association with human immunodeficiency virus (HIV) infection [44] although the evidence for a causative link remains correlative. In some patients partial recovery from ALS symptoms has been reported with antiretroviral treatment [44]. Another case study suggested that endogenous retroviral elements contribute in the pathophysiology of ALS, but again there is no evidence that they are the primary cause of the syndrome [45]. Armed military personnel deployed to the Persian Gulf War of 1990-1991 have twice the risk of getting ALS than military personnel who were not deployed [46, 47]. The increased incidence of ALS in this population has been attributed to an environmental factor although exact the cause remains unknown.

A closer link between ALS and environmental agents is evident by chronic exposure to the neurotoxin β-methylamino-L-alanine (BMAA) isolated from Cycas micronesica; a cycad plant produced by symbiotic cyanobacteria living in the roots [48]. BMAA found in cycad seeds are consumed in the diet of the Chamarro people of Guam [49]. A high content of cyanotoxins up to 50-100 times greater incidence of an ALS-complex disease is observed in Chamaro people [49]. However, more detailed epidemiological and toxicological studies have failed to support the hypothesis that these forms of ALS result from cyanotoxic effects.

1.5 Genetic causes of ALS

Known genetic causes of ALS now account for 11% of sALS and 68% of fALS [8]. A major advancement in the field was made in 2011 when a mutation in C9ORF72 repeat expansion of sequence GGGGCC (G_4C_2), was identified as the cause of 30% of fALS cases and 7% of sALS cases [17, 50]. However, superoxide dismutase 1 (SOD1) remains the earliest and most widely studied gene which accounts for 20% of fALS cases and 2% of all ALS [51]. Mutations in *TARDBP* encoding TDP-43 protein and FUS account for approximately 5% of fALS cases [52]. Importantly, misfolded, wild-type forms of SOD1, TDP-43 and FUS are also implicated in sALS

pathology, emphasising the overlap between sporadic and familial ALS [53-55]. Mutations in these four genes (*C9ORF72, SOD1, TARDBP, and FUS/TLS*) together account for over 50% of all fALS cases and hence are the most common genetic mutations which are discussed in the sections below [18]. Other genes identified are present in only a minority of cases of ALS (less than 1%) are also discussed.

Gene	Loca-tion	Inheritance	Familial ALS (%)	Sporadic ALS (%)	Reference
SOD1	**21q22**	**AD and AR**	**12**	**1–2**	**[51]**
C9ORF72	**9p21**	**AD**	**40**	**7**	**[17, 51]**
TARDBP	**1p36**	**AD**	**4**	**1**	**[56]**
FUS	**16p11**	**AD and AR**	**4**	**1**	**[57]**
UBQLN2	**Xp11**	**XD**	**<1**	**<1**	**[58]**
VCP	**9p13**	**AD**	**1**	**1**	**[59, 60]**
SQSTM1	**5q35**	**AD**	**1**	**<1**	**[61, 62]**
OPTN	**10p13**	**AR and AD**	**<1**	**<1**	**[63]**
PFN1	**17p13**	**AD**	**<1**	**<1**	**[64]**

Table 1 Genetic mutations associated with the most common forms of familial ALS. Values represent the percentage of ALS cases in European populations. AD, autosomal dominant; AR, autosomal recessive; XD, X-linked dominant.

Gene	Location	Predominant clinical syndromes	Reference
VAPB	**20q13**	PMA, fALS	**[65, 66]**
DCTN1	**2p13**	PMA; Perry syndrome	**[67-69]**
NEFH	**22q12**	fALS, sALS	**[70]**
PRPH	**12q12**	ALS, RP, mascular dystrophy	**[64]**
ALS2	**2q33**	Juvenile PLS; infantile HSP	**[71-73]**
FIG4	**6q21**	CMT; fALS	**[74, 75]**
CHMP2B	**3p11**	fALS; sALS; FTD	**[76]**
SETX	**9q34**	Juvenile ALS; ataxia with oculomotor apraxia	**[77]**
ANG	**14q11**	fALS; sALS	**[78]**
SPG11	**15q14**	Juvenile ALS; HSP	**[79, 80]**
DAO	**12q22-23**	ALS	**[81]**
TBK1	**12q14.2**	ALS	**[82]**
TAF15	**17q12**	ALS	**[83]**
MATR3	**5q31.2**	ALS	**[84]**
HNRNPA1	**12q13**	Multisystem proteinopathy; ALS	**[85]**
HNRNPA2B1	**7p15**	Multisystem proteinopathy; ALS	**[85]**
ELP3	**8p21**	sALS	**[86]**

Table 1. 2 Other genes (<1%) linked to implicated in the pathogenesis of disease. sALS - sporadic ALS, fALS - familial ALS, PMA - progressive muscular atrophy, FTD - frontotemporal dementia, HSP - hereditary spastic paraplegia, CMT-Charcot-Marie-Tooth disease; RP, retinitis pigmentosa, AOA2 - ataxia with oculomotor apraxia type 2.

1.6 Superoxide dismutase 1 (SOD1)

Human SOD1 is a homo-dimeric enzyme which is 32 kDa in size and the two subunits are linked non-covalently [87]. The dimer is formed by means of four hydrogen bonds with multiple hydrophobic and water mediated interactions [88]. The *SOD1* gene located on chromosome 21 codes for an intracellular metalloenzyme containing copper and zinc. SOD1 is predominately found in the cytoplasm and nucleus [89] and it catalyses the reduction of harmful, free superoxide radicals into molecular oxygen and hydrogen peroxide [90]. It is highly conserved and accounts for 1-2% of the total soluble protein found in the nervous system [91]. Therefore, this highly stable enzyme regulates oxidative stress and protects against oxygen radical-induced cellular stress [92]. SOD1 is stabilized by four cysteine residues present in each subunit two of which are linked by disulphide bonds [93]. The metal ions zinc and copper are present on each subunit and are essential for protein stability and catalytic activity of the enzyme [94].

Over 160 different ALS-linked SOD1 mutations have now been identified, throughout all five exons of the *SOD1* gene [95]. Most mutations cause single amino acid residue changes, however several deletions, insertions and truncation mutations are also present in disease. Around 95% of SOD1 missense mutations cause classic autosomal dominant ALS, although autosomal recessive inheritance occurs in rare instances involving specific SOD1 mutations such as D90A (aspartic acid to alanine) and D96N (aspartic acid to asparagine) [95-97]. The most commonly studied SOD1 mutations are A4V (alanine to valine), G93A (glycine to alanine) and G85R (glycine to arginine). The A4V mutation has a founder effect in the USA [98]. Some SOD1 mutations including H46R (histidine to arginine), disrupt binding to copper, which is required for the normal dismutase activity of the enzyme, and are therefore catalytically inactive. In contrast other ALS-linked SOD1 mutations including G93A retain normal metal binding and hence dismutase activity [60]. However, the dismutase activity of each ALS-linked mutant does not correlate with disease onset, severity or progression [99]. Inactive $SOD1^{H46R}$ associated with a slowly progressive disease, compared to active $SOD1^{G93A}$, which results in a classic, rapidly progressing disease [61-63]. Recent research has

identified misfolded wild-type SOD1 in non-SOD1-fALS and in sALS suggesting that it could play a role in the pathogenesis of ALS [100-102]. Misfolded SOD1 monomers have been observed in spinal cords of mice models of ALS-(G85R, G93A and G37R) using a specific SOD1-exposed dimer interface (SEDI) antibody. However another study demonstrated that misfolded SOD1 was specific to only fALS and was not observed in sporadic patients [103]. Over-expression of wild-type human SOD1 hastens disease in several mutant SOD1 transgenic mouse lines, indicating that even wild-type SOD1 could be involved in disease pathogenesis [89, 101].

Sporadic and SOD1-linked ALS are clinically indistinguishable and share many pathological hallmarks, signifying that an understanding of the SOD1-linked forms of disease should have broader application to all ALS cases.

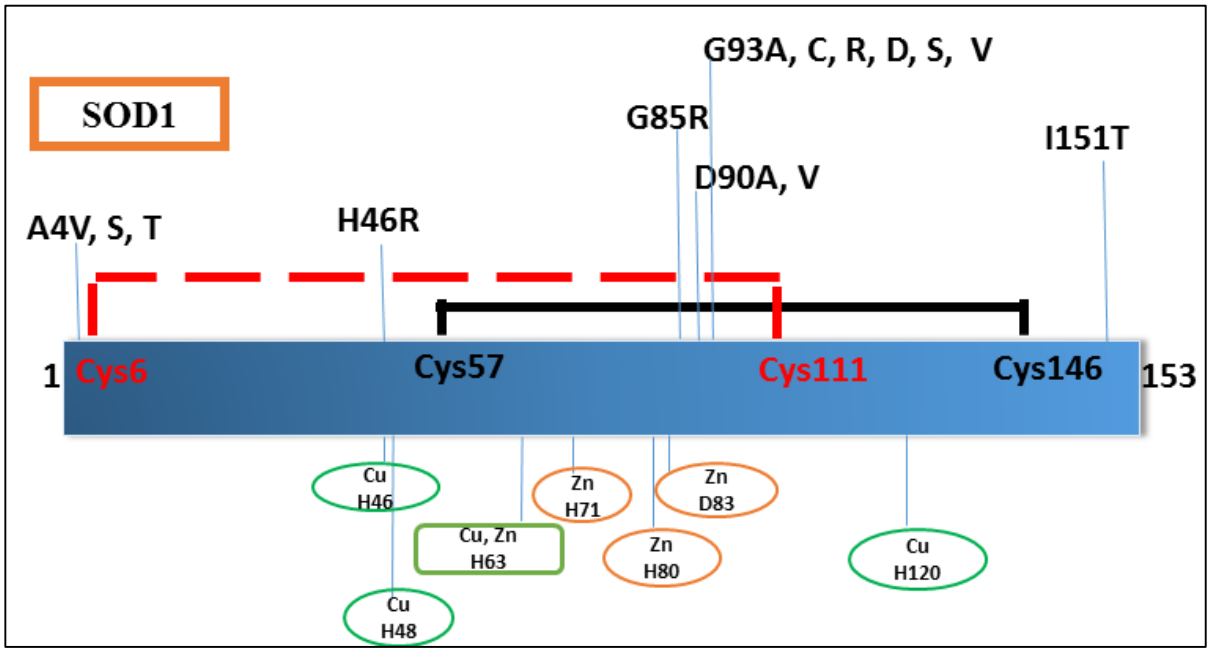

Figure 1 Schematic representation of SOD1 structural domain: displaying the location of several ALS causative mutations within the protein. The copper and zinc binding histidine residues and aspartic acid residues are also shown. The cysteine residues at position C57 and C146 forms an intrasubunit disulphide bond (black).

However, abnormal disulphide bonding is observed between C6 and C111 in ALS shown in red.

Mutant SOD1 proteins have a highly destabilized structure compared to wild-type protein and are much readily reduced into monomers [104]. Reduction of the disulphide bonds between C57 and C146 and demetallation at the dimer interface, could induce monomer formation [94, 105, 106]. Mutations in SOD1 also weaken the dimer interface thus increasing the load of unstable SOD1 monomer. Furthermore, oxidative modification of the amino acid residues present on the SOD1 dimer interface induces monomerisation and aggregation [105]. They induce toxicity in neuronal cell cultures and the toxicity of SOD1 is unrelated to its enzymatic behaviour [95, 107]. Accumulation of mutant SOD1 in affected neurons and astrocytes leads to the formation of insoluble, intracellular ubiquitin positive aggregates or inclusions [108]. Misfolded proteins underlie the formation of inclusions and these inclusions increase in number with the progression of disease [99]. Large SOD1 positive inclusions are visible by light microscopy in motor neurons of SOD1 patients and animal models [66]. SOD1 inclusions are also observed in the kidney and liver cells, although their relevance to disease remains unknown [67]. The exact mechanism by which mutant SOD1 causes neurodegeneration is unknown but several hypotheses are implicated including impairment of axonal transport, disruption of calcium homeostasis, dysfunction to ubiquitin-proteasome system, mitochondrial damage and dysregulation to autophagy [109, 110].

1.7 Animal disease models to investigate ALS

The first animal model of ALS, created in 1994, was the transgenic $SOD1^{G93A}$ mouse, following identification of mutations in SOD1 as a cause of fALS [111]. This model displays similar pathogenic features, including muscle denervation, muscle paralysis, motor dysfunction, and motor neuron death, to clinical cases of fALS and sALS. Several other transgenic mouse models based on SOD1 are now

available, including G37R, G85R, G127X, D90A and H46R [112-114]. Furthermore, disease models based on mutant SOD1 have also been developed in zebra fish, rodents and Drosophila [115-117]. While SOD1 transgenic models have provided significant insights into mechanisms of motor neuron degeneration, no therapeutic interventions that were successful in these animals have been validated in ALS patients [113]. Hence, this model has been extensively criticised. Furthermore, these mouse models may not replicate human disease accurately transgenic SOD1 G93A and D90A mice have been demonstrated to increase the load of mutant SOD1 in mitochondria in a non-physiological manner, inducing artifactual mitochondrial swelling [118]. Mice overexpressing wild-type SOD1 developed ALS like symptoms, although disease onset takes much longer compared to the $SOD1^{G93A}$ mice [119]. Similar pathological changes including loss of ventral horn neurons, vacuolisation and gliosis, were observed in both wild-type and mutant mice at disease end stages. However, ataxic staggering gait was observed in the mutant $SOD1^{G93A}$ mice only. The wobbler mouse, which bears a point mutation in the *Vps54* gene, demonstrates progressive degeneration of upper and lower motor neurons [120]. More recently, animal models have been generated based on mutations in TDP-43, FUS, and C9ORF72 [18, 121, 122], and ALS-associated mutant TDP-43 and FUS models have been developed in rat, zebra fish, yeast, roundworm, and Drosophila [123-128]. Transgenic TDP-43 mice carrying a human mutation (A315T) were developed several years ago but these animals do not replicate important features human ALS and die of gut pathology [129]. However, recently a novel mouse model based on wild-type TDP-43 lacking a NLS was developed, which displays a motor phenotype reminiscent of the SOD1 mouse models [130]. Furthermore, Drosophila and zebrafish models over-expressing hexanucleotide expansions in C9ORF72 have been recently developed [131]. Similarly, knock down of C9ORF72 in zebrafish models induces locomotion deficits and reduced axon lengths of motor neurons, although recent studies have argued against the loss of function as a novel pathogenic mechanism in ALS [132, 133].

1.8 Chromosome 9 open-reading frame 72 (C9ORF72)

The G_4C_2 hexanucleotide repeat expansion is present in the noncoding region of *C9ORF72* and it is a major cause of FTD as well as ALS [17, 50]. Bioinformatics studies show that the localisation of this protein is mostly cytoplasmic, and it is structurally related to DENN domain proteins conserved GDP-GTP exchange factors for RAB proteins [134]. However, normal cellular function of C9ORF72 and the exact mechanism by which it causes ALS is still under investigation. In normal individuals the G_4C_2 sequence is repeated 2-5 times and has not been detected above 30 times [135]. However, in ALS patients G_4C_2 is abnormally expanded from hundreds to thousands [135, 136]. A recent study demonstrated using epigenetic and RNA expression analyses that the small repeat expansions (less than 70 repeats) are multiple in origin and expand during parent-offspring transmission [137]. There are various hypotheses regarding how the C9ORF72 repeat expansion causes disease pathology including haploinsufficiency leading to loss of function of C9ORF72 encoded protein, RNA mediated toxicity and toxic dipeptides produced from repeat associated non-ATG (RAN) translation. The repeat expansion could potentially alter expression of the mutant allele, causing a decrease in expression of C9ORF72 transcripts. Alternatively, the G_4C_2 expansion could result in aberrant methylation of the cytosine phosphate guanine island near the repeat, resulting in down regulation of gene expression as studied in the Canadian patients [138]. Another mechanism is accumulation of abnormal repeat RNA transcripts that accumulate within nuclear foci in the brain and spinal cord of C9ORF72 expanded repeat carriers [17]. Similarly, other studies have also demonstrated the presence of RNA foci which may sequester RNA binding proteins in association with C9ORF72 ALS [139-141]. The repeat transcripts also undergo unusual RAN translation, thus generating peptides which aggregate in affected neurons and accumulate into distinct foci, causing ER stress and neurotoxicity in patients with ALS and FTD [142, 143]. These peptides affect transcription and translation, interfering with both mRNA splicing and the biogenesis of ribosomal RNA [144]. Expression of long G_4C_2 (78x) repeats forms intranuclear RNA foci that induce apoptosis in neuronal cell lines and zebrafish models, suggesting RNA toxicity and protein sequestration trigger neurodegeneration [145]. Recently,

nucleocytoplasmic shuttling of G_4C_2 expansion in C9ORF72 was demonstrated to induce toxicity in Drosophila models [146, 147].

1.9 TAR DNA-binding protein-43 (TDP-43)

TDP-43 is a widely-expressed protein encoded by the *TARDBP* gene located on human chromosome 1p36.22, with a molecular mass of 43 kDa [148, 149]. TDP-43 is a multifunctional RNA and DNA-binding protein which also interacts with other ribonuclear proteins. TDP-43 contains two RNA recognition motifs, a nuclear localization sequence (NLS), a nuclear export signal (NES) [150], and a glycine-rich C-terminus which facilitates protein interactions [151]. TDP-43 is generally localised in the nucleus, where it mediates RNA splicing and modulates microRNA biogenesis [152, 153]. It can also regulate the stability of its own mRNA, therefore it can auto regulate its protein levels [154]. Around one third of the cellular distribution of TDP-43 is cytoplasmic as it shuttles continuously between the nucleus and the cytoplasm [150, 155]. TDP-43 is a crucial component of dendritic and somatodendritic RNA transport granules in neurons [156, 157] and it plays an important role in neuronal plasticity by regulating local protein synthesis in dendrites of Drosophila models [158]. Knockdown of TDP-43 in mice models disrupts motor function and yields embryonic lethality [159]. TDP-43 is particularly significant under conditions of cellular stress as it is involved in the cytoplasmic stress granule response and forms protein complexes that sequester mRNAs redundant for survival [160].

Around 44 mutations in the *TARDBP* gene have been identified in both familial and sporadic ALS patients. These mutations are mostly clustered around the C-terminus of the protein and together they account for approximately 2% of total ALS cases, although TDP-43 pathology is rarely observed in fALS cases [56, 161-163]. TDP-43 is the major constituent of cytoplasmic and intranuclear inclusions in spinal cord neurons of patients with ALS and cortical neurons of FTD patients [54, 164]. Ubiquitinated TDP-43 positive inclusions are present in 97% of total ALS cases, emphasising the central role of TDP-43 pathology is importance in ALS [165, 166].

However, how TDP-43 dysfunction is associated with ALS remains largely unknown, although disease-specific fragmentation [56], aggregation of TDP-43 [167, 168], redistribution from the nucleus to the cytoplasm [169], loss of RNA processing [170] and axonal transport impairment [156] are key features linked to pathology [149]. Further discussion of the involvement of TDP-43 in ALS and results from investigations into the role of ER stress in TDP-43-linked disease are presented in Chapter 3.

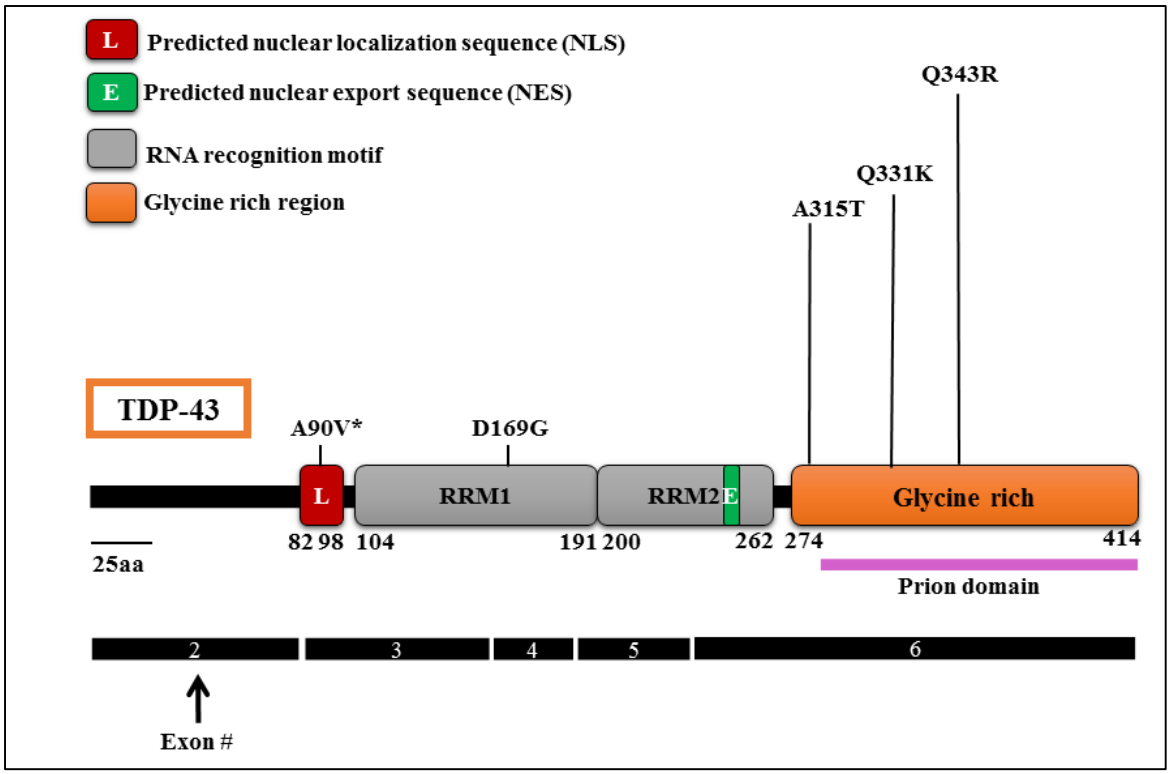

Figure 2 Schematic representation of the structural domains and motifs within TDP-43 domain: displaying ALS causative mutations within the protein. TDP-43 mutants A315T, Q331K and Q343R were used in this study.

1.10 Fused in Sarcoma (FUS)

Fused in sarcoma (FUS, also known as translocated in liposarcoma) is a multi-functional DNA/RNA-binding protein which belongs to the FET family, encoded

by the *FUS* gene located on human chromosome 16p11.2 [171]. TATA-binding protein associated factor 15 (TAF15) and Ewing sarcoma breakpoint region 1 (EWSR1) are other ALS genes that also belong to the same family of proteins [172]. FUS is 53 kDa in size and it bears similarities to TDP-43 in domain structure. FUS consists of a N-terminal serine-tyrosine-glutamine glycine (STQG) rich region, a glycine rich region, a conserved RNA recognition domain, a RanBP2-type zinc finger motif and multiple C-terminal arginine glycine-glycine motifs [173]. The C-terminus of FUS is thought to contain a specialised proline tyrosine nuclear localisation signal involved in RNA binding [174]. Although typically considered as a nuclear protein, FUS also plays a role in the nuclear-cytoplasmic shuttling of mRNA. FUS is also more immunodetectable in mature dendritic spines upon activation by metabolic glutamate receptor mGluR5 [175]. FUS regulates RNA metabolism, which includes transcription and post-transcriptional processing, such as pre-mRNA splicing and mRNA trafficking [176]. FUS-/- mice are not viable due to disruption of immune cell development and genomic instability [177]. Importantly, FUS knockdown in mice results in abnormal neuronal morphology signifying the role of FUS for neuronal structure and function [175].

In 2009 two groups identified mutations in the *FUS* gene causing around 5% of FUS linked fALS and less than 1% sALS. FUS in sALS cases however is controversial [57, 178]. Henceforth, FUS mutations have been shown in FTD, and in FTLD patients without motor impairment [179-181]. More recently, FUS mutation were also found in a family with hereditary essential tremors [182]. Most ALS associated FUS mutations are missense mutations and fewer cases of deletion and frame shift mutations have also been reported [153, 183]. FUS immunoreactivity has been detected with expanded poly-glutamine protein nuclear aggregates in cell culture [184]. These reports highlight the pathogenic overlap between ALS and other neurodegenerative diseases, indicating that similar dysfunctions could result in different clinical outcomes. Post mortem analysis of brain and spinal cord tissues of ALS patients with FUS mutations demonstrated that abnormal cytoplasmic inclusions containing FUS were present in neurons and glial cells in the absence of post-translational modifications such as

hyperphosphorylation and ubiquitination [57, 178]. FUS immunoreactivity is observed in inclusions of sporadic and TDP-43 mutant ALS patient spinal cords but not in patients with SOD1 mutations, similar to TDP-43 [55, 185].

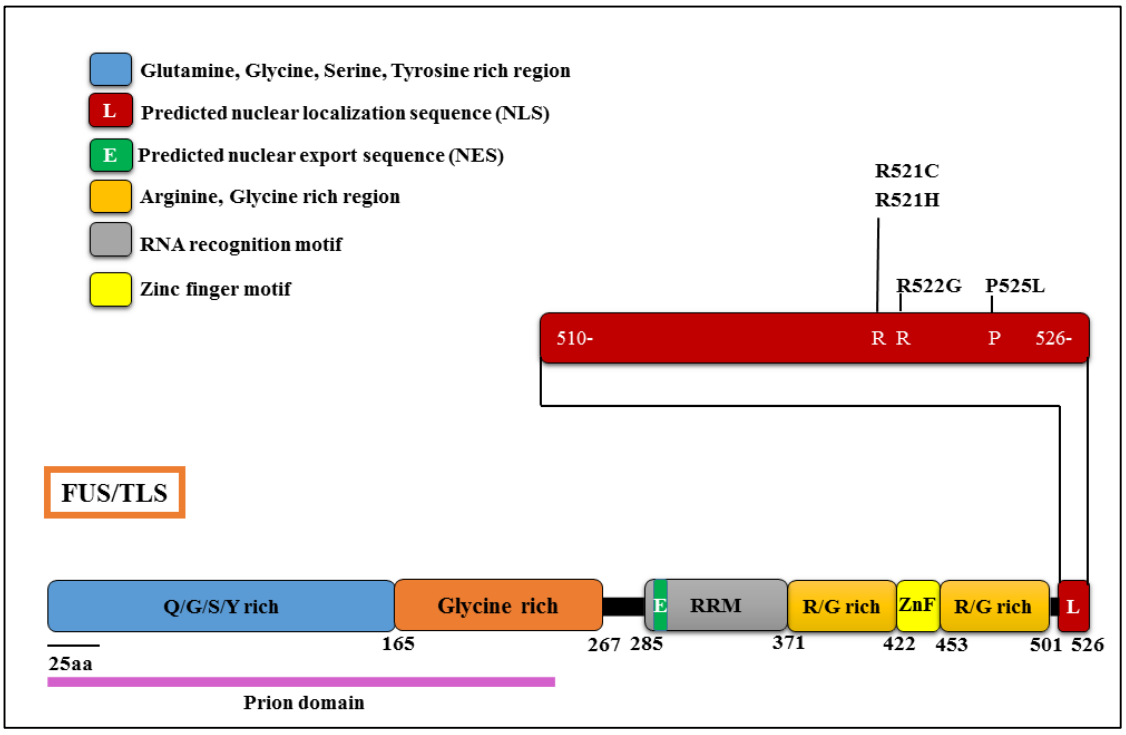

Figure 3 Schematic representation of the structural domains and motifs within FUS domain: displaying ALS causative mutations within the protein. FUS mutants R521C, R521H, R522G and P525L were used for this study.

Over 46 ALS causing FUS mutations have been identified, and most of these cluster around the C-terminus (515-524 amino acid) of the protein. In this region all 5 conserved arginine residues are mutated in ALS [52]. Several *in vitro* studies have shown that these mutations prevent nuclear import of FUS causing mislocalisation to the cytosol and the generation of transient stress granules (SGs) [186]. They also interrupt transportin mediated nuclear import of FUS [187]. The exact mechanism by which mutations in FUS cause ALS is still under investigation. However, loss of function due to incomplete disease penetrance in some FUS-linked ALS patients could be responsible [178, 179]. Though, most mutations are dominantly inherited,

suggesting that a gain of toxic function could be in operation in most cases. Moreover, different mutations in FUS may have different pathological effects. Expression of dominantly inherited mutant FUS R521G (arginine to glycine) induces cytoplasmic inclusion formation in neuroblastoma cells, however, expression of mutant H517Q (histidine to glutamine) FUS which is recessively inherited had no such effect [178]. Another truncated mutant R495X causes a severe ALS like phenotype leading to causing cytoplasmic distribution of FUS in HEK cells and zebrafish models [188]. Mutant R521C (arginine to cysteine) mislocalises and generates stress granules in primary cultured transgenic zebrafish models [189].

1.11 Mutations causing disturbance in protein homeostasis

1.11.1 Ubiquilin-2 (UBQLN2)

Ubiquilin-2 is encoded by the UBQLN2 gene and it is a member of the ubiquitin like protein family that all possesses a N-terminal ubiquitin like domain (UBL) and a C-terminal ubiquitin association domain (UAD) [190]. Ubiquilin-2 delivers ubiquitylated proteins to the proteasomal degradation machinery by simultaneously binding to these proteins through its UBA domain and to the proteasome through its UBL domain [191]. Mutations in UBQLN2 gene causes X-linked autosomal dominant form of classic ALS and frontotemporal lobar degeneration FTLD [58]. A PXX region located in the vicinity of the N-terminus of the UBA domain harbours the mutations associated with fALS and FTD [192, 193]. Ubiquilin-2 positive inclusions have been detected in motor neurons of patients with sALS or FTLD (in the absence of disease-linked UBQLN2 mutations) [58] as well as in patients with FUS mutations [192], suggesting that ubiquilin-2 may have a broader role in ALS additional to the association with mutations in fALS. It forms skein-like inclusions in association with TDP-43 in motor neurons of ALS patients. Furthermore, staining with C9ORF72 in ubiquilin-2 patients reveals abnormal pathology with dystrophic neurites and aggregates in the neocortex suggesting a common downstream pathway involving ubiquitin proteasome system in the disease pathology [194].

1.11.2 Valosin containing protein (VCP)

Also known as p97, VCP is an AAA ATPase associated with diverse cellular activities [195]. VCP is a multifunctional ubiquitin sensitive chaperone that unfolds and disassembles protein complexes [196]. It is ubiquitously expressed and plays an important role in ER associated degradation (ERAD) [197]. The N-terminal region of VCP assists in the transportation of misfolded proteins from the ER to the cytoplasm with its ATPase activity [198]. Misfolded proteins are attached to ubiquitin in the cytoplasm and degraded via the ubiquitin proteasome system [199]. ALS associated mutations in VCP disrupt ERAD function which is linked to disease pathology [200]. VCP is also involved in autophagy and it assists in the fusion of lysosomes with autophagosomes [201]. Knockdown of VCP increases the amount of ubiquitinated proteins and inhibit ubiquitin-proteasome system in Hela cells [202]. Decreased levels of cellular VCP also induces ER stress, due to reduced levels of ERAD substrates in Hela cells [203]. Mutations in VCP were first identified in patients with inclusion body myopathy with early onset Paget disease and FTD [59]. Exome sequencing further identified mutations in VCP clustered around the N-terminal of the protein in a small set of patients with fALS [60].

1.11.3 p62

The Sequestosome1 (*SQSTM1*) gene encodes p62, a major ubiquitin binding protein involved in protein degradation *via* the proteasome machinery [204]. p62 is a common constituent of neuronal and glial ubiquitin-positive inclusions in Alzheimer and Parkinson disease [205, 206]. Following the identification of ubiquilin-2 mutations in ALS the *p62* gene was investigated being a receptor for ubiquitylated proteins. Interestingly, mutations in *SQSTM1* were found in patients with fALS and in individuals with sALS [61]. p62 aggregates in fALS patients and in $SOD1^{G93A}$ mouse model of ALS [207, 208]. Over-expression of p62 with mutant SOD1 augments mutant SOD1 aggregate formation however this effect is reduced when the ubiquitin-associated domain of p62 is deleted in neuronal cell lines [207]. Mutant SOD1 is recognized by p62 in a ubiquitin-independent fashion and is targeted for autophagy [209]. Similarly, p62 co-localizes with TDP-43 inclusions

in FTD patients with ALS [210] and with FUS and TDP-43 ubiquitinated inclusions in motor neurons in spinal cords of sALS patients, non-SOD1 fALS and patients with ALS with dementia [55]. In addition, over-expression of p62 reduces TDP-43 aggregation in an autophagy-proteasome-dependent manner [211].

1.12 Mutations causing cytoskeleton/cellular transport defects

1.12.1 Optineurin (OPTN)

Optineurin is a cytoplasmic and Golgi-localised protein encoded by the gene *Optineurin (OPTN)* gene [212]. The main function of optineurin is to inhibit activation of transcription regulator nuclear factor kappa-light-chain-enhancer of activated B cells (NF-κB) by binding to the ubiquitylated receptor interacting protein [213]. Optineurin is also involved in vesicular trafficking, immune responses and transcriptional regulation [214, 215]. Additionally, the role of optineurin as an autophagy receptor has recently come into light. Optineurin interacts with lysosomes and promotes autophagosome fusion to lysosomes in neuronal cells, therefore it facilitates trafficking of lysosomes during autophagy in association with myosin VI [216]. Dominant missense, recessive deletion and non-sense optineurin mutations are observed in fALS and sALS patients [63]. Optineurin inclusions are present in the cytoplasm of sporadic ALS patients [217]. Mutations in the *OPTN* gene associated with aggressive form of ALS are also linked to adult-onset glaucoma [218]. Over-expression of wild-type optineurin in cell culture causes Golgi fragmentation and over-expression of mutant optineurin increases apoptosis [219, 220]. Recently, our group demonstrated that expression of mutant optineurin results in inhibition of secretory protein trafficking, ER stress and Golgi fragmentation in motor neuron-like NSC-34 cells [216]. These studies suggest that although only a minority of cases are associated with optineurin mutations optineurin is involved in several pathways linked to ALS which could be affected due to optineurin dysfunction. Consistent with this notion, our lab also detected loss of interaction of optineurin with myosin VI in sporadic ALS human spinal cords [216].

1.12.2 Vesicle-associated membrane protein-associated protein B (VAPB)

VAPB is a widely expressed, conserved, ER transmembrane protein, which is vital for microtubule transport [221]. It also plays an important role in ER-Golgi vesicle transport, modulating ER stress [221-223]. A missense P56S (proline to serine) mutation in VAPB is the most common mutation detected so far which causes a gradually progressing atypical form of ALS, autosomal dominant typical ALS or late-onset spinal muscular atrophy (SMA) in Brazilian and German cohorts [65, 224, 225]. However, little is known about the effect of another missense VAPB mutation T46I (threonine to isoleucine) in ALS [226]. Mutant P56S VAPB is ubiquitinated and insoluble, however, over-expression of wild-type VAPB induces the unfolded protein response (UPR) in NSC-34 cells [227]. Interestingly, mutant VAPB inhibits activation of ER stress sensor protein activating transcription factor 6 (ATF6) [228]. Mutant VAPB inclusions are ER derived, and colocalise with ER chaperone PDI [229], implying the importance of ER in disease pathology. VAPB is also important for Golgi maintenance and intracellular transport. Over-expression of mutant VAPB causes Golgi fragmentation in primary neurons [221, 223] and wild-type VAPB is required for Golgi-derived transport of lipids in HeLa cells [222]. No additional ALS-causative mutations in VAPB have been identified to date, indicating that VAPB mutations are a rare cause of ALS. However, decreased levels of VAPB mRNA and protein have been identified in both $SOD1^{G93A}$ transgenic mice models and in the spinal cord tissues of fALS and sALS patients without VAPB mutations [221, 230], suggesting that VAPB could also be involved in more common forms of disease.

1.12.3 Dynactin1 (DCTN1)

Identification of dynactin mutations in ALS indicates dysfunction to intracellular and axonal transport are determinant of motor neuron degeneration because dynactin is involved in microtubule and dynein based intracellular and axonal retrograde transport [231]. Dynactin mutations are rare in ALS and they were identified in the gene encoding the p150Glued subunit of the dynactin complex, *DCTN1* in patients with a form of autosomal dominant ALS, affecting lower motor-

neurons and causing early disease onset [232]. Additional p150Glued mutations in ALS and ALS-FTD patients were also subsequently identified [232]. The disease-linked G59S (glycine to serine) DCTN1 mutation disrupts microtubule binding [231], and transgenic mice expressing G59S develop progressive degeneration which is characterised by defects in vesicular trafficking, accumulation of ubiquitinated inclusions, abnormal ER morphology, an increase in the number of vesicles and autophagy activation [69, 233]. Conversely, few studies have not been successful in identifying disease-associated mutations, implying that dynactin mutations are important but an infrequent cause of ALS [234].

1.12.4 Neurofilament heavy chain NEFH

Neurofilaments are cytoskeleton proteins which are involved in maintaining axonal integrity [235].Heterozygous deletion and insertion mutations in the *NEFH* gene, encoding neurofilament heavy chain (NF-H), have been observed in a few cases (<1%) of sALS and fALS patients [70, 236, 237]. Phosphorylated neurofilament proteins accumulate in inclusions in motor neuron of fALS patients [238]. ALS causing mutations in NF-H are present in the region containing the phosphorylation site essential for neurofilament cross linking. These mutations result in toxicity due to neurofilament aggregation and disorganisation [239]. In the early stages of ALS pathology there is increased accumulation of neurofilaments in the LMN observed in patients [240]. Increased levels of phosphorylated NF-H are observed in the blood of $SOD1^{G93A}$ mice and ALS patients suggesting it may have potential as a ALS biomarker [241]. Despite these results, other studies have failed to identify an association between neurofilament gene mutations and ALS [155]. Furthermore, mutations in neurofilaments are also observed in normal controls as well as in ALS patients suggesting that they are not pathogenic [242]. However, modulating motor neuron degeneration in transgenic NF-H over-expressing mice supports the involvement of NF-H in ALS pathogenesis [156].

1.12.5 Peripherin (PRPH)

Expressed mainly in autonomic nerves and peripheral sensory neurons; peripherin is a neuronal intermediate filament that shares sequence similarity with neurofilament proteins [243]. Missense and frame-shift truncation mutations haven been identified in a few patients with either fALS or sALS, in the gene encoding *PRPH* [244, 245]. Peripherin is a constituent of the inclusions present in spinal cords of ALS patients, and also on over-expression of mutant peripherin in cell culture models [243, 244]. Furthermore, over-expression of peripherin inhibits axonal transport of neurofilament proteins [246], suggesting that disruption of the filament protein network, and changes in peripherin splicing and expression, could be general features of ALS [247]. Furthermore, over-expression of wild-type peripherin in which there is targeted disruption of the NFL gene in $SOD1^{G93A}$ transgenic mice results in selective degeneration of motor neurons and late onset disease [248]. Aggregate-inducing isoforms of peripherin are also up-regulated in $SOD1^{G37R}$ mice and ALS patients [247, 249].

1.12.6 Profilin 1 (PFN1)

Profilin 1 is a member of the profilin family of small actin-binding proteins and it is important for the polymerization of actin. Missense mutations C71G (cysteine to glycine) and M114T (methionine to threonine) in the *profilin (PFN1)* gene were first identified in fALS patients using exome sequencing [64]. Cells over-expressing PFN1 mutants formed ubiquitinated, insoluble aggregates colocalised with TDP-43. *In vitro* studies showed that PFN1 mutants reduced the actin-bound profilin levels and they inhibited axonal outgrowth by decreasing actin polymerisation in embryonic motor neurons [64]. These observations further emphasize that cytoskeletal pathway alterations contribute to ALS pathogenesis although certain studies do not find these mutations as a prominent cause of ALS [250], although profilin mutations are a rare cause of fALS cases. In Germany, the Nordic countries, and the United States a *PFN1* mutation T109M (threonine to methionine) was identified which abrogates a phosphorylation site in profilin 1

[251]. However, European and Chinese population may have low prevalence of profilin mutations [252, 253].

1.12.7 Alsin (ALS2)

The *ALS2* gene encodes for a guanine nucleotide exchange factor for the small GTPase Rab5, which is implicated in endosomal trafficking [254], endocytosis [255] and axonal outgrowth [256]. Mutations to the *ALS2* gene cause autosomal recessive juvenile onset familial ALS (ARJALS) or juvenile PLS and hereditary spastic paraplegia [73, 257, 258]. Loss of function of the wild-type alsin results neurotoxicity [259] Wild-type alsin associates with mutant SOD1 and increases reactive oxygen species [259, 260]. Over-expression of mutant alsin causes Golgi fragmentation and mitochondrial trafficking impairment in COS7 cells [261]. Alsin-deficient neurons have disrupted α-amino-3-hydroxy-5-methyl-4-isoxazolepropionic acid (AMPA) receptor trafficking and increased glutamate induced cytotoxicity [262]. Also knockdown of alsin in $SOD1^{H46R}$ mice caused early disease onset and reduced survival [263]. This was associated with defects in endolysosomal trafficking suggesting that some disease mechanisms overlap between mutant ALS2-linked and mutant SOD1-linked ALS [263].

1.12.8 Phosphatidylinositol 3,5-bisphosphate 5-phosphatase (encoded by FIG4)

FIG4 is found in vacuolar membranes, and it is essential for normal functioning of the endosome-lysosome system [264]. Mutations were first identified in pale tremor mice (a multi-system disorder) which develop neuronal degeneration, peripheral neuropathy and altered pigmentation [75]. Homozygous or compound heterozygous loss-of-function mutations in human FIG4 were further observed in patients with autosomal recessive hereditary motor and sensory neuropathy, designated as Charcot-Marie-Tooth disease type 4J (CMT4J) [75]. Dominant FIG4 mutations have been found in 1-2% of patients with autosomal dominant familial and sporadic PLS patients [75]. Also heterozygosity for a lethal allele of FIG4 has been found to be a risk factor for ALS [74]. These PLS and ALS patients retained one wild-type allele, in comparison to CMT4J patients, [43] suggesting, that

membrane and vesicle trafficking defects are common to peripheral neuropathies, such as PLS, as well as ALS.

1.12.9 Charged multivesicular body protein 2B /chromtin modifying protein 2b (CHMP2B)

CHMP2B regulates endosomal trafficking and it is involved in the sorting of integral membrane proteins in multivesicular bodies and subsequent clearance by autophagy [265]. Mutations in the gene encoding *CHMP2B* were initially identified in cases of FTD in a Danish family [76]. ALS cases from two separate familial groups that are affected by an ALS like phenotype were identified to possess mutations in CHMP2B [266]. Another study found several additional ALS specific CHMP2B mutations, and expressions of the mutants in cell culture demonstrated that altered lysosomal localisation and reduced autophagy function compared to wild-type protein [267]. However, due to the lack of additional studies linking CHMP2B mutations with sALS and fALS cases this is considered to be a rare cause of ALS [268].

1.13 Mutations causing RNA dysfunction

1.13.1 Senataxin (SETX)

Senataxin encoded by *SETX* gene, possesses a DNA/RNA helicase domain and it associates with the replication fork around the active transcriptional region where it facilitates DNA replication [269]. Senataxin is expressed generally in the nucleus, where it is protective against oxidative damage to DNA and it also functions in RNA transcription [270, 271]. Silencing senataxin inhibits neuritogenesis, neuronal differentiation and induces aberrant neurite growth [272]. Dominantly inherited missense or truncation mutations in the *SETX* gene cause an atypical juvenile form of ALS, characterised by symptom onset before 25 years of age [77, 273]. The symptoms include limb weakness with severe muscle wasting, however, the disease is slow progressing without the involvement of bulbar and respiratory muscles [273]. Ataxia may also be observed in some patients [274]. In

contrast, another SETX mutation T118I (threonine to isoleucine) was detected in patients with sporadic classical ALS, with disease onset at 42 years and rapid progression implying that senataxin is also involved in sALS disease pathology [275]. Mutant senataxin induces neurotoxicity by damaging DNA induced during replication and creating genomic instability [269].

1.13.2 Angiogenin (ANG)

Angiogenin is a member of the ribonuclease A (RNase A) superfamily of proteins and it is induced under hypoxic conditions to protect cells by regulating the activity of vascular endothelial growth factor (VEGF) [276, 277]. Angiogenin is also implicated in neurite outgrowth [278, 279]. More than 20 fALS mutations in the *ANG* gene have been observed in several distinct populations [78, 280, 281]. ALS patients with ANG mutations display TDP-43 accumulation and inclusion formation in motor neurons similar to patients with Parkinson disease, indicating similar biochemical pathways may be operating [282, 283]. ALS-linked mutant angiogenin protein possess show decreased ribonuclease activity compared to wild-type proteins *in vitro* suggesting that these mutations may involve a loss of function in disease [284]. Consistent with this idea, over-expression of angiogenin in $SOD1^{G93A}$ mice model ameliorates motor function and life span [277].

1.14 Excitotoxicity

1.14.1 D-amino acid oxidase D-amino acid oxidase (DAO)

DOA is an important co-agonist involved both in N-methyl d-aspartate receptor (NMDAR) mediated LTP and excitotoxicity [285, 286]. Recently, mutation R199W (arginine to tryptophan) DAO was shown to induce autophagy, aggregation and apoptosis, all of which processes were decreased by a d-serine/glycine site antagonist of the NMDAR [287]. DAO is a peroxisomal enzyme that functions as a neurotransmitter by oxidising its substrate D-serine, an NMDA-type glutamate receptor activator [288]. A single R199W missense mutation to DAO segregates with autosomal dominant ALS in a large multigenerational population

[81]. Over-expression of this mutant increases ubiquitinated inclusion formation and cell death in transduced primary motor neurons and diminished enzymatic activity of DAO is evident in neuronal cell culture [81]. Furthermore, dysregulation of the serine biosynthetic pathway has also been observed in the mutant $SOD1^{G93A}$ mice models [289].

1.15 DNA damage repair and autophagy

1.15.1 Spatacsin

Spatacsin protein is encoded by *SPG11* gene however, the exact function of spatacsin in humans is unknown. In zebra fish spatacsin is essential for axonal growth and muscular junction connectivity [290]. Mutations in spatacsin cause autosomal recessive hereditary spastic paraplegia with thin corpus callosum demonstrating overlap in phenotype between these two juvenile-onset movement disorders [80]. Additional homozygous or compound heterozygous mutations to spatacsin are also detected in patients with ARJALS [291]. This form of ALS has early onset (before the age of 25) and is characterised by bulbar symptoms, muscle weakness and dysfunction in both upper and lower motor neurons [291, 292].

1.15.2 Tank-binding kinase 1 (TBK1)

Due to advances in next generation sequencing techniques mutations in the *Tank-binding kinase 1(TBK1)* gene were recently identified in ALS patients [82]. Similarly, another study identified eight different loss-of-function mutations in TBK1 in fALS patients [293]. TBK1 is a multifunctional kinase which plays an important role in autophagy where it regulates autophagosome-mediated degradation of ubiquitinated cargo and inflammatory signalling [294]. Interestingly, both optineurin [295] and p62 [61] act as substrates for TBK1 [295]. Furthermore, biochemical studies indicated that haploinsufficiency of TBK1 or loss of interaction of the C-terminal TBK1 coiled-coil domain with its adaptor proteins are linked to both ALS and FTD [293].

1.16 Potential risk factors and other rare ALS causing genes

Recent advances in techniques for genome-wide association studies (GWAS) have facilitated significant contributions in our understanding of ALS genetics and allowed the identification of several novel variants which affect susceptibility to ALS. A number of susceptible loci have been identified by GWAS including FGGY [296], ITPR2 [297], chromogranin B [298, 299] and DPP6 [300] which did not replicate in large cohorts. Another risk factor UNC13A which is involved in synaptic glutamate release initially appeared to be robust, but exact replication of the locus in an independent cohort has not been achieved [301, 302]. Identification of variants of KAIFAP3 a molecular motor that mediate anterograde axonal transport, and EPH4A ephrin receptor have been reported to significantly affect survival in ALS patients [303, 304]. Similarly, other reports of linkage with several other loci were not replicated in independent populations [296, 305]. More recently, intronic variants of *PDA1* gene encoding PDI have also been reported as susceptible risk factors in ALS pathology [306]. These findings highlight the complications involved in identifying genetic risk factors for ALS.

Exome-wide sequencing also recently identified mutations in *TUBA4A*, the gene encoding the Tubulin isoform, Alpha 4A protein in fALS cases. Functional analyses revealed that these TUBA4A mutations destabilize the microtubule network by diminishing its re-polymerization capability [307]. Mutations in Sigma receptor 1 were identified in juvenile cases of ALS and FTD [308]. Sigma R1 is involved in calcium signalling in the ER and the ALS mutations in Sigma R1 causes abnormal ER morphology, mitochondrial abnormalities and impaired endosomal trafficking and autophagic degradation implying a loss of function [309, 310]. Mutant form of a RNA-DNA binding protein encoded by matrin 3 (MATR3) is also involved in fALS [84]. With the advances in the field of genomics, the complexity of disease is becoming resolved however, further investigations of potential genetic associations with disease is warranted. And validation of these new genes in additional families is also required.

1.17 ALS is a protein misfolding disorder

A common feature of neurodegenerative diseases is the presence of misfolded protein aggregates in affected regions of the nervous system. Aggregates are insoluble, non-native structures observed at aberrant subcellular localisation formed due to interactions between structured and partially folded proteins [311, 312]. Whereas inclusions are large polymers into which aggregated proteins are sequestered due to the self-assembly of non-native polymers [313].

Under non stressed conditions the cellular machinery prevents protein misfolding with the aid of protein chaperones that assists proteins to fold into their native configuration [314]. Alternatively, misfolded proteins are detected by cellular quality control machinery the ubiquitin proteasome system and autophagy, resulting in their degradation [315]. During neurodegenerative disease abnormal protein aggregation can inhibit indispensable cellular functions, causing dysregulation in the proteostasis and eventually neuronal loss. Proteins misfold by various mechanisms including genetic mutation, oxidation, post-translation modification, proteasomal dysregulation and seeded polymerisation [316]. The presence of large inclusions is a hallmark of ALS pathology as in other neurodegenerative diseases and these insoluble inclusions are observed at the onset of disease not only in the brain stem and spinal cord but also in the frontal and temporal cortices, hippocampus and cerebellum, where they progressively accumulate until disease end stage [317, 318].

In ALS the pathogenic inclusions are commonly Lewy body-like hyaline inclusions, skein like inclusions which are ubiquitin positive or Bunina bodies which are eosinophilic but ubiquitin-negative [319, 320]. The major pathogenic proteins, SOD1, TDP-43 [164] and FUS, misfold and form skein-like inclusions, while Bunina bodies are immunoreactive for cystatin C and neurofilament proteins [320, 321]. Unconventional translation of hexanucleotide repeat RNA in the hippocampus and cerebellum of C9ORF72 patients results in the accumulation of abnormal dipeptide repeat (DPR) proteins which are TDP-43-negative

ubiquitinated proteins [322-324]. All C9ORF72 cases are characterised by TDP-43 pathology in the motor cortex and spinal cord [149]. In a particular study the inclusions formed in patients with C9ORF72 mutation were TDP-43 positive and also partially co-localised with p62 and ubiquilin-2 [194]. Mutant SOD1 forms hyaline-like inclusions composed of granule coated fibrils immunoreactive for SOD1, in the spinal cord of fALS patients and transgenic SOD1 models [325-328]. Accumulation of mutant SOD1 monomers and high molecular weight oligomeric species that may contain non-native disulphide bonds are prominently associated with disease pathology in transgenic $SOD1^{G93A}$ mice [329]. Mutations in proteins that are involved in protein degradation including p62, ubiquilin-2 and VCP implicates disruption to protein clearance pathways as a pathogenic mechanism in ALS. Mutations in some rare genes causing ALS such as p62, ubiquilin-2, VCP leads to aggregation of TDP-43 [18]. In ALS patients with ubiquilin-2 mutation the ubiquitinated inclusions co-localise with ubiquilin-2 and also interact with TDP-43, FUS and optineurin [58, 192]. Both TDP-43 and FUS are aggregate prone *in vitro* [126, 330] and the prion domain may induce inclusion formation [331-333]. The role of inclusions in disease pathology is still controversial. However, increasing evidence suggests the monomeric and oligomeric species are related to toxicity rather than large inclusions visible by light microscope themselves [334].

Furthermore, wild-type forms of the same proteins mutated in fALS are also found in inclusions of sALS patients [53-55, 335]. Wild-type SOD1 has the propensity to misfold and aggregate under conditions of oxidative stress *in vitro* [101]. Furthermore, the misfolded, oxidised forms of wild-type SOD1 share similarity with the mutant form and impair axonal transport [53]. Similarly, wild-type TDP-43 is a major constituent of ubiquitinated proteins inclusions in nearly all sporadic ALS cases suggesting common possible mechanisms of toxicity. Furthermore, inclusions containing wild-type forms of FUS, ubiquilin-2 and optineurin are also observed in a proportion of sALS cases [55, 217]. Together these data suggest that dysfunction to proteostasis induced is possibly multifactorial in origin and it involves both a gain in toxic function and loss in normal function mechanisms.

1.18 Current Hypotheses linked with the pathogenesis of ALS

Neurons are highly susceptible to proteostatic dysregulation mainly due to their large size and high metabolic requirements [336]. Various hypotheses regarding how mutant proteins induce ALS pathology have been suggested including impaired axonal transport, abnormal RNA processing, mitochondrial dysfunction, redox dysregulation, glutamate excitotoxicity, proteasomal and autophagic dysfunction and ER-Golgi transport defects [100, 337, 338]. Importantly, ER stress is emerging as an important driver in neurodegeneration [339-341] however, ER folding and quality control mechanism are not well characterised during disease state [342]. The section below summarises current evidence to explain how mutant proteins induce disease pathology.

1.18.1 Impaired axonal transport

Axonal pathology is one of the key features of ALS observed during early disease [343]. Retraction and denervation of neurons, resulting in axonal connection failure and axonal dysfunction, is observed in the early stages in rodents and in ALS patients [344-346]. Motor neurons are highly polarized cells with very elongated axons (up to meter in length) that facilitate delivery of essential cellular components RNA, proteins and organelles [347]. Microtubule-dependent kinesin and cytoplasmic dynein molecular motors mediate anterograde and retrograde transport respectively [348]. Mutations in genes linked to axonal transport including *NEFH, PFN1, PRPH, dynactin* and *tubulin4*, further support the notion that axonal transport defects contribute to ALS pathogenesis. Recent evidence also demonstrated that SQSTM1 is essential for proper dynein motility and trafficking along microtubules [349]. Similarly, spatacsin is implicated in axonal maintenance and cargo trafficking [350].

Decreased levels of NFL mRNA encoded by *NEFL* gene were observed in ALS [351]. Proteomic studies demonstrated that knockdown of TDP-43 reduces the levels of intracellular transport proteins, RAN-binding protein 1 and chromogranin B, suggesting that loss of function of TDP-43 could induce transport defects [352].

TPD-43 and FUS transport mRNA which encodes for NFL to neuronal distal compartments however, mutations in TDP-43 inhibits axonal mRNA trafficking, presumably due to loss of function [156, 176]. Furthermore, mutations in TDP-43 and FUS may impair axonal transport by inducing stress granule formation and aggregation, or by reducing the availability of neurofilaments [157, 353, 354]. Mutations in FUS cause diminution in the number of SMN proteins (survival motor neuron) which are important in trafficking of mRNA [355, 356] in the axon by sequestration of SMN protein into cytoplasmic FUS aggregates [357]. Mutations in SOD1 also cause axonal transport disruption. Upon subcellular fractionation of the lumbar spinal cord of transgenic $SOD1^{G93A}$ mice accumulation of misfolded SOD1 was observed in the fraction dense with neurofilaments [358]. Mutant SOD1 aggregates associate with dynein, the motor responsible for retrograde transport. Furthermore, mutant SOD1 aggregation leads to alteration in the subcellular distribution of the dynein complex and inhibition of its function in the axon of cultured motor neurons [359]. Misfolded SOD1 associates with kinesin-associated protein 3 (KAP3), a cargo protein in $SOD1^{G93A}$ mice and sequestration of KAP3 into these aggregates inhibits trafficking [360]. Mutant SOD1 also activates neuronal p38, which inhibits kinesin-1 through activation of the MAP kinase pathway and impairs fast axonal transport in neuronal cultures, spinal cord lysates of mice and squid axoplasm [361].

1.18.2 Redox Dysregulation in ALS

Various cellular abnormalities associated with redox dysregulation including oxidative stress, mitochondrial dysfunction, glutamate excitotoxicity and lipid peroxidation are linked to ALS pathology. Supplementary Figure 2 consists of a review article written by the author that discusses in detail the consequences of the dysregulation of ALS and readers are directed here for comprehensive reading on this topic. Nonetheless, recent advances in this area are summarised below.

Oxidised DNA, lipids and proteins that serves as biomarkers of oxidative stress and nitrosative stress in tissues and biological fluids can aid in understanding ALS

pathology [362]. Depletion of antioxidant glutathione is observed in the cortex of ALS patients [363] and modulation of this redox regulator is linked to impaired mitochondrial pathology in mutant $SOD1^{G93A}$ mice [364]. Furthermore, reduction of glutathione is also associated with TDP-43 inclusion formation in sALS patients [365]. Expression of TDP-43 also increased the levels of oxidative stress markers in Drosophila models, suggesting that oxidative stress may trigger TDP-43 induced apoptosis [366]. Oxidative stress is further aggravated due to mutations in TDP-43 and FUS. Mutant FUS is directed to stress granules more rapidly during oxidative stress compared to wild-type FUS [188]. Likewise, TDP-43 is recruited to stress granules in conditions of oxidative stress [160]. ALS-linked mutation in TDP-43 induce oxidative stress and mitochondrial dysfunction by accumulation of nuclear factor E2 related factor 2 (Nrf2) which is a modulator of oxidative stress in neuronal cell cultures [367].

1.18.3 Mitochondrial dysfunction in ALS

Mitochondria are both a target and the main site of production of reactive oxygen species [368].Various studies have shown that mitochondrial dysfunction and abnormal mitochondrial morphology is associated with ALS pathology [369]. A recent study identified a missense mutation in the *CHCHD10* gene S59L (serine to leucine) which encodes a mitochondrial protein responsible for ALS and FTD [370]. Over-expression of a CHCHD10 mutant causes fragmentation of the mitochondrial network and ultrastructural defects including loss, disorganization and dilatation of cristae in Hela cells [370]. Mitochondrial dysfunction and oxidative stress induce mitophagy in cellular cultures expressing both wild-type and mutant TDP-43 [367, 371]. Mitochondria are either abnormal and unorganised in post-mortem neurons from juvenile ALS patients [372] and mitochondria are smaller in size in cultured motor neurons expressing cytoplasmic FUS mutants [373]. Additionally, over-expression of FUS mutant R521C cause Golgi fragmentation and aggregation of mitochondria in rats [374]. Recent studies in VCP mutant mouse demonstrated that these animals have increased accumulation of TDP-43 and accumulation of abnormal aggregated mitochondria, causing motor neuron loss [375, 376]. Furthermore, VCP deficiency results in mitochondrial

coupling which is associated with a reduction in mitochondrial membrane potential, increased mitochondrial oxygen consumption and abridged ATP production [377]. Increased vulnerability of mitochondria is associated with disturbance in calcium levels and has been extensively studied in SOD1 *in vitro* and *in vivo* models [378-380]. TDP-43 also perturbs ER-mitochondria interactions which is associated with disruption in cellular calcium homeostasis which effects the integrity of motor neurons [381].

Other studies have suggested that increased calcium levels in the mitochondria results in glutamate dysfunction [382, 383]. Motor neurons are highly vulnerable to excitotoxic insults and ALS mutations in DOA further highlights these mechanisms in ALS pathologies. A different study demonstrated that exposure to kainic acid leads to significant motor neuron death [287]. A more recent study using induced pluripotent stem cells (iPSCs) determined that C9ORF72 ALS iPSNs are highly susceptible to glutamate-mediated excitotoxicity [139].

1.18.4 Non cell autonomous toxicity

Non-neuronal cell types in the central nervous system (CNS) such as astrocytes and microglia are also implicated in modulation of ALS disease processes [384]. Astrocytes cultured from both fALS and sALS patients induced toxicity causing neuronal death [385]. Similar studies in $SOD1^{G85R}$ mice demonstrated that astrocytes and microglial cells contribute to disease onset and progression [386-388]. Similarly, reduced levels of mutant SOD1 in astroglia delay microglial activation and decelerate disease progression [386]. Furthermore, silencing mutant SOD1 expression in microglia also slows motor neuron loss and disease progression [387, 389]. The activation of glial cells during disease progression can be both protective and deleterious in patients and animal models and these mechanisms are not fully elucidated [390, 391]. Increased levels of hydrogen sulphide were detected in the CSF of ALS patients and in the media from $SOD1^{G93A}$ mouse astrocytes and microglia [392]. Loss of oligodendrocytes also induces ALS pathology as these cells express monocarboxylate lactate transporter, which is

important for axonal maintenance [393, 394]. Therefore, a better understanding of the role of non-neuronal cells in ALS pathology is necessary before disease processes can be fully understood.

1.18.5 Disruption in RNA homeostasis

Abnormal localisation and aggregation of essential RNA binding proteins are features of sporadic ALS, and mutations in these proteins are also linked to familial disease [18]. More importantly, dysregulation in the functions of TDP-43 and FUS which individually bind and regulate the transcription of nearly 30% of the transcriptome, could be deleterious [395]. As mentioned above ALS-linked mutations in other RNA-binding proteins have also been described including angiogenin [279], senataxin [77] and ataxin-2 [396]. The RNA binding domains in TDP-43 and FUS are essential for toxicity in ALS [397]. Increasing evidence suggests that the pathogenic mechanisms for TDP-43 and FUS are likely to be a combination of both loss of function and gain of toxic function properties [149, 153, 398]. TDP-43 levels are also important for normal RNA maturation. Silencing of TDP-43 in a normal mouse modulate the levels of 6000 mRNA's suggesting that the loss of function can result in major defects [399]. Mutant TDP-43-dependent degeneration of only lower motor neurons causes both loss and gain of splicing functions of selected RNA targets at early disease stages without aggregation or loss of nuclear protein [170]. TDP-43 and FUS are also both constituents of stress granules [353, 400]. Persistent TDP-43/FUS positive stress granules may induce pathogenicity by sequestering mRNA transcripts, other RNA binding proteins, and by providing a seed for the formation of pathological inclusions in ALS [353, 401]. Furthermore, the recruitment of TDP-43 and FUS to stress granules also suggests that a loss of function of each protein exists in ALS under these conditions. Upregulated TDP-43 levels in murine models results in neurodegeneration either due to the expression of RNAs that lack auto regulatory sequences, or due to disruption of auto regulation [129, 402, 403]. Another study suggested that TDP-43 and FUS translocate into the dendrites and bind to several RNA targets, that regulate synaptic function in response to neuronal activation [175, 404]. Therefore, dysfunction in TDP-43 or FUS may alter synaptic function [175, 404].

Mutant SOD1 can bind mRNA's and impair post-transcriptional regulation by sequestering key regulatory RNA-binding proteins including Hu Antigen R (HuR), and TIA-1-related protein (TIAR) [405]. Furthermore, wild-type SOD1 can interact with TDP-43, suggesting a possible common mechanism in regulation of specific RNA stability [354]. Neurodegeneration induced by C9ORF72 mutations are also linked to gain of RNA toxicity by the production of toxic RNA containing the repeat sequence [406]. Additional toxic mechanisms may be triggered from complementary repeat-containing RNA produced by bidirectional transcription [407] or RAN translation [408], leading to the production of potentially toxic RNA and protein species respectively. Expression of RAN polypeptides also reduced RNA-processing bodies and cytoplasmic stress granules preceded apoptosis suggesting that RNA homoeostasis is also perturbed by RAN translated peptides [409].

1.18.6 Prion like mechanism of Neurodegeneration

Increasing evidence suggests that misfolded proteins responsible for causing neurodegenerative diseases may have "prion-like" properties: the ability to sequester wild-type proteins and seed their aggregation or misfolding, and thus act as transmissible agents between cells [410, 411]. Prion proteins possess a 'prion-like domain', having similar amino acid composition to yeast prion proteins, which therefore have high propensity to aggregate [412]. In human patients, ALS spreads in a characteristic pattern from the site of onset through the neuroanatomy, hence it has been argued that prion-like mechanisms exist in ALS [413]. SOD1 displays prion-like properties *in vitro* and in animal models [384]. These mechanisms have implications for future therapy that will aim to halt the spread of pathology and also for pathogenesis in sALS, given the presence of aggregated SOD1 in sALS cases [53, 101, 414]. Similar evidence exists for TDP-43 which contains a prion like domain. The C-terminal glycine rich region of TDP-43 is involved in protein-protein interactions and is aggregation prone and it induces cellular toxicity in yeast models [415]. Exogenously applied insoluble aggregates of TDP-43 generated *in vitro* can be taken up human embryonic kidney cells where they act as a seed for aggregation of endogenous TDP-43 [416] Furthermore, the aggregates are similar

to pathological ubiquitinated TDP-43 in ALS patients suggesting that seeded aggregation of TDP-43 could be an important phenomenon in disease [416]. In addition aggregated TDP-43 isolated from the brains of ALS patients, when exogenously applied to human neuroblastoma cells in culture, served as a seed for propagation of additional ubiquitinated and phosphorylated TDP-43 aggregation [417]. This induced intracellular aggregated TDP-43 was toxic in neuronal cell culture, possibly due to proteasomal dysfunction [416]. FUS also contains a prion like domain and it requires the RNA binding and glycine rich region as well as its prion domain, to induce aggregation [330]. Similarly, mutations in the prion-like domains of hnRNPA2B1 and hnRNPA1 cause multisystem proteinopathy and ALS [331]. Nevertheless, further *in vivo* characterisation of the transmissibility misfolded proteins in ALS is required to determine the role of misfolded protein in ALS.

1.18.7 Autophagy

Autophagy is a protein degradation pathway for clearance of misfolded proteins, aggregates and the turnover of organelles within the cell to assist in maintaining neuronal homeostasis. This degradation is achieved through either macroautophagy, microautophagy and chaperone mediated autophagy [418]. However, autophagic dysfunction is linked to aggregation and inclusion formation in ALS [419]. Studies have demonstrated that the induction of autophagy markers in spinal cords of ALS animal models, sALS and fALS patients [420-422]. Autophagy is upregulated in spinal cords of $SOD1^{G93A}$ mice at the symptomatic stage, and increased levels of LC3-II which correspond to the extent of autophagosome formation [423, 424]. Autophagy is also activated in motor neurons of sALS patients evident by increased numbers of autophagosomes [425]. Furthermore, defects in endosomal sorting complexes required for transport (ESCRT)-III which are essential for fusion of autophagic vesicles within the endocytic pathway, cause accumulation of cytoplasmic inclusions containing ubiquitin, p62 and TDP-43 [426]. Moreover, C9ORF72 interacts with ubiquilin-2 and LC3-positive vesicles, and it co-migrates with lysosome-stained vesicles in neuronal cultures, providing further evidence that C9ORF72 may regulate autophagy [427].

Autophagy is upregulated due to cellular stress and it can promote cell survival. However, autophagy can also directly or indirectly induce cell death. Increasing evidence supports the notion that stimulation reduces pathological traits in ALS. Rapamycin, an activator of autophagy, reduces mutant FUS-positive stress granules, neurite fragmentation and apoptosis in neuronal cultures expressing mutant FUS under conditions of oxidative stress [428]. In a more recent study, induction of autophagy using rapamycin reduced the effect of over-expressing mutant optineurin by decreasing accumulated mutant optineurin inclusions thereby reducing adverse phenotype in rat models [429]. Administration of trehalose, an enhancer of mTOR independent autophagy in $SOD1^{G85R}$ mice, significantly decreased the accumulation of SOD1 aggregates, enhanced motor neuron survival, prolonged life-span and attenuated progression of disease [430]. A similar study with trehalose also delayed disease progression, and reduced motor neuron loss in spinal cord of $SOD1^{G93A}$ mice. Trehalose decreased the accumulation of SOD1 and p62 aggregates and it improved autophagic flux in motor neurons of transgenic mice $SOD1^{G93A}$ [431]. An additional autophagy inducing compound, methotrimeprazine improved TDP-43 clearance and localization, and enhanced survival in primary murine neurons, human stem cell-derived neurons, and astrocytes expressing mutant TDP-43 [432].

However, contradictory studies have shown that treatment with rapamycin can also exaggerate disease pathology. Treatment of $SOD1^{G93A}$ mice with rapamycin caused motor neuron loss and accelerated disease progression. Also rapamycin induced autophagic vacuoles failed to reduce the level of mutant SOD1 aggregation in ALS $SOD1^{G93A}$ mice [433]. Another report demonstrated that rapamycin had no protective effect on disease onset and survival in SOD1 H46R/H48Q mice [434]. In addition, using lithium to induce autophagy exaggerated disease progression in clinical patients and $SOD1^{G93A}$ transgenic models of ALS [435-437]. However, the exact mechanism by which autophagy affects disease pathogenesis remains controversial.

1.18.8 ER-Golgi transport defects

The ER-Golgi secretory pathway mediates the transportation of proteins and lipids between the ER and Golgi and it is instigated by collection of secretory cargo from within the ER lumen [438]. ER-Golgi transport is a vital gateway to the whole endomembrane system therefore defects may impact greatly on neuronal viability. Newly synthesized proteins in the ER are packed into vesicles and transported to Golgi apparatus *via* the ER-Golgi intermediate compartment (ERGIC) [439], and finally they are redistributed to their respective cellular destinations [440]. Efficient ER-Golgi transport depends on coat protein complexes (COPs) which recruit cargo proteins[441], COPII is an essential vesicle coat protein complex that mediate anterograde transport and hence mediates export of proteins from the ER to the Golgi [441]. Impairment of ER-Golgi transport increases the accumulation of secretory proteins within the ER lumen, resulting in ER stress and induction of the UPR [442, 443]. Moreover, disruption to this bidirectional transport also results in abnormal Golgi organisation and fragmentation [444, 445]. Defects in ER-Golgi trafficking may impact on several cellular processes including ER stress, axonal transport and autophagy.

Currently numerous studies suggest that disturbances and impairment in the neuronal secretory apparatus occurs early in ALS [446, 447]. Transportation of synaptic transporter-1 GAT1 (GABA) requires efficient ER export in neuronal cells, thus suggesting a link between axonal transport and ER Golgi trafficking [448]. Abnormal Golgi pathology is observed in neurons of transgenic $SOD1^{G93A}$ mice at preclinical stages of disease pathology [449]. Furthermore, Golgi fragmentation enhances with disease progression without accumulation of inclusions in mutant SOD1 mice [450]. ALS mutations in VAPB also disrupt in ER-Golgi vesicle transport [65]. Optineurin mutations in ALS also disrupt the interaction between optineurin and myosin VI, resulting in inhibition of secretory protein trafficking, ER stress and Golgi fragmentation in neuronal cell cultures [216].

The effects of SOD1 mutations in trafficking have been studied in ALS cellular and animal models. Mutant SOD1 interacts with dynein thus disrupting the dynein motor complex, in cultured cells and also in tissues of SOD1 G93A and G85R transgenic mice prior to onset of disease [451]. Mutant SOD1 also interacts with tubulin before disease onset and it recruits tubulin into inclusions, thus inhibiting tubulin polymerisation which is essential for microtubule organisation [452]. Our laboratory demonstrated that mutant SOD1 inhibits ER-Golgi transport [453]. Also, in cells expressing mutant SOD1, disruption in ER-Golgi trafficking preceded ER stress, Golgi fragmentation, protein aggregation and apoptosis *in vitro* [453]. Furthermore, over-expression of COPII subunits or Rab1 protected against inclusion formation and cell death in neuronal cultures and restored ER-Golgi transport suggesting a connection between neurodegeneration and ER Golgi transport defects in mutant SOD1 pathology [453]. In another study our laboratory demonstrated that extracellular aggregated wild-type and mutant SOD1 induced ER-Golgi trafficking defects in human neuronal cell lines, thus demonstrating that extracellular forms of wild-type SOD1 causes ER-Golgi transport impairment [454]. Our group further showed that C9ORF72 mediates endosomal trafficking by interacting with Rab proteins [427]. Consistent with previous bioinformatics predictions knockdown of C9ORF72 inhibited transport of Shiga toxin from the plasma membrane to Golgi apparatus in neuronal cell lines, primary cortical neurons and human spinal cord motor neurons [427]. Furthermore, greater colocalisation between C9ORF72 and Rab7 and Rab11 which are involved in endosomal transport was observed in motor neurons of ALS patients bearing the C9ORF72 repeat expansion suggesting that trafficking is dysregulated in ALS [427]. Therefore, further investigation into the relationship between ER-Golgi trafficking defects and ALS genes is warranted.

1.18.9 ER stress and the UPR signalling

ER is a vital cellular organelle which facilitates in the synthesis, folding, maturation and post-translational modification of proteins [455]. Nearly one third of all secretory proteins are synthesized in the ER and transported to their final destinations. In contrast, misfolded proteins are translocated into the cytoplasm for

ERAD [456, 457]. Therefore, efficient functioning of the ER is important in maintaining cellular protein homeostasis. The native folding of newly synthesised proteins is assisted by protein chaperones including PDI, ERp29, Hsp70 family members, immunoglobin binding protein (BiP), calnexin and calreticulin. ER stress is triggered when misfolded proteins accumulate in the ER and redox dysregulation, ER-Golgi vesicular trafficking defects, ER calcium imbalance, glucose deficiency or excess accumulation of mutant proteins can cause ER stress. [458]. This imbalance between the rate of protein synthesis and increased load of misfolded proteins activates the cellular stress response known as the unfolded protein response (UPR). The initial stages of UPR aims to restores normal cellular function by promoting protein folding and inhibiting protein translation *via* UPR sensor proteins to assist quality control cellular machinery to deal with the burden of misfolded proteins [459, 460].

The UPR initiates three crucial signalling branches, protein kinase RNA like endoplasmic reticulum kinase (PERK), inositol requiring kinase-1 (IRE-1) and activating transcription factor 6 (ATF6) [461]. Under non-stressed conditions BiP is bound to each UPR sensor protein which keeps them in an inactive state. However, during ER stress the load of misfolded proteins in the ER causes dissociation of BiP from each sensor protein leading to their activation [462]. Activation of PERK accelerates rapid and transient protein translation through inhibition and phosphorylation of the eukaryotic translation initiation factor 2α (eIF2α) which represses further entry of newly synthesised proteins in the ER [463]. Additionally, phosphorylation of eIF2α facilitates translation of mRNA encoding transcription factor ATF4, which regulates the expression of genes involved in redox function, apoptosis and autophagy. Activation of the second UPR signalling pathway results in dimerization of IRE1 and its auto-phosphorylation. This activates the transcription factor X-box binding protein 1 (XBP-1) by excision of a 26 base intron that introduces a frame shift in the XBP-1 mRNA. This stable, spliced XBP-1, regulates genes related to protein folding, ERAD and lipid synthesis [464]. C-Jun N-terminal kinase (JNK) and the apoptosis signal-regulating kinase 1 (ASK1) pathway are also activated by IRE-1α, by degrading a subset of specific mRNAs in

a tissue-specific manner through the binding of proteins. The third UPR signalling pathway involves the transcription factor ATF6 a basic leucine zipper that is anchored to the ER membrane under normal cellular conditions. However, during ER stress, ATF6 is cleaved by proteases to form an active 50 kDa transcription factor at the Golgi apparatus, and the cytosolic ATF6 fragment translocates to the nucleus to activate the transcription of ERAD genes and XBP-1 [465]. The collective action of ATF4, spliced XBP-1 and ATF6 upregulates the expression of chaperones that augment ER folding capacity and resolve the stress. PDI is one of the most important chaperones of the ER and the role of this protein in ALS is the main focus of author's thesis. The possible protective function of this protein is discussed below while the potential protection of other PDI family members, ERp57 and ERp72 in ALS are the focus of Chapter 5.

Whilst the UPR is primarily protective, an unresolved UPR, as observed in ALS, induces cell death. ER stress activates apoptosis *via* mitochondria-dependent and independent forms as well as facilitating Ca^{2+} release from the ER [466, 467]. Prolonged activation of PERK and ATF6 initiates a series of successive transcriptional responses arbitrated by ATF4, including up-regulation of pro-apoptotic ER stress specific transcription factor, C\EBP homologous protein (CHOP) [468] and pro-apoptotic components of the BCL-2 protein family. This cascade of events leads to the activation of BAX and BAK dependent apoptosis at the mitochondria and the induction of the caspase cascade [469]. CHOP regulates the cellular transition from pro-survival to pro-apoptotic signalling during ER stress [470]. Under unstressed conditions CHOP is found in the cytoplasm but it translocates to the nucleus during cellular stress [471]. Interestingly, ATF4 and CHOP were recently shown to induce cell death by accentuating protein synthesis during chronic conditions, resulting in ATP reduction, oxidative stress and apoptosis [472].

1.18.10 ER stress in ALS

ER stress and the UPR have been widely studied in neurodegenerative diseases, and emerging evidence highlights the UPR as a key pathological mechanism observed in both fALS and sALS patients [470, 473]. Induction of UPR sensors and chaperones was present in lumbar spinal cord of sALS patients and in the early stages of disease in $SOD1^{G93A}$ mice indicative of a protective role in ALS [474-476]. Similarly in another study up-regulation of PDI, ERp57, spliced XBP-1, ATF4 and phosphorylated eIF2α were detected in spinal cords of sALS patients [476]. Morphological abnormalities in the ER and accumulation of amorphous or granular materials within the ER lumen have also been demonstrated in patients with sporadic ALS [340, 477].Various studies have demonstrated that induction of ER stress is an early event in ALS animal models. Induction of BiP is also evident in spinal motor neurons of preclinical transgenic $SOD1^{L84V}$mice [478]. Saxena and group showed that a subtype-selective ER stress response impacts on disease manifestations. Vulnerable motor neurons are selectively more prone to ER stress and microglial activation compared to resistant motor neurons [341, 479]. Reduced levels of calreticulin were also observed in vulnerable motor neurons of $SOD1^{G93A}$ mice due to activation of FAS death receptor which induced muscle denervation, ER stress and apoptosis [480, 481]. Similarly, laser capture micro dissection and microarray analysis of motor neurons revealed activation of ATF4 at disease onset and significant up-regulation of CHOP at disease end stage in mutant $SOD1^{G93A}$ mice, relating ER stress with disease progression [482].

Our laboratory demonstrated that cells with mutant SOD1 inclusion bodies have high levels of activated CHOP and readily undergo apoptosis [483]. This occurs *via* activation of Bim [484]. Other studies have shown that mutant SOD1 interacts with an ER resident, Derlin-1, which is essential for ERAD function and this triggers ER stress-mediated cell death *via* ASK1 pathway [485]. Interestingly, we also found that misfolded aggregated wild-type SOD1 also induces ER stress to a similar degree as mutant SOD1 in neuronal cultures [454]. We also demonstrated that mutant TDP-43 induces ER stress and upregulates UPR markers CHOP, ATF6 and XBP-1 *in vitro* also ER stress further induced increased cytoplasmic translocation

of TDP-43 [486]. These studies are detailed further in Chapter 3. Similarly, cytoplasmic localised mutant FUS induces ER stress in neuronal cell lines [487]. Furthermore, neurotoxicity induced by $G_4C_{2\,(50)}$ in C9ORF72 is also associated with induction of ER stress in primary neuronal cultures [143]. Synthetically prepared poly GA RAN translated proteins induced CHOP and caspase-3 activation in primary neurons, which was inhibited on treatment with salubrinal, suggesting that ER stress is involved in C9ORF72 ALS pathology. Furthermore, salubrinal and other ER stress inhibitors such as guanabenz have been shown to reduce disease progression in SOD1 and TDP-43 transgenic models of ALS providing *in vivo* evidence that UPR is associated with disease pathology in ALS [341, 488, 489]. However in a recent study treatment with guanabenz hastened disease onset and progression in $SOD1^{G93A}$ mice [490]. In conclusion, these studies together imply that ER stress is a central and upstream mechanism in ALS pathogenesis, common to both familial and sporadic forms.

1.18.11 ER stress is linked to other pathogenic mechanism

ALS is a disease without a single cause, single mechanism or single phenotype. There is apparently interplay between the divergent causes and pathological mechanisms. As mentioned in the section above various pathological mechanisms - redox dysregulation, genetic mutations, ER-Golgi transport defects can cause ER stress trigger apoptosis. However, the exact relationship between ER pathology and ER stress in the disease progression are unclear. Glutamate excitotoxicity can result in protein accumulation and aggregation in the ER, suggesting a likely association with ER stress [491]. Kainic acid induces excitotoxic injury, requires activation of PERK, ATF6, IRE1, CHOP and caspase-12 in hippocampal neurons [491]. Furthermore, activated kainic acid fragments ER membrane in neurons, which is attributable to increased calcium influx and activation of glutamate receptors resulting in a vicious circle [491]. Another study demonstrated that JNK3 expression, a member of the JNK family is necessary for excitotoxic damage in the brain [492]. However, contrary evidence also demonstrated BiP protects neurons against glutamate-induced excitotoxicity [493].

ER stress induction, autophagy and dysfunction of the proteasomal system are also interconnected. Pharmacological stimulation of ER stress causes increased accumulation of ERAD substrates and therefore compromised function of the proteasome [494]. ER stress may accelerate autophagosome formation in neuronal cells, however, this effect is inhibited by IRE1 deficiency [495]. In addition, UPR induction leads to an increase in activity of the autophagy protein Atg1 [496], and UPR activation and disruption of calcium homeostasis induces autophagy *via* alterations in mammalian target of rapamycin (mTOR) [497]. Similarly, knockout of Atg7, which is essential for functional autophagy, increases PDI and BiP levels in the liver of transgenic mice [302], while knockdown of BiP in cell culture decreases ER stress-induced autophagosome formation [498]. Furthermore. knock-down of XBP-1 activates autophagy in $SOD1^{G86R}$ mice [420]. Additionally, changes in fatty acid composition, mitochondrial function and proteasome activity, which may be driven by excitotoxicity, lead to oxidative stress and finally contribute to ER stress in sporadic ALS [476]. Increased oxidative stress could lead to S-nitrosylation of ER chaperone PDI. The main function of PDI is to reduce protein misfolding hence S-nitrosylation in ALS patients may lead it to become non-functional and possibly further enhancing ER stress [483].

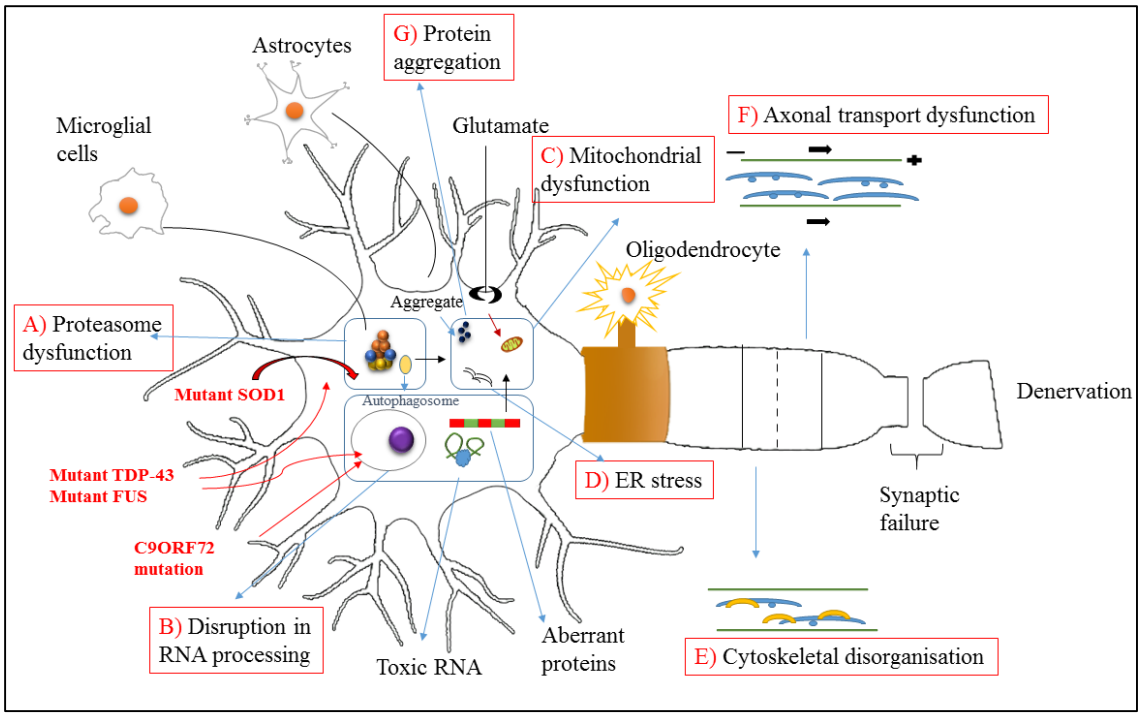

Figure 4 Overview of events associated with the pathogenesis of ALS. Motor neurons and neighbouring presynaptic neurons, astrocytes and microglia are affected by cellular disturbances in ALS. Refer to text for comprehensive descriptions of each process**.**

1.19 Protein disulphide isomerase (PDI)

PDI is multifunctional protein and the prototype of PDI family with more than 21 members involved in various cellular functions [499]. ERp57 and ERp72 are the closest homologues of PDI sharing similarity in function and structure (discussed in chapter 5). Recently, (May 2015) the author wrote a review article concerning the novel functions of PDI and its relevance in various diseases including ALS and the reader is directed to this review for more information (Supplementary Figure 1). However, a concise summary of the functions of PDI and its relation to ALS is presented below.

The biogenesis of secretory and cell surface proteins originates in the ER which is equipped with a variety of chaperones and folding factors. ER resident chaperones guide the unfolded polypeptide chains to achieve their native configuration by performing functions including post-translation modifications such as disulphide bond formation [500]. Chaperone such as members of the heat shock protein family, HSP70 (BiP) and HSP90, are abundantly found in the ER. They function as holdases by binding to the exposed hydrophobic region of non-native proteins thus reducing protein aggregation. However, whether HSP70 and HSP90 actively catalyse the formation of disulphide bonds (folding function) is unclear [501]. In contrast disulphide bonds are formed by PDI and PDI family of proteins due to the more oxidising environment of the ER (Eo'= -0.18 V) [502, 503]. Disulphide bonds are important for the structural stability of proteins and they promote assembly of the multi-protein complexes [503, 504].

PDI has two distinct functions. Firstly, it is an ER chaperone that assists in quality control by reducing misfolding and aggregation and secondly as a chaperone it is an isomerase that catalyses disulphide protein bond formation by the reduction and isomerisation of disulphide bonds of those proteins that traffic through the ER [505]. PDI is 55 kDa in size and the structure of yeast PDI has now been resolved [506]. PDI has four domains consisting of two thioredoxin-like domains namely (*a* and *a'*) and two homologous domains *(b* and *b')*. Each thioredoxin like domain contains the conserved active site sequence CGHC that facilitates the formation of disulphide bonds and are highly redox sensitive [506]. The homologous domains of PDI possess a linker region and an ER retrieval sequence - KDEL on the acidic C-terminus [507]. The *b'* domain is the main site for binding of protein substrates but other domains also assist in the attachment of misfolded proteins [508].The *b'* domain is also known as the chaperone domain that contains a large multivalent hydrophobic surface which forms a promiscuous binding site for substrates [509]. Although PDI is considered as being ER resident, it has been also observed in other sub-cellular locations, such as the extracellular matrix, cytosol and the nucleus under certain conditions [510].

1.19.1 PDI facilitates oxidative protein folding in the ER

Disulphide bonds are important for the structural stability of proteins and they also promote the assembly of multi-protein complexes [503, 504]. Disulphide bonds are introduced into protein substrates by a diverse set of pathways and the PDI family of proteins are key to this process [511]. PDI has two thioredoxin-like active sites, which both contain two cysteine residues. Disulphide bonds form between these two cysteines and the protein substrate, by oxidation. PDI is also responsible for the reduction and isomerization of these disulphide bonds. For PDI to catalyse the formation of disulphide bonds in unfolded proteins, it must be re-oxidized. ER oxidoreductin 1 (ERo1) is an oxidoreductase that utilises a redox cofactor, flavin adenine dinucleotide (FAD), and molecular oxygen, to generate disulphide bonds de novo. This reaction is catalysed by peroxiredoxin 4 and glutathione peroxidase, which produces hydrogen peroxide to oxidise PDI [512-514]. Additionally, oxidised glutathione (GSSG) and vitamin K oxidoreductase can reoxidise PDI after substrate oxidation, by directly interacting with PDI [515-517]. In contrast, quiescin sulfhydryl oxidase (QSQX) also facilitates disulphide bond formation by directly oxidising protein substrates [518, 519].

Substrate oxidation also results in the production of reduced PDI. Although the ER introduces disulphide bonds into substrate proteins with high precision, errors in this process can lead to the formation of non-native disulphide bonds in these substrates. The reduced form of PDI mediates isomerisation reactions in proteins, and reduced glutathione (GSH) delivers electrons directly to form reduced PDI [520]. Reduced forms of PDI and its other family members also function in the retrotranslocation of proteins from the ER to cytosol for degradation by ER associated degradation (ERAD) [521]. Hence, the redox state of PDI is essential for carrying out its normal functions involving both oxidation and reduction processes. PDI normally remains in a semi-oxidised state, however, PDI *a* domain stays in an oxidised state to aid in the formation of disulphide bonds whereas the other PDI *a'* domains remain in a reduced state to aid in the isomerisation reactions [522].

1.19.2 PDI in ALS

PDI is upregulated in spinal cords of $SOD1^{G93A}$ mice of ALS and in sporadic ALS patient spinal cords [523, 524]. Furthermore, PDI associates with abnormal inclusions in $SOD1^{G93A}$ mice and mutant SOD1 inclusions in neuronal cells in culture [523]. More importantly, PDI also colocalises and interacts with TDP-43 and FUS inclusions in the tissues of ALS patients [487, 525]. Similarly, PDI co-localises with the inclusions formed by ALS-linked proteins SOD1, TDP-43 [525, 526], FUS [527] VAPB [528], *in vitro* implying that PDI is linked to general protein misfolding in ALS. Over-expression of PDI reduces mutant SOD1 inclusions whereas silencing PDI expression increases the number of inclusions formed [483]. These data together suggest a protective role for PDI against abnormal protein aggregation and ER stress in ALS. Moreover, treatment of neuronal cells with (±)-trans-1,2-bis(mercaptoacetamido)cyclohexane (BMC) significantly reduced the formation of mutant SOD1 inclusions in a dose-dependent manner suggesting that pharmacological agents that mimic PDI's activity may have potential as a possible therapeutic target in ALS [529]. Also, PDI homologue ERp57 has been identified as potential biomarkers for ALS patients since it is closely associated with disease severity [530].The sub cellular distribution of PDI and its relocation from the ER which is mediated by reticulon protein in SOD1 mice during disease indicates PDI subcellular location importance in ALS pathology [531]. Although, PDI is normally is protective it is S-nitrosylated in transgenic mice models of ALS and patients suggesting that in disease it is unable to protect against protein misfolding [483]. In addition, S-nitrosylation of PDI increases the number of insoluble aggregated mutant SOD1 formed in ALS, suggesting that S-nitrosylated PDI has a toxic gain of function due to this post-translational modification [532, 533].

Accumulating evidence indicates that ER stress is a central upstream mechanism in ALS pathogenesis. Also, the ER chaperone, PDI is protective against misfolding and aggregation of misfolded proteins which is a key pathological hallmark of ALS. To investigate the role of PDI in ALS, each chapter of this thesis addresses specific aims, as described below.

Chapter 3 – The role of PDI against ER pathology in neuronal cells expressing mutant TDP-43, FUS or SOD1. The aims of the studies described in this chapter were to determine whether mutant TDP-43 induces ER stress in neuronal cell line and then study whether PDI is protective against ER stress, ER-Golgi transport defects and mislocalisation in the cytoplasm against fALS causing proteins in cell culture.

Chapter 4 – The mechanism of action of PDI in ALS. The aim of the studies described in this chapter was to determine whether the disulphide or the isomerase activity of PDI is responsible for the protective activity in ALS using PDI mutant constructs expressed in neuroblastoma cell models.

Chapter 5 – The role of other PDI family members in ALS. The aim of the studies described in this chapter was to determine whether other PDI family members besides PDI are also protective against ALS like pathology *in vitro* given they share similar structure and functional characteristics.

Chapter 6 –The subcellular location of PDI affects the protective activity of PDI. The aim of the studies described in this chapter was to determine whether the sub-cellular location of PDI determines the protective activity of PDI. A cytoplasmic PDI construct was generated with the aim to determine whether over-expression of cytoplasmicaly localised PDI was protective *in vitro*.

Chapter 2 Materials and Methods

This section lists general materials and methods, specific methods of chapter 6 are Subsequently described later.

2.1 Materials

2.1.1 Expression Constructs

Wild-type TDP-43 and mutant TDP-43 (Q343R and Q331K) constructs encoding enhanced green fluorescent protein (EGFP)-tagged human TDP-43 at the N-terminus were provided by Professor Benjamin Wolozin, Boston University, USA. Wild-type TDP-43 and mutant TDP-43 (A315T and Q331K) in pmCherry.N1 vector to allow expression of human TDP-43 with a C-terminal mCherry tag were as previously described [486]. Wild-type FUS and mutant FUS (P525L, R522G) constructs encoding hemaglutinin (HA)-tagged human FUS at the N-terminus were provided from Dr Dorothee Dormann, Munich University, Germany. VSVG tagged with mCherry was a generous gift from Dr Jennifer Lippincott-Schwartz and Dr George Patterson, National Institutes of Health, USA. Sequences containing either wild type FUS or C-terminal missense mutations R521C or R521H cDNAs were ligated into pFC8K-CMV Halo tag vector (Promega) with Halo tag positioned at the N-terminus of FUS as previously described [487]. The constructs wild-type SOD1 and $SOD1^{A4V}$ constructs encoding EGFP-tagged human SOD1 at the C-terminus were as described previously [534]. Previously generated pcDNA3.1(+) constructs encoding wild-type, PDI mutant in which the second cysteine of the *a* domain was mutated to serine (C2) (*CGHS, CGHC*) and PDI mutant in which the second cysteine of both the *a* and *a'* were mutated to serine (C26) (*CGHS, CGHS*) were provided by Professor, Neil Bulleid, University of Glasgow, UK [535]. The other PDI mutants - (PDI QUAD), (A), (A') were generated by a Masters student using site directed mutagenesis and cDNA was inserted into pcDNA3.1(+) vector which is 5428 base pairs with C-terminal V5 tag in it. Expression constructs for wild-type ERp57, mutant ERp57, wild-type ERp72 and mutant ERp72 constructed in pcDNA3.1(+) were also a generous gift from Professor Neil Bulleid [535, 536]. The expression constructs were resuspended in sterile Milli-Q water and transformed in XL1-Blue cells for further experiments.

2.2 Molecular biology

2.2.1 Luria-Bertani (LB) medium

Luria Bertani broth (10 g bacto-tryptone (Oxoid), 5 g yeast extract (Oxoid) and 10 g Nacl in 1 L dH_2O, pH adjusted with 200 µl of 5 M NaOH) was used as the liquid culture medium to maintain and support the growth of *E. coli*. The broth was autoclaved and antibiotics (ampicillin or kanamycin sulphate, Sigma) were added prior to usage. Antibiotic stock solutions were prepared at 100 mg/ml in dH_2O, filter sterilised and stored at -20°C. The final concentration of 50 µg/mL was used for ampicillin and 100 µg/mL for kanamycin. LB agar was prepared by dissolving 20 g of bacteriological Agar (Oxoid) to 1 L LB broth prior to autoclaving. And was used as the solid culture medium to support growth of *E. coli* in petri dishes. Appropriate antibiotic was added after autoclaving and LB-agar was poured into sterile petri dishes in a laminar flow hood. Plates were allowed to set, then used immediately or stored at 4°C.

2.2.2 Preparation of competent cells

The strain of *E. coli* XL1-Blue was inoculated in LB containing 10 µg/ml tetracycline. The overnight culture was added to fresh LB (80 ml) with starting OD_{600} as 0.1. The sample was grown until log phase and then centrifuged at 2000 *g* for 15 min. The supernatant was discarded and cell pellet was resuspended in 100 mM cold $CaCl_2$. The bacterial pellet was incubated on ice for 15 min and then centrifuged again at 2000 *g* for 10 min at 4°C. The pellet was gently resuspended in 85 mM $CaCl_2$ with 15% (v/v) glycerol. The mixture was aliquoted into 180 µl volumes and snap frozen in liquid nitrogen. The cells were stored at -80°C.

2.2.3 Transformation

Competent cells were thawed on ice. Appropriate volume of DNA plasmid was mixed with 50 µl of competent cells in a tube. Cells were incubated on ice for 15 min and then heat shocked at 42°C for 30 sec. The samples were immediately

incubated again on ice for 1 min. Aliquots of 50 µl of the mixture was spread on a LB agar plate containing appropriate antibiotics. The plates were incubated 37°C overnight.

2.2.4 Preparation of plasmids

The bacterial strain with the appropriate plasmid was inoculated in 10 ml of LB media and incubated overnight at 37°C. It was centrifuged at 4000 *g* for 5 min. The cultures were processed according to the manufacture's protocol and plasmid DNA was isolated using a plasmid midi kit (Qiagen). The DNA pellet was air-dried and resuspended in 400 µl of nuclease-free H_2O and stored at -20°C. DNA was quantified by agarose gel electrophoresis and spectrophotometry. Agarose gels 1% (w/v) prepared in TAE buffer (40 mM Tris-acetate, 1 mM EDTA, pH 8) and 0.1% (v/v) Gel Red (Biotium). Plasmid DNA samples were loaded with loading dye (0.25% bromophenol blue, 0.25% xylene cyanol, 30% glycerol) and with 1 Kb plus ladder (Invitrogen) as the standard marker. The gels were run at 110 V for 95 min and visualised under UV light on a gel doc system (UVP).

2.2.5 DNA quantification

The concentration of DNA was analysed directly by using a Nanodrop ND-1000 spectrophotometer. A conversion of 1.0 A260 = 50 ng/µL was used to determine the original DNA concentration, and the A260/A280 ratio was used to examine the purity of DNA, where A260<1.75/A280<1.85 was considered satisfactorily pure for transfection experiments.

2.2.6 DNA purification by ethanol precipitation

DNA purification was performed by mixing 1/10th volume sodium acetate (3 M, pH 5.2) and 2X volume of 100% ethanol (-20°C). The reaction mixture was placed at -20°C for approximately 30 to 120 min. To collect the precipitated DNA the sample was centrifuged at 16,100 *g* for 15 min at 4°C. The pellet was washed with 2X original volume of 70% ethanol and centrifuged at 16,100 *g* for 5 min at 4°C. The DNA pellet was air-dried at room temperature for 10 min or for 3 min

at 56°C. Precipitated DNA was then resuspended in appropriate volume of nuclease-free water.

2.3 Mammalian cell culture techniques

2.3.1 Fetal Calf serum (FCS) heat inactivation

FCS (Gibco) was removed from -20°C, allowed to thaw and was equilibrated to room temperature. FCS was then suspended in a 60°C water bath for 30 min with frequent mixing and was allowed to equilibrate. The heat-inactivated FCS was dispensed in 50 ml aliquots and stored at -20°C.

2.3.2 Cell culture maintenance

Mouse motor neuron-like NSC-34 cells (provided by Prof Neil Cashman, University of Toronto) and mouse neuroblastoma Neuro2a cells were used throughout this study. The cells were maintained in Dulbecco's modified eagle medium (DMEM) with 10% heat activated FCS, 100 µg/ml penicillin and 100 µg/ml streptomycin incubated at 37°C with 5% CO_2. Before the cells reached appropriate confluency they were washed with phosphate buffer saline (PBS, 3.2 mM Na_2HPO_4, 0.5 mM KH_2PO_4, 1.3 mM KCl, 135 mM NaCl, pH 7.4) and treated with 1 ml Trypsin-EDTA (Gibco) with incubation for 3 min at 37˚C to detach cells from the plate. The cells are resuspended in DMEM with 10% FCS and centrifuged at 500 *g* for 10 min. The pellet was resuspended in 1 ml DMEM with 10% FCS and the confluency of cells was determined by counting on a heamocytometer (Crown Scientific). Cell suspension (10 µL) was mixed with DMEM (90 µL) and trypan blue (100 µL, Invitrogen) to give a 1:20 dilution. The number of viable (non-blue stained) cells in each of four 1 mm^2 areas (100 nL volume) were counted and the mean number of cells was multiplied by dilution factor (20) to give 10^4 cell number per mL. Cells were then plated into 24-well plates or 6-well plates as required and subcultured in a fresh 10 cm plate.

2.3.3 Transfection

Neuro2a and NSC-34 cells were transfected using Lipofectamine2000 with PLUS reagent (Invitrogen) according to the manufacturer's protocols. Cells were typically grown to 75% confluency and $5x10^4$-$1x10^5$ cells were plated out in 24-well plates transfected with 250-1000 ng plasmid DNA. The cell number and DNA amount per well were kept constant within experiments, as appropriate. The cells were incubated in a 37°C incubator with 5% CO_2 and observed post-transfection.

2.3.4 Treatment with BMC

Treatment with trans-1,2-bis mercaptoacetamido cyclohexane (BMC) (Toronto-ResearchChemicals) was added from a stock dissolved at 25 uM in DMSO. BMC was added to the transfected cell expressing SOD1, TDP-43 and FUS post transfection.

2.3.5 Long-term storage of cell lines

Low passage number cells were collected by trypsinisation in antibiotic-free DMEM with 20% FCS. Approximately 1-$3x10^6$ cells were dispensed in the medium with 10% sterile DMSO to make the final volume of 1 mL in cryotubes (Nunc). Cells were cooled in an isopropanol-filled cryopresevative chamber at -80°C and then transferred to liquid nitrogen for long-term storage. Upon thawing, cells were rapidly warmed to 37°C and instantly plated in T75 flasks in DMEM with 10% FCS and 1% penicillin/streptomycin.

2.4 Microscopy

2.4.1 Fluorescence microscopy

After NSC-34 or Neuro2a cells were transfected with constructs, DMEM was removed from the wells of the 24-well plate and the cells washed with PBS. They were then fixed with freshly prepared 4% (w/v) paraformaldehyde and incubated in the dark for 15 min. The cells were washed again with PBS, treated with 500 ng/ml Hoechst 33528 stain and incubated in the dark for 20 min. They were then washed

twice with PBS and a drop of fluorescent mounting media (Dako) was added to a microscope slide. Coverslips were removed from the wells and placed on the fluorescent mounting media, cell side facing down. The slides were air dried and observed under 100X magnification on an Olympus 8212 epifluorescent microscope. DAPI (nuclie), FITC (EGFP fluorescence), TRITC (red fluorescence) filters were used for viewing and images taken using NIS-Elements BR 3.2 software. Confocal imaging was done using an Olympus Fluoview inverted confocal laser scanning microscope (Macquarie University).

2.4.2 Immunofluorescence microscopy

The cells were permeabilized with 0.1% (v/v) Triton-X in PBS for 5 min and blocked with 3% BSA in PBS for 30 min. After washing twice with PBS, appropriate primary antibody was added and the cells were incubated at 4°C overnight. The cells were washed again with PBS and the appropriate secondary antibody (Alexa Fluor 568- conjugated rabbit anti-mouse IgG (1:250) or Alexa Fluor 568- conjugated mouse anti-rabbit IgG (1:250) or Alexa Fluor 488-conjugated rabbit anti-mouse IgG (1:250), Alexa Fluor 488-conjugated mouse anti-rabbit IgG (1:250)) was added for 1 hr and incubated in the dark at room temperature. After washing, staining of nuclei was performed with Hoechst stain and mounted using fluorescent mounting media.

Protein (antigen)	Dilution factor	Species	Source
Anti-V5	1:200	Mouse	Abcam
β-actin	1:4000	Mouse	Sigma
CHOP	1:50	Mouse	Santa Cruz
Anti-HA	1:200	Rabbit	Sigma
Anti-Halo	1:250	Rabbit	Sigma
XBP-1	1:20	Rabbit	Santa Cruz
Anti-PDI	1:200	Mouse	Abcam
Anti-Calreticulin	1:250	Rabbit	Abcam

2.4.3 VSVG transport assay

Neuro2a cells were transiently transfected with appropriate plasmid and the VSVG-mCherry plasmid. Cells were incubated at 40˚C under 5% CO2 for 12.5 hr for SOD1, 16 hr for TDP-43 and 72 hr when the cells were transfected with FUS. The cells were then treated with cDMEM containing cycloheximide (20 μg/ml) and incubated at 32˚C for 30 min. Staining was performed with primary antibodies mouse anti-GM130 (1:250) (Golgi marker) (BD Transduction) and rabbit anti-calnexin (1:250) (ER marker) (Abcam) overnight. Secondary antibodies AlexaFluor 647 goat anti-mouse (1:200) and goat anti-rabbit (1;200) (Invitrogen) were used. Mander's coefficient (M) was used to determine the degree of co-localisation between VSVG-mCherry and ER or Golgi marker. Mander's coefficient was calculated for twenty cells by JACoP (Colocalisation Plugin) [537] in ImageJ (NIH).

2.4.4 Nuclear morphology apoptosis analysis

Neuro2a cells grown were transfected with appropriate plasmids, using Lipofectamine 2000 (Invitrogen) according to the manufacturer's protocol. Seventy hour post transfection cells were washed with PBS and fixed with 4% paraformaldehyde in PBS for 10 min. Cells were washed and treated with Hoechst 33342 (1:10,000) prior to mounting in fluorescent mounting medium (Dako). Images were acquired using an Olympus Fluoview inverted confocal laser-scanning microscope. Nuclei with abnormal morphology -condensed (under ~5 μm in diameter) or fragmented (multiple condensed Hoechst-positive structures in one cell), were defined as apoptotic nuclei. Apoptotic nuclei were counted as a percentage of non-apoptotic cells, from at least 100 cells coexpressing both plasmids per treatment in three independent experiments. Cells expressing only one transfected construct or undergoing cell division were excluded from analysis.

2.5 Statistical Analysis

The experiments were performed minimum three times on separate days with compulsory one blind experiment. The data are represented as the mean of ± SD or ±SEM value as applicable. The statistical significance of the data were analysed using ANOVA followed by Tukey *post hoc* test (GraphPad Prism, San Diego, CA, USA). P-values of 0.05 or less was considered significant where ***p<.001, **p<.01, *p<.05.

Chapter 3 PDI is protective against ER-Golgi Pathology in neuronal cells expressing TDP-43, FUS and SOD1

3.1 Introduction

Protein disulphide isomerase (PDI) accelerates the folding of disulphide-bonded proteins that enter the ER [538]. It also assists in rearranging disulphide bonds within incorrectly arranged disulphide bonded substrates. Alternatively, PDI acts as a chaperone by reducing the aggregation of misfolded proteins and translocating them into the cytoplasm for proteasomal degradation [539]. PDI inhibits the aggregation of proteins with or without the presence of disulphide bonds therefore, it acts as a vital cellular defence against general protein misfolding [540]. Furthermore, protein misfolding and ER stress are increasingly been implicated in various neurodegenerative diseases such as ALS, Parkinson and Alzheimer's disease suggesting PDI relevance in neurological disorders [541-543]. In ALS PDI is up-regulated in motor neurons of human patients and in animal models [339].

Various studies have proposed that induction of PDI is protective during ER stress since it decreases the load of misfolded proteins, restores proteostasis and increases neuronal viability [483, 533, 544]. However, recent studies indicate that the loss of function of PDI, due to aberrant post-translation modification, is associated with the pathogenesis of neurodegenerative diseases [540, 544]. Due to specific cellular stressors, such as oxidative stress, during disease states PDI becomes S-nitrosylated. S-nitrosylation is the covalent binding of nitric oxide (NO) groups to active site cysteine thiols in proteins [545]. S-nitrosylation of PDI under pathological conditions is an abnormal, irreversible process associated with protein misfolding, ER stress and apoptosis [546]. Increased levels of S-nitrosylated PDI are observed in the brains of Parkinson's, Alzheimer's and ALS patients [483, 544]. Moreover, S-nitrosylation reduces the protective effect of PDI in neurons and induces apoptosis by increasing ER stress, misfolded proteins or proteasome inhibition in these disorders [546]. A recent study using HEK cells revealed that the with active site domains of PDI are the main site of S-nitrosylation [547]. Therefore, this suggests that modifications in PDI can result in loss of its neuroprotective role.

3.1.1 S-nitrosylation of PDI

Redox-dependent post translational modifications of PDI are also linked to disease states. During some cellular conditions, high levels of reactive nitrogen species (RNS), hydrogen peroxide and reactive oxygen species (ROS) accumulate in cells, inducing nitrosative or oxidative stress. Nitrosative stress can lead to the post translation modification of PDI by addition of NO to active site cysteine residues, resulting in S-nitrosylation. Furthermore, proteins resident in the ER are particularly vulnerable to post translation modification due to the presence of critical thiol residues and redox regulated cysteines. Since PDI is a key enzyme that modifies protein disulphide bonds, the loss of function of PDI could increase general misfolding and increase ER stress. S-nitrosylation reduces both its chaperone and isomerase activity [544].

S-nitrosylation of PDI has been detected in postmortem brain tissues of patients with Alzheimer's and Parkinson's disease [544] as well as lumbar spinal cord tissues of ALS patients and $SOD1^{G93A}$ mice [483]. S-nitrosylation has also been reported in prion disease models triggering mitochondrial mediated apoptosis following prion infection [548]. Exposure of cultured neurons to N-methyl-D-aspartate receptor (NMDA), leading to calcium influx and nitric oxide production, also resulted in S-nitrosylation of PDI. S-nitrosylated PDI (SNO-PDI) increases the levels of polyubiquitinated proteins, triggering cell death, and it is also associated with hyper-activation of NMDA [546] and inhibition of mitochondria, leading to the generation of ROS and nitric oxide [549]. SNO-PDI accentuates the misfolding of synphilin in Parkinson disease [546] and S-nitrosylation also increases mutant SOD1 aggregation *via* incorrect disulphide cross-linking of the immature, misfolded mutant SOD1, leading to neuronal cell death [533]. Hence, these data imply that aberrant modifications of PDI lead directly to harmful effects as well as elimination of the normally protective properties of PDI.

3.1.2 ER stress and protein misfolding linked to mutant SOD1, TDP-43 and FUS

Protein misfolding and associated ER stress leading to apoptosis, are closely linked to ALS mutant SOD1. As mentioned earlier, mutant SOD1 induces ER stress in animal and cellular disease models based on mutant SOD1 [339, 478]. Previous studies have speculated mutant SOD1 is present in the ER, where it interacts with BiP [550]. Also SOD1 colocalised with ER markers and was present in the microsome fraction of cells *via* an ATP dependent mechanism [550, 551]. These studies suggest that mutant SOD1 directly induces ER stress from the ER. Apart from the conventional method of directly increasing the load of misfolded proteins within the ER, mutant SOD1 could induce ER stress through other, more indirect pathways, or from the cytoplasm. Mutant SOD1 interacts with Derlin-1, an ER protein involved in transport of misfolded proteins from the ER to the cytoplasm for degradation *via* ERAD [485]. Binding of mutant SOD1 to Derlin1 causes up-regulation of ER stress through activation of the IRE1-ASK1 pro-apoptotic pathway, in a Derlin1 binding-dependent manner during the later stages of disease in $SOD1^{G93A}$ mice [485]. This study also concluded that mutant SOD1 is not present within the ER, and it disputed previous findings of ER-localised SOD1, by showing that microsomes were contaminated with cytosolic SOD1 bound to the cytoplasmic face of the isolated vesicles [485]. Our laboratory also concluded, using multiple approaches, that mutant SOD1 is not present in the ER and that it triggers ER stress from the cytoplasm [552]. Moreover, we demonstrated that cytoplasmic mutant SOD1 inhibits ER-Golgi transport in neuronal cell lines, which subsequently induces ER stress [552]. ER-Golgi transport inhibition was observed prior to several other cellular events, including induction of ER stress, Golgi fragmentation, SOD1 aggregation and apoptosis. These data suggest that ER-Golgi transport defects could trigger ER stress and apoptosis in cellular models of ALS.

Similar to mutant SOD1, mutant FUS also induces ER stress in neuronal cells, [487]. Patients with mutations in FUS and SOD1 have different pathological signatures yet at a molecular level they induce the same pathological pathway, ER stress. Our laboratory previously showed that mutant FUS induces ER stress, including pro-apoptotic marker CHOP, specifically in those cells that mis-localise

to the cytoplasm, thus linking mutant FUS to ER-stress specific motor neuron death [487]. Mutant FUS also colocalised with ER maker calreticulin, suggesting that it is associated with the ER however, the exact mechanism by which mutant FUS induces ER stress requires clarification [487].

TDP-43 is structurally and functionally similar to FUS and several studies have shown that mutations in TDP-43 and FUS are clustered around the C-terminal nuclear localisation signal of each protein, which mediates cytoplasmic mis-localisation and prevents nuclear import [484, 485]. The TDP-43 and FUS inclusions present in human patient tissues are found in the cytoplasm, suggesting that they are associated with clearance of TDP-43 and FUS from the nucleus in disease, implying that redistribution of TDP-43 and FUS could be linked with pathogenesis [54, 89]. The reason for the presence of cytoplasmic TDP-43 remains unclear. However, previously there had been few studies linking ER stress to TDP-43. Mutations in VCP linked with FTLD induced alterations in TDP-43 localisation, triggered ER stress and cell death *in vitro* [553]. Though, whether induction of ER stress occurred before or after redistribution of TDP-43, and whether there was a causal link between the two processes, remained unknown. Another study showed that over-expression of TDP-43 induced neuronal cell death *in vitro* by the activation of Bim and down-regulation of the Bcl-1 family of proteins [554]. Increased levels of CHOP were detected in neuronal cells due to increased translation of CHOP mRNA and abrogation in the level of CHOP degradation, which was independent of activation of PERK/eIF2a/ATF4 or other UPR pathways after 24-48 post transfection [555]. However, the mechanism underlying this TDP-43 induced CHOP mRNA up-regulation wasn't previously defined. In another study, mutant TDP-43 induced Golgi fragmentation leading to neuronal loss in rat models, providing evidence for disruption in the ER-Golgi compartments [556]. However, mutant TDP-43 did not induce UPR or ER chaperone expression, but were depleted of XBP-1 suggesting that mutant TDP-43 could result in repression of UPR and ER chaperones such as PDI [556]. The first part of the studies outlined in this Chapter, which formed part of a manuscript published in 2013, demonstrate that mutant TDP-43 induces ER stress in neuronal cell lines, and that ER stress is

linked to redistribution of mutant TDP-43 from the ER to cytoplasm ([486], Supplementary Figure 3).

Recently, in a study involving the author (presented as Supplementary Figure 4), our laboratory demonstrated that mutant TDP-43 and mutant FUS inhibit protein transport between the ER-Golgi in neuronal cells, and this was linked to ER stress [557]. Mutant TDP-43 and mutant FUS both inhibited the assimilation of secretory protein cargo into COPII vesicles as they bud from the ER, and inhibited transport from ER to the ERGIC compartment. TDP-43 was observed on the cytoplasmic face of the ER membrane, whereas FUS was detected within the ER, suggesting that transport was inhibited from the cytoplasm by mutant TDP-43, and from the ER by mutant FUS. It was also demonstrated that mutant SOD1 destabilized microtubules and inhibited transport from the ERGIC compartment to Golgi, but not from ER to ERGIC. Whilst it appeared that the different mutant proteins were triggering different stages of ER-Golgi transport, each of these steps was Rab1-dependent [552]. Importantly, evidence was also provided that Rab1 is dysfunctional in human sporadic ALS: Rab1 was found to be misfolded and recruited to TDP-43 inclusions in human ALS motor neurons. Hence these findings imply that inhibition of ER-Golgi transport is a common pathogenic mechanism in ALS.

3.1.3 Aims of the Chapter

Despite their diversity, at the molecular level, ALS mutant proteins TDP-43, FUS and SOD1 share the same phenomenon of accumulating as abnormally folded proteins, and their expression triggers ER stress and inhibits ER-Golgi transport. The first aim of the studies presented in this Chapter was to investigate whether mutant TDP-43 induces ER stress in neuronal cell lines. Secondly, given that PDI is up-regulated during ALS, and given the association of PDI with mutant TDP-43, FUS and SOD1, it could be predicted that over-expression of PDI could protect against pathogenic processes triggered by these mutant proteins. Hence, the second aim of this Chapter was to investigate whether PDI is protective in cell lines expressing mutant TDP-43, FUS and SOD1 *in vitro*.

3.2 RESULTS

3.2.1 Over-expression of mutant TDP-43 induces ER stress to a greater extent than wild-type TDP-43 in neuronal cell lines.

It was first examined whether mutant TDP-43 induces ER stress in neuronal cell lines using immunochemistry for markers of the UPR: CHOP, ATF6 and XBP-1. Single cell analysis approach was used to detect only the cotransfected cells rather than the total cell population. Since, ER stress was only present in particular subtypes of cells and the analyses of the total cell populations would be improbable to reveal any differences between these populations.

Presence of nuclear XBP-1 was used as it detects the activation of the IRE-1 pathway during the early, pro-survival phases of UPR. Since, IRE-1 controls the cellular response to ER stress, and the extent of IRE1 signalling matches the magnitude of the stress [558]. Another UPR marker ATF6 translocates to the Golgi indicating activation of the ATF6 pathway of ER stress. CHOP a pro-apoptotic protein induced predominately *via* the PERK and ATF6 UPR pathways was also examined. Essentially, CHOP plays a role in facilitating the transition of the UPR from pro-survival to pro-apoptosis. Hence, the activation of CHOP directs the UPR into its apoptotic phase.

The study demonstrated that ALS mutant TDP-43 induces ER stress in neuronal cells. Neuro2a cells expressing mutant TDP-43 A315T had approximately 34% ($p<.01$) cells displaying nuclear XBP-1 immunoreactivity which was significantly higher than wild-type TDP-43. Similarly, ATF6 translocated to the Golgi in mutant Q331K expressing cells and 28% ($p<.05$) cells had ATF6 colocalising with the Golgi apparatus. Increased nuclear CHOP immunoreactivity was detected in Neuro2a cells expressing ALS mutant forms of TDP-43 (A315T, 33% $p<.05$ and Q331K, 35% $p<.01$) linked with mCherry and in Neuro2a cells expressing ALS mutant forms of TDP-43 (Q343R and Q331K, 35% $p<.05$) linked with EGFP.

The results are presented in the published manuscript: “Walker, A. K., et al. (2013) "ALS-associated TDP-43 induces endoplasmic reticulum stress, which drives cytoplasmic TDP-43 accumulation and stress granule formation." PloS one 8(11): e81170 “which is presented at the end of this chapter in Supplementary Figure 3. The author performed all the experiments presented in figure 4, described in the Results section of the manuscript on page e81170 titled ‘*Over-expression of mutant TDP-43 induces ER stress to a greater extent than wild-type TDP-43’*.

3.2.2 Over-expression of PDI reduces XBP-1 and CHOP activation induced by mutant TDP-43 in neuronal cell lines.

Our laboratory previously demonstrated that PDI is protective against mutant SOD1-induced ER stress, detected by nuclear immunoreactivity to CHOP in neuronal cell lines [483]. Hence, after demonstrating that mutant TDP-43 also induces ER stress, it was next examined whether PDI was protective against UPR induction in TDP-43 expressing cells.

Neuro2a cells were transfected with constructs expressing wild-type TDP-43 mCherry or mutant Q331K (a common mutation observed in sporadic ALS patients) tagged with mCherry as previously described [486]. Constructs expressing PDI-V5-pcDNA3.1 or empty vector in control cells were also cotransfected with TDP-43. Co-transfection was verified by detecting red fluorescence from mCherry from TDP-43 and using immunofluorescence with an Alexa Fluor 488-tagged secondary antibody to detect V5 tag of PDI. The mCherry tag is a commonly used tag to aid visualisation of the protein in neuronal cells, and it has previously demonstrated not to alter the native function or localisation of the protein of interest [559]. Also, V5 tag is a short peptide sequence of 14 amino acids that demonstrates high-affinity towards specific antibodies [560]. The overall transfection efficiency was found to be approximately 40% in Neuro2a cells when observed 18 hr post transfection. Co-expression of both PDI and TDP-43 proteins was confirmed by performing immunocytochemistry to detect V5 tag, followed by fluorescent microscopy to simultaneously detect the mCherry and V5 tags. Quantification of individual cells

revealed that over 96% of cells expressing TDP-43 were also expressing PDI (Figure 3.1). Hence, for subsequent studies involving ER stress markers (XBP-1 and CHOP) it was assumed that detection of TDP-43 expression in a cell reflected co-expression of both TDP-43 and PDI in the same cell.

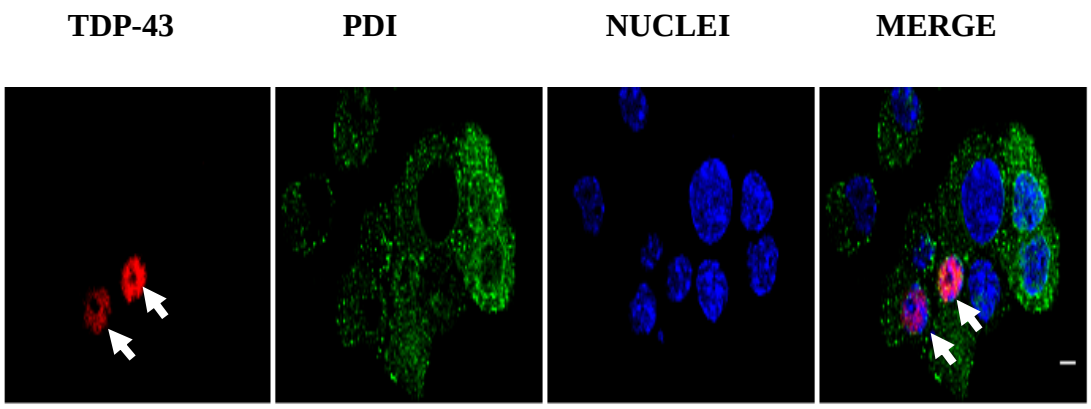

Figure 3.1 Co-expression of TDP mCherry and PDI V5 in Neuro2a cells. Representative confocal microscopy images of cells expressing wild-type TDP-43 mCherry (red) and PDI-V5 (green) and with Hoechst stained nuclei (blue) examined 18 hr post transfection. Transfection efficiency was approximately 40%. Image demonstrates cells expressing nuclear TDP-43 expression and with PDI in a reticulate distribution throughout the cytoplasm. Scale bar = 5 µm.

To investigate the effect of over-expression of PDI on ER stress induced by mutant TDP-43 two markers CHOP and XBP-1 were used to observe UPR indicating ER stress-induced apoptotic signalling pathway [486]. As previously established mutant TDP-43 induces UPR robustly at 18-24 hr post transfection, when it is predominantly expressed in the cytoplasm, because after this point it becomes more nuclear again [486]. Therefore, cells were examined at 18 hr post transfection. Neuro2a cells were transfected with wild-type TDP-43 or mutant TDP-43 (Q331K) and cotransfected with either empty vector or PDI. XBP-1 was used as a marker of

ER stress. Immunocytochemistry was performed using anti-XBP-1 antibody, where nuclear immunoreactivity to XBP-1 was indicative of ER stress.

In Neuro2a cells expressing mCherry alone a diffused localisation of fluorescence was observed in the cell throughout the entire cytoplasm and nucleus. Wild-type TDP-43 was mainly detected in the nucleus where it colocalised with the Hoechst stain. In the nucleus, wild-type TDP-43-mCherry fluorescence was punctate and particularly excluded from the nucleoli. Quantification of 100 transfected cells revealed that approximately 20% of cells expressing wild-type TDP-43-mCherry displayed cytoplasmic mCherry fluorescence, similar to other reports [561]. However, in contrast, in cells expressing mutant TDP-43 Q331K approximately 30% of cells displayed TDP-43 localised in the cytoplasm (discussed in section 3.1.7).

Cells expressing TDP-43 were then scored individually using fluorescence microscopy, according to whether XBP-1 was located in the cytoplasm or nucleus detected by the presence of green fluorescence (Figure 3.2 A). XBP-1 nuclear immunoreactivity was rarely detected in untransfected cells (UTR) (7% cells). Similar results were obtained when cells were transfected with empty vector mCherry as a control: nuclear immunoreactivity to XBP-1, indicating induction of ER stress, was present in only 6% cells. In cells expressing wild-type TDP-43, a slight, but non-significant activation of XBP-1 was detected in 20% of transfected cells. Expression of mutant TDP-43 Q331K with empty vector pcDNA3.1 resulted in significant increase in ER stress 34% as compared to cells expressing wild-type TDP-43, as detected by nuclear XBP-1 immunoreactivity, similar to the previous study. Interestingly, co-expression with PDI significantly reduced the proportion of cells with nuclear XBP-1 immunoreactivity, indicating induction of UPR to 26% ($p<.01$) (Figure 3.2 B).

A

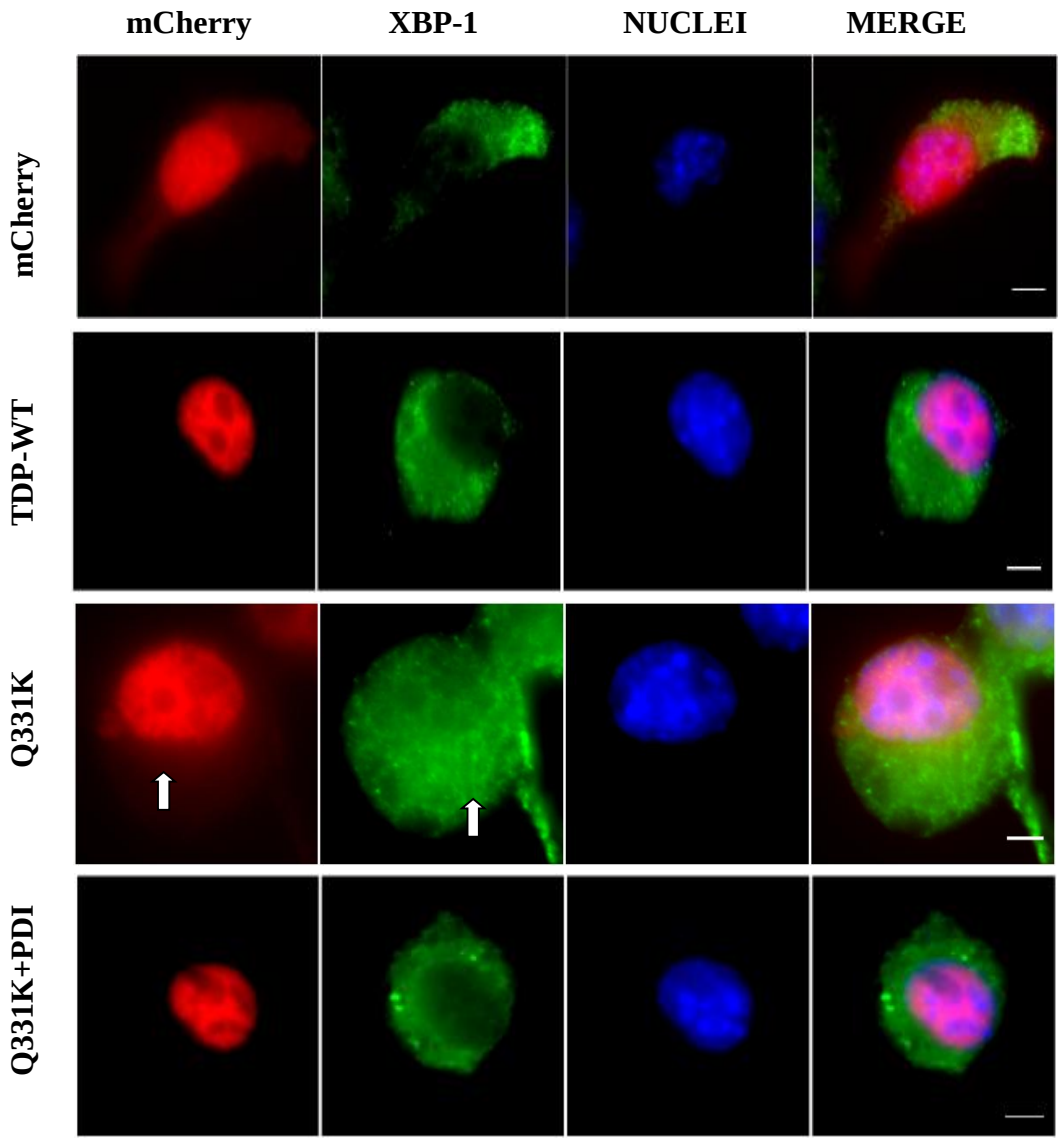
mCherry
XBP-1
NUCLEI
MERGE
mCherry
TDP-WT
Q331K
Q331K+PDI

B

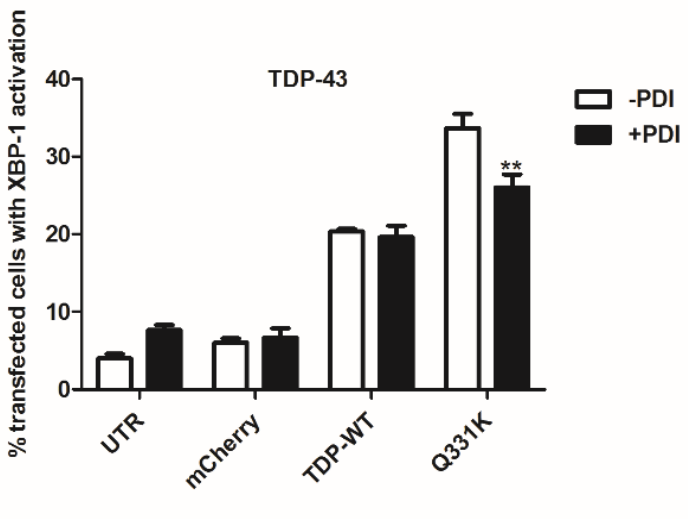
% transfected cells with XBP-1 activation
TDP-43
-PDI
+PDI
40
30
20
10
0
**
UTR
mCherry
TDP-WT
Q331K

Figure 3.2 Over-expression of PDI reduces XBP-1 activation, and hence ER stress, in Neuro2a cells. A) Cells were transfected with TDP-43 mCherry constructs and at 18 hr post-transfection, immunocytochemistry using anti-XBP-1 antibody and counter-staining with DAPI was performed. Cells expressing mCherry only (first panel) or wild-type TDP-43 (second panel, TDP-WT) display cytoplasmic expression of XBP-1, whereas mutant TDP-43 Q331K (third panel, Q331K) induced expression of XBP-1 in the nucleus (middle column), indicated with white arrow. However, after co-expression of PDI with TDP-43 Q331K fewer cells displayed nuclear XBP-1 expression (fourth panel), demonstrating a reduction in ER stress. Scale bar = 10 μm. **B)** Quantification of cells with and without co-expression of PDI using nuclear immunoreactivity for XBP-1 as a marker for ER stress. Cells expressing wild-type TDP-43 and mutant Q331K are shown, with those expressing mCherry only and untransfected control cells (UTR). A significant reduction (**) in the levels of ER stress was observed in cells expressing TDP-43 Q331K when cells were co-expressed with PDI. For each of 3 replicate experiments, 100 cells were scored for each population. Data are represented as mean ±standard error of the mean (SEM); n=3, **$p<0.01$ versus mCherry control by two-way ANOVA with Bonferroni's post test.

Next, the effect of PDI on ER stress-induced apoptotic signalling was examined in cells expressing mutant TDP-43, using nuclear immunoreactivity to CHOP as a marker. TDP-43 tagged mCherry wild-type TDP-43, Q331K, and a second mutant, A315T, which has been detected in multiple fALS pedigrees, were expressed with or without PDI in Neuro2a cells. Furthermore, to ensure that the mCherry tag does not induce deleterious effects TDP-43 constructs with an alternative tag, EGFP, were also expressed in Neuro2a cells. TDP-43-EGFP mutant Q331K, and a second familial ALS linked mutant, Q343R, which is aggregation prone and promotes toxicity in vivo were also examined (a EGFP-tagged A315T construct was not available).

Neuro2a cells were transfected with EGFP only, wild-type TDP-43 and mutant TDP-43 Q331K and Q343R for 18 hr, and the cells were then fixed and immunocytochemistry for CHOP was performed (Figure 3.3 A). CHOP nuclear immunoreactivity was rarely detected in untransfected cells (UTR) 6% cells. The expression of EGFP was diffused and observed throughout the cytoplasm and nucleus, and little ER stress was detected; only 6% of these cells displayed nuclear immunoreactivity to CHOP, indicating activation of the UPR. In cells expressing wild-type TDP-43, a slight, but non-significant activation of CHOP was detected in 21% of transfected cells. In contrast, cells expressing EGFP tagged Q331K 30% of cells or 39% of Q343R TDP-43 cells expressed nuclear CHOP, indicating activation of ER stress. However, when co-expressed with PDI there was a significant reduction in nuclear immunoreactivity to CHOP for all of the TDP-43 mutants; to 22% ($p<.05$) in Q331K cells and in mutant Q343R cells to 28% ($p<.01$) (Figure 3.3 B).

Similar observation was subsequently confirmed using TDP-43 mCherry constructs. Neuro2a cells were transfected with mCherry only, wild-type TDP-43 and mutant TDP-43 Q331K and A315T for 18 hr, and the cells were then fixed and immunocytochemistry for CHOP was performed. CHOP nuclear immunoreactivity was rarely detected in untransfected cells (UTR) 6% cells. The expression of mCherry was diffused and observed throughout the cytoplasm and nucleus, and little ER stress was detected; only 6% of these cells displayed nuclear immunoreactivity to CHOP, indicating activation of the UPR. In cells expressing wild-type TDP-43, a slight, but non-significant activation of CHOP was detected in 24% of transfected cells. In contrast, cells expressing mCherry tagged Q331K 34% of cells or 40% of A315T TDP-43 cells expressed nuclear CHOP, indicating activation of ER stress. However, when co-expressed with PDI there was a significant reduction in nuclear immunoreactivity to CHOP for all of the TDP-43 mutants; to 27% ($p<.01$) in Q331K cells and in mutant A315T cells to 32% ($p<.01$) (Figure 3.3 C).

Hence, the data demonstrated that PDI is protective against induction of ER stress and activation of both XBP-1 and CHOP in cells expressing three different TDP-43 mutants (Q331K, A315T and Q343R) during both early and late phases of UPR. Furthermore, similar levels of ER stress and the protective activities of PDI, were observed in cells expressing either mCherry or EGFP tagged mutant TDP-43 proteins, indicating that the tag did not impact on the findings.

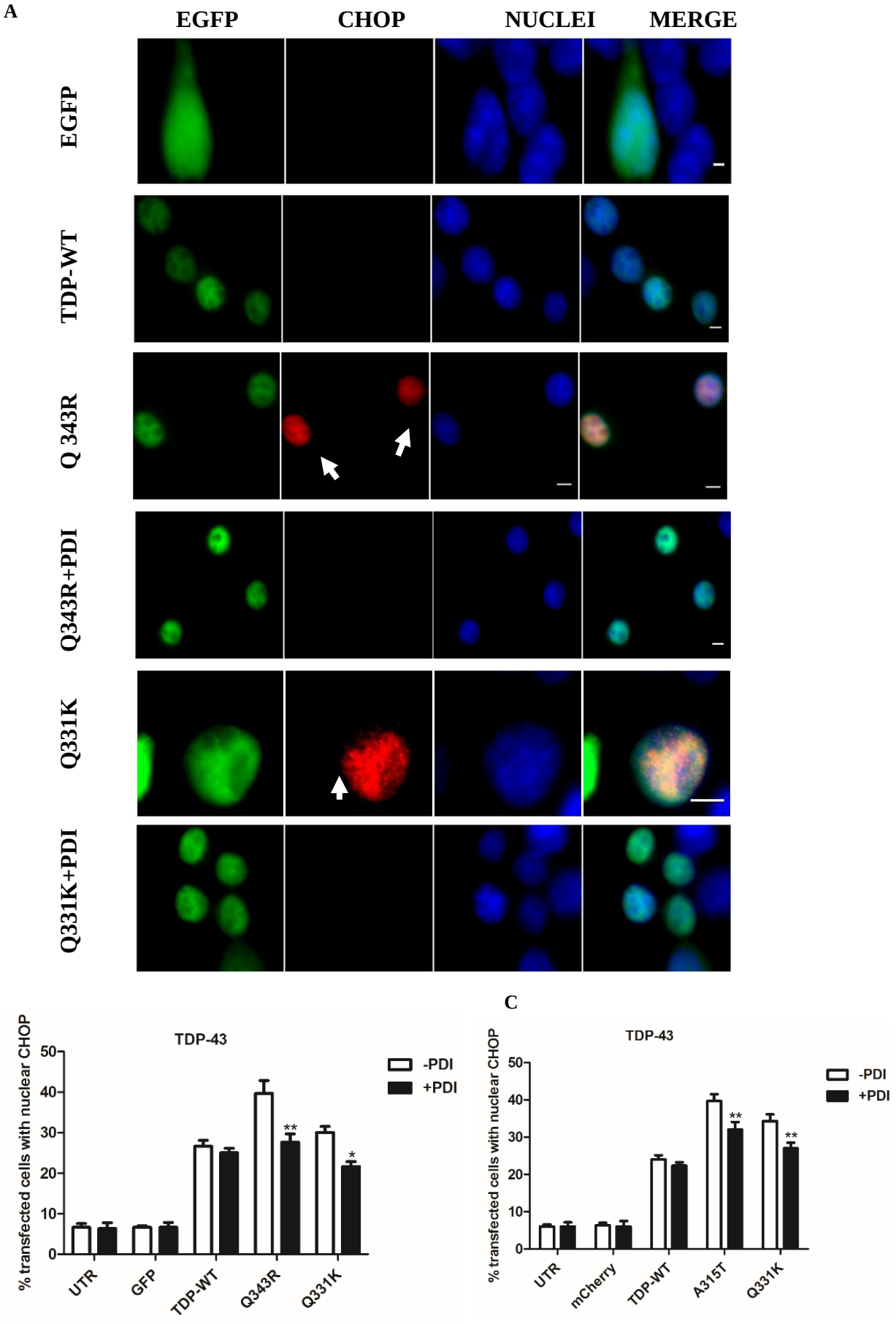
A
EGFP
CHOP
NUCLEI
MERGE
EGFP
TDP-WT
Q 343R
Q343R+PDI
Q331K
Q331K+PDI
B
TDP-43
% transfected cells with nuclear CHOP
-PDI
+PDI
UTR
GFP
TDP-WT
Q343R
Q331K
C
TDP-43
% transfected cells with nuclear CHOP
-PDI
+PDI
UTR
mCherry
TDP-WT
A315T
Q331K

Figure 3.3 Over-expression of PDI reduces nuclear immunoreactivity to CHOP, and hence ER stress, in mutant TDP-43 expressing cells. A) Neuro2a cells were transfected with EGFP only (first panel), wild-type TDP-43 EGFP (TDP-WT, second panel) or mutant TDP-43 Q343R EGFP or Q331K (third panel, fifth panel), at 18hr post-transfection. Immunocytochemistry was performed using anti-CHOP antibodies and counter-staining with DAPI. Control cells expressing EGFP only, and most cells expressing wild-type TDP-43 display little activation of CHOP. However, cells expressing TDP-43 mutant Q343R or Q331K induces ER stress, as detected by nuclear immunoreactivity to CHOP (middle panel) indicated with white arrows. However, co-expressing PDI reduces nuclear CHOP immunoreactivity in cells expressing both mutants (fourth panel and sixth panel). Scale bar = 10 µm **B** Quantification of cells expressing EGFP tagged TDP-43 proteins with and without co-expression of PDI using nuclear immunoreactivity to CHOP as a marker of ER-stress induced apoptotic signalling. A significant reduction (**) in the levels of ER stress was observed in cells expressing TDP-43 Q343R when cells were co-expressed with PDI. A significant reduction (*) in the levels of ER stress was observed in cells expressing TDP-43 Q331K when cells were co-expressed with PDI. 100 cells were scored for each population. Data represented as mean ±SEM, n=3, **p<0.01, *p<.05 versus EGFP controls by two-way ANOVA with Bonferroni's post test. PDI significantly reduces UPR activation in cells expressing mutant Q343R or Q331K. **C)** Quantification of cells expressing mCherry tagged TDP-43 proteins with and without co-expression of PDI using nuclear immunoreactivity to CHOP as a marker of ER-stress induced apoptotic signalling. A significant reduction (**) in the levels of ER stress was observed in cells expressing TDP-43 Q331K or A315T when cells were co-expressed with PDI. 100 cells were scored for each population. Data are represented as mean ±SEM, n=3, *p<.05 **p<0.01 versus mCherry controls by two-way ANOVA with Bonferroni's post-test. PDI significantly reduces UPR activation in cells expressing mutant A315T or Q331K.

3.2.3 Over-expression of PDI is protective against mutant TDP-43 induce ER-Golgi transport defects in neuronal cell lines.

Our lab recently demonstrated that mutant TDP-43 inhibit ER-Golgi transport in cellular models of ALS [552, 557]. It was next investigated whether PDI was protective against inhibition of ER-Golgi transport induced by mutant TDP-43. Vesicular stomatitis glycoprotein-ts045 (VSVG) protein is a widely used marker for studying ER-Golgi transport [562]. At 40°C VSVG misfolds and accumulates within the ER. However, at the permissive temperature, 32°C, VSVG is transported to the Golgi. Neuro2a cells were co-transfected with mCherry-tagged VSVG, EGFP tagged wild-type TDP-43 or mutant TDP-43 Q331K, and with either empty vector or V5-tagged PDI. The cells were incubated at 40°C for 16 hr to accumulate VSVG in the ER, before incubation at the permissive temperature for 30 min. Previous studies from our laboratory demonstrated that ER-Golgi transport was inhibited 16 hr post-transfection in cells expressing mutant TDP-43 Q331K [557] therefore, same time point was examined. After fixing the cells, immunocytochemistry was performed using antibodies for markers of the ER (calnexin) and Golgi (GM130) followed by fluorescent microscopy. Quantification of the localisation of VSVG in either the ER or Golgi was performed, using Mander's co-efficient, in the range from 0 to 1 representing 0-100% overlapping pixels as described previously [552, 563].

In untransfected cells (UTR), little VSVG 8% was retained in the ER and most 75% was transported to the Golgi apparatus after 30 min at the permissive temperature. Similarly, in cells expressing EGFP only 8% or wild-type TDP-43 11%, little VSVG was retained in the ER because most 72% was already transported to the Golgi at this time point. However, in cells expressing mutant TDP-43 Q331K, inhibition of ER-Golgi transport was detected relative to the other cell populations. In these cells, significantly more VSVG was retained in the ER 34% ($p<.01$) and less was transported to the Golgi after 30 min 43%, ($p<.05$), (Figure 3.4 A), similar to previous observations [557]. Conversely, when PDI was co-expressed with mutant TDP-43, transport between the ER-Golgi was restored only 14% VSVG was

retained in the ER 14% ($p<.01$) and 61% ($p<.05$) VSVG was transported to Golgi Therefore, these data suggest that over-expression of PDI rescued the inhibition of ER-Golgi transport induced by mutant TDP-43.

A

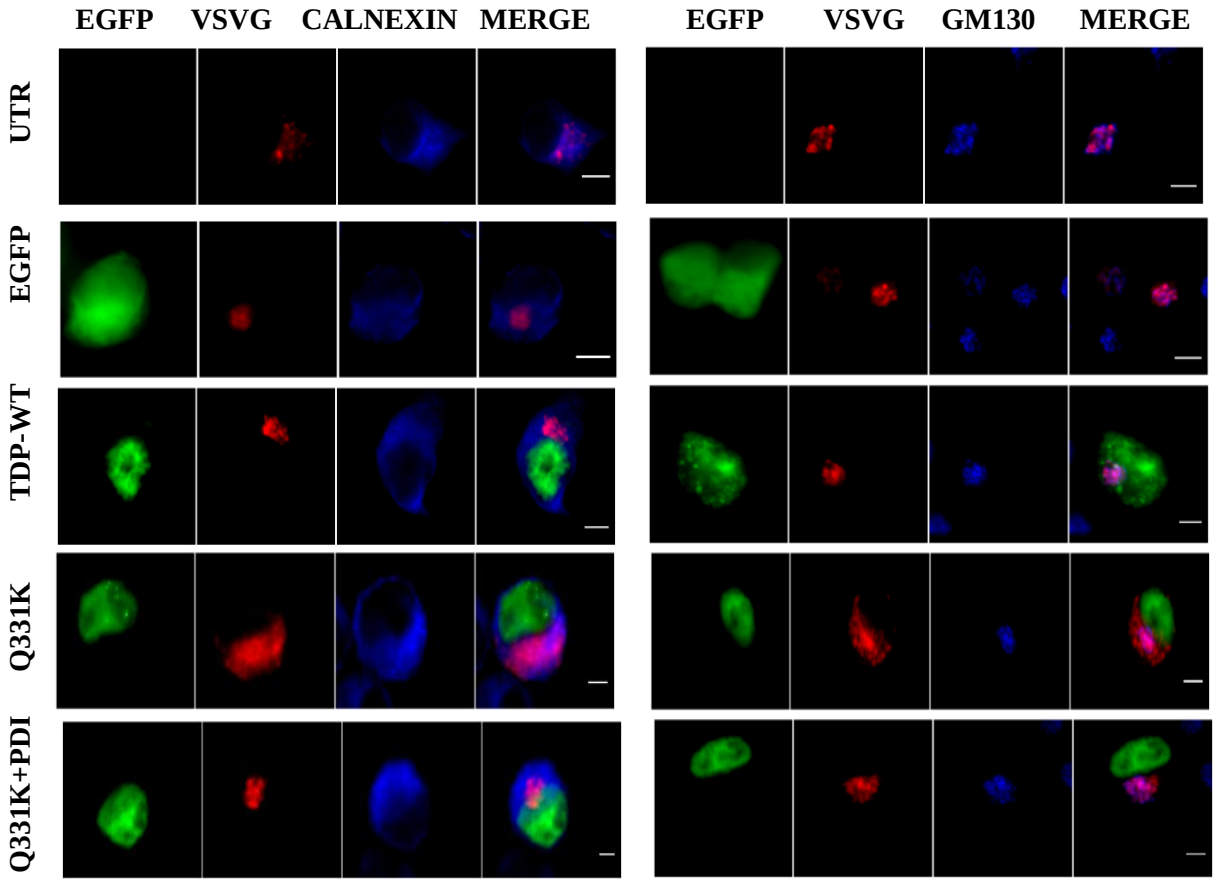
EGFP
VSVG
CALNEXIN
MERGE
EGFP
VSVG
GM130
MERGE
UTR
EGFP
TDP-WT
Q331K
Q331K+PDI

B

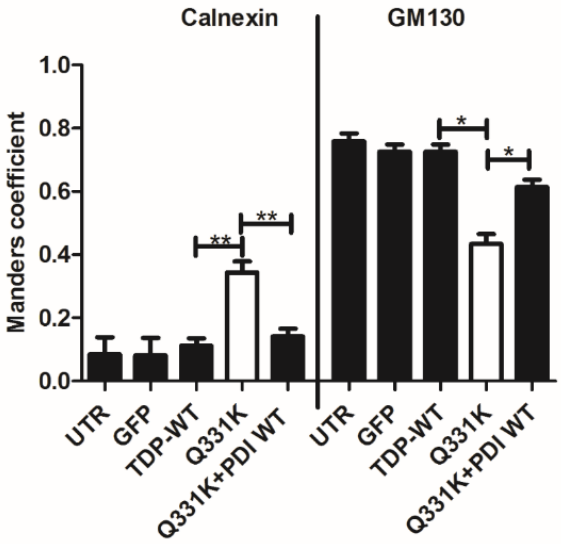
Calnexin
GM130
Manders coefficient
1.0
0.8
0.6
0.4
0.2
0.0
**
**
*
*
UTR
GFP
TDP-WT
Q331K
Q331K+PDI WT
UTR
GFP
TDP-WT
Q331K
Q331K+PDI WT

Figure 3.4 Over-expression of PDI reduces ER-Golgi transport defects in mutant TDP-43 expressing cells. A) Representative fluorescent images of co-expressing cells with enhanced green fluorescent protein (EGFP) tagged wild-type TDP-43 and Q331K and VSVGts045-mCherry with or without PDI at 16 hr post-transfection stained with markers of ER (calnexin) or Golgi apparatus (GM130). VSVGts045-mCherry was trapped in the ER at 40°C for 16 hr then cycloheximide was added and the temperature was shifted to the permissive temperature (32°C) for 30 min then cells were fixed with 4% paraformaldehyde (PFA) at 30 min at 32°C. At 32°C VSVG is transported to Golgi and does not colocalise with calnexin in untransfected cells (UTR) (first panel) and in cells expressing EGFP alone (second panel) or wild-type TDP-43 (TDP-WT, third panel). Inhibition of transportation was observed when Q331K was transfected and VSVG was found to colocalise more with calnexin and less with GM130 (fourth panel). On co-expressing PDI with Q331K transport was facilitated and VSVG colocalised more with GM130 and not with ER marker calnexin (fifth panel). Scale bar = 10 μm**.** **B)** Quantification of the degree of co-localization of VSVGts045-mCherry with calnexin or GM130 was quantified using Mander's coefficient in TDP-43 expressing cells. Data are presented as mean ± SEM, tested with one-way ANOVA and Tukey's post-test, n = 3. Significant difference was observed (**) $p<.01$ between cells expressing Q331K as compared to wild-type TDP-43 and when co-expressed with PDI when observed for co-localisation between VSVG and calnexin. Significant difference was observed (*) $p<.05$ when cells co-expressed Q331K as compared to wild-type TDP-43 with empty vector and when co-expressed with PDI when observed for co-localisation between VSVG and GM130.

3.2.4 Over-expression of PDI is protective against mutant FUS induced ER stress in neuronal cell lines.

Previous studies from our laboratory demonstrated that mutant FUS induces ER stress and mutant FUS expressing cells induced high levels of CHOP and XBP-1

[487]. Hence, it was next examined whether PDI could rescue ER stress in Neuro2a cells. Familial ALS associated FUS mutants R522G and P525L were examined in the study. These mutations are present in the NLS region and they result both in the formation of inclusions and abnormal cellular localization of FUS to the cytoplasm, in human neuroblastoma cells [564].

Similar to the TDP-43 studies described above, an initial experiment was performed to confirm that cells co-transfected with FUS HA-tagged constructs and PDI V5-tagged constructs coexpress both proteins in the same cells. Therefore, Neuro2a cells were co-transfected with wild-type FUS or mutant R522G or P525L-HA with PDI-V5. After 48 hr post-transfection, immunocytochemistry was performed using anti-HA and anti-V5 antibodies and counter-staining of the nucleus with DAPI. Fluorescence microscopy confirmed that 95% of all cells expressing FUS (wild-type and mutants) also express PDI (Figure 3.5).

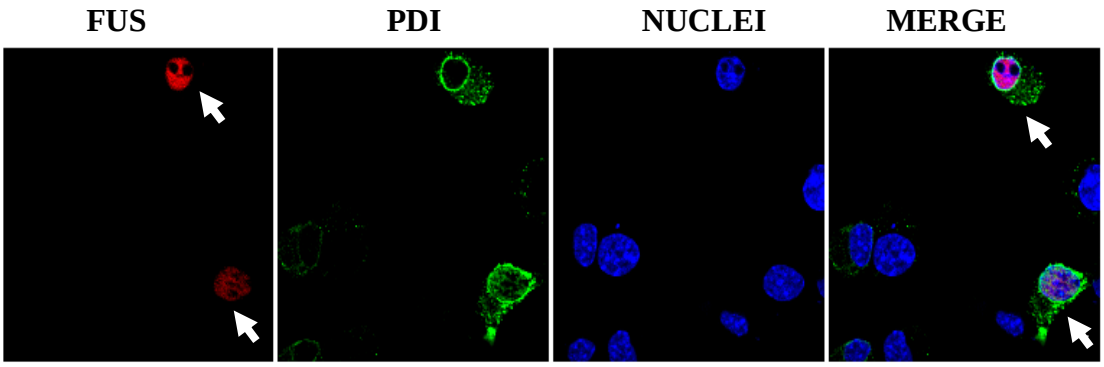

Figure 3.5 Co-expression of FUS HA and PDI V5 in Neuro2a cells. Representative confocal image of cells co-transfected mutant R522G FUS HA-tagged constructs with PDI V5-tagged constructs. After 48 hr post-transfection, cells were fixed then probed with HA-tag (first column), V5-tag (second column) antibodies then stained with DAPI (third column). The fourth column is a merge of the fluorescent images of HA-tag and V5-tag. Scale bar = 10 μm.

Neuro2a cells were transiently transfected with vectors encoding wild-type FUS or mutant FUS (R522G or P525L) with either empty vector pcDNA3.1 as a control or PDI tagged to V5. Immunocytochemistry was performed using anti-HA antibodies to detect FUS expression and anti-CHOP antibodies to detect ER stress. Transfected cells were observed 72 hr post transfection using fluorescence microscopy to detect nuclear CHOP immunoreactivity as a marker of induction of ER (Figure 3.6 A).

In untransfected cells (UTR) and cells expressing wild-type FUS, only a small proportion of cells (7% and 9% respectively) expressed nuclear CHOP, indicating induction of the UPR. However, cells expressing FUS mutants R522G or P525L with pcDNA3.1 only, a significantly greater proportion of cells displayed nuclear immunoreactivity to CHOP 37% compared to wild-type FUS expressing cells. Interestingly, when PDI was co-expressed with mutant FUS there was a significant reduction in nuclear immunoreactivity to CHOP, from 37% to 19% ($p<.001$) in cells expressing the R522G mutant, and to 12% ($p<.001$) in cells expressing the P525L mutant (Figure 3.6 B). Hence, over-expression of PDI significantly reduced ER stress-induced apoptotic signalling induced by mutant FUS R522G and P525L.

A

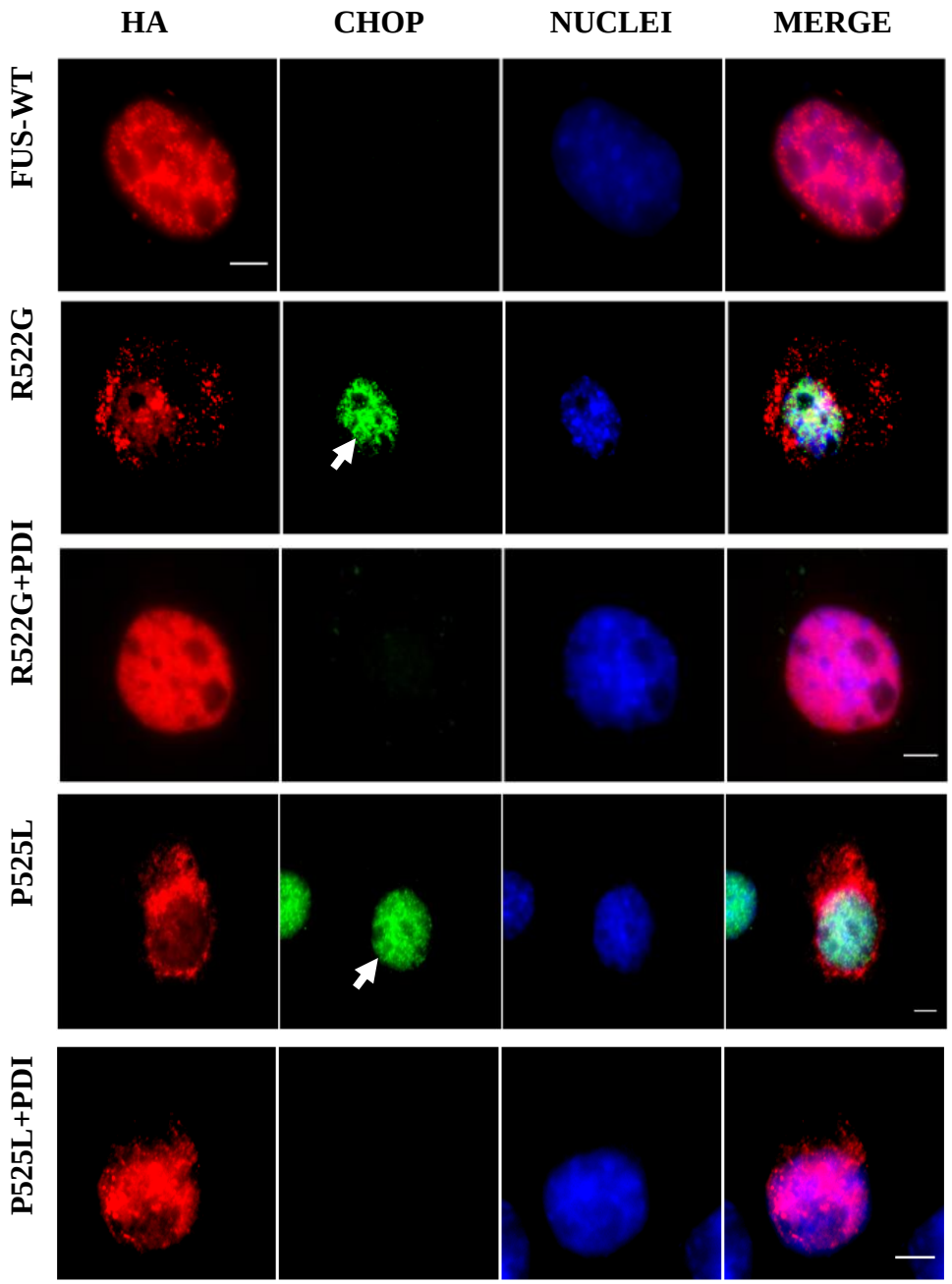
HA
CHOP
NUCLEI
MERGE
FUS-WT
R522G
R522G+PDI
P525L
P525L+PDI

B

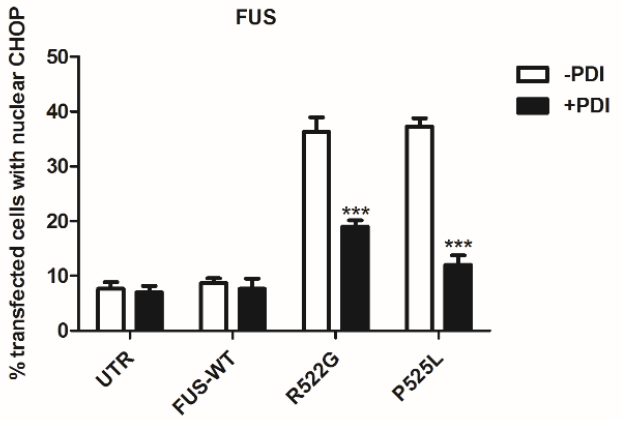
FUS
% transfected cells with nuclear CHOP
50
40
30
20
10
0
-PDI
+PDI
***
***
UTR
FUS-WT
R522G
P525L

Figure 3.6 Over-expression of PDI reduces nuclear immunoreactivity to CHOP, and hence ER stress, in mutant FUS expressing cells. A) Neuro2a cells were transfected with wild-type FUS (first panel) or mutant FUS R522G, P525L (second, fourth panel) at 72 hr post-transfection, and immunocytochemistry using anti-CHOP antibodies and counter-staining with DAPI was performed. Most cells expressing wild-type FUS display little activation of CHOP. However, cells expressing FUS mutant R522G and P525L induce ER stress, as detected by nuclear immunoreactivity to CHOP (middle panel) indicated with white arrows. However, over-expression of PDI reduces nuclear CHOP immunoreactivity in cells expressing both mutants (fourth and sixth panel). **B)** Quantification of cells expressing HA tagged FUS proteins with and without co-expression of PDI using nuclear immunoreactivity to CHOP as a marker of ER-stress induced apoptotic signalling. 100 cells were scored for each population. A significant reduction (***p<.001) in the levels of ER stress in cells expressing R522G or P525L when co-expressed with PDI. Data are represented as mean ±SEM, n=3, versus controls by two-way ANOVA with Bonferroni's post-test. PDI significantly reduces UPR activation in cells expressing mutant R522G or P525L.

3.2.5 Over-expression of PDI is protective against mutant FUS induced ER-Golgi transport defects in neuronal cell lines.

As mentioned earlier mutant FUS induces ER-Golgi transport defects in neuronal cultures [557]. As observed earlier, mutant TDP-43 also induced ER-Golgi transport defects in cell culture which was significantly facilitated when co-expressed with PDI (Result 3.2.3). It was imperative to investigate whether PDI could reduce transport defects induced by mutant FUS in neuronal cell lines. Neuro2a cells were co-transfected with mCherry-tagged VSVG, EGFP tagged wild-type FUS or mutant FUS R522G, and with either empty vector or V5-tagged PDI. The cells were incubated at 40°C to accumulate VSVG in the ER, before incubation at the permissive temperature for 30 min. After fixing the cells, immunocytochemistry was performed using antibodies for markers of the ER

(calnexin) and Golgi (GM130) followed by fluorescent microscopy (Figure 3.7 A). Quantification of the localisation of VSVG in either the ER or Golgi was performed, using Mander's co-efficient, in the range from 0 to 1 representing 0-100% overlapping pixels as described previously [552].

In untransfected cells (UTR), little VSVG 1% was retained in the ER and most 77% was transported to the Golgi apparatus after 30 min at the permissive temperature. Similarly, in cells expressing wild-type FUS 2%, little VSVG was retained in the ER because most was already transported to the Golgi 74% at this time point. However, in cells expressing mutant FUS R522G, inhibition of ER-Golgi transport was detected relative to the other cell populations. In these cells, significantly more VSVG was retained in the ER 43% ($p<.01$) and less was transported to the Golgi after 30 min 39%, ($p<.001$), (Figure 3.7 B). Conversely, when PDI was co-expressed with mutant FUS R522G, transport between the ER-Golgi was restored only 25% ($p<.05$) VSVG was retained in the ER and 60% ($p<.01$) VSVG was transported to Golgi Therefore, these data suggest that over-expression of PDI rescued the inhibition of ER-Golgi transport induced by mutant FUS.

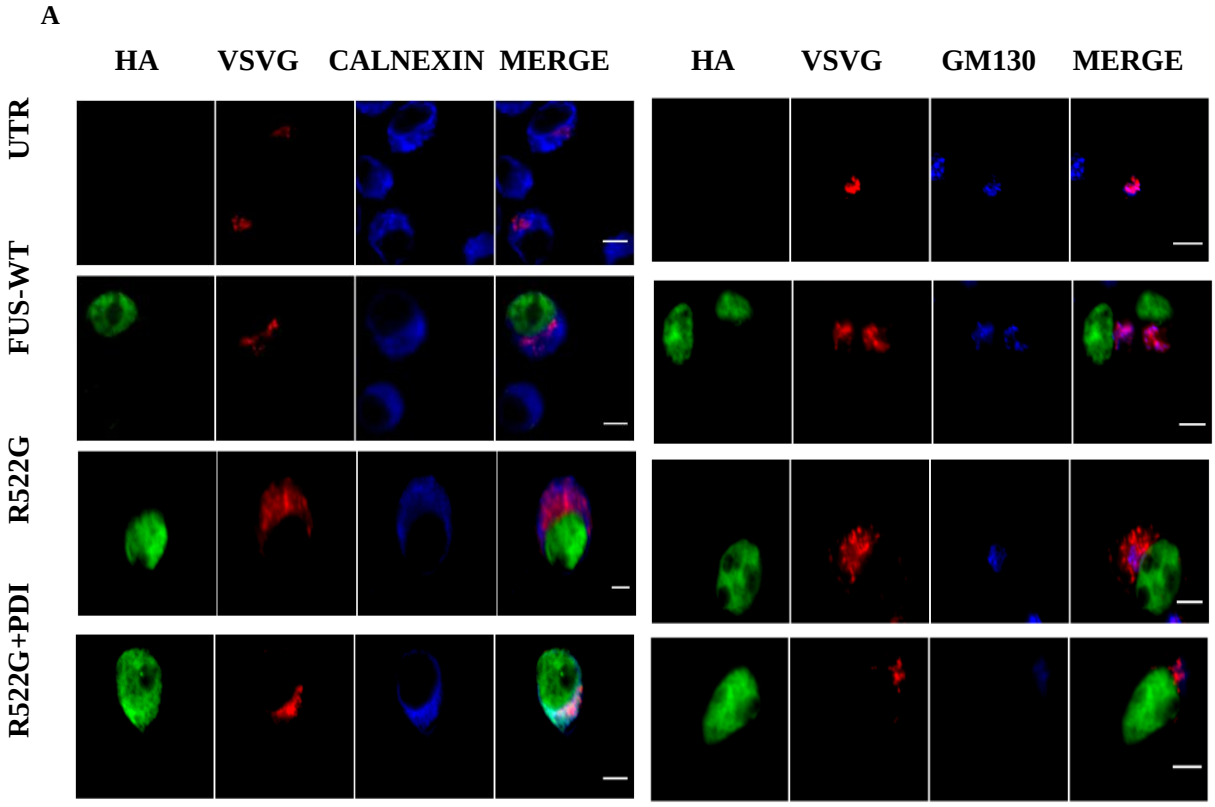
A
HA
VSVG
CALNEXIN
MERGE
HA
VSVG
GM130
MERGE
UTR
FUS-WT
R522G
R522G+PDI

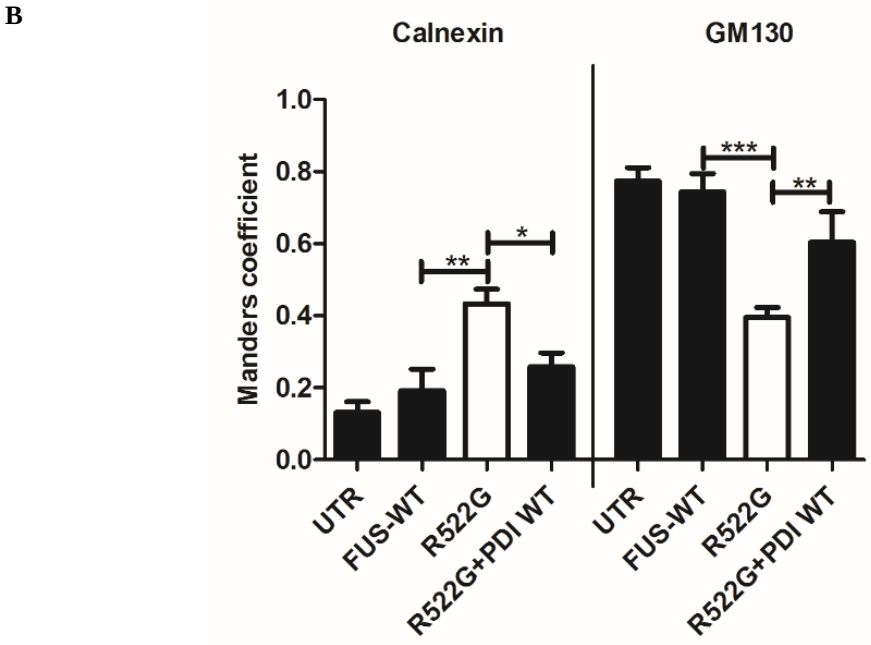
B
Calnexin
GM130
Manders coefficient
1.0
0.8
0.6
0.4
0.2
0.0
**
*
***
**
UTR
FUS-WT
R522G
R522G+PDI WT
UTR
FUS-WT
R522G
R522G+PDI WT

Figure 3.7 Over-expression of PDI reduces ER-Golgi transport defects in mutant FUS expressing cells. A) Representative fluorescent images of co-expressing cells with enhanced green fluorescent protein (EGFP) tagged wild-type FUS and R522G and VSVGts045-mCherry with or without PDI stained with markers of ER (calnexin) or Golgi apparatus (GM130). VSVGts045-mCherry was trapped in the ER at 40°C then cycloheximide was added and the temperature was shifted to the permissive temperature (32°C) for 30 min then cells were fixed with 4% paraformaldehyde (PFA) at 30 min at 32°C. At 32°C VSVG is transported to Golgi and does not colocalise with calnexin in untransfected cells (UTR) (first panel) and in cells expressing wild-type FUS (second panel, FUS-WT). Inhibition of transportation was observed when R522G was transfected and VSVG was found to colocalise more with calnexin and less with GM130 (third panel). On overexpressing PDI with R522G transport was facilitated and VSVG colocalised more with GM130 and not with ER marker calnexin (fourth panel). Scale bar = 10 μm. **B)** Quantification of the degree of co-localization of VSVGts045-mCherry with calnexin or GM130 was quantified using Mander's coefficient in FUS expressing cells. A significant difference was observed (**) $p<.01$ when cells were co-expressed with R522G as compared to wild-type FUS and (*) $p<.05$ between R522G and when co-expressed with PDI as observed for co-localisation between VSVG and calnexin. Significant difference was observed (***) $p<.001$ when cells were expressed with wild-type FUS as compared to R522G and (**) $p<.01$ between R522G and when co-expressed with PDI when observed for co-localisation between VSVG and GM130. Data are presented as mean ± SEM, tested with one-way ANOVA and Tukey's post-test, n = 3.

3.2.6 Over-expression of PDI is protective against mutant SOD1 induced ER-Golgi transport defects in neuronal cell lines.

Our group previously demonstrated that mutant SOD1 inhibits ER-Golgi transport in NSC-34 and SHSY5Y cells [454, 552], leading to induction of ER stress, in NSC-34 cells, and that PDI is protective against mutant SOD1 misfolding and ER stress

in this cell line [483]. However it had not been previously established whether PDI is also protective against inhibition of ER-Golgi transport in cells expressing mutant SOD1. Initial experiments performed in Neuro2a due to the higher transfection efficiency possible compared to NSC-34 cells demonstrated that at 12.5 hours post-transfection, mutant $SOD1^{A4V}$ first inhibited ER-Golgi trafficking, and at approximately 16 hours post-transfection, inclusions were first formed in these cells (data not shown). Therefore, ER-Golgi transport defects were examined in mutant SOD1 expressing Neuro2a cells at 12.5 hours post transfection.

Neuro2a cells were co-transfected with mCherry-tagged VSVG, EGFP tagged wild-type SOD1 or mutant $SOD1^{A4V}$, and with either empty vector or V5-tagged PDI. The cells were incubated at 40°C for 12.5 hours to accumulate VSVG in the ER, before incubation at the permissive temperature for 30 min. After fixing the cells, immunocytochemistry was performed using antibodies for markers of the ER (calnexin) and Golgi (GM130) followed by fluorescent microscopy (Figure 3.8 A). Quantification of the localisation of VSVG in either the ER or Golgi was performed, using Mander's co-efficient, in the range from 0 to 1 representing 0-100% overlapping pixels as described previously [552].

In untransfected cells (UTR), little VSVG 1% was retained in the ER and most 68% was transported to the Golgi apparatus after 30 min at the permissive temperature. Similarly, in cells expressing EGFP on its own or wild-type SOD1, little VSVG was retained in the ER 2% because most was already transported to the Golgi 70% in EGFP and in wild-type SOD1 68% at this time point. However, in cells expressing mutant $SOD1^{A4V}$, inhibition of ER-Golgi transport was detected relative to the other cell populations. In these cells, significantly more VSVG was retained in the ER 37% ($p<.01$) and less was transported to the Golgi after 30 min 42%, ($p<.01$), (Figure 3.8 B), similar to previous observations [552].

Conversely, when PDI was co-expressed with mutant $SOD1^{A4V}$, transport between the ER-Golgi was restored only 13% ($p<.01$) VSVG was retained in the

ER and 69% ($p<.01$) VSVG was transported to Golgi Therefore, these data suggest that over-expression of PDI rescued the inhibition of ER-Golgi transport induced by mutant SOD1.

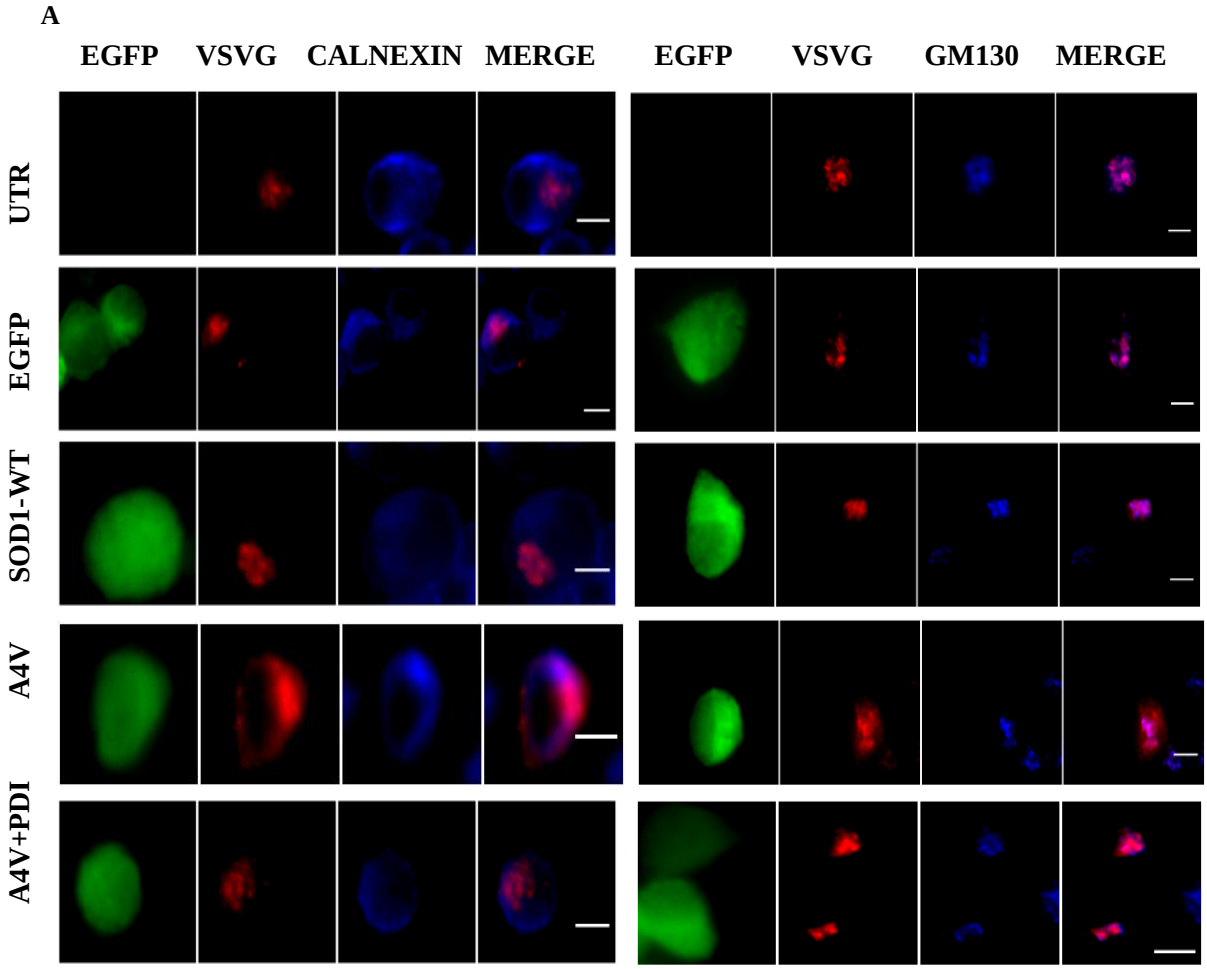
A
EGFP
VSVG
CALNEXIN
MERGE
EGFP
VSVG
GM130
MERGE
UTR
EGFP
SOD1-WT
A4V
A4V+PDI

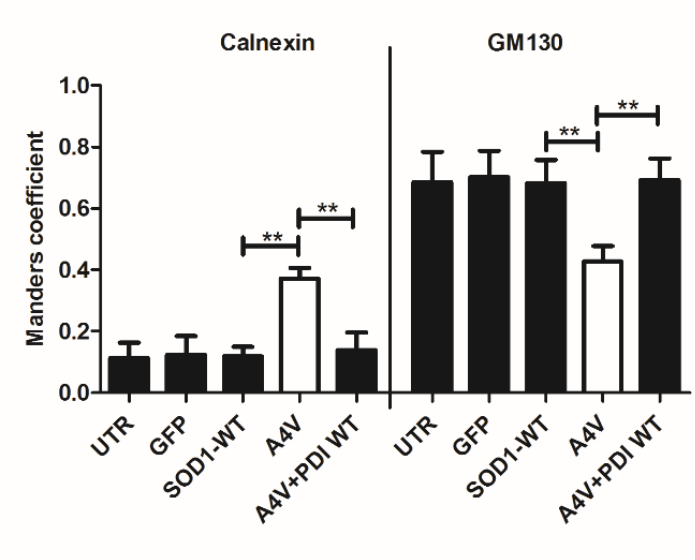
B
Calnexin
GM130
Manders coefficient
1.0
0.8
0.6
0.4
0.2
0.0
**
**
**
**
UTR
GFP
SOD1-WT
A4V
A4V+PDI WT
UTR
GFP
SOD1-WT
A4V
A4V+PDI WT

Figure 3.8 Over-expression of PDI reduces ER-Golgi transport defects in mutant SOD1 expressing cells. A) Representative fluorescent images of co-expressing cells with enhanced green fluorescent protein (EGFP) tagged wild-type SOD1 and $SOD1^{A4V}$ and VSVGts045-mCherry with or without PDI at 12.5 hr post-transfection stained with markers of ER (calnexin) or Golgi apparatus (GM130). VSVGts045-mCherry was trapped in the ER at 40°C for 12.5 hr then cycloheximide was added and the temperature was shifted to the permissive temperature (32°C) for 30 min then cells were fixed with 4% paraformaldehyde (PFA) at 30 min at 32°C. At 32°C VSVG is transported to Golgi and does not colocalise with calnexin in untransfected cells (UTR) (first panel) and in cells expressing EGFP alone (second panel) or wild-type SOD1 (SOD1-WT, third panel). Inhibition of transportation was observed when $SOD1^{A4V}$ was transfected and VSVG was found to colocalise more with calnexin and less with GM130 (fourth panel). On co-expressing PDI with $SOD1^{A4V}$ transport was facilitated and VSVG colocalised more with GM130 and not with ER marker calnexin (fifth panel). Scale bar = 10 μm. **B)** Quantification of the degree of co-localization of VSVGts045-mCherry with calnexin or GM130 was quantified using Mander's coefficient in SOD1 expressing cells. Data are presented as mean ± SEM, tested with one-way ANOVA and Tukey's post-test, n = 3. Significant difference was observed (**) p<.01 between cells expressing SOD1A4V as compared to wild-type SOD1 and when co-expressed with PDI when observed for co-localisation between VSVG and calnexin. Significant difference was observed (**) p<.01 when cells co-expressed $SOD1^{A4V}$ as compared to wild-type SOD1 with empty vector and when co-expressed with PDI when observed for co-localisation between VSVG and GM130.

Furthermore, the values obtained in this experiment "Neuro2a cells co-transfected with mCherry-tagged VSVG, EGFP tagged wild-type SOD1 or mutant $SOD1^{A4V}$" was also used for a manuscript to confirm that ER-Golgi transport is specifically inhibited by mutant SOD1. It was demonstrated that inhibition of ER-Golgi transport correlated with protein expression and fluorescence intensity. Individual cells expressing SOD1 were categorized according to their fluorescence intensity

which corresponded to protein expression. The arbitrary values of low, medium and high were calculated according to the pixel intensities quantified in each cells by using Image J, demonstrating the levels of expression of SOD1 protein. Using Mander's coefficient it was demonstrated that cells expressing highest expression of mutant $SOD1^{A4V}$ inhibited ER-Golgi transport the most.

The result is presented in the published manuscript: "Soo, K. Y., et al. (2015)."Rab1-dependent ER–Golgi transport dysfunction is a common pathogenic mechanism in SOD1, TDP-43 and FUS-associated ALS." Acta neuropathologica: 1-19" which is presented at the end of this chapter in (Supplementary Figure 4). The author performed all the experiments presented in figure 1e, described in the Results section of the manuscript on page 4 under the section of '*ER–Golgi transport is inhibited in cells expressing proteins associated with ALS'.*

3.2.7 Over-expression of PDI protects against mutant TDP-43 and mutant FUS mislocalisation in the cytoplasm in neuronal cell lines.

A common cellular event linked to both TDP-43 and FUS is the accumulation of each protein in the cytoplasm, rather than the nucleus, as observed in ALS patient motor neurons and ALS models during disease state [483]. However, the mechanism is poorly characterised. It was next investigated whether over-expression of PDI could protect against mutant TDP-43 and mutant FUS cytoplasmic mislocalisation in neuronal cells.

The effect of PDI on the cytoplasmic mislocalisation of mutant TDP-43 was examined using Neuro2a cells. (Figure 3.9 A). Since in our previous study [486], more mutant TDP-43 was present in the cytoplasm and ER stress was detected at 18-24 hr post-transfection, this time point was also used here [486]. Immunocytochemistry was performed using anti-V5 antibody to detect PDI expression. Transfected cells were observed 18 hr post transfection using fluorescence microscopy. Cells were considered nuclear when they completely

colocalised with the nuclear stain DAPI. However, cells displaying both nuclear and cytoplasmic localisation with fluorescence detected in both the cytoplasm and the nucleus were considered as cytoplasmic in TDP-43 expressing cells.

Expression of wild-type TDP-43 resulted in cytoplasmic TDP-43 distribution in 26% of cells, in accordance with the literature [150, 561]. Co-expression of PDI with wild-type TDP-43 did not alter the proportion of cells with cytoplasmic TDP-43 However, in cells expressing mutant TDP-43, significantly more cells displayed cytoplasmic localisation of TDP-43 (40% in A315T and 31% in Q331K) expressing cells compared to cells expressing wild-type TDP-43. Moreover, over-expression of PDI resulted in significantly fewer cells with cytoplasmic TDP-43 distribution; 28% in cells ($p < .05$) expressing A315T and 20% in cells expressing Q331K ($p < .05$, Figure 3.9 B). Therefore, this data reveals that over-expression of PDI is protective against the cytoplasmic mislocalisation of mutant TDP-43 in neuronal cells.

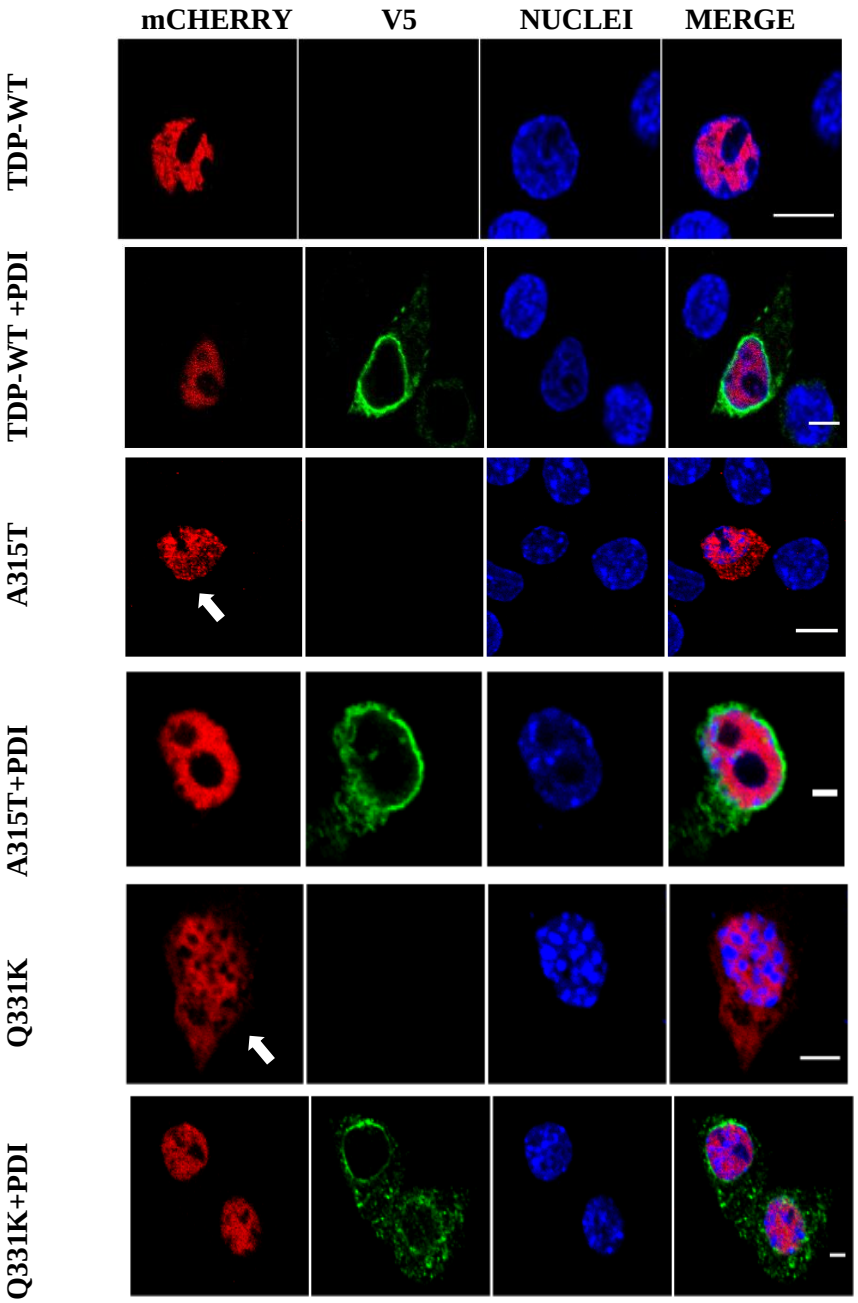
mCHERRY
V5
NUCLEI
MERGE
TDP-WT
TDP-WT +PDI
A315T
A315T+PDI
Q331K
Q331K+PDI

B

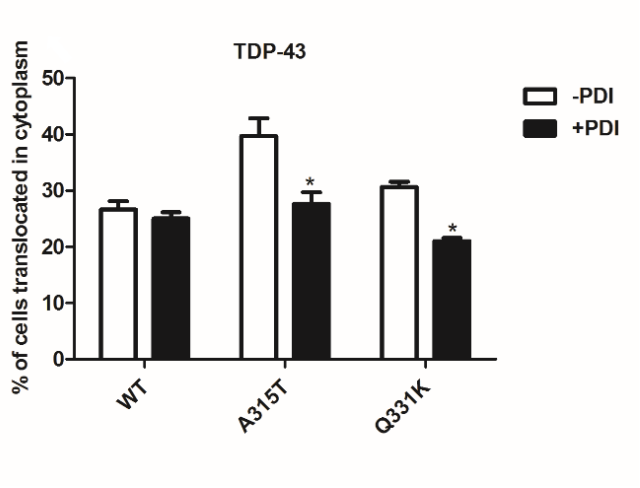

Figure 3.9 Over-expression of PDI decreases cytoplasmic distribution of mutant TDP-43 in the cytoplasm. A) Immunofluorescence images of Neuro2a cells co-expressing mutant TDP-43 with PDI. Neuro2a cells expressing wild-type TDP-43 (first panel. TDP-WT) displayed mainly nuclear TDP-43 localisation whereas more mutant TDP-43 A315T or Q331K (second, fourth panel) expressing cells were localised in the cytoplasm as indicated with white arrow. On co-expressing PDI with A315T or Q331K, fewer cells displayed cytoplasmic TDP-43 distribution (third and fifth panel). Scale bar = 10 µm. **B)** Quantification of cells in (A), displaying cytoplasmic distribution of mutant TDP-43. A significant difference in the proportion of cells displaying cytoplasmic TDP-43 was observed when A315T or Q331K cells were co-expressed with PDI (*). For each of 3 replicate experiments, 100 cells were scored for each population. Data are presented as mean ± SEM, tested with two-way ANOVA and Bonferroni's post-test, n = 3. Where *p<.05.

To examine the effect of PDI on mislocalisation induced by mutant FUS two frequently identified FUS ALS-associated mutations R521H and R521C were expressed in a cellular model of disease [153, 372, 565]. Neuro2a cells were transiently co-transfected with vectors encoding V5-tagged PDI and wild-type or mutant FUS constructs tagged with EGFP. Seventy two hr post transfection individual cells were examined by fluorescent microscopy and scored according to the cellular localization of fluorescence: nuclear (colocalising with DAPI) or cytoplasmic (completely excluded from the nucleus) (Figure 3.10 A) Cells with both nuclear and cytoplasmic distribution of FUS, were counted as nuclear [487]. Immunocytochemistry was performed using anti-Halo antibodies to detect FUS expression, and anti-V5 antibody to detect PDI expression.

As expected, in cells expressing wild-type FUS, the fluorescence was localized mainly in the nucleus and observed in the cytoplasm in only 15% of these cells. Co-expression of PDI with wild-type FUS did not alter the proportion of cells with cytoplasmic FUS. In contrast, in cells expressing mutant FUS R521C 64% or R521H 72% of cells respectively displayed cytoplasmic distribution of FUS. However, when PDI was co-expressed with mutant FUS, the proportion of cells with cytoplasmic FUS was significantly reduced, to 44% for each mutant ($p<.001$) (Figure 3.10 B). Hence these data imply that over-expression of PDI is protective against the cytoplasmic distribution of mutant FUS in neuronal cell lines.

A

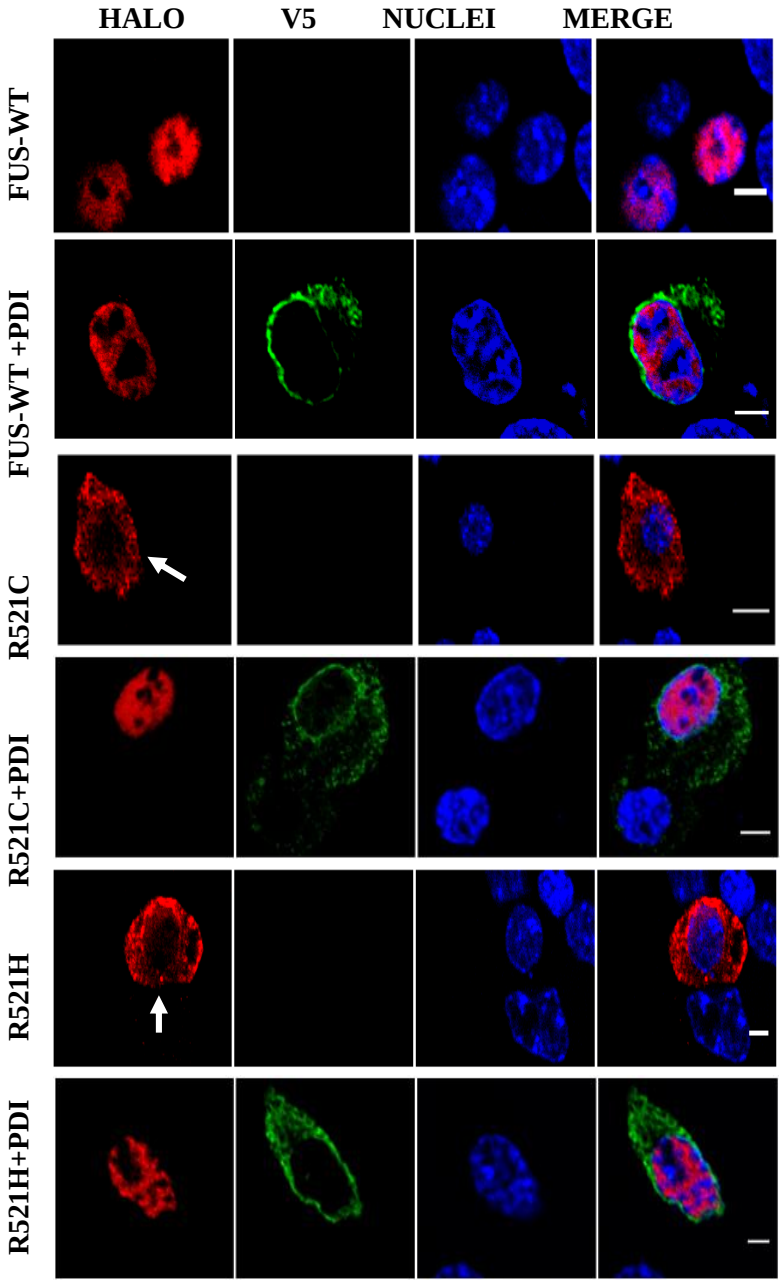
HALO
V5
NUCLEI
MERGE
FUS-WT
FUS-WT +PDI
R521C
R521C+PDI
R521H
R521H+PDI

B

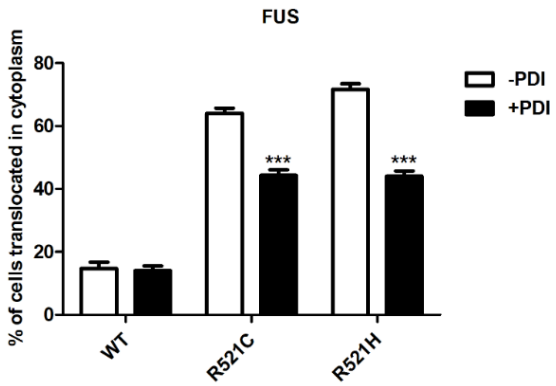
FUS
% of cells translocated in cytoplasm
80
60
40
20
0
-PDI
+PDI
***
***
WT
R521C
R521H

Figure 3.10 Over-expression of PDI decreases cytoplasmic distribution of mutant FUS in the cytoplasm. A) Immunofluorescence images of Neuro2a cells co-expressing mutant FUS with PDI. Neuro2a cells expressing wild-type FUS (first panel) or mutant FUS R521C, R521H (second, fourth panel) in the cytoplasm, as indicated with a white arrow. On co-expressing PDI fewer cells expressed mutant FUS in the cytoplasm (third and fifth panel). Scale bar = 10 μm. B) Quantification of cells in (A) co-expressing mutant FUS with PDI and displaying cytoplasmic localisation of FUS. A significant difference (***) in the proportion of cells expressing cytoplasmic FUS was observed when R521C or R521H cells were co-expressed with PDI. For each of 3 replicate experiments, 100 cells were scored for each population. Data are presented as mean ± SEM, tested with two-way ANOVA and Bonferroni's post test, n = 3. Where ***p<.001.

3.3 Discussion

Several proteins are genetically and pathologically linked to ALS, notably SOD1, TDP-43 and FUS, which together account for 30% of fALS cases [566]. Importantly, TDP-43 pathology is recognized as the signature pathological lesion of all sALS and some forms of fALS, because it is present in almost all cases of ALS (except SOD1-positive cases and FUS only positive cases) [567]. Despite the diverse functions of these proteins, ALS has a remarkably similar disease course and pathology. Significantly, ER stress is now recognised as a central mechanism leading to cell death in ALS, and it is induced by mutant forms of these proteins in neuronal cell cultures. This Chapter firstly demonstrates that mutant TDP-43 induces ER stress in neuronal cultures, as detected through activation of ER markers CHOP, XBP-1 and ATF6 [486]. Secondly, this Chapter demonstrates a protective role for PDI, which is upregulated during ER stress, *in vitro*. In Neuro2a cells expressing mutant TDP-43 or mutant FUS, over-expression of PDI was protective against ER stress, inhibition of ER-Golgi transport and mislocalisation of TDP-43 and FUS into the cytoplasm. These data are consistent with our previous studies that PDI is protective against mutant SOD1-induced apoptosis and ER stress [483]. Similarly, it was also demonstrated here that PDI restored ER-Golgi transport inhibition by mutant SOD1 in Neuro2a cells. In the previous study [483], we demonstrated that PDI is S-nitrosylated in ALS, suggesting that although PDI is up-regulated, it may not exert a protective effect during disease due to loss of its normal function. In this study, it was shown that over-expressing PDI is protective, hence it is possible that this protective activity may compensate for the loss of endogenous PDI, and thus overcome the cellular defects induced by mutant proteins. Whilst this chapter establishes that PDI, as a chaperone primarily located within the ER, is protective against mutant SOD1, TDP-43 and FUS, the mechanism involved remains undefined. Possible molecular mechanisms of protection by PDI in ALS were investigated further in the studies presented in Chapter 4.

Two UPR markers, XBP-1 and CHOP, were used to investigate ER stress in mutant TDP-43 expressing cell lines in this Chapter, representing markers of the early and late phases of UPR. Hence these data demonstrate the protective role of

PDI during early and later UPR induction in neuronal cell lines against mutant TDP-43 induced ER stress. Several different TDP-43 mutations involved in sporadic and familial cases of ALS were demonstrated to induce ER stress. PDI could inhibit ER stress in mutant TDP-43 expressing cells by either decreasing the load of misfolded proteins within the ER directly, or by indirect mechanisms, such as increasing the rate of ERAD, by retrotranslocation for degradation in the cytoplasm. Evidence have demonstrated that PDI facilitates ERAD activity in yeast models [568]. However, it was also demonstrated here that PDI restores ER-Golgi transport in cells expressing mutant TPD-43. Our data implicates inhibition of ER-Golgi transport as an important upstream trigger of ER stress [552]. Alternatively, as an oxidoreductase PDI could reduce aggregation of abnormally disulphide bonded, misfolded TDP-43 itself, since non-native disulphide bonds are implicated in the aggregation of mutant TDP-43 [569]. Our group recently demonstrated that mutant TDP-43 is present on the cytoplasmic face of the ER [557]. Therefore, PDI could physically interact with mutant TDP-43 in this location, and inhibit its aggregation, thus reducing adverse pathogenic mechanisms. This is in accordance with our previous study which demonstrated that PDI co-localises with TDP-43 inclusions and co-immunoprecipitates with mutant TDP-43 to a greater extent than wild-type TDP-43 [486].

Our group also demonstrated that ER stress induces TDP-43 localisation in the cytoplasm [486]. Therefore, it is possible that PDI reduces ER stress and hence prevents the associated cytoplasmic distribution of TDP-43 in cells. However, the exact mechanism involved in mislocalisation induced by TDP-43 is still under investigation. ALS mutations in the NLS region of TDP-43 result in cellular distribution to the cytoplasm, but cellular stressors including oxidative stress, and heat shock as well as ER stress, could also result in cytoplasmic re-distribution [150, 155, 570]. Alternatively, PDI may be protective by preventing misfolding of mutant TDP-43 in the cytoplasm, and this may be a primary driver of the protective effect rather than at mutant TDP-43 at the ER. Increased cytoplasmic mislocalisation of TDP-43 is toxic in primary rat cortical neurons [155] suggesting the importance of PDI protection against cytoplasmic distribution of TDP-43. It should be noted that

in the conditions used in these experiments, mutant TDP-43 inclusions were not formed in the cell lines used and is a limitation of using cell culture techniques. Additional strategies could be used to promote the formation of TDP-43 inclusions, such as using proteasome inhibitors. However, further investigations into the effect of PDI against mutant TDP-43 in primary cultures and animal model are therefore increasingly warranted.

Our laboratory previously showed that PDI immunoprecipitates with mutant FUS, co-localises with markers of the ER, and is present within the ER lumen [487, 557]. Hence, the findings obtained here that PDI is protective against ER stress in cells expressing mutant FUS is consistent with these data. The exact mechanism involved in mislocalisation induced by mutant FUS is unclear. However, cytoplasmic distribution of mutant FUS induces ER stress *in vitro,* and the induction of UPR correlates with the cytoplasmic localisation of mutant FUS [487]. Some studies propose that mutations in the C-terminal domain of FUS, containing the NLS, as the major cause of cytoplasmic mislocalisation [186, 187]. However, N-terminal mutations in FUS also induce cytoplasmic mislocalisation, suggesting that this is not the only factor to consider [571]. It is also possible that misfolded FUS could interfere with the normal shuttling of FUS from the nucleus to the cytoplasm, and hence this could mediate toxicity, as observed in yeast models [330]. Therefore, PDI may prevent FUS mislocalisation in the cytoplasm by reducing the load of misfolded proteins.

Mutant TDP-43 and FUS induce ER-Golgi transport defects in neuronal cell lines [557] and experiments performed in this Chapter demonstrate that PDI restores this transport. Although TDP-43 and FUS predominately localise in the nucleus our laboratory reported the presence of these proteins associated with the ER [487, 557]. Similarly, mutant TDP-43 inclusions disrupt ER-Golgi apparatus in neuronal cultures, providing further evidence for disruption of the ER-Golgi compartments [486]. Furthermore mutant FUS induces fragmentation of the Golgi apparatus in neuronal cell cultures [572].

Misfolded and incompletely folded proteins are excluded from export vesicles and do not leave ER exit sites during the first phases of ER-Golgi transport [573-575]. Inhibition of ER-Golgi traffic could increase the load of secretory proteins with the ER, inducing ER stress by this mechanism, even if this is initially triggered from the cytoplasm. PDI could therefore be protective by generally reducing the load of misfolded proteins within the ER, thus facilitating transport. In the case of mutant SOD1 and mutant TDP-43, ER-Golgi transport defects were shown to precede ER stress [552, 557] whereas ER-Golgi transport and ER stress were inhibited simultaneously in cells expressing mutant FUS [557]. This may reflect the direct ER-localisation of FUS and the cytoplasmic localisation of SOD1 and TDP-43 (although the latter was attached to the ER membrane). As mutant SOD1 and mutant TDP-43 induce ER stress from the cytoplasm, the question arises as to how PDI, a primarily ER resident protein, is recruited to interact with cytoplasmic proteins. However, PDI has been shown to be redistributed away from the ER as punctate vesicles by reticulon proteins (Rtn-1C), and in this location PDI was observed to have higher enzymatic activity [576]. This suggests that PDI in the cytoplasm could be mediating the protective effects outlined in this Chapter. Investigations into the subcellular locations where PDI is protective, and the resulting consequences, are presented in Chapter 6. In addition, knockdown of reticulon Rtn-4A and Rtn-4B has also been shown to induce axonal degeneration and early death of transgenic $SOD1^{G93A}$ mice [531]. These results suggest that redistribution of PDI modulates disease progression *in vivo*, although future demonstration of a beneficial effect by over-expression of reticulon proteins is necessary to confirm this possibility [577].

Given the innate limitations of investigations into a complex disease in cell culture, which is particularly affected by non-physiological, high levels of oxygen, it will be important in future studies to further investigate the protective role of PDI in ALS using *in vivo* models. Conditional knockout or transgenic PDI expression animal models could be employed to further investigate the role of PDI in ALS, and would allow examination of disease progression and onset, which is not possible using cell culture models only. It would be interesting in future studies to study the

effect of PDI on other ALS associated proteins, particularly those where a pathological association with the ER-Golgi compartments has been previously described. PDI interacts with VAPB inclusions in a *Drosophila melanogaster* model of ALS [229], and VAPB mutations cause ER stress [578]. The normal cellular functions of optineurin [63], alsin, VAPB [65] and VCP are associated with ER-Golgi trafficking, and ALS mutations in optineurin [216], VCP [203] and C9ORF72 [427] also induce ER stress. In particular, the effect of PDI on the C9ORF72 repeat expansion would be an interesting area of research, given that it causes the majority of fALS cases. Various other factors related to proteostasis should also be examined, such as the cells capacity to produce sufficient amounts of PDI. The association of PDI with other ER chaperones, to decrease the pathogenic processes should also be examined during disease progression.

In summary, in this study it was demonstrated that PDI is protective against mutant TDP-43, mutant FUS and mutant SOD1 induced ER stress, ER-Golgi transport defects and cytoplasmic localisation, in neuronal cells. These are important pathogenic mechanisms that are associated with cellular viability and apoptosis in ALS. Therefore, these studies suggest that PDI may have potential as a therapeutic target in ALS. Hence, understanding the underlying mechanism by which PDI is protective in ALS may help in designing more effective therapeutic targets, and studies investigating these processes are presented in Chapter 4.

Chapter 4 Mechanism of action of PDI against mutant SOD1, TDP-43 and FUS in neuronal cells

4.1 Introduction

Protein folding is a complex process and around one third of all proteins traverse the secretory pathway in humans [579]. Therefore, the ER is equipped with numerous ER-resident chaperones which mediate protein quality control mechanisms. The ER lumen provides an ideal environment for the oxidative folding of proteins. Furthermore, it possesses proficient oxidative pathways and contains chaperones, such as members of the PDI family, that generate disulphide bonds and thus assist in native oxidative folding of proteins [580]. Disulphide bond formation, meaning the covalent linkage between two cysteine residues in proteins, primarily occurs in the periplasmic space of the ER [581]. When a protein localized in the cytoplasm is correctly folded, the number of hydrophobic residues exposed on the surface of the protein is minimized. Conversely, membrane and secretory proteins are primarily folded in the ER, where oxidative folding occurs in addition to post-translational modifications such as N-glycosylation and disulphide bond formation [582].

Chronic ER stress, due to the accumulation of misfolded proteins in the ER, is now recognized to be an important pathology in protein misfolding disorders, including ALS [583]. Mutant proteins linked to fALS also have been shown to induce defects in ERAD machinery, ER-Golgi trafficking, the ER folding network, cellular redox conditions and protein degradation pathways [584]. Hence, ER stress could be a result or consequence of these cellular condition, subsequently leading to neuronal vulnerability and apoptosis [459, 476, 584].

The sections 4.1.2, 4.1.3 and 4.1.4 have been published in the manuscript “Novel Roles for Protein Disulphide Isomerase in Disease states: a Double Edged Sword?” which is also presented at the end of the chapter as (Supplementary Figure 1).

4.1.1 Structure of PDI

PDI is the prototype of the thioredoxin superfamily of proteins, and it consists of four domains, namely *a, b, b', a*' (Figure 4.1). The catalytically active *a* and *a'* domains share 47% similarity and contain the conserved active site motif, CGHC [585]. Only the active site cysteine residues interact with the thiol group of a newly synthesized protein substrate, hence these cysteines specifically mediate the formation and isomerisation of protein disulphide bonds [538]. The intermediate *b* and *b'* domains are 28% identical and they assist in the binding of protein substrates, but they lack the catalytically active cysteine residues [586]. PDI also contains a 'x' linker region and an acidic C terminus, containing a KDEL-ER retrieval sequence[509]. Whilst the three dimensional structure of human PDI is still under investigation, the structures of each single thioredoxin domain [587], and the domain combinations *bb'c* [509] and *bb'c*x*ac* [588], have been determined. However, the structure of yeast PDI has been solved [506], revealing that it adopts a 'U' shape structure, with the catalytic *a* and *a'* domains facing each other. NMR and x-ray crystallography studies have further demonstrated that the *b'* domain contains the chaperone activity responsible for binding ligands and protein substrates in its hydrophobic pocket [509]. The CGHC motif modulates the overall reduction potential of PDI and thus it regulates the catalytic ability of the active site cysteines to actively oxidize or reduce disulphide bonds [589]. The reduction potential of PDI is −180 mV, higher than other PDI family members, thus making it a strong oxidizing agent. The individual *a* and *a'* domains have similar oxidizing ability but conversely they have low isomerase activity. The *b'* domain is the main site for binding misfolded protein substrates but the other domains also assist in this process [508]. The catalytic domains can only catalyze basic disulphide exchange and all the domains are required to isomerize a protein substrate that has undergone conformational changes.

The crystal structure of the *bb'*x*a'* region of PDI suggested that PDI is a redox dependent chaperone [588]. Oxidation of PDI results in an open conformation, rendering the substrate-binding surface more exposed. This open conformation induces higher chaperone activity and prevents substrate aggregation during

refolding [588]. Binding of PDI to the unfolded proteins and assisting in the formation of disulphide bonds in turn reduces PDI. This results in a closed conformation which assists in the release of the folded substrates. Reduced PDI assists in the isomerisation of non-native disulphides in substrate proteins, and afterwards releases the folded substrates [590].

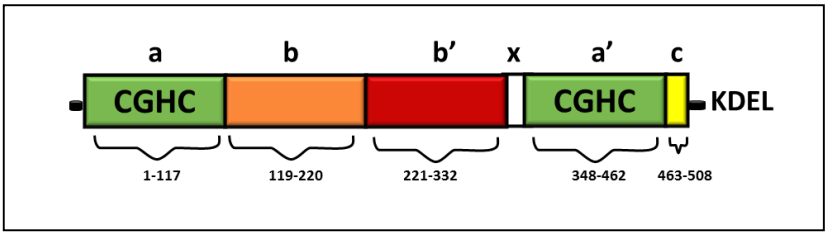

Figure 4.1 Schematic diagram representing the thioredoxin domains of PDI. The thioredoxin-like, catalytically active *a* and *a'* domains, containing the active site CGHC are shown in green, and the catalytically inactive and substrate binding *b* and *b '* domains are shown in orange and red respectively. White represents the linker region 'x' and the C-terminus is shown in yellow, which ends with the ER retrieval signal KDEL.

4.1.2 PDI is a chaperone present in the ER

PDI has the ability to distinguish between partially folded, unfolded and properly folded protein substrates, and it has a higher affinity to bind to misfolded proteins rather than native proteins through hydrophobic interactions [591]. These properties, together with its conformational flexibility, make PDI a highly effective chaperone [592]. PDI binds to a large number of protein substrates in the ER, although it is difficult to isolate and identify the individual substrates *in vivo.* Several methods are used to measure the chaperone activity of PDI *in vitro*. The rate of protein aggregation is assessed using protein substrates that do not possess cysteine residues, including GAPDH [540], rhodanese [593], citrate synthase, alcohol dehydrogenase [594], or EGFP, which on interaction with PDI causes increased fluorescent intensity due folding into its native conformation [595]. A major function of PDI is a chaperone upregulated during ER stress. Accumulation

of misfolded proteins within the ER activates the unfolded protein response (UPR). The UPR aims to reduce the load of unfolded proteins by increasing the curvature of ER, reducing protein synthesis and inducing PDI and other chaperones to further increase protein folding capacity [458]. This is achieved by activation of sensor ER proteins IRE-1, PERK, and ATF6, which subsequently activate UPR signaling pathways (detailed in [596]). While initially protective, prolonged UPR causes apoptosis [597]. PDI facilitates the degradation of misfolded proteins *via* ERAD, by translocation of these proteins from the ER to the cytoplasm, for subsequent degradation by the ubiquitin protease system. [598, 599]. It also assists in protein quality control by retaining unassembled procollagen until the correct native structure is achieved [600]. Other specific functions involving the chaperone activity of PDI have been described, including maintenance of the active conformation of the β subunit of collagen prolyl 4-hydroxylases [601], and stabilisation of the peptide loading complex (PLC) of the major histocompatibility complex (MHC), class 1 that mediates MHC class 1 folding. Interestingly, PDI exhibits both chaperone and anti-chaperone activity depending upon its initial concentration. When PDI's chaperone activity is dominant, virtually all of the substrate protein is correctly folded. However, at low concentrations, PD1 promotes intermolecular disulphide crosslinking of substrates into large inactive aggregates via anti-chaperone activity [602].

4.1.3 Disulphide interchange activity of PDI

Multiple studies have suggested that the disulphide interchange enzymatic activity of PDI is more important for its function than its chaperone activity. The two catalytically active thioredoxin domains, containing the CGHC sequences, and the C-terminal region of PDI, are responsible for its isomerase activity [603, 604]. When its catalytic cysteines are reduced, PDI is able to react with non-native disulphides of substrate proteins to form a mixed disulphide complex. PDI then catalyzes the rearrangement of incorrectly formed disulphide bonds *via* isomerisation reactions. This takes place with cycles of reduction (breaking of non-native disulphide bonds) and oxidation (to introduce correct pairing of cysteines) to eventually form the native disulphide bonds [605]. The tripeptide glutathione

constitutes the cellular redox buffer that maintains the redox environment of the ER [606]. After PDI has oxidized substrate proteins, it then has to be oxidized itself to complete the catalytic cycle. This function is carried out by a number of proteins, including FAD binding oxidases - Ero1α, oxidized glutathione, glutathione peroxidase 7, glutathione peroxidase 8 or quiescin sulfhydryl oxidase [607]. Interestingly, the chaperone activity of PDI is regulated by the redox state of its oxidized and reduced forms [608], thus suggesting a link between the two separate functions of PDI. Redox regulation of PDI can be examined experimentally *in vitro* using scrambled (inactive) RNAse, ribonuclease and bovine pancreatic trypsin inhibitor [609, 610]. Furthermore, prevention of mutant SOD1 aggregation by PDI could be modulated by disulphide bonding, since aggregation of mutant SOD1 is at least partially dependent upon disulphide bonds, with disulphide reduced monomers and high-molecular weight oligomers found in both cell and animal models of ALS [329, 611, 612].

4.1.4 Native and non-native disulphide bonds in SOD1

SOD1 is a 32 kDa cytoplasmic metalloenzyme [613]. The homo-dimer consists of two identical polypeptide chains which are non-covalently linked to each other [614]. Metal ions copper and zinc are present on each subunit and are critical for the stability and catalytic activity of the enzyme [615]. SOD1 consists of four cysteine residues at amino acid positions C6, C57, C111 and C146. The cysteine residues at positions C57 and C146 form an intrasubunit disulphide bond, which is important for correct native folding of the dimer [614]. This disulphide bond plays a vital role in stabilizing the structure of SOD1 and dissociation of the C57-C146 disulphide bond results in dimer destabilization [616]. The loop containing the C57 residue assists in the formation of the non-covalently bonded dimer interface.

Several studies have shown that in ALS transgenic models cellular stressors induce abnormal disulphide bonding between the C6 and C111 residues that do not normally form disulphide bonds [329, 617]. This leads to the formation of high molecular weight oligomers, containing non-native disulphide bonded aggregates. Small amounts of disulphide reduced monomeric species can induce aggregation of

other stable forms of SOD1 [618] and disulphide-reduced mutant SOD1 proteins show decreased metal binding and augmented misfolding [619]. Additionally, C111 is a target for oxidation, even in wild-type SOD1 [620]. Mutant SOD1 aggregates containing abnormal, non-native disulphide bonds have been detected in ALS linked mutant SOD1 animal and cellular models [621] and an increased proportion of disulphide-reduced SOD1 is observed in spinal cords of transgenic mutant SOD1 mice [618]. Conversely, some studies have also demonstrated that aberrant intermolecular disulphide bonding does not promote aggregation of mutant SOD1[622, 623].

Mutant SOD1 aggregation is linked with neuronal toxicity and correlates, with disease progression, suggesting that aggregation is associated with pathogenesis [114, 624]. Isomerisation of non-native disulphide bonds in mutant SOD1 reduces aggregation in neuronal cell cultures [625]. This suggests that reduction of aberrant non-native SOD1 disulphide bonds, or isomerisation of these intersubunit disulphide bonds, would be protective against mutant SOD1 aggregation and hence toxicity. Therefore, disulphide bond formation in SOD1 would lead to interaction of PDI with SOD1 (Figure 4.2). Hence it could also be predicted that by preventing the formation of non-native disulphide bonds in mutant SOD1, PDI could be protective in ALS.

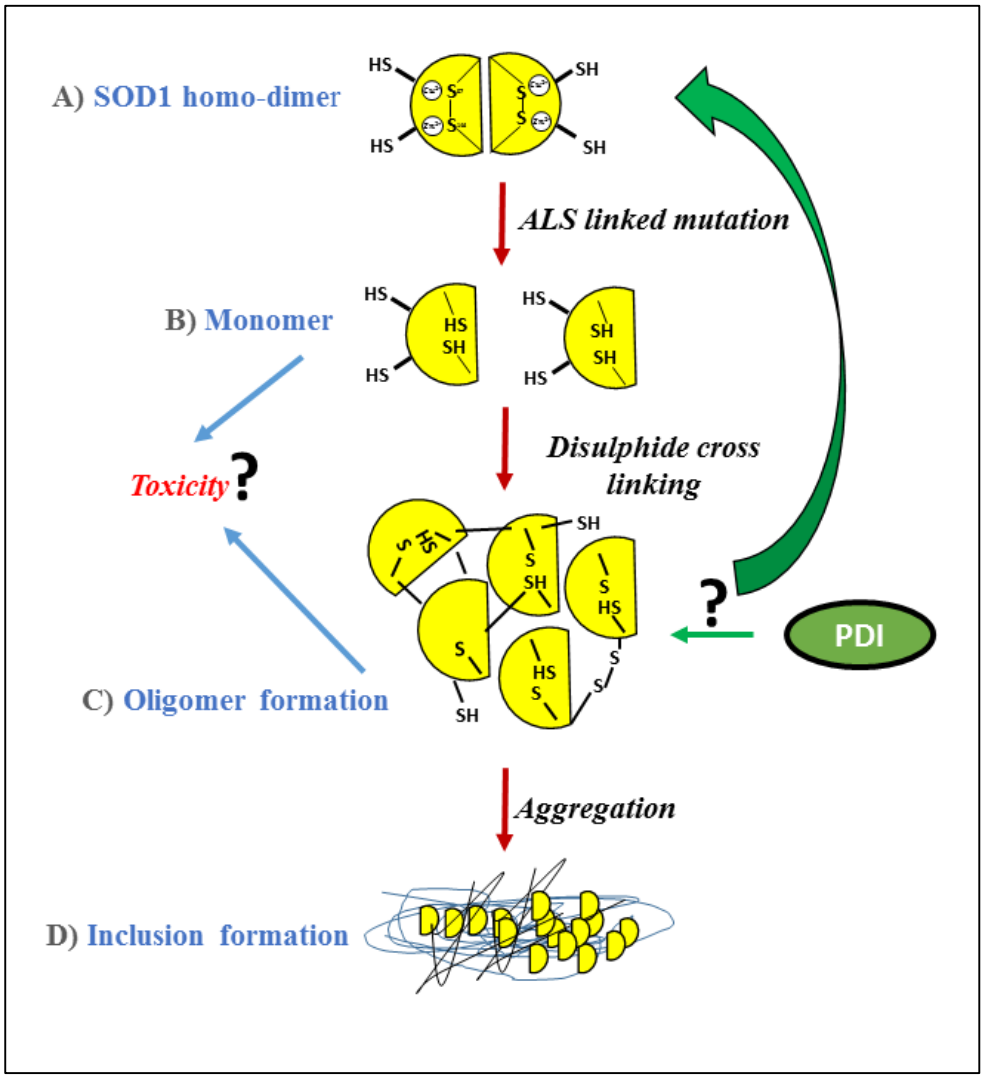

Figure 4.2 Schematic diagram representing the relationship between disulphide bond formation and aggregation of SOD1 and possible mode of action of PDI. A) Wild-type SOD1 is a homo-dimer stabilised by the presence of metal ions and an intramolecular disulphide bond between C57-C146, with two independent, cysteines at C6 and C111 per monomer. **B)** During SOD1-linked fALS, SOD1 mutations disrupt the normally stable dimer, leading to monomer formation and metal loss. **C)** Abnormal disulphide cross-linking, involving all four cysteine residues, leads to the formation of oligomers. Monomers and soluble oligomers are implicated as mediators of toxicity. PDI disulphide interchange activity could possibly reduce the non-native disulphide bonds, thus inhibiting the formation of the potentially toxic species. **D)** If the formation of aberrantly

disulphide-bonded mutant SOD1 oligomers is not prevented, insoluble intracellular mutant SOD1 inclusions result. The diagram is not to scale.

4.1.5 Disulphide bond formation in TDP-43

The presence of disulphide bonds in TDP-43 and FUS have not yet been investigated in detail. However, a study by Virginia Lee's group demonstrated that conserved redox regulated cysteine residues are present near the RNA recognition motif (RRM1) in TDP-43 [569]. Further characterization demonstrated the presence of an intra-molecular disulphide bond between residues C173 and C175 [569], and additional conserved cysteine residues (C198 and C244) in the RRM2 domain, identified using mass spectrometry, were also implicated in disulphide bond formation. This study also suggested that oxidation of conserved cysteine residues altered the conformation of TDP-43 and impaired its nuclear function, thus implying that these residues are important in TDP-43 structure and function. Moreover, TDP-43 aggregates with abnormal disulphide bonds were identified in brains of FTLD patients, suggesting that abnormal disulphide bond formation in TDP-43 is relevant to disease pathology [569]. A subsequent study further validated the presence of TDP-43 disulphide bonds, and also confirmed that oxidation of C173 and C175 in the RRM1 domain, and not N- terminal C39 and C50, formed oligomeric disulphide species in solution [626].

There is currently no evidence that FUS forms either native or non-native disulphide bonds. However, analysis of the primary sequence of FUS has revealed that the C-terminal zinc figure-like domain contains four cysteine residues [627]. Furthermore, NMR analysis of the zinc finger-like domain suggested that the zinc ion is coordinated *via* these four conserved cysteines [628]. However, further investigations into the possible existence of disulphide bonds in FUS, involving these four cysteine residues, is warranted.

4.1.6 Novel therapeutic approaches for ALS

Our laboratory previously demonstrated that a small molecule mimic of PDI disulphide interchange activity, -(±)-trans-1,2-Bis (2-mercaptoacetamido) cyclohexane (BMC), was protective against mutant SOD1 aggregation in neuronal cell lines [483]. BMC is a 262 Da synthetic dithiol which contains two hydrogen-sulphide bonds, which mimic the disulphide interchange activity [629]. BMC has been shown to assist in the formation and rearrangement of disulphide bonds *in vitro* and accelerate protein folding during the production of recombinant proteins [630]. In addition, BMC has the same reduction potential and acid dissociation constant as PDI, which determines the rate of disulphide bond formation [629]. However, BMC is not substrate specific because it cannot bind to a protein substrate [503]. Nevertheless the ability of BMC to mimic the disulphide interchange activity of PDI suggests that it may have potential as a novel therapeutic agent in ALS.

Another approach to reduce the cellular burden of abnormal mutant SOD1 disulphide bonds, which are implicated in toxicity in ALS, is to inhibit the expression of mutant SOD1. Down-regulation of SOD1 could be achieved through action of specific antisense peptide nucleic acids (PNA) sequences directed towards the mRNA of SOD1. PNA's are single stranded synthetic oligonucleotides designed to specifically bind to complementary mRNA targets through hydrogen bonding [631]. PNAs are currently being developed as probes for the detection and diagnosis of numerous diseases [632-634]. These DNA mimics have high affinity towards target sequences and low toxicity in cell models. However, due to their large size, they do not readily cross cell membranes and they have limited activity when delivered in animal models [635, 636]. Nevertheless, conjugation of vitamins to PNA's can subsequently improve the efficiency of delivery to cells and this strategy has been utilised for drug delivery [637]. PNA sequences have been previously shown to inhibit the expression of death signalling neurotrophic receptor ($p75^{NTR}$) which delays disease progression in $SOD1^{G93A}$ mice [638], suggesting that antisense therapies which are based on gene targeting of ALS mutant proteins using PNAs could be a useful therapeutic target in ALS.

4.1.7 Aims of the Chapter

PDI is a unique protein, which has two independent properties, a chaperone and as an isomerase. In Chapter 3 it was demonstrated that over-expression of PDI is protective in cells expressing mutant SOD1, TDP-43 and FUS. However, the exact mechanism of action against each misfolded protein remains unknown, whether this protection involves the chaperone or disulphide interchange activity of PDI. The aim of this chapter was to investigate these mechanisms and determine which activities of PDI are protective in each case, with the aim of facilitating futures studies to design possible therapeutics targets based on PDI. To perform these studies, PDI mutants were created in which the two active site cysteine's, which mediate the isomerisation activity of PDI, were removed. Hence, these mutants should only retain the chaperone activity. Furthermore, BMC, which mimics the disulphide interchange activity of PDI, was also examined in cells expressing ALS-mutants of SOD1, TDP-43 or FUS.

4.2 Results

4.2.1 Expression of PDI mutants in neuronal cell lines.

Wild-type PDI consists of two catalytically active domains, namely *a* and *a'*, with conserved active site motif CGHC, which is responsible for the disulphide interchange activity. To identify which activity of PDI is more important for its protective function, cysteine deficient mutants of PDI were examined. Previously generated pcDNA3.1 (+) constructs encoding wild-type PDI (PDI WT) with two native active sites (*CGHC, CGHC*) tagged with V5, a PDI mutant in which the second cysteine of the *a* domain was mutated to serine (C2) (*CGHS, CGHC*) and a PDI mutant in which the second cysteine of both the *a* and *a'* domains were mutated to serine (C26) (*CGHS, CGHS*), were provided by Professor. Neil Bulleid, Glasgow, UK [535] (Figure 4.3 A). Additional PDI mutants were previously generated by a Masters student in the laboratory, specifically; PDI QUAD, where all the four active site cysteine residues were mutated to serine (*SGHS SGHS*), PDI mutant (A) where both the vicinal cysteine residues were mutated to serine in the a domain (*SGHS CGHC*), and PDI mutant (A') in which both the cysteine residues were mutated to serine in the *a'* domain (*CGHC SGHS*).

PDI disulphide and isomerase activity are well characterised *in vitro* and various studies have demonstrated that mutating the active site cysteine residues does indeed inhibit the disulphide interchange activity of PDI. However, resulting mutants retain the chaperone activity of PDI [602, 609, 639-643]. However, PDI activity against mutant ALS proteins in neuronal cell culture has not been investigated.

The author transfected Neuro2a cells with all PDI mutant constructs. At 24 hr post transfection, cells were immunostained using anti-V5 antibodies to detect the sub-cellular localisation of PDI, and with anti-calreticulin antibodies to stain the ER, using confocal microscopy. The cells expressing wild-type PDI-V5 displayed reticulate expression of PDI in the ER, which was mostly excluded from the nucleus as expected. Similarly, PDI mutants all co-localised with calreticulin, suggesting ER localisation. Hence, the mutations did not alter the subcellular localisation of PDI, as shown in Figure 4.3 B.

A

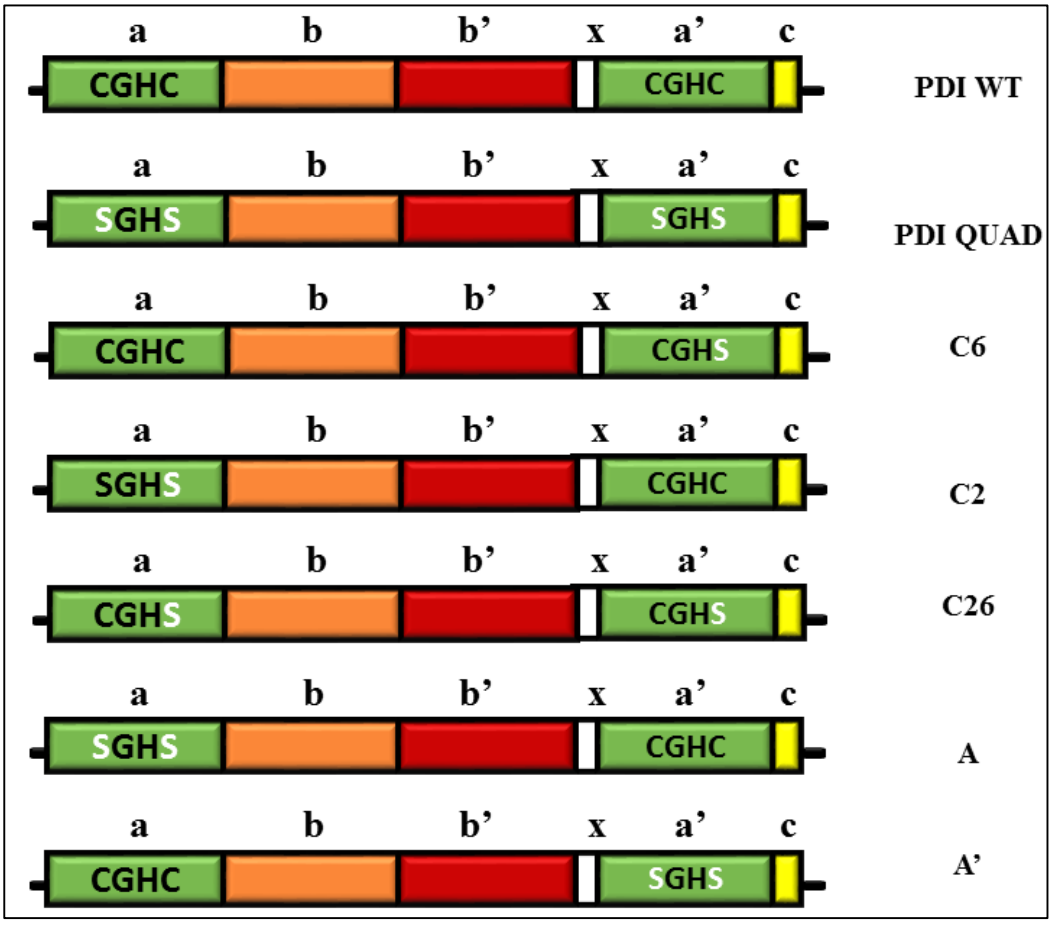

B

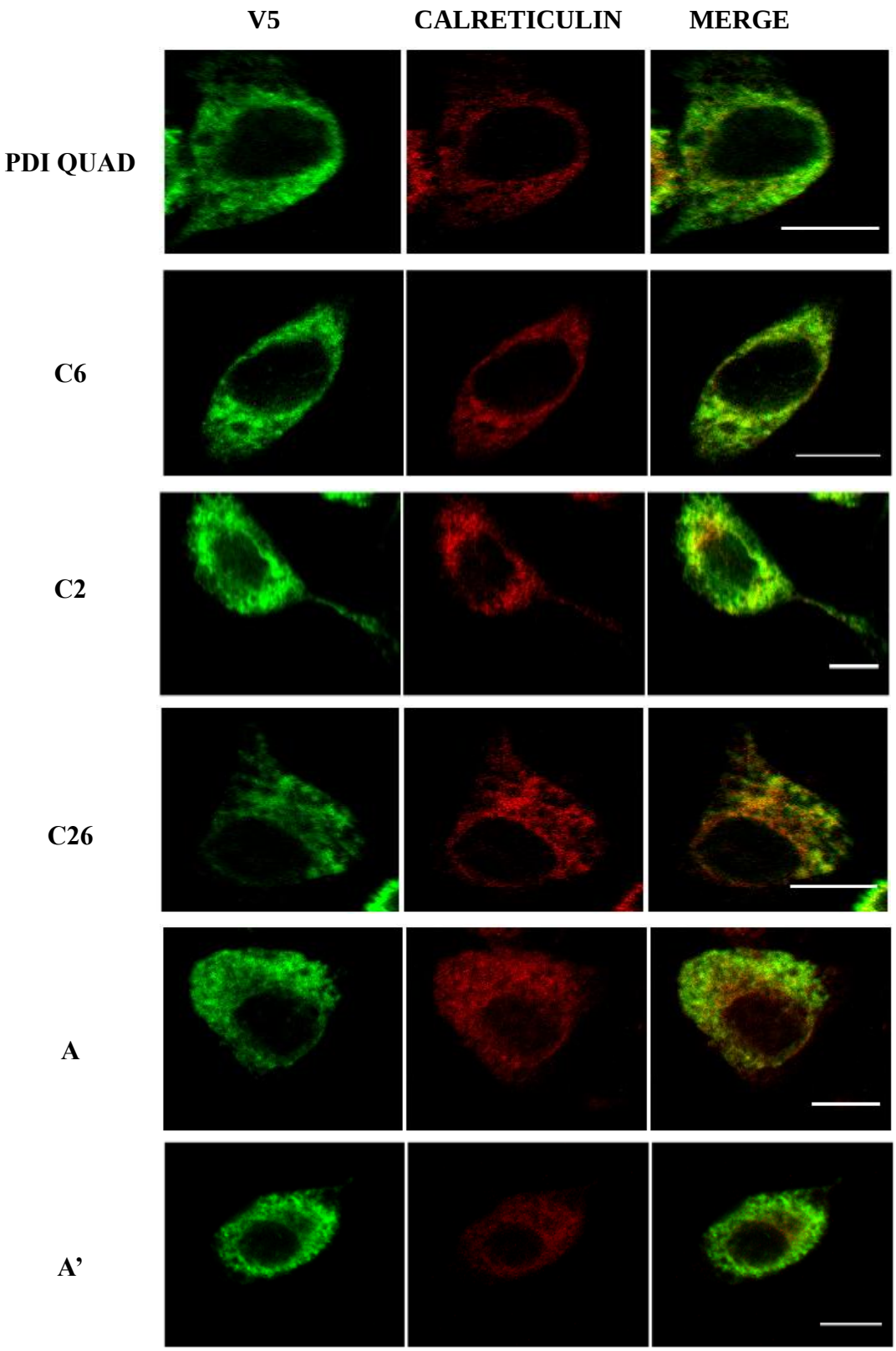

Figure 4.3 Expression of PDI mutants in Neuro2a cells A) Schematic representation of PDI mutants, illustrating their thioredoxin-like domains. The catalytic active domains *a* and *a'* are represented in green. The conserved residues (CGHC) are represented in black, and the cysteine residues mutated to serine are shown in white. The non-catalytic *b* domain is displayed in orange and the *b'* domain in red. The sequence coloured white represents the linker region (x). The C-terminus is represented in yellow. **B)** Confocal microscopy images of PDI mutants expressed in Neuro2a cells, examined 24 hr post-transfection Cells were fixed and probed with anti-V5 (first column) and anti-calreticulin (second column) antibodies using immunocytochemistry. The third column is a merge of the fluorescent images obtained from immunocytochemistry using anti-V5 and anti-calreticulin antibodies. Scale bar = 10 µm.

4.2.2) Disulphide interchange activity of PDI is protective against mutant SOD1 induced ER stress in neuronal cell lines.

Our laboratory previously demonstrated that PDI is protective against mutant SOD1-induced ER stress in neuronal cell lines [483]. However, the exact mechanism of protection remains unclear. This was investigated by examining the effect of PDI mutant proteins possessing only chaperone activity in cells expressing mutant SOD1. Therefore, Neuro2a cells were co-transfected with wild-type SOD1 or mutant $SOD1^{A4V}$, with either empty vector, wild-type PDI or mutant PDI for 72 hr.

An initial experiment was performed to confirm that cells co-transfected with SOD1 (wild-type or A4V) and mutant PDI V5-tagged constructs co-express both proteins together in the same cells. Immunocytochemistry was performed to detect the V5 tag, followed by fluorescent microscopy to simultaneously detect the EGFP and V5 tags. Quantification of individual cells revealed that over 98% of cells (200 cells quantified) expressing SOD1 were also expressing PDI. (Figure 4.4) Representative image of cells expressing $SOD1^{A4V}$ and PDI QUAD. Similar results were

demonstrated on expressing other PDI mutants (C6, C2 C26, A, A') (images not shown). The overall transfection efficiency was approximately 40% in Neuro2a cells observed 72 hr post transfection. Hence, for subsequent studies it was assumed that detection of SOD1 expression by the presence of EGFP, reflected co-expression of both SOD1 and PDI in the same cell

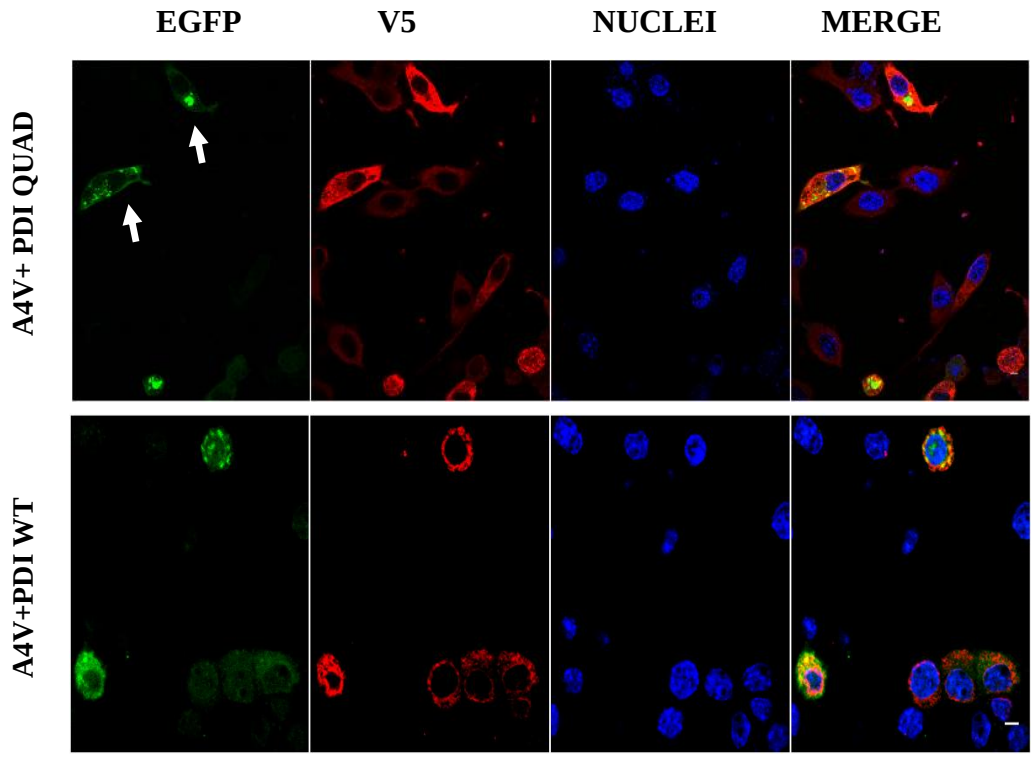

Figure 4.4 Co-expression of SOD1 and PDI in Neuro2a cells. Representative confocal microscopy images of cells co-expressing$SOD1^{A4V}$ (green) and PDI-QUAD (red) with Hoechst-stained nuclei (blue) (panel 1).Representative confocal microscopy images of cells co-expressing$SOD1^{A4V}$ (green) and PDI-WT (red) with Hoechst-stained nuclei (blue) (panel 2). Cells were examined 72 hr post transfection. The fourth column is a merge of the fluorescent images of EGFP and V5 tag. Scale bar = 10 µm.

To investigate the effect of over-expression of PDI mutants on ER stress induced by mutant SOD1, nuclear immunoreactivity to CHOP was examined as a marker of ER stress, as described previously [483]. Neuro2a cells were co-transfected with either wild-type SOD1 or $SOD1^{A4V}$ and either empty vector or PDI (Figure 4.5 A) and immunocytochemistry was performed using anti-CHOP antibodies.

As expected, only 17% of untransfected cells (UTR) or cells expressing EGFP, and only 21% of cells expressing wild-type SOD1, displayed nuclear CHOP immuno-reactivity. Furthermore, consistent with previous studies, a much greater proportion of cells (68%) expressing $SOD1^{A4V}$ displayed nuclear immunoreactivity to CHOP, indicating activation of the pro-apoptotic phases of the UPR in these cells. As previous, [483] co-expressing wild-type PDI with mutant $SOD1^{A4V}$ led to a significant reduction in the proportion of cells with nuclear CHOP immunoreactivity (38%, ***p<.001). In contrast, co-expression of PDI QUAD with $SOD1^{A4V}$, did not significantly decrease the proportion of cells with nuclear immunoreactivity to CHOP (63%, Figure 4.5 B). Similarly, all the other mutant PDI mutants examined did not significantly reduce the proportion of mutant $SOD1^{A4V}$ expressing cells with nuclear immunoreactivity to CHOP, with similar percentages of cells in each case: C6 (60%), C2 (59%), C26 (67%), A (64%) and A' (67%) (image not shown). Hence these data reveal that mutation of one or more cysteine residues in either the *a* or *a'* domain of PDI does not reduce ER stress in cells expressing with $SOD1^{A4V}$. These results therefore imply that the disulphide inter-change activity of PDI is required to protect against ER stress induced by mutant $SOD1^{A4V}$.

A

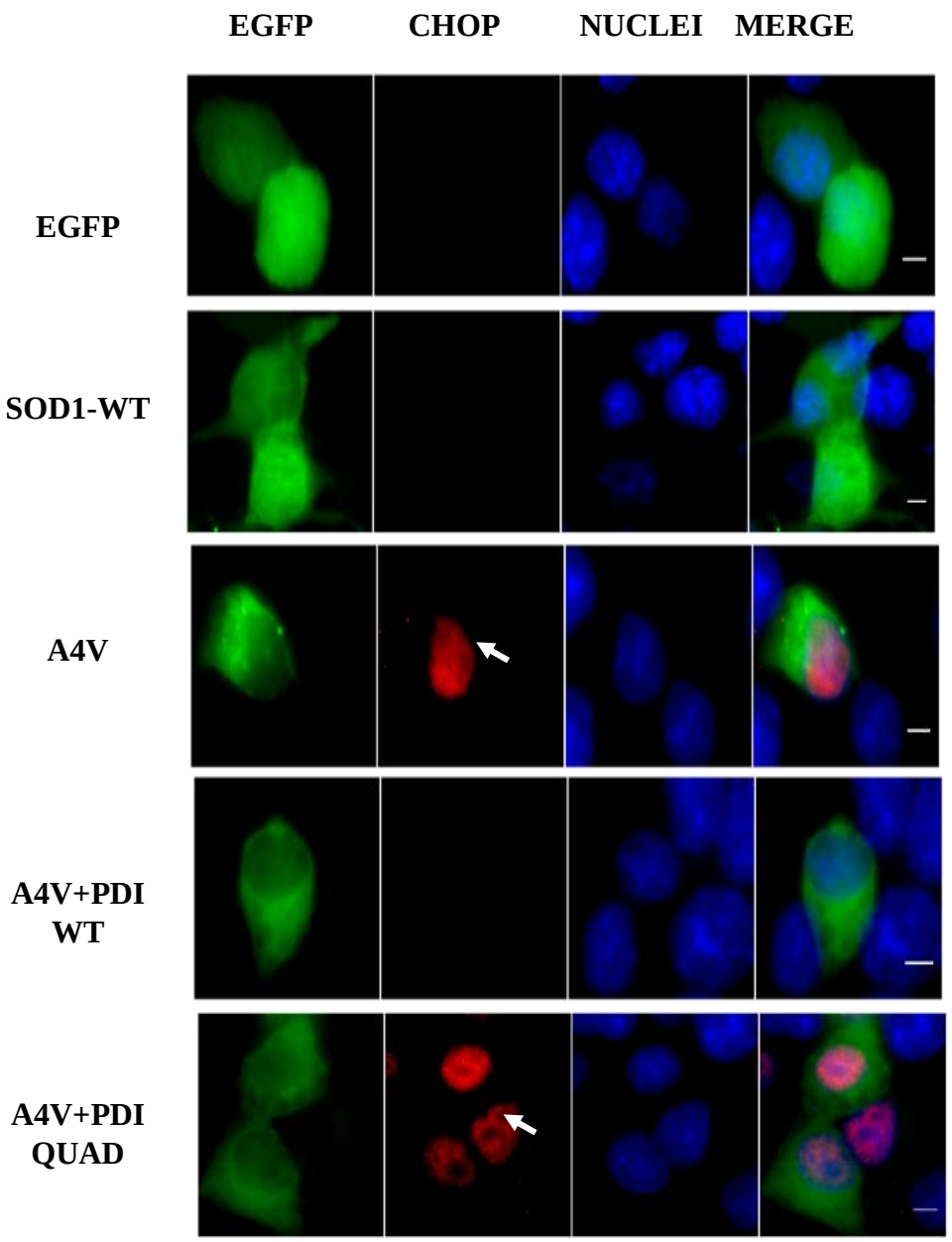
EGFP
CHOP
NUCLEI
MERGE
EGFP
SOD1-WT
A4V
A4V+PDI WT
A4V+PDI QUAD

B

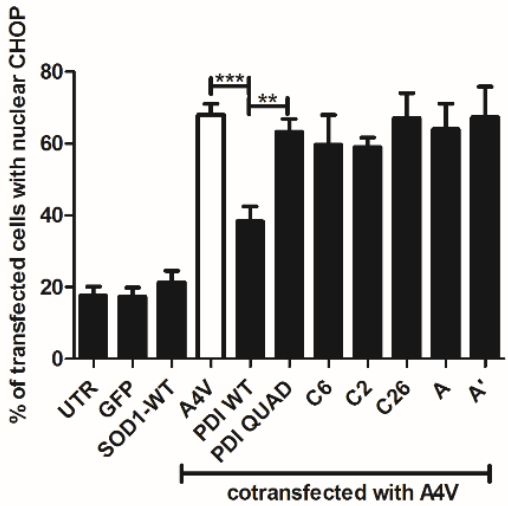
% of transfected cells with nuclear CHOP
80
60
40
20
0
***
**
UTR
GFP
SOD1-WT
A4V
PDI WT
PDI QUAD
C6
C2
C26
A
A'
cotransfected with A4V

Figure 4.5 Over-expression of PDI active site cysteine mutants is not protective against ER stress induced by mutant SOD1 in Neuro2a cells. A) Immunofluorescent detection of nuclear immunoreactivity to CHOP in wild-type SOD1 and $SOD1^{A4V}$ co-expressing Neuro2a cells with wild-type PDI or PDI mutants, visualised by confocal microscopy. Few cells expressing EGFP alone (panel 1) or wild-type (SOD1-WT, panel 2) displayed nuclear immunoreactivity to CHOP. In contrast, nuclear immunoreactivity to CHOP was significantly more frequent in cells expressing SOD1A4V (panel 3), indicating activation of the UPR, shown with white arrows (middle panel). However, fewer cells co-expressing $SOD1^{A4V}$ and wild-type PDI (panel 4) displayed nuclear CHOP immunoreactivity. In contrast, there was no difference in cells co-expressing $SOD1^{A4V}$ with vector only compared to $SOD1^{A4V}$ with PDI QUAD, indicating that PDI QUAD is not protective, unlike wild-type PDI (panel 5). Scale bar = 10 µm. **B)** Quantification of nuclear CHOP immunoreactivity in Neuro2a cells visualised in (A), co-expressing wild-type SOD1 or $SOD1^{A4V}$ with wild-type PDI or PDI QUAD. For each population, 100 transfected cells expressing CHOP in the nucleus were counted. The percentage of $SOD1^{A4V}$ cells expressing nuclear CHOP was significantly lower in cells co-expressing wild-type PDI compared to empty vector alone (***p<.001). There were also significantly fewer cells with CHOP activation when wild-type PDI was co-expressed with SOD1A4V, and between PDI QUAD and $SOD1^{A4V}$ (**p<.01). Data are represented as mean ±SD, n=3 with one-way ANOVA and Tukey's post-test.

4.2.3 Disulphide interchange activity of PDI is protective against mutant SOD1-induced inclusion formation in neuronal cell lines.

Mutant $SOD1^{A4V}$-EGFP forms prominent fluorescent inclusions, easily visible by microscopy, in neuronal cells [483]. Previously, over-expression of PDI was found to decrease the proportion of cells forming mutant $SOD1^{A4V}$ inclusions in neuronal cell lines [483]. Hence, it was next investigated whether over-expression of the PDI

mutants generated above was protective against inclusion formation induced by mutant SOD1. These results were consistent with the findings of our previous study, in which BMC, which mimics the disulphide interchange activity of PDI, was also protective against inclusions formation in cells expressing mutant SOD1 [483].

Neuro2a cells were co-transfected with wild-type and mutant SOD1-EGFP and wild-type and mutant PDI-V5 constructs. At 72 hr post transfection, cells were imaged using confocal fluorescent microscopy and the percentage of transfected cells (visualised by the presence of EGFP fluorescence) bearing fluorescent mutant SOD1 inclusions was quantified (Figure 4.6 A). Immunocytochemistry was performed using anti-V5 antibodies to detect PDI expression. Untransfected cells (UTR), cells expressing EGFP alone or wild-type SOD1 formed very few inclusions (<1%) as expected. Also, similar to previous observations, 34% of cells expressing mutant $SOD1^{A4V}$ formed inclusions [483]. However, when wild-type PDI was co-expressed with mutant $SOD1^{A4V}$ this proportion was significantly reduced, to 21% of cells (*p<.05), as demonstrated previously. In contrast, co-expression of PDI QUAD did not significantly alter the proportion of mutant $SOD1^{A4V}$ expressing cells bearing inclusions (34%, Figure 4.6 B). Quantification of cells coexpressing PDI QUAD and $SOD1^{A4V}$ demonstrated that 85% of SOD1 inclusion colocalised with PDI QUAD. Similarly, the other PDI mutants also did not prevent inclusion formation; 34% of C6 and C2 expressing cells, 35% of C26 expressing cells, and 32% of A' expressing cells formed inclusions, similar to PDI QUAD (microscopy images not shown). Hence these data suggest that the active cysteine residues of PDI are necessary to protect against SOD1 induced inclusion formation. Hence, similar to ER stress, the disulphide activity of PDI is required for protection against mutant SOD1 induced inclusion formation.

A

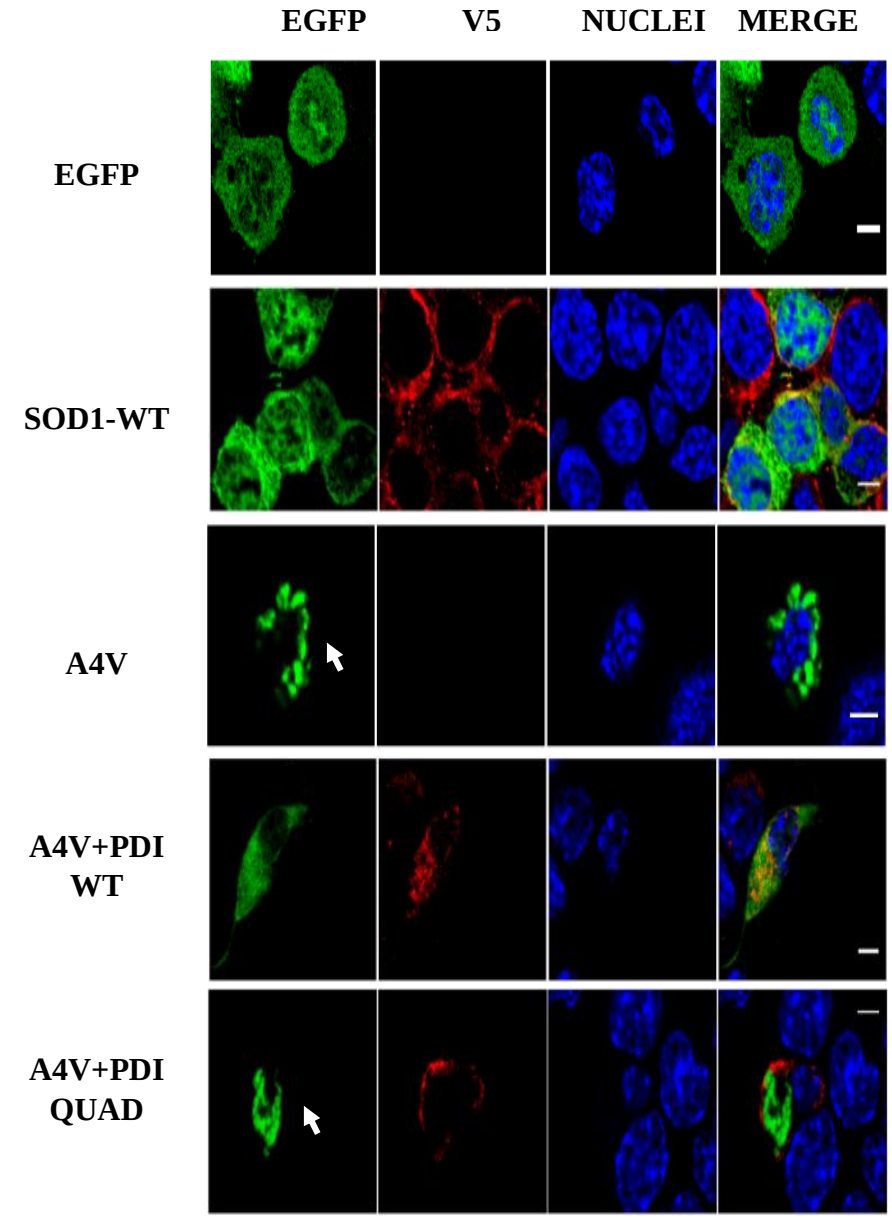
EGFP
V5
NUCLEI
MERGE
EGFP
SOD1-WT
A4V
A4V+PDI WT
A4V+PDI QUAD

B

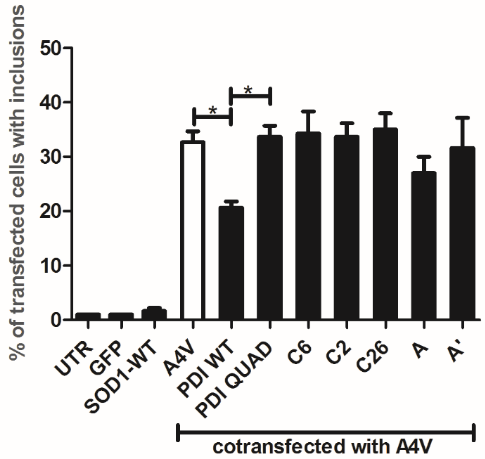
% of transfected cells with inclusions
50
40
30
20
10
0
*
*
UTR
GFP
SOD1-WT
A4V
PDI WT
PDI QUAD
C6
C2
C26
A
A'
cotransfected with A4V

Figure 4.6 Over-expression of PDI cysteine mutant is not protective against inclusion formation induced by mutant SOD1 in Neuro2a cells. A) Fluorescent detection of EGFP-positive inclusions present in Neuro2a cells expressing wild-type SOD1 (SOD1-WT) or $SOD1^{A4V}$ (A4V), co-expressing wild-type PDI or PDI QUAD (red), examined by confocal microscopy. Nuclei are visualised by Hoechst staining (blue). Cells expressing EGFP only (first panel) or wild-type SOD1 rarely form inclusions (second panel). In contrast, EGFP-positive inclusions were frequent in cells expressing $SOD1^{A4V}$ alone (third panel) or co-expressed with PDI QUAD (fifth panel), represented by white arrows. In contrast, fewer cells formed inclusions when wild-type PDI was over-expressed with $SOD1^{A4V}$ (third panel). Scale bar = 10 µm. **B)** Quantification of the percentage of transfected cells bearing EGFP-positive inclusions in Neuro2a cells represented in (A). Significantly fewer cells formed inclusions when wild-type PDI was co-expressed with $SOD1^{A4V}$ (*p<.05) compared to cells co-expressing PDI QUAD or vector only. Also when wild-type PDI was co-expressed with $SOD1^{A4V}$ and between PDI QUAD and SOD1A4V (*p<.05). Data are represented as mean ±SD, n=3 with one-way ANOVA and Tukey's post-test.

4.2.4) Both disulphide interchange activity and chaperone activity of PDI are protective against mutant SOD1 induced cell death in neuronal cell lines.

Our laboratory, as well as others, have previously demonstrated that mutant $SOD1^{A4V}$ induces apoptosis in neuronal cells [483, 624] but this is reduced by over-expression of PDI [483]. Hence, it was next examined whether the chaperone or disulphide interchange activity of PDI was protective against apoptosis induced by mutant SOD1 using the PDI mutants. Apoptosis was examined by nuclear morphology as described previously [483, 644], since fragmentation of DNA, visualised using DAPI, is one of the final stages of apoptosis.

Neuro2a cells were co-transfected with either SOD1-WT or $SOD1^{A4V}$ and either empty vector, wild-type PDI, or one of the PDI mutants, to examine apoptosis induced by mutant SOD1. Immunocytochemistry was performed using anti-V5 antibodies to detect PDI expression. Transfected cells were examined 72 hr post transfection using fluorescence microscopy and analysis of apoptosis was performed by quantification of the percentage of cells bearing apoptotic nuclei (Figure 4.7 A). Fragmented nuclei were rare in untransfected cells and cells transfected with empty vector EGFP (3% of cells – 3% for both UTR and vector only. As expected, only 5% of cells expressing wild-type SOD1 displayed apoptotic nuclei, whereas significantly more cells expressing mutant $SOD1^{A4V}$ were undergoing apoptosis (22%). In contrast, co-expression of wild-type PDI resulted in significantly fewer cells (11%, $p<.001$) with fragmented nuclei, indicating apoptosis. Interestingly, on co-expression of PDI QUAD with mutant $SOD1^{A4V}$ significantly fewer cells bore apoptotic nuclei 15% ($p<.01$) compared to cells transfected with vector only (Figure 4.7 B). Similarly, all of the other PDI mutants examined were also protective against apoptosis induced by mutant $SOD1^{A4V}$. Fragmented nuclei were detected in only 10% of C6 expressing cells, ($p<.001$), 12% of C2 or C26 expressing cells ($p<.001$), 15% of A expressing cells ($p<.01$) and 14% of A' expressing cells ($p<.01$). These data suggest that the cysteine residues of PDI are not necessary for its protective activity against apoptosis. Hence the chaperone activity of PDI is sufficient to protect against mutant $SOD1^{A4V}$ induced apoptosis in cell culture. Since the mutants of PDI examined in cells expressing mutant SOD1 (C6, C2, C26, A and A') produced similar findings to the PDI QUAD mutant, this suggests that mutation of a single cysteine residue resulted in similar effects as mutation of multiple cysteine, at least in terms of ER stress, inclusion formation and cell death. For all further analysis in the experiments described in this chapter involving mutant TDP-43 and mutant FUS, the PDI QUAD mutant was only examined.

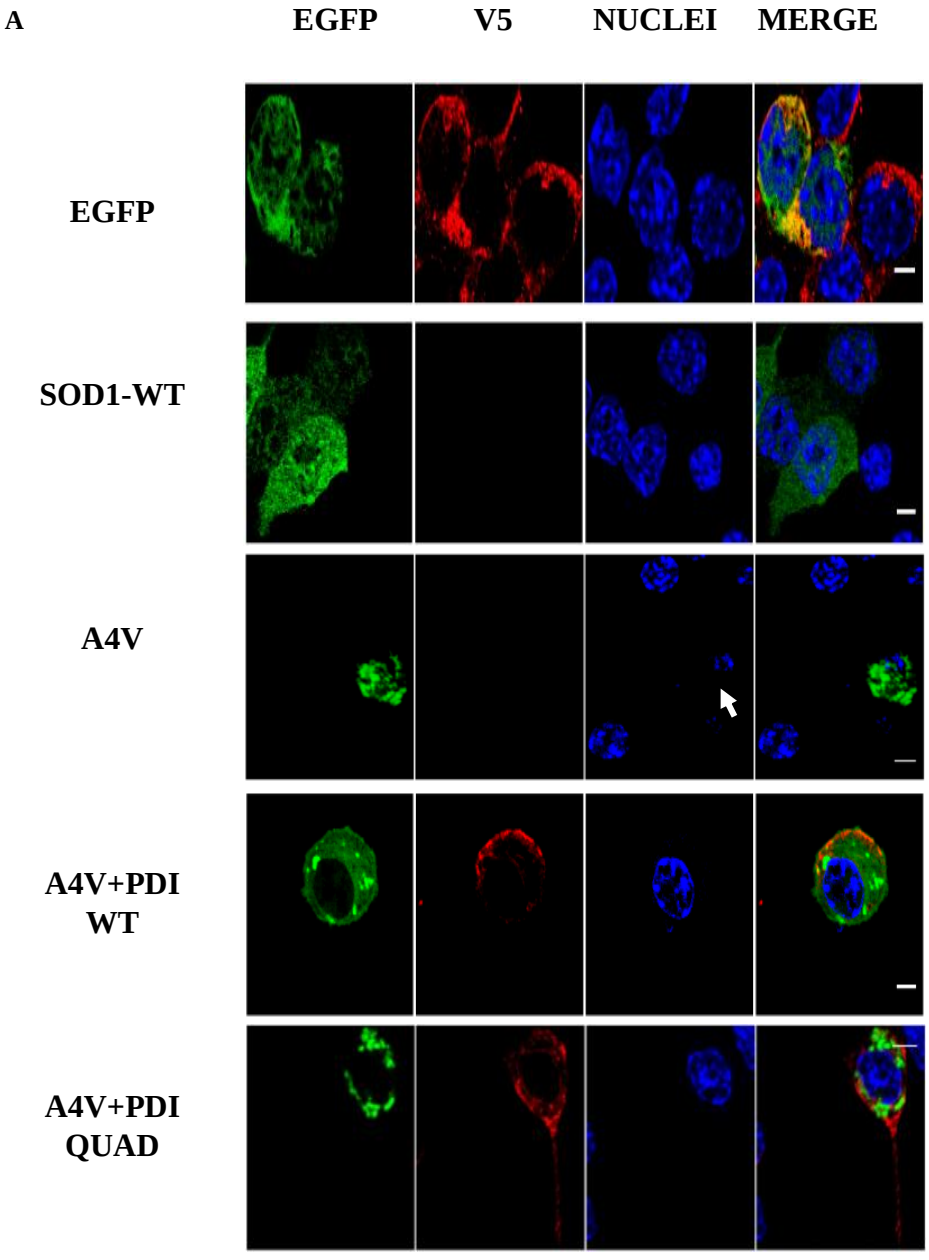
A
EGFP
V5
NUCLEI
MERGE
EGFP
SOD1-WT
A4V
A4V+PDI WT
A4V+PDI QUAD
B
% of apoptotic nuclei
30
20
10
0
UTR
GFP
SOD1-WT
A4V
PDI WT
PDI QUAD
C6
C2
C26
A
A'
cotransfected with A4V

Figure 4.7 Over-expression of PDI mutants is protective against mutant SOD1 induced apoptosis in Neuro2a cells. A) Immunofluorescent images of Neuro2a cells co-expressing mutant SOD1A4V with wild-type PDI or PDI mutants. Nuclei are shown by Hoechst stain (blue). Arrow represents condensed nuclei, indicating apoptosis is underway. Neuro2a cells expressing control EGFP only (first panel), wild-type SOD1 (second panel) or SOD1A4V with fragmented nuclei (A4V, third panel), indicated with white arrow. On co-expressing wild-type PDI (fourth panel) or PDI QUAD (fifth panel) fewer cells were undergoing apoptosis. Scale bar = 10 μm. **B)** Quantification of apoptotic nuclei in cells in (A), expressing SOD1 and PDI. There was a significant difference in the population of apoptotic nuclei observed between SOD1A4V co-expressed with vector only and when co-expressed with wild-type PDI, C6, C2 , C26 (***, $p<.001$), or co-expressed with PDI QUAD, A,A'(** $p<.01$).

4.2.5) Disulphide interchange activity of PDI is protective against mutant SOD1 induced ER-Golgi transport defects in neuronal cell lines.

Our laboratory previously established that mutant SOD1 inhibits ER-Golgi transport in neuronal cell lines [552]. Furthermore, the studies described in Chapter 3 demonstrated that over-expression of PDI was protective against these ER-Golgi trafficking defects. It was next examined whether the disulphide interchange activity of PDI was protective against the inhibition of ER-Golgi transport. For this purpose, the PDI QUAD mutant was used to investigate whether the chaperone activity retains the protective activity of PDI. Similarly, as BMC mimics the disulphide interchange activity of PDI, it was also investigated whether BMC was protective against the inhibition of ER-Golgi transport, assayed using VSVG [562], in Neuro2a cells expressing mutant $SOD1^{A4V}$.

Neuro2a cells were co-transfected with mCherry-tagged VSVG, either EGFP tagged wild-type SOD1 or mutant $SOD1^{A4V}$, and either empty vector or V5-tagged

PDI (wild-type PDI or PDI QUAD). The cells were incubated at 40°C for 12.5 hours to accumulate VSVG in the ER, before incubation at the permissive temperature for 30 min. In a separate group of cells co-transfected with mCherry-tagged VSVG and either EGFP tagged wild-type SOD1 or mutant $SOD1^{A4V}$, BMC (25 µm) was administered 1 hr post-transfection followed by incubation at 37°C for 12.5 hr. Similarly, control cells co-expressing $SOD1^{A4V}$ and VSVG were treated with DMSO for the same period. After fixing the cells, immunocytochemistry was performed using antibodies for markers of the ER (calnexin) and Golgi (GM130), followed by fluorescent microscopy (Figure 4.8 A). Quantification of the localisation of VSVG in either the ER or Golgi compartments was performed using Mander's co-efficient, in the range from 0 to 1, representing 0-100% overlapping pixels, as described previously [552].

In untransfected cells (UTR) and EGFP only expressing cells, little VSVG (2%) was retained in the ER and most (70%) was transported to the Golgi apparatus after 30 min at the permissive temperature. Similarly, in cells expressing wild-type SOD1, little VSVG (10%) was retained in the ER and most was transported to the Golgi (68%) at this time point. However, in cells expressing mutant $SOD1^{A4V}$, inhibition of ER-Golgi transport was detected relative to the other cell populations. In these cells, significantly more VSVG was retained in the ER (40% , $p<.01$) and less was transported to the Golgi after 30 min (43, $p<.01$), (Figure 4.8 B), similar to previous observations [552]. However, as in the results described in Chapter 3, when wild-type PDI was co-expressed with mutant $SOD1^{A4V}$, transport between the ER-Golgi was restored. There was no significant difference and only 16% ($p<.01$) VSVG was retained in the ER and 70% ($p<.001$) VSVG was transported to Golgi. In contrast however, when PDI QUAD was co-expressed with mutant $SOD1^{A4V}$, transport between ER-Golgi was again inhibited, and significantly more VSVG was retained in the ER (30%) and significantly less was transported to the Golgi after 30 min (50%) compared to cells expressing wild-type SOD1 or control cells. Also as a control, ER-Golgi transport was not inhibited in cells co-expressing PDI QUAD with mCherry-tagged VSVG as little VSVG (1%) was retained in the ER and most (73%) was transported to Golgi, demonstrating that expression of PDI QUAD alone does not inhibit transport (data not shown). Interestingly, when BMC

was administered to the cells, VSVG transport was also restored, and there was no significant difference between BMC-treated cells and cells expressing wild-type SOD1 or control cells; 16% ($p<.01$) VSVG was retained in the ER and 66% ($p<.001$) was transported to the Golgi. Therefore, these data reveal that wild-type PDI and BMC, which possess the disulphide interchange activity of PDI, can restore ER-Golgi transport inhibited by mutant SOD1. However, in contrast, the PD1 QUAD mutant, which has lost the disulphide interchange activity but retains the chaperone activity, is not protective against inhibition of ER-Golgi transport.

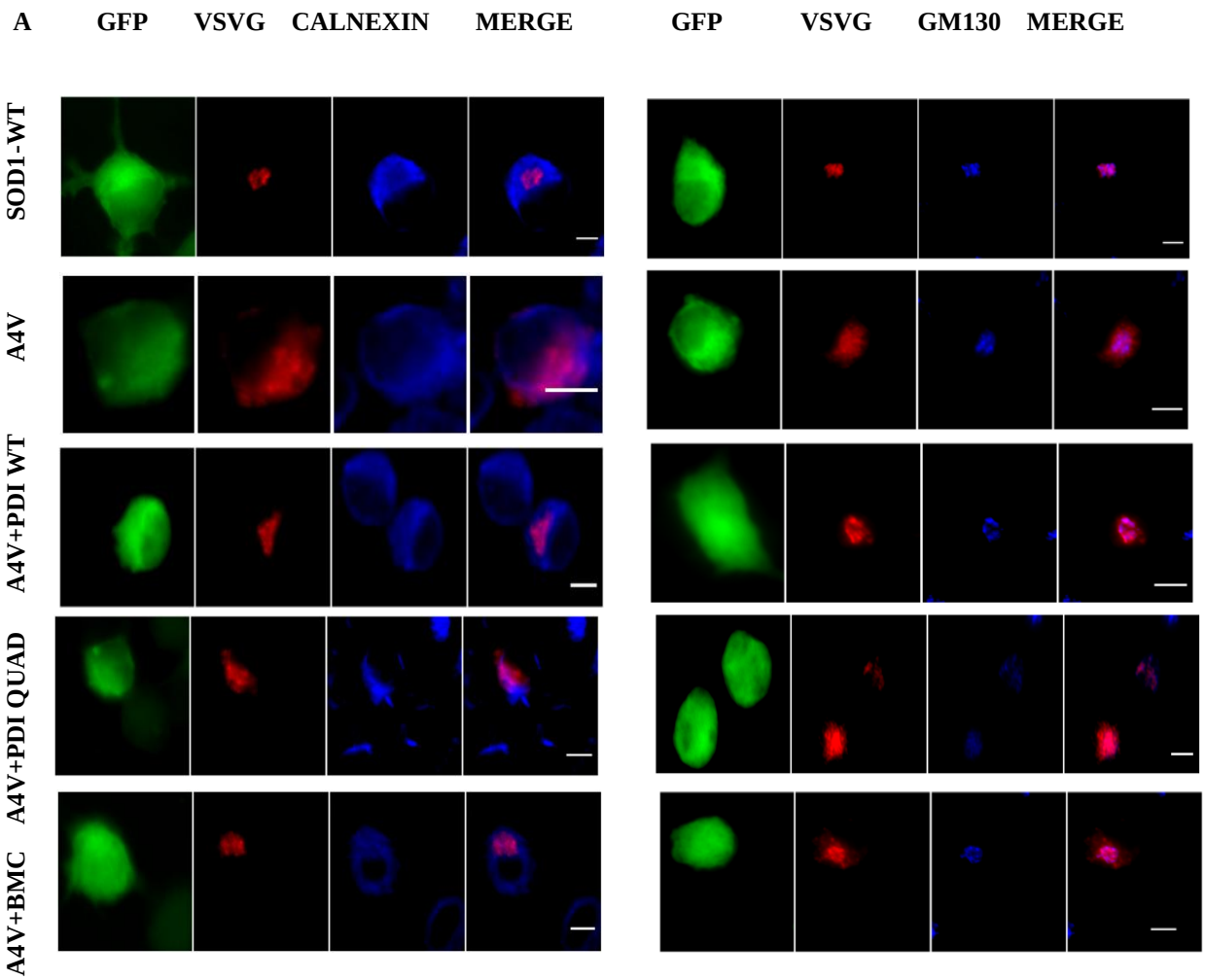
A
GFP
VSVG
CALNEXIN
MERGE
GFP
VSVG
GM130
MERGE
SOD1-WT
A4V
A4V+PDI WT
A4V+PDI QUAD
A4V+BMC

B

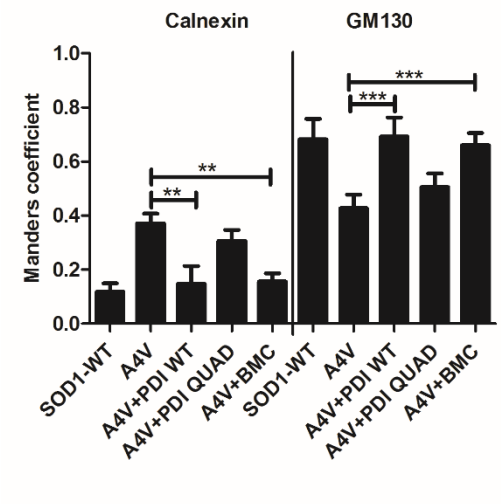
Calnexin
GM130
Manders coefficient
1.0
0.8
0.6
0.4
0.2
0.0
**
**
***
***
SOD1-WT
A4V
A4V+PDI WT
A4V+PDI QUAD
A4V+BMC
SOD1-WT
A4V
A4V+PDI WT
A4V+PDI QUAD
A4V+BMC

Figure 4.8 The disulphide interchange activity of PDI is protective against inhibition of ER-Golgi transport in mutant SOD1 expressing cells. A) Representative fluorescent images of cells co-expressing VSVGts045-mCherry, either EGFP enhanced green fluorescent protein tagged wild-type SOD1 or $SOD1^{A4V}$ VSVGts045-mCherry, and either empty vector or PDI (wild-type or QUAD) at 12.5 hr post-transfection, stained with markers of ER (calnexin) or Golgi apparatus (GM130). VSVGts045-mCherry was trapped in the ER at 40°C for 12.5 hr, then cycloheximide was added and the temperature was shifted to the permissive temperature (32°C) for 30 min. Cells were then fixed with 4% paraformaldehyde at 30 min at 32°C. At 32°C VSVG is transported to Golgi and little co-localises with calnexin in untransfected cells or wild-type SOD1 expressing cells (SOD1-WT, first panel). However, inhibition of ER-Golgi transport was observed in cells expressing $SOD1^{A4V}$ with vector alone or co-expressing PDI QUAD more VSVG co-localise with calnexin and less with GM130 (second panel and fifth panel). In contrast, on co-expressing wild-type PDI with $SOD1^{A4V}$, or administrating BMC, ER-Golgi transport was restored and VSVG co-localised more with GM130 rather than calnexin (third panel and fifth panel). Scale bar = 10 μm. **B)** Quantification of the degree of co-localization of VSVGts045-mCherry with calnexin or GM130 of cells in (A), using Mander's coefficient. Data are presented as mean ± SEM, tested with one-way ANOVA and Tukey's post-test, n = 3. A significant difference in co-localisation between VSVG and calnexin was observed (**) $p<.01$ between cells expressing $SOD1^{A4V}$ with empty vector compared to those co-expressing PDI or treated with BMC when observed for co-localisation between VSVG and calnexin. Significant difference was observed (***) $p<.001$ when cells co-expressed SOD1A4V with empty vector and when coexpressed with PDI or when administered with BMC when observed for co-localisation between VSVG and GM130.

4.2.6) The disulphide interchange activity of PDI is necessary for protection against mutant TDP-43 induced ER stress in neuronal cell lines.

As previously demonstrated in Chapter 3, PDI is protective against mutant TDP-43 induced ER stress in neuronal cultures. To investigate whether the disulphide inter-change activity or the chaperone activity of PDI is necessary for this protection in cells expressing mutant TDP-43, induction of ER stress was examined using nuclear immunoreactivity to CHOP as a marker as above. Neuro2a cells were co-transfected with mCherry only, wild-type TDP-43 or mutant TDP-43 Q331K, with either empty vector or either wild-type PDI or PDI QUAD. BMC was administered to the cells 4 hr post transfection (Figure 4.9 A). The cells were then fixed and immunocytochemistry for CHOP was performed at 18 hr post transfection.

CHOP nuclear immunoreactivity was detected in only 7% of untransfected cells (UTR) as expected. Similarly, only 6% of cells expressing mCherry only displayed nuclear immunoreactivity to CHOP. In cells expressing wild-type TDP-43, a slight, but non-significant activation of CHOP was detected, as 22% of transfected cells displayed nuclear immunoreactivity to CHOP. In contrast, significantly more cells expressing mCherry-tagged Q331K (39%, $p<.001$) expressed nuclear CHOP, indicating activation of ER stress, but this was significantly reduced to 30% ($p<.01$) in TDP-43 Q331K cells when wild-type PDI was co-expressed (Figure 4.9 B). Similarly, administering BMC to mutant Q331K cells significantly reduced ER stress, as only 28% ($p<.01$) cells displayed nuclear immunoreactivity to CHOP. However, when PDI QUAD was co-expressed with TDP-43 Q331K, 35% cells displayed nuclear CHOP immunoreactivity, which was not significantly different to those cells expressing vector only. Hence these data demonstrate that the PDI QUAD mutant was not protective against induction of ER stress by mutant TDP-43. This indicates that the disulphide activity of PDI is essential for protection against ER stress induced by mutant TDP-43.

A

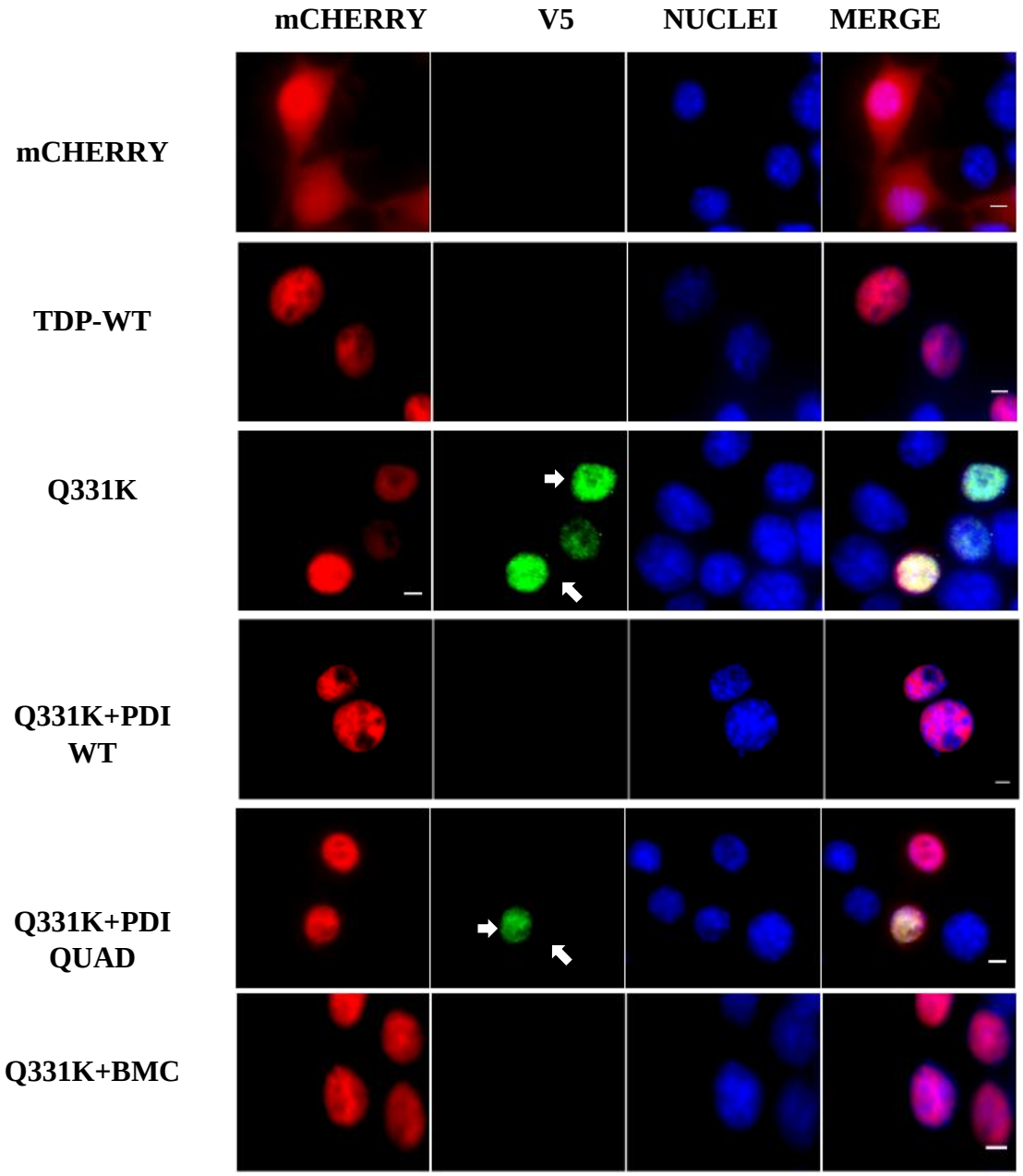
mCHERRY
V5
NUCLEI
MERGE
mCHERRY
TDP-WT
Q331K
Q331K+PDI WT
Q331K+PDI QUAD
Q331K+BMC

B

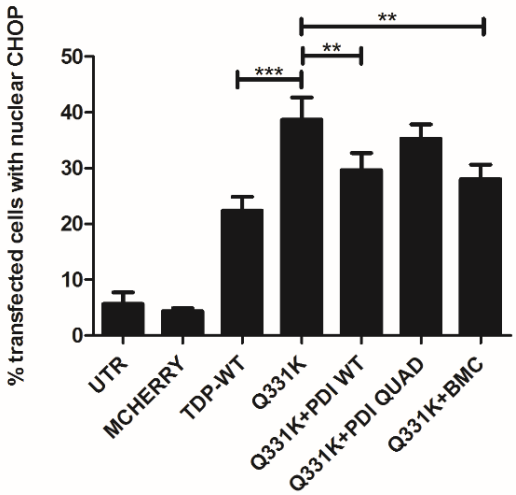
% transfected cells with nuclear CHOP
50
40
30
20
10
0
***
**
**
UTR
MCHERRY
TDP-WT
Q331K
Q331K+PDI WT
Q331K+PDI QUAD
Q331K+BMC

Figure 4.9 The disulphide interchange activity of PDI is protective against nuclear CHOP activation in Neuro2a cells. A) Neuro2a cells were transfected with mCherry only (first panel), wild-type TDP-43 (TDP-WT, second panel) or mutant TDP-43 Q331K (third panel), for 18 hr. Immunocytochemistry was performed using anti-CHOP antibodies and counter-staining with DAPI (blue). Few control cells expressing mCherry only, or cells expressing wild-type TDP-43, display nuclear immunoreactivity to CHOP. However, significantly more cells expressing TDP-43 mutant Q331K induce ER stress, as detected by nuclear immunoreactivity to CHOP (middle panel), indicated with white arrows. However, coexpression of wild-type PDI or administration of BMC reduces nuclear CHOP immunoreactivity in cells expressing Q331K (fourth panel and sixth panel). In contrast, co-expressing PDI QUAD with Q331K did not significantly reduce the proportion of cells with nuclear CHOP immunoreactivity, indicating ER stress (fifth panel). Scale bar = 10 µm. **B)** Quantification of cells in (A), expressing mCherry tagged TDP-43 proteins with and without co-expression of PDI (wild-type of QUAD) or administrating BMC using nuclear immunoreactivity to CHOP as a marker of ER-stress induced apoptotic signalling. Significantly fewer cells were detected with activation of the UPR (***) $p<.001$ in cells co-expressing wild-type TDP-43 with empty vector compared to TDP-43 Q331K coexpressed with empty vector, and between cells co-expressing TDP-43 Q331K with wild-type PDI or administered with BMC (**) $p <.01$. However there was no difference in cells with ER stress in TDP-43 Q331K cells expressing vector alone compared to PDI QUAD. For each of 3 replicate experiments, 100 cells were scored for each population. Data are presented as mean ± SEM, tested with one-way ANOVA and Tukey's post-test, $n = 3$.

4.2.7) The disulphide interchange activity of PDI is necessary for protection against mutant TDP-43 induced inhibition of ER-Golgi transport in neuronal cell lines.

To investigate whether the disulphide interchange or chaperone activity of PDI is protective against inhibition of ER-Golgi transport, transport of VSVG-mCherry was examined in Q331K cells co-expressing PDI QUAD or treated with BMC. Neuro-2a cells were co-transfected with mCherry-tagged VSVG, either EGFP tagged wild-type TDP-43 or mutant TDP-43 Q331K, and either empty vector or V5-tagged PDI (wild-type or QUAD). The cells were incubated at 40°C for 16 hr to accumulate VSVG in the ER, before incubation at the permissive temperature for 30 min. BMC was administered to the cells 1 hr post-transfection in cells expressing mutant TDP-43 followed by incubation at 37°C for 16 hr. Control cells expressing Q331K were treated with DMSO instead of BMC. After fixing the cells, immunocytochemistry was performed using antibodies for markers of the ER (calnexin) and Golgi (GM130) followed by fluorescent microscopy. Quantification of the localisation of VSVG in either the ER or Golgi compartments was performed using Mander's co-efficient, in the range from 0 to 1, representing 0-100% overlapping pixels, as described previously in Chapter 3.

In untransfected cells and in EGFP expressing cells, little VSVG (8%) was retained in the ER and most (75%) was transported to the Golgi apparatus after 30 min at the permissive temperature, as in Chapter 3 (data not shown). Similarly, in cells expressing wild-type TDP-43, little VSVG was retained in the ER (13%) and most (72%) was had already reached the Golgi at this time point. However, in cells expressing mutant TDP-43 Q331K, inhibition of ER-Golgi transport was detected relative to the other cell populations. In these cells, significantly more VSVG was retained in the ER (37%) and significantly less (42%) was transported to the Golgi after 30 min, (Figure 4.10 A). When wild-type PDI was co-expressed with mutant TDP-43, transport between the ER-Golgi was restored, and little (16%, $p<.01$) VSVG was retained in the ER because most (63%, $p<.05$) was transported to Golgi, and there was no significant difference to cells expressing wild-type TDP-43 or

control cells. Similarly, treatment with BMC also restored transport, little VSVG (17%, $p<.05$) was retained in the ER and most (64%, $p<.01$) was transported to the Golgi. However, co-expression of PDI QUAD with Q331K VSVG did not significantly alter the proportion of VSVG retained in the ER (26%) or transported to the Golgi 49% compared to vecto4r only treated cells (Figure 4.10 B). Therefore, because BMC was protective and PDI QUAD was not protective, these data suggest that the disulphide interchange activity of PDI is necessary for protection against inhibition of ER-Golgi transport induced by mutant TDP-43.

A

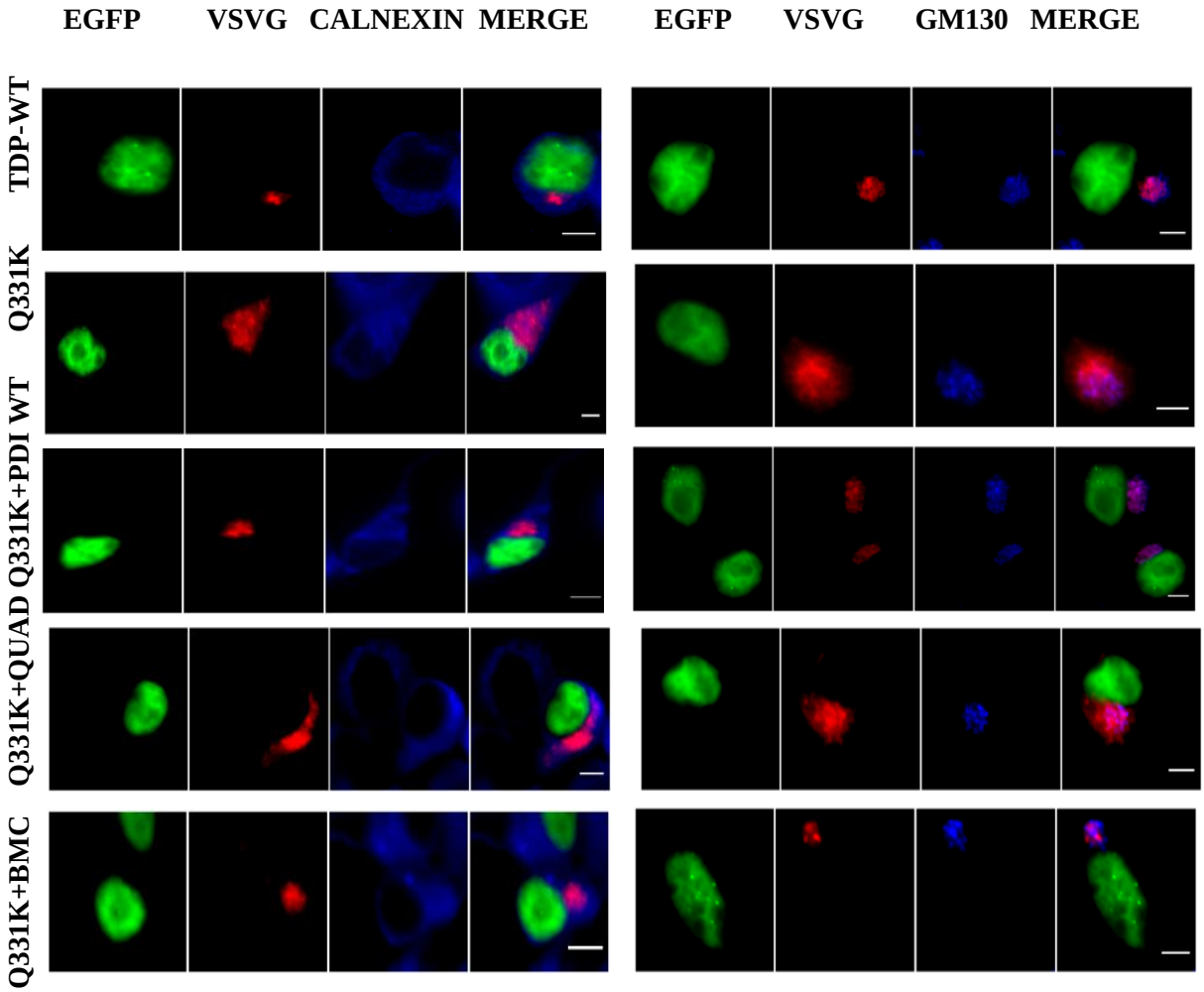
EGFP
VSVG
CALNEXIN
MERGE
EGFP
VSVG
GM130
MERGE
TDP-WT
Q331K
Q331K+PDI WT
Q331K+QUAD
Q331K+BMC

B

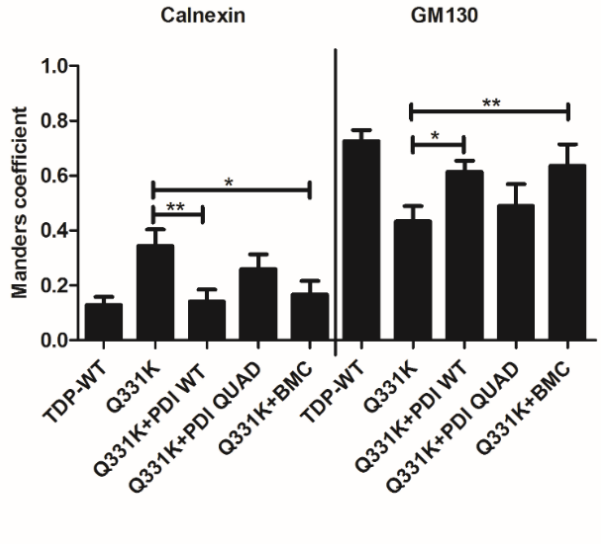
Calnexin
GM130
Manders coefficient
1.0
0.8
0.6
0.4
0.2
0.0
**
*
**
*
TDP-WT
Q331K
Q331K+PDI WT
Q331K+PDI QUAD
Q331K+BMC
TDP-WT
Q331K
Q331K+PDI WT
Q331K+PDI QUAD
Q331K+BMC

Figure 4.10 The disulphide interchange activity of PDI is protective against inhibition of ER-Golgi transport in mutant TDP-43 expressing cells. A) Representative fluorescent images of cells co-expressing VSVGts045-mCherry with EGFP-tagged wild-type TDP-43 or Q331K, and PDI (wild-type or QUAD) or vector only at 16 hr post-transfection. VSVGts045-mCherry was trapped in the ER at 40°C for 16 hr and the temperature was then shifted to the permissive temperature (32°C) for 30 min. After fixing cells with 4% paraformaldehyde at 30 min at 32°C, immunocytochemistry was performed using markers of the ER (calnexin) or Golgi apparatus (GM130). VSVG is transported to the Golgi and little co-localises with the ER in cells expressing wild-type TDP-43 (TDP-WT, first panel). Inhibition of ER-Golgi transport is observed when TDP-43 Q331K is expressed with empty vector or coexpressed with PDI QUAD, more VSVG colocalises with calnexin and less with GM130 (second and fourth panel). However on co-expressing wild-type PDI or administering BMC with Q331K, transport was restored and VSVG co-localised more with GM130 rather than calnexin (third and fifth panel). Scale bar = 10 μm. **B)** Quantification of the degree of co-localization of cells in (A) using Mander's coefficient. Data are presented as mean ± SEM, tested with one-way ANOVA and Tukey's post-test, n = 3. A significant difference was observed (**, $p<.01$) between cells expressing Q331K with empty vector and PDI or (*, $p<.05$) treatment with BMC for co-localisation between VSVG and calnexin. Significant difference was observed (*, $p<.05$) between cells expressing Q331K and PDI and when Q331K administered with BMC (**, $p<.01$) when observed for co-localisation between VSVG and GM130.

4.2.8 The disulphide interchange activity of PDI is necessary for protection against mutant TDP-43 mislocalisation in the cytoplasm in neuronal cell lines.

In chapter 3 it was demonstrated that PDI prevents the re-distribution of mutant TDP-43 from the nucleus to cytoplasm. It was next examined which properties of PDI (disulphide interchange or chaperone activities) are necessary for its protective

ability in Neuro2a cells. In our previous study [486], as outlined in Chapter 3, it was demonstrated that more mutant TDP-43 was present in the cytoplasm at 18-24 hr post-transfection compared to later time points [486]. Hence, cells were transfected with PDI and TDP-43 constructs as above for 18-24 hr. Immunocytochemistry was then performed using anti-V5 antibodies to detect PDI expression, with counter-staining for DAPI to identify the nucleus. The cellular distribution of TDP-43 was examined in individual cells using fluorescence microscopy. TDP-43 was considered nuclear when it completely co-localised with DAPI. However, cells in which TDP-43 was expressed in both the nucleus and cytoplasm were categorised as containing cytoplasmic TDP-43. (Figure 4.11 A).

Wild-type TDP-43 was expressed in the cytoplasm in 23% of cells, in accordance with the literature [150, 561], and co-expressing wild-type PDI, PDI QUAD or treatment with BMC did not affect the proportion of cells with cytoplasmic TDP-43 (25%, 29% or 23% of cells respectively, images not shown). As expected, significantly more mutant TDP-43 cells expressed TDP-43 in the cytoplasm compared to cells expressing wild-type TDP-43; 41% ($p<.001$) of Q343R cells and 36% ($p<.01$) of Q331K expressing cells. However, co-expression of mutant TDP-43 and wild-type PDI resulted in significantly fewer cells with cytoplasmic TDP-43 compared to cells transfected with vector only; 28% of Q343R expressing cells ($p <.01$) and 22% of Q331K expressing cells ($p<.01$, Figure 4.11 B). Furthermore, treatment with BMC also significantly reduced the proportion of cells with cytoplasmic TDP-43 24% of Q343R expressing cells ($p <.001$) and 23% of Q331K expressing cells ($p<.01$, Figure 4.12 B) compared to cells transfected with vector only. However, in contrast, co-expressing PDI QUAD did not reduce the proportion of cells expressing mutant TDP-43 in the cytoplasm; 34% of Q343R expressing cells and 28% of Q331K expressing cells. Therefore, these data reveal that the disulphide interchange activity of PDI is protective against the redistribution of mutant TDP-43 from the nucleus to the cytoplasm in neuronal cells.

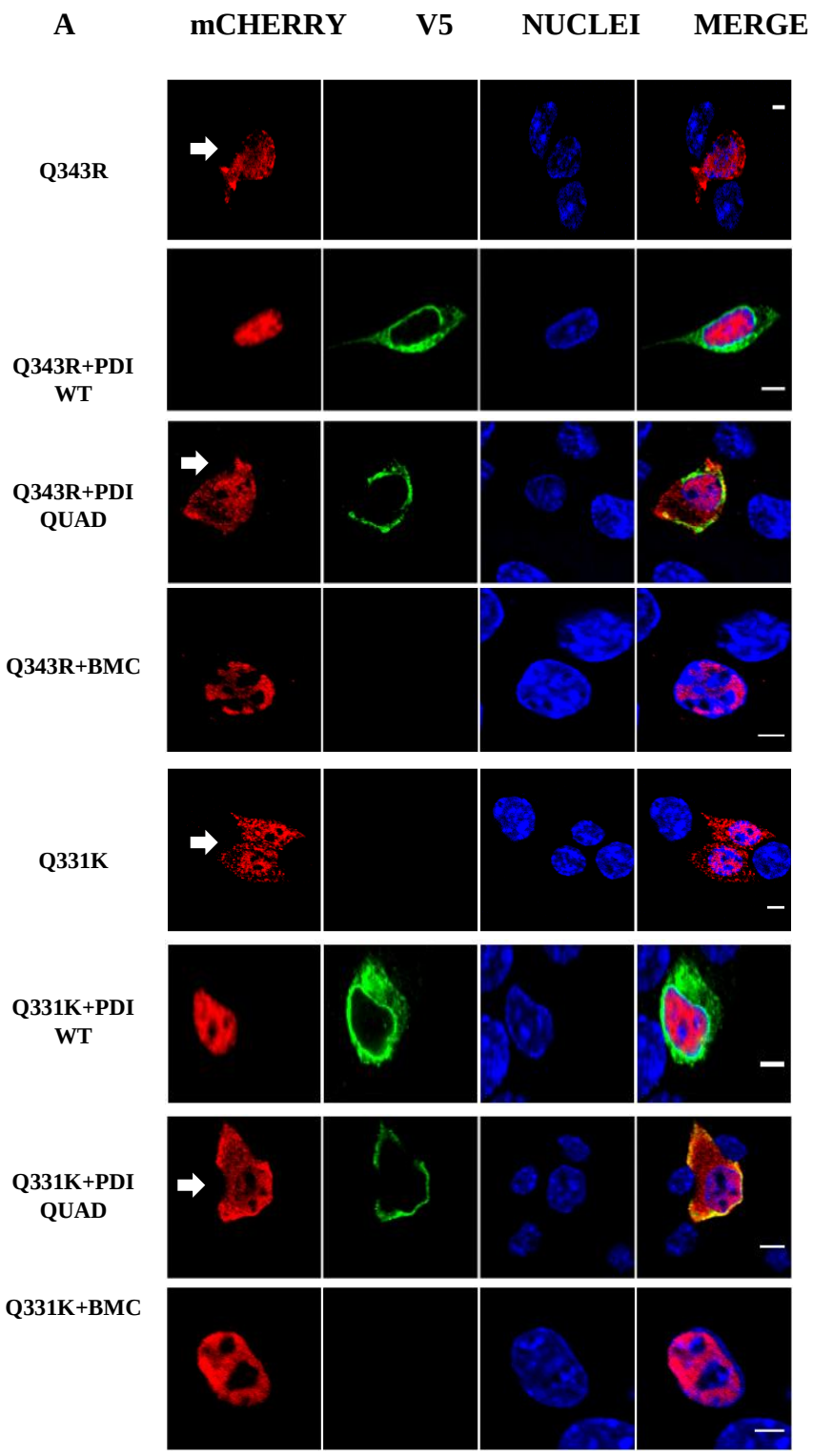
A
mCHERRY
V5
NUCLEI
MERGE
Q343R
Q343R+PDI WT
Q343R+PDI QUAD
Q343R+BMC
Q331K
Q331K+PDI WT
Q331K+PDI QUAD
Q331K+BMC

B

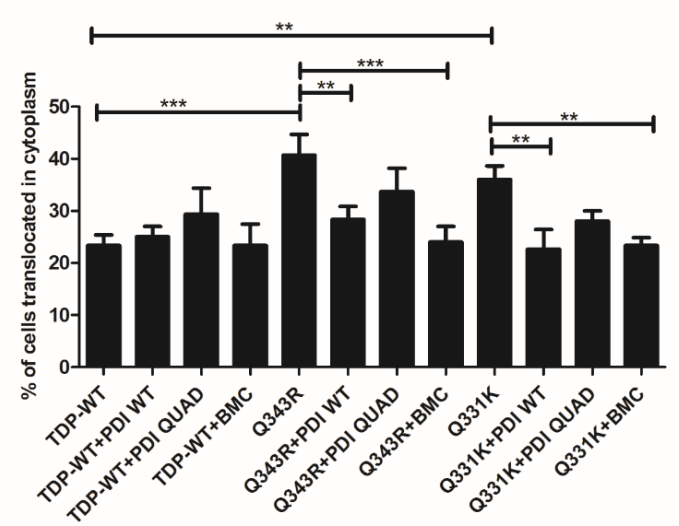

Figure 4.11 The disulphide interchange activity of PDI is protective against the cytoplasmic localisation of mutant TDP-43. A) Immunofluorescent images of Neuro2a cells co-expressing mutant TDP-43 with PDI (wild-type or QUAD). Mutant TDP-43 Q343R or Q331K (first, fifth panel) localises more in the cytoplasm compared to wild-type TDP-43, indicated with white arrow. However, on co-expression with wild-type PDI fewer cells express mutant TDP-43 in the cytoplasm (second and sixth panel). In contrast, expression of PDI QUAD did not alter the proportion of cells expressing mutant TDP-43 in the cytoplasm compared to vector only transfected cells, indicated with white arrow (third and seventh panel). Conversely on treatment with BMC, significantly fewer cells expressed mutant TDP-43 in the cytoplasm compared to vector only transfected Q343R or Q331K cells (fourth and eighth panel). Scale bar = 10 µm. **B)** Quantification of cells in (A), representing the cytoplasmic distribution of TDP-43. A significant difference in the proportion of cells expressing TDP-43 in the cytoplasm was observed between wild-type TDP-43 and mutant TDP-43 Q343R (***p<001) or Q331K (**p<.01) expressing cells. Similarly, a significant difference in the proportion of cells with cytoplasmic mutant TDP-43 was observed when Q343R or Q331K cells were co-expressed with wild-type PDI (**), or treated with BMC; Q343R (***p<.01) or (**p<.01) Q331K cells. However, there was no significant difference between the proportion of cells with cytoplasmic mutant TDP-43 in vector only or PDI QUAD transfected cells. For each of 3 replicate experiments, 100 cells were scored for each

population. Data are presented as mean ± SEM, tested with one-way ANOVA and Tukey's post-test, n = 3.

4.2.9) The disulphide interchange and chaperone activities of PDI are protective against inhibition of ER-Golgi transport in mutant FUS expressing neuronal cell lines.

A PhD student in our laboratory, Jessica Sultana, investigated the effect of expression of PDI QUAD or treatment with BMC in neuronal cell lines expressing mutant FUS. The data is presented only for reference and comparison. PDI QUAD was co-expressed with FUS in Neuro2a cells, and BMC was administered to mutant FUS expressing cells, following the same procedures as outlined in Chapter 3. Interestingly it was demonstrated that both BMC and co-expression of PDI QUAD prevented nuclear immunoreactivity to CHOP and hence the induction of ER stress, and the mislocalisation of FUS in the cytoplasm in neuronal cells expressing mutant FUS R522G and P525L. It was demonstrated that both the chaperone and the disulphide activity of PDI are protective against induction of ER stress and the cytoplasmic localisation of FUS in mutant FUS expressing cells.

The author performed additional experiments examining which of PDI's activities are protective against inhibition of ER-Golgi trafficking induced by mutant FUS (described in Chapter 3). Neuro-2a cells were co-transfected with mCherry-tagged VSVG, either EGFP-tagged wild-type FUS or mutant FUS R522G, and either empty vector or V5-tagged PDI (wild-type or QUAD). The cells were incubated at 40°C to accumulate VSVG in the ER, before incubation at the permissive temperature for 30 min. In separate groups of mutant FUS expressing cells, 25 µm BMC or DMSO vehicle control were administered 1 hr post-transfection. After fixing the cells, immunocytochemistry was performed using antibodies for markers of the ER (calnexin) and Golgi (GM130) followed by fluorescent microscopy (Figure 4.12 A). Quantification of the localisation of VSVG in either the ER or Golgi compartments was performed, using Mander's co-efficient, in the

range from 0 to 1 representing 0-100% overlapping pixels as described previously in chapter 3.

In untransfected cells (UTR) and EGFP expressing cells, as before, little VSVG (15%) was retained in the ER and most (77%) was transported to the Golgi apparatus after 30 min at the permissive temperature. Similarly, in cells expressing wild-type FUS, little (19%) VSVG was retained in the ER, because most was already transported to the Golgi (74%) at this time point. However, in cells expressing mutant FUS R522G, inhibition of ER-Golgi transport was detected relative to the other cell populations. In these cells, significantly more VSVG was retained in the ER (43%) and significantly less was transported to the Golgi after 30 min (40%). As previously described in Chapter 3 when wild-type PDI was co-expressed with mutant FUS R522G, transport between the ER-Golgi was restored to levels found in control cells; only 24% ($p<.05$) VSVG was retained in the ER and 62% ($p<.01$) VSVG was transported to Golgi. Interestingly, co-expressing PDI QUAD with mutant FUS was also found to significantly restore transport to levels that were similar to control cells. Little VSVG was retained in the ER (23%, $p<.01$) and most (60%, $p<.01$) was transported to the Golgi (Figure 4.12 B). Similarly, BMC also rescued inhibition of transport in cells expressing mutant FUS; little (21%, $p<.01$) VSVG was detected in the ER and most (61%, $p<.01$) VSVG was transported to the Golgi in BMC-treated cells. Hence, transfection with PDI QUAD or treatment with BMC are both protective against inhibition of ER-Golgi transport induced by mutant FUS. Therefore, these data suggest that both the chaperone activity and disulphide activity of PDI are protective against the inhibition of ER-Golgi transport induced by mutant FUS.

A

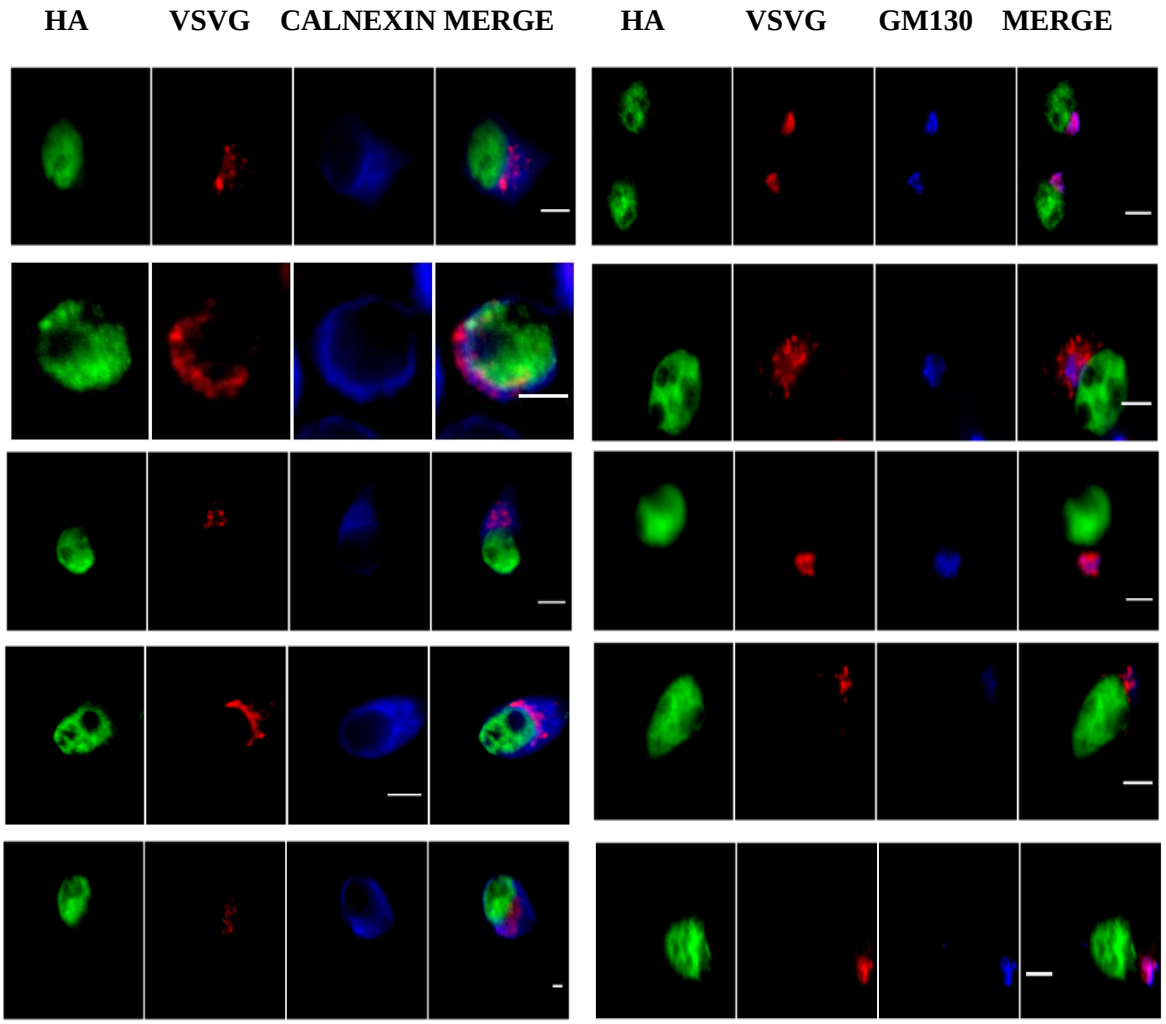
HA
VSVG
CALNEXIN
MERGE
HA
VSVG
GM130
MERGE

B

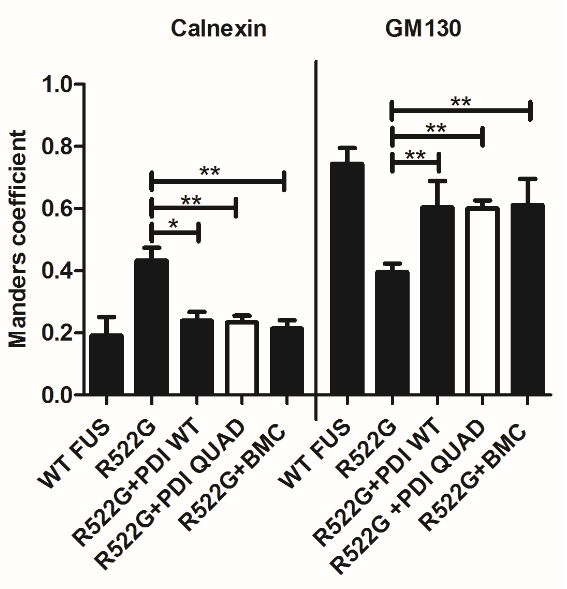
Calnexin
GM130
Manders coefficient
1.0
0.8
0.6
0.4
0.2
0.0
**
**
*
**
**
**
WT FUS
R522G
R522G+PDI WT
R522G+PDI QUAD
R522G+BMC
WT FUS
R522G
R522G+PDI WT
R522G +PDI QUAD
R522G+BMC

Figure 4.12 Both the disulphide interchange and chaperone activities of PDI are protective against inhibition of ER-Golgi transport in mutant FUS expressing cells. A) Representative fluorescent images of cells co-expressing VSVGts045-mCherry, either EGFP-tagged wild-type FUS or mutant FUS R522G, and either wild-type PDI or PDI QUAD, stained with markers of the ER (calnexin) or Golgi apparatus (GM130). VSVGts045-mCherry was trapped in the ER at 40°C and the temperature was then shifted to the permissive temperature (32°C) for 30 min, followed by fixing with 4% paraformaldehyde (PFA) at 30 min at 32°C. At 32°C VSVG is transported to Golgi and little co-localises with the ER in cells expressing wild-type FUS (first panel, FUS-WT). In contrast, in mutant FUS R522G expressing cells, VSVG co-localises significantly more with the ER and less with the Golgi (second panel). However, on over-expressing either wild-type PDI or PDI QUAD, transport was restored in mutant FUS expressing cells: VSVG co-localised more with the Golgi rather than the ER (third and fourth panel). Similarly treatment of R522G expressing cells with BMC restored transport to the Golgi (fifth panel). Scale bar = 10 μm**. B)** Quantification of the degree of co-localization of VSVGts045-mCherry with either calnexin or GM130 in FUS expressing cells in (A), using Mander's coefficient. A significant difference in the localization of VSVG within the ER was detected in mutant FUS R522G cells treated with BMC (**, p<.01), or co-expressed with either wild-type PDI (*, p<.05), or PDI QUAD (**, p<.01). Similarly, significantly more VSVG co-localised with the Golgi (**, p<.01) in mutant FUS R522G cells co-expressing either PDI wild-type, PDI QUAD or treated with BMC. Data are presented as mean ± SEM, tested with one-way ANOVA and Tukey's post-test, n = 3.

4.2.10 Administering BMC reduces the loss of motor neurons in SOD1^{G93A} mice.

Our group previously demonstrated that treatment with BMC protects against mutant SOD1 induced inclusion formation and aggregation *in vitro* [483]. It was next investigated whether BMC could recapitulate similar effects *in vivo*. The experiment was performed in collaboration with Dr. Bradley Turner, (Florey

Institute of Neuroscience and Mental Health, The University of Melbourne, Australia) who performed these *in vivo* experiments using SOD1^{G93A} mice.

At postnatal day 90 (P90), mice were anesthetized as demonstrated previously [534]. Surgical implantation of mini-osmotic pumps (Alzet model 2006, 0.15 µl per hr for 6 weeks) filled with BMC solution or PBS (vehicle control, VEH) at a dosage of 0.1 ml/10 g body weight, with 2 mice per group (total 6 animals). Lumbar spinal cord motor neurons were quantified in wild-type SOD1 transgenic mice (WT), SOD1^{G93A} mice (VEH) and BMC-treated SOD1^{G93A} mice (BMC). Administering BMC to SOD1^{G93A} mice significantly reduced the loss of motor neurons (Figure 4.13) as compared to the vehicle-treated mice alone. Motor neuron counts in treated animals were similar to non-transgenic control animals when administered with BMC. Hence, these data demonstrated that the molecular mimic of the PDI active site, BMC, is protective against motor neuron loss *in vivo*.

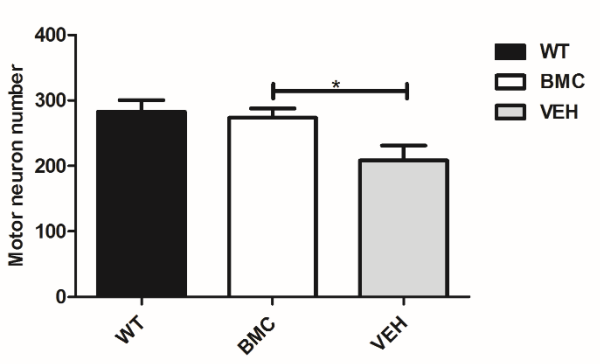

Figure 4.13 Administration of BMC rescues the loss of motor neurons in SOD1^{G93A} mice. Quantitation of the number of ventral horn motor neurons within lumbar spinal cord sections of SOD1^{G93A} mice. Data are presented as mean ± SEM, ($p<.05$) n=6. Administering BMC significantly reduced the loss of motor neuron as compared to the vehicle.

4.2.11 PNA-targeting SOD1 reduce mutant SOD1 induced inclusion formation and ER stress in neuronal cell lines.

Another therapeutic strategy, based on knockdown of SOD1 using PNAs, was next examined. Dr Belinda Abbott, La Trobe University, Melbourne, Australia, prepared a series of PNAs targeting SOD1. The results are discussed in the manuscript "Efficacy of peptide nucleic acid and conjugates against specific cellular pathologies of Amyotrophic Lateral Sclerosis" which is presented at the end of the Chapter as (Supplementary Figure 5). The author performed all the immunocytochemistry and immunoblotting experiments described on page 11 (Figure 4), page 13 (Figure 5) and page 15 (Figure 6) of the manuscript. These studies demonstrated that administration of PNA1, 6-PNA1, 7-PNA1, 8-PNA1 and 9 PNA1 all reduced the expression levels of mutant $SOD1^{A4V}$. PNA1, 6-PNA1 and 7-PNA1 reduce mutant $SOD1^{A4V}$ inclusion formation and PNA1 and 6-PNA1 reduced ER stress in neuronal cells expressing mutant $SOD1^{A4V}$. The manuscript describing these findings is currently under review at "Organic and Biomolecular Chemistry".

4.3 Discussion

PDI is the archetype of a family of chaperones that perform two major functions; (i) the formation and isomerisation of native disulphide bonds in proteins *via* disulphide interchange (oxido-reductase activity) and (ii) general chaperone activity [645]. However, the normally protective properties of PDI are probably inactivated in ALS, rendering it non-functional [483]. In Chapter 3 it was demonstrated that over-expression of PDI is protective in cells expressing mutant SOD1, mutant TDP-43 or mutant FUS in neuronal cultures. Hence, identification of the specific requirements that facilitate the protective abilities of PDI, would assist in the development of novel therapeutics that may target diverse forms of disease linked to SOD1, TDP-43 or FUS. The aim of the studies outlined in this Chapter was to investigate whether the disulphide interchange (isomerase) or chaperone activities are protective in cells expressing mutant ALS proteins; SOD1, TDP-43 and FUS. For this purpose, PDI mutants with mutations in active site cysteine residues were investigated. PDI active site mutants were previously shown to retain the chaperone activity and were unable perform disulphide isomerisation functions [602, 639, 640]. BMC has been previously developed to mimic the disulphide interchange activity of PDI [629]. The findings outlined in this chapter demonstrate that the disulphide interchange activity of PDI is necessary for its protective ability against ER stress, inclusion formation and cytoplasmic localisation of mutant TDP-43, because each of these properties were lost when the PDI QUAD mutant was co-expressed in Neuro2a cells. In contrast, the PDI QUAD mutant, which possesses only chaperone activity, reduced the proportion of mutant SOD1 expressing cells undergoing apoptosis and the proportion of mutant FUS expressing cells that induce ER stress or express mutant FUS in the cytoplasm.

Mutations in SOD1 cause conformational changes that have been linked to the formation of intermolecular disulphide bonds between non-native cysteine residues that induce aggregation [646]. Furthermore, those SOD1 mutations with the highest propensity to aggregate are the most unstable, and cause the most aggressive and rapidly progressing form of ALS [647, 648]. The PDI QUAD mutant and the other PDI mutants (C2, C6, C26, A and A') were not protective

against the formation of mutant SOD1 inclusions. This implies that the disulphide interchange activity of PDI is essential for its protection against mutant SOD1. Conversely, another study previously demonstrated that a similar PDI mutant with all four cysteine residues deleted (SXXS SXXS) was protective against mutant SOD1 G93A aggregation, demonstrated using biochemical western analysis although wild-type PDI was considerably more effective. However, HEK cells rather than neuronal cells were used in this study, and mutant SOD1 may be less prone to aggregation in these cells than in neuronal cells. Similarly, neuronal cells might be more vulnerable than other cell types to the effect of inclusion formation [533].

All cysteine deficient PDI mutants demonstrated similar properties to the PDI QUAD mutant. Hence, mutation in a single cysteine residue of only one active site resulted in loss of protective effects of PDI against mutant SOD1. It has been previously demonstrated that PDI mutants in which mutation in a single residue in only one active site are less effective than wild-type PDI as catalysis of disulphide rearrangements is slowed. Hence, a similar pattern may exist in this study [649]. The active site cysteine residues are clearly important in terms of PDI function as they bind to misfolded proteins and therefore contribute to protein stabilization [506]. Hence, here PDI may bind to mutant SOD1 oligomers and hence reduce SOD1 misfolding, which would further inhibit the formation of inclusions. It should be noted that inclusions per se may not directly trigger cell death [650, 651]. Consistent with this notion, other studies have suggested that the monomeric and oligomeric forms of misfolded ALS linked SOD1 are the actual toxic species to motor neurons [334]. Therefore, in future studies it would be worth examining the effect of PDI on SOD1 monomer or oligomer formation directly, to further understand the mode of protection It is possible that PDI stabilises the formation of the SOD1 dimer *via* its disulphide interchange activity, in order to prevent monomerisation, oligomerisation and thus prevent inclusion formation. It would also be worthwhile to further probe the structural regions of PDI using site-directed mutagenesis, so that the protective properties could be further refined. These

investigations may be lead to the design of novel therapeutic compounds based on the protective properties of PDI.

Although PDI is an ER chaperone and therefore inhibits protein misfolding, the PDI mutants with only chaperone activity, were not protective against ER stress induced by mutant SOD1. The reasons for this are unclear but may also relate to protein aggregation of mutant SOD1 as described above. Alternatively, the disulphide interchange activity of PDI may assist in the isomerisation and formation of disulphide bonds in other proteins, which may generally decrease the levels of stress within the ER. The substrate binding *b* and *b'* domains of PDI which are essential for the chaperone activity of PDI bind to the hydrophobic regions of misfolded proteins However, complex isomerisation reactions that involve extensive conformational changes in the substrate require all of the PDI domains together [508], suggesting that the chaperone activity of PDI alone cannot protect against the load of misfolded proteins and induction of ER stress. Another possibility is that since mutant SOD1 interacts with PDI [447], this interaction could perturb the chaperone activity of PDI, rendering it non-functional. Also, mutant SOD1 association and disruption of important ERAD proteins such as Derlin-1 could induce irreversible ER stress which could explain the loss of protective chaperone function [485]. Similar observations were made when examining the effect of PDI QUAD on inhibition of ER-Golgi transport in mutant SOD1 expressing neuronal cells. The PDI QUAD did not restore transport of VSVG, suggesting that the disulphide interchange activity of PDI is also necessary for this protective activity in neuronal cells.

However, all PDI mutants were protective against the formation of apoptotic nuclei in cells expressing mutant SOD1. DNA fragmentation is considered as a late marker of apoptosis, hence these data suggest that the chaperone activity of PDI is protective during the final stages of apoptosis. However, it would be worthwhile also investigating the effect of mutant PDI constructs on early markers of apoptosis, such as activation of recruitment of Bax [572, 624] to confirm the finding that the

chaperone activity of PDI is protective against apoptotic cell death. It remains unclear as to why the chaperone activity is protective however, it could be speculated that this mechanism is used by the cell as a last resort to restore cellular homeostasis.

Mutant TDP-43 has been demonstrated to form aberrant, non-native disulphide bonds, which contribute to aggregation under cellular stress conditions *in vitro* [652]. Hence, it could be speculated that the disulphide interchange activity of PDI assists in preventing the formation of these mutant TDP-43 aggregates. This is consistent with the finding that the PDI QUAD mutant was not protective against ER stress, ER-Golgi transport defects and mislocalisation in the cytoplasm in mutant TDP-43 expressing cells. This implies that the non-native disulphide bonds in mutant TDP-43 produce aggregates that contribute to ER stress, ER-Golgi transport inhibition and mislocalisation to the cytoplasm. However, it should be noted that there was a slight, but non-significant decrease, in the proportion of mutant TDP-43 expressing cells displaying these cellular pathologies when the PDI QUAD was over-expressed. Further studies may be required to investigate this further because it is possible that the use of other assays, with greater sensitivities than the ones used here, may've resulted in more pronounced differences when PDI QUAD was overexpressed with mutant TDP-43. Therefore, we cannot completely eliminate the possibility that the chaperone activity has some protective effects against mutant TDP-43.

However, contrasting results were obtained in cells expressing mutant FUS. Over-expression of PDI QUAD was protective against ER stress, ER-Golgi transport defects and mislocalisation of mutant FUS to the cytoplasm in these cells. TDP-43 and FUS have similar structures and functions and they share some DNA/RNA targets [153]. However, they do bind to different sets of cytoplasmic mRNAs in neuronal cultures [653]. Hence, it could be speculated that the two proteins may be involved in pathology *via* different mechanisms.

FUS contains 4 cysteine residues but the presence of disulphide bonds in FUS has not been demonstrated [654]. In preliminary experiments by our laboratory we could not detect the presence of disulphide bonds in FUS. Hence, there is currently no evidence that the aggregation of FUS is linked to disulphide bond formation, unlike mutant TDP-43 and mutant SOD1. It is possible that the disulphide inter-change activity of PDI is not necessary for its protective activity in cells expressing mutant FUS. The differences between the results obtained for SOD1, TDP-43 and FUS imply that aberrant disulphide bonds could be primary drivers of pathology in cells expressing mutant SOD1 or mutant TDP-43, but this is not the case for FUS, revealing important differences in pathological processes in each case. FUS bears prion-like domain and its aggregation has been previously linked to the presence of this domain [655]. Furthermore, PDI interacts with prion-like misfolded proteins [656]. This implies that PDI acts as a general chaperone by binding to FUS *via* the prion-like domain and thus may exert its protective activity by refolding misfolded FUS proteins. However, the chaperone activity is not the only factor to consider since BMC was also protective in cells expressing mutant FUS. Therefore, this finding suggests that the disulphide interchange activity of PDI is also essential for protection against mutant FUS. It could also be postulated that BMC is protective in an indirect way, such as by preventing the misfolding of other disulphide bonded proteins in cells expressing FUS, and thus overall improving disulphide bond formation in the cell.

Our laboratory previously demonstrated that BMC was protective against mutant SOD1 aggregation and inclusion formation in cellular ALS models [483]. In preliminary studies, its importance was also validated *in vivo*, suggesting that PDI mimics may be relevant to disease pathology. In this study, BMC was protective against inhibition of ER-Golgi transport and ER stress in cells expressing mutant SOD1, TDP-43 or FUS, and it was also protective against mislocalisation of mutant TDP-43 or mutant FUS in the cytoplasm in cell culture. BMC possesses similar oxidoreductase properties and possess the equivalent reduction potential as that of the active site of PDI [629]. BMC could induce the efficient folding of protein substrates by acting as a direct catalyst and thus assisting the protein folding

machinery to reach a redox active state. Administration of BMC may induce an oxidising environment in the cells as observed *in vitro* addition of 10 µm BMC increases the yield of native disulphide bonded proinsulin by two fold [657]. Also 100 µm BMC increases the secretion of recombinant immunoglobins expressed in Chinese Hamster Ovary (CHO) cells [658]. Since BMC is a reducing agent it may also influence the mitochondrial redox potential. Furthermore the presence of BMC in the ER may be an important consideration for BMC to mimic the properties of PDI. One study demonstrated that administration of BMC increases the secretion of heterologous proteins in yeast cells and that BMC was able to enter the ER [629].

Our findings show it mimics the same protective activities of PDI in cells expressing mutant SOD1, TDP-43 or FUS. These results further validate that the disulphide interchange activity of PDI is protective in ALS. Hence it is possible that other mimics of PDI such as active-site bis (cysteinyl) fragments may be beneficial against these ALS mutant proteins [630]. Furthermore, CGC peptide has been demonstrated to perform isomerisation functions *in vitro* [659]. However, a mono-thiol analogue (CxxC) of BMC was inefficient in reducing protein aggregation suggesting that the presence of all four cysteine residues in the active site are necessary for the formation of native disulphide bonds [649, 660], which is consistent with the findings obtained here using the panel of PDI mutants BMC is not substrate specific, hence, administration of BMC may be creating a more reducing cellular environment. This in turn may facilitate more efficient disulphide bond formation and isomerisation by endogenous PDI, because PDI is known to require these conditions for activity [661].

PDI is a redox dependent chaperone, and cellular redox conditions also determine the oxidoreductase properties of PDI [538]. The oxidative environment of the ER assists PDI in the formation of disulphide bonds in proteins. However, during unfavourable conditions it becomes more reducing [662, 663]. Therefore, specific experiments should be conducted in the future to investigate how cellular redox conditions regulate PDI function in relation to SOD1, TDP-43 and FUS, and also if

or how this becomes altered during ALS, which would help elucidate the mechanism of action of PDI in this disorder. PDI may act as a redox-dependent switch, and it acts as a chaperone or an isomerase depending upon the redox conditions. Since the active cysteine residues are also redox defined by post-translation modifications due to cellular stressors, this may also similarly regulate the chaperone or isomerase activity. Site-directed mutagenesis of PDI (removal of domains/modification of the redox active sites of PDI) could further assist in understanding of the minimum requirements necessary for the protective activity of PDI, which would be beneficial in designing new therapeutics based on PDI's function. Furthermore, to completely understand the mechanistic details of PDI function, the substrate specificity of PDI should also be investigated, since it binds non-specifically to aggregated proteins and assists in their native folding [539]. Furthermore, studies leading to identification of other proteins that interact with PDI, whether or how PDI collaborates with other ER residents, and investigations of possible substitutive pathways for disulphide formation, are therefore warranted. The PDI family members are able to recompense for each other, and they may also assist in shedding light on the mechanisms of action of PDI, which is discussed further in Chapter 5.

In summary, this study reveals that the disulphide interchange activity of PDI is an important feature of PDI activity in ALS, and it is protective in cells expressing mutant SOD1, TDP-43 and FUS in cellular models of ALS. Furthermore, the chaperone activity is also protective in the case of mutant FUS. Understanding the key features that mediate the protective activity of PDI may facilitate future studies that aim to develop therapeutic targets in protein misfolding disorders. The preliminary findings that BMC is protective *in vivo* add weight to this argument and investigations into the protective abilities of PDI mimics of PDI are therefore warranted.

Chapter 5 Examining the role of PDI family members ERp57 and ERp72 in ALS

5.1 Introduction

The PDI family comprises of more than 21 members that share similar signal sequence, active site motif (CXXC) and at least one thioredoxin-like domain [505]. Although it is implied that all PDI family members possess the ability to rearrange disulphide bonds, only some members have been shown to actually perform these physiological activities *in vivo* and the rest are associated to the PDI family through evolution rather than function [664]. The PDI family members that possess disulphide interchange activity assist in the formation and isomerisation of disulphide bonds within protein substrates, thereby assisting proteins to achieve their active confirmation in their fully folded states [665]. In addition, some members also possess chaperone-like activities and assist in the degradation of misfolded proteins [666]. PDI family members primarily vary in their substrate specificity and enzymatic activity due to their differing redox potentials [535]. The enzymatic activity relies on the sequence of the active site generally, and the residues around the active site that modulate the cysteine residues [666].

Sequence alignment reveals that PDI family members ERp57 and ERp72 are the most similar to PDI [667, 668]. The PDI members that have been studied in most detail are ERp44, ERp18, ERdj5 and PDIp (Figure 5.1). ERp57 and PDIp share the same active site motif (CXXC), and the same domain architecture (*a-b-b'-a'-c)* with PDI. However, ERp57 mediates disulphide bond formation primarily in glycosylated proteins by interacting with the ER-resident lectins, calnexin or calreticulin [669]. Conversely, PDI can bind non-specifically to a large number of substrates, including non-glycosylated proteins [670]. PDIp is only expressed in pancreatic cells suggesting that it functions as a protein-folding catalyst for secretory digestive enzymes [671]. ERp72 is the second largest protein in the PDI family, which possess three catalytically active domains and has an overall (31%) sequence similarity to PDI [672]. Since PDI family members share sequence similarities with the archetype PDI, it is possible that ERp57 and ERp72, which are the closest homologues of PDI may have interchangeable and overlapping functions. Therefore, this chapter focuses on the role of the PDI family members

ERp57 and ERp72 and their effect on the pathological effects triggered by mutant SOD1, FUS and TDP-43 in neuronal cells.

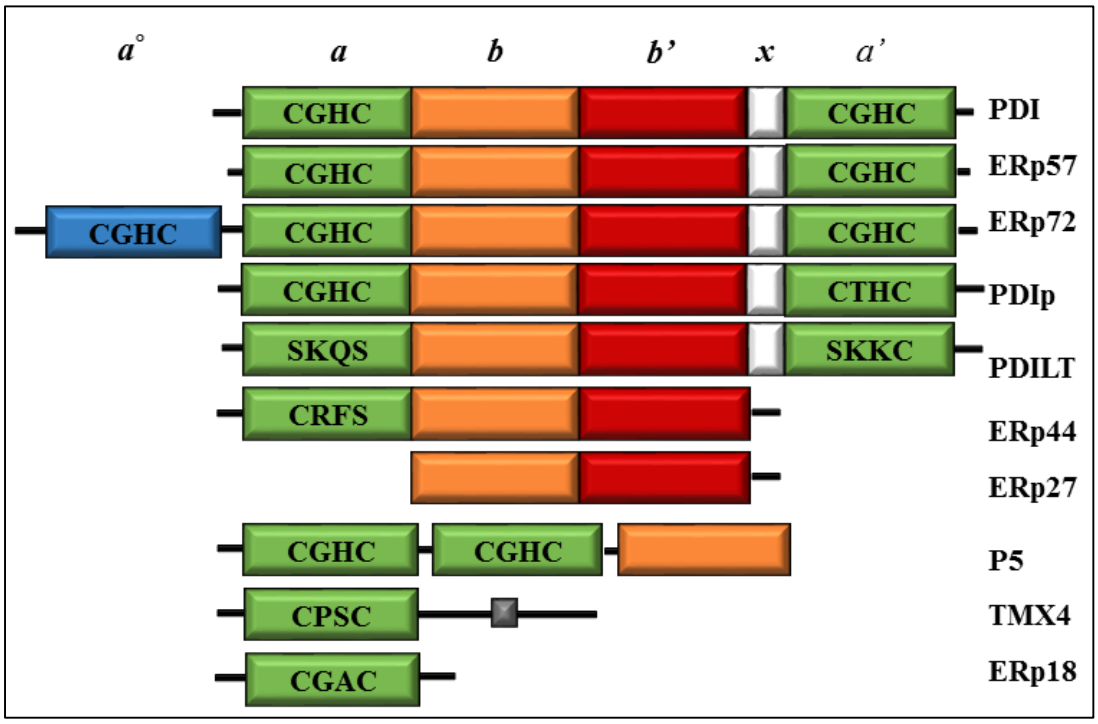

Figure 5.1 Schematic diagram of the most common PDI family members. Green represents the catalytic domains, *a* and *a'*. The domains coloured orange represent the non-catalytic *b* domains, and red represents the *b'* domains that facilitate substrate binding. The sequence coloured white represents the linker region (x) which allows flexibility between domains. Finally, the transmembrane region is represented in grey. ERp72 is the only PDI family member which has three catalytic domains. The third catalytic domain of ERp72 is termed '*a°'* and is represented here in blue.

5.1.1 Endoplasmic Reticulum protein 57 (ERp57)

ERp57, which is also known as PDIA3 or HIP-70, is the second most abundant soluble protein after PDI found in the ER. It can also localise in other non-ER compartments such as the cytosol, mitochondria, cell surface and the nucleus, under varied conditions [673]. It was first discovered in the hamster fibroblast cell

line K12 and it was originally named ‘glucose regulated protein (GRp58)’ since its expression increased after glucose depletion [674]. Encoded by the gene *PDIA3*, human ERp57 is situated on chromosome 15, and is 505 amino acids long, with a molecular weight of 57 kDa. ERp57 is ubiquitously distributed in most tissues however, it is expressed at considerably higher levels in secretory cells compared to other tissues [675]. ERp57 has an overall 33% sequence similarity with PDI making it the closest homologue. However, extremely low sequence similarity (17%) is observed in the substrate binding *b’* domain [538, 676]. The redox potential, which determines the catalytic properties of ERp57, is less than that of PDI, making ERp57 more reducing in nature [677, 678]. ERp57 performs numerous activities such as accelerating the oxidative refolding of RNase B [678], participating in the assembly of the major histocompatibility complex (MHC) class I peptide (independent of its enzymatic activity) [679], and folding and maturation of influenza heamagglutinin in association with the chaperone tapasin [680, 681]. Recently, it was demonstrated that ERp57 assists peripheral nerve regeneration in ERp57 transgenic mice [682]. Predominately, like PDI, the main function of ERp57 is an oxidoreductase to facilitate the isomerisation and formation of native disulphide bonds in proteins [674].

Studies have demonstrated that ERp57 also assists PDI and other PDI family members in protein folding, and that ERp57 reacts non-specifically with small ligands and some macromolecules [673]. ERp57 and PDI participate simultaneously in the formation of disulphide-linked complexes with thyroglobulin, during the production and isomerisation of its new disulphide bonds [683]. PDI and ERp57 are also crucial for the optimal folding of transferrin [684]. Furthermore, knockdown of both PDI and ERp57 together leads to protein misfolding and impaired export of proteins such as α-fetoprotein from the ER in human hepatoma cells [685]. ERp57 has also been shown to interact with ERp27 in a similar method ERp57 interacts with calreticulin. However, the exact cellular function of this interaction with ERp27 is unknown, although it is hypothesised to play a role in quality control of non-glycosylated proteins [686]. Deletion of ERp57 using siRNA in fibroblasts does not induce ER stress, and neither is the oxidation

of glycoproteins affected [687]. However, ERp57 deficiency is lethal in mice at early embryonic stages, possibly due to modulation of signal transducer and activator of transcription 3 (STAT3) signalling [688].

5.1.2 Structure of ERp57

ERp57 contains four analogous domains to PDI (*a*-*b*-*b'*-*a'*). Most similarity (46%) to PDI is found between the *a* and *a'* domain, whereas there is lesser similarity (~20%) between the *b* and *b'* domains [689]. All the four domains together assist in the formation and isomerisation of disulphide bonds within the unfolded protein substrate [674]. Crystallographic studies reveal that the four domains of human ERp57 form a U-shaped struture, allowing the two terminal *a* and *a'* domains to face each other and interact together with other proteins [684]. The two central domains of ERp57 *b* and *b'*, form the binding site for calreticulin and calnexin [690]. However, the PDI substrate binding *b'* domain is different to that of ERp57 in that it binds to small ligands and not these lectin chaperones [508]. The *b* and *b'* domains of ERp57 contain the basic residues K214, K274 and R282, which are highly conserved and are essential for binding to lectin-like chaperones [691]. The *b* domain of ERp57 interacts with the arm-like P-domains of calnexin and calreticulin [21]. For both ERp57 and PDI the oxidative and catalytic properties depends on charged glutamic acid and lysine residues, found near the active CGHC site [505].

5.1.3 Role of ERp57 in neurodegenerative diseases

ERp57 has been linked to several neurodegenerative diseases. ERp57 has been detected in the CSF of Alzheimer's patients, where it physically associates and reduces the aggregation of β-amyloid peptides [692]. ERp57 and PDI were found to be up-regulated in two gene profile studies in cellular models of Parkinson Disease (PD), where they were identified as a global response to ER stress [693, 694]. However, oxidation of ERp57 due to oxidative stress causes accumulation of

high molecular weight ERp57-containing aggregates in PD *in vitro* models [695]. In prion disorders, misfolded prion proteins induce ER stress in neuronal cell cultures, and the levels of ERp57 correlate with the levels of prion misfolding [696]. However, ERp57 levels were inversely correlated with the degree of neuronal injury in murine models, suggesting ERp57 has a protective role against prion neurotoxicity [696]. ERp57 has also been previously linked to ALS. Both ERp57 and PDI are up-regulated during ER stress in transgenic $SOD1^{G93A}$ mice, and also in lumbar spinal cord tissues and CSF of sALS patients [470]. PDI and ERp57 were also identified as potential biomarkers for ALS using peripheral blood mononuclear cells [530]. Recently, missense variants in the *PDIA1* and *ERp57* genes were detected in ALS patients using exome sequencing, suggesting a possible contribution of these genetic mutations to disease pathology [697].

5.1.4 Endoplasmic reticulum protein 72 (ERp72)

ERp72 is a 72 kDa protein which is predominately found in the lumen of the ER, but it has also been detected on the cell membrane [668, 698]. ERp72 is also known as protein disulphide isomerase 4 (PDIA4) or calcium binding protein (CaBP2) [699]. It is the only member of the PDI family with three catalytic domains (containing active site residues, CGHC), thus it possesses similar redox properties to PDI and ERp57 [700]. The catalytic domain (*a* and *a'*) of ERp72 is similar to PDI, showing 48% sequence similarity, but overall ERp72 has lower sequence similarity to PDI [672, 701]. ERp72 has an overall structural similarity of 40% with ERp57 (more than ERp57 has with PDI), and it may also substitute for ERp57 in the folding of specific proteins [687], although it does not bind to glycoproteins. Because ERp72 has interchangeable activities with ERp57, it has been suggested to compensate for deficiency of ERp57 in knockout cells [702]. The similarities observed between PDI and ERp57 imply that ERp72 has a role in the rearrangement of disulphide bonds. Furthermore, ERp72 has been detected in complexes with class II MHC and it may therefore assist in the assembly of these molecules [703]. ERp72 is part of a large complex of chaperones, including PDI and BiP, which forms an ER network that binds to unfolded protein substrates, instead of existing as free

molecules [704]. ERp72 is important for the isomerisation of disulphide bonds in bovine pancreatic trypsin inhibitor [705], and it associates with transporter associated with antigen processing (TAP), and assists TAP in transporting peptides to ER [700]. ERp72 also associates with BiP and together the ERp72-BiP complex assists in the folding of apolipoprotein B [706].

5.1.5 Structure of ERp72

The structure of ERp72 is composed of five thioredoxin-like domains (*a°-a-a'-b-b')* , and the conserved CGHC motif is found in all three active catalytic domains, *a°*, *a* and *a'* [691]. The non-catalytic domains *b* and *b'* bind substrates, although not much information is available regarding the substrate specificity of ERp72. Analysis from small angle x-ray scattering studies in rat suggests that the structure of ERp72 adopts a crescent shape, where the *a°* domain is situated in the same plane as the other two catalytic domains *a* and *a'* [672]. The *a'* domain of ERp72 is structurally similar to the *a'* domain of PDI (48%) [707], whereas the *a°* domain of ERp72 is more analogous to the *a* domain of PDI, (54% identity, rather than the *a'* domain of PDI. This implies that duplication of the *a* domain may have occurred during evolution [672]. Following the *a°* domain is a repetitive stretch of aspartic acid and glutamic acid residues, which are responsible for binding to calcium ions and positively charged ER substrates [699]. The non-catalytic *b* and *b'* domains of ERp72 are 22% and 35% similar to the *b* and *b'* domains of ERp57 [707]. ERp72 does not bind to lectin chaperones as it lacks positive residues in the *bb'* fragment, which are responsible for binding of substrates [707]. The C-terminus of ERp72 consists of negatively charged residues similar to PDI [510]. It possess a KEEL sequence instead of the conventional KDEL sequence for ER retention [708].

5.1.6 Aim

The PDI family members ERp57 and ERp72 have structural and functional similarities to PDI, but they have not been studied before in relation to protection

in ALS. However it could be hypothesized that they might be protective against mutant SOD1, TDP-43 and FUS, due to their similarity to PDI. The aim of the studies described in this chapter was to investigate the role of PDI family members ERp57 and ERp72 in ALS. Studies were performed in which the effect of ERp57 in neuronal cells expressing mutant SOD1 was examined. The findings of these experiments, that ERp57 was protective against mutant SOD1 inclusion formation, ER stress and apoptosis, is presented as a manuscript in the (Supplementary Figure 6). Investigations into whether ERp57 and ERp72 were protective in cells expressing mutant FUS or TDP-43 are presented below. In all of these studies, catalytically inactive mutants of ERp57 and ERp72 were also examined, to provide insights into the mechanism of these proteins in their protective activities.

5.2 Results

5.2.1 Expression of ERp57 and ERp72 constructs in Neuro2a cells.

Previously generated pcDNA3.1(+) constructs encoding wild-type ERp57, mutant ERp57 (C24A_ERp57), wild-type ERp72 or mutant ERp72 (C26A_ERp72) were a generous gift from Dr Neil Bullied, Glasgow, UK [536]. The mutant constructs contain mutations in the active site of either ERp57 or ERp72, where the second cysteine residue of each catalytic domain is mutated to alanine (CGHC - CGHA). In C24A_ERp57 one cysteine residue in both the *a* and *a'* domains were mutated to alanine, whereas in C26A_ERp72, cysteine residues of only two of the catalytic domains, *a°* and *a',* were mutated to alanine (Figure 5.2 A).

Neuro2a cells were transfected with ERp57 and ERp72 and examined at 72 hr post transfection. The cells were fixed and then probed with anti-V5-tag and anti-calreticulin antibodies using immunocytochemistry. The subcellular localization of wild-type ERp57, C24A_ERp57, ERp72 wild-type and C26A_ERp72 expressed in these cells was examined using confocal fluorescent microscopy (Figure 5.2.B). Both wild-type and mutant forms of ERp57 and ERp72 co-localised with ER marker calreticulin, thus confirming their subcellular localisation in the ER, as expected. These data also demonstrate that the cysteine mutations do not alter the cellular localisation of C24A_ERp57 or C26A_ERp72.

A

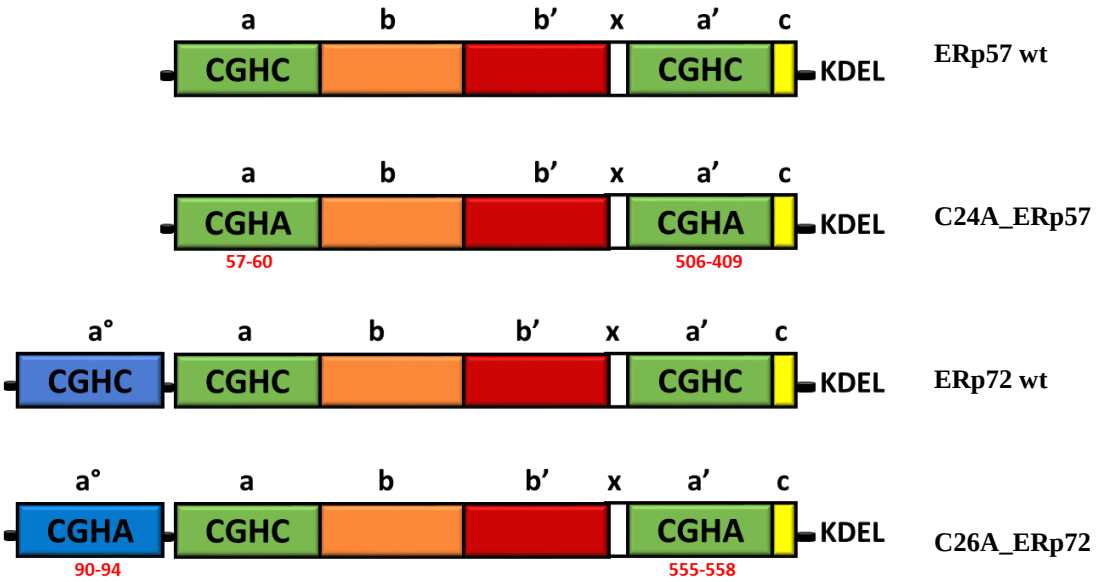
a
b
b'
x
a'
c
CGHC
CGHC
KDEL
ERp57 wt
CGHA
CGHA
57-60
506-409
C24A_ERp57
a°
CGHC
ERp72 wt
CGHA
90-94
555-558
C26A_ERp72

B

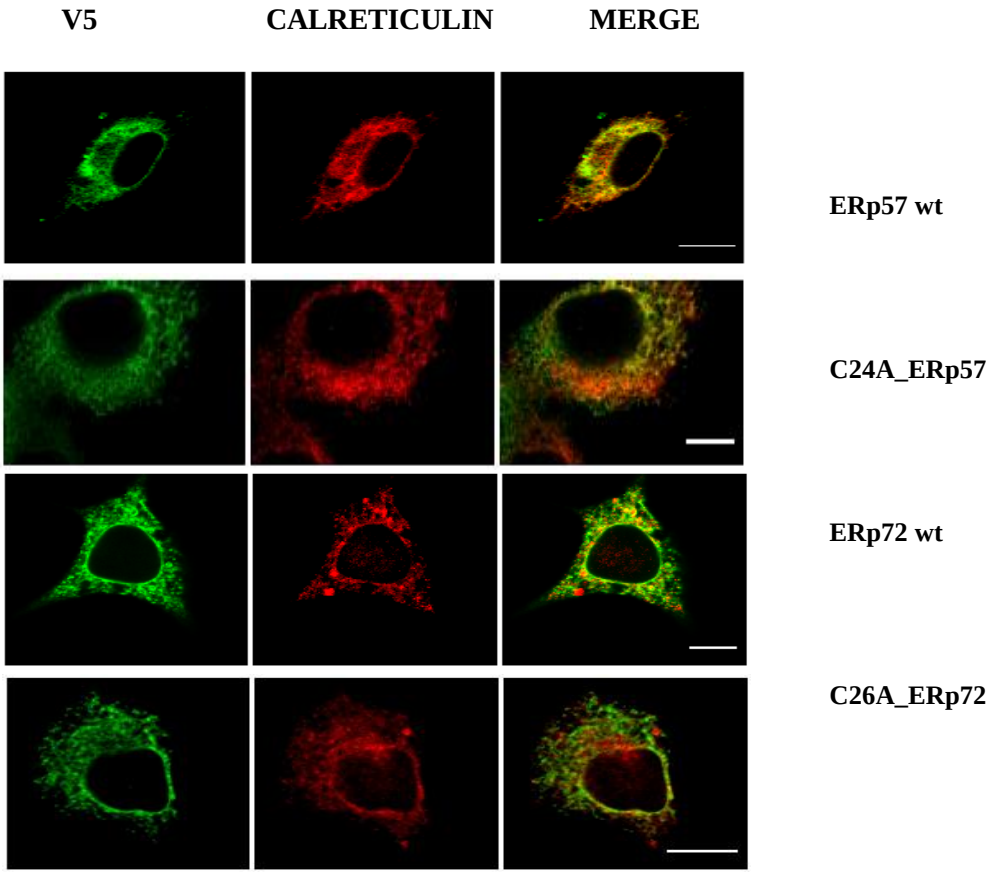
V5
CALRETICULIN
MERGE
ERp57 wt
C24A_ERp57
ERp72 wt
C26A_ERp72

Figure 5.2 Expression of ERp57 and ERp72 in Neuro2a cells A) Schematic representation of wild-type ERp57, C24A_ERp57, wild-type ERp72 and C26A_ERp72.The active site residues CGHC in the catalytic a and a' domains, which are shown in green, were mutated to CGHA in the construct expressing C24A_ERp57. Similarly, cysteine residues of catalytic domains a° and a', were mutated in the construct expressing same C26A_ERp72, as shown in blue and green. Numbers represent the position in the amino acid sequence on the active site residues. **B)** Confocal microscopy images of wild-type and mutant forms of ERp57 and ERp72 expressed in Neuro2a cells. ERp57 and ERp72 expressing cells were examined after 72 hr post-transfection and the cells were fixed and then probed with anti-V5-tag (first column) and anti-calreticulin (second column) antibodies using immunocytochemistry. The third column is a merge of the fluorescent images obtained from immunocytochemistry using anti-V5 and anti-calreticulin antibodies. Scale bar = 10µm.

5.2.2 Over-expression of ERp57 is protective against ALS mutant SOD1 expressed in neuronal cell culture.

The results of this section are discussed in the manuscript "ERp57 protects against toxicity induced by mutant SOD1 in ALS". The author performed all the experiments described in the manuscript except where acknowledgments are made. This manuscript is presented in the (Supplementary Figure 6) to this chapter.

5.2.3 Over-expression of ERp72 is not protective against mutant SOD1 inclusion formation in neuronal cultures.

This result was obtained as a part of the author's Masters Research study, and hence is only presented for reference and comparison. The author examined whether over-expression of ERp72 was protective against mutant SOD1 inclusion formation. ERp72 was co-expressed with SOD1 in neuronal cell lines (NSC-34 and Neuro2a) following the same procedures as for PDI, as outlined in Chapter 4. Unlike the results obtained for PDI, no decrease in the number of transfected cells forming inclusions was observed when ERp72 was co-expressed with mutant $SOD1^{A4V}$ and

$SOD1^{G85R}$. Hence these data imply that ERp72 is not protective against mutant SOD1 inclusion formation.

5.2.4 Over-expression of ERp57 and ERp7 is protective against mutant FUS induced ER stress in neuronal cultures.

In chapter 4 it was previously established that over-expression of either wild-type PDI or the PDI QUAD was protective against ER stress induced by mutant FUS. Therefore, it was examined whether PDI family members ERp57 and ERp72 were also protective against ER stress induced by mutant FUS. Neuro2a cells were transfected with wild-type FUS (FUS-WT) or mutant FUS (R522G) and co-transfected with either wild-type ERp57, C24A_ERp57, wild-type ERp72 or C26A_ERp72. Immunocytochemistry was performed using anti-HA antibodies to detect FUS expression and anti-CHOP antibodies to detect ER stress. Transfected cells were observed 72 hr post transfection using fluorescence microscopy to detect nuclear CHOP immunoreactivity as a marker of induction of ER stress (Figure 5.3 A).

Only 11% of untransfected cells were found to display nuclear CHOP immunoreactivity. Similarly, in wild-type FUS expressing cells, few cells (11%) cells expressed CHOP in the nucleus. However, in contrast, 67% of cells expressing mutant FUS R522G displayed nuclear CHOP immunoreactivity (Figure 5.3 B), but this was significantly reduced to 43% ($p<.01$) upon co-expression with wild-type ERp57. Hence ERp57 is protective against ER stress induced by mutant FUS. Similarly, when wild-type ERp72 was co-expressed with mutant FUS R522G, significantly fewer cells (48%, $p<.05$) displayed nuclear CHOP immunoreactivity, indicating that ERp72 is also protective against ER stress induced by mutant FUS. Next, C24A_ERp57 and C26A_ERp72 were over-expressed with FUS R522G. Similar to wildtype ERp57, significantly fewer cells co-expressing C24A_ERp57 with FUS displayed nuclear CHOP immunoreactivity (44% $p<.01$) compared to cells expressing vector alone. In contrast, no significant difference in

nuclear CHOP immunoreactivity was observed between cells co-expressing C26A_ERp72 (66%) and those expressing vector only. These results suggest that wild-type ERp57, C24A_ERp57 and wild-type ERp72 are protective against ER stress-induced by mutant FUS.

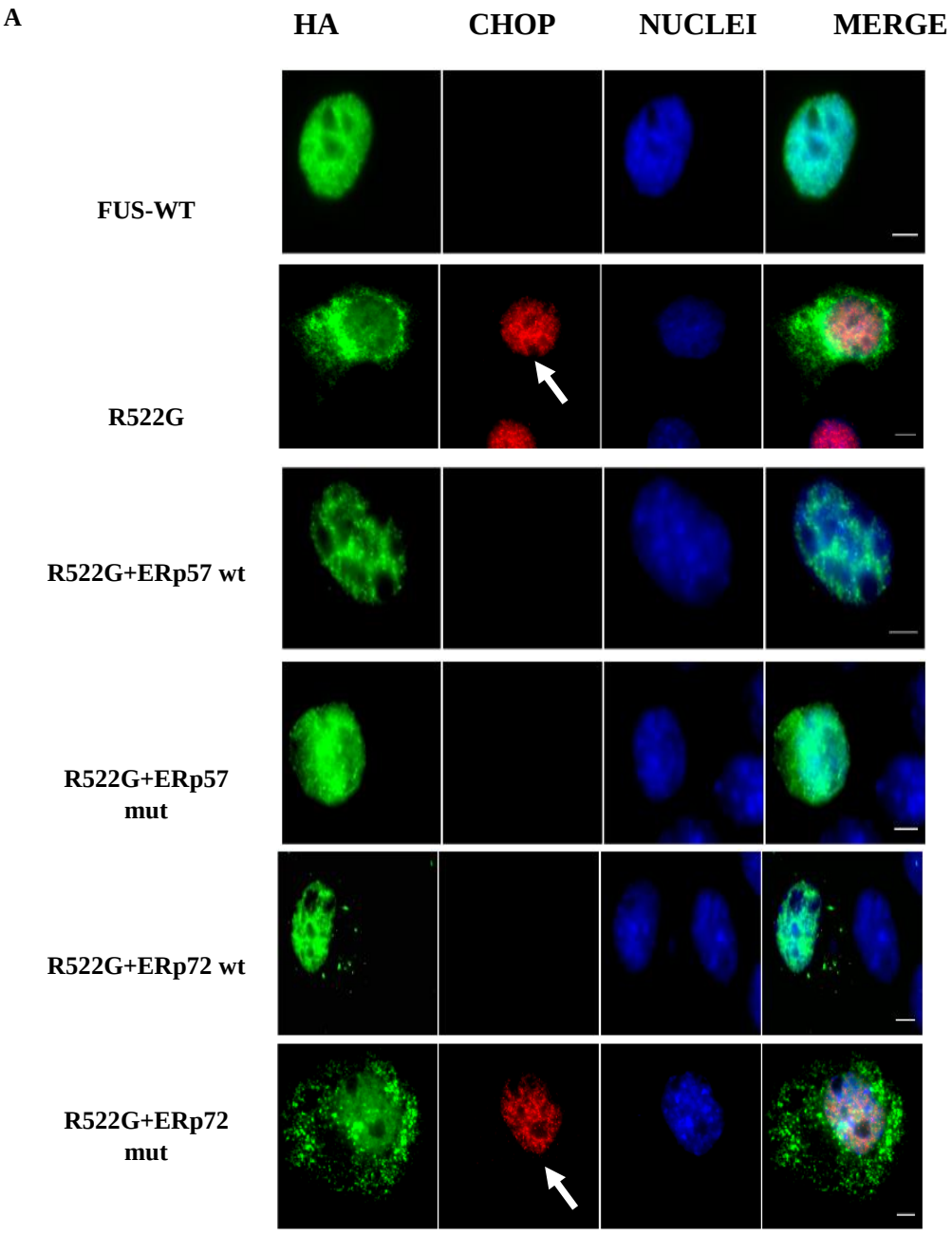
A
HA
CHOP
NUCLEI
MERGE
FUS-WT
R522G
R522G+ERp57 wt
R522G+ERp57 mut
R522G+ERp72 wt
R522G+ERp72 mut

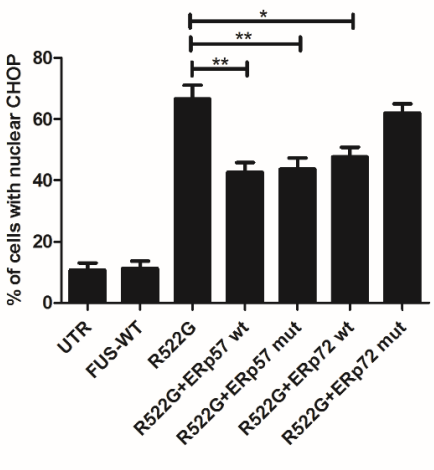
% of cells with nuclear CHOP
0
20
40
60
80
*
**
**
UTR
FUS-WT
R522G
R522G+ERp57 wt
R522G+ERp57 mut
R522G+ERp72 wt
R522G+ERp72 mut

Figure 5.3 Over-expression of wild-type ERp57, C24A_ERp57 and wild-type ERp72 reduces CHOP activation induced by mutant FUS in Neuro2a cells. A) Immunofluorescence images of Neuro2a cells co-expressing mutant FUS R522G with ERp57 and ERp72. Neuro2a cells expressing wild-type FUS (first panel) or mutant FUS R522G (second panel), which induces nuclear CHOP expression (middle panel), indicating activation of the UPR, as indicated by the white arrow. On co-expressing wild-type ERp57, C24A_ERp57 or wild-type ERp72 with FUS R522G, fewer cells displayed nuclear CHOP expression and hence ER stress (third, fourth and fifth panel). However, on co-expressing C26A_ERp72 with FUS R522G there was no significant difference in nuclear CHOP immunoreactivity to cells expressing vector only (sixth panel). White arrows indicate nuclear CHOP immunoreactivity, as marker of ER stress. Scale bar = 10 µm. **B)** Quantification of cells with nuclear CHOP immunoreactivity induced by mutant FUS, co-expressed with ERp57 or ERp72. A significant difference (**) in the proportion of cells displaying nuclear CHOP immunoreactivity was observed when FUS R522G was co-expressed with ERp57 (wild-type or mutant) or (*) co-expressed with ERp72. For each of 3 replicate experiments, 100 cells were scored for each population. Data are presented as mean ± SEM, tested with one-way ANOVA and Tukey's post-test, n = 3. Where *p<.05, **p<.01.

5.2.5 Over-expression of ERp57 and ERp72 is protective against mutant FUS mislocalisation into the cytoplasm in neuronal cultures.

After observing that wild-type ERp57, C24A_ERp57 and wild-type ERp72 were protective against ER stress induced by mutant FUS, the cellular distribution of FUS (cytoplasmic or nuclear) was next examined. Neuro2a cells were co-transfected with wild-type FUS (FUS-WT) or mutant FUS (R522G) and either wild-type ERp57, C24A_ERp57, wild-type ERp72 or C26A_ERp72. Immunocytochemistry was performed using anti-HA antibodies to detect FUS expression, and anti-V5 antibodies to detect ERp57 and ERp72 expression.

Transfected cells were observed 72 hr post transfection using fluorescence microscopy (Figure 5.4 A).

Consistent with earlier reports as expected only 19% of vector only transfected Neuro2a cells expressed FUS in the cytoplasm [487]. Conversely, significantly more (66%) R522G mutant cells displayed FUS expressed in the cytoplasm. However, significantly fewer cells expressed cytoplasmic FUS when wild-type ERp57 47% ($p<.01$) or wild-type ERp72 49% ($p<.01$) was co-expressed with mutant FUS. Hence these data reveal that ERp57 and ERp72 are protective against the mislocalisation of mutant FUS to the cytoplasm. Similarly, over-expression of C24A_ERp57 was also protective, as it significantly reduced the proportion of cells expressing mutant FUS in the cytoplasm to 49% ($p<01$). However, in contrast C26A_ERp72 did not reduce the proportion of cells with cytoplasmic FUS: there was no significant difference between the proportions of vector only transfected cells expressing mutant FUS compared to cells expressing C26A_ERp72 (64%) (Figure 5.4 B). Hence these data suggest that the chaperone activity of ERp57, but not ERp72, is protective against the mislocalisation of mutant FUS to the cytoplasm.

A

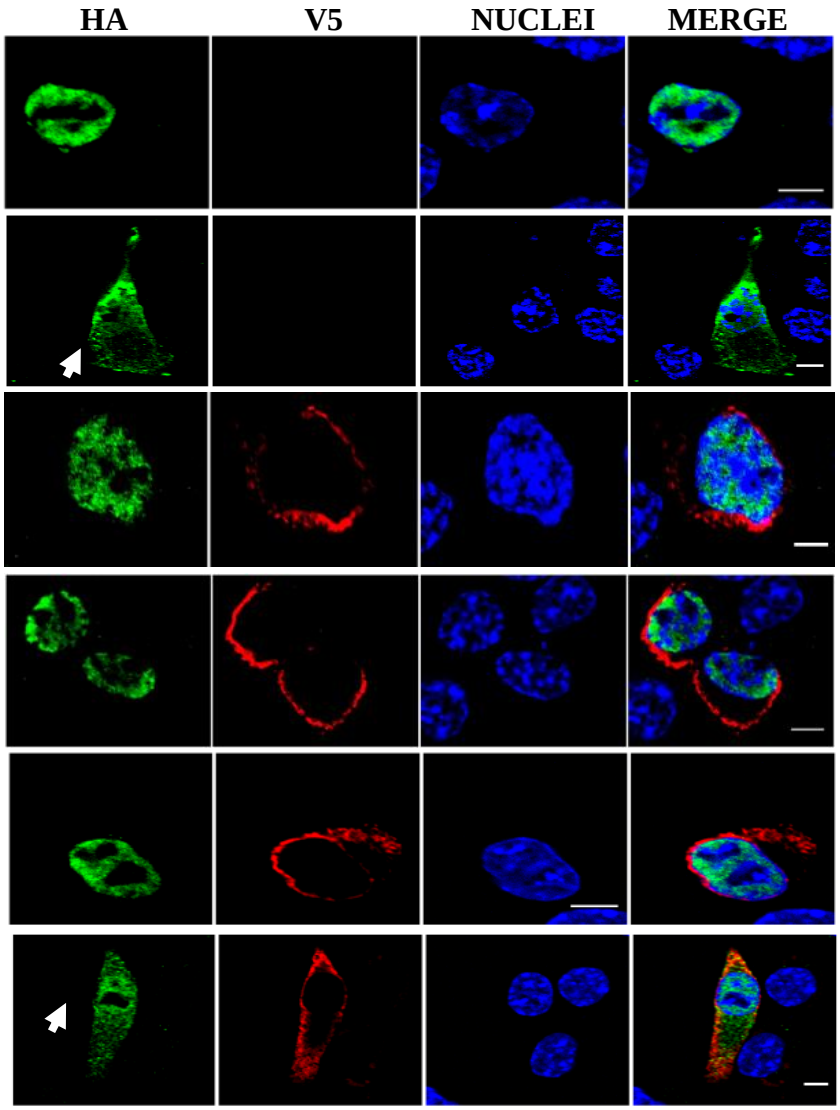
HA
V5
NUCLEI
MERGE
FUS-WT
R522G
R522G+ERp57 wt
R522G+ERp57 mut
R522G+ERp72 wt
R522G+ERp72 mut

B

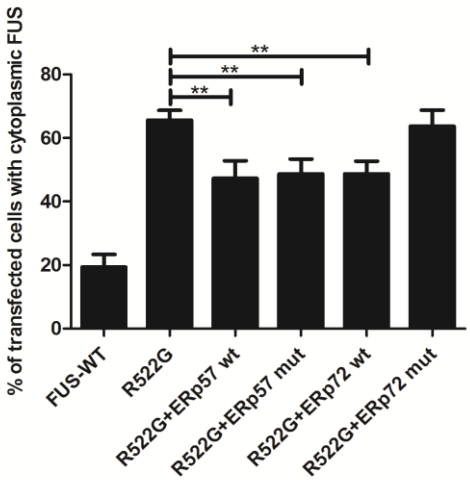
% of transfected cells with cytoplasmic FUS
0
20
40
60
80
**
**
**
FUS-WT
R522G
R522G+ERp57 wt
R522G+ERp57 mut
R522G+ERp72 wt
R522G+ERp72 mut

Fig 5.4 Wild-type ERp57, C24A_ERp57 and wild-type ERp72 decrease the proportion of cells with FUS localisation in the cytoplasm. A) Immunofluorescence images of Neuro2a cells co-expressing mutant FUS R521G with ERp57 and ERp72. Neuro2a cells expressing wild-type FUS (first panel) or mutant FUS R522G (second panel) in the cytoplasm, as indicated with a white arrow. On overexpressing wild-type ERp57, C24A_ERp57or wild-type ERp72 fewer cells expressed mutant FUS in the cytoplasm (third panel, fourth and fifth panel). However, co-expression of mutant ERp72 with R522G had no effect on the proportion of cells with cytoplasmic mutant FUS (sixth panel). Scale bar = 10 μm. **B)** Quantification of cells in (A) co-expressing mutant FUS with ERp57 or ERp72 and displaying cytoplasmic localisation of FUS. A significant difference (**) in the proportion of cells expressing cytoplasmic FUS was observed when R522G cells were co-expressed with ERp57, wild-type ERp72 or C24A_ERp57. For each of 3 replicate experiments, 100 cells were scored for each population. Data are presented as mean ± SEM, tested with one-way ANOVA and Tukey's post-test, n = 3. Where *p<.05. **p<.01 and ***p<.001.

The author supervised an Honours student who examined whether ERp57 and ERp72 was protective against ER stress and mislocalisation of TDP-43 in the cytoplasm in mutant TDP-43 expressing cells. The following results, presented in sections 5.2.6 and 5.2.7, were performed by Honours student Emma Perri, under the supervision of the author.

5.2.6 Over-expression of ERp57 and ERp72 are protective against mutant TDP-43 induced ER stress in neuronal cultures.

The effect of ERp57 and ERp72 on ER stress induced by mutant TDP-43 was examined in neuronal cell culture. Neuro2a cells were transfected with wild-type TDP-43 (TDP-43 WT) or mutant TDP-43 (Q331K) and cotransfected with either wild-type ERp57, C24A_ERp57, wild-type ERp72 or C26A_ERp72. XBP-1 was

used as a marker of ER stress. Immunocytochemistry was performed using anti-XBP-1 antibodies, where nuclear immunoreactivity to XBP-1 was indicative of ER stress. Transfected cells were observed 18 hr post transfection using fluorescence microscopy (Figure 5.5 A).

XBP-1 nuclear immunoreactivity was rarely detected in untransfected cells (UTR) (4% cells). Similar results were obtained when cells were transfected with empty vector mCherry as a control: nuclear immunoreactivity to XBP-1, indicating induction of ER stress, was present in only 5% cells. In cells expressing wild-type TDP-43, a slight, but non-significant activation of XBP-1 was detected in 16% of transfected cells. In contrast, in cells expressing Q331K, the proportion of cells with XBP-1 activation increased significantly to 39% ($p<.01$), as expected (Chapter 3). However, in cells co-expressing wild-type ERp57 and Q331K, there was a significant decrease in the proportion of cells with ER stress, as only 23% ($p<.05$) of these cells displayed nuclear XBP-1 immunoreactivity. Whereas, co-expression of C24A_ERp57 with TDP-43 Q331K did not significantly reduce the proportion of transfected cells with XBP-1 activation (39%) compared to vector only transfected cells. Conversely, there was a significant decrease in the proportion of cells co-expressing wild-type ERp72 and mutant FUS with nuclear XBP-1 immunoreactivity, compared to cells transfected with mutant FUS and vector only (23% $p<.05$). However, there was no significant difference between the proportion of cells co-expressing C26A_ERp72 and TDP-43 Q331K with nuclear XBP-1 immunoreactivity compared to those expressing TDP-43 Q331K and vector only (Figure 5.5 B). These results indicate that both wild-type ERp57 and wild-type ERp72 are protective against ER stress induced by mutant TDP-43. However, neither C24A_ERp57 nor C26A_ERp72 are protective, indicating that the disulphide interchange activity of both ERp57 and ERp72 are necessary for this activity.

A

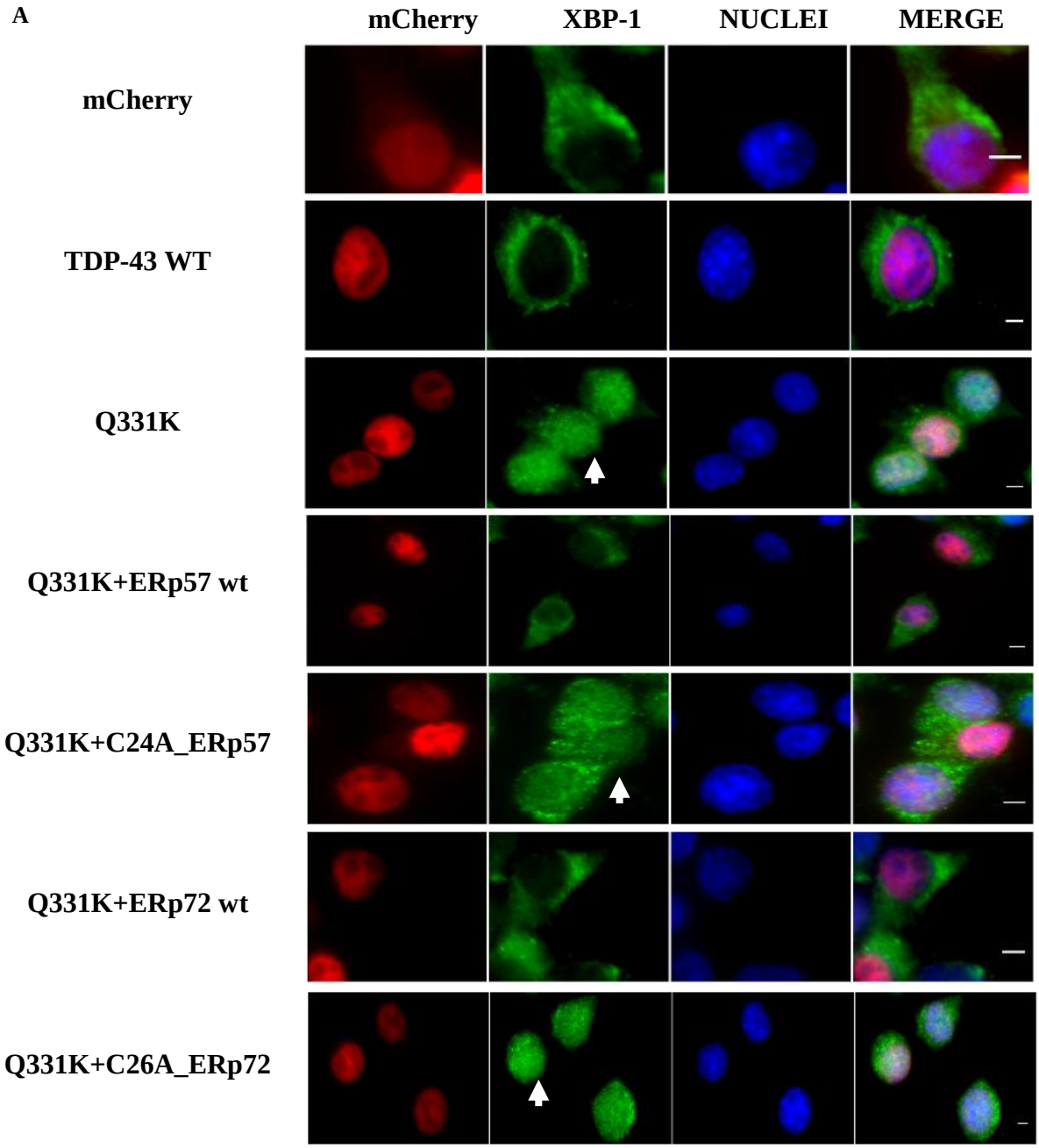
mCherry
XBP-1
NUCLEI
MERGE
mCherry
TDP-43 WT
Q331K
Q331K+ERp57 wt
Q331K+C24A_ERp57
Q331K+ERp72 wt
Q331K+C26A_ERp72

B

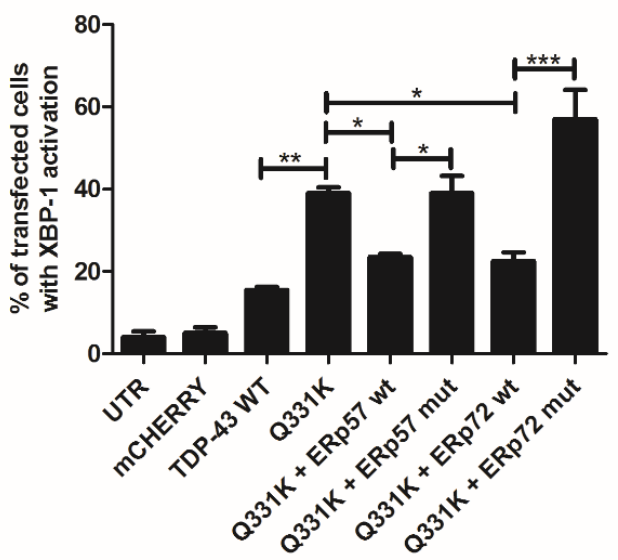
% of transfected cells with XBP-1 activation
80
60
40
20
0
**
*
*
*
***
UTR
mCHERRY
TDP-43 WT
Q331K
Q331K + ERp57 wt
Q331K + ERp57 mut
Q331K + ERp72 wt
Q331K + ERp72 mut

Figure 5.5 Over-expression of wild-type ERp57 and wild-type ERp72 reduces the proportion of Neuro2a cells with nuclear XBP-1 immunoreactivity. A) Immunofluorescence images of cells co-expressing mutant TDP-43 Q331K with ERp57 or ERp72. Neuro2a cells expressing empty vector only (first panel), wild-type TDP-43 (second panel), or mutant TDP-43 Q331K (third panel) are shown. Nuclear XBP-1 immunoreactivity induced by mutant FUS (middle panel) is indicated by white arrows. On co-expressing wild-type ERp57 or wild-type ERp72 with TDP-43 Q331K fewer cells displayed nuclear XBP-1 immunoreactivity compared to cells transfected with TDP-43 Q331K and vector only (fourth panel and sixth panel). However, on co-expressing C24A_ERp57 or C26A_ERp72 with TDP-43 Q331K there was no significant difference in the proportion of cells with nuclear XBP-1 immunoreactivity compared to cells transfected with TDP-43 Q331K and vector only (fifth panel and seventh panel).White arrows indicate nuclear XBP-1 immunoreactivity, indicating induction of ER stress. Scale bar = 10 µm**. B)** Quantification of mutant TDP-43 Q331K cells with nuclear XBP-1 immunoreactivity co-expressing either ERp57 or ERp72. A significant difference in the proportion of cells displaying nuclear XBP-1 (*) immunoreactivity was observed when ERp57 or ERp72 (wild-type) was co-expressed with TDP-43 Q331K. For each of 3 replicate experiments, 100 cells were scored for each population. Data are presented as mean ± SEM, tested with one-way ANOVA and Tukey's post-test, n = 3. Where *p<.05, **p<.01 and ***p<.001.

5.2.7 Over-expression of ERp57 and ERp72 are protective against mislocalisation of mutant TDP-43 into the cytoplasm in neuronal cells

Neuro2a cells were co-transfected with wild-type TDP-43 or mutant TDP-43 (Q331K) and either wild-type ERp57, C24A_ERp57, wild-type ERp72 or C26A_ERp72. Immunocytochemistry was performed using anti-V5 antibodies to detect ERp57 and ERp72 expression. Transfected cells were observed 72 hr post transfection using fluorescence microscopy (Figure 5.6 A).

In Neuro2a cells expressing wild-type TDP-43, only 6% of transfected cells displayed cytoplasmic localisation of TDP-43, whereas in TDP-43 Q331K expressing cells, this proportion was significantly increased to (19%, $p<.001$) of transfected cells. However, in cells co-expressing Q331K with wild-type ERp57, significantly fewer transfected cells expressed TDP-43 in the cytoplasm (10%, $p<.01$), in comparison to cells expressing Q331K alone. Similarly, there was a significant reduction (13%, $p<.05$) in the proportion of cells with cytoplasmic TDP-43 when mutant Q331K was co-expressed with wild-type ERp72. However, co-expression of TDP-43 Q331K with either C24A_ERp57 or C26A_ERp72 did not significantly reduce the proportion of transfected cells with cytoplasmic localisation of TDP-43 (20%, Figure 5.6 B). These data reveal that both wild-type ERp57 and ERp72 are protective against mutant TDP-43 mislocalisation to the cytoplasm. However, C24A_ERp57 and C26A_ERp72 were not protective against cytoplasmic localisation of TDP-43, thus implying that the disulphide interchange activity is necessary for this activity.

A

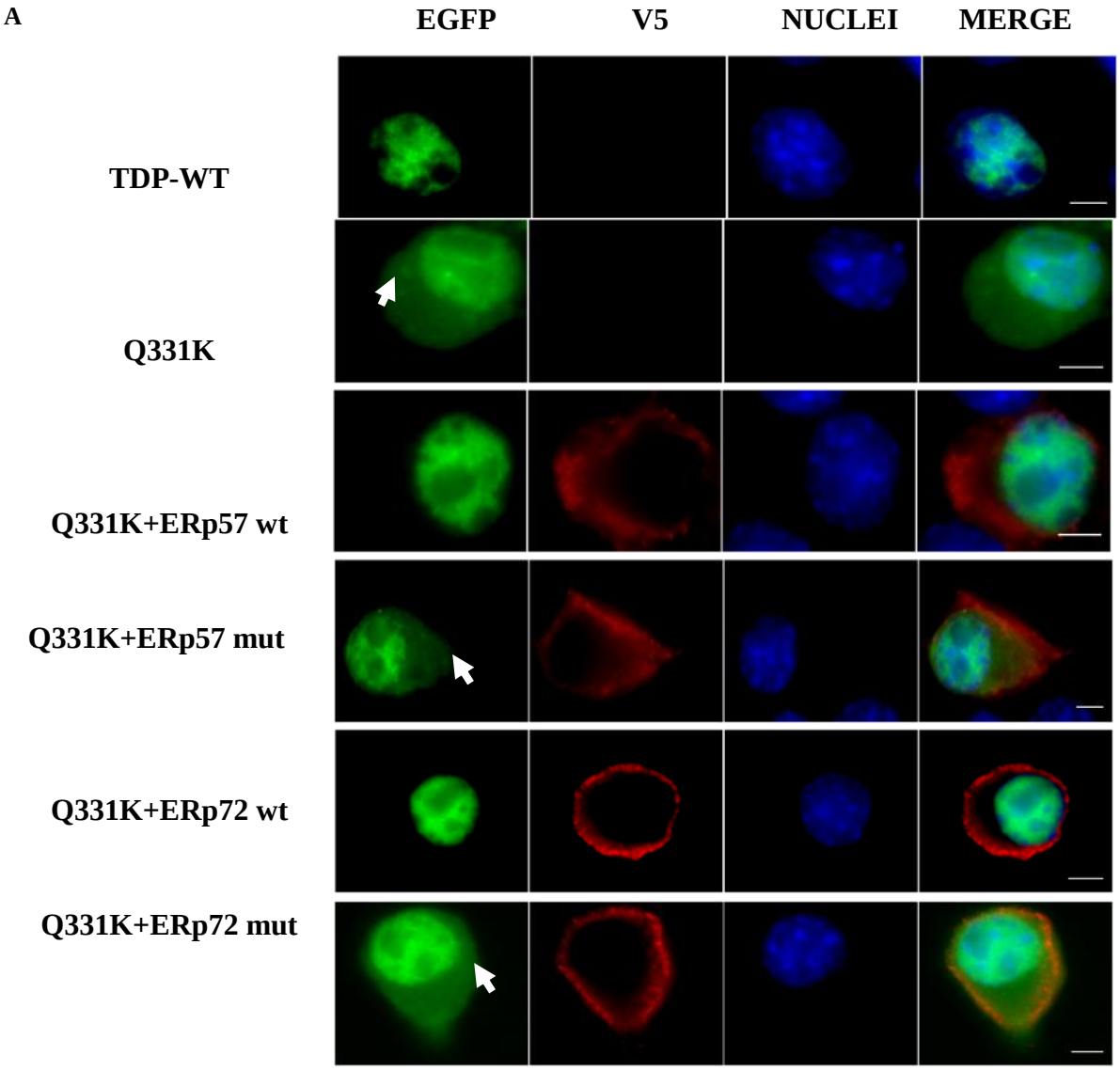
EGFP
V5
NUCLEI
MERGE
TDP-WT
Q331K
Q331K+ERp57 wt
Q331K+ERp57 mut
Q331K+ERp72 wt
Q331K+ERp72 mut

B

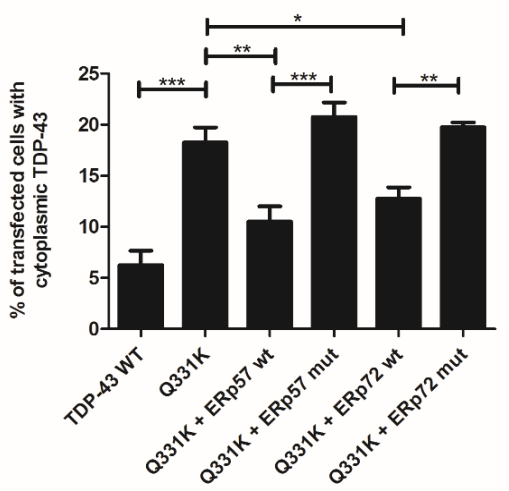
% of transfected cells with cytoplasmic TDP-43
25
20
15
10
5
0
*
**
***
***
**
TDP-43 WT
Q331K
Q331K + ERp57 wt
Q331K + ERp57 mut
Q331K + ERp72 wt
Q331K + ERp72 mut

Fig 5.6 ERp57 and ERp72 reduce the proportion of cells with TDP-43 localisation in the cytoplasm. A) Immunofluorescence images of Neuro2a cells co-expressing mutant TDP-43 Q331K with ERp57 or ERp72. Neuro2a cells expressing wild-type TDP-43 (first panel) displayed mainly nuclear TDP-43 localisation whereas more mutant TDP-43 Q331K expressing cells were localised in the cytoplasm (second panel), as indicated with white arrow. On co-expressing wild-type ERp57 or wild-type ERp72 with Q331K, fewer cells displayed cytoplasmic TDP-43 distribution (third panel and fifth panels). However, co-expressing Q331K with either C24A_ERp57 or C26A_ERp72 cells did not change the proportion of cells with cytoplasmic TDP-43 (fourth panel and sixth panel). Scale bar = 10 µm**. B)** Quantification of cells in (A), displaying cytoplasmic distribution of mutant TDP-43. A significant difference in the proportion of cells displaying cytoplasmic TDP-43 was observed when Q331K cells were expressed with wild type ERp57 (**) or with (*) wild-type ERp72, but not C24A_ERp57 or C26A_ERp72. For each of 3 replicate experiments, 100 cells were scored for each population. Data are presented as mean ± SEM, tested with one-way ANOVA and Tukey's post-test, n = 3. Where *p<.05. **p<.01 and ***p<.001.

5.3 Discussion

It was previously demonstrated in chapter 4 that over-expression of PDI is protective against mutant TDP-43 and FUS in neuronal cultures. Furthermore, experiments performed by our laboratory demonstrated that PDI is non-functional due to S-nitrosylation as observed in ALS patients which may contribute to disease progression [483]. Since, PDI is the prototype of the PDI family which comprises of proteins with similar structure and functions [664]. In this study the role of the other most extensively studied family members ERp57 and ERp72 was observed. Due to the similarities between these proteins and PDI it was interesting to investigate their role against mutant SOD1, TDP-43 and FUS. The study focussing the role of ERp57 on mutant SOD1 induced toxicity in cell culture is presented as a separate manuscript and is not a part of this discussion below.

Mutant Protein	Pathology	wild-type ERp57	C24A_ERp57
FUS R522G	ER stress	✓	✓
FUS R522G	Mislocalisation in cyto-plasm	✓	✓
TDP-43 Q331K	ER stress	✓	X
TDP-43 Q331K	Mislocalisation in cyto-plasm	✓	X
Mutant Protein	**Pathology**	**wild-type ERp72**	**C26A_ERp72**
FUS R522G	ER stress	✓	X
FUS R522G	Mislocalisation in cyto-plasm	✓	X
TDP-43 Q331K	ER stress	✓	X
TDP-43 Q331K	Mislocalisation in cyto-plasm	✓	X

Table 5.1 Summary of the effect of wild-type ERp57 and C24A_ERp57 against mutant TDP-43 and FUS in neuronal cell lines and the effect of ERp72 wild-type and C26A_ERp72 against mutant TDP-43 and FUS in neuronal cell lines.

To investigate whether ERp57 had similar protective function as that of PDI, ERp57 was co-expressed with mutant FUS. In this study it was demonstrated that ERp57 is protective against ER stress and mislocalisation induced by mutant FUS and TDP-43 in neuronal cell cultures. Since, ERp57 is also found in the nucleus and

cytosol it could interact with the predominately nuclear localised proteins TDP-43 and FUS accessible in non-ER locations [709]. Additionally, ERp57 in the cytoplasm has been postulated to protect against oxidative stress which could further prevent mislocalisation of mutant TDP-43 and FUS into the cytoplasm [710]. Another possible mechanism through with ERp57 could be protective is by directly interacting with them as it has been shown to participate in regulatory events in the nucleus where it was found to associate with several transcription factors [710, 711].

Furthermore, co-expression of either wild-type or C24A_ERp57 was protective against ER stress and mislocalisation into the cytoplasm in cells expressing mutant FUS. The mutation in the active site of C24A_ERp57 did not hinder its protective ability against mutant FUS. The data implies that with mutant FUS the chaperone activity along with the disulphide interchange activity of ERp57 plays a protective role. Since there is absence of disulphide bonding in FUS protein the chaperone activity of ERp57 could assist in reducing the detrimental effects of mutant FUS [628]. ERp57 is upregulated during ER stress in ALS [709]. Therefore, ERp57 could be preventing the aggregation of misfolded mutant FUS proteins by functioning as a holdase and assist in the degradation of misfolded proteins. This data is also similar to observation made in Chapter 4 where mutant PDI QUAD which had mutation in the active site of PDI was also protective against FUS pathology.

The effect of ERp57 on mutant TDP-43 induced ER stress and mislocalisation was different from FUS. Co-expression of wild-type ERp57 significantly reduced ER stress and mislocalisation of mutant TDP-43 into the cytoplasm. However, C24A_ERp57 was not protective against ER stress and cytoplasmic TDP-43 localisation in cells expressing mutant TDP-43. Co-expression of C24A_ERp57 with mutant TDP-43 had similar or more devastating effect than mutant TDP-43 co-expressed with empty vector which suggests that mutation in a single cysteine residue of the active site could make ERp57 non-functional. This result is in

accordance with the observation that against mutant TDP-43 the mode of action of protection is through the disulphide interchange activity. Since the cysteine residues in TDP-43 could cross-link during stress and could alter conformations and function of proteins [569]. Hence, it is tempting to speculate that protection by ERp57 is a cellular response to prevent further aggregation of abnormally disulphide bonded and misfolded TDP-43 a mechanism similar to mutant SOD1. Furthermore it also validates the result obtained with BMC which only has the disulphide interchange activity and catalyses reactions like PDI in protection against mutant TDP-43 and mutant SOD1 [712].

The presence of three active sites in ERp72 makes it exclusive amongst PDI family members and a potential candidate in mimicking the role of PDI. ERp72 was co-expressed with either mutant FUS or TDP-43 and the effect on ER stress and mislocalisation was observed in neuronal cell cultures. It was observed that wild-type ERp72 was protective against mutant TDP-43 and FUS. However, co-expressing with C26A_ERp72 had no effect on mutant TDP-43 or FUS expressing cells. This ER chaperone may be reducing the load of misfolded proteins and reducing stress as it is involved in the disulphide bond oxidation and isomerisation and has also been confirmed *in vitro* [713]. ERp72 is more similar to ERp57, since many of the residues that are implicated in ERp57 are conserved in ERp72. This suggests that ERp72 could be compensating the function of ERp57 or indirectly PDI. It could also associate and modulate the redox state of ERdj5 which is a major regulator of the degradation of misfolding proteins in the ER [714, 715]. Or could be protective *via* a network of chaperone in a multi protein complex and interact with misfolded proteins [704]. However, since the C26A_ERp72 was not protective other contributing factors such as substrate specificity, redox conditions, cellular localisation and abundance in the cell could also play a role in the protection.

Although ERp57 and ERp72 were protective against mutant TDP-43 and FUS in neuronal cell lines, interaction with these proteins is warranted. ERp57 interacts with glycosylated substrates contrarily ERp72 substrate specificity is still unclear

[716]. A study reported endogenous protein substrates of PDI family members including PDI, ERp72, ERp57, ERp18, ERp46 and PDIA6 using active site cysteine trapping mutants to isolate PDI proteins that had formed mixed disulphide bonds with substrates, and demonstrated that the different PDI family members have different substrate specificities [535]. Furthermore, both PDI and ERp57 had broader substrate specificity than ERp72 [535]. However, TDP-43 and FUS have never been studied as potential substrates of PDI family members. It would be intriguing to observe whether ERp57 or ERp72 colocalise with TDP-43 and FUS inclusions in patients tissues and provide a cellular defence. It could also be useful to perform immunoprecipitation studies to examine whether ERp57 or ERp72 forms complexes with mutant TDP-43 or FUS. Further detailed investigation of the substrate specificity of the PDI family members can be beneficial in understanding their specific functions.

To understand the mechanism of action of these proteins, more specific approach could be utilised. Since induction of XBP-1, an early ER stress marker was used to study mutant TDP-43 co-expression with ERp57 and CHOP a late apoptotic marker was observed for mutant FUS co-expression with ERp72. Other ER stress markers such as BiP, ATF6, and PERK could be studied to understand the occurrence of induction of these ER chaperones which would further help in understanding the mechanism of action. Also observing the effect of ERp57 and ERp72 under different stressors such as oxidative stress in cellular models could provide insight into the mechanism of action.

It is probable that like PDI, ERp57 and ERp72 could also be non-functional during disease state. Evidence suggests that both ERp57 and ERp72 have the presence of phosphorylation sites and ERp57 could be phosphorylated on the tyrosine and ERp72 on serine residues [717-719]. Additionally, PDI plays an important role in oxidising the other PDI family members such as ERp57 *via* the ERo1α pathway and accelerates formation and isomerisation of disulphide bonds in substrates [720]. It

could be postulated that loss of function of PDI could affect the function ERp57 and ERp72 during disease state.

A detailed investigation of the role of the other PDI family members is also warranted following the outcome of this study. Since PDI family members complement and overlap each other's function a thorough investigation on structures of PDIs in complex with their substrates or functional partners is essential for fully understanding how PDIs fulfil their distinguished functions to maintain cellular homeostasis. ERp27 which lacks the catalytic domains but the *b'* domain is identical PDI and assists in binding misfolded proteins should also be investigated to understand which key domain is important in protection [686].

In summary, in this study it was demonstrated that ERp57 and ERp72 protect against mutant TDP-43 and FUS induced ER stress and cytoplasmic localisation in neuronal cells. It was further demonstrated that the mode of action of protection is different among PDI family members. The disulphide interchange activity of ERp57 is important for protecting against mutant TDP-43 pathology. Whereas, C24A_ERp57 with most chaperone activity was protective against mutant FUS induced ER stress and cytoplasmic distribution. Another ER chaperone, ERp72 was also protective against mutant TDP-43 and FUS pathology. PDIs undergo significant dynamics in conformation and cellular localization in response to various conditions and situations. Therefore, further investigation of these ER proteins could help in elucidating ER stress and also the functions of other PDI family members. This study also suggests that like PDI, other members of the PDI family may also have specific roles in protein misfolding and protection against ALS pathology.

Chapter 6 Cytoplasmic PDI is protective against mutant SOD1, TDP-43 and FUS in neuronal cell cultures

6.1 Introduction

Traditionally, PDI is recognised as being resident within the ER, where it is highly expressed, with ER concentrations of 0.2–0.5 mM range [721]. The oxidising environment of ER lumen provides an ideal condition for protein folding and post-translational modifications for the efficient functioning of PDI [722]. Indeed, PDI is retained in the ER lumen due to the presence of a short signal peptide at the N-terminus and a classic Lys-Asp-Glu-Leu (KDEL) motif at the C-terminus end [582]. The KDEL tagged PDI is retrieved back into the ER *via* a retrograde pathway through non-covalent interaction with the KDEL receptors localised on the ER and cis-Golgi membrane [723]. However, various reports have identified roles for PDI in other cellular locations, where important functions have been ascribed.

6.1.1 PDI in Non-ER locations

The exact mechanism by which PDI escapes from the ER is poorly defined. However, numerous theories have been proposed, related to redox modulation, saturation of the ER-retention machinery or removal of the KDEL sequence [510]. PDI acts as a reductase in non-ER locations, including the cytosol, endosomes, and plasma membrane, due to the reducing environment of these cellular locations. Specific functions of PDI have been described in these locations [724]. For example, in the cytosolic fraction of human liver cells, PDI is involved in the metabolism of insulin [725]. PDI is also expressed in the cytoplasm in leukocytes and megakaryocytes, although the concentrations of cytosolic PDI are considerably lower than the levels of ER-localized PDI found in other cells [726]. Cytoplasmic PDI is observed in glial astrocytes, where PDI regulates actin polymerisation [727]. PDI is also present on the cell surface, although the exact mechanism of how PDI positions itself on the membrane is unclear. However, electrostatic charges have been implicated in this process [728]. Cell surface PDI is involved in cell signalling through interaction with membrane receptors. The thioredoxin like domains of PDI assist in catalysis of disulphide bonds in lymphocytes [729, 730].

Cell surface PDI is also involved in adhesion of leukocytes, where more reducing PDI is required for its conformational stability [731]. The reducing activity of cell surface PDI assists in the interaction with thyroid stimulating hormone receptor of thyrocytes [732]. Furthermore, PDI has been detected in the nuclear matrix of human lymphocytes and monocytes [733]. PDI in the nucleus has been associated with various transcription factors where it activates the binding of immunoglobulin enhancer-binding factors (E2A) and NF- kB *via* a redox regulated mechanism [734, 735]. PDI is also secreted from a variety of cell types, such as hepatocytes, pancreatic exocrine cells and endothelial cells, although the biological relevance is still unclear [728, 736, 737].

PDI also has detrimental effects and is implicated in mediating the entry of pathogens during infectious disease. Cell surface PDI mediates infection of HeLa cells by mouse polyoma virus [738], and it also facilitates the entry of cholera toxin [739]. The oxidized form of PDI mediates translocation of cholera toxin into the host cell cytoplasm [740] whereas the reduced form of PDI leads to its unfolding. In rat models of Huntington and Alzheimer's disease, PDI accumulation at the ER-mitochondrial junction triggers apoptosis *via* mitochondrial outer membrane permeabilisation [741]. This effect is specific for the accumulation of misfolded proteins, but not other triggers of apoptosis, suggesting a specific role for pro-apoptotic PDI in neurodegenerative disease.

6.1.2 Reticulon-mediated redistribution of PDI in ALS

The distribution of PDI from the ER to other cellular locations, mediated *via* reticulon proteins, was demonstrated in two independent studies [531, 576]. From these studies the importance of the reticulon family of proteins as regulators of PDI activity was shown. Reticulons are membrane-bound proteins residing in the ER that possess a uniquely conserved C-terminus and a variable N-terminal region [742, 743]. They maintain the curvature of the ER membrane and are also associated with ER-Golgi trafficking, ER stress, vesicle formation, membrane morphogenesis and apoptosis [742, 744, 745]. Four reticulon proteins have been

identified in mammals, namely Rtn-1, Rtn-2, Rtn-3 and Rtn-4 (Nogo): the latter is also a specific neurite outgrowth inhibitor. It was demonstrated that Rtn1-C induced a punctate localisation of PDI, that was distinct from the ER, without affecting the overall morphology of the ER in neuronal cell lines [576]. Furthermore, this redistribution was associated with a significant increase in PDI enzymatic activity, which also reduced the intracellular levels of S-nitrosylated PDI [576]. Another study demonstrated that the punctate redistribution of PDI could also be modulated by reticulon-4A (NogoA) [531]. Over-expression of NogoA induced a punctate redistribution of PDI both *in vitro* and *in vivo*. Moreover, knock-down of NogoA accelerated motor neuron degeneration in $SOD1^{G93A}$ mice [531], suggesting that the localisation of PDI in punctate structures away from the ER could be protective in ALS. However, the study did not define the exact cellular compartment in which PDI was distributed. A range of markers were examined, including Golgi and endosomal markers, but they did not colocalise with the PDI-positive vesicular structures.

6.1.3 Aim

PDI is conventionally recognized as being ER-resident, but it is also present in other cellular locations including the nucleus, extra-cellular matrix and on the cell surface. However, the functional consequence of PDI in non-ER compartments is poorly understood. Given that over-expression of PDI was protective against mutant SOD1, TDP-43 and FUS in neuronal cultures (Chapter 3), it was important to define the sub-cellular compartment in which this protection occurs since this could provide further clues as to disease pathogenesis. In this study, construct was designed to express PDI in the cytoplasm, by deleting the signal peptide and KDEL retention signal. The localisation of PDI in the cytoplasm was confirmed using subcellular fractionation and confocal microscopy. Furthermore, the protective role of cytoplasmic PDI in cells expressing mutant SOD1, TDP-43 and FUS in neuronal cell lines was investigated.

6.2 Methods and Materials

6.2.1 Materials

Restriction enzymes were purchased from New England Biolabs (NEB, http://www.neb.com/) and PCR primers were purchased from Gene Works (http://www.geneworks.com.au/). The pcDNA3.1 empty vector was provided by Dr. Hamsa Puthalakath, La Trobe Institute for Molecular Science, Melbourne, Australia. PDI WT pcDNA3.1 was provided from Prof Neil Bullied, Glasgow, UK. For cloning *E.coli* XL1-Blue strain was used and was purchased from Stratagene.

6.2.2 Bioinformatics tools

The cDNA sequences were analyzed using the National Centre for Biotechnology Information (NCBI) and ExPASY translate tools were used to translate protein sequences and to confirm molecular weights. A plasmid Editor program - ApE (University of Utah, USA) was used to create vector maps and to analyse nucleotide sequences.

6.2.3 Polymerase chain reaction (PCR)

To amplify the cDNA insert from the CYTO PDI pcDNA3.1 construct without the ER targeting signal sequence and ER retention signal sequence specific primers were designed. The forward (5′ AAAGAATTCATGGACGCCCCCGAG-GAGGA 3′) and reverse (5′ AAAGCGGCCGCTCAAGTAGAATCAAGACCAA-GAA 3′) primers were used to amplify 52-1555 nucleotide region. A start codon and an *EcoR*I restriction enzyme site were introduced in the forward primer, and a stop codon and *Not*I restriction enzyme site were introduced in the reverse primer to enable cloning into the pcDNA3.1 vector. PCR reactions were prepared with 1× Thermopol buffer, 10 µM of forward and reverse primers, 10 mM of dNTPS (dGTP, dATP, dCTP, dTTP), 1 ng of template DNA, and 10 U of *Taq* and *Vent* polymerase in a total volume of 50 µl. The DNA was amplified in a thermocycler (Thermo Scientific) using an initial denaturation temperature

of 95°C for 5 min, followed by 30 cycles of denaturation at 95°C for 30 sec; annealing at 60°C for 30 sec; extension at 72°C for 2 min and a final extension at 72°C for 5 min.

6.2.4 Restriction Enzyme Digest and agarose gel electrophoresis

For the cloning of CYTO PDI-pcDNA3.1 restriction enzyme digest reaction mixtures were prepared in NEB buffer 3.1 with 4 µg of DNA, 20 U of *EcoRI* and 10 U of *NotI* restriction enzymes in a total volume of 20 µl and incubated at 37°C for 4 hr. The DNA samples were mixed with DNA loading dye (3.7 mM bromophenol blue, 4.6 mM xylene cyanol and 33% glycerol) and loaded onto a 1% (w/v) agarose gel prepared in TAE buffer (40 mM Tris, 1 mM EDTA, 0.114% v/v glacial acetic acid) and 0.1% (v/v) Gel Red (Biotium). The size of DNA fragments was estimated using DNA 1Kb plus ladder (Invitrogen) as the standard marker. The gels was run at 110 V for 90 min in TAE buffer and visualized under UV light on chemidoc imaging system (Biorad).

6.2.5 Gel extraction

The restriction digest products and PCR amplicons were run on 1% (w/v) low melting agarose gel at 80 V for 3 hr. Target fragments were excised using a scalpel and extraction was performed using a QIAquick Gel Extraction Kit (Qiagen) as per the manufacturer's protocol.

6.2.6 Ligation

Ligation reaction was performed to ligate the gel extracted CYTO PDI pcDNA3.1 insert into the pcDNA3.1 vector. The reaction mixture was prepared in T4 DNA ligase buffer (Promega) containing 1:4 molar ratios of vector and insert DNA and 1 U of T4 DNA ligase (Promega). The ligation mixture was incubated at 4°C overnight.

6.2.7 Sequencing

Sequencing samples were prepared by mixing 0.5 µg of plasmid DNA with 1 pmol of T7 forward or BGH reverse primer for CYTO PDI pCDNA3.1. Sequencing of the samples were performed at the Australian Genome Research Facility (AGRF) by using DNA Big Dye Terminator (BDT) sequencing method. The results were examined using Basic Local Alignment Search Tool (BLAST) and the chromatographs were analyzed by using Chromas v2.1 software (Technelysium, Brisbane) to determine the accuracy of the sequence.

6.2.8 Primary neurons

Primary neurons were harvested from the cortex of C57BL/6 mouse embryos at embryonic (E) day 14.5 by washing the cortex in cell plating medium (Neuro-basal™ medium (Gibco), 2% B27 supplement, 10% fetal calf serum (Gibco), 0.5 mm glutamine, 25 µm glutamate and 1% antibiotic/antimycotic (Gibco) followed by treatment with 0.125% Trypsin-EDTA (Gibco) (37 C for 5 min) and mechanical titration using a 1 ml pipette. Cell viability and density were assessed using a trypan blue exclusion assay. Cells were plated onto poly-l-lysine-coated 13 mm coverslips in 24-well plates at a concentration of 50 000 cells per coverslip. The following day, the media was changed to cell maintenance media consisting of plating media without the fetal calf serum and glutamate. Cells were grown in 5% CO_2 at 37°C for 5 days and then fixed with 4 % paraformaldehyde and immunocytochemistry was performed.

6.2.9 Subcellular fractionation Assay

Neuro2a cells were grown ($4*10^{6}$) and transfected with either CYTO PDI pcDNA3.1, wild-type PDI pcDNA3.1 or PDI QUAD pcDNA3.1 for 72 hr. The culture media was removed and cells were trypsinised using Trypsin and incubated at 37°C for 5 min. The cells were dislodged and aspirated with cold culture media containing 10% Fetal Bovine Serum to quench the Trypsin. Cells were centrifuged at 100 RCF at 4°C to pellet the cells. The supernatant was washed with ice cold

PBS and the cell suspension was centrifuged at 100 *g* at 4°C to pellet the cells. The cells were resuspended in 400 µl of ice cold Digitonin Buffer (150 mM NaCl, 50 mM HEPES pH 7.425, µg/ml digitonin (SIGMA #D141)) containing protease inhibitors. The cell suspension was incubated at 4°C for 10 min and then centrifuged at 2,000 *g* to pellet the cells. The supernatant was collected which contained the cytosol-enriched fraction. The cell pellet was resuspended by vortexing in 400 µl of cold NP40 Buffer (150 mM NaCl, 50 mM HEPES pH 7.4,1 % NP40). The pellet was incubated on ice for 30 min and then centrifuged at 7,000 *g* to pellet nuclei and cell debris. The supernatant, comprising membrane bound organelles including the ER proteins was collected. The resulting extracts were analysed by 12% SDS PAGE followed by Western blotting and probed using antibodies against markers of the ER (IRE-1α or calnexin) and cytoplasm (GAPDH).

6.2.10 Immunoblotting

Protein concentrations of the different cell fractions were determined using the BCA protein assay (Thermo scientific) by comparison with bovine serum albumin (BSA) standards. Protein samples (20 µg) were electrophorezed through 12% SDS–polyacrylamide gels and transferred to nitrocellulose membranes. Membranes were blocked with 5% skim-milk in Tris-buffered saline pH 8.0 for 30 min, then incubated with the appropriate primary antibodies at 4°C for 16 hr anti Ire-1a (1:500, Santa Cruz), or anti-calnexin (1:1000, Abcam) or anti-GAPDH (1;4000, Milipore). Membranes were incubated for 1 hr at room temperature with appropriate secondary antibodies (1:4000, HRP-conjugated goat anti rabbit, or HRP-conjugated goat anti mouse Chemicon), and were detected using ECL reagent (Biorad) on Chemidoc XRS (Biorad). Precision plus Protein^{TM} (Biorad) molecular marker was used to identify the approximate protein size.

6.3 Results

6.3.1 Design and Characterization of Cytoplasmic PDI

PDI consists of 508 amino acids and it contains an ER signal sequence, comprising of 17 amino acids at the N-terminus, and an ER retention motif, KDEL, at the C-terminus. In this study, a construct was designed to encode a 407 amino acid PDI protein whose expression was restricted to the cytoplasm (CYTO PDI pcDNA3.1). This plasmid was constructed by deleting the KDEL sequence and the first 17 secretory peptide sequence from a PDI expression vector based on pcDNA3.1, tagged with a V5 tag. A schematic diagram of the designed CYTO PDI protein encoded by this plasmid is presented in (Figure 6.1 A). The amino acid sequence of PDI, highlighting the active site motifs CGHC and the V5 tag for detection of expression, is presented in (Figure 6.1 B). A DNA sequence is shown in the Appendix section.

The CYTO PDI pcDNA3.1 insert was cloned into a mammalian expression vector pcDNA3.1 using *EcoRI* and *NotI* restriction enzymes. The CYTO PDI pcDNA3.1 insert band was gel extracted and ligated into the *EcoRI* and *NotI* digested vector pcDNA3.1. The ligation reactions were then transformed into XL1-Blue *E.Coli* cells and plasmid DNA was isolated from positive colonies. The successful ligation of the insert to vector was confirmed by restriction enzyme digest of the plasmid DNA with *EcoRI* and *NotI* enzymes. The correct sequence in the resulting CYTO PDI pcDNA3.1 construct was confirmed by DNA sequencing.

A

B

DAPEEEDHVLVLRKSNFAEALAAHKYLLVEFYAPW
CGHCAAEYAKAAGKLKAEGSEIRLAKVDATEESDL
AQQYGVRGYPTIKFFRNGDTASPKEYTAGREADDI
VNWLKKRGPAATTLPDGAAAESLVESEVAVIGFFK
DVESDSAKQFLQAAEAIDDIPFGITSNSDVSKYQL
DKDGVVLFKKFDEGRNNFEGEVTKENLLDFIKHNQ
LPLVIEFTEQTAPKIFGGEIKTHILLFLPKSVSDY
DGKLSNFKTAAESFKGKILFIFIDSDHTDNQRILE
FFGLKKEECPAVRLITLEEEMTKYKPESEELTAER
ITEFCHRFLEKIKPHLMSQELPEDWDKQPVKVLVG
KNFEDVAFDEKKNVFVEFYAWCGCKQLAPIWDKLG
ETYKDHENIVIAKMDSTANEVEAVKVHSFPTLKFF
PASADRTVIDYNGERTLDGFKKFLESGGQDGAGDD
DDLEDLEEAEEPDMEEDDDQKAVGKPIPNPLLGLD
ST

Figure 6.1: Domain organization and amino acid sequence of the CYTO PDI protein. A) Domain map of CYTO PDI showing the deleted ER targeting signal sequence and KDEL sequence. **B)** Amino acid sequence of full length CYTO PDI, with the active site CGHC highlighted in red and the V5 tag shown in purple.

6.3.2 Expression of CYTO PDI, wild-type PDI and PDI QUAD in Neuro2a cells

The localisation of the expressed PDI protein (CYTO PDI) in the cytoplasm was confirmed using confocal microscopy (Figure 6.2 A) Neuro2a cells were transfected with the construct encoding CYTO PDI and observed 24 hr post-transfection. Immunocytochemistry was performed using anti-V5 antibodies to detect expression of CYTO PDI, and anti-calreticulin antibodies as an ER marker.

Confocal microscopy was performed to verify the localisation of the expressed protein. CYTO PDI displayed a diffuse, cytoplasmic staining pattern, which lacked any distinct punctate structures. Calreticulin was present in the typical perinuclear pattern characteristic of the ER. When the PDI and calreticulin images were merged, there was no clear co-localisation of CYTO PDI with calreticulin. This was further confirmed by observing the orthogonal section of the z stack image (Figure 6.2 B).

As a comparison, the cellular distribution of endogenous PDI, and wild-type PDI and PDI QUAD expressed in Neuro2a cells was also examined Firstly, the cellular localisation of endogenous PDI in primary cortical neurons was examined at 24 hr post plating. Cortical neurons were fixed and stained using anti-PDI antibodies, to observe the expression of endogenous PDI, and anti-calreticulin antibodies, as a marker of ER. Confocal microscopy demonstrated that PDI in primary neurons co-localised with ER marker calreticulin, confirming that normally PDI is expressed principally within neurons in the ER, as expected (Figure 6.2 C, D).

To further confirm the cellular localisation of endogenous PDI in neuronal cell lines, subcellular fractionation of Neuro2a cells was also performed. Neuro2a cells were plated and after 24 hr cells were harvested and subcellular fractionation was performed accordingly to the protocol mentioned in (6.2.9). The generated fractions were analysed by 12% SDS PAGE followed by Western blotting, and then probed using antibodies against calnexin (ER marker), GAPDH (cytoplasmic marker) and PDI to detect endogenous PDI expression. The total cell lysate was used as a control fraction. The integrity of the fractions was confirmed by expression of GAPDH only in the cytoplasmic fraction and calnexin only in the ER fraction. PDI was present only in the ER fraction: a faint band of approximately 59 kDa was present (Figure 6.2 E).

A

B

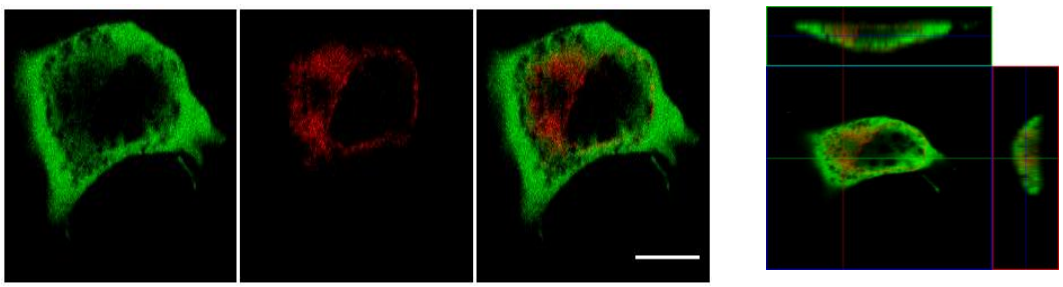
CYTO PDI
CALRETICULIN
MERGE

C

D

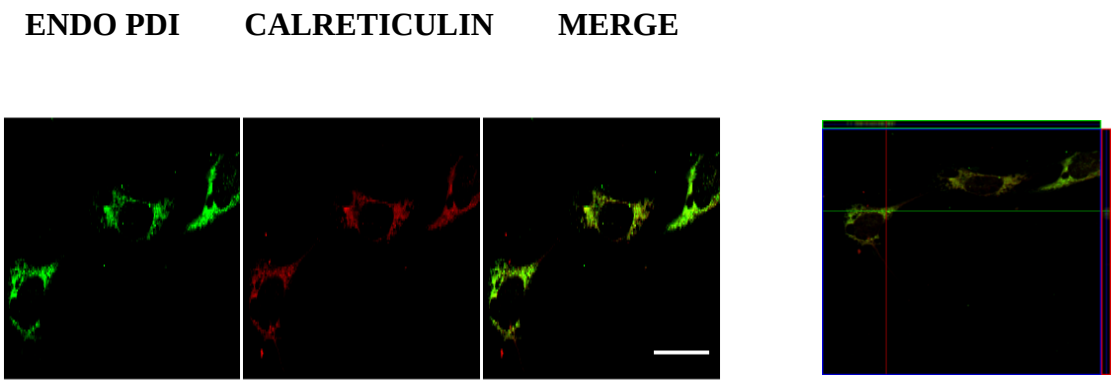
ENDO PDI
CALRETICULIN
MERGE

E

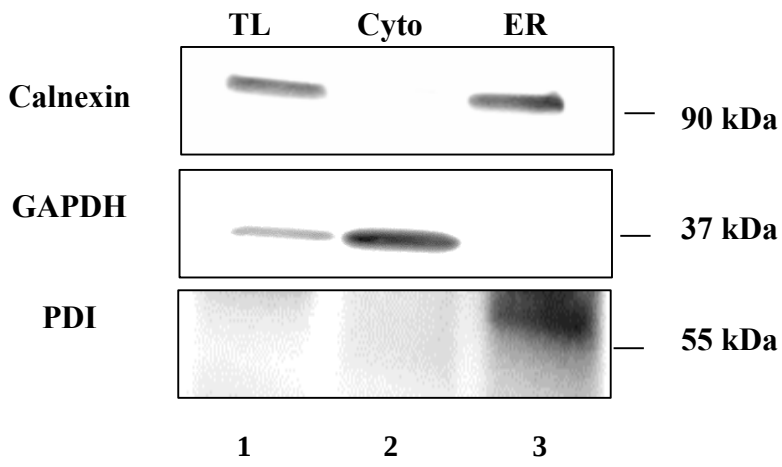
TL
Cyto
ER
Calnexin
90 kDa
GAPDH
37 kDa
PDI
55 kDa
1
2
3

Figure 6.2 Characterization of the subcellular location of CYTO PDI, PDI WT, PDI QUAD and endogenous PDI. A) Confocal microscopy images of Neuro2a cells expressing CYTO PDI (green) immunostained using antibodies against ER marker calreticulin (red). CYTO PDI does not co-localise with calreticulin and its distribution appeared cytoplasmic, as observed in the merge image. **B)** Orthogonal section of confocal images in (A) confirming that CYTO PDI does not co-localise with ER marker calreticulin. Scale bar = 10 µm. **C)** Confocal microscopy images of mouse primary cortical neurons immunostained using antibodies against PDI (green) in and ER marker calreticulin (red). Endogenous mouse PDI colocalises with calreticulin as observed in the merge image, demonstrating ER-localisation. Scale bar = 10 µm. **D)** Orthogonal section of the confocal images in H, showing co-localisation of endogenous PDI in primary neurons with ER marker calreticulin. **E)** Western blot demonstrating subcellular fractionation of Neuro2a cell lysates. Calnexin was used as an ER marker (~ 90 kDa) and GAPDH was used as a cytoplasmic marker (37 kDa). Lane 1-total cell lysate (TL), 2-Cytoplamic fraction, 3-ER fraction. Total cell lysate was used as a control. Endogenous PDI was observed in the ER fraction only (lane 3).

The cellular distribution of wild-type PDI and PDI QUAD expressed in Neuro2a cells was also examined. Neuro2a cells were transfected with constructs encoding either wild-type PDI or PDI QUAD and observed 24 hr post transfection using confocal microscopy. Immunocytochemistry was performed using anti-V5 antibodies to detect wild-type PDI and PDI QUAD expression, and anti-calreticulin antibodies as an ER marker. Confocal microscopy was performed to verify the localisation of these proteins. Both wild-type PDI and PDI QUAD co-localised with ER marker calreticulin, confirming their subcellular localisation in the ER, as expected (Figure 6.3 A, C). This was further confirmed by observing the orthogonal section of the z stack image (Figure 6.3 B, D).

The localisation of wild-type PDI, PDI QUAD and CYTO PDI was further confirmed using subcellular fractionation experiments. Neuro2a cells were transfected with wild-type PDI, PDI QUAD or CYTO PDI in pcDNA3.1 and 72 hr post transfection harvested and subcellular fractionation was performed. The fractions generated were analysed by 12% SDS PAGE followed by Western blotting and probed with antibodies against Ire-1α (ER marker), GAPDH (cytoplasmic marker) and V5 to detect expression of PDI. The total cell lysate was used as a control and as expected, contained GAPDH, which is normally present in the cytoplasmic fraction, and Ire1-a, which is normally present in the ER fraction. Both wild-type PDI and PDI QUAD were expressed in the ER and the cytoplasmic fractions. However, in contrast, CYTO PDI was only present in the cytoplasmic fraction, and not in the ER fraction (Figure 6.3 E), demonstrating that targeting to the cytoplasm only was successful.

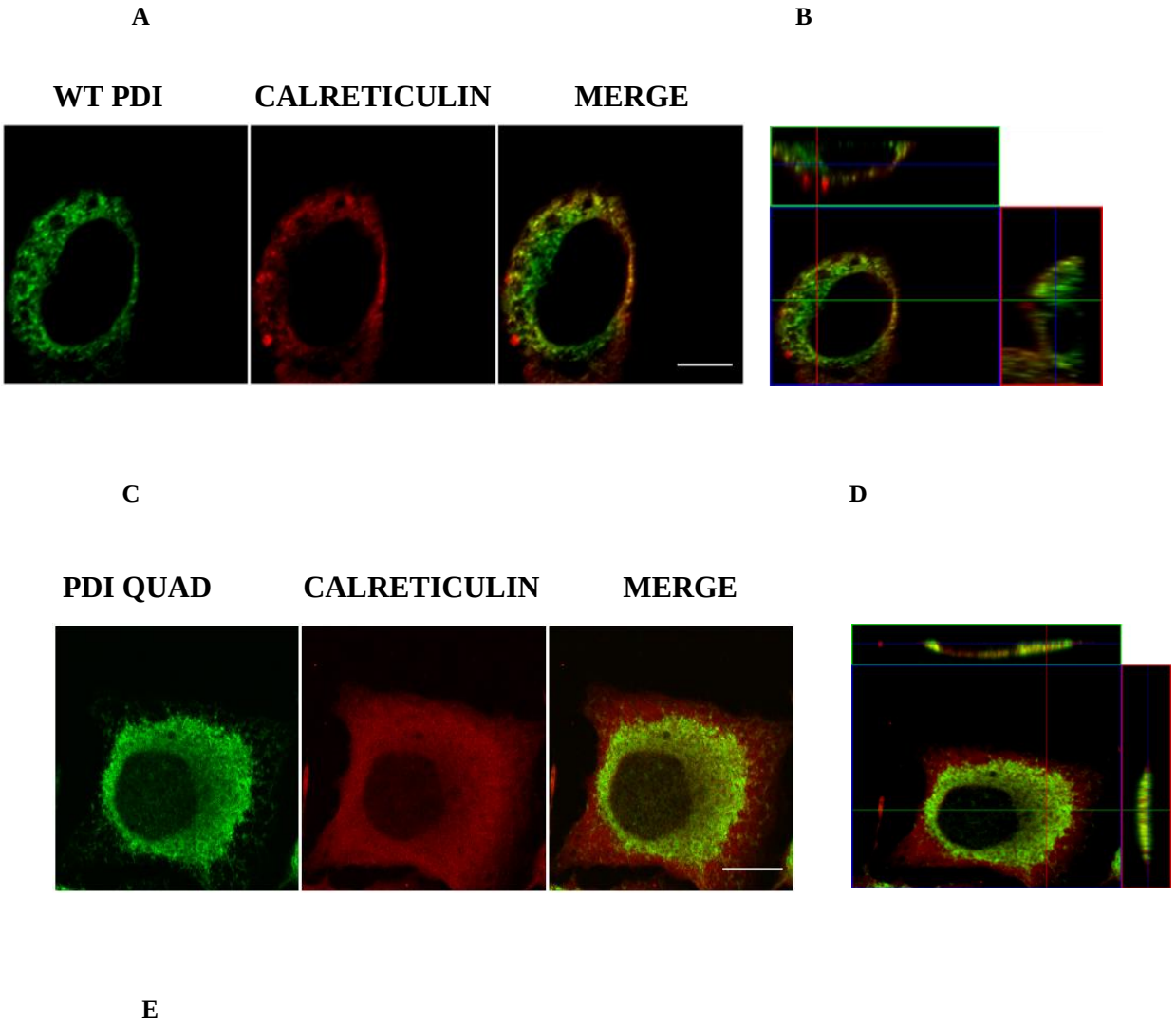
A
B
WT PDI
CALRETICULIN
MERGE
C
D
PDI QUAD
CALRETICULIN
MERGE
E
Lysate
PDI WT
CYTO PDI
PDI QUAD
TL
E
C
E
C
E
C
V5
70 kDa
GAPDH
37 KDa
Ire-1a
125 kDa
1
2
3
4
5
6
7

Figure 6.3 Characterization of the subcellular location of CYTO PDI, wild-type PDI and PDI QUAD. A) Confocal microscopy images of Neuro2a cells expressing wild-type PDI (green) immunostained using antibodies against ER marker calreticulin (red). Wild-type PDI co-localised with calreticulin as observed in the merge image. Scale bar = 10 µm. **B)** Orthogonal section of the confocal images in C, showing co-localisation of wild-type PDI with ER marker calreticulin. **C)** Confocal microscopy images of Neuro2a cells expressing PDI QUAD (green) immunostained with antibodies against ER marker calreticulin (red). PDI QUAD co-localises with calreticulin, as observed in the merge image. Scale bar = 10 µm. Orthogonal section of confocal images in F, showing co-localisation of PDI QUAD with the ER marker calreticulin. Scale bar = 10 µm. **E)** Western blot demonstrating subcellular fractionation of wild-type PDI, PDI CYTO and PDI QUAD cell lysate extracts. Total cell lysate is represented as (TL), ER-rich fraction as (E) and the cytoplasmic fraction as (C). Ire-1α was used as an ER marker (125 kDa), and GAPDH was used as a cytoplasmic marker (37 kDa). Lane 1-total lysate (TL), 2-ER rich fraction for wild-type PDI overexpressing cells, 3-Cytoplasmic fraction for wild-type PDI overexpressing cells, 4-ER fraction for CYTO PDI overexpressing cells, 5-Cytoplasmic fraction for CYTO-PDI overexpressing cells, 6-ER fraction for PDI QUAD overexpressing cells, 7-Cytoplasmic fraction for PDI QUAD. Total cell lysate was used as a control. Wild-type PDI (lane 2, 3) and PDI QUAD (lane 6, 7) were observed in both the ER and the cytoplasmic fractions. However in contrast, CYTO PDI was only detected in the cytoplasmic fraction (lane 5) and not in the ER fraction**.**

6.3.3 Over-expression of CYTO PDI is protective against mutant SOD1 induced ER stress in neuronal cell lines

Previously in Chapter 4 it was demonstrated that over-expression of wild-type PDI (CGHC CGHC) was protective against mutant SOD1 induced ER stress, inclusion formation and cell death in neuronal cell lines. However PDI QUAD, containing mutations in the active site regions (SGHS SGHS) was not protective. Hence, it was next examined whether CYTO PDI was also protective against mutant SOD1 expressed in neuronal cells, to address where the subcellular location where this protection is mediated. Neuro2a cells were co-transfected with wild-type SOD1 or $SOD1^{A4V}$ with empty vector and wild-type PDI, PDI QUAD or CYTO PDI. Immunocytochemistry was performed using anti-CHOP antibodies to examine nuclear immunoreactivity to CHOP, used as a marker of ER stress. Transfected cells were observed 72 hr post transfection using fluorescence microscopy (Figure 6.4 A).

As expected, few control untransfected cells (5%), and cells expressing EGFP or wild-type SOD1 (7%) induced ER stress. as indicated by nuclear CHOP immuno-reactivity, similar to the results presented in Chapter 4. In contrast, in Neuro2a expressing mutant $SOD1^{A4V}$, that were also co-transfected with empty vector pcDNA3.1, 50% of cells displayed nuclear CHOP immunoreactivity. Interestingly, co-expressing either CYTO PDI or wild-type PDI WT with $SOD1^{A4V}$ had a protective effect. Co-expression of wild-type PDI reduced nuclear CHOP immunoreactivity to only 28% ($p<.001$) of transfected cells. Similarly, there was a significant reduction in the proportion of CYTO PDI expressing cells with ER stress, as only 35% ($p<.001$) cells displayed nuclear CHOP immunoreactivity (Figure 6.4 B). Similar to the results obtained in Chapter 4, co-expression of PDI QUAD with $SOD1^{A4V}$, did not reduce the proportion of cells with nuclear immunoreactivity 42% cells. These data imply that PDI localised in the cytoplasm is protective against ER stress induced by mutant $SOD1^{A4V}$.

A

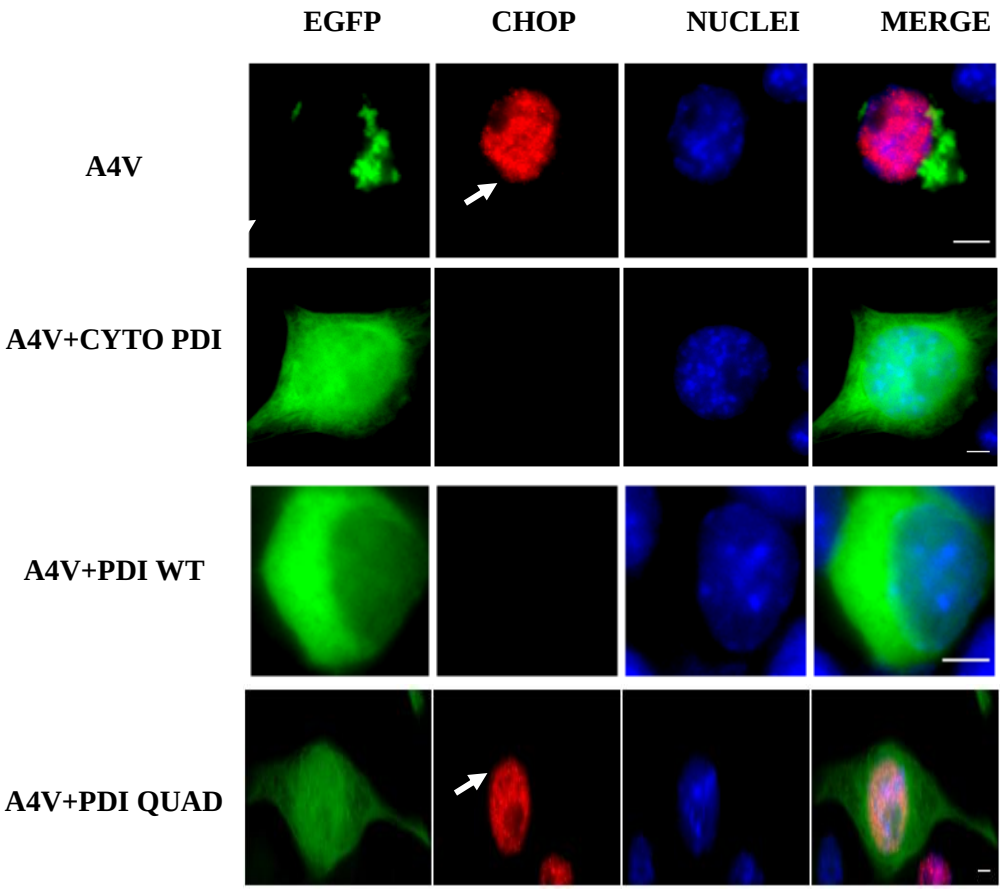
EGFP
CHOP
NUCLEI
MERGE
A4V
A4V+CYTO PDI
A4V+PDI WT
A4V+PDI QUAD

B

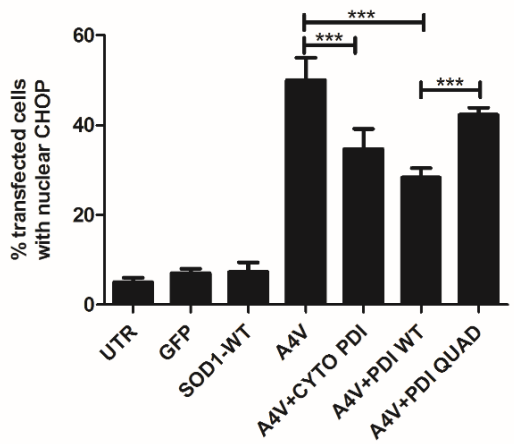
% transfected cells with nuclear CHOP
60
40
20
0
***
***
***
UTR
GFP
SOD1-WT
A4V
A4V+CYTO PDI
A4V+PDI WT
A4V+PDI QUAD

Figure 6.4 CYTO PDI and wild-type PDI are protective against ER stress induced by mutant SOD1 in Neuro2a cells. A) Immunofluorescent images of Neuro2a cells co-expressing mutant $SOD1^{A4V}$ with PDI CYTO, wild-type PDI or PDI QUAD. Neuro2a cells expressing $SOD1^{A4V}$ (A4V, first panel), immunostained using anti-CHOP antibodies, (middle panel) nuclear immunoreactivity to CHOP indicated with white arrow. Co-expression of CYTO PDI (second panel) or wild-type PDI (third panel), but not PDI QUAD (fourth panel), leads to a reduction in ER stress. Scale bar = 10 μm. **B)** Quantification of nuclear CHOP immunoreactivity in Neuro2a cells visualised in (A), co-expressing wild-type SOD1 or $SOD1^{A4V}$ with PDI CYTO, wild-type PDI or PDI QUAD. Significantly fewer cells were detected with nuclear CHOP immunoreactivity (***, $p<.001$) between $SOD1^{A4V}$ cells transfected with vector alone compared to those co-expressing CYTO PDI or wild-type PDI. 100 successfully transfected cells expressing CHOP in the nucleus were counted in each case. For each of 3 replicate experiments, 100 cells were scored for each population. Data are presented as mean ± SEM, tested with one-way ANOVA and Tukey's post-test, n = 3.

6.3.4 CYTO PDI is protective against the formation of mutant SOD1 inclusions and cell death in neuronal cell lines

Since CYTO PDI was protective against mutant SOD1 induced ER stress, the effect of CYTO PDI on inclusion formation and cell death induced by mutant SOD1 in neuronal cultures was next observed. Neuro2a cells were co-transfected with wild-type SOD1 or $SOD1^{A4V}$ with empty vector or CYTO PDI, wild-type PDI or PDI QUAD. Transfected cells were observed 72 hr post transfection using fluorescence microscopy and the percentage of transfected cells bearing mutant SOD1 inclusions was quantified by visualising the presence of EGFP fluorescence (Figure 6.5 A). As expected, Neuro2a cells expressing EGFP vector or wild-type SOD1 formed very few inclusions (<1%). Conversely, 21% of cells expressing mutant $SOD1^{A4V}$ with empty vector pcDNA3.1 formed inclusions, similar to

previous results. Co-expression of wild-type PDI significantly reduced the proportion of cells with mutant $SOD1^{A4V}$ inclusions, as previous 16% ($p<.01$). However, importantly, co-expression of CYTO PDI with mutant $SOD1^{A4V}$ resulted in a significant reduction in the proportion of cells forming inclusions, to only 12% ($p<.001$) of cells (Figure 6.5 B). CYTO PDI was significantly protective suggesting that cytoplasmic location of PDI preserves its protective ability. As in Chapter 4, co-expression of PDI QUAD did not significantly reduce inclusion formation.

A

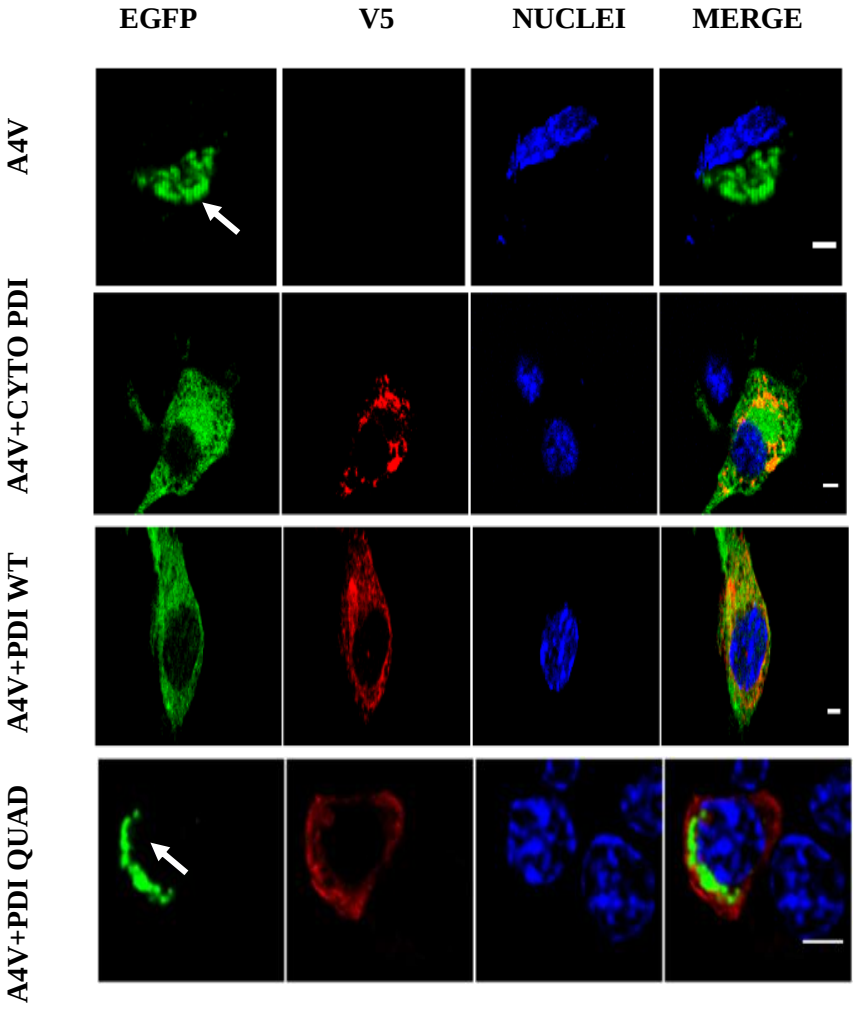
EGFP
V5
NUCLEI
MERGE
A4V
A4V+CYTO PDI
A4V+PDI WT
A4V+PDI QUAD

B

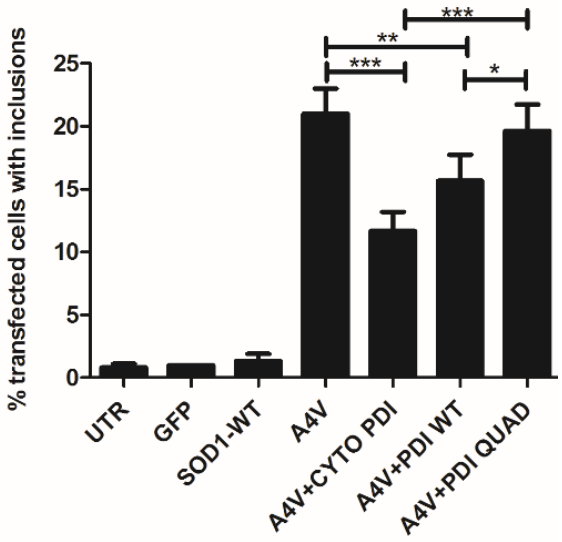
% transfected cells with inclusions
25
20
15
10
5
0
***
**
***
*
UTR
GFP
SOD1-WT
A4V
A4V+CYTO PDI
A4V+PDI WT
A4V+PDI QUAD

Figure 6.5 CYTO PDI is protective against inclusion formation induced by mutant SOD1. A) Immunofluorescent images of Neuro2a cells co-expressing mutant $SOD1^{A4V}$ with PDI CYTO, wild-type PDI or PDI QUAD. Neuro2a cells expressing $SOD1^{A4V}$ that form inclusions (A4V, first panel), indicated with white arrow. On co-expressing CYTO PDI (second panel) or wild-type PDI (third panel) significantly fewer cells formed inclusions. However, co-expressing PDI QUAD (fourth panel) did not alter the percentage of inclusion positive cells. Scale bar = 10 μm. **B)** Quantification of the percentage of transfected Neuro2a cells bearing inclusions, visualised in (A), co-expressing wild-type SOD1 or $SOD1^{A4V}$ with PDI CYTO, wild-type PDI or PDI QUAD. There was a significant difference in the percentage of cells forming inclusions, between $SOD1^{A4V}$ alone and when co-transfected with (**p<.01) wild-type PDI, and (***p<.001) CYTO PDI. There was also a significant difference in the percentage of cells forming inclusions, between (***p<.001) $SOD1^{A4V}$ with CYTO PDI and $SOD1^{A4V}$ with PDI QUAD. 100 cells expressing mutant SOD1 were counted. For each of 3 replicate experiments, 100 cells were scored for each population. Data are presented as mean ± SEM, tested with one-way ANOVA and Tukey's post-test, n = 3. Where *p<.05, **p<.01 and ***p<.001.

Next, cell death was examined in cells expressing mutant SOD1, using nuclear morphology analysis. Neuro2a cells were co-transfected with wild-type SOD1 or $SOD1^{A4V}$ with empty vector or wild-type PDI, PDI QUAD or CYTO PDI. Immuno-cytochemistry was performed using anti-V5 antibodies to detect the expression of PDI. Transfected cells were observed 72 hr post transfection using fluorescence microscopy, and quantification of apoptosis was performed by examining the cells for the presence of fragmented nuclei, indicative of apoptosis [483, 644]. Fragmented nuclei and nuclei without detectable DAPI were significantly more common (12%) in cells expressing $SOD1^{A4V}$ than in those expressing wild-type SOD1 ($p<.001$), consistent with previous observations (Figure 6.6 A). Also as previous, co-expressing wild-type PDI or PDI QUAD with mutant $SOD1^{A4V}$ resulted in significantly fewer cells with apoptotic nuclei 8%, $p<.01$ and 9%, $p<.05$ (Figure 6.6 B). Interestingly, co-expressing CYTO PDI with mutant $SOD1^{A4V}$ significantly reduced the proportion of cells with apoptotic nuclei to only 6% ($p<.001$). These data suggest that PDI located in cytoplasm is protective against apoptotic cell death induced by mutant SOD1.

A

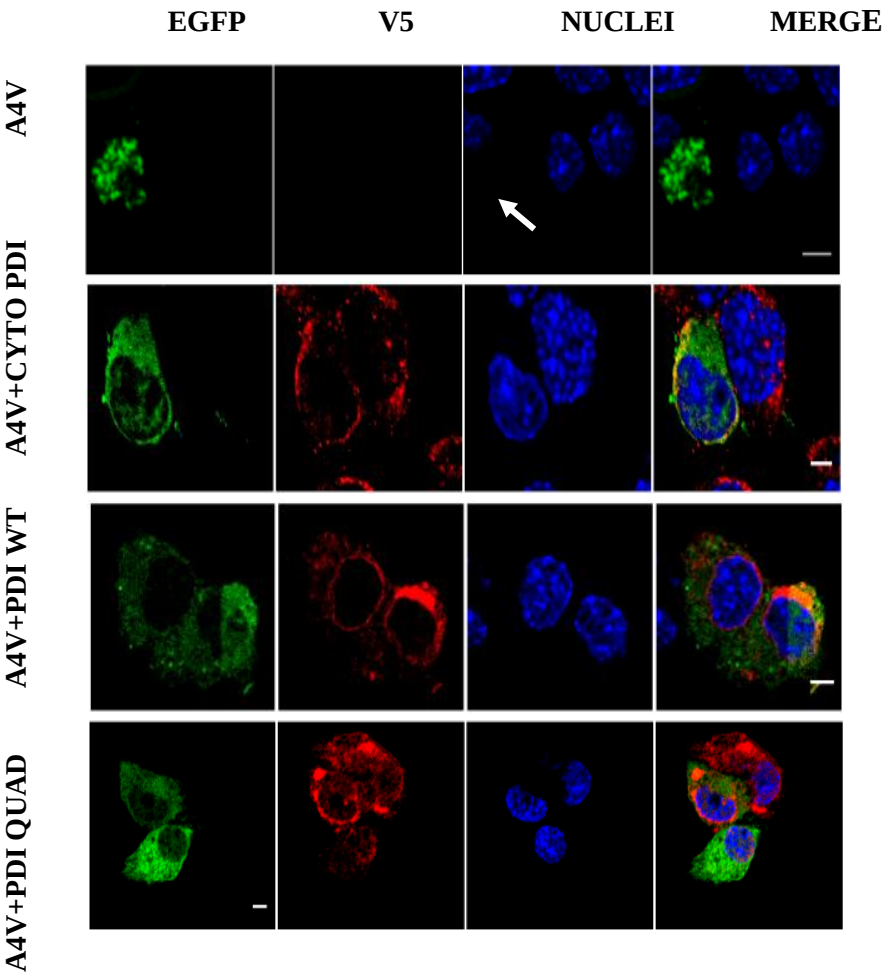
EGFP
V5
NUCLEI
MERGE
A4V
A4V+CYTO PDI
A4V+PDI WT
A4V+PDI QUAD

B

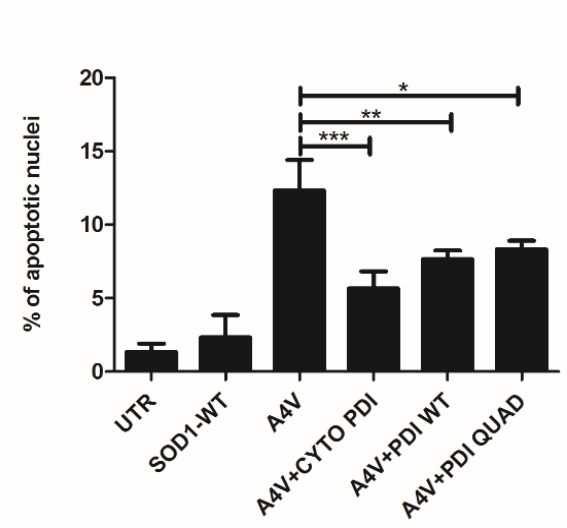
% of apoptotic nuclei
20
15
10
5
0
*
**
***
UTR
SOD1-WT
A4V
A4V+CYTO PDI
A4V+PDI WT
A4V+PDI QUAD

Figure 6.6 CYTO PDI is protective against apoptotic cell death induced by mutant SOD1. A) Immunofluorescent images of Neuro2a cells co-expressing mutant $SOD1^{A4V}$ with PDI CYTO, wild-type PDI or PDI QUAD. Nuclei are visualised using Hoechst staining (blue). Arrow represents nuclei without detectable DAPI, indicating that apoptosis is underway. Neuro2a cells expressing $SOD1^{A4V}$ with fragmented nuclei (A4V, first panel), indicated with white arrow. On co-expressing CYTO PDI (second panel), wild-type PDI (third panel), PDI QUAD (fourth panel) fewer cells were undergoing apoptosis. Scale bar = 10 μm. **B)** Quantification of apoptotic nuclei in cells shown in (A), expressing SOD1 and PDI. There was a significant difference in the proportion of $SOD1^{A4V}$ expressing cells with apoptotic nuclei between cells co-transfected with empty vector compared to those co-expressing (**, $p<.01$) wild-type PDI, (***, $p<.001$) CYTO PDI and (*, $p<.05$) PDI QUAD. For each of 3 replicate experiments, 100 cells were scored for each population. Data are presented as mean ± SEM, tested with one-way ANOVA and Tukey's post-test, n = 3.

6.3.5 CYTO PDI is protective against mislocalisation of TDP-43 in the cytoplasm and induction of ER stress in neuronal cell lines

As CYTO PDI was protective in neuronal cell lines expressing mutant SOD1, it was next examined whether CYTO PDI was also protective against ER stress and mislocalisation induced by mutant TDP-43. Neuro2a cells were co-transfected with wild-type TDP-43 or mutant TDP-43 (Q331K), and empty vector or either CYTO PDI, wild-type PDI or PDI QUAD (Figure 6.7 A). Immunocytochemistry was performed using anti-CHOP antibodies to examine nuclear immunoreactivity as a marker for ER stress. Transfected cells were observed 18 hr post transfection using fluorescence microscopy.

In control, untransfected cells (UTR) and cells transfected with empty vector few cells (5%) displayed nuclear CHOP immunoreactivity, similar to results presented in Chapter 4. In Neuro2a cells expressing wild-type TDP-43, 30% of cells displayed

nuclear CHOP immunoreactivity, and this was significantly increased in cells expressing mutant TDP-43 Q331K, where 40% of cells ($p<.01$) expressed nuclear CHOP. Interestingly, co-expression of mutant TDP-43 Q331K with CYTO PDI significantly fewer cells displayed nuclear CHOP immunoreactivity, indicating ER stress (28%,$p<.01$) (Figure 6.7 B). Similar results were obtained by co-expressing wild-type PDI with mutant TDP-43 Q331K, 28% of cells ($p<.01$) displayed nuclear immunoreactivity to CHOP. Hence both wild-type PDI and CYTO PDI were protective against ER stress induced by mutant TDP-43. In contrast, co-expression of PDI QUAD did not significantly reduce the proportion of cells with nuclear CHOP (35% cells). These data suggests that PDI localised in the cytoplasm is protective against ER stress induced by mutant TDP-43.

A

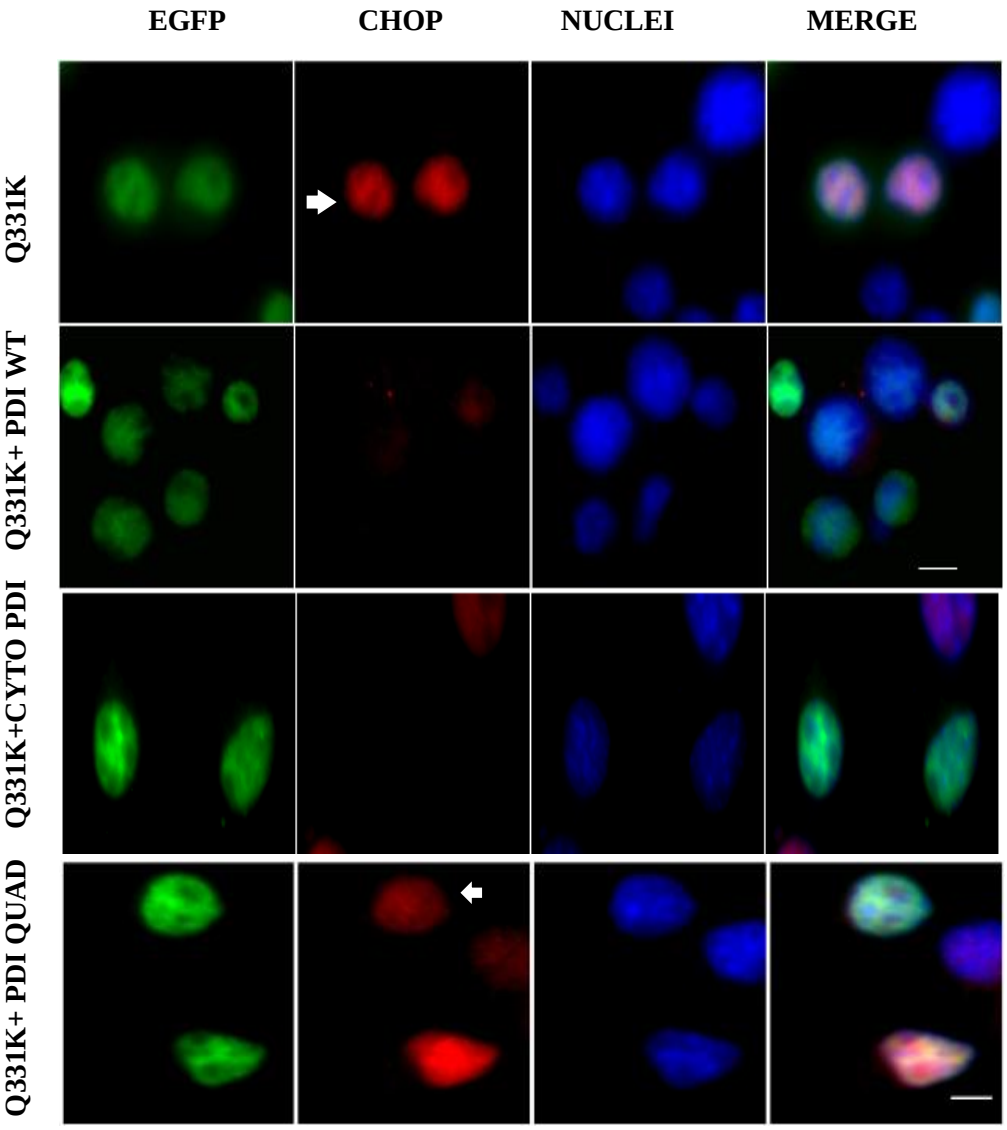
EGFP
CHOP
NUCLEI
MERGE
Q331K
Q331K+ PDI WT
Q331K+CYTO PDI
Q331K+ PDI QUAD

B

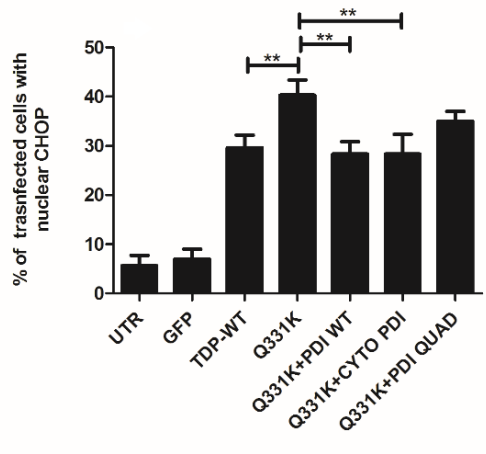
% of trasnfected cells with nuclear CHOP
50
40
30
20
10
0
**
**
**
UTR
GFP
TDP-WT
Q331K
Q331K+PDI WT
Q331K+CYTO PDI
Q331K+PDI QUAD

Figure 6.7 CYTO PDI is protective against the induction of ER stress. A) Immunofluorescent images of cells co-expressing mutant TDP-43 (Q331K) with CYTO PDI, wild-type PDI or PDI QUAD. Neuro2a cells expressing Q331K (first panel) display nuclear CHOP immunoreactivity as a marker of ER stress (middle panel), indicated using white arrows. However, co-expression of CYTO PDI or wild-type PDI with Q331K resulted in fewer cells with nuclear CHOP expression (second panel and third panel). In contrast, co-expression of PDI QUAD with Q331K did not alter the proportion of cells with nuclear CHOP expression (fourth panel), indicated by white arrow. Scale bar = 10 μm**. B)** Quantification of mutant TDP-43 Q331K expressing cells with nuclear CHOP immunoreactivity in (A), co-expressed with CYTO PDI, wild-type PDI or PDI QUAD. A significant difference in the proportion of cells displaying nuclear CHOP (** $p<.01$) was observed between wild-type TDP and Q331K expressing cells transfected with empty vector, and Q331K expressing cells cotransfected with either wild-type PDI or with CYTO PDI, compared to vector only. For each of 3 replicate experiments, 100 cells were scored for each population. Data are presented as mean ± SEM, tested with one-way ANOVA and Tukey's post-test, n = 3.

The effect of CYTO PDI on the cytoplasmic localisation of mutant TDP-43 was next examined. Neuro2a cells were co-transfected with wild-type TDP-43 or mutant TDP-43 (Q331K), with empty vector or CYTO PDI, wild-type PDI or PDI QUAD (Figure 6.8 A). Immunocytochemistry was performed using anti-V5 antibodies to detect the expression of PDI. Transfected cells were observed 18 hr post transfection using fluorescence microscopy.

In Neuro2a cells expressing wild-type TDP only 25% of transfected cells displayed cytoplasmic localisation of TDP-43. As expected, in comparison, an increased proportion of cells expressed TDP-43 in the cytoplasm in mutant TDP-43 Q331K cells (36% cells, $p<.01$). However, on co-expression of mutant TDP-43 Q331K cells with CYTO PDI, significantly fewer cells expressed TDP-43 in the cytoplasm compared to cells expressing Similar to previous results (Chapter 4), significantly fewer transfected cells expressing wild-type PDI 26% ($p<.01$) displayed cytoplasmic TDP-43. Hence both CYTO PDI and wild-type PDI were protective against the cytoplasmic localisation of mutant TDP-43. In contrast, PDI QUAD did not reduce the proportion of cells with TDP-43 31% of transfected cells were detected with cytoplasmic localisation (Figure 6.7 B).

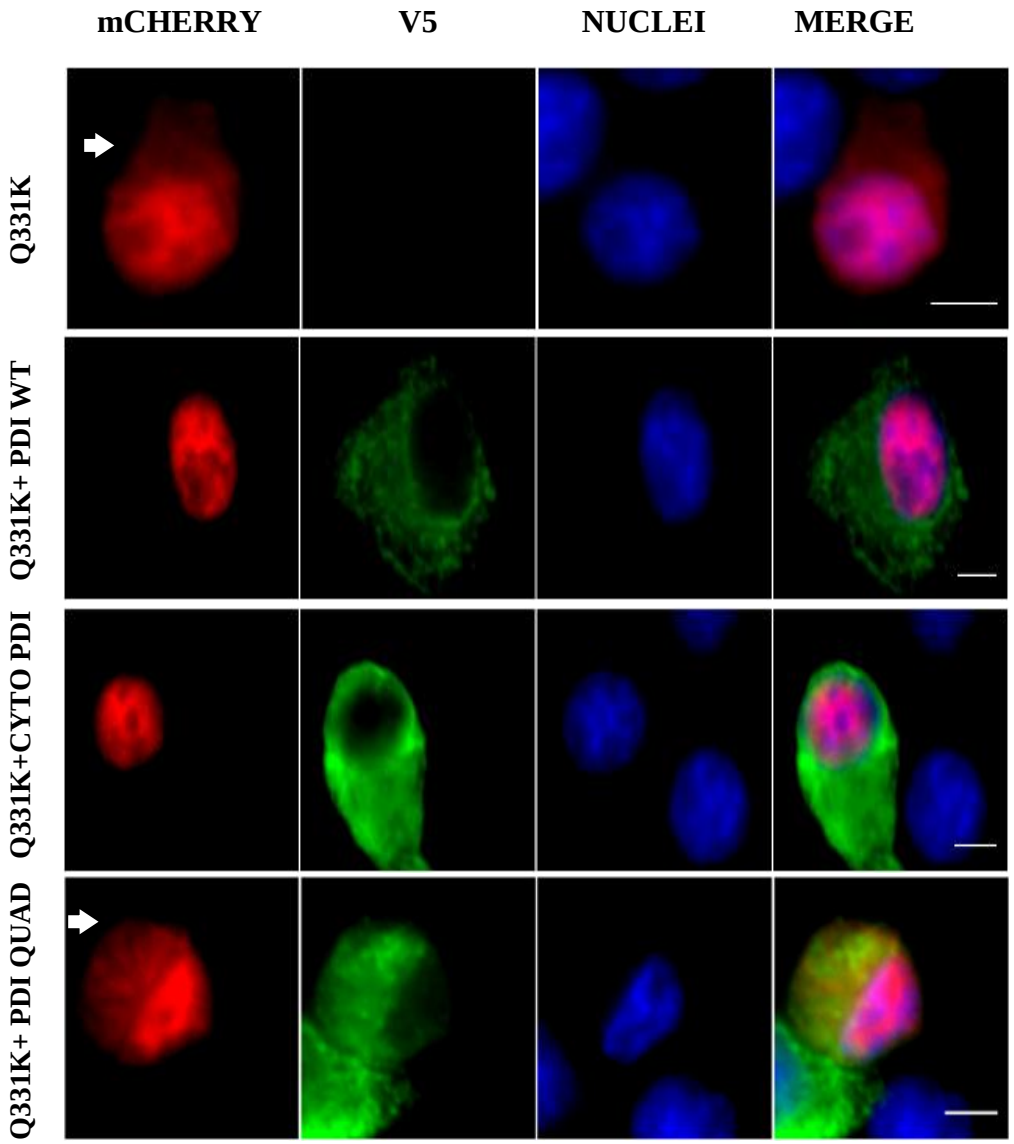
mCHERRY
V5
NUCLEI
MERGE
Q331K
Q331K+ PDI WT
Q331K+CYTO PDI
Q331K+ PDI QUAD

B

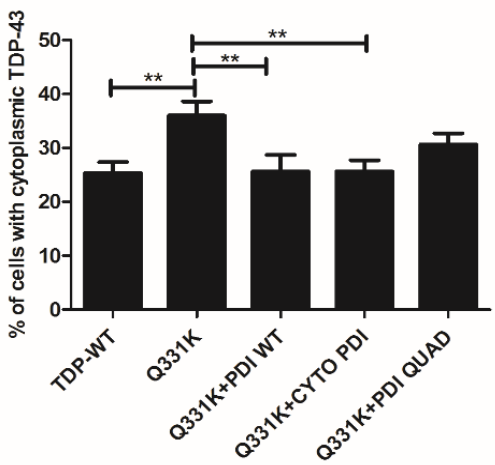
% of cells with cytoplasmic TDP-43
50
40
30
20
10
0
**
**
**
TDP-WT
Q331K
Q331K+PDI WT
Q331K+CYTO PDI
Q331K+PDI QUAD

Figure 6.7 CYTO PDI is protective against the localisation of TDP-43 in the cytoplasm. A) Immunofluorescent images of Neuro2a cells co-expressing TDP-43 and PDI. Significantly more cells expressed TDP-43 in the cytoplasm in mutant TDP-43 Q331K cells compared to wild-type TDP-43 cells (first panel), indicated using white arrows. On overexpressing wild-type PDI or CYTO PDI significantly fewer cells displayed cytoplasmic localisation of mutant TDP-43 Q331K (second and third panel). However, on co-expressing PDI QUAD with Q331K the cytoplasmic distribution did not change (fourth panel). **B)** Quantification of mutant TDP-43 and- PDI expressing cells in (A) that display cytoplasmic distribution of TDP-43. A significant difference in the proportion of cells with cytoplasmic TDP-43 was observed between cells expressing wild-type TDP and Q331K (**) $p<.01$, and between Q331K cells expressing vector only, and (**) wild-type PDI or CYTO PDI. For each of 3 replicate experiments, 100 cells were scored for each population. Data are presented as mean ± SEM, tested with one-way ANOVA and Tukey's post-test, $n = 3$.

6.3.6 CYTO PDI is protective against induction of ER stress and mislocalisation of FUS in the cytoplasm in neuronal cell lines

As CYTO PDI was protective in neuronal cell lines expressing mutant SOD1 and TDP-43, it was next examined whether CYTO PDI was also protective against ER stress and mislocalisation induced by mutant FUS.Neuro2a cells were co-transfected with wild-type FUS (FUS-WT) or mutant FUS (R522G) with empty vector or either CYTO PDI or wild-type PDI or PDI QUAD (Figure 6.9 A). Immunocytochemistry was performed using anti-CHOP antibodies to detect nuclear immunoreactivity to CHOP, indicating activation of ER stress. Transfected cells were observed 72 hr post transfection using fluorescence microscopy.

In Neuro2a cells expressing wild-type FUS, only 14% of cells displayed nuclear CHOP immunoreactivity, compared to approximately 50% of cells expressing mutant FUS R522G, similar to previous findings. Notably, on co-expressing CYTO PDI with mutant FUS R522G, significantly fewer cells expressed nuclear CHOP immunoreactivity (37%, $p<.05$) of transfected cells, (Figure 6.9 B). Similarly, co-expressing either wild-type PDI or PDI QUAD also reduced the proportion of cells with nuclear CHOP immunoreactivity, to 34% ($p<.01$) and 38% ($p<.05$) of transfected cells respectively. These data reveal that CYTO PDI is also protective against ER stress induced by mutant FUS R522G.

A

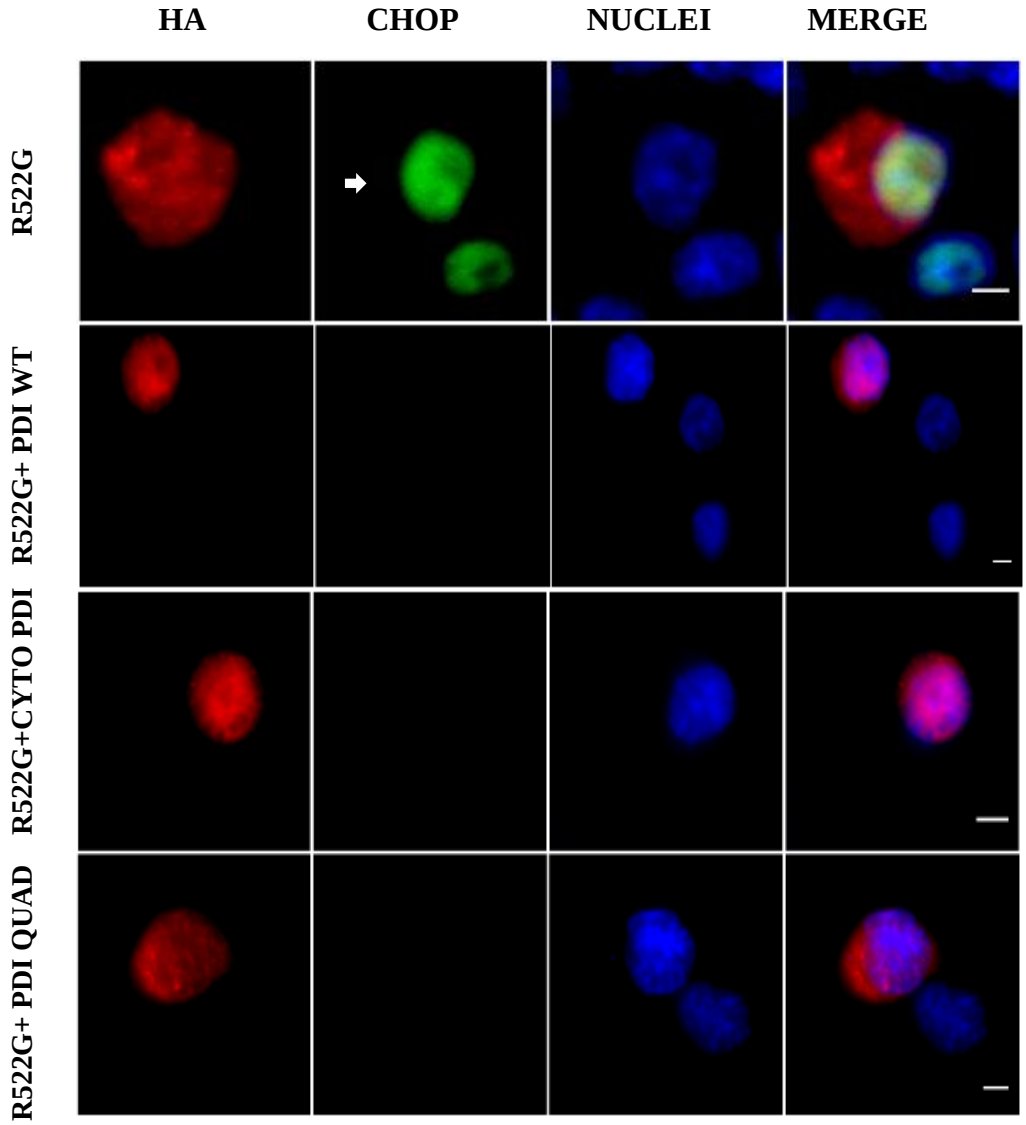
HA
CHOP
NUCLEI
MERGE
R522G
R522G+ PDI WT
R522G+CYTO PDI
R522G+ PDI QUAD

B

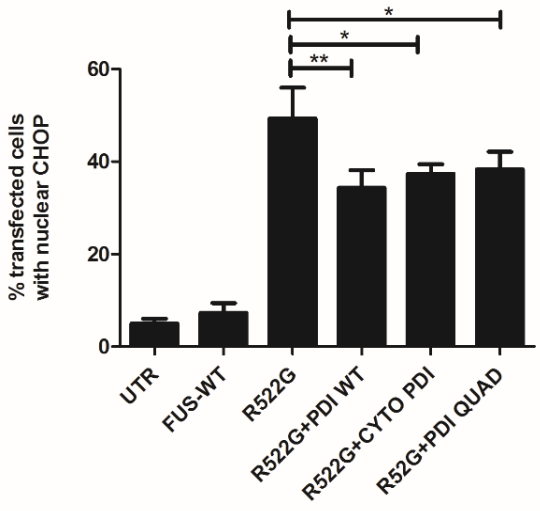
% transfected cells with nuclear CHOP
60
40
20
0
*
*
**
UTR
FUS-WT
R522G
R522G+PDI WT
R522G+CYTO PDI
R52G+PDI QUAD

Fig 6.9 CYTO PDI reduces the proportion of cells with ER stress in Neuro2a cells. A) Immunofluorescent images of Neuro2a cells co-expressing mutant FUS R522G with PDI proteins. Neuro2a cells expressing mutant FUS R522G (first panel) display nuclear CHOP immunoreactivity, (middle panel) indicated with white arrow. On over-expressing wild-type PDI, CYTO PDI or PDI QUAD significantly fewer cells displayed nuclear CHOP immunoreactivity, indicating ER stress (second, third panel, fourth panel). Scale bar = 10 µm. **B)** Quantification of mutant FUS expressing cells with nuclear CHOP immunoreactivity, co-expressing wild-type PDI, CYTO PDI or PDI QUAD, in (A). A significant difference (**) in the proportion of FUS R522G cells displaying nuclear CHOP immunoreactivity was observed when cells were co-transfected with wild-type PDI, (*) CYTO PDI or PDI QUAD. For each of 3 replicate experiments, 100 cells were scored for each population. Data are presented as mean ± SEM, tested with one-way ANOVA and Tukey's post-test, n = 3, where *p<.05. **p<.01.

Furthermore, the effect of CYTO PDI against the cytoplasmic localisation of mutant FUS was examined. Neuro2a cells were co-transfected with wild-type FUS or mutant FUS (R522G) and with empty vector or either CYTO PDI, wild-type PDI or PDI QUAD (Figure 6.10 A). Immunocytochemistry was performed using anti-HA antibodies to detect the expression of FUS, and anti-V5 antibodies to detect the expression of PDI. Transfected cells were observed 72 hr post transfection using fluorescence microscopy.

In Neuro2a cells expressing wild-type FUS only 18% of transfected cells expressed FUS in the cytoplasm. Conversely, 70% cells expressing FUS mutant P525L displayed cytoplasmic localisation of FUS ($p<.001$). However, when CYTO PDI was co-expressed with mutant FUS, significantly fewer cells expressed FUS in the cytoplasm (48%, $p<.01$) compared to mutant FUS cells co-transfected with empty vector. Hence these data suggest that PDI located in the cytoplasm is protective against the mislocalisation of mutant FUS in the cytoplasm. (Figure 6.10 B). Similar results were obtained when wild-type PDI or PDI QUAD were co-expressed with mutant FUS: significantly fewer cells of expressing FUS in the cytoplasm (49%, $p<.01$) and (53%, $p<.01$) respectively.

A

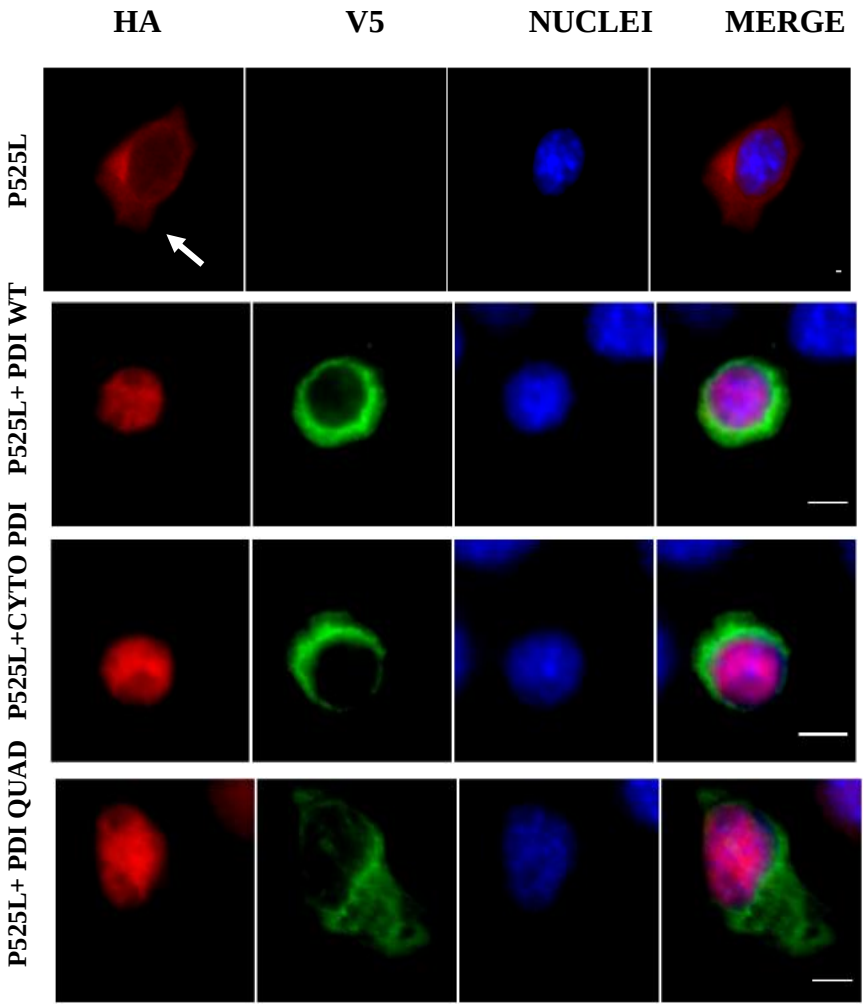
HA
V5
NUCLEI
MERGE
P525L
P525L+ PDI WT
P525L+CYTO PDI
P525L+ PDI QUAD

B

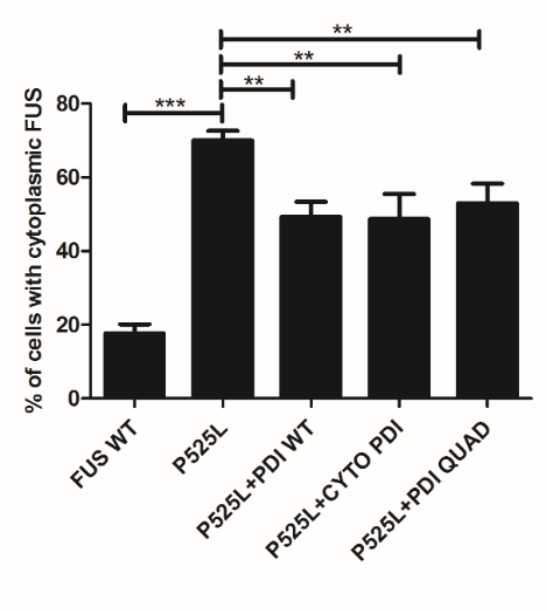
% of cells with cytoplasmic FUS
0
20
40
60
80
***
**
**
**
FUS WT
P525L
P525L+PDI WT
P525L+CYTO PDI
P525L+PDI QUAD

Fig 6.10 CYTO PDI reduces the proportion of cells localised in the cytoplasm. **A)** Immunofluorescent images of Neuro2a cells co-expressing mutant FUS P525L with PDI proteins. A proportion of Neuro2a cells express mutant FUS P525L (first panel) in the cytoplasm, indicated with white arrow. On over-expressing wild-type PDI, CYTO PDI or PDI QUAD, fewer cells displayed cytoplasmic FUS distribution (second, third panel, fourth panel). Scale bar = 10 μm. **B)** Quantification of cells in (A), with cytoplasmic distribution of mutant FUS. A significant difference in the proportion of cells expressing FUS in the cytoplasm was observed between wild-type FUS and P525L (***), and between cells co-expressing mutant FUS P525L with CYTO PDI, wild-type PDI or PDI QUAD (**). For each of 3 replicate experiments, 100 cells were scored for each population. Data are presented as mean ± SEM, tested with one-way ANOVA and Tukey's post-test, n = 3, where **p<.01 and ***p<.001.

6.3 Discussion

The main findings of this study are that by restricting the subcellular location of PDI to the cytoplasm, its protective activities could be retained, suggesting that the cytoplasm is the subcellular compartment where protection occurs. Cytoplasmic PDI (CYTO PDI) was generated by deleting the signal peptide and KDEL sequence from PDI, which are responsible for targeting to the ER, and retention in the ER, respectively. The cytoplasmic location of CYTO PDI and its exclusion from the ER was confirmed using confocal microscopy and subcellular fractionation. Interestingly, CYTO PDI was protective against mutant SOD1 induced ER stress, inclusion formation and apoptosis in neuronal cell lines. Similarly, CYTO PDI protected against mutant TDP-43 and FUS induced ER stress and mislocalisation to the cytoplasm.

SOD1 is predominately cytoplasmic and pathological forms of TDP-43 and FUS are present in the cytoplasm [89, 746, 747]. The reasons why cytoplasmic PDI is protective remain unclear. However, CYTO PDI could be protective due to availability of the substrate, or due to augmented interaction with the mutant ALS proteins in the cytoplasm compared to the ER. Alternatively, the reducing environment of the cytoplasm could assist in isomerisation of non-native disulphide bonds and may prevent the misfolding of ALS mutant proteins SOD1, TDP-43 and FUS.

Additionally, CYTO PDI was protective against the formation of mutant SOD1 inclusions in neuronal cell lines. This finding suggests that CYTO PDI could possibly interact better with misfolded mutant SOD1, which localises in the same compartment, and hence exert more protection. Similarly, CYTO PDI also reduced SOD1 induced apoptosis. PDI assists in the retrotranslocation of misfolded proteins into the cytosol for proteolysis [748]. Hence, CYTO PDI may recognise misfolded proteins in the cytoplasm and therefore degrade them more efficiently, thus reducing toxicity. It is possible that the interaction of PDI with other cytosolic

proteins not yet identified is involved. PDI family members have the ability to form multiprotein complex *via* a network of chaperones against protein misfolding [704]. Therefore, cytoplasmic PDI may also interact with other PDI family members and chaperones localised in the cytoplasm, thus enhancing the beneficial effect.

The findings of this study suggest that expression of PDI in the cytoplasm is beneficial in neuronal cultures expressing ALS-mutant proteins. Interestingly, sub-cellular fractionation experiments demonstrated that wild-type PDI and PDI QUAD localised both in the ER and the cytoplasm. However, it should be noted that expression of PDI in the cytoplasm could be an artefact, since experimental over-expression is not physiological and it is possible that highly expressed recombinant proteins mis-localised or leak into the cytoplasm. Also in preparations of ER compartment the danger of a presence of other membrane bound organelles such as the Golgi or some nuclear lumenal proteins is quite real. The studies with endogenous PDI here, consistent with previous studies, have shown that PDI is expressed profusely in the ER region surrounding the nuclear membrane [510]. However, the non-ER localisation of PDI has been substantiated by multiple experimental approaches, in numerous studies, thus arguing against the possibility that cytoplasmic PDI is due entirely to contamination [510, 725, 749, 750]. Similar PDI redistribution has been detected in ALS, and hence may occur primarily during disease states.

The localisation of PDI may affect its protein folding ability and thus influence its function during disease states. PDI is highly expressed in spinal cord motor neurons and is protective against misfolded proteins but undergoes aberrant post-translational modification in ALS [483]. This study shows that cytoplasmic PDI is protective effect, hence it could be postulated that during disease states, induction of ER stress could lead to the leakage of endogenous PDI in the cytoplasm where it may more favourably interact with cytoplasmic protein substrates. It has been demonstrated that PDI is released in the cytoplasm during ER stress-induced apoptosis in a Bax-dependent manner [751]. Therefore, an indirect mechanism may

explain the protective effect of cytoplasmic PDI, possibly *via* a non-classical ER stress pathway. Recently our group demonstrated that mutant TDP-43, FUS and SOD1 inhibit ER-Golgi transport in neuronal cultures [552, 557]. Furthermore, mutant TDP-43 was observed at the cytoplasmic face of the ER and inhibited ER-Golgi transport from the cytoplasm. Hence, PDI available in the cytoplasm would be beneficial against such cellular defects induced by mutant proteins. However, due to S-nitrosylation, PDI may be non-functional in the cytoplasm. This would be important to examine in sporadic ALS, where the exact role of PDI remains poorly defined.

Another possible explanation for the protective effect of PDI could be reticulon-modulated re-distribution of PDI. Previous evidence suggests that PDI redistributes away from the ER in ALS, where enhanced enzymatic activity was demonstrated. However, in this study the precise localisation of punctate PDI that was associated with protection could not clearly be define [531]. Although the oxidation of newly formed disulphide bonds in substrate proteins is difficult in the cytoplasm due to the reducing environment, other possible mechanisms have been proposed through which PDI could isomerise disulphide bonds in proteins in the cytoplasm [511].The reduced form glutathione in the cytoplasm assists PDI in the non-native disulphide bond rearrangements [752].

A key question which arises from the studies presented in this Chapter is, if distribution of PDI is protective in ALS, at what stage during the disease process does PDI become distributed away from the ER. Reticulon-1C mediated distribution of PDI did not affect ER morphology and also did not induce UPR [576]. However, other cellular insults, such as oxidative stress and heat shock, could be responsible for the cellular distribution of PDI in non-ER locations. Therefore, investigating the mechanism by which reticulons mediate PDI re-distribution is an exciting question that should be addressed in future studies. Similarly, it would also be interesting to investigate the role of a cytoplasmic version of the PDI QUAD mutant in future studies. These type of studies would further assist in understanding

the precise role of the disulphide interchange activity of PDI and its beneficial role against mutant proteins linked to ALS, since cytoplasmic PDI was protective against three major misfolded proteins in this study. The findings of these studies may provide new clues in designing novel therapeutics which could be targeted to the cytosol rather than other cellular compartments. This may also explain how BMC, a synthetic mimic of PDI which is not confined to the ER, was protective as described previously.

Hence, in summary in the studies outlined in this Chapter, the subcellular location of PDI was examined in relation to its protective activity. It was demonstrated that the disulphide interchange activity of PDI, when localised in the cytoplasm, is protective in cells expressing the major misfolded proteins linked to ALS, mutant SOD1, TDP-43 and FUS. Hence, small molecules that mimic the protective activity of cytoplasmic PDI, may be a novel therapeutic target, and relevant to multiple forms of ALS.

.

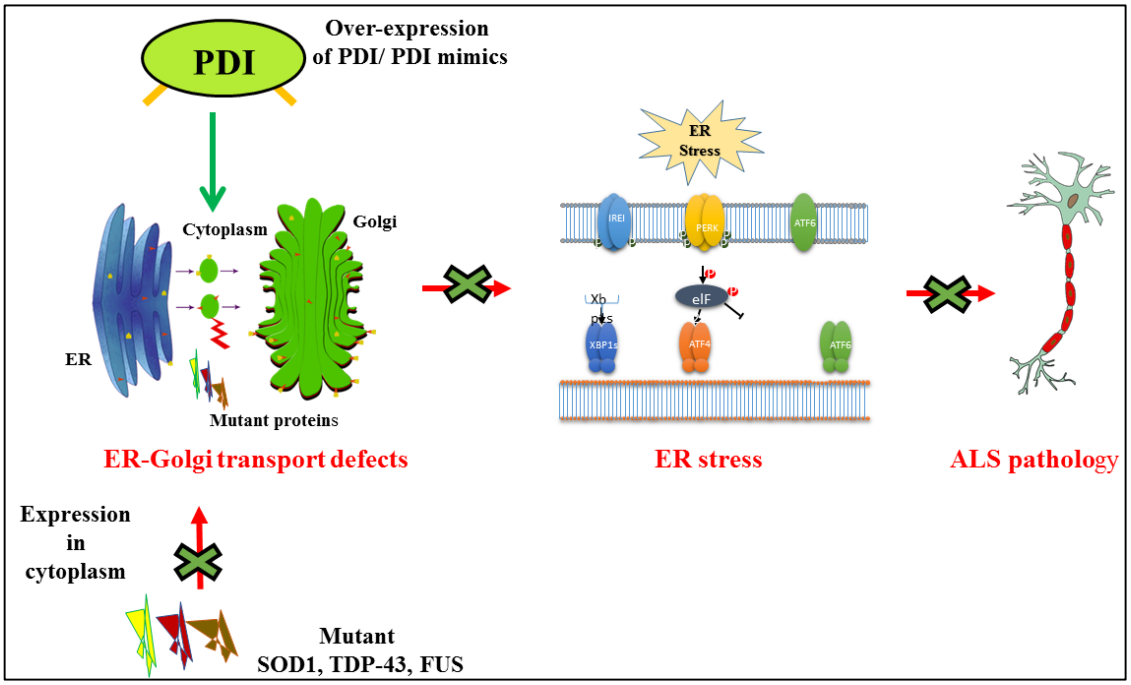

Figure 6.7 Schematic representation outlining the possible mechanism of action of CYTO PDI in ALS. This schematic diagram summarizes how PDI may be protective in ALS. During disease states, the cysteine residues of PDI become modified by S-nitrosylation, rendering PDI, nonfunctional. Furthermore, mutant, misfolded forms of SOD1, TDP-43 and FUS mislocalise to the cytoplasm, where they inhibit ER-Golgi transport, trigger ER stress, leading to apoptosis. However, on over-expression of CYTO PDI, PDI becomes accessible to these mutant proteins either through the disulphide interchange activity or chaperone activity and thus is protective. Therefore, a molecular mimic of PDI, which could compensate loss of endogenous PDI in the cytoplasm, may be a beneficial therapeutic target in ALS. The diagram is not to scale.

General Discussion

7.1 General Discussion

7.1.1 Summary of the main findings from this thesis

The main findings of this study demonstrate an important neuroprotective role for PDI against several of the major misfolded proteins associated with ALS; TDP-43, FUS and SOD1. These proteins are structurally and functionally different however, they portray a similar clinical pattern. Over-expression of PDI was protective against mutant SOD1, TDP-43 and FUS induced ER stress, ER-Golgi transport defects and mislocalisation into the cytoplasm in neuronal cell cultures. Importantly, insights into the mechanism of protection of PDI were also provided in this study. The disulphide interchange activity of PDI was found to be essential for protection against mutant SOD1 and mutant TDP-43, and it was also protective against mutant FUS. However, the chaperone activity was also protective against mutant FUS, unlike mutant TDP-43 and mutant SOD1. The molecular mimic of PDI - BMC was further protective against these mutant proteins, and administration of BMC rescued the loss of motor neurons in $SOD1^{G93A}$ mice, suggesting it is relevant to disease pathology. Furthermore, the involvement of other PDI family members, ERp57 and ERp72, in cellular models of ALS was investigated. Like PDI, ERp57 was found to be protective in cells expressing mutant SOD1, mutant TDP-43, and mutant FUS. Another homologue, ERp72, was also protective against mutant TDP-43 and mutant FUS, however it was not protective against mutant SOD1. These data suggest that specificity exists amongst PDI family members against these proteins. Lastly, the role of PDI in the cytoplasm was examined. By modulating the location of PDI in the cytoplasm, its protection could be preserved against mutant SOD1, TDP-43 and FUS in cellular cultures, suggesting that the cytoplasm is a primary location where PDI is protective. Moreover, the studies outlined in this thesis raise the possibility of utilising oxidoreductase chaperones such as PDI for designing therapeutic agents that could be trialled in ALS.

Mutant protein	*Pathology*	*PDI WT/BMC*	*PDI QUAD*	*CYTO PDI*
SOD1 - A4V	ER stress	✓	X	✓
SOD1 - A4V	ER-Golgi transport defects	✓	X	–
SOD1 - A4V	Inclusion formation	✓	X	✓
SOD1 - A4V	Apoptosis	✓	X	✓
TDP-43 - Q331K, Q343R, A315T	ER stress	✓	X	✓
TDP-43 - Q331K	ER-Golgi transport defects	✓	X	–
TDP-43 - Q331K, Q343R	Mislocalisation in cytoplasm	✓	X	✓
FUS - R522G, P525L	ER stress	✓	✓	✓
FUS - R522G	ER-Golgi transport defects	✓	✓	–
FUS - R522G, P525L R521C,R521H	Mislocalisation in cytoplasm	✓	✓	✓

Table 7.1 Summary of the results obtained from the thesis. Wild-type PDI with the disulphide interchange activity and BMC treatment were protective against all three mutant proteins – SOD1, TDP-43 and FUS. Similarly, CYTO PDI, localised only in the cytoplasm instead of the ER, was also protective against mutant SOD1, TDP-43 and FUS. The PDI

QUAD mutant, which only possessed chaperone activity, was only protective against mutant FUS.

7.1.2 PDI is protective against mutant TDP-43, FUS and SOD1 in neuronal cell lines.

The findings described in Chapter 3 highlight the importance of PDI in ALS and its broad role in disorders related to protein aggregation. Neurodegenerative diseases are associated with the accumulation and aggregation of misfolded proteins that are associated with induction of ER stress and apoptosis [316, 753]. Neuroblastoma cell culture models were used to demonstrate that over-expression of PDI protects against mutant TDP-43 and FUS induced ER stress, ER-Golgi transport defects and mislocalisation in the cytoplasm. Furthermore, PDI also protected against ER-Golgi transport defects induced by mutant SOD1 in Neuro2a cells, adding to previous findings from our group that PDI is protective against ER stress and apoptosis in cells expressing mutant SOD1 [483].

Protein misfolding is a common and intrinsic propensity of most proteins, even those that do not bear mutations, and it is influenced by amino acid composition and cellular conditions that can induce conformational changes [754]. Misfolded proteins display normally buried hydrophobic regions at their surfaces, which can lead to accumulation into protein aggregates, which may be toxic. Therefore, the normal cellular machinery is equipped with chaperones to refold aberrantly folded proteins and degrade protein aggregates [755]. PDI has distinctive properties that makes it an effective catalyst, such assist conformational flexibility, rapid ligand exchange, broad substrate specificity and ability to differentiate between unfolded and partial folded proteins [592]. Other chaperones, such as the heat shock proteins, are holdases and only decrease protein aggregation. However, PDI is unique since it reduces aggregation either by degrading misfolded proteins or by isomerising disulphide bonds present within the protein substrate, until the correct confirmation is achieved. This dual property of PDI could be particularly important in ALS and

other neurodegenerative conditions as pathogenic processes may induce autophagy failure and/or disturbance in the proteasome ubiquitin degradation system, which would further exacerbate protein misfolding [756].

However, PDI is S-nitrosylated in patients with ALS as well as in other neurodegenerative disorders [483]. This aberrant post-translational modification could therefore mask the normal protective function of PDI during disease states [483]. PDI S-nitrosylation may compromise its oxidoreductase functions, as well as its chaperone functions, further aggravating protein misfolding and ER stress in these conditions. Protein misfolding could additionally further deplete chaperones by sequestration, thus reducing the effective cellular pool of chaperones. This vicious circle may trigger the onset of disease due to the collapse of multiple cellular processes, thus dysregulating proteostasis [757].

The possibility of an alternative protective mechanism of PDI, unrelated to its chaperone or oxidoreductase activity, cannot be eliminated. Among the various important functions ascribed to PDI are that it is also involved in cytoskeleton reorganisation of actin *via* interaction with cysteine residues [758]. Since cytoskeletal defects are common in ALS pathology [759, 760], multifunctional PDI may exert protection *via* these types of processes, thus reducing the pathological consequences. Consistent with this notion, large motor neurons are particularly vulnerable to neurofilament abnormalities. Misfolded proteins can also induce axonal transport defects, which is a well described pathogenic process in ALS [343]. Hence, compensating PDI levels may facilitate axonal transport, which could have a beneficial effect on other related cellular processes, such as ER-Golgi transport. Alternatively, the ER-Golgi transport defects we have describe may underlie the axonal transport dysfunction identified in ALS, because these processes are clearly linked [448, 761].

The studies described in this thesis imply that the normal function of PDI is to protect against pathogenic processes induced by mutant ALS proteins. However,

due to unfavourable conditions, such as oxidative stress PDI can become non-functional, and other studies have demonstrated it acquires a toxic gain of function [741] and even becomes apoptotic [663, 762]. Therefore, it is possible that with PDI, both loss of its normal function and gain of aberrant, toxic functions, come into play. PDI may therefore act as a regulatory switch, in which PDI is initially protective against protein misfolding and aggregation. However, in response to unknown triggers, when proteostasis cannot otherwise be resolved, PDI subsequently becomes apoptotic (Figure 7.1), in what may be ultimately a protective mechanism to protect the organism from the burden of misfolded proteins. Therefore, aberrant post-translational modifications, together with the pro-apoptotic function of PDI, could further accentuate the adverse effects of PDI. This raises the possibility that therapeutic elevation of PDI activity, either by increasing the cellular levels of PDI, by administration of small molecular mimics of PDI activity, could be beneficial. In addition, reversal of PDI inhibition, or prevention of nitrosative stress, could also increase the protective capabilities of PDI [763]. Alternatively, it is also possible that the pro-apoptotic activities of PDI could be targeted as a possible therapeutic strategy, as was described in a study that identified PDI inhibitors such as muscimol that were protective in Huntington models [741].

It is important to mention some caveats to this study. The studies in this thesis incorporated the use of cell culture models overexpressing mutant proteins linked to ALS. The rationale with using these models is to gain a simplified, yet accelerated, view of the pathological consequences of expression of these mutant proteins and also investigate the effect of PDI. The microscopic techniques used allow us to examine the fate of a single transfected cell, rather than the total population, which is therefore not dependent on transfection efficiency. Immunoblotting assays can sometimes be less accurate because they sample the whole cell population, even though only a percentage of the cells actually express that protein [764]. However, it should be noted that transient transfections result in high levels of expression of mutant proteins, which may be non-physiological and therefore give rise to phenotypes not directly relevant to the disorder. Investigating cellular pathologies using stable cell lines expressing PDI, may eliminate aberrantly

levels of expression. Alternatively, in future studies other approaches could be used to express mutant proteins in cell culture, such as the use of the CRISPR/Cas9 technology, which could possibly give more physiological levels of expression [765]. This thesis shows that over-expression of ER targeted proteins results in expression in the cytoplasm, so these approaches may assist in understanding the effect of different localisation of PDI. Other improvements and better approaches would be to examine live cells using more advanced techniques such as foster resonance energy transfer (FRET) methods [766], since these techniques are efficient in determining the compartmentalization and functional organization of living cells [767]. FRET methods could assist in efficient characterisation of PDI subcellular localisation.

Furthermore, in future studies it would be worthwhile to investigate other pathologies related to the ER in relation to ALS, including dysregulation in the levels of calcium, the redox state of ER, or in ERAD function, which could impact on the protective functions of PDI. Fluorescence recovery after photobleaching (FRAP) could be utilised to directly determine the burden of misfolded protein within the ER using novel techniques and reagents recently developed [768, 769] that directly monitor the activities of chaperones such as BiP or PDI. ERAD substrates should also be monitored since they can provide insights into the functionality of the ER folding environment [770]. It would be worthwhile to investigate additional pathogenic events such as oxidative stress, response to heat or toxins. PDI might be selectively protective against particular events linked to ER however it might not exert similar protective against other cellular stressors.

Also in this thesis, VSVG was the only method examined to investigate ER-Golgi transport, and this is an overexpressed, non-physiological marker. Therefore, other alternative approaches are warranted, such as examining normal proteins secreted by neurons. Recently, a novel method of examining cellular transport using flow cytometry was described, which could be used in future studies to confirm the results obtained here [771]. Furthermore, the data obtained from the VSVG assay using Manders coefficient could further be validated and compared to data obtained

using Pearson correlation coefficient, which excludes background pixels [772]. These additional experiments could further strengthen the findings obtained in this study that elucidate the role of PDI in the pathogenesis of ALS.

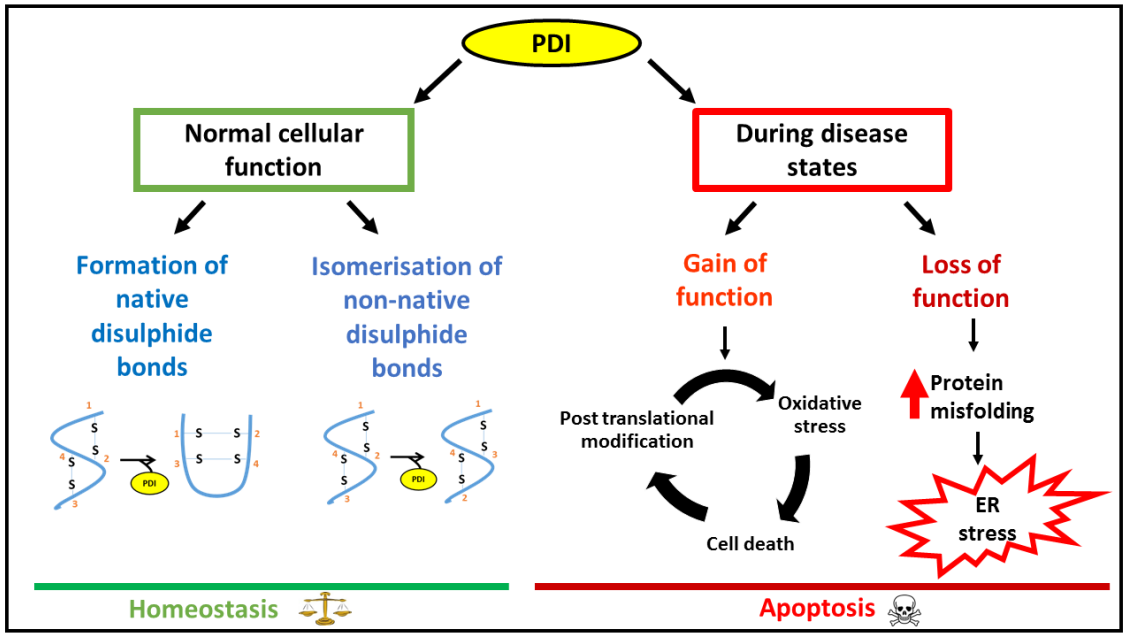

Figure 7.1 Schematic diagram outlining the dual nature of PDI in ALS. Under normal conditions, PDI reduces the load of misfolded proteins either by its chaperone activity or by isomerization of non-native bonds. However, during disease states, loss of the normal protective function of PDI as well as the gain of additional, toxic functions, leads to PDI becoming apoptotic, thus contributing to disease pathology.

7.1.3 Mechanism of action of PDI against mutant SOD1, TDP-43 and FUS in neuronal cell lines.

In order to exploit the protective ability of PDI and to develop therapeutic targets it is important to determine which key property of PDI makes it protective. In this study it was demonstrated that the disulphide interchange activity of PDI is

protective against mutant SOD1, mutant FUS and mutant TDP-43 in neuronal cell lines. Furthermore, BMC, the molecular mimic of the active site of PDI, was protective against all the three mutant proteins observed in this study *in vitro*. The disulphide residues of PDI are important for various functions in the cell, such as the specific recognition of misfolded proteins in the ER [773]. These residues are essential for interaction with other chaperones such as BiP. According to a proposed model, BiP and PDI form a multiprotein complex, where BiP binds to unfolded polypeptide chains, thus allowing PDI to access cysteine residues which otherwise are buried [774]. Additionally, reduction of disulphide bridges in substrate proteins by the cysteine residues of PDI are a prerequisite for their retro-translocation into the cytoplasm [775]. Although cysteine residues are important for the function of PDI, they are also susceptible to be modified by oxidative stress [547], which would consequently leading to redox dysregulation and loss of PDI function.

One gap in our knowledge of the function of PDI is whether the redox status of PDI could affect its protective ability. Since PDI is a redox regulated protein, it is important to understand the changes in the redox state during ER stress. An ER-targeted GFP that has been modified to become redox sensitive could be utilised to examine changes in ER redox potential in the presence of aberrant disulphide bond formation [776]. However, since the redox state of PDI *in vivo* is determined by numerous factors such as the redox environment of the ER, the availability and the concentration of glutathione and the specific substrate, it is hard to replicate similar conditions *in vitro*. Investigations using Dsb (bacterial disulphide oxido-reductase) rather than PDI may also assist in understanding the redox regulation conditions necessary for the protective function of PDI in ALS because the redox machinery is simpler in DsbA and its redox requirements are now well understood [586, 777, 778]. BMC was protective both *in vitro* and *in vivo* models, and more detailed experiments to investigate how BMC delays symptom onset and progression in $SOD1^{G93A}$ mice and reduces neuropathology, are now in progress in our laboratory.

7.1.4 Role of PDI family members Erp57 and ERp72 against mutant SOD1, TDP-43 and FUS in neuronal cell lines.

The reasons why so many PDI family members exist remains unclear since the PDI proteins have very similar functions in the isomerisation and refolding of misfolded proteins. The results in this thesis also demonstrate the protective role of PDI family members ERp57 and ERp72 in cellular models of ALS. Therefore, further detailed investigations into the role of other PDI family members in ALS is warranted. Specific PDI family members could be involved in preventing misfolding of certain specific misfolded protein substrates, or alternatively they may function in a cell-type specific manner. Sequence comparisons of the substrate binding domains of these proteins has suggested that there are similarities between PDIp, PDILT, ERp27, ERp44 and PDI [686], suggesting that these family members could also bind to misfolded proteins similar to PDI. Similarly, understanding how PDI family members compensate each other's function would be another approach to understand the mechanism of protection of PDI. Given that ER stress is a central process in ALS, it would also be worthwhile investigating other ER chaperones related to PDI to provide further insights into how this family of proteins function in ALS. Peptidyl prolyl isomerase is an ER chaperone that also assists in the isomerisation of disulphide bonds in proteins [773]. This could be an important molecule to investigate to further understand if indeed the disulphide interchange activity of PDI is the key feature which protects against mutant proteins.

The PDI family of proteins may have broader functions than just isomerisation and formation of disulphide bonds. There is some evidence that they regulate quality control mechanisms and therefore regulating ER homeostatic mechanism. ERdj5 is a co-chaperone of BiP that directs BiP to bind to unfolded proteins during UPR induction [704]. Some PDI family members also interact with heat shock proteins, including HSP70 [505, 779]. However, defining the *in vivo* functions of chaperone proteins is difficult to determine due to their intrinsically complex substrate specificity. Hence knock down studies, in which the activity of each protein is negligible, would assist in examining the role of individual PDI family members.

However, the presence of active site cysteine residues in all PDI family members, may render them susceptible to post-translational modifications, and hence they may be non-functional during disease state.

7.1.5 Role of Cytoplasmic PDI against mutant SOD1, TDP-43 and FUS in neuronal cell lines.

The studies outlined in chapter 6 demonstrate that PDI in the cytoplasm is protective against mutant SOD1, TDP-43 and FUS in neuronal cultures. By deletion of the signal peptide and the ER retention signal KDEL, the cellular localisation of PDI was directed to the cytoplasm, and we confirmed that PDI was no longer expressed in the ER. Cytoplasmic PDI was efficient in rescuing several pathological processes induced by mutant SOD1, TDP-43 and FUS, implying that the subcellular location of PDI does affect its protective functions. However, this observation has opened up several questions which should be investigated in future studies. For example, does the cell modulate the location of PDI as a defence against different stressors, to facilitate augmented protein folding? Furthermore, what levels of PDI are optimal to protect the cell against these stressors during disease states, given that the cytoplasm does not ideally favour disulphide bond formation? It would therefore be worthwhile to determine the binding partners of PDI which assist in its protective function in the cytoplasm. Conversely, it should be noted that PDI in non-ER locations can have adverse effects. Cell surface PDI facilitates the entry of nitric oxide into the cell, which subsequently can induce post-translational modifications into proteins [780]. Furthermore, PDI at the mitochondrial-associated ER membrane (MAM) regulates apoptotic signalling in Huntington models, and induces apoptosis [741]. Therefore the role of PDI within different cellular locations is clearly important in terms of its function and therefore needs detailed investigation in the future.

7.2 Concluding remarks

ALS is a late onset disease which is coupled with decreased cellular defences and increased protein misfolding. PDI is an efficient catalyst and protein chaperone. It

has the ability to restore proteostasis by catalysing the efficient folding of newly synthesized proteins, and it plays an important role in protein quality control. The protective functions of PDI may be modulated by the subcellular location of PDI, levels of ER stress, redox environment and post-translational modification. In this study, over-expression of PDI positively modified the deleterious cellular features of pathogenic SOD1, TDP-43 and FUS mutations, thereby reducing the vicious stress cycle. Elevation of the levels of total PDI, with the aim of restoring PDI function and therefore reduce protein misfolding, could be an effective therapeutic approach in ALS. Similarly, reducing the levels of aberrantly modified PDI might also be necessary in neurodegeneration, in order to defend against the pro-apoptotic properties of PDI. Taken together these findings suggest that PDI may have therapeutic potential for the treatment of ALS and related neurodegenerative disorders associated with protein misfolding, which should be investigated in the future in *in vivo* approaches.

References

1. Wood, E.M., *Amyotrophic Lateral Sclerosis*, in *Genetic Counseling for Adult Neurogenetic Disease*. 2015, Springer. p. 163-182.

2. Rosenfeld, J. and M.J. Strong, *Challenges in the Understanding and Treatment of Amyotrophic Lateral Sclerosis/Motor Neuron Disease.* Neurotherapeutics, 2015: p. 1-9.

3. Ajroud-Driss, S. and T. Siddique, *Sporadic and hereditary amyotrophic lateral sclerosis (ALS).* Biochimica et Biophysica Acta (BBA)-Molecular Basis of Disease, 2014.

4. Rutkove, S.B., *Clinical Measures of Disease Progression in Amyotrophic Lateral Sclerosis.* Neurotherapeutics, 2015: p. 1-10.

5. Miller, R.G., et al., *Riluzole for amyotrophic lateral sclerosis (ALS)/motor neuron disease (MND).* The Cochrane Library, 2007.

6. Bensimon, G., L. Lacomblez, and V.f. Meininger, *A controlled trial of riluzole in amyotrophic lateral sclerosis.* New England Journal of Medicine, 1994. **330**(9): p. 585-591.

7. Matus, S., D.B. Medinas, and C. Hetz, *Common Ground: Stem Cell Approaches Find Shared Pathways Underlying ALS.* Cell stem cell, 2014. **14**(6): p. 697-699.

8. Renton, A.E., A. Chiò, and B.J. Traynor, *State of play in amyotrophic lateral sclerosis genetics.* Nature neuroscience, 2014. **17**(1): p. 17-23.

9. Laferrière, F. and M. Polymenidou, *Advances and challenges in understanding the multifaceted pathogenesis of amyotrophic lateral sclerosis.* Swiss medical weekly, 2015. **145**: p. w14054.

10. Ravits, J.M. and A.R. La Spada, *ALS motor phenotype heterogeneity, focality, and spread Deconstructing motor neuron degeneration.* Neurology, 2009. **73**(10): p. 805-811.

11. Sabatelli, M., et al., *Uncovering amyotrophic lateral sclerosis phenotypes: clinical features and long-term follow-up of upper motor neuron-dominant ALS.* Amyotrophic Lateral Sclerosis, 2011. **12**(4): p. 278-282.

12. Rosenfeld, J. and M. Swash, *What's in a name? Lumping or splitting ALS, PLS, PMA, and the other motor neuron diseases.* Neurology, 2006. **66**(5): p. 624-625.

13. Turner, M.R., et al., *The diagnostic pathway and prognosis in bulbar-onset amyotrophic lateral sclerosis.* Journal of the neurological sciences, 2010. **294**(1): p. 81-85.

14. Lomen-Hoerth, C., T. Anderson, and B. Miller, *The overlap of amyotrophic lateral sclerosis and frontotemporal dementia.* Neurology, 2002. **59**(7): p. 1077-1079.

15. Hodges, J., et al., *Survival in frontotemporal dementia.* Neurology, 2003. **61**(3): p. 349-354.

16. Burrell, J.R., et al., *Motor neuron dysfunction in frontotemporal dementia.* Brain, 2011: p. awr195.

17. DeJesus-Hernandez, M., et al., *Expanded GGGGCC hexanucleotide repeat in noncoding region of C9ORF72 causes chromosome 9p-linked FTD and ALS.* Neuron, 2011. **72**(2): p. 245-256.

18. Ling, S.-C., M. Polymenidou, and D.W. Cleveland, *Converging mechanisms in ALS and FTD: disrupted RNA and protein homeostasis.* Neuron, 2013. **79**(3): p. 416-438.

19. Haverkamp, L.J., V. Appel, and S.H. Appel, *Natural history of amyotrophic lateral sclerosis in a database population Validation of a scoring system and a model for survival prediction.* Brain, 1995. **118**(3): p. 707-719.

20. Londral, A., et al., *Quality of life in ALS patients and caregivers: impact of assistive communication from early stages.* Muscle & nerve, 2015.

21. Rollins, Y.D., B. Oskarsson, and S.P. Ringel, *Primary lateral sclerosis.* 2009.

22. Sakowski, S.A. and E.L. Feldman, *The Spectrum of Motor Neuron Diseases: From Childhood Spinal Muscular Atrophy to Adult Amyotrophic Lateral Sclerosis.* Neurotherapeutics, 2015: p. 1-3.

23. Abrahams, S., et al., *Relation between cognitive dysfunction and pseudobulbar palsy in amyotrophic lateral sclerosis.* Journal of Neurology, Neurosurgery & Psychiatry, 1997. **62**(5): p. 464-472.

24. Valdmanis, P.N. and G.A. Rouleau, *Genetics of familial amyotrophic lateral sclerosis.* Neurology, 2008. **70**(2): p. 144-152.

25. Beghi, E., et al., *The epidemiology of ALS and the role of population-based registries.* Biochimica et Biophysica Acta (BBA)-Molecular Basis of Disease, 2006. **1762**(11): p. 1150-1157.

26. Majoor, I., *Krakauer D, Willems PJ, Hofman A.* Genetic epidemiology of amyotrophic lateral sclerosis. Clin Genet, 2003. **63**: p. 83-101.

27. Manjaly, Z.R., et al., *The sex ratio in amyotrophic lateral sclerosis: a population based study.* Amyotrophic Lateral Sclerosis, 2010. **11**(5): p. 439-442.

28. Laaksovirta, H., et al., *Chromosome 9p21 in amyotrophic lateral sclerosis in Finland: a genome-wide association study.* The Lancet Neurology, 2010. **9**(10): p. 978-985.

29. Cronin, S., O. Hardiman, and B.J. Traynor, *Ethnic variation in the incidence of ALS A systematic review.* Neurology, 2007. **68**(13): p. 1002-1007.

30. Gordon, P.H., et al., *Incidence of amyotrophic lateral sclerosis among American Indians and Alaska natives.* JAMA neurology, 2013. **70**(4): p. 476-480.

31. Zaldivar, T., et al., *Reduced frequency of ALS in an ethnically mixed population A population-based mortality study.* Neurology, 2009. **72**(19): p. 1640-1645.

32. Mehta, P., et al., *Prevalence of amyotrophic lateral sclerosis-United States, 2010-2011.* MMWR Surveill Summ, 2014. **63**(suppl 7): p. 1-14.

33. Kiernan, M.C., et al., *Amyotrophic lateral sclerosis.* The Lancet, 2011. **377**(9769): p. 942-955.

34. Al-Chalabi, A. and O. Hardiman, *The epidemiology of ALS: a conspiracy of genes, environment and time.* Nature Reviews Neurology, 2013. **9**(11): p. 617-628.

35. Pupillo, E., et al., *Trauma and amyotrophic lateral sclerosis: a case–control study from a population-based registry.* European Journal of Neurology, 2012. **19**(12): p. 1509-1517.

36. Armon, C. and S.M. Albert, *A blow to the head trauma–ALS hypothesis.* Neurology, 2015: p. 10.1212/WNL. 0000000000001528.

37. Valenti, M., et al., *Amyotrophic lateral sclerosis and sports: a case–control study.* European journal of neurology, 2005. **12**(3): p. 223-225.

38. Sutedja, N.A., et al., *Exposure to chemicals and metals and risk of amyotrophic lateral sclerosis: a systematic review.* Amyotrophic Lateral Sclerosis, 2009. **10**(5-6): p. 302-309.

39. Fang, F. and W. Ye, *Smoking may be considered an established risk factor for sporadic ALS.* Neurology, 2010. **74**(23): p. 1927-1929.

40. Armon, C., *Smoking may be considered an established risk factor for sporadic ALS.* Neurology, 2009. **73**(20): p. 1693-1698.

41. Gallo, V., et al., *Smoking and risk for amyotrophic lateral sclerosis: analysis of the EPIC cohort.* Annals of neurology, 2009. **65**(4): p. 378-385.

42. Alonso, A., et al., *Association of smoking with amyotrophic lateral sclerosis risk and survival in men and women: a prospective study.* BMC neurology, 2010. **10**(1): p. 6.

43. Wang, H., et al., *Smoking and risk of amyotrophic lateral sclerosis: a pooled analysis of 5 prospective cohorts.* Archives of neurology, 2011. **68**(2): p. 207-213.

44. Verma, A. and J.R. Berger, *ALS syndrome in patients with HIV-1 infection.* Journal of the neurological sciences, 2006. **240**(1): p. 59-64.

45. Alfahad, T. and A. Nath, *Retroviruses and amyotrophic lateral sclerosis.* Antiviral research, 2013. **99**(2): p. 180-187.

46. Coffman, C.J., et al., *Estimating the occurrence of amyotrophic lateral sclerosis among Gulf War (1990-1991) veterans using capture-recapture methods.* Neuroepidemiology, 2004. **24**(3): p. 141-150.

47. Horner, R.D., J.R. Feussner, and E.J. Kasarskis, *Neurological mortality among Gulf War veterans.* American journal of industrial medicine, 2010. **53**(5): p. 548-549.

48. Cox, P.A., S.A. Banack, and S.J. Murch, *Biomagnification of cyanobacterial neurotoxins and neurodegenerative disease among the Chamorro people of Guam.* Proceedings of the National Academy of Sciences, 2003. **100**(23): p. 13380-13383.

49. Banack, S.A. and S.J. Murch, *Multiple neurotoxic items in the Chamorro diet link BMAA with ALS/PDC.* Amyotrophic Lateral Sclerosis, 2009. **10**(S2): p. 34-40.

50. Renton, A.E., et al., *A hexanucleotide repeat expansion in C9ORF72 is the cause of chromosome 9p21-linked ALS-FTD.* Neuron, 2011. **72**(2): p. 257-268.

51. Rosen, D.R., et al., *Mutations in Cu/Zn superoxide dismutase gene are associated with familial amyotrophic lateral sclerosis.* Nature, 1993. **362**(6415): p. 59-62.

52. Lagier-Tourenne, C. and D.W. Cleveland, *Rethinking als: The fus about tdp-43.* Cell, 2009. **136**(6): p. 1001-1004.

53. Forsberg, K., et al., *Novel antibodies reveal inclusions containing non-native SOD1 in sporadic ALS patients.* PloS one, 2010. **5**(7): p. e11552.

54. Neumann, M., et al., *Ubiquitinated TDP-43 in frontotemporal lobar degeneration and amyotrophic lateral sclerosis.* Science, 2006. **314**(5796): p. 130-133.

55. Deng, H.X., et al., *FUS-immunoreactive inclusions are a common feature in sporadic and non-SOD1 familial amyotrophic lateral sclerosis.* Annals of neurology, 2010. **67**(6): p. 739-748.

56. Sreedharan, J., et al., *TDP-43 mutations in familial and sporadic amyotrophic lateral sclerosis.* Science, 2008. **319**(5870): p. 1668-1672.

57. Vance, C., et al., *Mutations in FUS, an RNA processing protein, cause familial amyotrophic lateral sclerosis type 6.* Science, 2009. **323**(5918): p. 1208-1211.

58. Deng, H.-X., et al., *Mutations in UBQLN2 cause dominant X-linked juvenile and adult-onset ALS and ALS/dementia.* Nature, 2011. **477**(7363): p. 211-215.

59. Watts, G.D., et al., *Inclusion body myopathy associated with Paget disease of bone and frontotemporal dementia is caused by mutant valosin-containing protein.* Nature genetics, 2004. **36**(4): p. 377-381.

60. Johnson, J.O., et al., *Exome sequencing reveals VCP mutations as a cause of familial ALS.* Neuron, 2010. **68**(5): p. 857-864.

61. Fecto, F., et al., *SQSTM1 mutations in familial and sporadic amyotrophic lateral sclerosis.* Archives of neurology, 2011. **68**(11): p. 1440-1446.

62. Laurin, N., et al., *Recurrent mutation of the gene encoding sequestosome 1 (SQSTM1/p62) in Paget disease of bone.* The American Journal of Human Genetics, 2002. **70**(6): p. 1582-1588.

63. Maruyama, H., et al., *Mutations of optineurin in amyotrophic lateral sclerosis.* Nature, 2010. **465**(7295): p. 223-226.

64. Wu, C.-H., et al., *Mutations in the profilin 1 gene cause familial amyotrophic lateral sclerosis.* Nature, 2012. **488**(7412): p. 499-503.

65. Nishimura, A.L., et al., *A mutation in the vesicle-trafficking protein VAPB causes late-onset spinal muscular atrophy and amyotrophic lateral sclerosis.* The American Journal of Human Genetics, 2004. **75**(5): p. 822-831.

66. Landers, J., et al., *New VAPB deletion variant and exclusion of VAPB mutations in familial ALS.* Neurology, 2008. **70**(14): p. 1179-1185.

67. Farrer, M.J., et al., *DCTN1 mutations in Perry syndrome.* Nature genetics, 2009. **41**(2): p. 163-165.

68. Puls, I., et al., *Distal spinal and bulbar muscular atrophy caused by dynactin mutation.* Annals of neurology, 2005. **57**(5): p. 687-694.

69. Münch, C., et al., *Point mutations of the p150 subunit of dynactin (DCTN1) gene in ALS.* Neurology, 2004. **63**(4): p. 724-726.

70. Figlewicz, D.A., et al., *Variants of the heavy neurofilament subunit are associated with the development of amyotrophic lateral sclerosis.* Human Molecular Genetics, 1994. **3**(10): p. 1757-1761.

71. Panzeri, C., et al., *The first ALS2 missense mutation associated with JPLS reveals new aspects of alsin biological function.* Brain, 2006. **129**(7): p. 1710-1719.

72. Devon, R., et al., *The first nonsense mutation in alsin results in a homogeneous phenotype of infantile-onset ascending spastic paralysis with bulbar involvement in two siblings.* Clinical genetics, 2003. **64**(3): p. 210-215.

73. Yang, Y., et al., *The gene encoding alsin, a protein with three guanine-nucleotide exchange factor domains, is mutated in a form of recessive amyotrophic lateral sclerosis.* Nature genetics, 2001. **29**(2): p. 160-165.

74. Chow, C.Y., et al., *Deleterious variants of FIG4, a phosphoinositide phosphatase, in patients with ALS.* The American Journal of Human Genetics, 2009. **84**(1): p. 85-88.

75. Chow, C.Y., et al., *Mutation of FIG4 causes neurodegeneration in the pale tremor mouse and patients with CMT4J.* Nature, 2007. **448**(7149): p. 68-72.

76. Skibinski, G., et al., *Mutations in the endosomal ESCRTIII-complex subunit CHMP2B in frontotemporal dementia.* Nature genetics, 2005. **37**(8): p. 806-808.

77. Chen, Y.-Z., et al., *DNA/RNA helicase gene mutations in a form of juvenile amyotrophic lateral sclerosis (ALS4).* The American Journal of Human Genetics, 2004. **74**(6): p. 1128-1135.

78. Greenway, M., et al., *A novel candidate region for ALS on chromosome 14q11. 2.* Neurology, 2004. **63**(10): p. 1936-1938.

79. Orlacchio, A., et al., *SPATACSIN mutations cause autosomal recessive juvenile amyotrophic lateral sclerosis.* Brain, 2010: p. awp325.

80. Stevanin, G., et al., *Mutations in SPG11, encoding spatacsin, are a major cause of spastic paraplegia with thin corpus callosum.* Nature genetics, 2007. **39**(3): p. 366-372.

81. Mitchell, J., et al., *Familial amyotrophic lateral sclerosis is associated with a mutation in D-amino acid oxidase.* Proceedings of the National Academy of Sciences, 2010. **107**(16): p. 7556-7561.

82. Cirulli, E.T., et al., *Exome sequencing in amyotrophic lateral sclerosis identifies risk genes and pathways.* Science, 2015. **347**(6229): p. 1436-1441.

83. Ticozzi, N., et al., *Mutational analysis reveals the FUS homolog TAF15 as a candidate gene for familial amyotrophic lateral sclerosis.* American Journal of Medical Genetics Part B: Neuropsychiatric Genetics, 2011. **156**(3): p. 285-290.

84. Johnson, J.O., et al., *Mutations in the Matrin 3 gene cause familial amyotrophic lateral sclerosis.* Nature neuroscience, 2014. **17**(5): p. 664-666.

85. Kim, H.J., et al., *Prion-like domain mutations in hnRNPs cause multisystem proteinopathy and ALS.* Nature, 2013. **495**(7442): p. 467.

86. Simpson, C.L., et al., *Variants of the elongator protein 3 (ELP3) gene are associated with motor neuron degeneration.* Human molecular genetics, 2009. **18**(3): p. 472-481.

87. Doucette, P.A., et al., *Dissociation of Human Copper-Zinc Superoxide Dismutase Dimers Using Chaotrope and Reductant.* Journal of Biological Chemistry, 2004. **279**(52): p. 54558-54566.

88. Keerthana, S. and P. Kolandaivel, *Interaction between dimer interface residues of native and mutated SOD1 protein: a theoretical study.* JBIC Journal of Biological Inorganic Chemistry, 2015. **20**(3): p. 509-522.

89. Zelko, I.N., T.J. Mariani, and R.J. Folz, *Superoxide dismutase multigene family: a comparison of the CuZn-SOD (SOD1), Mn-SOD (SOD2), and EC-SOD (SOD3) gene structures, evolution, and expression.* Free Radical Biology and Medicine, 2002. **33**(3): p. 337-349.

90. McCord, J.M. and I. Fridovich, *Superoxide dismutase. An enzymic function for erythrocuprein (hemocuprein).* Journal of Biological Chemistry, 1969. **244**(22): p. 6049-55.

91. Pardo, C.A., et al., *Superoxide dismutase is an abundant component in cell bodies, dendrites, and axons of motor neurons and in a subset of other neurons.* Proceedings of the National Academy of Sciences, 1995. **92**(4): p. 954-958.

92. Byung Pal, Y., *Cellular defenses against damage from reactive oxygen species.* Physiological Reviews, 1994. **v74**(n1): p. p139(24).

93. Arnesano, F., et al., *The unusually stable quaternary structure of human Cu,Zn-superoxide dismutase 1 is controlled by both metal occupancy and disulfide status.* Journal of Biological Chemistry, 2004. **279**(46): p. 47998-8003.

94. Arnesano, F., et al., *The unusually stable quaternary structure of human Cu, Zn-superoxide dismutase 1 is controlled by both metal occupancy and disulfide status.* Journal of Biological Chemistry, 2004. **279**(46): p. 47998-48003.

95. Saccon, R.A., et al., *Is SOD1 loss of function involved in amyotrophic lateral sclerosis?* Brain, 2013: p. awt097.

96. Andersen, P.M., et al., *Amyotrophic lateral sclerosis associated with homozygosity for an Asp90Ala mutation in CuZn-superoxide dismutase.* Nature genetics, 1995. **10**(1): p. 61-66.

97. Hand, C.K., et al., *Compound heterozygous D90A and D96N SOD1 mutations in a recessive amyotrophic lateral sclerosis family.* Annals of neurology, 2001. **49**(2): p. 267-271.

98. Saeed, M., et al., *Age and founder effect of SOD1 A4V mutation causing ALS.* Neurology, 2009. **72**(19): p. 1634-1639.

99. Cleveland, D.W. and J.D. Rothstein, *From Charcot to Lou Gehrig: deciphering selective motor neuron death in ALS.* Nature Reviews Neuroscience, 2001. **2**(11): p. 806-819.

100. Rotunno, M.S. and D.A. Bosco, *An emerging role for misfolded wild-type SOD1 in sporadic ALS pathogenesis.* Frontiers in Cellular Neuroscience, 2013. **7**.

101. Bosco, D.A., et al., *Wild-type and mutant SOD1 share an aberrant conformation and a common pathogenic pathway in ALS.* Nature neuroscience, 2010. **13**(11): p. 1396-1403.

102. Guareschi, S., et al., *An over-oxidized form of superoxide dismutase found in sporadic amyotrophic lateral sclerosis with bulbar onset shares a toxic mechanism with mutant SOD1.* Proceedings of the National Academy of Sciences, 2012. **109**(13): p. 5074-5079.

103. Liu, H.N., et al., *Lack of evidence of monomer/misfolded superoxide dismutase-1 in sporadic amyotrophic lateral sclerosis.* Annals of neurology, 2009. **66**(1): p. 75-80.

104. Hough, M.A., et al., *Dimer destabilization in superoxide dismutase may result in disease-causing properties: Structures of motor neuron disease mutants.* Proceedings of the National Academy of Sciences of the United States of America, 2004. **101**(16): p. 5976-5981.

105. Rakhit, R., et al., *Monomeric Cu, Zn-superoxide dismutase is a common misfolding intermediate in the oxidation models of sporadic and familial amyotrophic lateral sclerosis.* Journal of Biological Chemistry, 2004. **279**(15): p. 15499-15504.

106. Tiwari, A. and L.J. Hayward, *Familial amyotrophic lateral sclerosis mutants of copper/zinc superoxide dismutase are susceptible to disulfide reduction.* Journal of Biological Chemistry, 2003. **278**(8): p. 5984-5992.

107. Bruijn, L.I., et al., *Aggregation and motor neuron toxicity of an ALS-linked SOD1 mutant independent from wild-type SOD1.* Science, 1998. **281**(5384): p. 1851-4.

108. Matsumoto, G., et al., *Structural properties and neuronal toxicity of amyotrophic lateral sclerosis–associated Cu/Zn superoxide dismutase 1 aggregates.* The Journal of Cell Biology, 2005. **171**(1): p. 75-85.

109. Bruijn, L.I., T.M. Miller, and D.W. Cleveland, *UNRAVELING THE MECHANISMS INVOLVED IN MOTOR NEURON DEGENERATION IN ALS.* Annual Review of Neuroscience, 2004. **27**(1): p. 723-749.

110. Bunton-Stasyshyn, R.K., et al., *SOD1 Function and Its Implications for Amyotrophic Lateral Sclerosis Pathology New and Renascent Themes.* The Neuroscientist, 2014: p. 1073858414561795.

111. Gurney, M.E., et al., *Motor neuron degeneration in mice that express a human Cu, Zn superoxide dismutase mutation.* Science, 1994. **264**(5166): p. 1772-1775.

112. Ripps, M.E., et al., *Transgenic mice expressing an altered murine superoxide dismutase gene provide an animal model of amyotrophic lateral sclerosis.* Proceedings of the National Academy of Sciences, 1995. **92**(3): p. 689-693.

113. Wong, P.C., et al., *An adverse property of a familial ALS-linked SOD1 mutation causes motor neuron disease characterized by vacuolar degeneration of mitochondria.* Neuron, 1995. **14**(6): p. 1105-1116.

114. Turner, B.J. and K. Talbot, *Transgenics, toxicity and therapeutics in rodent models of mutant SOD1-mediated familial ALS.* Progress in neurobiology, 2008. **85**(1): p. 94-134.

115. McGown, A., et al., *Early interneuron dysfunction in ALS: insights from a mutant sod1 zebrafish model.* Annals of neurology, 2013. **73**(2): p. 246-258.

116. Watson, M.R., et al., *A drosophila model for amyotrophic lateral sclerosis reveals motor neuron damage by human SOD1.* Journal of Biological Chemistry, 2008. **283**(36): p. 24972-24981.

117. Sakowski, S.A., et al., *Neuromuscular effects of G93A-SOD1 expression in zebrafish.* Molecular neurodegeneration, 2012. **7**(1): p. 1-15.

118. Bergemalm, D., et al., *Overloading of stable and exclusion of unstable human superoxide dismutase-1 variants in mitochondria of murine amyotrophic lateral sclerosis models.* The Journal of neuroscience, 2006. **26**(16): p. 4147-4154.

119. Graffmo, K.S., et al., *Expression of wild-type human superoxide dismutase-1 in mice causes amyotrophic lateral sclerosis.* Human molecular genetics, 2012: p. dds399.

120. Moser, J.M., P. Bigini, and T. Schmitt-John, *The wobbler mouse, an ALS animal model.* Molecular Genetics and Genomics, 2013. **288**(5-6): p. 207-229.

121. Walker, A.K., et al., *Functional recovery in new mouse models of ALS/FTLD after clearance of pathological cytoplasmic TDP-43.* Acta neuropathologica, 2015. **130**(5): p. 643-660.

122. Chew, J., et al., *C9ORF72 repeat expansions in mice cause TDP-43 pathology, neuronal loss, and behavioral deficits.* Science, 2015. **348**(6239): p. 1151-1154.

123. Zhou, H., et al., *Transgenic rat model of neurodegeneration caused by mutation in the TDP gene.* PLoS Genet, 2010. **6**(3): p. e1000887.

124. Huang, C., et al., *FUS transgenic rats develop the phenotypes of amyotrophic lateral sclerosis and frontotemporal lobar degeneration.* PLoS Genet, 2011. **7**(3): p. e1002011.

125. Liachko, N.F., C.R. Guthrie, and B.C. Kraemer, *Phosphorylation promotes neurotoxicity in a Caenorhabditis elegans model of TDP-43 proteinopathy.* The Journal of Neuroscience, 2010. **30**(48): p. 16208-16219.

126. Johnson, B.S., et al., *TDP-43 is intrinsically aggregation-prone, and amyotrophic lateral sclerosis-linked mutations accelerate aggregation and increase toxicity.* Journal of Biological Chemistry, 2009. **284**(30): p. 20329-20339.

127. Vaccaro, A., et al., *Methylene blue protects against TDP-43 and FUS neuronal toxicity in C. elegans and D. rerio.* PLoS One, 2012. **7**(7): p. e42117-e42117.

128. Armstrong, G.A. and P. Drapeau, *Loss and gain of FUS function impair neuromuscular synaptic transmission in a genetic model of ALS.* Human molecular genetics, 2013. **22**(21): p. 4282-4292.

129. Wegorzewska, I., et al., *TDP-43 mutant transgenic mice develop features of ALS and frontotemporal lobar degeneration.* Proceedings of the National Academy of Sciences, 2009. **106**(44): p. 18809-18814.

130. Walker, A.K., et al., *Functional recovery in new mouse models of ALS/FTLD after clearance of pathological cytoplasmic TDP-43.* Acta neuropathologica, 2015: p. 1-18.

131. Stepto, A., et al., *Modelling C9ORF72 hexanucleotide repeat expansion in amyotrophic lateral sclerosis and frontotemporal dementia.* Acta neuropathologica, 2014. **127**(3): p. 377-389.

132. Ciura, S., et al., *Loss of function of C9orf72 causes motor deficits in a zebrafish model of Amyotrophic Lateral Sclerosis.* Annals of neurology, 2013. **74**(2): p. 180-187.

133. Koppers, M., et al., *C9orf72 ablation in mice does not cause motor neuron degeneration or motor deficits.* Annals of neurology, 2015. **78**(3): p. 426-438.

134. Levine, T.P., et al., *The product of C9orf72, a gene strongly implicated in neurodegeneration, is structurally related to DENN Rab-GEFs.* Bioinformatics, 2013. **29**(4): p. 499-503.

135. Majounie, E., et al., *Frequency of the C9orf72 hexanucleotide repeat expansion in patients with amyotrophic lateral sclerosis and frontotemporal dementia: a cross-sectional study.* The Lancet Neurology, 2012. **11**(4): p. 323-330.

136. Dols-Icardo, O., et al., *Characterization of the repeat expansion size in C9orf72 in amyotrophic lateral sclerosis and frontotemporal dementia.* Human molecular genetics, 2014. **23**(3): p. 749-754.

137. Xi, Z., et al., *Jump from pre-mutation to pathologic expansion in C9orf72.* The American Journal of Human Genetics, 2015. **96**(6): p. 962-970.

138. Xi, Z., et al., *Hypermethylation of the CpG island near the G 4 C 2 repeat in ALS with a C9orf72 expansion.* The American Journal of Human Genetics, 2013. **92**(6): p. 981-989.

139. Donnelly, C.J., et al., *RNA toxicity from the ALS/FTD C9ORF72 expansion is mitigated by antisense intervention.* Neuron, 2013. **80**(2): p. 415-428.

140. Gendron, T.F., et al., *Antisense transcripts of the expanded C9ORF72 hexanucleotide repeat form nuclear RNA foci and undergo repeat-associated non-ATG translation in c9FTD/ALS.* Acta neuropathologica, 2013. **126**(6): p. 829-844.

141. Lagier-Tourenne, C., et al., *Targeted degradation of sense and antisense C9orf72 RNA foci as therapy for ALS and frontotemporal degeneration.* Proceedings of the National Academy of Sciences, 2013. **110**(47): p. E4530-E4539.

142. Ash, P.E., et al., *Unconventional translation of C9ORF72 GGGGCC expansion generates insoluble polypeptides specific to c9FTD/ALS.* Neuron, 2013. **77**(4): p. 639-646.

143. Zhang, Y.-J., et al., *Aggregation-prone c9FTD/ALS poly (GA) RAN-translated proteins cause neurotoxicity by inducing ER stress.* Acta neuropathologica, 2014. **128**(4): p. 505-524.

144. Kwon, I., et al., *Poly-dipeptides encoded by the C9orf72 repeats bind nucleoli, impede RNA biogenesis, and kill cells.* Science, 2014. **345**(6201): p. 1139-1145.

145. Lee, Y.-B., et al., *Hexanucleotide repeats in ALS/FTD form length-dependent RNA foci, sequester RNA binding proteins, and are neurotoxic.* Cell reports, 2013. **5**(5): p. 1178-1186.

146. Xiao, S., et al., *Isoform-specific antibodies reveal distinct subcellular localizations of C9orf72 in amyotrophic lateral sclerosis.* Annals of neurology, 2015. **78**(4): p. 568-583.

147. Freibaum, B.D., et al., *GGGGCC repeat expansion in C9orf72 compromises nucleocytoplasmic transport.* Nature, 2015.

148. Wang, H.-Y., et al., *Structural diversity and functional implications of the eukaryotic TDP gene family.* Genomics, 2004. **83**(1): p. 130-139.

149. Scotter, E.L., H.-J. Chen, and C.E. Shaw, *TDP-43 Proteinopathy and ALS: Insights into Disease Mechanisms and Therapeutic Targets.* Neurotherapeutics, 2015. **12**(2): p. 352-363.

150. Winton, M.J., et al., *Disturbance of nuclear and cytoplasmic TAR DNA-binding protein (TDP-43) induces disease-like redistribution, sequestration, and aggregate formation.* Journal of Biological Chemistry, 2008. **283**(19): p. 13302-13309.

151. Buratti, E., et al., *TDP-43 Binds Heterogeneous Nuclear Ribonucleoprotein A/B through Its C-terminal Tail AN IMPORTANT REGION FOR THE INHIBITION OF CYSTIC FIBROSIS TRANSMEMBRANE CONDUCTANCE REGULATOR EXON 9 SPLICING.* Journal of Biological Chemistry, 2005. **280**(45): p. 37572-37584.

152. Buratti, E. and F.E. Baralle, *TDP-43: gumming up neurons through protein–protein and protein–RNA interactions.* Trends in biochemical sciences, 2012. **37**(6): p. 237-247.

153. Lagier-Tourenne, C., M. Polymenidou, and D.W. Cleveland, *TDP-43 and FUS/TLS: emerging roles in RNA processing and neurodegeneration.* Human molecular genetics, 2010. **19**(R1): p. R46-R64.

154. Ayala, Y.M., et al., *TDP-43 regulates its mRNA levels through a negative feedback loop.* The EMBO journal, 2011. **30**(2): p. 277-288.

155. Barmada, S.J., et al., *Cytoplasmic mislocalization of TDP-43 is toxic to neurons and enhanced by a mutation associated with familial amyotrophic lateral sclerosis.* The Journal of Neuroscience, 2010. **30**(2): p. 639-649.

156. Alami, N.H., et al., *Axonal transport of TDP-43 mRNA granules is impaired by ALS-causing mutations.* Neuron, 2014. **81**(3): p. 536-543.

157. Liu-Yesucevitz, L., et al., *ALS-linked mutations enlarge TDP-43-enriched neuronal RNA granules in the dendritic arbor.* The Journal of Neuroscience, 2014. **34**(12): p. 4167-4174.

158. Diaper, D.C., et al., *Loss and gain of Drosophila TDP-43 impair synaptic efficacy and motor control leading to age-related neurodegeneration by loss-of-function phenotypes.* Human molecular genetics, 2013. **22**(8): p. 1539-1557.

159. Kraemer, B.C., et al., *Loss of murine TDP-43 disrupts motor function and plays an essential role in embryogenesis.* Acta neuropathologica, 2010. **119**(4): p. 409-419.

160. Colombrita, C., et al., *TDP-43 is recruited to stress granules in conditions of oxidative insult.* Journal of neurochemistry, 2009. **111**(4): p. 1051-1061.

161. Van Deerlin, V.M., et al., *TARDBP mutations in amyotrophic lateral sclerosis with TDP-43 neuropathology: a genetic and histopathological analysis.* The Lancet Neurology, 2008. **7**(5): p. 409-416.

162. Rutherford, N.J., et al., *Novel mutations in TARDBP (TDP-43) in patients with familial amyotrophic lateral sclerosis.* PLoS genetics, 2008. **4**(9): p. e1000193.

163. Del Bo, R., et al., *TARDBP (TDP-43) sequence analysis in patients with familial and sporadic ALS: identification of two novel mutations.* European journal of neurology, 2009. **16**(6): p. 727-732.

164. Arai, T., et al., *TDP-43 is a component of ubiquitin-positive tau-negative inclusions in frontotemporal lobar degeneration and amyotrophic lateral sclerosis.* Biochemical and biophysical research communications, 2006. **351**(3): p. 602-611.

165. Mackenzie, I.R., et al., *Pathological TDP-43 distinguishes sporadic amyotrophic lateral sclerosis from amyotrophic lateral sclerosis with SOD1 mutations.* Annals of neurology, 2007. **61**(5): p. 427-434.

166. Maekawa, S., et al., *TDP-43 is consistently co-localized with ubiquitinated inclusions in sporadic and Guam amyotrophic lateral sclerosis but not in familial amyotrophic lateral sclerosis with and without SOD1 mutations.* Neuropathology, 2009. **29**(6): p. 672-683.

167. Budini, M., et al., *Role of selected mutations in the Q/N rich region of TDP-43 in EGFP-12xQ/N-induced aggregate formation.* Brain research, 2012. **1462**: p. 139-150.

168. Nonaka, T., et al., *Truncation and pathogenic mutations facilitate the formation of intracellular aggregates of TDP-43.* Human molecular genetics, 2009. **18**(18): p. 3353-3364.

169. Han, J.-H., et al., *ALS/FTLD-linked TDP-43 regulates neurite morphology and cell survival in differentiated neurons.* Experimental cell research, 2013. **319**(13): p. 1998-2005.

170. Arnold, E.S., et al., *ALS-linked TDP-43 mutations produce aberrant RNA splicing and adult-onset motor neuron disease without aggregation or loss of nuclear TDP-43.* Proceedings of the National Academy of Sciences, 2013. **110**(8): p. E736-E745.

171. Mackenzie, I.R. and M. Neumann, *FET proteins in frontotemporal dementia and amyotrophic lateral sclerosis.* Brain research, 2012. **1462**: p. 40-43.

172. Neumann, M., et al., *FET proteins TAF15 and EWS are selective markers that distinguish FTLD with FUS pathology from amyotrophic lateral sclerosis with FUS mutations.* Brain, 2011. **134**(9): p. 2595-2609.

173. Yang, S., et al., *Fused in sarcoma/translocated in liposarcoma: a multifunctional DNA/RNA binding protein.* The international journal of biochemistry & cell biology, 2010. **42**(9): p. 1408-1411.

174. Zakaryan, R.P. and H. Gehring, *Identification and characterization of the nuclear localization/retention signal in the EWS proto-oncoprotein.* Journal of molecular biology, 2006. **363**(1): p. 27-38.

175. Fujii, R., et al., *The RNA binding protein TLS is translocated to dendritic spines by mGluR5 activation and regulates spine morphology.* Current Biology, 2005. **15**(6): p. 587-593.

176. Fujii, R. and T. Takumi, *TLS facilitates transport of mRNA encoding an actin-stabilizing protein to dendritic spines.* Journal of cell science, 2005. **118**(24): p. 5755-5765.

177. Hicks, G.G., et al., *Fus deficiency in mice results in defective B-lymphocyte development and activation, high levels of chromosomal instability and perinatal death.* Nature genetics, 2000. **24**(2): p. 175-179.

178. Kwiatkowski, T.J., et al., *Mutations in the FUS/TLS gene on chromosome 16 cause familial amyotrophic lateral sclerosis.* Science, 2009. **323**(5918): p. 1205-1208.

179. Blair, I.P., et al., *FUS mutations in amyotrophic lateral sclerosis: clinical, pathological, neurophysiological and genetic analysis.* Journal of Neurology, Neurosurgery & Psychiatry, 2010. **81**(6): p. 639-645.

180. Corrado, L., et al., *Mutations of FUS gene in sporadic amyotrophic lateral sclerosis.* Journal of medical genetics, 2010. **47**(3): p. 190-194.

181. Belzil, V., et al., *Mutations in FUS cause FALS and SALS in French and French Canadian populations.* Neurology, 2009. **73**(15): p. 1176-1179.

182. Merner, N.D., et al., *Exome sequencing identifies FUS mutations as a cause of essential tremor.* The American Journal of Human Genetics, 2012. **91**(2): p. 313-319.

183. Hewitt, C., et al., *Novel FUS/TLS mutations and pathology in familial and sporadic amyotrophic lateral sclerosis.* Archives of neurology, 2010. **67**(4): p. 455-461.

184. Doi, H., et al., *The RNA-binding protein FUS/TLS is a common aggregate-interacting protein in polyglutamine diseases.* Neuroscience research, 2010. **66**(1): p. 131-133.

185. DeJesus-Hernandez, M., et al., *De novo truncating FUS gene mutation as a cause of sporadic amyotrophic lateral sclerosis.* Human mutation, 2010. **31**(5): p. E1377-E1389.

186. Gal, J., et al., *Nuclear localization sequence of FUS and induction of stress granules by ALS mutants.* Neurobiology of aging, 2011. **32**(12): p. 2323. e27-2323. e40.

187. Dormann, D., et al., *ALS-associated fused in sarcoma (FUS) mutations disrupt Transportin-mediated nuclear import.* The EMBO journal, 2010. **29**(16): p. 2841-2857.

188. Bosco, D.A., et al., *Mutant FUS proteins that cause amyotrophic lateral sclerosis incorporate into stress granules.* Human molecular genetics, 2010. **19**(21): p. 4160-4175.

189. Acosta, J.R., et al., *Mutant human FUS is ubiquitously mislocalized and generates persistent stress granules in primary cultured transgenic zebrafish cells.* PloS one, 2014. **9**(6): p. e90572.

190. Zhang, K.Y., et al., *Ubiquilin 2: A component of the ubiquitin–proteasome system with an emerging role in neurodegeneration.* The international journal of biochemistry & cell biology, 2014. **50**: p. 123-126.

191. Ko, H.S., et al., *Ubiquilin interacts with ubiquitylated proteins and proteasome through its ubiquitin-associated and ubiquitin-like domains.* FEBS letters, 2004. **566**(1): p. 110-114.

192. Williams, K.L., et al., *UBQLN2/ubiquilin 2 mutation and pathology in familial amyotrophic lateral sclerosis.* Neurobiology of aging, 2012. **33**(10): p. 2527. e3-2527. e10.

193. Synofzik, M., et al., *Screening in ALS and FTD patients reveals 3 novel UBQLN2 mutations outside the PXX domain and a pure FTD phenotype.* Neurobiology of aging, 2012. **33**(12): p. 2949. e13-2949. e17.

194. Brettschneider, J., et al., *Pattern of ubiquilin pathology in ALS and FTLD indicates presence of C9ORF72 hexanucleotide expansion.* Acta neuropathologica, 2012. **123**(6): p. 825-839.

195. Zhang, X., et al., *Structure of the AAA ATPase p97.* Molecular cell, 2000. **6**(6): p. 1473-1484.

196. Vij, N., *AAA ATPase p97/VCP: cellular functions, disease and therapeutic potential.* Journal of cellular and molecular medicine, 2008. **12**(6a): p. 2511-2518.

197. Meyer, H., M. Bug, and S. Bremer, *Emerging functions of the VCP/p97 AAA-ATPase in the ubiquitin system.* Nature cell biology, 2012. **14**(2): p. 117-123.

198. Song, C., Q. Wang, and C.-C.H. Li, *ATPase activity of p97-valosin-containing protein (VCP) D2 mediates the major enzyme activity, and D1 contributes to the heat-induced activity.* Journal of Biological Chemistry, 2003. **278**(6): p. 3648-3655.

199. Bonifacino, J.S. and A.M. Weissman, *Ubiquitin and the control of protein fate in the secretory and endocytic pathways 1.* Annual review of cell and developmental biology, 1998. **14**(1): p. 19-57.

200. Weihl, C.C., et al., *Inclusion body myopathy-associated mutations in p97/VCP impair endoplasmic reticulum-associated degradation.* Human molecular genetics, 2006. **15**(2): p. 189-199.

201. Ju, J.-S., et al., *Valosin-containing protein (VCP) is required for autophagy and is disrupted in VCP disease.* The Journal of cell biology, 2009. **187**(6): p. 875-888.

202. Wojcik, C., M. Yano, and G.N. DeMartino, *RNA interference of valosin-containing protein (VCP/p97) reveals multiple cellular roles linked to ubiquitin/proteasome-dependent proteolysis.* Journal of cell science, 2004. **117**(2): p. 281-292.

203. Nowis, D., E. McConnell, and C. Wójcik, *Destabilization of the VCP-Ufd1-Npl4 complex is associated with decreased levels of ERAD substrates.* Experimental cell research, 2006. **312**(15): p. 2921-2932.

204. Seibenhener, M.L., et al., *Sequestosome 1/p62 is a polyubiquitin chain binding protein involved in ubiquitin proteasome degradation.* Molecular and cellular biology, 2004. **24**(18): p. 8055-8068.

205. Zatloukal, K., et al., *p62 Is a common component of cytoplasmic inclusions in protein aggregation diseases.* The American journal of pathology, 2002. **160**(1): p. 255-263.

206. Nakano, T., et al., *Expression of ubiquitin-binding protein p62 in ubiquitin-immunoreactive intraneuronal inclusions in amyotrophic lateral sclerosis with dementia: analysis of five autopsy cases with broad clinicopathological spectrum.* Acta neuropathologica, 2004. **107**(4): p. 359-364.

207. Gal, J., et al., *p62 accumulates and enhances aggregate formation in model systems of familial amyotrophic lateral sclerosis.* Journal of Biological Chemistry, 2007. **282**(15): p. 11068-11077.

208. Mizuno, Y., et al., *Immunoreactivities of p62, an ubiqutin-binding protein, in the spinal anterior horn cells of patients with amyotrophic lateral sclerosis.* Journal of the neurological sciences, 2006. **249**(1): p. 13-18.

209. Gal, J., et al., *Sequestosome 1/p62 links familial ALS mutant SOD1 to LC3 via an ubiquitin-independent mechanism.* Journal of neurochemistry, 2009. **111**(4): p. 1062-1073.

210. Hiji, M., et al., *White matter lesions in the brain with frontotemporal lobar degeneration with motor neuron disease: TDP-43-immunopositive inclusions co-localize with p62, but not ubiquitin.* Acta neuropathologica, 2008. **116**(2): p. 183-191.

211. Brady, O.A., et al., *Regulation of TDP-43 aggregation by phosphorylation andp62/SQSTM1.* Journal of neurochemistry, 2011. **116**(2): p. 248-259.

212. Ying, H., et al., *Posttranslational modifications, localization, and protein interactions of optineurin, the product of a glaucoma gene.* PLoS One, 2010. **5**(2): p. e9168.

213. Zhu, G., et al., *Optineurin negatively regulates TNFα-induced NF-κB activation by competing with NEMO for ubiquitinated RIP.* Current Biology, 2007. **17**(16): p. 1438-1443.

214. Nagabhushana, A., et al., *Regulation of endocytic trafficking of transferrin receptor by optineurin and its impairment by a glaucoma-associated mutant.* BMC cell biology, 2010. **11**(1): p. 4.

215. Chalasani, M.L., G. Swarup, and D. Balasubramanian, *Optineurin and its mutants: molecules associated with some forms of glaucoma.* Ophthalmic Res, 2009. **42**(4): p. 176-84.

216. Sundaramoorthy, V., et al., *Defects in optineurin and myosin VI mediated cellular trafficking in amyotrophic lateral sclerosis.* Human molecular genetics, 2015: p. ddv126.

217. Deng, H.-X., et al., *Differential involvement of optineurin in amyotrophic lateral sclerosis with or without SOD1 mutations.* Archives of neurology, 2011. **68**(8): p. 1057-1061.

218. Kumar, A., et al., *Role of CYP1B1, MYOC, OPTN and OPTC genes in adult-onset primary open-angle glaucoma: predominance of CYP1B1 mutations in Indian patients.* Molecular vision, 2007. **13**: p. 667.

219. Park, B.-C., et al., *Studies of optineurin, a glaucoma gene: Golgi fragmentation and cell death from overexpression of wild-type and mutant optineurin in two ocular cell types.* The American journal of pathology, 2006. **169**(6): p. 1976-1989.

220. Koga, T., et al., *Differential effects of myocilin and optineurin, two glaucoma genes, on neurite outgrowth.* The American journal of pathology, 2010. **176**(1): p. 343-352.

221. Teuling, E., et al., *Motor neuron disease-associated mutant vesicle-associated membrane protein-associated protein (VAP) B recruits wild-*

type VAPs into endoplasmic reticulum-derived tubular aggregates. The Journal of Neuroscience, 2007. **27**(36): p. 9801-9815.

222. Peretti, D., et al., *Coordinated lipid transfer between the endoplasmic reticulum and the Golgi complex requires the VAP proteins and is essential for Golgi-mediated transport.* Molecular biology of the cell, 2008. **19**(9): p. 3871-3884.

223. Fasana, E., et al., *A VAPB mutant linked to amyotrophic lateral sclerosis generates a novel form of organized smooth endoplasmic reticulum.* The FASEB Journal, 2010. **24**(5): p. 1419-1430.

224. Nishimura, A.L., A. Al-Chalabi, and M. Zatz, *A common founder for amyotrophic lateral sclerosis type 8 (ALS8) in the Brazilian population.* Human genetics, 2005. **118**(3-4): p. 499-500.

225. Funke, A., et al., *The p. P56S mutation in the VAPB gene is not due to a single founder: the first European case.* Clinical genetics, 2010. **77**(3): p. 302-303.

226. Chen, H.-J., et al., *Characterization of the properties of a novel mutation in VAPB in familial amyotrophic lateral sclerosis.* Journal of Biological Chemistry, 2010. **285**(51): p. 40266-40281.

227. Kanekura, K., et al., *Characterization of amyotrophic lateral sclerosis-linked P56S mutation of vesicle-associated membrane protein-associated protein B (VAPB/ALS8).* Journal of Biological Chemistry, 2006. **281**(40): p. 30223-30233.

228. Gkogkas, C., et al., *VAPB interacts with and modulates the activity of ATF6.* Human molecular genetics, 2008. **17**(11): p. 1517-1526.

229. Tsuda, H., et al., *The amyotrophic lateral sclerosis 8 protein VAPB is cleaved, secreted, and acts as a ligand for Eph receptors.* Cell, 2008. **133**(6): p. 963-977.

230. Anagnostou, G., et al., *Vesicle associated membrane protein B (VAPB) is decreased in ALS spinal cord.* Neurobiology of aging, 2010. **31**(6): p. 969-985.

231. Puls, I., et al., *Mutant dynactin in motor neuron disease.* Nature genetics, 2003. **33**(4): p. 455-456.

232. Munch, C., et al., *Heterozygous R1101K mutation of the DCTN1 gene in a family with ALS and FTD.* Annals of neurology, 2005. **58**(5): p. 777-780.

233. Laird, F.M., et al., *Motor neuron disease occurring in a mutant dynactin mouse model is characterized by defects in vesicular trafficking.* The Journal of Neuroscience, 2008. **28**(9): p. 1997-2005.

234. Schymick, J., K. Talbot, and B. Traynor, *Genetics of sporadic amyotrophic lateral sclerosis.* Human Molecular Genetics, 2007. **16**(R2): p. R233-R242.

235. Gentil, B.J., M. Tibshirani, and H.D. Durham, *Neurofilament dynamics and involvement in neurological disorders.* Cell and tissue research, 2015: p. 1-12.

236. Al-Chalabi, A., et al., *Deletions of the heavy neurofilament subunit tail in amyotrophic lateral sclerosis.* Human molecular genetics, 1999. **8**(2): p. 157-164.

237. Tomkins, J., et al., *Novel insertion in the KSP region of the neurofilament heavy gene in amyotrophic lateral sclerosis (ALS).* Neuroreport, 1998. **9**(17): p. 3967-3970.

238. Mizusawa, H., et al., *Focal accumulation of phosphorylated neurofilaments within anterior horn cell in familial amyotrophic lateral sclerosis.* Acta neuropathologica, 1989. **79**(1): p. 37-43.

239. Brettschneider, J., et al., *Axonal damage markers in cerebrospinal fluid are increased in ALS.* Neurology, 2006. **66**(6): p. 852-856.

240. Delisle, M.B. and S. Carpenter, *Neurofibrillary axonal swellings and amyotrophic lateral sclerosis.* Journal of the neurological sciences, 1984. **63**(2): p. 241-250.

241. Boylan, K., et al., *Immunoreactivity of the phosphorylated axonal neurofilament H subunit (pNF-H) in blood of ALS model rodents and ALS patients: evaluation of blood pNF-H as a potential ALS biomarker.* Journal of neurochemistry, 2009. **111**(5): p. 1182-1191.

242. Garcia, M.L., et al., *Mutations in neurofilament genes are not a significant primary cause of non-SOD1-mediated amyotrophic lateral sclerosis.* Neurobiology of disease, 2006. **21**(1): p. 102-109.

243. Gros-Louis, F., et al., *A frameshift deletion in peripherin gene associated with amyotrophic lateral sclerosis.* Journal of Biological Chemistry, 2004. **279**(44): p. 45951-45956.

244. Leung, C.L., et al., *A pathogenic peripherin gene mutation in a patient with amyotrophic lateral sclerosis.* Brain pathology, 2004. **14**(3): p. 290-296.

245. Corrado, L., et al., *A novel peripherin gene (PRPH) mutation identified in one sporadic amyotrophic lateral sclerosis patient.* Neurobiology of aging, 2011. **32**(3): p. 552. e1-552. e6.

246. Millecamps, S., et al., *Defective axonal transport of neurofilament proteins in neurons overexpressing peripherin.* Journal of neurochemistry, 2006. **98**(3): p. 926-938.

247. Xiao, S., et al., *An aggregate-inducing peripherin isoform generated through intron retention is upregulated in amyotrophic lateral sclerosis and associated with disease pathology.* The Journal of Neuroscience, 2008. **28**(8): p. 1833-1840.

248. Beaulieu, J.-M., M.D. Nguyen, and J.-P. Julien, *Late onset death of motor neurons in mice overexpressing wild-type peripherin.* The Journal of cell biology, 1999. **147**(3): p. 531-544.

249. Robertson, J., et al., *A neurotoxic peripherin splice variant in a mouse model of ALS.* The Journal of cell biology, 2003. **160**(6): p. 939-949.

250. Lattante, S., et al., *Mutations in the PFN1 gene are not a common cause in patients with amyotrophic lateral sclerosis and frontotemporal lobar degeneration in France.* Neurobiology of aging, 2013. **34**(6): p. 1709. e1-1709. e2.

251. Ingre, C., et al., *A novel phosphorylation site mutation in profilin 1 revealed in a large screen of US, Nordic, and German amyotrophic lateral sclerosis/frontotemporal dementia cohorts.* Neurobiology of aging, 2013. **34**(6): p. 1708. e1-1708. e6.

252. Zou, Z.-Y., et al., *Mutations in the profilin 1 gene are not common in amyotrophic lateral sclerosis of Chinese origin.* Neurobiology of aging, 2013. **34**(6): p. 1713. e5-1713. e6.

253. Daoud, H., et al., *Mutation analysis of PFN1 in familial amyotrophic lateral sclerosis patients.* Neurobiology of aging, 2013. **34**(4): p. 1311. e1-1311. e2.

254. Otomo, A., et al., *ALS2, a novel guanine nucleotide exchange factor for the small GTPase Rab5, is implicated in endosomal dynamics.* Human molecular genetics, 2003. **12**(14): p. 1671-1687.

255. Kunita, R., et al., *The Rab5 activator ALS2/alsin acts as a novel Rac1 effector through Rac1-activated endocytosis.* Journal of Biological Chemistry, 2007. **282**(22): p. 16599-16611.

256. Otomo, A., et al., *ALS2/alsin deficiency in neurons leads to mild defects in macropinocytosis and axonal growth.* Biochemical and biophysical research communications, 2008. **370**(1): p. 87-92.

257. Hadano, S., et al., *A gene encoding a putative GTPase regulator is mutated in familial amyotrophic lateral sclerosis 2.* Nature genetics, 2001. **29**(2): p. 166-173.

258. Chandran, J., J. Ding, and H. Cai, *Alsin and the molecular pathways of amyotrophic lateral sclerosis.* Molecular neurobiology, 2007. **36**(3): p. 224-231.

259. Kanekura, K., et al., *Alsin, the product of ALS2 gene, suppresses SOD1 mutant neurotoxicity through RhoGEF domain by interacting with SOD1 mutants.* Journal of Biological Chemistry, 2004. **279**(18): p. 19247-19256.

260. Li, Q., et al., *Alsin and SOD1G93A proteins regulate endosomal reactive oxygen species production by glial cells and proinflammatory pathways responsible for neurotoxicity.* Journal of Biological Chemistry, 2011. **286**(46): p. 40151-40162.

261. Millecamps, S., et al., *Alsin is partially associated with centrosome in human cells.* Biochimica et Biophysica Acta (BBA)-Molecular Cell Research, 2005. **1745**(1): p. 84-100.

262. Lai, C., et al., *Amyotrophic lateral sclerosis 2-deficiency leads to neuronal degeneration in amyotrophic lateral sclerosis through altered AMPA receptor trafficking.* The Journal of neuroscience, 2006. **26**(45): p. 11798-11806.

263. Hadano, S., et al., *Loss of ALS2/Alsin exacerbates motor dysfunction in a SOD1H46R-expressing mouse ALS model by disturbing endolysosomal trafficking.* PLoS One, 2010. **5**(3): p. e9805.

264. Michell, R.H., et al., *Phosphatidylinositol 3, 5-bisphosphate: metabolism and cellular functions.* Trends in biochemical sciences, 2006. **31**(1): p. 52-63.

265. Filimonenko, M., et al., *Functional multivesicular bodies are required for autophagic clearance of protein aggregates associated with neurodegenerative disease.* The Journal of cell biology, 2007. **179**(3): p. 485-500.

266. Parkinson, N., et al., *ALS phenotypes with mutations in CHMP2B (charged multivesicular body protein 2B).* Neurology, 2006. **67**(6): p. 1074-1077.

267. Cox, L.E., et al., *Mutations in CHMP2B in lower motor neuron predominant amyotrophic lateral sclerosis (ALS).* PLoS One, 2010. **5**(3): p. e9872.

268. Blair, I.P., et al., *CHMP2B mutations are not a common cause of familial or sporadic amyotrophic lateral sclerosis.* Journal of Neurology, Neurosurgery & Psychiatry, 2008. **79**(7): p. 849-850.

269. Alzu, A., et al., *Senataxin associates with replication forks to protect fork integrity across RNA-polymerase-II-transcribed genes.* Cell, 2012. **151**(4): p. 835-846.

270. Suraweera, A., et al., *Senataxin, defective in ataxia oculomotor apraxia type 2, is involved in the defense against oxidative DNA damage.* The Journal of cell biology, 2007. **177**(6): p. 969-979.

271. Suraweera, A., et al., *Functional role for senataxin, defective in ataxia oculomotor apraxia type 2, in transcriptional regulation.* Human molecular genetics, 2009. **18**(18): p. 3384-3396.

272. Vantaggiato, C., et al., *Senataxin modulates neurite growth through fibroblast growth factor 8 signalling.* Brain, 2011. **134**(6): p. 1808-1828.

273. Chen, Y.-Z., et al., *Senataxin, the yeast Sen1p orthologue: characterization of a unique protein in which recessive mutations cause ataxia and dominant mutations cause motor neuron disease.* Neurobiology of disease, 2006. **23**(1): p. 97-108.

274. Hirano, M., et al., *Senataxin mutations and amyotrophic lateral sclerosis.* Amyotrophic Lateral Sclerosis, 2011. **12**(3): p. 223-227.

275. Zhao, Z.-h., et al., *A novel mutation in the senataxin gene identified in a Chinese patient with sporadic amyotrophic lateral sclerosis.* Amyotrophic Lateral Sclerosis, 2009. **10**(2): p. 118-122.

276. Sebastia, J., et al., *Angiogenin protects motoneurons against hypoxic injury.* Cell Death & Differentiation, 2009. **16**(9): p. 1238-1247.

277. Kieran, D., et al., *Control of motoneuron survival by angiogenin.* The Journal of Neuroscience, 2008. **28**(52): p. 14056-14061.

278. Subramanian, V., B. Crabtree, and K.R. Acharya, *Human angiogenin is a neuroprotective factor and amyotrophic lateral sclerosis associated angiogenin variants affect neurite extension/pathfinding and survival of motor neurons.* Human molecular genetics, 2008. **17**(1): p. 130-149.

279. Greenway, M.J., et al., *ANG mutations segregate with familial and'sporadic'amyotrophic lateral sclerosis.* Nature genetics, 2006. **38**(4): p. 411-413.

280. Conforti, F., et al., *A novel Angiogenin gene mutation in a sporadic patient with amyotrophic lateral sclerosis from southern Italy.* Neuromuscular Disorders, 2008. **18**(1): p. 68-70.

281. Gellera, C., et al., *Identification of new ANG gene mutations in a large cohort of Italian patients with amyotrophic lateral sclerosis.* Neurogenetics, 2008. **9**(1): p. 33-40.

282. Seilhean, D., et al., *Accumulation of TDP-43 and α-actin in an amyotrophic lateral sclerosis patient with the K17I ANG mutation.* Acta neuropathologica, 2009. **118**(4): p. 561-573.

283. van Es, M.A., et al., *Angiogenin variants in Parkinson disease and amyotrophic lateral sclerosis.* Annals of neurology, 2011. **70**(6): p. 964-973.

284. Thiyagarajan, N., et al., *Structural and molecular insights into the mechanism of action of human angiogenin-ALS variants in neurons.* Nature communications, 2012. **3**: p. 1121.

285. Mothet, J.-P., et al., *D-serine is an endogenous ligand for the glycine site of the N-methyl-D-aspartate receptor.* Proceedings of the National Academy of Sciences, 2000. **97**(9): p. 4926-4931.

286. Li, Y., et al., *Identity of endogenous NMDAR glycine site agonist in amygdala is determined by synaptic activity level.* Nature communications, 2013. **4**: p. 1760.

287. Paul, P. and J. de Belleroche, *Experimental approaches for elucidating co-agonist regulation of NMDA receptor in motor neurons: therapeutic implications for amyotrophic lateral sclerosis (ALS).* Journal of pharmaceutical and biomedical analysis, 2015.

288. Snyder, S.H. and P.M. Kim, *D-amino acids as putative neurotransmitters: focus on D-serine.* Neurochemical research, 2000. **25**(5): p. 553-560.

289. Lobsiger, C.S., S. Boillée, and D.W. Cleveland, *Toxicity from different SOD1 mutants dysregulates the complement system and the neuronal regenerative response in ALS motor neurons.* Proceedings of the National Academy of Sciences, 2007. **104**(18): p. 7319-7326.

290. Martin, E., et al., *Spatacsin and spastizin act in the same pathway required for proper spinal motor neuron axon outgrowth in zebrafish.* Neurobiology of disease, 2012. **48**(3): p. 299-308.

291. Orlacchio, A., et al., *SPATACSIN mutations cause autosomal recessive juvenile amyotrophic lateral sclerosis.* Brain, 2010. **133**(2): p. 591-598.

292. Daoud, H., et al., *Exome sequencing reveals SPG11 mutations causing juvenile ALS.* Neurobiology of aging, 2012. **33**(4): p. 839. e5-839. e9.

293. Freischmidt, A., et al., *Haploinsufficiency of TBK1 causes familial ALS and fronto-temporal dementia.* Nature neuroscience, 2015.

294. Weidberg, H. and Z. Elazar, *TBK1 mediates crosstalk between the innate immune response and autophagy.* Science signaling, 2011. **4**(187): p. pe39-pe39.

295. Pilli, M., et al., *TBK-1 promotes autophagy-mediated antimicrobial defense by controlling autophagosome maturation.* Immunity, 2012. **37**(2): p. 223-234.

296. Chiò, A., et al., *A two-stage genome-wide association study of sporadic amyotrophic lateral sclerosis.* Human molecular genetics, 2009. **18**(8): p. 1524-1532.

297. Kwee, L.C., et al., *A high-density genome-wide association screen of sporadic ALS in US veterans.* PLoS One, 2012. **7**(3): p. e32768.

298. Gros-Louis, F., et al., *Chromogranin B P413L variant as risk factor and modifier of disease onset for amyotrophic lateral sclerosis.* Proceedings of the National Academy of Sciences, 2009. **106**(51): p. 21777-21782.

299. van Vught, P.W., J.H. Veldink, and L.H. van den Berg, *P413L CHGB is not associated with ALS susceptibility or age at onset in a Dutch population.* Proceedings of the National Academy of Sciences, 2010. **107**(19): p. E77-E77.

300. Fogh, I., et al., *No association of DPP6 with amyotrophic lateral sclerosis in an Italian population.* Neurobiology of aging, 2011. **32**(5): p. 966-967.

301. Daoud, H., et al., *Analysis of the UNC13A gene as a risk factor for sporadic amyotrophic lateral sclerosis.* Archives of neurology, 2010. **67**(4): p. 516-517.

302. Consortium, A., *Age of onset of amyotrophic lateral sclerosis is modulated by a locus on 1p34. 1.* Neurobiology of aging, 2013. **34**(1): p. 357. e7-357. e19.

303. Landers, J.E., et al., *Reduced expression of the Kinesin-Associated Protein 3 (KIFAP3) gene increases survival in sporadic amyotrophic lateral sclerosis.* Proceedings of the National Academy of Sciences, 2009. **106**(22): p. 9004-9009.

304. Van Hoecke, A., et al., *EPHA4 is a disease modifier of amyotrophic lateral sclerosis in animal models and in humans.* Nature medicine, 2012. **18**(9): p. 1418-1422.

305. Daoud, H., et al., *Analysis of DPP6 and FGGY as candidate genes for amyotrophic lateral sclerosis.* Amyotrophic Lateral Sclerosis, 2010. **11**(4): p. 389-391.

306. Gonzalez-Perez, P., et al., *Identification of Rare Protein Disulfide Isomerase Gene Variants in Amyotrophic Lateral Sclerosis patients.* Gene, 2015.

307. Smith, B.N., et al., *Exome-wide rare variant analysis identifies TUBA4A mutations associated with familial ALS.* Neuron, 2014. **84**(2): p. 324-331.

308. Al-Saif, A., F. Al-Mohanna, and S. Bohlega, *A mutation in sigma-1 receptor causes juvenile amyotrophic lateral sclerosis.* Annals of neurology, 2011. **70**(6): p. 913-919.

309. Hayashi, T. and T.-P. Su, *Sigma-1 receptor chaperones at the ER-mitochondrion interface regulate Ca 2+ signaling and cell survival.* Cell, 2007. **131**(3): p. 596-610.

310. Vollrath, J., et al., *Loss of function of the ALS protein SigR1 leads to ER pathology associated with defective autophagy and lipid raft disturbances.* Cell death & disease, 2014. **5**(6): p. e1290.

311. Fink, A.L., *Protein aggregation: folding aggregates, inclusion bodies and amyloid.* Folding and design, 1998. **3**(1): p. R9-R23.

312. Speed, M.A., D.I. Wang, and J. King, *Specific aggregation of partially folded polypeptide chains: the molecular basis of inclusion body composition.* Nature biotechnology, 1996. **14**(10): p. 1283-1287.

313. Kopito, R.R., *Aggresomes, inclusion bodies and protein aggregation.* Trends in cell biology, 2000. **10**(12): p. 524-530.

314. Reynaud, E., *Protein misfolding and degenerative diseases.* Nat Educ, 2010. **3**(9): p. 28.

315. Ciechanover, A. and Y.T. Kwon, *Degradation of misfolded proteins in neurodegenerative diseases: therapeutic targets and strategies.* Experimental & molecular medicine, 2015. **47**(3): p. e147.

316. Soto, C., *Unfolding the role of protein misfolding in neurodegenerative diseases.* Nature Reviews Neuroscience, 2003. **4**(1): p. 49-60.

317. Watanabe, M., et al., *Histological evidence of protein aggregation in mutant SOD1 transgenic mice and in amyotrophic lateral sclerosis neural tissues.* Neurobiology of disease, 2001. **8**(6): p. 933-941.

318. Al-Chalabi, A., et al., *The genetics and neuropathology of amyotrophic lateral sclerosis.* Acta neuropathologica, 2012. **124**(3): p. 339-352.

319. Piao, Y.S., et al., *Neuropathology with clinical correlations of sporadic amyotrophic lateral sclerosis: 102 autopsy cases examined between 1962 and 2000.* Brain pathology, 2003. **13**(1): p. 10-22.

320. Furukawa, Y., *Protein aggregates in pathological inclusions of amyotrophic lateral sclerosis*. 2012: INTECH Open Access Publisher.

321. Wood, J., T. Beaujeux, and P. Shaw, *Protein aggregation in motor neurone disorders.* Neuropathology and applied neurobiology, 2003. **29**(6): p. 529-545.

322. Al-Sarraj, S., et al., *p62 positive, TDP-43 negative, neuronal cytoplasmic and intranuclear inclusions in the cerebellum and hippocampus define the pathology of C9orf72-linked FTLD and MND/ALS.* Acta neuropathologica, 2011. **122**(6): p. 691-702.

323. May, S., et al., *C9orf72 FTLD/ALS-associated Gly-Ala dipeptide repeat proteins cause neuronal toxicity and Unc119 sequestration.* Acta neuropathologica, 2014. **128**(4): p. 485-503.

324. Zu, T., et al., *RAN proteins and RNA foci from antisense transcripts in C9ORF72 ALS and frontotemporal dementia.* Proceedings of the National Academy of Sciences, 2013. **110**(51): p. E4968-E4977.

325. Kato, S., et al., *New consensus research on neuropathological aspects of familial amyotrophic lateral sclerosis with superoxide dismutase 1 (SOD1) gene mutations: inclusions containing SOD1 in neurons and astrocytes.* Amyotrophic Lateral Sclerosis, 2000. **1**(3): p. 163-184.

326. Shibata, N., et al., *Immunohistochemical study on superoxide dismutases in spinal cords from autopsied patients with amyotrophic lateral sclerosis.* Developmental neuroscience, 1996. **18**(5-6): p. 492-498.

327. Bruijn, L., et al., *ALS-linked SOD1 mutant G85R mediates damage to astrocytes and promotes rapidly progressive disease with SOD1-containing inclusions.* Neuron, 1997. **18**(2): p. 327-338.

328. Bruijn, L.I., T.M. Miller, and D.W. Cleveland, *Unraveling the mechanisms involved in motor neuron degeneration in ALS.* Annu. Rev. Neurosci., 2004. **27**: p. 723-749.

329. Furukawa, Y., et al., *Disulfide cross-linked protein represents a significant fraction of ALS-associated Cu, Zn-superoxide dismutase aggregates in spinal cords of model mice.* Proceedings of the National Academy of Sciences, 2006. **103**(18): p. 7148-7153.

330. Sun, Z., et al., *Molecular determinants and genetic modifiers of aggregation and toxicity for the ALS disease protein FUS/TLS.* PLoS biology, 2011. **9**(4): p. e1000614.

331. Kim, H.J., et al., *Mutations in prion-like domains in hnRNPA2B1 and hnRNPA1 cause multisystem proteinopathy and ALS.* Nature, 2013. **495**(7442): p. 467-473.

332. Kato, M., et al., *Cell-free formation of RNA granules: low complexity sequence domains form dynamic fibers within hydrogels.* Cell, 2012. **149**(4): p. 753-767.

333. Han, T.W., et al., *Cell-free formation of RNA granules: bound RNAs identify features and components of cellular assemblies.* Cell, 2012. **149**(4): p. 768-779.

334. Guo, Y., et al., *Ultrastructural diversity of inclusions and aggregations in the lumbar spinal cord of SOD1-G93A transgenic mice.* Brain research, 2010. **1353**: p. 234-244.

335. Blokhuis, A.M., et al., *Protein aggregation in amyotrophic lateral sclerosis.* Acta neuropathologica, 2013. **125**(6): p. 777-794.

336. Carr, F., *Neurodegeneration: Selective vulnerability.* Nature Reviews Neuroscience, 2015. **16**(3): p. 123-123.

337. Robberecht, W. and T. Philips, *The changing scene of amyotrophic lateral sclerosis.* Nature Reviews Neuroscience, 2013.

338. Ravits, J., et al., *Deciphering amyotrophic lateral sclerosis: what phenotype, neuropathology and genetics are telling us about pathogenesis.* Amyotrophic Lateral Sclerosis and Frontotemporal Degeneration, 2013. **14**(S1): p. 5-18.

339. Atkin, J.D., et al., *Endoplasmic reticulum stress and induction of the unfolded protein response in human sporadic amyotrophic lateral sclerosis.* Neurobiology of disease, 2008. **30**(3): p. 400-407.

340. Sasaki, S., *Endoplasmic reticulum stress in motor neurons of the spinal cord in sporadic amyotrophic lateral sclerosis.* Journal of Neuropathology & Experimental Neurology, 2010. **69**(4): p. 346-355.

341. Saxena, S., E. Cabuy, and P. Caroni, *A role for motoneuron subtype–selective ER stress in disease manifestations of FALS mice.* Nature neuroscience, 2009. **12**(5): p. 627-636.

342. Claudio, H. and M. Bertrand, *Disturbance of endoplasmic reticulum proteostasis in neurodegenerative diseases.* Nature Reviews Neuroscience, 2014. **15**(4): p. 233-249.

343. Bilsland, L.G., et al., *Deficits in axonal transport precede ALS symptoms in vivo.* Proceedings of the National Academy of Sciences, 2010. **107**(47): p. 20523-20528.

344. Frey, D., et al., *Early and selective loss of neuromuscular synapse subtypes with low sprouting competence in motoneuron diseases.* The Journal of Neuroscience, 2000. **20**(7): p. 2534-2542.

345. Fischer, L.R., et al., *Amyotrophic lateral sclerosis is a distal axonopathy: evidence in mice and man.* Experimental neurology, 2004. **185**(2): p. 232-240.

346. Williamson, T.L. and D.W. Cleveland, *Slowing of axonal transport is a very early event in the toxicity of ALS–linked SOD1 mutants to motor neurons.* Nature neuroscience, 1999. **2**(1): p. 50-56.

347. Morfini, G.A., et al., *Axonal transport defects in neurodegenerative diseases.* The Journal of Neuroscience, 2009. **29**(41): p. 12776-12786.

348. Ferraiuolo, L., et al., *Molecular pathways of motor neuron injury in amyotrophic lateral sclerosis.* Nature Reviews Neurology, 2011. **7**(11): p. 616-630.

349. Calderilla-Barbosa, L., et al., *Interaction of SQSTM1 with the motor protein dynein–SQSTM1 is required for normal dynein function and trafficking.* Journal of cell science, 2014. **127**(18): p. 4052-4063.

350. Pérez-Brangulí, F., et al., *Dysfunction of spatacsin leads to axonal pathology in SPG11 linked hereditary spastic paraplegia.* Human molecular genetics, 2014: p. ddu200.

351. Bergeron, C., et al., *Neurofilament light and polyadenylated mRNA levels are decreased in amyotrophic lateral sclerosis motor neurons.* Journal of Neuropathology & Experimental Neurology, 1994. **53**(3): p. 221-230.

352. Štalekar, M., et al., *Proteomic analyses reveal that loss of TDP-43 affects RNA processing and intracellular transport.* Neuroscience, 2015. **293**: p. 157-170.

353. Li, Y.R., et al., *Stress granules as crucibles of ALS pathogenesis.* The Journal of cell biology, 2013. **201**(3): p. 361-372.

354. Volkening, K., et al., *Tar DNA binding protein of 43 kDa (TDP-43), 14-3-3 proteins and copper/zinc superoxide dismutase (SOD1) interact to modulate NFL mRNA stability. Implications for altered RNA processing in amyotrophic lateral sclerosis (ALS).* Brain research, 2009. **1305**: p. 168-182.

355. Fallini, C., et al., *The survival of motor neuron (SMN) protein interacts with the mRNA-binding protein HuD and regulates localization of poly (A) mRNA in primary motor neuron axons.* The Journal of Neuroscience, 2011. **31**(10): p. 3914-3925.

356. Dombert, B., et al., *Presynaptic Localization of Smn and hnRNP R in Axon Terminals of Embryonic and Postnatal Mouse Motoneurons.* PloS one, 2014. **9**(10): p. e110846.

357. Groen, E.J., et al., *ALS-associated mutations in FUS disrupt the axonal distribution and function of SMN.* Human molecular genetics, 2013: p. ddt222.

358. Tateno, M., et al., *Calcium-permeable AMPA receptors promote misfolding of mutant SOD1 protein and development of amyotrophic lateral sclerosis in a transgenic mouse model.* Human molecular genetics, 2004. **13**(19): p. 2183-2196.

359. Ligon, L.A., et al., *Mutant superoxide dismutase disrupts cytoplasmic dynein in motor neurons.* Neuroreport, 2005. **16**(6): p. 533-536.

360. Tateno, M., et al., *Mutant SOD1 impairs axonal transport of choline acetyltransferase and acetylcholine release by sequestering KAP3.* Human molecular genetics, 2009. **18**(5): p. 942-955.

361. Morfini, G.A., et al., *Inhibition of fast axonal transport by pathogenic SOD1 involves activation of p38 MAP kinase.* PloS one, 2013. **8**(6): p. e65235.

362. D'Amico, E., et al., *Clinical perspective on oxidative stress in sporadic amyotrophic lateral sclerosis.* Free Radical Biology and Medicine, 2013. **65**: p. 509-527.

363. Weiduschat, N., et al., *Motor cortex glutathione deficit in ALS measured in vivo with the J-editing technique.* Neuroscience letters, 2014. **570**: p. 102-107.

364. Vargas, M.R., D.A. Johnson, and J.A. Johnson, *Decreased glutathione accelerates neurological deficit and mitochondrial pathology in familial ALS-linked hSOD1 G93A mice model.* Neurobiology of disease, 2011. **43**(3): p. 543-551.

365. Iguchi, Y., et al., *Oxidative stress induced by glutathione depletion reproduces pathological modifications of TDP-43 linked to TDP-43 proteinopathies.* Neurobiology of disease, 2012. **45**(3): p. 862-870.

366. Zhan, L., Q. Xie, and R.S. Tibbetts, *Opposing roles of p38 and JNK in a Drosophila model of TDP-43 proteinopathy reveal oxidative stress and innate immunity as pathogenic components of neurodegeneration.* Human molecular genetics, 2014: p. ddu493.

367. Duan, W., et al., *Mutant TAR DNA-binding protein-43 induces oxidative injury in motor neuron-like cell.* Neuroscience, 2010. **169**(4): p. 1621-1629.

368. Carrì, M.T., et al., *Oxidative stress and mitochondrial damage: importance in non-SOD1 ALS.* Frontiers in cellular neuroscience, 2015. **9**.

369. Cozzolino, M., et al., *Mitochondrial dynamism and the pathogenesis of Amyotrophic Lateral Sclerosis.* Name: Frontiers in Cellular Neuroscience, 2015. **9**: p. 31.

370. Bannwarth, S., et al., *A mitochondrial origin for frontotemporal dementia and amyotrophic lateral sclerosis through CHCHD10 involvement.* Brain, 2014. **137**(8): p. 2329-2345.

371. Hong, K., et al., *Full-length TDP-43 and its C-terminal fragments activate mitophagy in NSC34 cell line.* Neuroscience letters, 2012. **530**(2): p. 144-149.

372. Huang, E.J., et al., *Extensive FUS-Immunoreactive Pathology in Juvenile Amyotrophic Lateral Sclerosis with Basophilic Inclusions.* Brain Pathology, 2010. **20**(6): p. 1069-1076.

373. Tradewell, M.L., et al., *Arginine methylation by PRMT1 regulates nuclear-cytoplasmic localization and toxicity of FUS/TLS harbouring ALS-linked mutations.* Human molecular genetics, 2012. **21**(1): p. 136-149.

374. Huang, C., et al., *Entorhinal cortical neurons are the primary targets of FUS mislocalization and ubiquitin aggregation in FUS transgenic rats.* Human molecular genetics, 2012: p. dds299.

375. Yin, H., et al., *Slow development of ALS-like spinal cord pathology in mutant valosin-containing protein gene knock-in mice.* Cell death & disease, 2012. **3**(8): p. e374.

376. Nalbandian, A., et al., *A progressive translational mouse model of human valosin-containing protein disease: The VCPR155H/+ mouse.* Muscle & nerve, 2013. **47**(2): p. 260-270.

377. Bartolome, F., et al., *Pathogenic VCP mutations induce mitochondrial uncoupling and reduced ATP levels.* Neuron, 2013. **78**(1): p. 57-64.

378. Jaiswal, M.K. and B.U. Keller, *Cu/Zn superoxide dismutase typical for familial amyotrophic lateral sclerosis increases the vulnerability of mitochondria and perturbs Ca2+ homeostasis in SOD1G93A mice.* Molecular pharmacology, 2009. **75**(3): p. 478-489.

379. Jaiswal, M.K., et al., *Impairment of mitochondrial calcium handling in a mtSOD1 cell culture model of motoneuron disease.* BMC neuroscience, 2009. **10**(1): p. 64.

380. Barrett, E.F., J.N. Barrett, and G. David, *Dysfunctional mitochondrial Ca2+ handling in mutant SOD1 mouse models of fALS: integration of findings from motor neuron somata and motor terminals.* Frontiers in cellular neuroscience, 2014. **8**.

381. Stoica, R., et al., *ER–mitochondria associations are regulated by the VAPB–PTPIP51 interaction and are disrupted by ALS/FTD-associated TDP-43.* Nature communications, 2014. **5**.

382. Keelan, J., O. Vergun, and M.R. Duchen, *Excitotoxic mitochondrial depolarisation requires both calcium and nitric oxide in rat hippocampal neurons.* The Journal of physiology, 1999. **520**(3): p. 797-813.

383. Kruman, I.I., et al., *ALS-linked Cu/Zn–SOD mutation increases vulnerability of motor neurons to excitotoxicity by a mechanism involving increased oxidative stress and perturbed calcium homeostasis.* Experimental neurology, 1999. **160**(1): p. 28-39.

384. Ilieva, H., M. Polymenidou, and D.W. Cleveland, *Non–cell autonomous toxicity in neurodegenerative disorders: ALS and beyond.* The Journal of cell biology, 2009. **187**(6): p. 761-772.

385. Haidet-Phillips, A.M., et al., *Astrocytes from familial and sporadic ALS patients are toxic to motor neurons.* Nature biotechnology, 2011. **29**(9): p. 824-828.

386. Yamanaka, K., et al., *Astrocytes as determinants of disease progression in inherited amyotrophic lateral sclerosis.* Nature neuroscience, 2008. **11**(3): p. 251-253.

387. Boillée, S., C.V. Velde, and D.W. Cleveland, *ALS: a disease of motor neurons and their nonneuronal neighbors.* Neuron, 2006. **52**(1): p. 39-59.

388. Wang, L., D.H. Gutmann, and R.P. Roos, *Astrocyte loss of mutant SOD1 delays ALS disease onset and progression in G85R transgenic mice.* Human Molecular Genetics, 2010: p. ddq463.

389. Beers, D.R., et al., *Wild-type microglia extend survival in PU. 1 knockout mice with familial amyotrophic lateral sclerosis.* Proceedings of the National Academy of Sciences, 2006. **103**(43): p. 16021-16026.

390. Philips, T. and W. Robberecht, *Neuroinflammation in amyotrophic lateral sclerosis: role of glial activation in motor neuron disease.* The Lancet Neurology, 2011. **10**(3): p. 253-263.

391. Appel, S., et al., *The microglial-motoneuron dialogue in ALS.* Acta Myologica, 2011. **30**(1): p. 4.

392. Davoli, A., et al., *Evidence of hydrogen sulfide involvement in amyotrophic lateral sclerosis.* Annals of neurology, 2015. **77**(4): p. 697-709.

393. Lee, Y., et al., *Oligodendroglia metabolically support axons and contribute to neurodegeneration.* Nature, 2012. **487**(7408): p. 443-448.

394. Philips, T., et al., *Oligodendrocyte dysfunction in the pathogenesis of amyotrophic lateral sclerosis.* Brain, 2013. **136**(2): p. 471-482.

395. Lagier-Tourenne, C., et al., *Divergent roles of ALS-linked proteins FUS/TLS and TDP-43 intersect in processing long pre-mRNAs.* Nature neuroscience, 2012. **15**(11): p. 1488-1497.

396. Elden, A.C., et al., *Ataxin-2 intermediate-length polyglutamine expansions are associated with increased risk for ALS.* Nature, 2010. **466**(7310): p. 1069-1075.

397. Barmada, S.J., *Linking RNA dysfunction and neurodegeneration in amyotrophic lateral sclerosis.* Neurotherapeutics, 2015. **12**(2): p. 340-351.

398. Sun, S., et al., *ALS-causative mutations in FUS/TLS confer gain and loss of function by altered association with SMN and U1-snRNP.* Nature communications, 2015. **6**.

399. Polymenidou, M., et al., *Long pre-mRNA depletion and RNA missplicing contribute to neuronal vulnerability from loss of TDP-43.* Nature neuroscience, 2011. **14**(4): p. 459-468.

400. Dewey, C.M., et al., *TDP-43 is directed to stress granules by sorbitol, a novel physiological osmotic and oxidative stressor.* Molecular and cellular biology, 2011. **31**(5): p. 1098-1108.

401. Bentmann, E., *Stress granule recruitment and deposition of proteins of the FET family and TDP-43 in ALS and FTD*. 2014, lmu.

402. Wils, H., et al., *TDP-43 transgenic mice develop spastic paralysis and neuronal inclusions characteristic of ALS and frontotemporal lobar degeneration.* Proceedings of the National Academy of Sciences, 2010. **107**(8): p. 3858-3863.

403. Igaz, L.M., et al., *Dysregulation of the ALS-associated gene TDP-43 leads to neuronal death and degeneration in mice.* The Journal of clinical investigation, 2011. **121**(2): p. 726.

404. Wang, I., et al., *TDP-43, the signature protein of FTLD-U, is a neuronal activity-responsive factor.* Journal of neurochemistry, 2008. **105**(3): p. 797-806.

405. Lu, L., et al., *Amyotrophic Lateral Sclerosis-linked Mutant SOD1 Sequesters Hu Antigen R (HuR) and TIA-1-related Protein (TIAR) IMPLICATIONS FOR IMPAIRED POST-TRANSCRIPTIONAL REGULATION OF VASCULAR ENDOTHELIAL GROWTH FACTOR.* Journal of Biological Chemistry, 2009. **284**(49): p. 33989-33998.

406. La Spada, A.R. and J.P. Taylor, *Repeat expansion disease: progress and puzzles in disease pathogenesis.* Nature Reviews Genetics, 2010. **11**(4): p. 247-258.

407. Moseley, M.L., et al., *Bidirectional expression of CUG and CAG expansion transcripts and intranuclear polyglutamine inclusions in spinocerebellar ataxia type 8.* Nature genetics, 2006. **38**(7): p. 758-769.

408. Zu, T., et al., *Non-ATG–initiated translation directed by microsatellite expansions.* Proceedings of the National Academy of Sciences, 2011. **108**(1): p. 260-265.

409. Wen, X., et al., *Antisense proline-arginine RAN dipeptides linked to C9ORF72-ALS/FTD form toxic nuclear aggregates that initiate in vitro and in vivo neuronal death.* Neuron, 2014. **84**(6): p. 1213-1225.

410. Polymenidou, M. and D.W. Cleveland, *Prion-like spread of protein aggregates in neurodegeneration.* The Journal of experimental medicine, 2012. **209**(5): p. 889-893.

411. Aguzzi, A. and A.M. Calella, *Prions: protein aggregation and infectious diseases.* Physiological reviews, 2009. **89**(4): p. 1105-1152.

412. Maniecka, Z. and M. Polymenidou, *From nucleation to widespread propagation: A prion-like concept for ALS.* Virus research, 2015.

413. Ravits, J., et al., *Deciphering amyotrophic lateral sclerosis: what phenotype, neuropathology and genetics are telling us about pathogenesis.* Amyotrophic Lateral Sclerosis and Frontotemporal Degeneration, 2013. **14**(sup1): p. 5-18.

414. Grad, L.I. and N.R. Cashman, *Prion-like activity of Cu/Zn superoxide dismutase: implications for amyotrophic lateral sclerosis.* Prion, 2014. **8**(1): p. 33-41.

415. Johnson, B.S., et al., *A yeast TDP-43 proteinopathy model: Exploring the molecular determinants of TDP-43 aggregation and cellular toxicity.* Proceedings of the National Academy of Sciences, 2008. **105**(17): p. 6439-6444.

416. Furukawa, Y., et al., *A seeding reaction recapitulates intracellular formation of Sarkosyl-insoluble transactivation response element (TAR) DNA-binding protein-43 inclusions.* Journal of Biological Chemistry, 2011. **286**(21): p. 18664-18672.

417. Nonaka, T., et al., *Prion-like properties of pathological TDP-43 aggregates from diseased brains.* Cell reports, 2013. **4**(1): p. 124-134.

418. Klionsky, D.J. and S.D. Emr, *Autophagy as a regulated pathway of cellular degradation.* Science, 2000. **290**(5497): p. 1717-1721.

419. Nakano, I., T. Shibata, and Y. Uesaka, *On the possibility of autolysosomal processing of skein-like inclusions: Electron microscopic observation in a case of amyotrophic lateral sclerosis.* Journal of the neurological sciences, 1993. **120**(1): p. 54-59.

420. Hetz, C., et al., *XBP-1 deficiency in the nervous system protects against amyotrophic lateral sclerosis by increasing autophagy.* Genes & development, 2009. **23**(19): p. 2294-2306.

421. Tian, F., et al., *In vivo optical imaging of motor neuron autophagy in a mouse model of amyotrophic lateral sclerosis.* Autophagy, 2011. **7**(9): p. 985-992.

422. Crippa, V., et al., *The small heat shock protein B8 (HspB8) promotes autophagic removal of misfolded proteins involved in amyotrophic lateral sclerosis (ALS).* Human molecular genetics, 2010. **19**(17): p. 3440-3456.

423. Morimoto, N., et al., *Increased autophagy in transgenic mice with a G93A mutant SOD1 gene.* Brain research, 2007. **1167**: p. 112-117.

424. Li, L., X. Zhang, and W. Le, *Altered macroautophagy in the spinal cord of SOD1 mutant mice.* Autophagy, 2008. **4**(3): p. 290-293.

425. Sasaki, S., *Autophagy in spinal cord motor neurons in sporadic amyotrophic lateral sclerosis.* Journal of Neuropathology & Experimental Neurology, 2011. **70**(5): p. 349-359.

426. Rusten, T.E. and A. Simonsen, *ESCRT functions in autophagy and associated disease.* Cell Cycle, 2008. **7**(9): p. 1166-1172.

427. Farg, M.A., et al., *C9ORF72, implicated in amytrophic lateral sclerosis and frontotemporal dementia, regulates endosomal trafficking.* Human molecular genetics, 2014: p. ddu068.

428. Ryu, H.-H., et al., *Autophagy regulates amyotrophic lateral sclerosis-linked fused in sarcoma-positive stress granules in neurons.* Neurobiology of aging, 2014. **35**(12): p. 2822-2831.

429. Ying, H., et al., *Induction of autophagy in rats upon overexpression of wild-type and mutant optineurin gene.* BMC Cell Biol, 2015. **16**(1): p. 14.

430. Castillo, K., et al., *Trehalose delays the progression of amyotrophic lateral sclerosis by enhancing autophagy in motoneurons.* Autophagy, 2013. **9**(9): p. 1308-1320.

431. Zhang, X., et al., *MTOR-independent, autophagic enhancer trehalose prolongs motor neuron survival and ameliorates the autophagic flux defect in a mouse model of amyotrophic lateral sclerosis.* Autophagy, 2014. **10**(4): p. 588-602.

432. Barmada, S.J., et al., *Autophagy induction enhances TDP43 turnover and survival in neuronal ALS models.* Nature chemical biology, 2014. **10**(8): p. 677-685.

433. Zhang, X., et al., *Rapamycin treatment augments motor neuron degeneration in SOD1G93A mouse model of amyotrophic lateral sclerosis.* Autophagy, 2011. **7**(4): p. 412-425.

434. Bhattacharya, A., et al., *Dietary restriction but not rapamycin extends disease onset and survival of the H46R/H48Q mouse model of ALS.* Neurobiology of aging, 2012. **33**(8): p. 1829-1832.

435. Group, U.-L.S., *Lithium in patients with amyotrophic lateral sclerosis (LiCALS): a phase 3 multicentre, randomised, double-blind, placebo-controlled trial.* The Lancet Neurology, 2013. **12**(4): p. 339-345.

436. Pizzasegola, C., et al., *Treatment with lithium carbonate does not improve disease progression in two different strains of SOD1 mutant mice.* Amyotrophic lateral sclerosis, 2009. **10**(4): p. 221-228.

437. Verstraete, E., et al., *Lithium lacks effect on survival in amyotrophic lateral sclerosis: a phase IIb randomised sequential trial.* Journal of Neurology, Neurosurgery & Psychiatry, 2012. **83**(5): p. 557-564.

438. Watson, P. and D.J. Stephens, *ER-to-Golgi transport: form and formation of vesicular and tubular carriers.* Biochimica et Biophysica Acta (BBA)-Molecular Cell Research, 2005. **1744**(3): p. 304-315.

439. Marie, M., et al., *Take the 'A' train: on fast tracks to the cell surface.* Cellular and molecular life sciences : CMLS, 2008. **65**(18): p. 2859-74.

440. Emr, S., et al., *Journeys through the Golgi--taking stock in a new era.* The Journal of cell biology, 2009. **187**(4): p. 449-53.

441. Barlowe, C., et al., *COPII: a membrane coat formed by Sec proteins that drive vesicle budding from the endoplasmic reticulum.* Cell, 1994. **77**(6): p. 895-907.

442. Boslem, E., et al., *Alteration of endoplasmic reticulum lipid rafts contributes to lipotoxicity in pancreatic β-cells.* Journal of Biological Chemistry, 2013. **288**(37): p. 26569-26582.

443. Preston, A., et al., *Reduced endoplasmic reticulum (ER)-to-Golgi protein trafficking contributes to ER stress in lipotoxic mouse beta cells by promoting protein overload.* Diabetologia, 2009. **52**(11): p. 2369-2373.

444. Storrie, B., et al., *Recycling of Golgi-resident glycosyltransferases through the ER reveals a novel pathway and provides an explanation for nocodazole-induced Golgi scattering.* The Journal of cell biology, 1998. **143**(6): p. 1505-1521.

445. Lucocq, J., G. Warren, and J. Pryde, *Okadaic acid induces Golgi apparatus fragmentation and arrest of intracellular transport.* Journal of Cell Science, 1991. **100**(4): p. 753-759.

446. Soo, K.Y., M. Farg, and J.D. Atkin, *Molecular motor proteins and amyotrophic lateral sclerosis.* International journal of molecular sciences, 2011. **12**(12): p. 9057-9082.

447. Atkin, J.D., et al., *Induction of the unfolded protein response in familial amyotrophic lateral sclerosis and association of protein-disulfide isomerase with superoxide dismutase 1.* Journal of Biological Chemistry, 2006. **281**(40): p. 30152-30165.

448. Reiterer, V., et al., *Sec24-and ARFGAP1-dependent trafficking of GABA transporter-1 is a prerequisite for correct axonal targeting.* The Journal of Neuroscience, 2008. **28**(47): p. 12453-12464.

449. Mourelatos, Z., et al., *The Golgi apparatus of spinal cord motor neurons in transgenic mice expressing mutant Cu, Zn superoxide dismutase becomes fragmented in early, preclinical stages of the disease.* Proceedings of the National Academy of Sciences, 1996. **93**(11): p. 5472-5477.

450. Stieber, A., et al., *The neuronal Golgi apparatus is fragmented in transgenic mice expressing a mutant human SOD1, but not in mice expressing the human NF-H gene.* Journal of the neurological sciences, 2000. **173**(1): p. 63-72.

451. Zhang, F., et al., *Interaction between familial amyotrophic lateral sclerosis (ALS)-linked SOD1 mutants and the dynein complex.* Journal of Biological Chemistry, 2007. **282**(22): p. 16691-16699.

452. Kabuta, T., et al., *Familial amyotrophic lateral sclerosis-linked mutant SOD1 aberrantly interacts with tubulin.* Biochemical and biophysical research communications, 2009. **387**(1): p. 121-126.

453. Atkin, J.D., et al., *Mutant SOD1 inhibits ER-Golgi transport in amyotrophic lateral sclerosis.* Journal of Neurochemistry, 2014. **129**(1): p. 190-204.

454. Sundaramoorthy, V., et al., *Extracellular wildtype and mutant SOD1 induces ER–Golgi pathology characteristic of amyotrophic lateral sclerosis in neuronal cells.* Cellular and Molecular Life Sciences, 2013. **70**(21): p. 4181-4195.

455. Rutkowski, D.T. and R.J. Kaufman, *A trip to the ER: coping with stress.* Trends in Cell Biology, 2004. **14**(1): p. 20-8.

456. Ellgaard, L. and A. Helenius, *Quality control in the endoplasmic reticulum.* Nature Reviews Molecular Cell Biology, 2003. **4**(3): p. 181-91.

457. Braakman, I. and N.J. Bulleid, *Protein folding and modification in the mammalian endoplasmic reticulum.* Annual review of biochemistry, 2011. **80**: p. 71-99.

458. Hetz, C. and B. Mollereau, *Disturbance of endoplasmic reticulum proteostasis in neurodegenerative diseases.* Nature Reviews Neuroscience, 2014. **15**(4): p. 233-249.

459. Hetz, C., *The unfolded protein response: controlling cell fate decisions under ER stress and beyond.* Nature reviews Molecular cell biology, 2012. **13**(2): p. 89-102.

460. Walter, P. and D. Ron, *The unfolded protein response: from stress pathway to homeostatic regulation.* Science, 2011. **334**(6059): p. 1081-1086.

461. Wang, S. and R.J. Kaufman, *The impact of the unfolded protein response on human disease.* The Journal of cell biology, 2012. **197**(7): p. 857-867.

462. Shen, J., et al., *Stable binding of ATF6 to BiP in the endoplasmic reticulum stress response.* Molecular & Cellular Biology, 2005. **25**(3): p. 921-32.

463. Schröder, M. and R.J. Kaufman, *The mammalian unfolded protein response.* Annu. Rev. Biochem., 2005. **74**: p. 739-789.

464. Hetz, C., et al., *The unfolded protein response: integrating stress signals through the stress sensor IRE1α.* Physiological reviews, 2011. **91**(4): p. 1219-1243.

465. Shoulders, M.D., et al., *Stress-independent activation of XBP1s and/or ATF6 reveals three functionally diverse ER proteostasis environments.* Cell reports, 2013. **3**(4): p. 1279-1292.

466. Shore, G.C., F.R. Papa, and S.A. Oakes, *Signaling cell death from the endoplasmic reticulum stress response.* Current opinion in cell biology, 2011. **23**(2): p. 143-149.

467. Tabas, I. and D. Ron, *Integrating the mechanisms of apoptosis induced by endoplasmic reticulum stress.* Nature cell biology, 2011. **13**(3): p. 184-190.

468. Rao, R.V., et al., *Coupling endoplasmic reticulum stress to the cell death program. Mechanism of caspase activation.* Journal of Biological Chemistry, 2001. **276**(36): p. 33869-74.

469. Scorrano, L., et al., *BAX and BAK regulation of endoplasmic reticulum Ca2+: a control point for apoptosis.* Science, 2003. **300**(5616): p. 135-139.

470. Atkin, J.D., et al., *Induction of the unfolded protein response in familial amyotrophic lateral sclerosis and association of protein-disulfide isomerase with superoxide dismutase 1.* Journal of Biological Chemistry, 2006. **281**(40): p. 30152-65.

471. Oyadomari, S. and M. Mori, *Roles of CHOP//GADD153 in endoplasmic reticulum stress.* Cell Death Differ, 2003. **11**(4): p. 381-389.

472. Han, J., et al., *ER-stress-induced transcriptional regulation increases protein synthesis leading to cell death.* Nature cell biology, 2013. **15**(5): p. 481-490.

473. Walker, A.K. and J.D. Atkin, *Stress signaling from the endoplasmic reticulum: A central player in the pathogenesis of amyotrophic lateral sclerosis.* IUBMB life, 2011. **63**(9): p. 754-763.

474. Atkin, J.D., et al., *Endoplasmic reticulum stress and induction of the unfolded protein response in human sporadic amyotrophic lateral sclerosis.* Neurobiology of Disease, 2008. **30**(3): p. 400-7.

475. Ito, Y., et al., *Involvement of CHOP, an ER-stress apoptotic mediator, in both human sporadic ALS and ALS model mice.* Neurobiology of disease, 2009. **36**(3): p. 470-476.

476. Ilieva, E.V., et al., *Oxidative and endoplasmic reticulum stress interplay in sporadic amyotrophic lateral sclerosis.* Brain, 2007. **130**(12): p. 3111-3123.

477. Oyanagi, K., et al., *Spinal anterior horn cells in sporadic amyotrophic lateral sclerosis show ribosomal detachment from, and cisternal distention of the rough endoplasmic reticulum.* Neuropathology and applied neurobiology, 2008. **34**(6): p. 650-658.

478. Tobisawa, S., et al., *Mutant SOD1 linked to familial amyotrophic lateral sclerosis, but not wild-type SOD1, induces ER stress in COS7 cells and*

transgenic mice. Biochemical and biophysical research communications, 2003. **303**(2): p. 496-503.

479. Carr, F., *Neurodegeneration: Selective vulnerability.* Nat Rev Neurosci, 2015. **16**(3): p. 123-123.

480. Bernard-Marissal, N., et al., *Calreticulin levels determine onset of early muscle denervation by fast motoneurons of ALS model mice.* Neurobiology of disease, 2015. **73**: p. 130-136.

481. Bernard-Marissal, N., et al., *Reduced calreticulin levels link endoplasmic reticulum stress and Fas-triggered cell death in motoneurons vulnerable to ALS.* The Journal of Neuroscience, 2012. **32**(14): p. 4901-4912.

482. Ferraiuolo, L., et al., *Microarray analysis of the cellular pathways involved in the adaptation to and progression of motor neuron injury in the SOD1 G93A mouse model of familial ALS.* The Journal of Neuroscience, 2007. **27**(34): p. 9201-9219.

483. Walker, A.K., et al., *Protein disulphide isomerase protects against protein aggregation and is S-nitrosylated in amyotrophic lateral sclerosis.* Brain, 2010. **133**(1): p. 105-116.

484. Soo, K.Y., et al., *Bim links ER stress and apoptosis in cells expressing mutant SOD1 associated with amyotrophic lateral sclerosis.* PLoS One, 2012. **7**(4): p. e35413.

485. Nishitoh, H., et al., *ALS-linked mutant SOD1 induces ER stress-and ASK1-dependent motor neuron death by targeting Derlin-1.* Genes & development, 2008. **22**(11): p. 1451-1464.

486. Walker, A.K., et al., *ALS-associated TDP-43 induces endoplasmic reticulum stress, which drives cytoplasmic TDP-43 accumulation and stress granule formation.* PloS one, 2013. **8**(11): p. e81170.

487. Farg, M.A., et al., *Mutant FUS induces endoplasmic reticulum stress in amyotrophic lateral sclerosis and interacts with protein disulfide-isomerase.* Neurobiology of aging, 2012. **33**(12): p. 2855-2868.

488. Vaccaro, A., et al., *Pharmacological reduction of ER stress protects against TDP-43 neuronal toxicity in vivo.* Neurobiology of disease, 2013. **55**: p. 64-75.

489. Jiang, H.-Q., et al., *Guanabenz delays the onset of disease symptoms, extends lifespan, improves motor performance and attenuates motor neuron loss in the SOD1 G93A mouse model of amyotrophic lateral sclerosis.* Neuroscience, 2014. **277**: p. 132-138.

490. Vieira, F.G., et al., *Guanabenz Treatment Accelerates Disease in a Mutant SOD1 Mouse Model of ALS.* PloS one, 2015. **10**(8): p. e0135570.

491. Sokka, A.-L., et al., *Endoplasmic reticulum stress inhibition protects against excitotoxic neuronal injury in the rat brain.* the Journal of Neuroscience, 2007. **27**(4): p. 901-908.

492. Yang, D.D., et al., *Absence of excitotoxicity-induced apoptosis in the hippocampus of mice lacking the Jnk3 gene.* Nature, 1997. **389**(6653): p. 865-870.

493. Yu, Z., et al., *The endoplasmic reticulum stress-responsive protein GRP78 protects neurons against excitotoxicity and apoptosis: suppression of oxidative stress and stabilization of calcium homeostasis.* Experimental neurology, 1999. **155**(2): p. 302-314.

494. Menéndez-Benito, V., et al., *Endoplasmic reticulum stress compromises the ubiquitin–proteasome system.* Human molecular genetics, 2005. **14**(19): p. 2787-2799.

495. Ogata, M., et al., *Autophagy is activated for cell survival after endoplasmic reticulum stress.* Molecular and cellular biology, 2006. **26**(24): p. 9220-9231.

496. Yorimitsu, T., et al., *Endoplasmic reticulum stress triggers autophagy.* Journal of Biological Chemistry, 2006. **281**(40): p. 30299-30304.

497. Høyer-Hansen, M. and M. Jäättelä, *Connecting endoplasmic reticulum stress to autophagy by unfolded protein response and calcium.* Cell Death & Differentiation, 2007. **14**(9): p. 1576-1582.

498. Li, J., et al., *The unfolded protein response regulator GRP78/BiP is required for endoplasmic reticulum integrity and stress-induced autophagy in mammalian cells.* Cell Death & Differentiation, 2008. **15**(9): p. 1460-1471.

499. Okumura, M., H. Kadokura, and K. Inaba, *Structures and functions of protein disulfide isomerase family members involved in proteostasis in the endoplasmic reticulum.* Free Radical Biology and Medicine, 2015.

500. Halperin, L., J. Jung, and M. Michalak, *The many functions of the endoplasmic reticulum chaperones and folding enzymes.* IUBMB life, 2014. **66**(5): p. 318-326.

501. Chambers, J.E. and S.J. Marciniak, *Cellular Mechanisms of Endoplasmic Reticulum Stress Signaling in Health and Disease. 2. Protein misfolding and ER stress.* American Journal of Physiology-Cell Physiology, 2014. **307**(8): p. C657-C670.

502. Wilkinson, B. and H.F. Gilbert, *Protein disulfide isomerase.* Biochimica et Biophysica Acta (BBA) - Proteins and Proteomics, 2004. **1699**(1–2): p. 35-44.

503. Woycechowsky, K.J. and R.T. Raines, *Native disulfide bond formation in proteins.* Current Opinion in Chemical Biology, 2000. **4**(5): p. 533-539.

504. Frand, A.R. and C.A. Kaiser, *The ERO1gene of yeast is required for oxidation of protein dithiols in the endoplasmic reticulum.* Molecular cell, 1998. **1**(2): p. 161-170.

505. Ellgaard, L. and L.W. Ruddock, *The human protein disulphide isomerase family: substrate interactions and functional properties.* EMBO Reports, 2005. **6**(1): p. 28-32.

506. Tian, G., et al., *The Crystal Structure of Yeast Protein Disulfide Isomerase Suggests Cooperativity between Its Active Sites.* Cell, 2006. **124**(1): p. 61-73.

507. Darby, N.J., J. Kemmink, and T.E. Creighton, *Identifying and Characterizing a Structural Domain of Protein Disulfide Isomerase.* Biochemistry, 1996. **35**(32): p. 10517-10528.

508. Klappa, P., et al., *The b' domain provides the principal peptide-binding site of protein disulfide isomerase but all domains contribute to binding of misfolded proteins.* The EMBO journal, 1998. **17**(4): p. 927-935.

509. Denisov, A.Y., et al., *Solution structure of the bb' domains of human protein disulfide isomerase.* FEBS journal, 2009. **276**(5): p. 1440-1449.

510. Turano, C., et al., *Proteins of the PDI family: unpredicted non-ER locations and functions.* Journal of cellular physiology, 2002. **193**(2): p. 154-163.

511. Bulleid, N.J. and L. Ellgaard, *Multiple ways to make disulfides.* Trends in biochemical sciences, 2011. **36**(9): p. 485-492.

512. Nguyen, V.D., et al., *Two endoplasmic reticulum PDI peroxidases increase the efficiency of the use of peroxide during disulfide bond formation.* Journal of molecular biology, 2011. **406**(3): p. 503-515.

513. Zito, E., et al., *Oxidative protein folding by an endoplasmic reticulum-localized peroxiredoxin.* Molecular cell, 2010. **40**(5): p. 787-797.

514. Wang, L., et al., *Glutathione peroxidase 7 utilizes hydrogen peroxide generated by Ero1α to promote oxidative protein folding.* Antioxidants & redox signaling, 2014. **20**(4): p. 545-556.

515. Ruddock, L.W., *Low-molecular-weight oxidants involved in disulfide bond formation.* Antioxidants & redox signaling, 2012. **16**(10): p. 1129-1138.

516. Appenzeller-Herzog, C., et al., *Disulphide production by Ero1α–PDI relay is rapid and effectively regulated.* The EMBO journal, 2010. **29**(19): p. 3318-3329.

517. Lappi, A.-K. and L.W. Ruddock, *Reexamination of the role of interplay between glutathione and protein disulfide isomerase.* Journal of molecular biology, 2011. **409**(2): p. 238-249.

518. Raje, S. and C. Thorpe, *Inter-domain redox communication in flavoenzymes of the quiescin/sulfhydryl oxidase family: role of a thioredoxin domain in disulfide bond formation.* Biochemistry, 2003. **42**(15): p. 4560-4568.

519. Codding, J.A., B.A. Israel, and C. Thorpe, *Protein substrate discrimination in the quiescin sulfhydryl oxidase (QSOX) family.* Biochemistry, 2012. **51**(20): p. 4226-4235.

520. Chakravarthi, S. and N.J. Bulleid, *Glutathione is required to regulate the formation of native disulfide bonds within proteins entering the secretory pathway.* Journal of Biological Chemistry, 2004. **279**(38): p. 39872-39879.

521. Kojer, K. and J. Riemer, *Balancing oxidative protein folding: the influences of reducing pathways on disulfide bond formation.* Biochimica et Biophysica Acta (BBA)-Proteins and Proteomics, 2014. **1844**(8): p. 1383-1390.

522. Appenzeller-Herzog, C. and L. Ellgaard, *In vivo reduction-oxidation state of protein disulfide isomerase: the two active sites independently occur in the reduced and oxidized forms.* Antioxidants & redox signaling, 2008. **10**(1): p. 55-64.

523. Atkin, J.D., et al., *Induction of the unfolded protein response in familial amyotrophic lateral sclerosis and association of protein-disulfide isomerase with superoxide dismutase 1.* J Biol Chem, 2006. **281**(40): p. 30152-65.

524. Atkin, J.D., et al., *Endoplasmic reticulum stress and induction of the unfolded protein response in human sporadic amyotrophic lateral sclerosis.* Neurobiol Dis, 2008. **30**(3): p. 400-7.

525. Honjo, Y., et al., *Protein disulfide isomerase-immunopositive inclusions in patients with amyotrophic lateral sclerosis.* Amyotrophic Lateral Sclerosis, 2011. **12**(6): p. 444-450.

526. Walker, A.K., et al., *ALS-Associated TDP-43 Induces Endoplasmic Reticulum Stress, Which Drives Cytoplasmic TDP-43 Accumulation and Stress Granule Formation.* PLoS One, 2013. **8**(11).

527. Farg, M.A., et al., *Mutant FUS induces endoplasmic reticulum stress in amyotrophic lateral sclerosis and interacts with protein disulfide-isomerase.* Neurobiol Aging, 2012. **33**(12): p. 2855-68.

528. Tsuda, H., et al., *The Amyotrophic Lateral Sclerosis 8 Protein VAPB Is Cleaved, Secreted, and Acts as a Ligand for Eph Receptors.* Cell, 2008. **133**(6): p. 963-977.

529. Walker, A.K., et al., *Protein disulphide isomerase protects against protein aggregation and is S-nitrosylated in amyotrophic lateral sclerosis.* Brain, 2010. **133**(Pt 1): p. 105-16.

530. Nardo, G., et al., *Amyotrophic lateral sclerosis multiprotein biomarkers in peripheral blood mononuclear cells.* PloS one, 2011. **6**(10): p. e25545.

531. Yang, Y.S., N.Y. Harel, and S.M. Strittmatter, *Reticulon-4A (Nogo-A) redistributes protein disulfide isomerase to protect mice from SOD1-dependent amyotrophic lateral sclerosis.* The Journal of Neuroscience, 2009. **29**(44): p. 13850-13859.

532. Chen, X., et al., *S-nitrosylated protein disulfide isomerase contributes to mutant SOD1 aggregates in amyotrophic lateral sclerosis.* Journal of neurochemistry, 2013. **124**(1): p. 45-58.

533. Jeon, G.S., et al., *Potential effect of S-nitrosylated protein disulfide isomerase on mutant SOD1 aggregation and neuronal cell death in amyotrophic lateral sclerosis.* Molecular neurobiology, 2014. **49**(2): p. 796-807.

534. Turner, B.J., et al., *Impaired extracellular secretion of mutant superoxide dismutase 1 associates with neurotoxicity in familial amyotrophic lateral sclerosis.* The Journal of neuroscience, 2005. **25**(1): p. 108-117.

535. Jessop, C.E., et al., *Protein disulphide isomerase family members show distinct substrate specificity: P5 is targeted to BiP client proteins.* Journal of cell science, 2009. **122**(23): p. 4287-4295.

536. Jessop, C.E., et al., *ERp57 is essential for efficient folding of glycoproteins sharing common structural domains.* The EMBO journal, 2007. **26**(1): p. 28-40.

537. Bolte, S. and F. Cordelieres, *A guided tour into subcellular colocalization analysis in light microscopy.* Journal of microscopy, 2006. **224**(3): p. 213-232.

538. Wang, L., X. Wang, and C.-c. Wang, *Protein disulfide–isomerase, a folding catalyst and a redox-regulated chaperone.* Free Radical Biology and Medicine, 2015. **83**: p. 305-313.

539. Quan, H., G. Fan, and C.-c. Wang, *Independence of the chaperone activity of protein disulfide isomerase from its thioredoxin-like active site.* Journal of Biological Chemistry, 1995. **270**(29): p. 17078-17080.

540. Cai, H., C.-C. Wang, and C.-L. Tsou, *Chaperone-like activity of protein disulfide isomerase in the refolding of a protein with no disulfide bonds.* Journal of Biological Chemistry, 1994. **269**(40): p. 24550-24552.

541. QIAN, J. and J. GUO, *Regulating mechanism of protein-disulphide isomerase in neurodegenerative diseases.* International Journal of Pathology and Clinical Medicine, 2009. **3**: p. 010.

542. Cheng, H., L. Wang, and C.-c. Wang, *Domain a'of protein disulfide isomerase plays key role in inhibiting α-synuclein fibril formation.* Cell Stress and Chaperones, 2010. **15**(4): p. 415-421.

543. Lee, J.H., et al., *Induction of the unfolded protein response and cell death pathway in Alzheimer's disease, but not in aged Tg2576 mice.* Experimental & molecular medicine, 2010. **42**(5): p. 386-394.

544. Uehara, T., et al., *S-nitrosylated protein-disulphide isomerase links protein misfolding to neurodegeneration.* Nature, 2006. **441**(7092): p. 513-517.

545. Nakamura, T., et al., *Aberrant protein S-nitrosylation contributes to the pathophysiology of neurodegenerative diseases.* Neurobiology of disease, 2015.

546. Forrester, M.T., M. Benhar, and J.S. Stamler, *Nitrosative stress in the ER: a new role for S-nitrosylation in neurodegenerative diseases.* ACS chemical biology, 2006. **1**(6): p. 355-358.

547. Conway, M.E. and M. Harris, *S-nitrosylation of the thioredoxin-like domains of protein disulfide isomerase and its role in neurodegenerative conditions.* Frontiers in chemistry, 2015. **3**.

548. Wang, S.-B., et al., *Protein disulfide isomerase regulates endoplasmic reticulum stress and the apoptotic process during prion infection and PrP mutant-induced cytotoxicity.* PloS one, 2012. **7**(6): p. e38221.

549. Halloran, M., S. Parakh, and J. Atkin, *The role of S-nitrosylation and S-glutathionylation of protein disulphide isomerase in protein misfolding and neurodegeneration.* International journal of cell biology, 2013. **2013**.

550. Kikuchi, H., et al., *Spinal cord endoplasmic reticulum stress associated with a microsomal accumulation of mutant superoxide dismutase-1 in an ALS model.* Proceedings of the National Academy of Sciences, 2006. **103**(15): p. 6025-6030.

551. Urushitani, M., et al., *The endoplasmic reticulum-Golgi pathway is a target for translocation and aggregation of mutant superoxide dismutase linked to ALS.* The FASEB Journal, 2008. **22**(7): p. 2476-2487.

552. Atkin, J.D., et al., *Mutant SOD1 inhibits ER-Golgi transport in amyotrophic lateral sclerosis.* Journal of neurochemistry, 2014. **129**(1): p. 190-204.

553. Gitcho, M.A., et al., *VCP mutations causing frontotemporal lobar degeneration disrupt localization of TDP-43 and induce cell death.* Journal of Biological Chemistry, 2009. **284**(18): p. 12384-12398.

554. Suzuki, H., K. Lee, and M. Matsuoka, *TDP-43-induced death is associated with altered regulation of BIM and Bcl-xL and attenuated by caspase-mediated TDP-43 cleavage.* Journal of Biological Chemistry, 2011. **286**(15): p. 13171-13183.

555. Suzuki, H. and M. Matsuoka, *TDP-43 toxicity is mediated by the unfolded protein response-unrelated induction of C/EBP homologous protein expression.* Journal of neuroscience research, 2012. **90**(3): p. 641-647.

556. Tong, J., et al., *XBP1 depletion precedes ubiquitin aggregation and Golgi fragmentation in TDP-43 transgenic rats.* Journal of neurochemistry, 2012. **123**(3): p. 406-416.

557. Soo, K.Y., et al., *Rab1-dependent ER–Golgi transport dysfunction is a common pathogenic mechanism in SOD1, TDP-43 and FUS-associated ALS.* Acta neuropathologica, 2015: p. 1-19.

558. Pincus, D., et al., *BiP binding to the ER-stress sensor Ire1 tunes the homeostatic behavior of the unfolded protein response.* PLoS biology, 2010. **8**(7): p. e1000415.

559. Shaner, N.C., P.A. Steinbach, and R.Y. Tsien, *A guide to choosing fluorescent proteins.* Nature methods, 2005. **2**(12): p. 905-909.

560. Terpe, K., *Overview of tag protein fusions: from molecular and biochemical fundamentals to commercial systems.* Applied microbiology and biotechnology, 2003. **60**(5): p. 523-533.

561. Wang, I.-F., N.M. Reddy, and C.-K.J. Shen, *Higher order arrangement of the eukaryotic nuclear bodies.* Proceedings of the National Academy of Sciences, 2002. **99**(21): p. 13583-13588.

562. Hirschberg, K., et al., *Kinetic analysis of secretory protein traffic and characterization of Golgi to plasma membrane transport intermediates in living cells.* The Journal of cell biology, 1998. **143**(6): p. 1485-1503.

563. Manders, E., F. Verbeek, and J. Aten, *Measurement of co-localization of objects in dual-colour confocal images.* Journal of microscopy, 1993. **169**(3): p. 375-382.

564. Shelkovnikova, T., et al. *FUS gene mutations associated with familiar forms of amyotrophic lateral sclerosis affect cellular localization and aggregation properties of the encoded protein*. in *Doklady Biochemistry and Biophysics*. 2011. Springer.

565. Bäumer, D., et al., *Juvenile ALS with basophilic inclusions is a FUS proteinopathy with FUS mutations.* Neurology, 2010. **75**(7): p. 611-618.

566. Chen, S., et al., *Genetics of amyotrophic lateral sclerosis: an update.* Mol Neurodegener, 2013. **8**(1): p. 28.

567. Geser, F., et al., *Evidence of multisystem disorder in whole-brain map of pathological TDP-43 in amyotrophic lateral sclerosis.* Archives of Neurology, 2008. **65**(5): p. 636-641.

568. Sakoh-Nakatogawa, M., S.-i. Nishikawa, and T. Endo, *Roles of protein-disulfide isomerase-mediated disulfide bond formation of yeast Mnl1p in endoplasmic reticulum-associated degradation.* Journal of Biological Chemistry, 2009. **284**(18): p. 11815-11825.

569. Cohen, T.J., et al., *Redox signalling directly regulates TDP-43 via cysteine oxidation and disulphide cross-linking.* The EMBO journal, 2012. **31**(5): p. 1241-1252.

570. Nonaka, T., et al., *Phosphorylated and ubiquitinated TDP-43 pathological inclusions in ALS and FTLD-U are recapitulated in SH-SY5Y cells.* FEBS letters, 2009. **583**(2): p. 394-400.

571. Kino, Y., et al., *Intracellular localization and splicing regulation of FUS/TLS are variably affected by amyotrophic lateral sclerosis-linked mutations.* Nucleic acids research, 2011. **39**(7): p. 2781-2798.

572. Farg, M.A., et al., *Ataxin-2 interacts with FUS and intermediate-length polyglutamine expansions enhance FUS-related pathology in amyotrophic lateral sclerosis.* Human molecular genetics, 2013. **22**(4): p. 717-728.

573. Mezzacasa, A. and A. Helenius, *The transitional ER defines a boundary for quality control in the secretion of tsO45 VSV glycoprotein.* Traffic, 2002. **3**(11): p. 833-849.

574. Aridor, M., et al., *Cargo selection by the COPII budding machinery during export from the ER.* The Journal of cell biology, 1998. **141**(1): p. 61-70.

575. Fromme, J.C., *Membrane Trafficking: Licensing a Cargo Receptor for ER Export.* Current Biology, 2015. **25**(2): p. R67-R68.

576. Bernardoni, P., et al., *Reticulon1-C modulates protein disulphide isomerase function.* Cell death & disease, 2013. **4**(4): p. e581.

577. Walker, A.K., *Protein disulfide isomerase and the endoplasmic reticulum in amyotrophic lateral sclerosis.* The Journal of Neuroscience, 2010. **30**(11): p. 3865-3867.

578. Suzuki, H., et al., *ALS-linked P56S-VAPB, an aggregated loss-of-function mutant of VAPB, predisposes motor neurons to ER stress-related death by inducing aggregation of co-expressed wild-type VAPB.* Journal of neurochemistry, 2009. **108**(4): p. 973-985.

579. Fewell, S.W., et al., *The action of molecular chaperones in the early secretory pathway.* Annual review of genetics, 2001. **35**(1): p. 149-191.

580. Hudson, D.A., S.A. Gannon, and C. Thorpe, *Oxidative protein folding: From thiol–disulfide exchange reactions to the redox poise of the endoplasmic reticulum.* Free Radical Biology and Medicine, 2015. **80**: p. 171-182.

581. Nguyen, V.D., *MECHANISMS AND APPLICATIONS OF DISULFIDE BOND FORMATION.*

582. Dudek, J., et al., *Protein transport into the human endoplasmic reticulum.* Journal of molecular biology, 2015. **427**(6): p. 1159-1175.

583. Matus, S., L.H. Glimcher, and C. Hetz, *Protein folding stress in neurodegenerative diseases: a glimpse into the ER.* Current opinion in cell biology, 2011. **23**(2): p. 239-252.

584. Nassif, M., et al., *Amyotrophic lateral sclerosis pathogenesis: a journey through the secretory pathway.* Antioxidants & redox signaling, 2010. **13**(12): p. 1955-1989.

585. Kemmink, J., et al., *Structure determination of the N-terminal thioredoxin-like domain of protein disulfide isomerase using multidimensional heteronuclear 13C/15N NMR spectroscopy.* Biochemistry, 1996. **35**(24): p. 7684-7691.

586. Gruber, C.W., et al., *Protein disulfide isomerase: the structure of oxidative folding.* Trends in biochemical sciences, 2006. **31**(8): p. 455-464.

587. Nguyen, V.D., et al., *Alternative conformations of the x region of human protein disulphide-isomerase modulate exposure of the substrate binding b'domain.* Journal of molecular biology, 2008. **383**(5): p. 1144-1155.

588. Wang, C., et al., *Human protein-disulfide isomerase is a redox-regulated chaperone activated by oxidation of domain a'.* Journal of Biological Chemistry, 2012. **287**(2): p. 1139-1149.

589. Quan, S., et al., *The CXXC motif is more than a redox rheostat.* Journal of Biological Chemistry, 2007. **282**(39): p. 28823-28833.

590. Irvine, A.G., et al., *Protein disulfide-isomerase interacts with a substrate protein at all stages along its folding pathway.* PloS one, 2014. **9**(1).

591. Klappa, P., H.C. Hawkins, and R.B. Freedman, *Interactions between protein disulphide isomerase and peptides.* European Journal of Biochemistry, 1997. **248**(1): p. 37-42.

592. Irvine, A.G., et al., *Protein disulfide-isomerase interacts with a substrate protein at all stages along its folding pathway.* PloS one, 2014. **9**(1): p. e82511.

593. Song, J.l. and C.c. Wang, *Chaperone-like activity of protein disulfide-isomerase in the refolding of rhodanese.* European Journal of Biochemistry, 1995. **231**(2): p. 312-316.

594. Primm, T.P., K.W. Walker, and H.F. Gilbert, *Facilitated Protein Aggregation EFFECTS OF CALCIUM ON THE CHAPERONE AND ANTI-CHAPERONE ACTIVITY OF PROTEIN DISULFIDE-ISOMERASE.* Journal of Biological Chemistry, 1996. **271**(52): p. 33664-33669.

595. Mares, R.E., S.G. Meléndez-López, and M.A. Ramos, *Acid-denatured Green Fluorescent Protein (GFP) as model substrate to study the chaperone activity of protein disulfide isomerase.* International journal of molecular sciences, 2011. **12**(7): p. 4625-4636.

596. Sovolyova, N., et al., *Stressed to death–mechanisms of ER stress-induced cell death.* Biological chemistry, 2014. **395**(1): p. 1-13.

597. Schroder, M. and R.J. Kaufman, *ER stress and the unfolded protein response.* Mutation Research/Fundamental and Molecular Mechanisms of Mutagenesis, 2005. **569**(1): p. 29-63.

598. Lee, S.O., et al., *Protein disulphide isomerase is required for signal peptide peptidase-mediated protein degradation.* The EMBO journal, 2010. **29**(2): p. 363-375.

599. Molinari, M., et al., *Sequential assistance of molecular chaperones and transient formation of covalent complexes during protein degradation from the ER.* The Journal of cell biology, 2002. **158**(2): p. 247-257.

600. Bottomley, M.J., et al., *Quality control in the endoplasmic reticulum: PDI mediates the ER retention of unassembled procollagen C-propeptides.* Current Biology, 2001. **11**(14): p. 1114-1118.

601. Vuori, K., et al., *Characterization of the human prolyl 4-hydroxylase tetramer and its multifunctional protein disulfide-isomerase subunit synthesized in a baculovirus expression system.* Proceedings of the National Academy of Sciences of the United States of America, 1992. **89**(16): p. 7467.

602. Puig, A. and H.F. Gilbert, *Protein disulfide isomerase exhibits chaperone and anti-chaperone activity in the oxidative refolding of lysozyme.* Journal of Biological Chemistry, 1994. **269**(10): p. 7764-7771.

603. Hawkins, H.C. and R.B. Freedman, *The reactivities and ionization properties of the active-site dithiol groups of mammalian protein disulphide-isomerase.* Biochem. J, 1991. **275**: p. 335-339.

604. Hawkins, H.C., E. Blackburn, and R.B. Freedman, *Comparison of the activities of protein disulphide-isomerase and thioredoxin in catalysing disulphide isomerization in a protein substrate.* Biochem. J, 1991. **275**: p. 349-353.

605. Schwaller, M., B. Wilkinson, and H.F. Gilbert, *Reduction-reoxidation cycles contribute to catalysis of disulfide isomerization by protein-disulfide isomerase.* Journal of Biological Chemistry, 2003. **278**(9): p. 7154-7159.

606. Hwang, C., A.J. Sinskey, and H.F. Lodish, *Oxidized redox state of glutathione in the endoplasmic reticulum.* Science, 1992. **257**(5076): p. 1496-1502.

607. Wilkinson, B. and H.F. Gilbert, *Protein disulfide isomerase.* Biochimica et Biophysica Acta (BBA)-Proteins and Proteomics, 2004. **1699**(1): p. 35-44.

608. Wang, C., et al., *Structural insights into the redox-regulated dynamic conformations of human protein disulfide isomerase.* Antioxidants & redox signaling, 2013. **19**(1): p. 36-45.

609. Darby, N.J., E. Penka, and R. Vincentelli, *The multi-domain structure of protein disulfide isomerase is essential for high catalytic efficiency.* Journal of molecular biology, 1998. **276**(1): p. 239-247.

610. Xiao, R., et al., *Combinations of protein-disulfide isomerase domains show that there is little correlation between isomerase activity and wild-type growth.* Journal of Biological Chemistry, 2001. **276**(30): p. 27975-27980.

611. Jonsson, P.A., et al., *Disulphide-reduced superoxide dismutase-1 in CNS of transgenic amyotrophic lateral sclerosis models.* Brain, 2006. **129**(2): p. 451-464.

612. Nagano, S., et al., *A cysteine residue affects the conformational state and neuronal toxicity of mutant SOD1 in mice: relevance to the pathogenesis of ALS.* Human molecular genetics, 2015. **24**(12): p. 3427-3439.

613. Fridovich, I., *Superoxide dismutases.* Annual review of biochemistry, 1975. **44**(1): p. 147-159.

614. Valentine, J.S., P.A. Doucette, and S. Zittin Potter, *Copper-zinc superoxide dismutase and amyotrophic lateral sclerosis.* Annu. Rev. Biochem., 2005. **74**: p. 563-593.

615. Kitamura, F., et al., *Structural instability and Cu-dependent pro-oxidant activity acquired by the apo form of mutant SOD1 associated with amyotrophic lateral sclerosis.* Biochemistry, 2011. **50**(20): p. 4242-4250.

616. Hennig, J., et al., *Local Destabilization of the Metal-Binding Region in Human Copper–Zinc Superoxide Dismutase by Remote Mutations Is a Possible Determinant for Progression of ALS.* Biochemistry, 2015. **54**(2): p. 323-333.

617. Niwa, J.-i., et al., *Disulfide bond mediates aggregation, toxicity, and ubiquitylation of familial amyotrophic lateral sclerosis-linked mutant SOD1.* Journal of Biological Chemistry, 2007. **282**(38): p. 28087-28095.

618. Chattopadhyay, M., et al., *Initiation and elongation in fibrillation of ALS-linked superoxide dismutase.* Proceedings of the National Academy of Sciences, 2008. **105**(48): p. 18663-18668.

619. Kayatekin, C., J.A. Zitzewitz, and C.R. Matthews, *Disulfide-reduced ALS variants of Cu, Zn superoxide dismutase exhibit increased populations of unfolded species.* Journal of molecular biology, 2010. **398**(2): p. 320-331.

620. Fujiwara, N., et al., *Oxidative modification to cysteine sulfonic acid of Cys111 in human copper-zinc superoxide dismutase.* Journal of Biological Chemistry, 2007. **282**(49): p. 35933-35944.

621. Banci, L., et al., *SOD1 and amyotrophic lateral sclerosis: mutations and oligomerization.* PLoS One, 2008. **3**(2): p. e1677.

622. Roberts, B.L., et al., *Role of disulfide cross-linking of mutant SOD1 in the formation of inclusion-body-like structures.* 2012.

623. Karch, C.M., et al., *Role of mutant SOD1 disulfide oxidation and aggregation in the pathogenesis of familial ALS.* Proceedings of the National Academy of Sciences, 2009. **106**(19): p. 7774-7779.

624. Soo, K.Y., et al., *Recruitment of mitochondria into apoptotic signaling correlates with the presence of inclusions formed by amyotrophic lateral sclerosis-associated SOD1 mutations.* Journal of neurochemistry, 2009. **108**(3): p. 578-590.

625. Cozzolino, M., et al., *Cysteine 111 affects aggregation and cytotoxicity of mutant Cu, Zn-superoxide dismutase associated with familial amyotrophic lateral sclerosis.* Journal of Biological Chemistry, 2008. **283**(2): p. 866-874.

626. Chang, C.-k., et al., *Molecular mechanism of oxidation-induced TDP-43 RRM1 aggregation and loss of function.* FEBS letters, 2013. **587**(6): p. 575-582.

627. Morohoshi, F., et al., *Genomic structure of the human RBP56/hTAFII68 and FUS/TLS genes.* Gene, 1998. **221**(2): p. 191-198.

628. Iko, Y., et al., *Domain architectures and characterization of an RNA-binding protein, TLS.* Journal of Biological Chemistry, 2004. **279**(43): p. 44834-44840.

629. Woycechowsky, K.J., K.D. Wittrup, and R.T. Raines, *A small-molecule catalyst of protein folding in vitro and in vivo.* Chemistry & biology, 1999. **6**(12): p. 871-879.

630. Kersteen, E.A. and R.T. Raines, *Catalysis of protein folding by protein disulfide isomerase and small-molecule mimics.* Antioxidants and Redox Signaling, 2003. **5**(4): p. 413-424.

631. Nielsen, P.E., M. Egholm, and O. Buchardt, *Peptide nucleic acid (PNA). A DNA mimic with a peptide backbone.* Bioconjugate chemistry, 1994. **5**(1): p. 3-7.

632. Ray, A. and B. Nordén, *Peptide nucleic acid (PNA): its medical and biotechnical applications and promise for the future.* The FASEB Journal, 2000. **14**(9): p. 1041-1060.

633. Shi, H., et al., *A review: Fabrications, detections and applications of peptide nucleic acids (PNAs) microarray.* Biosensors and Bioelectronics, 2015. **66**: p. 481-489.

634. Shakeel, S., S. Karim, and A. Ali, *Peptide nucleic acid (PNA)—a review.* Journal of Chemical Technology and Biotechnology, 2006. **81**(6): p. 892-899.

635. Nielsen, P.E., *Peptide nucleic acids (PNA) in chemical biology and drug discovery.* Chemistry & biodiversity, 2010. **7**(4): p. 786-804.

636. Sazani, P., et al., *Systemically delivered antisense oligomers upregulate gene expression in mouse tissues.* Nature biotechnology, 2002. **20**(12): p. 1228-1233.

637. Browne, E.C., S.J. Langford, and B.M. Abbott, *Synthesis and effects of conjugated tocopherol analogues on peptide nucleic acid hybridisation.* Organic & biomolecular chemistry, 2013. **11**(39): p. 6744-6750.

638. Turner, B.J., et al., *Antisense peptide nucleic acid-mediated knockdown of the p75 neurotrophin receptor delays motor neuron disease in mutant SOD1 transgenic mice.* Journal of neurochemistry, 2003. **87**(3): p. 752-763.

639. Whiteley, E.M., T.-A. Hsu, and M.J. Betenbaugh, *Thioredoxin domain non-equivalence and anti-chaperone activity of protein disulfide isomerase mutants in vivo.* Journal of Biological Chemistry, 1997. **272**(36): p. 22556-22563.

640. Hashimoto, S., K. Okada, and S. Imaoka, *Interaction between bisphenol derivatives and protein disulphide isomerase (PDI) and inhibition of PDI functions: requirement of chemical structure for binding to PDI.* Journal of biochemistry, 2008. **144**(3): p. 335-342.

641. Walker, K.W., M.M. Lyles, and H.F. Gilbert, *Catalysis of oxidative protein folding by mutants of protein disulfide isomerase with a single active-site cysteine.* Biochemistry, 1996. **35**(6): p. 1972-1980.

642. Puig, A., et al., *The role of the thiol/disulfide centers and peptide binding site in the chaperone and anti-chaperone activities of protein disulfide isomerase.* Journal of Biological Chemistry, 1994. **269**(29): p. 19128-19135.

643. Laboissiere, M.C., S.L. Sturley, and R.T. Raines, *The essential function of protein-disulfide isomerase is to unscramble non-native disulfide bonds.* Journal of Biological Chemistry, 1995. **270**(47): p. 28006-28009.

644. Hawkins, C.J. and D.L. Vaux, *Analysis of the Role of bcl-2 in Apoptosis.* Immunological reviews, 1994. **142**(1): p. 127-139.

645. Parakh, S. and J.D. Atkin, *Novel roles for protein disulphide isomerase in disease states: a double edged sword?* Frontiers in Cell and Developmental Biology, 2015. **3**: p. 30.

646. Wang, J., G. Xu, and D.R. Borchelt, *Mapping superoxide dismutase 1 domains of non-native interaction: roles of intra-and intermolecular*

disulfide bonding in aggregation. Journal of neurochemistry, 2006. **96**(5): p. 1277-1288.

647. Prudencio, M., et al., *Variation in aggregation propensities among ALS-associated variants of SOD1: correlation to human disease.* Human molecular genetics, 2009. **18**(17): p. 3217-3226.

648. Wang, Q., et al., *Protein aggregation and protein instability govern familial amyotrophic lateral sclerosis patient survival.* PLoS biology, 2008. **6**(7): p. e170.

649. Walker, K.W. and H.F. Gilbert, *Scanning and escape during protein-disulfide isomerase-assisted protein folding.* Journal of Biological Chemistry, 1997. **272**(14): p. 8845-8848.

650. Lee, J., et al., *No correlation between aggregates of Cu/Zn superoxide dismutase and cell death in familial amyotrophic lateral sclerosis.* Journal of neurochemistry, 2002. **82**(5): p. 1229-1238.

651. Oh, Y.K., et al., *Superoxide dismutase 1 mutants related to amyotrophic lateral sclerosis induce endoplasmic stress in neuro2a cells.* Journal of neurochemistry, 2008. **104**(4): p. 993-1005.

652. Cohen, T.J., et al., *Redox signalling directly regulates TDP-43 via cysteine oxidation and disulphide cross-linking.* The EMBO Journal, 2011. **31**(5): p. 1241-1252.

653. Colombrita, C., et al., *TDP-43 and FUS RNA-binding proteins bind distinct sets of cytoplasmic messenger RNAs and differently regulate their post-transcriptional fate in motoneuron-like cells.* Journal of Biological Chemistry, 2012. **287**(19): p. 15635-15647.

654. Iko, Y., et al., *Domain Architectures and Characterization of an RNA-binding Protein, TLS.* Journal of Biological Chemistry, 2004. **279**(43): p. 44834-44840.

655. Gitler, A.D. and J. Shorter, *RNA-binding proteins with prion-like domains in ALS and FTLD-U.* brain, 2011. **2**: p. 4.

656. Watts, J.C., et al., *Interactome analyses identify ties of PrP and its mammalian paralogs to oligomannosidic N-glycans and endoplasmic reticulum-derived chaperones.* PLoS Pathog, 2009. **5**(10): p. e1000608.

657. Winter, J., H. Lilie, and R. Rudolph, *Recombinant expression and in vitro folding of proinsulin are stimulated by the synthetic dithiol Vectrase-P.* FEMS microbiology letters, 2002. **213**(2): p. 225-230.

658. Pflugh, D.L., S.E. Maher, and A.L. Bothwell, *Ly-6 superfamily members Ly-6A/E, Ly-6C, and Ly-6I recognize two potential ligands expressed by B lymphocytes.* The Journal of Immunology, 2002. **169**(9): p. 5130-5136.

659. Woycechowsky, K.J. and R.T. Raines, *The CXC motif: a functional mimic of protein disulfide isomerase.* Biochemistry, 2003. **42**(18): p. 5387-5394.

660. Nørgaard, P. and J.R. Winther, *Mutation of yeast Eug1p CXXS active sites to CXXC results in a dramatic increase in protein disulphide isomerase activity.* Biochemical Journal, 2001. **358**(Pt 1): p. 269-274.

661. Mezghrani, A., et al., *Manipulation of oxidative protein folding and PDI redox state in mammalian cells.* The EMBO journal, 2001. **20**(22): p. 6288-6296.

662. Merksamer, P.I., A. Trusina, and F.R. Papa, *Real-time redox measurements during endoplasmic reticulum stress reveal interlinked protein folding functions.* Cell, 2008. **135**(5): p. 933-947.

663. Parakh, S., et al., *Redox Regulation in Amyotrophic Lateral Sclerosis.* Oxidative Medicine and Cellular Longevity, 2013. **2013**: p. 408681.

664. Galligan, J.J. and D.R. Petersen, *The human protein disulfide isomerase gene family.* Human genomics, 2012. **6**(1): p. 1-15.

665. Sato, Y., et al., *Synergistic cooperation of PDI family members in peroxiredoxin 4-driven oxidative protein folding.* Scientific reports, 2013. **3**.

666. Kozlov, G., et al., *A structural overview of the PDI family of proteins.* FEBS journal, 2010. **277**(19): p. 3924-3936.

667. Maattanen, P., et al., *ERp57 and PDI: multifunctional protein disulfide isomerases with similar domain architectures but differing substrate-partner associations This paper is one of a selection of papers published in this Special Issue, entitled CSBMCB-Membrane Proteins in Health and Disease.* Biochemistry and cell biology, 2006. **84**(6): p. 881-889.

668. Mazzarella, R.A., et al., *ERp72, an abundant luminal endoplasmic reticulum protein, contains three copies of the active site sequences of protein disulfide isomerase.* Journal of Biological Chemistry, 1990. **265**(2): p. 1094-1101.

669. Leach, M.R., et al., *Localization of the lectin, ERp57 binding, and polypeptide binding sites of calnexin and calreticulin.* Journal of Biological Chemistry, 2002. **277**(33): p. 29686-29697.

670. Oliver, J.D., et al., *Interaction of the thiol-dependent reductase ERp57 with nascent glycoproteins.* Science, 1997. **275**(5296): p. 86-8.

671. Xinmiao, F., et al., *PDIp is a major intracellular oestrogen-storage protein that modulates tissue levels of oestrogen in the pancreas.* Biochemical Journal, 2012. **447**(1): p. 115-123.

672. Kozlov, G., et al., *Structure of the noncatalytic domains and global fold of the protein disulfide isomerase ERp72.* Structure, 2009. **17**(5): p. 651-659.

673. Grillo, C., et al., *Cooperative activity of Ref-1/APE and ERp57 in reductive activation of transcription factors.* Free Radical Biology and Medicine, 2006. **41**(7): p. 1113-1123.

674. Hirano, N., et al., *Molecular cloning of the human glucose-regulated protein ERp57/GRP58, a thiol-dependent reductase. Identification of its secretory form and inducible expression by the oncogenic transformation.* European Journal of Biochemistry, 1995. **234**(1): p. 336-42.

675. Marcus, N., et al., *Tissue distribution of three members of the murine protein disulfide isomerase (PDI) family.* Biochimica et Biophysica Acta (BBA)-Gene Structure and Expression, 1996. **1309**(3): p. 253-260.

676. Inaba, K., et al., *Crystal structures of human Ero1α reveal the mechanisms of regulated and targeted oxidation of PDI.* The EMBO journal, 2010. **29**(19): p. 3330-3343.

677. Bourdi, M., et al., *cDNA cloning and baculovirus expression of the human liver endoplasmic reticulum P58: characterization as a protein disulfide isomerase isoform, but not as a protease or a carnitine acyltransferase.* Archives of Biochemistry & Biophysics, 1995. **323**(2): p. 397-403.

678. Frickel, E.M., et al., *ERp57 is a multifunctional thiol-disulfide oxidoreductase.* Journal of Biological Chemistry, 2004. **279**(18): p. 18277-87.

679. Garbi, N., et al., *Impaired assembly of the major histocompatibility complex class I peptide-loading complex in mice deficient in the oxidoreductase ERp57.* Nature immunology, 2006. **7**(1): p. 93-102.

680. Daniels, R., et al., *N-linked glycans direct the cotranslational folding pathway of influenza hemagglutinin.* Molecular cell, 2003. **11**(1): p. 79-90.

681. Bouvier, M., *Accessory proteins and the assembly of human class I MHC molecules: a molecular and structural perspective.* Molecular Immunology, 2003. **39**(12): p. 697-706.

682. Castillo, V., et al., *Functional Role of the Disulfide Isomerase ERp57 in Axonal Regeneration.* PLoS ONE, 2015. **10**(9): p. e0136620.

683. Di Jeso, B., et al., *Mixed-disulfide folding intermediates between thyroglobulin and endoplasmic reticulum resident oxidoreductases ERp57 and protein disulfide isomerase.* Molecular and cellular biology, 2005. **25**(22): p. 9793-9805.

684. Kozlov, G., et al., *Crystal structure of the bb' domains of the protein disulfide isomerase ERp57.* Structure, 2006. **14**(8): p. 1331-1339.

685. Rutkevich, L.A., et al., *Functional relationship between protein disulfide isomerase family members during the oxidative folding of human secretory proteins.* Molecular biology of the cell, 2010. **21**(18): p. 3093-3105.

686. Alanen, H.I., et al., *ERp27, a new non-catalytic endoplasmic reticulum-located human protein disulfide isomerase family member, interacts with ERp57.* Journal of Biological Chemistry, 2006. **281**(44): p. 33727-33738.

687. Solda, T., et al., *Consequences of ERp57 deletion on oxidative folding of obligate and facultative clients of the calnexin cycle.* Journal of Biological Chemistry, 2006. **281**(10): p. 6219-26.

688. Coe, H., et al., *ERp57 modulates STAT3 signaling from the lumen of the endoplasmic reticulum.* Journal of Biological Chemistry, 2010. **285**(9): p. 6725-6738.

689. Pirneskoski, A., et al., *Molecular characterization of the principal substrate binding site of the ubiquitous folding catalyst protein disulfide isomerase.* Journal of Biological Chemistry, 2004. **279**(11): p. 10374-81.

690. Russell, S.J., et al., *The primary substrate binding site in the b' domain of ERp57 is adapted for endoplasmic reticulum lectin association.* Journal of Biological Chemistry, 2004. **279**(18): p. 18861-18869.

691. Maattanen, P., et al., *ERp57 and PDI: multifunctional protein disulfide isomerases with similar domain architectures but differing substrate–partner associationsThis paper is one of a selection of papers published in this Special Issue, entitled CSBMCB — Membrane Proteins in Health and Disease.* Biochemistry and Cell Biology, 2006. **84**(6): p. 881-889.

692. Erickson, R.R., et al., *In cerebrospinal fluid ER chaperones ERp57 and calreticulin bind β-amyloid.* Biochemical and biophysical research communications, 2005. **332**(1): p. 50-57.

693. Holtz, W.A. and K.L. O'Malley, *Parkinsonian mimetics induce aspects of unfolded protein response in death of dopaminergic neurons.* Journal of Biological Chemistry, 2003. **278**(21): p. 19367-19377.

694. Ryu, E.J., et al., *Endoplasmic reticulum stress and the unfolded protein response in cellular models of Parkinson's disease.* The Journal of Neuroscience, 2002. **22**(24): p. 10690-10698.

695. Kim-Han, J.S. and K.L. O'Malley, *Cell stress induced by the parkinsonian mimetic, 6-hydroxydopamine, is concurrent with oxidation of the chaperone, ERp57, and aggresome formation.* Antioxidants & redox signaling, 2007. **9**(12): p. 2255-2264.

696. Hetz, C., et al., *The disulfide isomerase Grp58 is a protective factor against prion neurotoxicity.* The Journal of neuroscience, 2005. **25**(11): p. 2793-2802.

697. Gonzalez-Perez, P., et al., *Identification of rare protein disulfide isomerase gene variants in amyotrophic lateral sclerosis patients.* Gene, 2015. **566**(2): p. 158-165.

698. Chen, W., et al., *A possible biochemical link between NADPH oxidase (Nox) 1 redox-signalling and ERp72.* Biochem. J, 2008. **416**: p. 55-63.

699. Van, P.N., et al., *CaBP2 is a rat homolog of ERp72 with proteindisulfide isomerase activity.* European Journal of Biochemistry, 1993. **213**(2): p. 789-795.

700. Spee, P., J. Subjeck, and J. Neefjes, *Identification of Novel Peptide Binding Proteins in the Endoplasmic Reticulum: ERp72, Calnexin, and grp170†.* Biochemistry, 1999. **38**(32): p. 10559-10566.

701. Okumura, M., H. Kadokura, and K. Inaba, *Structures and functions of protein disulfide isomerase family members involved in proteostasis in the endoplasmic reticulum.* Free Radical Biology and Medicine, 2015. **83**: p. 314-322.

702. Soldà, T., et al., *Consequences of ERp57 deletion on oxidative folding of obligate and facultative clients of the calnexin cycle.* Journal of Biological Chemistry, 2006. **281**(10): p. 6219-6226.

703. Schaiff, W.T., et al., *HLA-DR associates with specific stress proteins and is retained in the endoplasmic reticulum in invariant chain negative cells.* The Journal of experimental medicine, 1992. **176**(3): p. 657-666.

704. Meunier, L., et al., *A subset of chaperones and folding enzymes form multiprotein complexes in endoplasmic reticulum to bind nascent proteins.* Molecular biology of the cell, 2002. **13**(12): p. 4456-4469.

705. Freedman, R.B., T.R. Hirst, and M.F. Tuite, *Protein disulphide isomerase: building bridges in protein folding.* Trends in Biochemical Sciences, 1994. **19**(8): p. 331-6.

706. Linnik, K.M. and H. Herscovitz, *Multiple Molecular Chaperones Interact with Apolipoprotein B during Its Maturation.* Journal of Biological Chemistry, 1998. **273**(33): p. 21368-21373.

707. Kozlov, G., et al., *Structure of the Noncatalytic Domains and Global Fold of the Protein Disulfide Isomerase ERp72.* Structure (London, England : 1993), 2009. **17**(5): p. 651-659.

708. Mazzarella, R.A., et al., *ERp72, an abundant luminal endoplasmic reticulum protein, contains three copies of the active site sequences of protein disulfide isomerase.* Journal of Biological Chemistry, 1990. **265**(2): p. 1094-101.

709. Turano, C., et al., *Proteins of the PDI family: Unpredicted non-ER locations and functions.* Journal of Cellular Physiology, 2002. **193**(2): p. 154-163.

710. Turano, C., et al., *ERp57/GRP58: a protein with multiple functions.* Cellular & molecular biology letters, 2011. **16**(4): p. 539-563.

711. Andreu, C.I., et al., *Protein disulfide isomerases in neurodegeneration: from disease mechanisms to biomedical applications.* FEBS letters, 2012. **586**(18): p. 2826-2834.

712. Woycechowsky, K.J. and R.T. Raines, *The CXC Motif: A Functional Mimic of Protein Disulfide Isomerase†.* Biochemistry, 2003. **42**(18): p. 5387-5394.

713. Rupp, K., et al., *Effects of CaBP2, the rat analog of ERp72, and of CaBP1 on the refolding of denatured reduced proteins. Comparison with protein disulfide isomerase.* Journal of Biological Chemistry, 1994. **269**(4): p. 2501-2507.

714. Ushioda, R., et al., *ERdj5 is required as a disulfide reductase for degradation of misfolded proteins in the ER.* Science, 2008. **321**(5888): p. 569-572.

715. Kadokura, H., et al., *Identification of the redox partners of ERdj5/JPDI, a PDI family member, from an animal tissue.* Biochemical and biophysical research communications, 2013. **440**(2): p. 245-250.

716. Jessop, C.E., et al., *ERp57 is essential for efficient folding of glycoproteins sharing common structural domains.* EMBO Journal, 2007. **26**(1): p. 28-40.

717. Donella-Deana, A., et al., *Isolation from Spleen of a 57-kDa Protein Substrate of the Tyrosine Kinase Lyn.* European Journal of Biochemistry, 1996. **235**(1-2): p. 18-25.

718. Chen, N., et al., *Evidence that casein kinase 2 phosphorylates hepatic microsomal calcium-binding proteins 1 and 2 but not 3.* Biochemistry, 1996. **35**(25): p. 8299-8306.

719. Casoni, F., et al., *Protein Nitration in a Mouse Model of Familial Amyotrophic Lateral Sclerosis POSSIBLE MULTIFUNCTIONAL ROLE IN THE PATHOGENESIS.* Journal of Biological Chemistry, 2005. **280**(16): p. 16295-16304.

720. Araki, K., et al., *Ero1-α and PDIs constitute a hierarchical electron transfer network of endoplasmic reticulum oxidoreductases.* The Journal of cell biology, 2013. **202**(6): p. 861-874.

721. Zapun, A., et al., *Folding in vitro of bovine pancreatic trypsin inhibitor in the presence of proteins of the endoplasmic reticulum.* Proteins: Structure, Function, and Bioinformatics, 1992. **14**(1): p. 10-15.

722. Laurindo, F.R., L.A. Pescatore, and D. de Castro Fernandes, *Protein disulfide isomerase in redox cell signaling and homeostasis.* Free Radical Biology and Medicine, 2012. **52**(9): p. 1954-1969.

723. Pelham, H.R., *The Florey lecture, 1992: the secretion of proteins by cells.* Proceedings of the Royal Society of London B: Biological Sciences, 1992. **250**(1327): p. 1-10.

724. Noiva, R. *Protein disulfide isomerase: the multifunctional redox chaperone of the endoplasmic reticulum*. in *Seminars in cell & developmental biology*. 1999. Elsevier.

725. Wroblewski, V.J., et al., *Mechanisms involved in degradation of human insulin by cytosolic fractions of human, monkey, and rat liver.* Diabetes, 1992. **41**(4): p. 539-547.

726. Essex, D., K. Chen, and M. Swiatkowska, *Localization of protein disulfide isomerase to the external surface of.* Blood, 1995. **86**(6): p. 2168-2173.

727. SAFRAN, M. and J.L. LEONARD, *Characterization of a N-bromoacetyl-L-thyroxine affinity-labeled 55-kilodalton protein as protein disulfide isomerase in cultured glial cells.* Endocrinology, 1991. **129**(4): p. 2011-2016.

728. Terada, K., et al., *Secretion, surface localization, turnover, and steady state expression of protein disulfide isomerase in rat hepatocytes.* Journal of Biological Chemistry, 1995. **270**(35): p. 20410-20416.

729. Jiang, X.-M., et al., *Redox control of exofacial protein thiols/disulfides by protein disulfide isomerase.* Journal of Biological Chemistry, 1999. **274**(4): p. 2416-2423.

730. Lawrence, D.A., R. Song, and P. Weber, *Surface thiols of human lymphocytes and their changes after in vitro and in vivo activation.* Journal of leukocyte biology, 1996. **60**(5): p. 611-618.

731. Bennett, T.A., et al., *Sulfhydryl regulation of L-selectin shedding: phenylarsine oxide promotes activation-independent L-selectin shedding from leukocytes.* The Journal of Immunology, 2000. **164**(8): p. 4120-4129.

732. Delom, F., et al., *Role of extracellular molecular chaperones in the folding of oxidized proteins refolding of colloidal thyroglobulin by protein disulfide isomerase and immunoglobulin heavy chain-binding protein.* Journal of Biological Chemistry, 2001. **276**(24): p. 21337-21342.

733. Gerner, C., et al., *Reassembling proteins and chaperones in human nuclear matrix protein fractions.* Journal of cellular biochemistry, 1999. **74**(2): p. 145-151.

734. Clive, D.R. and J.J. Greene, *Cooperation of protein disulfide isomerase and redox environment in the regulation of NF-κB and AP1 binding to DNA.* Cell biochemistry and function, 1996. **14**(1): p. 49-55.

735. Markus, M. and R. Benezra, *Two isoforms of protein disulfide isomerase alter the dimerization status of E2A proteins by a redox mechanism.* Journal of Biological Chemistry, 1999. **274**(2): p. 1040-1049.

736. Hotchkiss, K.A., L.J. Matthias, and P.J. Hogg, *Exposure of the cryptic Arg-Gly-Asp sequence in thrombospondin-1 by protein disulfide isomerase.* Biochimica et Biophysica Acta (BBA)-Protein Structure and Molecular Enzymology, 1998. **1388**(2): p. 478-488.

737. Yoshimori, T., et al., *Protein disulfide-isomerase in rat exocrine pancreatic cells is exported from the endoplasmic reticulum despite possessing the retention signal.* Journal of Biological Chemistry, 1990. **265**(26): p. 15984-15990.

738. Gilbert, J., et al., *Downregulation of protein disulfide isomerase inhibits infection by the mouse polyomavirus.* Journal of virology, 2006. **80**(21): p. 10868-10870.

739. Stolf, B.S., et al., *Protein disulfide isomerase and host-pathogen interaction.* The Scientific World Journal, 2011. **11**: p. 1749-1761.

740. Tsai, B., et al., *Protein disulfide isomerase acts as a redox-dependent chaperone to unfold cholera toxin.* Cell, 2001. **104**(6): p. 937-948.

741. Hoffstrom, B.G., et al., *Inhibitors of protein disulfide isomerase suppress apoptosis induced by misfolded proteins.* Nature chemical biology, 2010. **6**(12): p. 900-906.

742. Yang, Y.S. and S.M. Strittmatter, *The reticulons: a family of proteins with diverse functions.* Genome Biol, 2007. **8**(12): p. 234.

743. Oertle, T., et al., *Genomic structure and functional characterisation of the promoters of human and mouse nogo/rtn4.* Journal of molecular biology, 2003. **325**(2): p. 299-323.

744. Iwahashi, J. and N. Hamada, *Human reticulon 1-A and 1-B interact with a medium chain of the AP-2 adaptor complex.* Cellular and molecular biology (Noisy-le-Grand, France), 2002. **49**: p. OL467-71.

745. Steiner, P., et al., *Reticulon 1-C/neuroendocrine-specific protein-C interacts with SNARE proteins.* Journal of neurochemistry, 2004. **89**(3): p. 569-580.

746. Ayala, Y.M., et al., *Structural determinants of the cellular localization and shuttling of TDP-43.* Journal of cell science, 2008. **121**(22): p. 3778-3785.

747. Zinszner, H., et al., *TLS (FUS) binds RNA in vivo and engages in nucleo-cytoplasmic shuttling.* Journal of cell science, 1997. **110**(15): p. 1741-1750.

748. Gillece, P., et al., *Export of a cysteine-free misfolded secretory protein from the endoplasmic reticulum for degradation requires interaction with protein disulfide isomerase.* The Journal of cell biology, 1999. **147**(7): p. 1443-1456.

749. Johnson, S., et al., *The ins and outs of calreticulin: from the ER lumen to the extracellular space.* Trends in cell biology, 2001. **11**(3): p. 122-129.

750. Rigobello, M.P., et al., *Isolation, purification, and characterization of a rat liver mitochondrial protein disulfide isomerase.* Free Radical Biology and Medicine, 2000. **28**(2): p. 266-272.

751. Wang, X., et al., *Bcl-2 proteins regulate ER membrane permeability to luminal proteins during ER stress-induced apoptosis.* Cell Death & Differentiation, 2011. **18**(1): p. 38-47.

752. Tu, B.P. and J.S. Weissman, *Oxidative protein folding in eukaryotes mechanisms and consequences.* The Journal of cell biology, 2004. **164**(3): p. 341-346.

753. Raj, K., S.I. Chanu, and S. Sarkar, *Protein misfolding and aggregation in neurodegenerative disorders: focus on chaperone-mediated protein folding machinery.* International Journal of Neurology Research, 2015. **1**(2): p. 72-78.

754. Herczenik, E. and M.F. Gebbink, *Molecular and cellular aspects of protein misfolding and disease.* The FASEB Journal, 2008. **22**(7): p. 2115-2133.

755. Duncan, E.J., et al., *The Role of HSP70 and Its Co-chaperones in Protein Misfolding, Aggregation and Disease*, in *The Networking of Chaperones by Co-chaperones*. 2015, Springer. p. 243-273.

756. Robberecht, W. and T. Philips, *The changing scene of amyotrophic lateral sclerosis.* Nature Reviews Neuroscience, 2013. **14**(4): p. 248-264.

757. Yu, A., et al., *Protein aggregation can inhibit clathrin-mediated endocytosis by chaperone competition.* Proceedings of the National Academy of Sciences, 2014. **111**(15): p. E1481-E1490.

758. Sobierajska, K., et al., *Protein disulfide isomerase directly interacts with β-Actin Cys374 and regulates cytoskeleton reorganization.* Journal of Biological Chemistry, 2014. **289**(9): p. 5758-5773.

759. Moloney, E.B., F. de Winter, and J. Verhaagen, *ALS as a distal axonopathy: molecular mechanisms affecting neuromuscular junction stability in the presymptomatic stages of the disease.* Frontiers in Neuroscience, 2014. **8**: p. 252.

760. Shaw, P. and C. Eggett, *Molecular factors underlying selective vulnerability of motor neurons to neurodegeneration in amyotrophic lateral sclerosis.* Journal of neurology, 2000. **247**(1): p. I17-I27.

761. Hammerschlag, R., et al., *Evidence that all newly synthesized proteins destined for fast axonal transport pass through the Golgi apparatus.* The Journal of cell biology, 1982. **93**(3): p. 568-575.

762. Parakh, S. and J. Atkin, *Novel roles for protein disulphide isomerase in disease states: a double edged sword?* Frontiers in Cell and Developmental Biology, 2015. **3**.

763. Nakamura, T. and S.A. Lipton, *Preventing Ca 2+-mediated nitrosative stress in neurodegenerative diseases: possible pharmacological strategies.* Cell calcium, 2010. **47**(2): p. 190-197.

764. Sigal, A., et al., *Variability and memory of protein levels in human cells.* Nature, 2006. **444**(7119): p. 643-646.

765. Tu, Z., et al., *CRISPR/Cas9: a powerful genetic engineering tool for establishing large animal models of neurodegenerative diseases.* Molecular neurodegeneration, 2015. **10**(1): p. 1-8.

766. Lajoie, P., E.N. Fazio, and E.L. Snapp, *Approaches to imaging unfolded secretory protein stress in living cells.* Endoplasmic reticulum stress in diseases, 2014. **1**(1): p. 27-39.

767. Sekar, R.B. and A. Periasamy, *Fluorescence resonance energy transfer (FRET) microscopy imaging of live cell protein localizations.* The Journal of cell biology, 2003. **160**(5): p. 629-633.

768. Lajoie, P., et al., *Kar2p availability defines distinct forms of endoplasmic reticulum stress in living cells.* Molecular biology of the cell, 2012. **23**(5): p. 955-964.

769. Snapp, E.L., *Fluorescent proteins: a cell biologist's user guide.* Trends in cell biology, 2009. **19**(11): p. 649-655.

770. Cabantous, S., T.C. Terwilliger, and G.S. Waldo, *Protein tagging and detection with engineered self-assembling fragments of green fluorescent protein.* Nature biotechnology, 2005. **23**(1): p. 102-107.

771. Toh, W.H., et al., *Application of Flow Cytometry to Analyze Intracellular Location and Trafficking of Cargo in Cell Populations.* Membrane Trafficking: Second Edition, 2015: p. 227-238.

772. Adler, J. and I. Parmryd, *Quantifying colocalization by correlation: the Pearson correlation coefficient is superior to the Mander's overlap coefficient.* Cytometry Part A, 2010. **77**(8): p. 733-742.

773. Maattanen, P., et al. *Protein quality control in the ER: the recognition of misfolded proteins*. in *Seminars in cell & developmental biology*. 2010. Elsevier.

774. Mayer, M., et al., *BiP and PDI Cooperate in the Oxidative Folding of Antibodiesin Vitro.* Journal of Biological Chemistry, 2000. **275**(38): p. 29421-29425.

775. Moore, P., K.M. Bernardi, and B. Tsai, *The Ero1α-PDI redox cycle regulates retro-translocation of cholera toxin.* Molecular biology of the cell, 2010. **21**(7): p. 1305-1313.

776. Björnberg, O., H. Østergaard, and J.R. Winther, *Measuring intracellular redox conditions using GFP-based sensors.* Antioxidants & redox signaling, 2006. **8**(3-4): p. 354-361.

777. Wunderlich, M. and R. Glockshuber, *In vivo control of redox potential during protein folding catalyzed by bacterial protein disulfide-isomerase (DsbA).* Journal of Biological Chemistry, 1993. **268**(33): p. 24547-24550.

778. Heras, B., et al., *DSB proteins and bacterial pathogenicity.* Nature Reviews Microbiology, 2009. **7**(3): p. 215-225.

779. Hosoda, A., et al., *JPDI, a novel endoplasmic reticulum-resident protein containing both a BiP-interacting J-domain and thioredoxin-like motifs.* Journal of Biological Chemistry, 2003. **278**(4): p. 2669-2676.

780. Ramachandran, N., et al., *Mechanism of transfer of NO from extracellular S-nitrosothiols into the cytosol by cell-surface protein disulfide isomerase.* Proceedings of the National Academy of Sciences, 2001. **98**(17): p. 9539-9544.

7.2.1 Sequence of CYTO PDI without signal sequence or KDEL:

atgGACGCCCCCGAGGAGGAGGACCACGTCCTGGTGCTGCG-
GAAAAGCAACTTCGCGGAGGCGCTGGCGGCCCACAAGTAC-
CTGCTGGTGGAGTTCTATGCCCCTTGGTGTGGCCACTG-
CAAGGCTCTGGCCCCTGAGTATGCCAAAGCCGCTGGGAA-
GCTGAAGGCAGAAGGTTCCGAGATCAGGTTGGCCAAGGTG-
GACGCCACGGAGGAGTCTGACCTGGCCCAGCAGTAC-
GGCGTGCGCGGCTATCCCACCATCAAGTTCTTCAG-
GAATGGAGACACGGCTTCCCCCAAGGAATATACAGCTGG-
CAGAGAGGCTGATGACATCGTGAACTGGCTGAAGAAGCG-
CACGGGCCCGGCTGCCACCACCCTGCCTGACGGCGCAGCTG-
CAGAGTCCTTGGTGGAG-
TCCAGCGAGGTGGCTGTCATCGGCTTCTTCAAGGACGTG-
GAGTCGGACTCTGCCAAGCAGTTTTTGCAGGCAG-
CAGAGGCCATCGATGACATACCATTTGGGATCAC-
TTCCAACAGTGACGTGTTCTCCAAATACCAGCTCGACAAA-
GATGGGGTTGTCCTCTTTAAGAAGTTTGATGAAGGCCG-
GAACAACTTTGAAGGGGAGGTCACCAAGGAGAACCTGCTG-
GACTTTATCAAACACAACCAGCTGCCCCTTGTCATCGAG-
TTCACCGAGCAGACAGCCCCGAAGATTTTT-
GGAGGTGAAATCAAGACTCACATCCTGCTGTTCTTGCCCAA-
GAGTGTGTCTGACTATGACGGCAAACTGAG-
CAACTTCAAAACAGCAGCCGAGAGCTTCAAGGGCAA-
GATCCTGTTCATCTTCATCGACAGCGACCACACCGACAAC-
CAGCGCATCCTCGAGTTCTTTGGCCTGAAGAAGGAAGAG-
TGCCCGGCCGTGCGCCTCATCACCCTGGAGGAGGAGATGAC-
CAAGTACAAGCCCGAATCGGAGGAGCTGACGGCAGAGAG-
GATCACAGAGTTCTGCCACCGCTTCCTGGAGGG-
CAAAATCAAGCCCCACCTGATGAGCCAGGAGCTGCCGGAG-
GACTGGGACAAGCAGCCTGTCAAGGTGCTTGTTGGGAA-
GAACTTTGAAGACGTGGCTTTTGATGAGAAAAAAAAC-
GTCTTTGTGGAGTTCTATGCCCCATGGTGTGGTCACTG-
CAAACAGTTGGCTCCCATTTGGGATAAACTGGGAGAGAC-
GTACAAGGACCATGAGAACATCGTCATCGCCAA-
GATGGACTCGACTGCCAACGAGGTGGAGGCCGTCAAAGTG-
CACAGCTTCCCCACACTCAAGTTCTTTCCTGCCAG-
TGCCGACAGGACGGTCATTGATTACAACGGGGAACGCAC-
GCTGGATGGTTTTAAGAAATTCCTGGAGAGCGGTGGCCAG-
GATGGGGCAGGGGATGATGACGATCTCGAGGACCTGGAA-
GAAGCAGAGGAGCCAGACATGGAGGAAGAC-
GATGATCAGAAAGCTGTGGGTAAAC-
CTATTCCTAATCCTCTTCTTGGTCTTGATTCTACTTGA

7.2.2 Supplementary Figure 1

The published review article: Parakh S and Atkin J (2015) ***"Novel roles for protein disulphide isomerase in disease states: a double edged sword".*** *Frontiers in Cell and Developmental Biology* **3:** 1-11 was written by the author with the guidance of supervisor Julie Atkin.

frontiers in Cell and Developmental Biology

REVIEW
published: 21 May 2015
doi: 10.3389/fcell.2015.00030

Novel roles for protein disulphide isomerase in disease states: a double edged sword?

Sonam Parakh[1] *and Julie D. Atkin*[1,2]*

[1] Department of Biomedical Sciences, Faculty of Medicine and Health Sciences, Macquarie University, Sydney, NSW, Australia, [2] Department of Biochemistry, La Trobe Institute for Molecular Science, La Trobe University, Bundoora, VIC, Australia

Protein disulphide isomerase (PDI) is a multifunctional redox chaperone of the endoplasmic reticulum (ER). Since it was first discovered 40 years ago the functions ascribed to PDI have evolved significantly and recent studies have recognized its distinct functions, with adverse as well as protective effects in disease. Furthermore, post translational modifications of PDI abrogate its normal functional roles in specific disease states. This review focusses on recent studies that have identified novel functions for PDI relevant to specific diseases.

Keywords: protein disulfide isomerase family, neurodegenerative diseases, protein chaperones, post-translational modifications, cancer, amyotrophic lateral sclerosis

OPEN ACCESS

Edited by:
Bulent Mutus, University of Windsor, Canada

Reviewed by:
Ruchi Chaube, Case Western Reserve University, USA
Daniel Sexton, Dyax Corp., USA

***Correspondence:**
Julie D. Atkin, Department of Biomedical Sciences, Faculty of Medicine and Health Sciences, Macquarie University, 2 Technology Place, Sydney, NSW 2109, Australia
julie.atkin@mq.edu.au; website:www.medicine.mq.edu.au

Specialty section:
This article was submitted to Cellular Biochemistry, a section of the journal Frontiers in Cell and Developmental Biology

Received: *30 January 2015*
Accepted: *28 April 2015*
Published: *21 May 2015*

Citation:
Parakh S and Atkin JD (2015) Novel roles for protein disulphide isomerase in disease states: a double edged sword? Front. Cell Dev. Biol. 3:30. doi: 10.3389/fcell.2015.00030

Introduction

Protein disulphide isomerase (PDI) was the first folding catalyst isolated from rat liver (Goldberger et al., 1963) and it is found abundantly in many tissues, accounting for 0.8% of total cellular protein (Freedman et al., 1994). PDI is induced during endoplasmic reticulum (ER) stress (Wilkinson and Gilbert, 2004) and it serves as a vital cellular defense against general protein misfolding via its chaperone activity. It is also responsible for the isomerization, formation, and rearrangement of protein disulphide bonds, thereby providing another mechanism by which native protein conformation is maintained. Disulphide bonds play an important role in the folding and stability of proteins and they are present in more than 30% of all human proteins that traverse the secretory pathway (Fewell et al., 2001). Since most cellular compartments are reducing environments, protein disulphide bonds are usually unstable in the cytosol, although there are exceptions (Frand et al., 2000). PDI assists in redox protein folding, involving oxidation, multiple intramolecular thiol-disulphide exchanges, and isomerization (reduction) activities and it is highly specific in its interaction with different substrates. Whilst PDI is considered to be resident primarily within the ER, nonetheless it has been detected in many other diverse cellular locations, including the cell surface, cytosol, mitochondria, and extracellular matrix (Turano et al., 2002). However, the mechanism by which PDI escapes from the ER is still unclear. PDI is also present in the extracellular medium where it facilitates protein folding and reduces protein aggregation (Delom et al., 2001). Furthermore, specific functions of cell surface PDI have been identified in hepatocytes, platelets, and endothelial cells (Turano et al., 2002). This review focusses on recent advances recognizing the versatile roles of PDI in normal cellular function and also in disease states. These studies highlight novel therapeutic possibilities based on the functional properties of PDI.

Structure and Superfamily of PDI

PDI is a soluble 55-kDa protein that is the prototype of the PDI family of proteins which all contain the thioredoxin-like βαβαβαββα domain (Kemmink et al., 1997). Thioredoxins are a class of oxidoreductase enzymes containing a dithiol-disulphide active site that are involved in redox signaling (Moran et al., 2001). Besides PDI, 21 more family members have been described (Kozlov et al., 2010). However, the enzymatic properties of these proteins differ in their redox potential and hence substrate specificity (Jessop et al., 2009), the sequence of their active site and the pKa of the active site cysteine residues (Ellgaard and Ruddock, 2005). They are primarily localized in the ER where they maintain an oxidative environment and thereby contribute to ER homeostasis (Anelli et al., 2002).

Full length PDI contains 508 amino acids and consists of four domains namely *a, b, b', a'* **(Figure 1)**. The homologous *a* and *a'* domains share 47% similarity and contain the active site, CGHC (Kemmink et al., 1996). The active site cysteine residues interact with the thiol group of a newly synthesized substrate, thus mediating the formation and isomerization of protein disulphide bonds (Gilbert, 1998). The intermediate *b* and *b'* domains are 28% identical and they assist in the binding of protein substrates but they lack the catalytically active cysteine residues (Gruber et al., 2006). PDI also contains a *x* linker region and an acidic C terminus containing a KDEL-ER retrieval sequence (Darby et al., 1996). Whilst the three dimensional structure of human PDI is still under investigation, the structures of each single thioredoxin domain (Nguyen et al., 2008) and the domain combinations *bb'c* (Denisov et al., 2009) and *bb'cxac* (Wang et al., 2012a) have been determined. However, the structure of yeast PDI has been solved (Tian et al., 2006) revealing that it adopts a U shape structure, with the catalytic *a* and *a'* domains facing each other. NMR and x-ray crystallography has further demonstrated that the *b'* domain contains the chaperone activity responsible for binding ligands and protein substrates in its hydrophobic pocket (Denisov et al., 2009).

The CGHC motif modulates the overall reduction potential of PDI and thus it regulates the catalytic ability of the active site cysteines to actively oxidize or reduce disulphide bonds (Chivers et al., 1997). The reduction potential of PDI is −180 mV, higher than other PDI family members, thus making it a strong oxidizing agent. The individual *a* and *a'* domains have similar oxidizing ability but conversely they have low isomerase activity

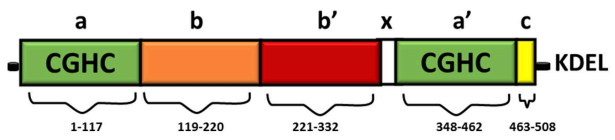

FIGURE 1 | Domain structure of PDI. The thioredoxin-like domains are shown in green, representing the catalytically active domains *a* and *a'*. The catalytically inactive *b* domain and *b'* domains are illustrated in orange and red respectively. The linker region x (shown in white) is responsible for the U shape structure of PDI. The C terminus is illustrated in yellow, followed by an ER retrieval signal, KDEL.

(Darby et al., 1998). The *b'* domain is the main site for binding misfolded protein substrates but the other domains also assist in this process (Klappa et al., 1998). The catalytic domains can only catalyze basic disulphide exchange and all the domains are required to isomerize a protein substrate that has undergone conformational changes (Darby et al., 1996). Deletion of the C-terminal residues of PDI results in deactivation of its chaperone-like activity and its peptide binding ability, but this does not affect its catalytic activity in disulphide bond formation (Dai and Wang, 1997).

Although it is implied that all PDI family members possess the ability to rearrange disulphide bonds, only a few members have actually been demonstrated to perform these activities and the rest are linked to the family through evolution rather than function (Galligan and Petersen, 2012). The most commonly studied members of the PDI family after PDI are ERp57, ERp72, ERp29, ERp44, and PDIA2 (Appenzeller-Herzog and Ellgaard, 2008). There appears to be an interplay of functions amongst the PDI family and some family members are able to recompense for each other. For example, ERp72 is known to compensate for ERp57 deficiency, where it can assist in folding specific proteins (Solda et al., 2006). Certain protein substrates also appear to interact simultaneously with PDI and its family members. ERp57 and PDI engage simultaneously in forming mixed disulphides with thyroglobulin during the production and isomerization of new disulphide bonds. In addition both ERp57 and PDI are released from thyroglobulin when it dissociates from the ER (Di Jeso et al., 2005). Transferrin also requires both PDI and ERp57 for optimal folding. Furthermore, depletion of both PDI and ERp57 leads to generalized protein misfolding, impaired export from the ER, and degradation in human hepatoma cells, implying that these proteins function together (Rutkevich et al., 2010). Functional analysis in yeast revealed that ERp46 substitutes for PDI-mediated disulphide bond formation *in vivo* (Knoblach et al., 2003). However, PDI itself plays a key role in oxidative protein folding and no other family member can entirely compensate for its loss (Rutkevich et al., 2010).

There is also evidence that PDI family members dimerise and that this property is involved in its function. PDI was recently shown to form disulphide-independent dimers *in vivo* suggesting that dimerization may control efficient protein folding in the ER (Bastos-Aristizabal et al., 2014). This may be achieved by generating a reserve of inactive protein that allows the ER to respond competently to an abrupt increase in substrate availability (Bastos-Aristizabal et al., 2014). PDI family member ERp29 also dimerises, and it acts as an escort protein in the binding of thyroglobulin in the ER (Rainey-Barger et al., 2007). It has been suggested that the formation of a dimer of PDIA2, which is mediated through glycosylation (Walker et al., 2013), is increased under conditions of oxidative stress, and this dimer has increased chaperone activity compared to the monomeric form (Fu and Zhu, 2009). Several excellent recent reviews have discussed the structural aspects of the PDI family in more detail and the reader is directed to these for further information (Hatahet and Ruddock, 2009; Kozlov et al., 2010; Galligan and Petersen, 2012). This review will focus on recent advances made into the functional roles of PDI.

Functions of PDI

PDI is found in all eukaryotic organisms, whereas in prokaryotes a related homolog, Dsb, performs similar functions in facilitating protein folding (Inaba, 2009). The importance of PDI in cellular function was first realized in yeast, where PDI was found to be essential for cellular viability (LaMantia et al., 1991). To date, no viable PDI knockout strain has been reported in rodents, further emphasizing the importance of PDI in normal cellular physiology (Hatahet and Ruddock, 2009). The disulphide interchange and chaperone functions of PDI are well documented and will be summarized briefly below. Emerging evidence describing novel functions for PDI will then be described.

PDI is a Chaperone Present in the ER

PDI has the ability to distinguish between partially folded, unfolded, and properly folded protein substrates, and it has a higher affinity to bind to misfolded proteins rather than native proteins through hydrophobic interactions (Klappa et al., 1997). These properties, together with its conformational flexibility, make PDI a highly effective chaperone (Irvine et al., 2014). PDI binds to a large number of protein substrates in the ER, although it is difficult to isolate and identify the individual substrates *in vivo*. Several methods are used to measure the chaperone activity of PDI *in vitro*. The rate of protein aggregation is assessed using protein substrates that do not possess cysteine residues, including GAPDH (Cai et al., 1994), rhodanese (Song and Wang, 1995), citrate synthase, alcohol dehydrogenase (Primm et al., 1996), or GFP, which on interaction with PDI causes increased fluorescent intensity as it folds into its native conformation (Mares et al., 2011).

A major function of PDI is a chaperone upregulated during ER stress. Accumulation of misfolded proteins within the ER activates the unfolded protein response (UPR). The UPR aims to reduce the load of unfolded proteins by increasing the curvature of ER, reducing protein synthesis, and by the induction of PDI and other chaperones to further increase the protein folding capacity (Hetz and Mollereau, 2014). This is achieved by activation of sensor ER proteins inositol requiring enzyme-1(IRE-1), protein kinase RNA like ER kinase (PERK), and activating transcription factor kinase 6 (ATF6), which subsequently activate UPR signaling pathways [detailed in (Sovolyova et al., 2014)]. While initially protective, prolonged UPR causes apoptosis (Schroder and Kaufman, 2005).

PDI facilitates the degradation of misfolded proteins *via* ER association degradation (ERAD) by translocation of these proteins from the ER to the cytoplasm, for subsequent degradation by the ubiquitin protease system. (Molinari et al., 2002; Lee et al., 2010b). It also helps in protein quality control by retaining unassembled procollagen until the correct native structure is achieved (Bottomley et al., 2001).

Other specific functions involving the chaperone activity of PDI have been described, including maintenance of the active conformation of the β subunit of collagen prolyl 4-hydroxylase (Vuori et al., 1992) and stabilization of the major histocompatibility complex's (MHC) class 1 peptide loading complex (PLC) that mediates MHC class 1 folding. Interestingly, PDI exhibits both chaperone and anti-chaperone activity depending upon its initial concentration. When PDI's chaperone activity is dominant, virtually all of the substrate protein is correctly folded. However, at low concentrations, PD1 promotes intermolecular disulphide crosslinking of substrates into large inactive aggregates via anti-chaperone activity (Puig and Gilbert, 1994).

Redox Regulation of PDI

Multiple studies have suggested that the disulphide interchange enzymatic activity of PDI is more important for its function than its chaperone activity. When its catalytic cysteines are reduced, PDI is able to react with non-native disulphides of substrate proteins to form a mixed disulphide complex. PDI then catalyzes the rearrangement of incorrectly formed disulphide bonds via isomerization reactions. This takes place with cycles of reduction (breaking of non-native disulphide bonds) and oxidation (to introduce correct pairing of cysteines) to eventually form the native disulphide bonds (Schwaller et al., 2003). The tripeptide glutathione constitutes the cellular redox buffer that maintains the redox environment of the ER (Hwang et al., 1992). After PDI has oxidized substrate proteins, it then has to be oxidized itself to complete the catalytic cycle. This function is carried out by a number of proteins including FAD binding oxidases, Ero1α, oxidized glutathione, glutathione peroxidase 7, glutathione peroxidase 8 or quiescin sulfhydryl oxidase (Wilkinson and Gilbert, 2004) **(Figure 2)**. Interestingly, the chaperone activity of PDI is regulated by the redox state of its oxidized and reduced forms (Wang et al., 2013), suggesting a link between the two separate functions of PDI. Redox regulation of PDI can be examined experimentally *in vitro* using scrambled RNAse, ribonuclease and bovine pancreatic trypsin inhibitor (Darby et al., 1998; Xiao et al., 2001).

The *in vivo* redox state of PDI is complex and determined by numerous factors including the reduction potential of PDI, the glutathione redox state in the ER, and the potential reductase activity of the substrate and its availability. However, redox conditions can have a major impact on the functions of PDI. For example, PDI regulates the organization of the cytoskeleton by forming a disulphide bond to Cys 374 of β-actin *via* a redox dependent mechanism (Sobierajska et al., 2014).

PDI in Disease States

Recent studies provide compelling evidence for a role for PDI in both the physiology and pathophysiology of disease states including diabetes (Grek and Townsend, 2014), cardiovascular diseases (Khan and Mutus, 2014), cancer (Xu et al., 2014), neurodegenerative conditions (Andreu et al., 2012) and the entry of pathogens in infectious diseases (Benham, 2012). However, precise roles for PDI in these diseases have not yet been elucidated. PDI is upregulated in various tissues during disease and surprisingly, both protective and detrimental effects have been described. These effects relate to either a loss of its normal protective function in some situations, or gain of toxic function in others. While the association between the PDI family and human disease states still requires further validation, current

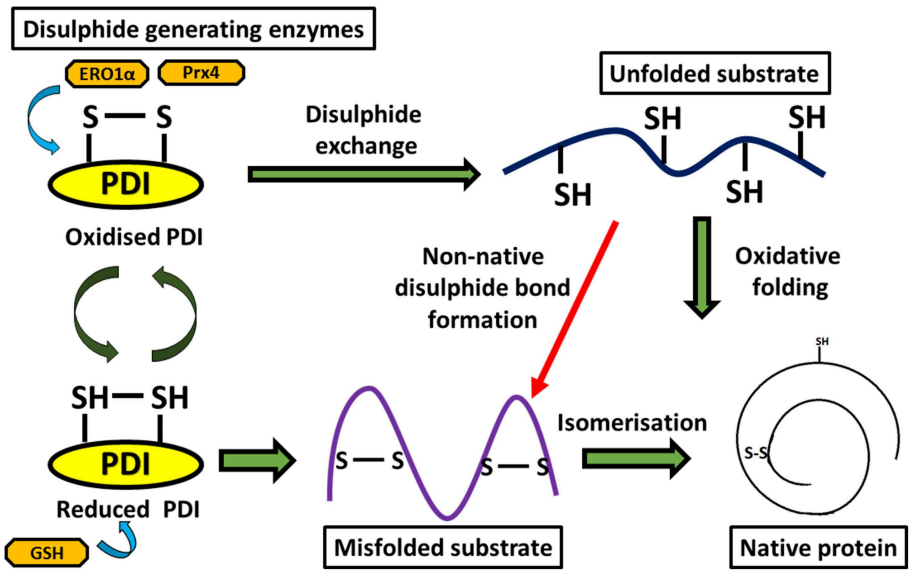

FIGURE 2 | Diagram representing disulphide bond formation in the eukaryotic ER and redox reactions involving PDI. Oxidative folding of PDI leads to disulphide bond formation in native protein substrates. Reduced PDI facilitates isomerization of non-native bonds in protein substrates.

improvements in our understanding of the functional roles of PDI provide new insights into the physiological contribution of PDI *in vivo*.

PDI in Cancer

PDI is highly expressed and up-regulated in numerous cancer cell types, including kidney, lung, brain, ovarian, melanoma, prostrate, and male germ cell tumors (Xu et al., 2014). Also, lower levels of PDI are associated with a higher survival rate in patients with breast cancer and glioblastoma (Thongwatchara et al., 2011), suggesting that PDI promotes the survival of cancer cells. Consistent with this notion, knockdown of PDI induces cytotoxicity in human breast cancer and neuroblastoma cell lines due to caspase activation (Hashida et al., 2011). Suppression of apoptosis by PDI has been proposed as mechanism for tumor growth and metastasis. Over-expression of PDI may therefore serve as a diagnostic marker for cancer, as suggested for glial cell cancer (Goplen et al., 2006), colorectal cancer (Ataman-Onal et al., 2013), and breast cancer (Thongwatchara et al., 2011). Cell surface PDI is also associated with cancer progression and administering of anti-PDI monoclonal antibodies inhibits the invasion of glioma cells (Goplen et al., 2006).

As increasing evidence suggests that PDI supports the survival and progression of various cancers, inhibitors of PDI may therefore have a therapeutic role against cancer progression (Xu et al., 2014). A synthesized series of PACMA (propynoic acid carbamoyl methyl amides) compounds demonstrated anticancer activity in human ovarian cancer *in vitro* and *in vivo* by a mechanism involving inhibition of PDI (Xu et al., 2012). Bacitracin, a pharmacological inhibitor of PDI, reduced the *in vitro* migration and invasion of human brain glial cells (Goplen et al., 2006). However, the specificity of bacitracin as an inhibitor of PDI has recently been questioned (Karala and Ruddock, 2010). Small-molecule inhibitors of PDI which bind to the CGHC active site may also have potential for improving the efficacy of chemotherapy in melanoma, as inhibition of PDI function proliferates apoptosis (Lovat et al., 2008). However, the effect of PDI in supporting tumor survival is based on the specific type of cancer and may be cell type dependent. Hence it is important to recognize the specific type of cancer cell for future applications in cancer therapy.

PDI in Neurodegenerative Disorders

Neurodegenerative diseases are also known as protein misfolding disorders due to their characteristic property of accumulating insoluble ubiquitinated aggregated proteins within affected tissues. Protein misfolding within the ER triggers ER stress, and hence up-regulation of PDI, and ER stress is increasingly implicated in these diseases (Hetz and Mollereau, 2014). Most studies suggest that the induction of PDI during ER stress in neurodegenerative diseases reduces the load of misfolded proteins, and is therefore protective thus restoring proteostasis and increasing neuronal viability.

PDI is upregulated in dopaminergic neurons and Lewy bodies of patients with Parkinson's disease. Similarly PDI reduces aggregation of the Parkinson's disease-associated protein synphilin-1 in neuroblastoma cells, an activity which relies on the presence of the CGHC active site motif (Uehara et al., 2006). Similarly, PDI also prevents aggregation of another Parkinson's associated protein, α-synuclein, in cell-free *in vitro* systems (Cheng et al., 2010). PDI also co-localizes with neurofibrillary tangles in Alzheimer's disease patient brain tissue, and is upregulated in brains of Alzheimer's rodent models (Lee et al., 2010a) implying a role in refolding misfolded proteins in these conditions. Consistent with this notion, ERp57 is present in CSF, where it binds and reduces aggregation of β-amyloid peptides

(Erickson et al., 2005). Furthermore, PDI is upregulated in response to hypoxia in the brain and PDI prevents neuronal and cardiomyocyte apoptosis, triggered by hypoxia-ischaemia in cell culture and in rodent models, by decreasing protein misfolding (Tanaka et al., 2000). In prion disorders, Wang and group suggested a pleiotropic role of PDI in the cellular management of misfolded prion protein (Wang et al., 2012b) because PDI and ERp57 are protective against prion induced toxicity *in vitro* (Hetz et al., 2005) and inhibition of PDI increases the production of misfolded prion proteins (Watts et al., 2009).

An important role for PDI has been implicated in amyotrophic lateral sclerosis (ALS). PDI is up-regulated and recruited to misfolded protein aggregates in sporadic human ALS (Atkin et al., 2008). PDI is also up-regulated in lumbar spinal cords from transgenic $SOD1^{G93A}$ mice, the most widely used animal disease model (Atkin et al., 2006). Furthermore, over-expression of PDI is protective against the formation of mutant SOD1 inclusions and ER stress, whereas knockdown of PDI using siRNA increases mutant SOD1 aggregation and inclusion formation (Walker et al., 2010). Similarly, a small molecule mimic of PDI reduces mutant SOD1 aggregation *in vitro* (Walker et al., 2010). Endogenous PDI co-localizes with mutant superoxide dismutase 1 (SOD1) (Atkin et al., 2006), TAR DNA-binding protein-43 (TDP-43) (Honjo et al., 2011), vesicle associated protein B (VAPB) (Tsuda et al., 2008), and Fused in Sarcoma (FUS) (Farg et al., 2012) in neuronal cells. PDI and ERp57 were identified as potential biomarkers for ALS using peripheral blood mononuclear cells (Nardo et al., 2011) and mutations in intronic variants of PDI are predicted to be a risk factor in ALS (Kwok et al., 2013).

There is also evidence that the cellular location of PDI is linked to disease outcomes in ALS. PDI is redistributed away from the ER via a reticulon-dependent process in transgenic $SOD1^{G93A}$ mice (Yang et al., 2009). The reticulon family of proteins function in maintaining the curvature of ER and several members of this family modulate the re-distribution of PDI away from the ER when overexpressed (Bernardoni et al., 2013). Furthermore, deletion of reticulon 4a,b enhances disease progression in $SOD1^{G93A}$ mice (Yang et al., 2009), highlighting the importance of a non-ER location of PDI in ALS.

Roles of PDI in Cardiovascular Disease

Both beneficial and harmful roles for PDI in cardiovascular disease have been proposed. PDI prevents protein misfolding in the myocardium during ischemic myocardial injury (Toldo et al., 2011). PDI is also up-regulated in hypoxia induced in myocardial capillary endothelial cells (Tian et al., 2009) and this is linked to significant decreases in the rate of cardiomyocyte apoptosis in murine models (Severino et al., 2007). Similarly, PDI is also involved in endothelial cell endurance (Severino et al., 2007) and it is required for platelet derived growth factor (PDGF)-induced vascular smooth muscle cell migration (Primm and Gilbert, 2001) which is an important therapeutic target in atherosclerosis (Pescatore et al., 2012). Furthermore, increased expression of PDI is protective against endothelial cellular migration, adhesion, and tubular formation in mice suggesting an important role for PDI in angiogenesis (Tian et al., 2009). Hence these studies raise the possibility that upregulating PDI has possible future pharmacological applications in treating ischemic cardiomyopathy (Severino et al., 2007).

Diabetes is associated with coronary artery disease and an increased risk of heart failure, and PDI function is impaired in mouse models of diabetes. This may be due to alterations in its oxidoreductive state (Toldo et al., 2011). Reduced PDI has been detected in the diabetic heart after ischemia, which could explain why PDI is not protective in diabetes (Toldo et al., 2011).

However, in contrast to these protective functions, PDI has also been implicated in detrimental activities in cardiovascular diseases. Over-expression of PDI in myocytes attenuates the levels of misfolded pro-insulin while decreasing glucose stimulated insulin secretion, thereby inducing ER stress and apoptosis (Zhang et al., 2009). PDI on the surface of platelets plays an important role in thrombus formation and it is vital for the aggregation of platelets (Kim et al., 2013). Similarly, PDI is also present on at the surface of human B-lymphocytes where it has a putative role in regulating leukocyte adhesion (Bennett et al., 2000). PDI has also been implicated in platelet integrin function, tissue-factor activation, and in mice, it accumulates during fibrin and thrombus formation at sites of vascular injury (Jurk et al., 2011). PDI inhibition prevents both platelet accumulation and fibrin generation during thrombus formation (Jasuja et al., 2012). Therefore, inhibition of PDI could prevent thrombosis in coronary artery disease, suggesting that PDI inhibitors have potential as antithrombotic agents (Jasuja et al., 2012).

PDI Mediates Pathogen Entry in Infectious Diseases

PDI is also implicated in mediating the entry of pathogens during infectious disease. Over-expression of PDI increases the fusion of viral membranes, leading to internalization of HIV-1 (Auwerx et al., 2009). Similarly, cell surface PDI facilitates infection of HeLa cells by mouse polyoma virus (Gilbert et al., 2006), and it also mediates the entry of cholera toxin (Stolf et al., 2011). The chaperone activity of PDI is important for folding cholera toxin subunit A1 and reducing its aggregation (Taylor et al., 2011). However, cholera intoxication is a redox dependent process. The oxidized form of PDI mediates translocation of cholera toxin into the host cell cytoplasm (Tsai et al., 2001) whereas the reduced form of PDI leads to its unfolding.

Post Translational Modification of PDI

Redox-dependent post translational modifications of PDI are also linked to disease states. Due to cellular conditions, high levels of reactive nitrogen species (RNS), hydrogen peroxide and reactive oxygen species (ROS) can accumulate in cells, inducing nitrosative or oxidative stress. Nitrosative stress can lead to post translation modification of PDI by the addition of NO to active site cysteine residues, resulting in S-nitrosylation. S-nitrosylation of proteins under pathological conditions is an abnormal, irreversible process that is linked to protein misfolding, ER stress and apoptosis. Furthermore, proteins resident in the ER are particularly vulnerable to post translation modification due to

the presence of critical redox regulated cysteines. Since PDI is the major enzyme responsible for modification of protein disulphide bonds, the loss of function of PDI could increase cellular protein misfolding and thus increase ER stress. S-nitrosylation of PDI inhibits its normal enzymatic activity and hence the beneficial effects of PDI, and S-nitrosylated PDI has been detected in several neurodegenerative diseases (Nakamura and Lipton, 2011; Chen et al., 2012). S-nitrosylation reduces both its chaperone and isomerase activity (Uehara et al., 2006).

S-nitrosylation of PDI has been detected in postmortem brain tissues of patients with Alzheimer's disease, Parkinson's disease (Uehara et al., 2006) and in lumbar spinal cord tissues of ALS patients and transgenic $SOD1^{G93A}$ mice (Walker et al., 2010). S-nitrosylation has also been reported in prion disease models using brain tissues of scrapie-263K-infected hamsters (Wang et al., 2012b). Exposure of cultured neurons to N-methyl-D-aspartate receptor (NMDA), leading to calcium influx and nitric oxide production, also resulted in the S-nitrosylation of PDI (Forrester et al., 2006). S-nitrosylated PDI (SNO-PDI) increases the levels of polyubiquitinated proteins and triggers cell death, and it is also associated with hyper-activation of NMDA (Forrester et al., 2006) and inhibition of mitochondria, leading to the generation of ROS and nitric oxide (Halloran et al., 2013). SNO-PDI accentuates the misfolding of synphilin in Parkinson disease (Forrester et al., 2006) and S-nitrosylation also increases mutant SOD1 aggregation via incorrect disulphide cross-linking of the immature, misfolded mutant SOD1, leading to neuronal cell death (Jeon et al., 2014).

As well as S-nitrosylation, other aberrant post-translational modifications of PDI have been described, including carbonylation and S-glutathionylation. Oxidized low density lipoproteins induce carbonylation, which disrupts the catalytic activity of PDI, inducing ER stress and apoptosis in vascular cells (Muller et al., 2013). Furthermore, carbonylated PDI detected in the lipid rich atherosclerotic region of human endothelial cells activates CHOP and XBP1 and induces apoptosis (Muller et al., 2013). S-glutathionylation is induced by reactive oxygen or nitrogen species and it results in formation of a disulphide bond between GSH and a cysteine residue of another protein (Xiong et al., 2011). S-glutathionylation, leading to increased protein misfolding and enhancement of the UPR (Townsend et al., 2009), has been detected primarily in relation to cancer. S-glutathionylation of PDI obliterates estrogen receptor α stability in breast cancer cells, which prevents binding of PDI to the receptor. This subsequently leads to dysregulation in ERα signaling (Xiong et al., 2012), and cell death via UPR induction (Xiong et al., 2012). S-glutathionylation also reduces the isomerase activity of PDI in ovarian cancer cells and human leukemia cells and it also decreases chaperone activity. In cultured astrocytes after cerebral ischemic reperfusion, SNO-PDI increases the levels of ubiquitinated aggregates that co-localize with SOD1 (Chen et al., 2012). These modifications can further attenuate UPR and cause neuronal cell death. Hence, aberrant modifications of PDI lead directly to harmful effects as well as loss of the normally protective properties of PDI.

PDI Causes Oxidative Stress

Recent evidence implicates PDI in increasing the levels of ROS, thus directly inducing oxidative stress and apoptosis *via* its chaperone activity rather than the disulphide interchange activity (Fernandes et al., 2009). Similarly, only oxidized PDI triggers the production of ROS, whereas reduced PDI inhibits the production of ROS (Paes et al., 2011). PDI associates with the NAPDH peroxidase complex (Nox), a major source of ROS, where it stabilizes and associates with the oxidase subunit of Nox in vascular smooth muscle cells (Janiszewski et al., 2005). Similar effects are observed in macrophages and murine microglial cells, where PDI interacts with Nox and increases the levels of ROS (Fernandes et al., 2009). PDI also activates the transcription factors NF-kB and AP-1, thus promoting their binding to DNA (Clive and Greene, 1996). PDI is also a major catalyst of trans-nitrosation reactions, mediating nitric oxide internalization from extracellular S-nitrosothiols (Zai et al., 1999), thus further promoting the production of SNO proteins (Ramachandran et al., 2001).

PDI Causes Apoptosis

Whilst SNO-PDI is implicated in triggering apoptosis, recent studies have revealed a direct role for unmodified PDI in apoptosis. In rat models of Huntington and Alzheimer's disease, PDI accumulation at the ER-mitochondrial junction triggers apoptosis *via* mitochondrial outer membrane permeabilisation (Hoffstrom et al., 2010). This effect is specific for the accumulation of misfolded proteins, but not other triggers of apoptosis, suggesting a specific role for pro-apoptotic PDI in neurodegenerative disease. Inhibitors of PDI including hypotaurine, thiomuscimol, and shRNA that inhibited the activity of PDI, were found to suppress the toxicity associated with misfolded Huntingtin and β-amyloid proteins.

Summary

PDI is an important cellular protein given its abundance, multiple biological functions, versatile redox behavior, interaction with other proteins and its implied role in various diseases. However, many issues remain unresolved that warrant further investigation, in particular the role of PDI in non-ER sub-cellular locations, and substrate specificity of the PDI family members. In future studies it will be important to replicate the precise functions of PDI in the ER and other cellular locations, separately from roles ascribed *in vitro*, before its normal cellular roles are fully understood.

PDI performs an impressive array of cellular functions and the up-regulation of PDI is a cellular defensive mechanism to restore proteostasis. However, despite this up-regulation, the functional properties of PDI can become abrogated due to aberrant post translational modifications. This is of particular relevance in neurodegenerative diseases where disruption to redox regulation is implicated (Parakh et al., 2013). Furthermore, neurons are particularly susceptible to ROS/RNS damage due to their high oxygen demand and a lower availability of antioxidants. Recent evidence implicates PDI as a trigger for apoptosis specifically in relation to the accumulation of misfolded

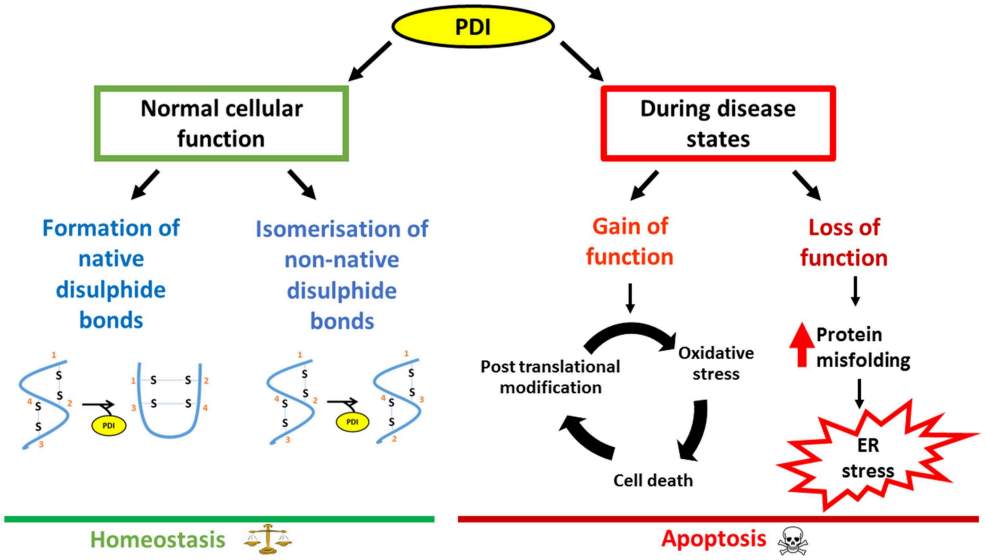

FIGURE 3 | Schematic diagram outlining the dual nature of PDI, focusing on neurodegenerative disorders as an example. Under normal conditions, PDI reduces the load of misfolded proteins either by its chaperone activity or by isomerization of non-native bonds. However, during disease states, loss of the normal protective function of PDI as well as the gain of additional, toxic functions, leads to PDI becoming apoptotic, thus contributing to pathology.

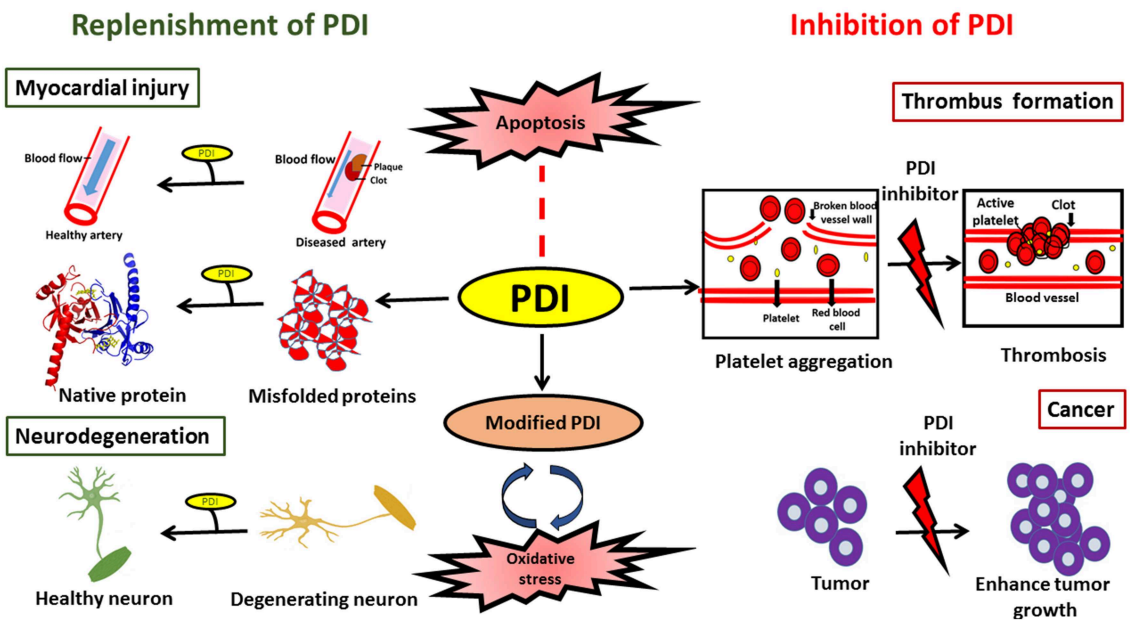

FIGURE 4 | Schematic diagram illustrating possible therapeutic applications to modulate PDI function.

proteins. PDI may therefore act as a regulatory switch, in which PDI is initially is protective against protein misfolding and aggregation. However, in response to an unknown trigger PDI subsequently becomes apoptotic when proteostasis cannot otherwise be resolved (**Figure 3**). Therefore aberrant post translational modifications together with the pro-apoptotic function of PDI could further accentuate the adverse effects of PDI.

In conclusion, PDI is an efficient catalyst and protein chaperone. It has the ability to restore proteostasis by catalyzing the efficient folding of newly synthesized proteins, and it plays an important role in protein quality control and ERAD by

reducing the burden of misfolded proteins, thus inhibiting abnormal protein aggregation. The protective or harmful functions of PDI may be modulated by the subcellular location of PDI, levels of ER stress and the redox environment. While further investigations are clearly needed in this area, PDI has the potential to be exploited therapeutically in a variety of diseases. However, specific approaches depending on the disease in question will be required. In neurodegenerative conditions, elevation of the levels of total PDI, with the aim of restoring PDI function to reduce protein misfolding, could be an effective therapeutic approach. However, in contrast, reduction of the levels of PDI might be an appropriate strategy in cancer or cardiovascular diseases **(Figure 4)**. Similarly, reducing the levels of aberrantly modified PDI might also be necessary in neurodegeneration in order to defend against the pro-apoptotic properties of PDI. At the cellular level there are important unanswered questions that need addressing, before the therapeutic applications of PDI can become realized in the future.

Acknowledgments

This work was supported by the National Health and Medical Research Council of Australia (NHMRC) Project grants (1006141 and 1030513), Bethlehem Griffiths Research Foundation, and Motor Neurone Disease Research Institute of Australia Angie Cunningham Laugh to Cure MND Grant, Zo-ee Research Grant and Grants in Aid. SP is supported by a Macquarie University Postgraduate Research Scholarship, and previously by a La Trobe Post Graduate Research Scholarship.

References

Andreu, C. I., Woehlbier, U., Torres, M., and Hetz, C. (2012). Protein disulfide isomerases in neurodegeneration: from disease mechanisms to biomedical applications. *FEBS Lett*. 586: 2826–2834. doi: 10.1016/j.febslet.2012.07.023

Anelli, T., Alessio, M., Mezghrani, A., Simmen, T., Talamo, F., Bachi, A., et al. (2002). ERp44, a novel endoplasmic reticulum folding assistant of the thioredoxin family. *EMBO J*. 21, 835–844. doi: 10.1093/emboj/21.4.835

Appenzeller-Herzog, C., and Ellgaard, L. (2008). The human PDI family: versatility packed into a single fold. *Biochim. Biophys. Acta* 1783, 535–548. doi: 10.1016/j.bbamcr.2007.11.010

Ataman-Onal, Y., Beaulieu, C., Busseret, S., Charrier, J.-P., Choquet-Kastylevsky, G., Rolland, D., et al. (2013). Protein disulfide isomerase assay method for the in vitro diagnosis of colorectal cancer. *Patents* 1–30.

Atkin, J. D., Farg, M. A., Turner, B. J., Tomas, D., Lysaght, J. A., Cheema, S. S., et al. (2006). Induction of the unfolded protein response in familial amyotrophic lateral sclerosis and association of protein-disulfide isomerase with superoxide dismutase 1. *J. Biol. Chem*. 281, 30152–30165. doi: 10.1074/jbc.M603393200

Atkin, J. D., Farg, M. A., Walker, A. K., McLean, C., Tomas, D., and Horne, M. K. (2008). Endoplasmic reticulum stress and induction of the unfolded protein response in human sporadic amyotrophic lateral sclerosis. *Neurobiol. Dis.* 30, 400–407. doi: 10.1016/j.nbd.2008.02.009

Auwerx, J., Isacsson, O., Söderlund, J., Balzarini, J., Johansson, M., and Lundberg, M. (2009). Human glutaredoxin-1 catalyzes the reduction of HIV-1 gp120 and CD4 disulfides and its inhibition reduces HIV-1 replication. *Int. J. Biochem. Cell Biol*. 41, 1269–1275. doi: 10.1016/j.biocel.2008.10.031

Bastos−Aristizabal, S., Kozlov, G., and Gehring, K. (2014). Structural insight into the dimerization of human protein disulfide isomerase. *Protein Sci*. 23, 618–626. doi: 10.1002/pro.2444

Benham, A. M. (2012). The protein disulfide isomerase family: key players in health and disease. *Antioxid. Redox Signal.* 16, 781–789. doi: 10.1089/ars.2011.4439

Bennett, T. A., Edwards, B. S., Sklar, L. A., and Rogelj, S. (2000). Sulfhydryl regulation of L-selectin shedding: phenylarsine oxide promotes activation-independent L-selectin shedding from leukocytes. *J. Immunol*. 164, 4120–4129. doi: 10.4049/jimmunol.164.8.4120

Bernardoni, P., Fazi, B., Costanzi, A., Nardacci, R., Montagna, C., Filomeni, G., et al. (2013). Reticulon1-C modulates protein disulphide isomerase function. *Cell Death Dis.* 4:e581. doi: 10.1038/cddis.2013.113

Bottomley, M. J., Batten, M. R., Lumb, R. A., and Bulleid, N. J. (2001). Quality control in the endoplasmic reticulum: PDI mediates the ER retention of unassembled procollagen C-propeptides. *Curr. Biol*. 11, 1114–1118. doi: 10.1016/S0960-9822(01)00317-7

Cai, H., Wang, C.-C., and Tsou, C.-L. (1994). Chaperone-like activity of protein disulfide isomerase in the refolding of a protein with no disulfide bonds. *J. Biol. Chem*. 269, 24550–24552.

Chen, X., Guan, T., Li, C., Shang, H., Cui, L., Lui, X.-M., et al. (2012). SOD1 aggregation in astrocytes following ischemia/reperfusion injury: a role of NO-mediated S-nitrosylation of protein disulfide isomerase (PDI). *J. Neuroinflammation* 9:237. doi: 10.1186/1742-2094-9-237

Cheng, H., Wang, L., and Wang, C.-C. (2010). Domain a'of protein disulfide isomerase plays key role in inhibiting α-synuclein fibril formation. *Cell Stress Chaperones*. 15, 415–421. doi: 10.1007/s12192-009-0157-2

Chivers, P. T., Prehoda, K. E., and Raines, R. T. (1997). The CXXC motif: a rheostat in the active site. *Biochemistry* 36, 4061–4066. doi: 10.1021/bi9628580

Clive, D. R., and Greene, J. J. (1996). Cooperation of protein disulfide isomerase and redox environment in the regulation of NF−κB and AP1 binding to DNA. *Cell Biochem. Funct*. 14, 49–55. doi: 10.1002/cbf.638

Dai, Y., and Wang, C.-C. (1997). A mutant truncated protein disulfide isomerase with no chaperone activity. *J. Biol. Chem*. 272, 27572–27576. doi: 10.1074/jbc.272.44.27572

Darby, N. J., Kemmink, J., and Creighton, T. E. (1996). Identifying and characterizing a structural domain of protein disulfide isomerase. *Biochemistry* 35, 10517–10528.

Darby, N. J., Penka, E., and Vincentelli, R. (1998). The multi-domain structure of protein disulfide isomerase is essential for high catalytic efficiency. *J. Mol. Biol*. 276, 239–247. doi: 10.1006/jmbi.1997.1504

Delom, F., Mallet, B., Carayon, P., and Lejeune, P.-J. (2001). Role of extracellular molecular chaperones in the folding of oxidized proteins refolding of colloidal thyroglobulin by protein disulfide isomerase and immunoglobulin heavy chain-binding protein. *J. Biol. Chem*. 276, 21337–21342. doi: 10.1074/jbc.M101086200

Denisov, A. Y., Määttänen, P., Dabrowski, C., Kozlov, G., Thomas, D. Y., Gehring, K., et al. (2009). Solution structure of the bb' domains of human protein disulfide isomerase. *FEBS J*. 276, 1440–1449. doi: 10.1111/j.1742-4658.2009.06884.x

Di Jeso, B., Park, Y.-N., Ulianich, L., Treglia, A. S., Urbanas, M. L., High, S., et al. (2005). Mixed-disulfide folding intermediates between thyroglobulin and endoplasmic reticulum resident oxidoreductases ERp57 and protein disulfide isomerase. *Mol. Cell. Biol.* 25, 9793–9805. doi: 10.1128/MCB.25.22.9793-9805.2005

Ellgaard, L., and Ruddock, L. W. (2005). The human protein disulphide isomerase family: substrate interactions and functional properties. *EMBO Rep*. 6, 28–32. doi: 10.1038/sj.embor.7400311

Erickson, R. R., Dunning, L. M., Olson, D. A., Cohen, S. J., Davis, A. T., and Holtzman, J. L., et al. (2005). In cerebrospinal fluid ER chaperones ERp57 and calreticulin bind β-amyloid. *Biochem. Biophys. Res. Commun*. 332, 50–57. doi: 10.1016/j.bbrc.2005.04.090

Farg, M. A., Soo, K. Y., Walker, A. K., Pham, H., Orian, J. and Atkin, J. D., et al. (2012). Mutant FUS induces endoplasmic reticulum stress in amyotrophic lateral sclerosis and interacts with protein disulfide-isomerase. *Neurobiol. Aging* 33, 2855–2868. doi: 10.1016/j.neurobiolaging.2012.02.009

Fernandes, D. C., Manoel, A. H. O., Wosniak, J. Jr., and Laurindo, F. R. (2009). Protein disulfide isomerase overexpression in vascular smooth muscle cells induces spontaneous preemptive NADPH oxidase activation and Nox1 mRNA

expression: effects of nitrosothiol exposure. *Arch. Biochem. Biophys.* 484, 197–204. doi: 10.1016/j.abb.2009.01.022

Fewell, S. W., Travers, K. J., Weissman, J. S., and Brodsky, J. L. (2001). The action of molecular chaperones in the early secretory pathway. *Annu. Rev. Genet.* 35, 149–191. doi: 10.1146/annurev.genet.35.102401.090313

Forrester, M. T., Benhar, M., and Stamler, J. S. (2006). Nitrosative stress in the ER: a new role for S-nitrosylation in neurodegenerative diseases. *ACS Chem. Biol.* 1, 355–358. doi: 10.1021/cb600244c

Frand, A. R., Cuozzo, J. W., and Kaiser, C. A. (2000). Pathways for protein disulphide bond formation. *Trends Cell Biol.* 10, 203–210. doi: 10.1016/S0962-8924(00)01745-1

Freedman, R. B., Hirst, T. R., and Tuite, M. F. (1994). Protein disulphide isomerase: building bridges in protein folding. *Trends Biochem. Sci.* 19, 331–336. doi: 10.1016/0968-0004(94)90072-8

Fu, X.-M., and Zhu, B. T. (2009). Human pancreas-specific protein disulfide isomerase homolog (PDIp) is an intracellular estrogen-binding protein that modulates estrogen levels and actions in target cells. *J. Steroid Biochem. Mol. Biol.* 115, 20–29. doi: 10.1016/j.jsbmb.2009.02.008

Galligan, J. J., and Petersen, D. R. (2012). The human protein disulfide isomerase gene family. *Hum. Genomics* 6, 1–15. doi: 10.1186/1479-7364-6-6

Gilbert, H. F. (1998). Protein disulfide isomerases. *Meth. Enzymol.* 290, 26–50. doi: 10.1016/S0076-6879(98)90005-2

Gilbert, J., Ou, W., Silver, J., and Benjamin, T. (2006). Downregulation of protein disulfide isomerase inhibits infection by the mouse polyomavirus. *J. Virol.* 80, 10868–10870. doi: 10.1128/JVI.01117-06

Goldberger, R. F., Epstein, C. J., and Anfinsen, C. B. (1963). Acceleration of reactivation of reduced bovine pancreatic ribonuclease by a microsomal system from rat liver. *J. Biol. Chem.* 238, 628–635.

Goplen, D., Wang, J., Enger, P. Ø., Tysnes, B. B., Terzis, A., and Bjerkvig, R., et al. (2006). Protein disulfide isomerase expression is related to the invasive properties of malignant glioma. *Cancer Res.* 66, 9895–9902. doi: 10.1158/0008-5472.CAN-05-4589

Grek, C., and Townsend, D. (2014). Protein disulfide isomerase superfamily in disease and the regulation of apoptosis. *Endoplasmic Reticulum Stress Dis.* 1, 4–17. doi: 10.2478/ersc-2013-0001

Gruber, C. W., Čemažar, M., Heras, B., Martin, J. L., and Craik, D. J. (2006). Protein disulfide isomerase: the structure of oxidative folding. *Trends Biochem. Sci.* 31, 455–464. doi: 10.1016/j.tibs.2006.06.001

Halloran, M., Parakh, S., and Atkin, J. (2013). The role of S-nitrosylation and S-glutathionylation of protein disulphide isomerase in protein misfolding and neurodegeneration. *Int. J. Cell Biol.* 2013:797914. doi: 10.1155/2013/797914

Hashida, T., Kotake, Y., and Ohta, S. (2011). Protein disulfide isomerase knockdown-induced cell death is cell-line-dependent and involves apoptosis in MCF-7 cells. *J. Toxicol. Sci.* 36, 1–7. doi: 10.2131/jts.36.1

Hatahet, F., and Ruddock, L. W. (2009). Protein disulfide isomerase: a critical evaluation of its function in disulfide bond formation. *Antioxid. Redox Signal.* 11, 2807–2850. doi: 10.1089/ars.2009.2466

Hetz, C., and Mollereau, B. (2014). Disturbance of endoplasmic reticulum proteostasis in neurodegenerative diseases. *Nat. Rev. Neurosci.* 15, 233–249. doi: 10.1038/nrn3689

Hetz, C., Russelakis-Carneiro, M., Wälchli, S., Carboni, S., Vial-Knecht, E., Maundrell, K., et al. (2005). The disulfide isomerase Grp58 is a protective factor against prion neurotoxicity. *J. Neurosci.* 25, 2793–2802. doi: 10.1523/JNEUROSCI.4090-04.2005

Hoffstrom, B. G., Kaplan, A., Letso, R., Schmid, R. S., Turmel, G. J. and Stockwell, B. R., et al. (2010). Inhibitors of protein disulfide isomerase suppress apoptosis induced by misfolded proteins. *Nat. Chem. Biol.* 6, 900–906. doi: 10.1038/nchembio.467

Honjo, Y., Kaneko, S., Ito, H., Horibe, T., Nagashima, M., Nakamura, M., et al. (2011). Protein disulfide isomerase-immunopositive inclusions in patients with amyotrophic lateral sclerosis. *Amyotroph. Lateral Scler.* 12, 444–450. doi: 10.3109/17482968.2011.594055

Hwang, C., Sinskey, A. J., and Lodish, H. F. (1992). Oxidized redox state of glutathione in the endoplasmic reticulum. *Science* 257, 1496–1502. doi: 10.1126/science.1523409

Inaba, K. (2009). Disulfide bond formation system in *Escherichia coli*. *J. Biochem.* 146, 591–597. doi: 10.1093/jb/mvp102

Irvine, A. G., Wallis, A. K., Sanghera, N., Rowe, M. L., Ruddock, L. W., Freedman, R. B., et al. (2014). Protein disulfide-isomerase interacts with a substrate protein at all stages along its folding pathway. *PLoS ONE* 9:e82511. doi: 10.1371/journal.pone.0082511

Janiszewski, M., Lopes, L. R., Carmo, A. O., Pedro, M. A., Brandes, R. P., Laurindo, F. R., et al. (2005). Regulation of NAD (P) H oxidase by associated protein disulfide isomerase in vascular smooth muscle cells. *J. Biol. Chem.* 280, 40813–40819. doi: 10.1074/jbc.M509255200

Jasuja, R., Passam, F. H., Kennedy, D. R., Kim, S. H., van Hessem, L., Furie, B., et al. (2012). Protein disulfide isomerase inhibitors constitute a new class of antithrombotic agents. *J. Clin. Invest.* 122, 2104–2113. doi: 10.1172/JCI61228

Jeon, G. S., Nakamura, T., Lee, W.-J., Choi, S.-W., Ahn, K.-W., Lipton, S. A., et al. and (2014). Potential effect of S-nitrosylated protein disulfide isomerase on mutant SOD1 aggregation and neuronal cell death in amyotrophic lateral sclerosis. *Mol. Neurobiol.* 49, 796–807. doi: 10.1007/s12035-013-8562-z

Jessop, C. E., Watkins, R. H., Simmons, J. J., Tasab, M., and Bulleid, N. J. (2009). Protein disulphide isomerase family members show distinct substrate specificity: P5 is targeted to BiP client proteins. *J. Cell Sci.* 122, 4287. doi: 10.1242/jcs.059154

Jurk, K., Lahav, J., Van Aken, H., Brodde, M., Nofer, J. R., and Kehrel, B. (2011). Extracellular protein disulfide isomerase regulates feedback activation of platelet thrombin generation via modulation of coagulation factor binding. *J. Thromb. Haemost.* 9, 2278–2290. doi: 10.1111/j.1538-7836.2011.04509.x

Karala, A. R., and Ruddock, L. W. (2010). Bacitracin is not a specific inhibitor of protein disulfide isomerase. *FEBS J.* 277, 2454–2462. doi: 10.1111/j.1742-4658.2010.07660.x

Kemmink, J., Darby, N. J., Dijkstra, K., Nilges, M., and Creighton, T. E. (1996). Structure determination of the N-terminal thioredoxin-like domain of protein disulfide isomerase using multidimensional heteronuclear 13C/15N NMR spectroscopy. *Biochemistry* 35, 7684–7691. doi: 10.1021/bi960335m

Kemmink, J., Darby, N. J., Dijkstra, K., Nilges, M., and Creighton, T. E. (1997). The folding catalyst protein disulfide isomerase is constructed of active and inactive thioredoxin modules. *Curr. Biol.* 7, 239–245. doi: 10.1016/S0960-9822(06)00119-9

Khan, H. A., and Mutus, B. (2014). Protein disulfide isomerase a multifunctional protein with multiple physiological roles. *Front. Chem.* 2:70. doi: 10.3389/fchem.2014.00070

Kim, K., Hahm, E., Li, J., Holbrook, L.-M., Sasikumar, P., Cho, J., et al. (2013). Platelet protein disulfide isomerase is required for thrombus formation but not for hemostasis in mice. *Blood* 122, 1052–1061. doi: 10.1182/blood-2013-03-492504

Klappa, P., Hawkins, H. C., and Freedman, R. B. (1997). Interactions between protein disulphide isomerase and peptides. *Eur. J. Biochem.* 248, 37–42. doi: 10.1111/j.1432-1033.1997.t01-1-00037.x

Klappa, P., Ruddock, L. W., Darby, N. J., and Freedman, R. B. (1998). The b domain provides the principal peptide-binding site of protein disulfide isomerase but all domains contribute to binding of misfolded proteins. *EMBO J.* 17, 927–935.

Knoblach, B., Keller, B. O., Groenendyk, J., Aldred, S., Zheng, J., Michalak, M., et al. (2003). ERp19 and ERp46, new members of the thioredoxin family of endoplasmic reticulum proteins. *Mol. Cell. Proteomics* 2, 1104–1119. doi: 10.1074/mcp.M300053-MCP200

Kozlov, G., Määttänen, P., Thomas, D. Y., and Gehring, K. (2010). A structural overview of the PDI family of proteins. *FEBS J.* 277, 3924–3936. doi: 10.1111/j.1742-4658.2010.07793.x

Kwok, C. T., Morris, A. G., Frampton, J., Smith, B., Shaw, C. E., de Belleroche, J., et al. (2013). Association studies indicate that protein disulfide isomerase is a risk factor in amyotrophic lateral sclerosis. *Free Radic. Biol. Med.* 58, 81–86. doi: 10.1016/j.freeradbiomed.2013.01.001

LaMantia, M., Miura, T., Tachikawa, H., Kaplan, H. A., Lennarz, W. J., Mizunaga, T., et al. (1991). Glycosylation site binding protein and protein disulfide isomerase are identical and essential for cell viability in yeast. *Proc. Natl. Acad. Sci. U.S.A.* 88, 4453–4457. doi: 10.1073/pnas.88.10.4453

Lee, J. H., Won, S. M., Suh, J., Son, S. J., Moon, G. J., Park, U.-J., et al. (2010a). Induction of the unfolded protein response and cell death pathway in Alzheimer's disease, but not in aged Tg2576 mice. *Exp. Mol. Med.* 42, 386–394. doi: 10.3858/emm.2010.42.5.040

Lee, S. O., Cho, K., Cho, S., Kim, I., Oh, C., and Ahn, K. (2010b). Protein disulphide isomerase is required for signal peptide peptidase−mediated protein degradation. *EMBO J.* 29, 363–375. doi: 10.1038/emboj.2009.359

Lovat, P. E., Corazzari, M., Armstrong, J. L., Martin, S., Pagliarini, V., Redfern, C. P., et al. (2008). Increasing melanoma cell death using inhibitors of protein disulfide isomerases to abrogate survival responses to endoplasmic reticulum stress. *Cancer Res.* 68, 5363–5369. doi: 10.1158/0008-5472.CAN-08-0035

Mares, R. E., Meléndez-López, S. G., and Ramos, M. A. (2011). Acid-denatured Green Fluorescent Protein (GFP) as model substrate to study the chaperone activity of protein disulfide isomerase. *Int. J. Mol. Sci.* 12, 4625–4636. doi: 10.3390/ijms12074625

Molinari, M., Galli, C., Piccaluga, V., Pieren, M., and Paganetti, P. (2002). Sequential assistance of molecular chaperones and transient formation of covalent complexes during protein degradation from the ER. *J. Cell Biol.* 158, 247–257. doi: 10.1083/jcb.200204122

Moran, L. K., Gutteridge, J., and Quinlan, G. J. (2001). Thiols in cellular redox signalling and control. *Curr. Med. Chem.* 8, 763–772. doi: 10.2174/0929867013372904

Muller, C., Bandemer, J., Vindis, C., Camaré, C., Mucher, E., Guéraud, F., et al. (2013). Protein disulfide isomerase modification and inhibition contribute to ER stress and apoptosis induced by oxidized low density lipoproteins. *Antioxid. Redox Signal.* 18, 731–742.

Nakamura, T., and Lipton, S. A. (2011). S-nitrosylation of critical protein thiols mediates protein misfolding and mitochondrial dysfunction in neurodegenerative diseases. *Antioxid. Redox Signal.* 14, 1479–1492. doi: 10.1089/ars.2010.3570

Nardo, G., Pozzi, S., Pignataro, M., Lauranzano, E., Spano, G., Garbelli, S., et al. (2011). Amyotrophic lateral sclerosis multiprotein biomarkers in peripheral blood mononuclear cells. *PLoS ONE* 6:e25545. doi: 10.1371/journal.pone.0025545

Nguyen, V. D., Wallis, K., Howard, M. J., Haapalainen, A. M., Salo, K. E., Ruddock, L. W., et al. (2008). Alternative conformations of the x region of human protein disulphide-isomerase modulate exposure of the substrate binding b'domain. *J. Mol. Biol.* 383, 1144–1155. doi: 10.1016/j.jmb.2008.08.085

Paes, A. M. D. A., Veríssimo-Filho, S., Guimarães, L. L., Silva, A. C. B., Takiuti, J. T. Lopes, L. R., et al. (2011). Protein disulfide isomerase redox-dependent association with p47phox: evidence for an organizer role in leukocyte NADPH oxidase activation. *J. Leukoc. Biol.* 90, 799–810. doi: 10.1189/jlb.0610324

Parakh, S., Spencer, D. M., Halloran, M. A., Soo, K. Y., and Atkin, J. D. (2013). Redox regulation in amyotrophic lateral sclerosis. *Oxid. Med. Cell. Longev.* 2013:408681. doi: 10.1155/2013/408681

Pescatore, L. A., Bonatto, D., Forti, F. L., Sadok, A., Kovacic, H., Laurindo, F. R., et al. (2012). Protein disulfide isomerase is required for platelet-derived growth factor-induced vascular smooth muscle cell migration, Nox1 NADPH oxidase expression, and RhoGTPase activation. *J. Biol. Chem.* 287, 29290–29300. doi: 10.1074/jbc.M112.394551

Primm, T. P., and Gilbert, H. F. (2001). Hormone binding by protein disulfide isomerase, a high capacity hormone reservoir of the endoplasmic reticulum. *J. Biol. Chem.* 276, 281–286. doi: 10.1074/jbc.M007670200

Primm, T. P., Walker, K. W., and Gilbert, H. F. (1996). Facilitated protein aggregation effects of calcium on the chaperone and anti-chaperone activity of protein disulfide-isomerase. *J. Biol. Chem.* 271, 33664–33669. doi: 10.1074/jbc.271.52.33664

Puig, A., and Gilbert, H. F. (1994). Protein disulfide isomerase exhibits chaperone and anti-chaperone activity in the oxidative refolding of lysozyme. *J. Biol. Chem.* 269, 7764–7771.

Rainey-Barger, E. K., Mkrtchian, S., and Tsai, B. (2007). Dimerization of ERp29, a PDI-like protein, is essential for its diverse functions. *Mol. Biol. Cell.* 18, 1253–1260. doi: 10.1091/mbc.E06-11-1004

Ramachandran, N., Root, P., Jiang, X.-M., Hogg, P. J., and Mutus, B. (2001). Mechanism of transfer of NO from extracellular S-nitrosothiols into the cytosol by cell-surface protein disulfide isomerase. *Proc. Natl. Acad. Sci. U.S.A.* 98, 9539–9544. doi: 10.1073/pnas.171180998

Rutkevich, L. A., Cohen-Doyle, M. F., Brockmeier, U., and Williams, D. B. (2010). Functional relationship between protein disulfide isomerase family members during the oxidative folding of human secretory proteins. *Mol. Biol. Cell.* 21, 3093–3105. doi: 10.1091/mbc.E10-04-0356

Schroder, M., and Kaufman, R. J. (2005). ER stress and the unfolded protein response. mutation research/fundamental and molecular mechanisms of mutagenesis. *Mutat. Res.* 569, 29–63. doi: 10.1016/j.mrfmmm.2004.06.056

Schwaller, M., Wilkinson, B., and Gilbert, H. F. (2003). Reduction-reoxidation cycles contribute to catalysis of disulfide isomerization by protein-disulfide isomerase. *J. Biol. Chem.* 278, 7154–7159. doi: 10.1074/jbc.M211036200

Severino, A., Campioni, M., Straino, S., Salloum, F. N., Schmidt, N., and Bussani, R., et al. (2007). Identification of protein disulfide isomerase as a cardiomyocyte survival factor in ischemic cardiomyopathy. *J. Am. Coll. Cardiol.* 50, 1029–1037. doi: 10.1016/j.jacc.2007.06.006

Sobierajska, K., Skurzynski, S., Stasiak, M., Kryczka, J., Cierniewski, C. S., Swiatkowska, M., et al. (2014). Protein disulfide isomerase directly interacts with β-Actin Cys374 and regulates cytoskeleton reorganization. *J. Biol. Chem.* 289, 5758–5773. doi: 10.1074/jbc.M113.479477

Solda, T., Garbi, N., Hämmerling, G. J., and Molinari, M. (2006). Consequences of ERp57 deletion on oxidative folding of obligate and facultative clients of the calnexin cycle. *J. Biol. Chem.* 281, 6219–6226. doi: 10.1074/jbc.M513595200

Song, J. L., and Wang, C. C. (1995). Chaperone−like activity of protein disulfide−isomerase in the refolding of rhodanese. *Eur. J. Biochem.* 231, 312–316. doi: 10.1111/j.1432-1033.1995.tb20702.x

Sovolyova, N., Healy, S., Samali, A., and Logue, S. E. (2014). Stressed to death–mechanisms of ER stress-induced cell death. *Biol. Chem.* 395, 1–13. doi: 10.1515/hsz-2013-0174

Stolf, B. S., Smyrnias, I., Lopes, L. R., Vendramin, A., Goto, H., Santos, C. X., et al. (2011). Protein disulfide isomerase and host-pathogen interaction. *ScientificWorldJournal* 11, 1749–1761. doi: 10.1100/2011/289182

Tanaka, S., Uehara, T., and Nomura, Y. (2000). Up-regulation of protein-disulfide isomerase in response to hypoxia/brain ischemia and its protective effect against apoptotic cell death. *J. Biol. Chem.* 275, 10388–10393. doi: 10.1074/jbc.275.14.10388

Taylor, M., Banerjee, T., Ray, S., Tatulian, S. A., and Teter, K. (2011). Protein-disulfide isomerase displaces the cholera toxin A1 subunit from the holotoxin without unfolding the A1 subunit. *J. Biol. Chem.* 286, 22090–22100. doi: 10.1074/jbc.M111.237966

Thongwatchara, P., Promwikorn, W., Srisomsap, C., Chokchaichamnankit, D., Boonyaphiphat, P., Thongsuksai, P., et al. (2011). Differential protein expression in primary breast cancer and matched axillary node metastasis. *Oncol. Rep.* 26, 185–191. doi: 10.3892/or.2011.1266

Tian, F., Zhou, X., Wikström, J., Karlsson, H., Sjöland, L.-M., Gan, J.,et al. (2009). Protein disulfide isomerase increases in myocardial endothelial cells in mice exposed to chronic hypoxia: a stimulatory role in angiogenesis. *Am. J. Physiol.* 297, H1078–H1086. doi: 10.1152/ajpheart.00937.2008

Tian, G., Xiang, S., Noiva, R., Lennarz, W., and Schindelin, H. (2006). The crystal structure of yeast protein disulfide isomerase suggests cooperativity between its active sites. *Cell* 124, 61–73. doi: 10.1016/j.cell.2005.10.044

Toldo, S., Boccellino, M., Rinaldi, B., Seropian, I. M., Mezzaroma, E., Paolisso, G., et al. (2011). Altered oxido-reductive state in the diabetic heart: loss of cardioprotection due to protein disulfide isomerase. *Mol. Med.* 17, 1012. doi: 10.2119/molmed.2011.00100

Townsend, D. M., Manevich, Y., He, L., Xiong, Y., Bowers, R., Tew, K. D., et al. (2009). Nitrosative stress–induced S-glutathionylation of protein disulfide isomerase leads to activation of the unfolded protein response. *Cancer Res.* 69, 7626–7634. doi: 10.1158/0008-5472.CAN-09-0493

Tsai, B., Rodighiero, C., Lencer, W. I., and Rapoport, T. A. (2001). Protein disulfide isomerase acts as a redox-dependent chaperone to unfold cholera toxin. *Cell* 104, 937–948. doi: 10.1016/S0092-8674(01)00289-6

Tsuda, H., Han, S. M., Yang, Y., Tong, C., Lin, Y. Q., Kwan, J., et al. (2008). The amyotrophic lateral sclerosis 8 protein VAPB is cleaved, secreted, and acts as a ligand for Eph receptors. *Cell* 133, 963–977. doi: 10.1016/j.cell.2008.04.039

Turano, C., Coppari, S., Altieri, F., and Ferraro, A. (2002). Proteins of the PDI family: unpredicted non−ER locations and functions. *J. Cell. Physiol.* 193, 154–163. doi: 10.1002/jcp.10172

Uehara, T., Nakamura, T., Yao, D., Shi, Z.-Q., Gu, Z., Lipton, S. A., et al. (2006). S-nitrosylated protein-disulphide isomerase links protein misfolding to neurodegeneration. *Nature* 441, 513–517. doi: 10.1038/nature04782

Vuori, K., Pihlajaniemi, T., Marttila, M., and Kivirikko, K. I. (1992). Characterization of the human prolyl 4-hydroxylase tetramer and its

multifunctional protein disulfide-isomerase subunit synthesized in a baculovirus expression system. *Proc. Natl. Acad. Sci. U.S.A.* 89, 7467.

Walker, A. K., Farg, M. A., Bye, C. R., McLean, C. A., Horne, M. K., Atkin, J. D., et al. (2010). Protein disulphide isomerase protects against protein aggregation and is S-nitrosylated in amyotrophic lateral sclerosis. *Brain* 133, 105–116. doi: 10.1093/brain/awp267

Walker, A. K., Soo, K. Y., Levina, V., Talbo, G. H., and Atkin, J., D. (2013). N–linked glycosylation modulates dimerization of protein disulfide isomerase family A member 2 (PDIA2). *FEBS J.* 280, 233–243. doi: 10.1111/febs.12063

Wang, C., Li, W., Ren, J., Fang, J., Ke, H., Gong, W., et al. (2013). Structural insights into the redox-regulated dynamic conformations of human protein disulfide isomerase. *Antioxid. Redox Signal.* 19, 36–45. doi: 10.1089/ars.2012.4630

Wang, C., Yu, J., Huo, L., Wang, L., Feng, W., Wang, C.-C., et al. (2012a). Human protein-disulfide isomerase is a redox-regulated chaperone activated by oxidation of domain a'. *J. Biol. Chem.* 287, 1139–1149. doi: 10.1074/jbc.M111.303149

Wang, S.-B., Shi, Q., Xu, Y., Xie, W.-L., Zhang, J., Chen, C., et al (2012b). Protein disulfide isomerase regulates endoplasmic reticulum stress and the apoptotic process during prion infection and PrP mutant-induced cytotoxicity. *PLoS ONE* 7:e38221. doi: 10.1371/journal.pone.0038221

Watts, J. C., Huo, H., Bai, Y., Ehsani, S., Won, A. H., Xu, L., et al. (2009). Interactome Analyses identify ties of PrPC and its mammalian paralogs to oligomannosidic N-Glycans and endoplasmic reticulum-derived chaperones. *PLoS Pathog.* 5:e1000608. doi: 10.1371/journal.ppat.1000608

Wilkinson, B., and Gilbert, H. F. (2004). Protein disulfide isomerase. *Biochim. Biophys. Acta* 1699, 35–44. doi: 10.1016/j.bbapap.2004.02.017

Xiao, R., Solovyov, A., Gilbert, H. F., Holmgren, A., and Lundström-Ljung, J. (2001). Combinations of protein-disulfide isomerase domains show that there is little correlation between isomerase activity and wild-type growth. *J. Biol. Chem.* 276, 27975–27980. doi: 10.1074/jbc.M104203200

Xiong, Y., Manevich, Y., Tew, K. D., and Townsend, D. M. (2012). S-glutathionylation of protein disulfide isomerase regulates estrogen receptor stability and function. *Int. J. Cell Biol.* 2012:273549. doi: 10.1155/2012/273549

Xiong, Y., Uys, J. D., Tew, K. D., and Townsend, D. M. (2011). S-glutathionylation: from molecular mechanisms to health outcomes. *Antioxid. Redox Signal.* 15, 233–270. doi: 10.1089/ars.2010.3540/

Xu, S., Butkevich, A. N., Yamada, R., Zhou, Y., Debnath, B., Neamati, N., et al (2012). Discovery of an orally active small-molecule irreversible inhibitor of protein disulfide isomerase for ovarian cancer treatment. *Proc. Natl. Acad. Sci. U.S.A.* 109, 16348–16353. doi: 10.1073/pnas.1205226109

Xu, S., Sankar, S., and Neamati, N. (2014). Protein disulfide isomerase: a promising target for cancer therapy. *Drug Discov. Today* 19, 222–240. doi: 10.1016/j.drudis.2013.10.017

Yang, Y. S., Harel, N. Y., and Strittmatter, S. M. (2009). Reticulon-4A (Nogo-A) redistributes protein disulfide isomerase to protect mice from SOD1-dependent amyotrophic lateral sclerosis. *J. Neurosci.* 29, 13850–13859. doi: 10.1523/JNEUROSCI.2312-09.2009

Zai, A., Rudd, M. A., Scribner, A. W., and Loscalzo, J. (1999). Cell-surface protein disulfide isomerase catalyzes transnitrosation and regulates intracellular transfer of nitric oxide. *J. Clin. Invest.* 103, 393–399. doi: 10.1172/JCI4890

Zhang, L., Lai, E., Teodoro, T., and Volchuk, A. (2009). GRP78, but not protein-disulfide isomerase, partially reverses hyperglycemia-induced inhibition of insulin synthesis and secretion in pancreatic β-cells. *J. Biol. Chem.* 284, 5289–5298. doi: 10.1074/jbc.M805477200

Conflict of Interest Statement: The authors declare that the research was conducted in the absence of any commercial or financial relationships that could be construed as a potential conflict of interest.

7.2.3 Supplementary Figure 2

The published review article: Parakh S, Spencer DM, Halloran MA, Soo KY, Atkin JD (2012) "***Redox Regulation in Amyotrophic Lateral Sclerosis".*** *Oxidative Medicine and Cellular Longevity* **408681:**1-12 was written by the author with the guidance of supervisor Julie Atkin except;

Section 3.4 Lipid Peroxidation and Cholesterol Esterification-kindly contributed by Mark Halloran, La Trobe University, Melbourne, Australia.

Section 3.5 Mitochondrial Dysfunction - kindly contributed by Dr Damian Spencer, La Trobe University, Melbourne, Australia.

Section 3.6 Impaired Axonal transport - kindly contributed by Dr Kai Soo, La Trobe University, Melbourne, Australia.

Hindawi Publishing Corporation
Oxidative Medicine and Cellular Longevity
Volume 2013, Article ID 408681, 12 pages
http://dx.doi.org/10.1155/2013/408681

Review Article

Redox Regulation in Amyotrophic Lateral Sclerosis

Sonam Parakh,[1] Damian M. Spencer,[1] Mark A. Halloran,[2] Kai Y. Soo,[1] and Julie D. Atkin[1,3]

[1] *Department of Biochemistry, La Trobe Institute for Molecular Science, La Trobe University, Vic 3086, Australia*
[2] *School of Psychological Science, La Trobe University, Vic 3086, Australia*
[3] *Florey Department of Neuroscience, University of Melbourne, Parkville, Vic 3010, Australia*

Correspondence should be addressed to Julie D. Atkin; j.atkin@latrobe.edu.au

Received 17 October 2012; Revised 7 January 2013; Accepted 10 January 2013

Academic Editor: Jeannette Vasquez-Vivar

Amyotrophic lateral sclerosis (ALS) is a neurodegenerative disease that results from the death of upper and lower motor neurons. Due to a lack of effective treatment, it is imperative to understand the underlying mechanisms and processes involved in disease progression. Regulations in cellular reduction/oxidation (redox) processes are being increasingly implicated in disease. Here we discuss the possible involvement of redox dysregulation in the pathophysiology of ALS, either as a cause of cellular abnormalities or a consequence. We focus on its possible role in oxidative stress, protein misfolding, glutamate excitotoxicity, lipid peroxidation and cholesterol esterification, mitochondrial dysfunction, impaired axonal transport and neurofilament aggregation, autophagic stress, and endoplasmic reticulum (ER) stress. We also speculate that an ER chaperone protein disulphide isomerase (PDI) could play a key role in this dysregulation. PDI is essential for normal protein folding by oxidation and reduction of disulphide bonds, and hence any disruption to this process may have consequences for motor neurons. Addressing the mechanism underlying redox regulation and dysregulation may therefore help to unravel the molecular mechanism involved in ALS.

1. Introduction

Cellular oxidation/reduction (redox) states regulate various aspects of cellular function and maintain homeostasis [1]. Moderate levels of reactive oxygen species/reactive nitrogen species (ROS/RNS) function as signals to promote cell proliferation, regulation, and survival [2], whereas increased levels of ROS/RNS can induce cell death [1, 2]. Under normal physiological conditions, cells maintain redox homeostasis through generation of ROS which include free radical species such as superoxide (O_2^-) hydroxyl radicals (OH^-) and non-radical species such as hydrogen peroxide (H_2O_2); and RNS, which includes nitric oxide (NO), nitronium ion (NO_2^+), nitrogen dioxide ($NO_2^\bullet$), and peroxynitrite ($ONOO^-$) [3–5]. RNS are by-products of nitric oxide synthase (NOS) and NADPH oxidase [6]. Increased levels of NOS have been observed in the motor neurons of amyotrophic lateral sclerosis (ALS) patients suggesting a role of RNS in pathology [7]. Higher levels of RNS can react with other free radicals such as superoxide and undergo complex reactions to form the strong oxidant $ONOO^-$ which causes cellular damage [8–10].

Cells are equipped with antioxidant systems to eliminate ROS/RNS and maintain redox homeostasis, which include enzymatic antioxidants such as superoxide dismutase (SOD), peroxidase, oxidase, catalase, and nonenzymatic oxidants such as glutathione [3, 11]. Glutaredoxin and thioredoxin are redox active molecules which undergo cysteine dependent modifications, also making them preferential targets for direct oxidation [12].

Redox regulation is a fundamental cellular process involving enzymes that maintain the appropriate environment for metabolic activities and proper functioning of the cell [13]. Normally, redox homeostasis ensures that cells respond to stressors such as oxidative or nitrative stress efficiently but when it is disturbed, neurodegeneration and apoptosis can occur [11, 14]. Neurons are particularly susceptible to degeneration via redox dysregulation as the high consumption of oxygen by the brain results in a significant production of ROS [15]. Disruption in redox regulation is implicated in the pathogenesis of neurodegeneration disorders, including ALS. Interestingly, several pathogenic mechanisms linked to ALS involve redox-sensitive proteins, such as SOD1, and proteins with active-site cysteine residues, including protein

disulphide isomerase (PDI), thioredoxin, and glutathione [16–20]. These proteins contain a thiol group which is highly sensitive to changes in redox conditions [12, 21]. Even slight modulations in redox state are capable of producing neurotoxic species such as NO_2^+, $NO_2^\bullet$, and $ONOO^-$ [14], suggesting that redox stress could be of importance in disease [9].

2. Amyotrophic Lateral Sclerosis (ALS)

ALS, also known as Charcot's or Lou Gehrig's disease, is a fatal neurodegenerative disorder that affects the upper and lower motor neurons of the primary cortex, brainstem, and spinal cord [22, 23]. The symptoms include muscle weakness and muscle spasticity eventually resulting in paralysis [24] with ALS patients generally dying from respiratory failure within 3–5 years of diagnosis. Approximately 2 per 100,000 people worldwide are affected by ALS every year [22]. Riluzole is the only FDA-approved drug currently available for ALS. Riluzole has modest efficacy. It slows disease progression and a dose of 100 mg per day also improves limb function and muscle strength although it increases life span by an average of only 2-3 months [25, 26]. Therefore, a greater understanding of the molecular mechanisms causing ALS is important in order to develop better therapeutic solutions.

Approximately 90% of ALS cases have no genetic association and are known as sporadic ALS (SALS). However mutations in genes such as copper/zinc superoxide dismutase (*SOD1*), fused in sarcoma (*FUS*) and TAR DNA binding protein (*TARDBP*), have also been described in SALS patients; also environmental causes such as smoking and viral infection are linked to ALS [24, 27–31]. Studies have shown higher prevalence of ALS in people with a history of trauma [32] and involvement in physical activities such as soccer has also been observed in ALS patients [33, 34]; however the exact aetiology is unknown. The remaining 10% of ALS cases, known as familial ALS (FALS), are linked to mutations in specific genes [35] including SOD1, TDP-43, FUS, vesicle associated membrane protein-B (VAPB), optineurin, alsin, and ubiquilin-2 [18, 36–43]. Recently a noncoding mutation in C9ORF72 was shown to cause the greatest proportion of FALS cases [44]. SOD1 causes 15–20% of all FALS cases and was the first described and hence most widely researched gene linked to ALS [18]. Transgenic mice overexpressing ALS-associated mutant SOD1 proteins have been used extensively as disease models [45–47]. Similar to other protein disorders, the pathological hallmark of ALS is the presence of intracellular protein inclusions [48]. Misfolded wild-type and mutant forms of SOD1, FUS, and TDP-43 [41, 49, 50] are present on the inclusions found in affected tissues of ALS patients [41, 51–53]. SALS and FALS have similar symptoms and are clinically and pathologically indistinguishable.

Wild-type SOD1 is a highly stable homodimeric protein, explained in part by the presence of an intrasubunit disulphide bond between cysteine 57 and cysteine 146 [54]. It contains both copper and zinc ions which are essential for the catalytic activity and stability, respectively [55]. Reduction of the disulphide bond results in dissociation of the dimer and the resulting protein is highly unstable and prone to aggregation [56, 57].

Dysfunction in multiple cellular mechanisms is linked to ALS pathology reviewed recently by Cozzolino and coworkers [58]. Many of these events are linked to redox regulation including oxidative stress, protein misfolding and aggregation, excitotoxicity, lipid peroxidation and cholesterol esterification, mitochondrial dysfunction, impaired axonal transport and neurofilament aggregation, autophagy, and ER stress [46, 59–68]. However, there is a complex interplay between these processes and the exact aetiology of the disease is unclear. It is debatable whether redox dysregulation is a primary effect or a secondary consequence of other pathologies and the association of redox regulation and cysteine rich redox regulated proteins with these mechanisms is unclear. This paper discusses the main redox linked mechanisms which are involved in ALS and their association with redox or cysteine dependent proteins.

3. Possible Redox Regulated Cellular Mechanisms Involved in ALS

3.1. Oxidative Stress. Oxidative stress arises when the levels of ROS/RNS exceed the amounts required for normal redox signalling. While oxidative stress has been implicated as a pathological mechanism in ALS the exact role of ROS/RNS in disease processes is unclear [9, 69]. ROS causes permanent oxidative damage to major cellular components such as proteins, DNA, lipids, and cell membranes [70–72]. ROS has been detected in the spinal cord and cerebrospinal fluid (CSF) of SALS patients [17]. Increased levels of H_2O_2 and oxidative damage to protein and DNA have also been observed in SOD1 transgenic mice [73]. Defects in the Rac/Nox pathway leading to redox dysregulation are also linked to $SOD1^{G93A}$ mice [74]. Furthermore dysregulation of redox regulated-tumour protein 1, ubiquitin carboxyl-terminal hydrolase isoenzyme L1, and αB crystallin has been observed in transgenic $SOD1^{G93A}$ mice [75].

Altered redox homeostasis regulates gene expression of transcriptional factors such as nuclear factor kappa-light-chain-enhancer of activated B cells (NF-κB), activator protein 1 (AP-1), and hypoxia inducible factor 1α (HIF-1α) [76]. These transcriptional factors help in maintaining homeostasis by regulating gene expression. They have a redox regulated cysteine residue at their DNA binding site [76] which can be affected due to thiol oxidation and could be influenced by ROS [77]. A direct relation between the transcription factors and redox regulation in ALS is unknown; nevertheless dysregulation in the levels of NF-κB and HIF-1α has been observed in SALS patients, and activation of AP-1 in mutant SOD1 expressing cells, suggesting potential involvement of redox regulation in ALS pathology [78, 79].

SOD1 and its antioxidant properties have been studied extensively from the perspective of redox regulation in ALS [80, 81]. SOD1 catalyses the conversion of superoxide into hydrogen peroxide and oxygen and it undergoes cyclic reduction and oxidation of its copper ions [82]. Initially, it

was proposed that ALS mutations in SOD1 result in the loss of its ability to act as an antioxidant, but further research showed that disease is not associated with its enzymatic activity [83]. However, mutations in SOD1 could produce $ONOO^-$ or OH^- and lower its ability to catalyse superoxide [84] by reacting with nitric oxide [85]. These intermediate products are highly unstable and have been detected with other amino acids such as tyrosine. Nitrated proteins and high levels of nitrotyrosine have been detected in the CSF of both SALS and FALS patients suggesting that posttranslational modification via free radical production is present in ALS [17, 86–88]. Oxidised wild-type SOD1 in the lymphoblasts of SALS patients associates with mitochondrial Bcl-2 which causes mitochondrial damage [89]. Oxidative damage is an important phenomenon; however, treatment with antioxidants has not been very successful [90].

3.2. Protein Aggregation and Misfolding. Redox dysregulation may not only increase the production of ROS/RNS but also affect protein conformation and structure. Posttranslational modification of SOD1 such as oxidation has an adverse effect on the conformational arrangement of SOD1 [91]. Glutathionylation, a posttranslational modification of the 111 cysteine residue, causes destabilisation of SOD1 structure [92]. Wild-type SOD1 has been shown in inclusions of SALS patients suggesting its involvement in causing neurotoxicity [93]. Evidence suggests that oxidised wild-type SOD1 has the ability to misfold and form aggregates and gain similar conformation as the mutant and has toxic functions *in vitro* [89, 94]. SOD1 depleted zinc and copper have altered redox activity and are more prone to oxidation [95].

An oxidising environment also causes abnormal disulphide linkages and protein aggregation in ALS [80, 96]. SOD1 containing aberrant disulphide bonds involves the normally unpaired cysteine residues cysteine 6 and cysteine 111 in the spinal cord of ALS transgenic mice models [96]. Studies show that mutant TDP-43 aggregation is caused due to increased disulphide bonds [97]. Similarly oxidative stress causes aberrant disulphide cross-linking and subcellular localisation of TDP-43 [97] as well as accumulation of FUS into the cytoplasm [98]. Mutant SOD1 readily forms monomers, oligomers, or inclusions which are insoluble [55]. It is unclear how conformational changes cause misfolding but one possible explanation could be the modification and alteration of protein structure by ROS through oxidisation of the thiol group, forming aberrant disulphide bonds.

3.3. Glutamate Excitotoxicity. The levels of glutamate present in mammalian CNS are much higher than those of other neurotransmitters (5–10 mmol/kg) indicating the importance of glutamate in neuronal function [99]. However, excitotoxicity occurs when the levels of glutamate are increased in neurons, resulting in increased calcium intake and neuronal injury [100, 101]. Motor neurons are particularly susceptible to high levels of glutamate [102]. Glutamate uptake from the synapse is controlled by glutamate transporters astroglial GLAST, GLT1, and neuronal EAAC1 which possess a redox regulated cysteine residue [103]. N-methyl-D aspartic acid (NMDA) glutamate receptors are also redox regulated suggesting that redox dysfunction may further affect glutamate regulation. Increased levels of intracellular glutamate and decreased uptake of glutamate from the synapse have been observed in ALS patients [104, 105]. Indeed, Rothstein and coworkers showed an absence of GLT1 transporter in ALS patients [106]. ROS can reduce the uptake of glutamate in mammals [107]; however, increased calcium levels in the mitochondria due to dysfunctional glutamate regulation can result in overproduction of ROS and cause oxidative stress [108]. The question remains whether oxidative stress causes glutamate dysregulation or vice versa.

3.4. Lipid Peroxidation and Cholesterol Esterification. The ER is also the main site of lipid and sterol synthesis [109]. Lipids are major targets of oxidative stress, resulting in lipid peroxidation via a chain-reaction process [11]. Sphingolipids are localised in the plasma membrane and ER membranes and, with cholesterol, are processed into domains known as lipid rafts [68]. Lipid rafts can form macroplatforms for redox signalling, providing critical mediation for cellular functioning [110]. Lipid peroxidation and cholesterol esterification have been implicated in the pathogenesis of ALS [68, 69, 111]. Excitotoxicity and oxidative stress alter sphingolipid metabolism resulting in the accumulation of long-chain ceramides, sphingomyelin, and cholesterol esters in the spinal cords of ALS patients and Cu/Zn SOD1 mice. This occurs at the early presymptomatic stage of disease in the SOD1 mice [68] thus implicating aberrant lipid metabolism in the pathophysiology of ALS. Further evidence of lipid dysregulation in ALS comes from studies which reported that ALS patients demonstrated a tendency towards hyperlipidemia. Additionally, correlational studies have shown that ALS patients with the highest low density lipoprotein (LDL)/ high density lipoprotein (HDL) ratio have a significant increase in survival time and respiratory function [112, 113]. Furthermore, recently, an interaction between SOD1 aggregates with lipid was found to alter lipid membrane permeability [114].

Lipid peroxidation products such as 4-hydroxynonenal have been detected at higher levels in ALS patients spinal cord than controls, and this has been linked to modification of astrocytic glutamate transporter EAAT2 and excitotoxicity [111]. Excitotoxicity was also linked to upregulation of sterol regulatory binding element 1 (SREBP1) in the spinal cords of FALS and SALS patients, and $SOD1^{G93A}$ transgenic mice suggesting cholesterol depletion [115]. Furthermore, the link between ALS and statins, a class of drug which inhibit 3-hydroxy-3-methylglutaryl coenzyme A (HMG-CoA) reductase, may suggest that suppressing cholesterol synthesis increases the incidence [116, 117], progression, and severity of ALS [118], although this has been questioned [119]. Lipid raft alteration has also been linked to the pathogenesis of ALS. Endogenous, wild-type and mutant $SOD1^{G93A}$ proteins were recruited into lipid rafts isolated from spinal cords of transgenic SOD1 mice [120]. Hence, together the data suggest that oxidative stress may alter sphingolipid and cholesterol metabolism and deregulate lipid raft redox signalling leading

to the accumulation of toxic ceramides and cholesterol esters which may ultimately result in motor neuron death [68].

3.5. Mitochondrial Dysfunction. Mitochondria are important players in redox regulation and oxidative stress has the potential to cause mitochondrial dysfunction [70, 121]. Indeed, damaged mitochondria are observed in the spinal cord cells of SALS patients [122–124]. The mitochondrial genome is particularly susceptible to oxidative damage [125], hence any increase in cellular ROS would potentially perturb mitochondrial functions. Mitochondria participate in neuronal apoptotic signalling pathways through the release of mitochondrial proteins including cytochrome c into the cytoplasm [126]. There is substantial evidence that molecular components of mitochondrial apoptosis play a role in neurodegeneration in both SOD1 rodents and in mutant SOD1 overexpressed in cell culture [127]. The enzymatic activity of cytochrome c oxidase (COX) in mitochondria is also reduced in the spinal cord cells of SALS patients [122–124, 128, 129]. Mitochondria have been well studied in relation to ALS pathogenesis. Degenerating or abnormal mitochondria have been described in mouse models [62, 130], cultured neuronal cellular models [131, 132], and ALS patients [133, 134], although how nonfunctioning mitochondria relate to ALS is unclear. Possible explanations include inhibition of axonal transport, dysregulation of calcium buffering [135], or activation of mitochondrial-dependent apoptosis [128, 136]. Recent studies have shown that overexpression of TDP-43 causes mitochondrial dysfunction and induces mitophagy in cell culture [137]. The presence of ROS and impairment of the mitochondrial respiratory chain have also been observed in TDP-43 models [138, 139].

Mutant SOD1 has also been implicated in mitochondrial respiratory complex impairment [140] and a shift in the redox state of mitochondria towards oxidation [141]. How SOD1 functions in the mitochondria is still not clear, although some data suggests that SOD1 is crucial for maintenance of the mitochondrial redox state [142, 143] and that ALS mutations affect the localisation or function of SOD1 in mitochondria [135]. However, mutant misfolded SOD1 has been found localised with various compartments of the mitochondria [144]. Significantly, any pathological changes in regulation of the electron transport chain would result in more oxidative stress [145] triggering further cellular redox dysregulation, leading to a potential vicious cycle of damage and degeneration.

3.6. Impaired Axonal Transport. Axonal transport is a key mechanism required for cellular viability in neuronal cells. Most proteins required in the axon and in synaptic terminals must be transported along the axon after synthesis in the cell body. Similarly RNA and organelles also need to be transported over long distances, and these transport processes require molecular motors, such as kinesins, dyneins, and myosins that operate along the cellular cytoskeleton. Dysfunction of axonal transport has now been well documented in ALS [61]. Whilst many of these studies implicate dynein in this process [146], several also highlight the importance of kinesin in ALS, particularly kinesin heavy chains KIF5A and KIF1Bβ, which transport mitochondria, synaptic vesicles, and macromolecular complexes. Interestingly, a recent study demonstrated that oxidised wild-type SOD1 immunopurified from SALS patient tissues inhibited kinesin-based axonal transport in a manner similar to mutant SOD1 in FALS providing evidence for common pathogenic mechanisms in both SALS and FALS [94].

Neurofilaments (NF) accumulation in motor neurons is another histopathological hallmark of ALS [147, 148]. Also, transgenic mice that overexpress NF subunits in motor neurons develop a motor neuron disease with impaired axonal flow, as axonal defects cause delay in transportation of components required for the maintenance of axon [149]. However, $ONOO^-$ formed during oxidative stress from nitrooxide and superoxide can affect NF assembly and cause NF accumulation in motor neurons [8]. Chou and coworkers showed NF aggregations are associated with SOD1 and nitric oxide synthase activities leading to nitrotyrosine formation on NF [150]. Nitrotyrosine can inhibit phosphorylation of heavy or light NF subunits and may alter axonal transport and trigger motor neuron death [150]. Taken together, these findings suggest a relation between redox regulation and axonal transport dysfunctions in ALS.

3.7. Autophagy. Autophagy is a normal homeostatic mechanism to dispose large protein aggregates, damaged organelles, and long-lived proteins. Autophagic stress results when the number of autophagosomes increases relative to the proportion of degradable proteins. The presence of high levels of superoxide and hydrogen peroxide species can induce autophagy *in vitro* [151], but consequently, autophagy can further induce oxidative or nitrative stress thus creating a vicious cycle [152]. Dysregulated redox activity also influences autophagy. Cathepsin, a class of proteases which have highly regulated thiol groups [152] and other key regulatory autophagic complexes such as Beclin 1 and Rubicon, also have the presence of cysteine residues [152]. The presence of cysteine residues suggests that they are redox regulated and likely to be affected by ROS. ATG 4, another protease, is a target of oxidation by hydrogen peroxide. However, direct association of these with ALS has not yet been identified. Altered autophagic levels have been observed in $SOD1^{G93A}$ mice and sporadic and familial patients but whether the increased levels are protective or not is still questionable [153–156].

3.8. ER Stress and Protein Disulphide Isomerase (PDI) in ALS. The ER is redox regulated and another important location for the production of ROS. It plays key roles in protein and lipid synthesis and protein folding. Protein misfolding within the ER triggers ER stress which induces the unfolded protein response (UPR) a distinct signalling pathway which aims to relieve stress [157]. While initially protective, prolonged UPR causes apoptosis [158, 159]. Recent studies suggest that ER stress is an early and important pathogenic mechanism in ALS [66, 158, 160]. ER stress is induced in animal models of SOD1, in cells expressing mutant FUS and in patients

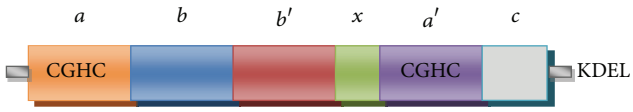

Figure 1: Schematic diagram showing domain structure of PDI. Thioredoxin-like *a* domain (orange) and a' domain (purple) possessing the catalytic motif, catalytically inactive *b* domain (blue), and b' domain (red). Green represents the linker region *x* which allows flexibility between domains. The C terminal domain is shown in grey followed by the ER retrieval signal KDEL.

[20, 161]. Oxidative stress driven by changes in fatty acid composition, mitochondrial function, and/or proteosome activity leads to oxidative stress and contributes to ER stress in SALS patients [162, 163]. PDI is an ER chaperone which is induced during UPR and has been implicated in several neurodegenerative disorders including ALS [164–166].

PDI is a member of an extended family of foldases and chaperones which are responsible for the formation and isomerisation of protein disulphide bonds [167]. The PDI family comprises 21 members which have structural similarities but different functions [168] and all have a similar active site to thioredoxin [169]. Thioredoxin is an intracellular protein which regulates redox conditions and which is effective against oxidative stress [170]. PDI is most abundant in the ER but it is also found in other subcellular locations such as the nucleus and extracellular matrix [171] and it constitutes 0.8% of the total cellular protein [172]. The yeast PDI crystal structure was recently solved [173] which suggests that *a* and a' domains are responsible for the formation of disulphide bonds (Figure 1). These domains contain a redox active CGHC motif which isomerases protein disulphide bonds and is involved in redox regulation [173]. PDI also contains *b* and b' domains which are responsible for substrate binding [174, 175]. Misfolded proteins attach to the hydrophobic region of an inverted U shape structure [173, 176]. The C-terminal region also aids in polypeptide binding and contributes chaperone activity [177]. Compared to other family members, PDI has broad substrate specificities and can interact with glycosylated as well as nonglycosylated proteins [178].

4. PDI and Redox Regulation

PDI forms protein disulphide bonds by the oxidation of thiols within the PDI active site cysteine residues [179, 180]. When PDI is in an oxidised state it transfers a disulphide to the substrates thereby oxidising the substrate and becoming reduced itself. Conversely, substrates which need disulphide bond rearrangement are reduced by PDI in the reduced state thus oxidising PDI in the process [168, 181]. This continual cycling regulates redox conditions within the ER. A thiol containing tripeptide protein and glutathione also maintains ER redox homeostasis by similar shuffling between oxidized and reduced cysteine residues. Glutathione is also required for the isomerisation and rearrangement of disulphide bonds [182]. The redox potential of PDI (−110 mV) is lower than other family members [183] due to intervening residues present between the reactive cysteines thus facilitating disulphide bonds [183]. ERO1 oxidises PDI also aiding disulphide bond formations [184], but PDI is also oxidised through peroxiredoxin 4, vitamin K, glutathione peroxidase, and quiescin sulfhydryl oxidase [181]. During ER stress high levels of ERO1 have been observed which accelerates protein oxidation suggesting interplay between oxidative stress and ER stress. The transfer of electrons from the thiol group of PDI to ERO1 results in the production of excess ROS, decreasing the levels of glutathione available for reduction and increasing ERO1 thus altering the redox conditions [185, 186]. Hence, imbalance in the redox state of the ER may result in dysregulation of thiol containing proteins and triggers.

4.1. The Role of PDI in ALS. Due to its function in preventing protein misfolding, PDI is important in protein quality control [166]; also deletion of PDI is embryonically lethal [187]. Hence, regulated expression of PDI is critical for normal cellular function. There is now growing evidence for a role of PDI in ALS. PDI levels are upregulated in transgenic models of ALS and spinal cord tissues of ALS patients [66, 158]. Overexpression of PDI is also protective against mutant SOD1 mediated aggregation and reduces cell death *in vitro* [20]. PDI coimmunoprecipitates with both SOD1 and FUS [158, 161]; it also colocalises with SOD1, TDP-43, and FUS in ALS patients suggesting a physical interaction exists between PDI and other key misfolded proteins in ALS [66, 161, 188]. Similarly, PDI also colocalises with TDP-43 in ALS tissues and with VAPB inclusions in a *Drosophila melanogaster* model of ALS [188, 189]. A small mimic of the active site of PDI, dithiol (±)-trans-1,2-bis (mercaptoacetamido) cyclohexane (BMC), is also protective in cell culture and it reduces mutant SOD1 aggregation in a dose dependent manner [20]. Further evidences for a role for disulphide interchange activity in ALS comes from studies showing that another PDI family member ERp57 is also upregulated in transgenic SOD1 mice and ALS patients [66]. Furthermore, thioredoxin is also upregulated in the erythrocytes of FALS patients [19].

The upregulation of these thiol containing proteins in ALS suggests a cellular defensive mechanism is triggered in disease as a defence against oxidative stress. However, there is evidence that normal protective function of PDI is inhibited in disease [20]. Modifications of active site thiol groups through direct oxidation, S-glutathiolation and S-nitrosylation, can lead to inactivation of the normal enzymatic activity of PDI [13, 190, 191]. PDI was recently shown to be S-nitrosylated in ALS [20, 192] as in other neurodegenerative disorders such as Parkinson's and Alzheimer's disease. [191]. S-nitrosylation occurs when there is an increased production of RNS during oxidative stress resulting in addition of a nitrogen monoxide group to the thiol side of PDI [20, 164]. Experiments performed by Chen and coworkers suggested that in the presence of S-nitrosylated PDI, the formation of mutant SOD1 aggregates increases *in vitro* [192]. It is also likely that inactivation of PDI could lead to activation of the UPR as observed in other neurodegenerative disorders [191]. The loss of PDI functional activity can directly lead to

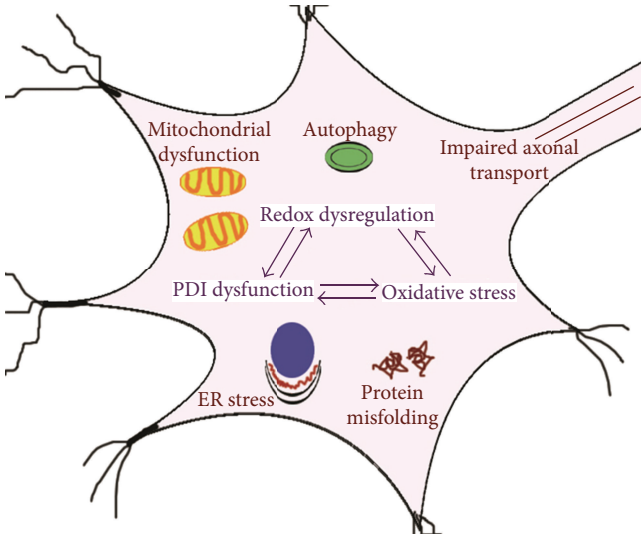

Figure 2: Redox dysfunction and its relationship to other pathologies in ALS. Alteration in the enzymatic activity of PDI due to redox dysregulation and oxidative stress can further increase the load of misfolded proteins, ER stress, oxidative stress, autophagy, mitochondrial dysfunction, and axonal impairment leading to neuronal cell death.

apoptosis, or indirectly to a range of cellular abnormalities such as oxidative stress and protein misfolding, which again lead to cell death [164, 166]. Hence the redox regulation of PDI is a crucial component in the maintenance of a balanced redox environment, and inhibition of its enzymatic activity will lead to important consequences for the cell (Figure 2).

Neurons are highly susceptible to redox dysregulation due to their high metabolic requirements, large size, and lower ability to maintain the balance between antioxidants and ROS [15]. In disease states such as ALS, oxidative stress, and altered enzymatic activity of PDI, which normally reduces ROS and the burden of misfolded protein, can cause serious damage to the neuron. Since multiple mechanisms are involved in neurodegeneration, any imbalance in redox regulation can lead to an imbalance in the production of free radical species, which consequently cause mitochondrial damage and excitotoxicity, thus elevating the levels of free radicals [193]. Furthermore, an excess of free radicals can also lead to DNA damage and may also result in aggregation of NF [194] and structural destabilization of other proteins, thus inducing ER stress and apoptosis. Since ALS is a slow progressive disorder it could be hypothesised that these cyclic events, due to loss of functional activity of PDI, may gradually lead to neuronal degradation. In such a scenario, the redox regulatory function of PDI may therefore have an important protective effect.

5. Conclusion

Redox regulation is an important mechanism of homeostasis in eukaryotic cells, especially neuronal cells where oxygen levels are high [15]. Many cellular processes rely on it, including proper functioning of the mitochondria and ER, calcium regulation, axonal transport, regulated autophagy, and protein folding. Links between redox dysregulation and ALS are becoming well documented in the literature, although the directionality of these links and their underlying cause are still quite unknown. One possible key player in redox regulation in ALS is PDI, whose role in ALS pathogenesis is the topic of much new research. As the critical protein involved in thiol reduction, any dysregulation of PDI activity can lead to oxidative stress and redox dysregulation. Due to its activity, PDI itself also contains an active site thiol group suggesting that it can also be affected by oxidative stress, leading to an escalating cycle that perpetuates redox dysregulation. How PDI becomes nonfunctional in the first place is still unclear, although some papers point to S-nitrosylation as having a role [20]. Regardless of its exact role, any mechanism to improve the catalytic activity of PDI should have a reductive effect on oxidative stress levels in neurons. It is therefore tempting to speculate about PDI as a possible therapeutic target in the treatment of ALS.

Acknowledgments

This work was supported by the National Health and Medical Research Council of Australia (project Grants 454749, 1006141, and 1030513), Amyotrophic Lateral Sclerosis Association (USA), MND Research Institute of Australia, Bethlehem Griffiths Research Council, Henry H Roth Charitable Foundation Grant for MND Research, Australian Rotary Health, and the Brain Foundation. S. Parakh holds a La Trobe University Post Graduate Research Scholarship.

References

[1] H. Kamata and H. Hirata, "Redox regulation of cellular signalling," *Cellular Signalling*, vol. 11, no. 1, pp. 1–14, 1999.

[2] A. R. Cross and O. T. G. Jones, "Enzymic mechanisms of superoxide production," *Biochimica et Biophysica Acta*, vol. 1057, no. 3, pp. 281–298, 1991.

[3] V. Adler, Z. Yin, K. D. Tew, and Z. Ronai, "Role of redox potential and reactive oxygen species in stress signaling," *Oncogene*, vol. 18, no. 45, pp. 6104–6111, 1999.

[4] J. Nordberg and E. S. J. Arnér, "Reactive oxygen species, antioxidants, and the mammalian thioredoxin system," *Free Radical Biology and Medicine*, vol. 31, no. 11, pp. 1287–1312, 2001.

[5] M. G. Espey, K. M. Miranda, D. D. Thomas et al., "A chemical perspective on the interplay between NO, reactive oxygen species, and Reactive Nitrogen Oxide Species," *Annals of the New York Academy of Sciences*, vol. 962, pp. 195–206, 2002.

[6] W. A. Pryor and G. L. Squadrito, "The chemistry of peroxynitrite: a product from the reaction of nitric oxide with superoxide," *American Journal of Physiology-Lung Cellular and Molecular Physiology*, vol. 268, no. 5, pp. L699–L722, 1995.

[7] K. Abe, L. H. Pan, M. Watanabe, H. Konno, T. Kato, and Y. Itoyama, "Upregulation of protein-tyrosine nitration in the anterior horn cells of amyotrophic lateral sclerosis," *Neurological Research*, vol. 19, no. 2, pp. 124–128, 1997.

[8] J. S. Beckman, M. Carson, C. D. Smith, and W. H. Koppenol, "ALS, SOD and peroxynitrite," *Nature*, vol. 364, no. 6438, p. 584, 1993.

[9] S. C. Barber and P. J. Shaw, "Oxidative stress in ALS: key role in motor neuron injury and therapeutic target," *Free Radical Biology and Medicine*, vol. 48, no. 5, pp. 629–641, 2010.

[10] M. C. Martínez and R. Andriantsitohaina, "Reactive nitrogen species: molecular mechanisms and potential significance in health and disease," *Antioxidants and Redox Signaling*, vol. 11, no. 3, pp. 669–702, 2009.

[11] D. Trachootham, W. Lu, M. A. Ogasawara, N. R. D. Valle, and P. Huang, "Redox regulation of cell survival," *Antioxidants and Redox Signaling*, vol. 10, no. 8, pp. 1343–1374, 2008.

[12] C. E. Cooper, R. P. Patel, P. S. Brookes, and V. M. Darley-Usmar, "Nanotransducers in cellular redox signaling: modification of thiols by reactive oxygen and nitrogen species," *Trends in Biochemical Sciences*, vol. 27, no. 10, pp. 489–492, 2002.

[13] H. Nakamura, K. Nakamura, and J. Yodoi, "Redox regulation of cellular activation," *Annual Review of Immunology*, vol. 15, pp. 351–369, 1997.

[14] S. A. Lipton, Y. B. Choi, Z. H. Pan et al., "A redox-based mechanism for the neuroprotective and neurodestructive effects of nitric oxide and related nitroso-compounds," *Nature*, vol. 364, no. 6438, pp. 626–632, 1993.

[15] B. Halliwell, "Oxidative stress and neurodegeneration: where are we now?" *Journal of Neurochemistry*, vol. 97, no. 6, pp. 1634–1658, 2006.

[16] R. P. Guttmann and T. J. Powell, "Redox regulation of cysteine-dependent enzymes in neurodegeneration," *International Journal of Cell Biology*, vol. 2012, Article ID 703164, 8 pages, 2012.

[17] H. Tohgi, T. Abe, K. Yamazaki, T. Murata, E. Ishizaki, and C. Isobe, "Increase in oxidized NO products and reduction in oxidized glutathione in cerebrospinal fluid from patients with sporadic form of amyotrophic lateral sclerosis," *Neuroscience Letters*, vol. 260, no. 3, pp. 204–206, 1999.

[18] D. R. Rosen, T. Siddique, D. Patterson et al., "Mutations in Cu/Zn superoxide dismutase gene are associated with familial amyotrophic lateral sclerosis," *Nature*, vol. 362, no. 6415, pp. 59–62, 1993.

[19] Y. Ogawa, H. Kosaka, T. Nakanishi et al., "Stability of mutant superoxide dismutase-1 associated with familial amyotrophic lateral sclerosis determines the manner of copper release and induction of thioredoxin in erythrocytes," *Biochemical and Biophysical Research Communications*, vol. 241, no. 2, pp. 251–257, 1997.

[20] A. K. Walker, M. A. Farg, C. R. Bye, C. A. McLean, M. K. Horne, and J. D. Atkin, "Protein disulphide isomerase protects against protein aggregation and is S-nitrosylated in amyotrophic lateral sclerosis," *Brain*, vol. 133, no. 1, pp. 105–116, 2010.

[21] M. W. Akhtar, C. R. Sunico, T. Nakamura, and S. A. Lipton, "Redox regulation of protein function via cysteine S-nitrosylation and its relevance to neurodegenerative diseases," *International Journal of Cell Biology*, vol. 2012, Article ID 463756, 9 pages, 2012.

[22] J. D. Rothstein, "Current hypotheses for the underlying biology of amyotrophic lateral sclerosis," *Annals of Neurology*, vol. 65, no. 1, pp. S3–S9, 2009.

[23] J. Mitchell and G. Borasio, "Amyotrophic lateral sclerosis," *Lancet*, vol. 369, no. 9578, pp. 2031–2041, 2007.

[24] L. C. Wijesekera and P. N. Leigh, "Amyotrophic lateral sclerosis," *Orphanet Journal of Rare Diseases*, vol. 4, no. 1, p. 3, 2009.

[25] G. Bensimon, L. Lacomblez, and V. Meininger, "A controlled trial of riluzole in amyotrophic lateral sclerosis," *New England Journal of Medicine*, vol. 330, no. 9, pp. 585–591, 1994.

[26] R. G. Miller, J. D. Mitchell, M. Lyon, and D. H. Moore, "Riluzole for amyotrophic lateral sclerosis (ALS)/motor neuron disease (MND)," *Cochrane Database of Systematic Reviews*, no. 1, Article ID CD001447, 2007.

[27] A. Alonso, G. Logroscino, S. S. Jick, and M. A. Hernán, "Association of smoking with amyotrophic lateral sclerosis risk and survival in men and women: a prospective study," *BMC Neurology*, vol. 10, no. 1, p. 6, 2010.

[28] A. Verma and J. R. Berger, "ALS syndrome in patients with HIV-1 infection," *Journal of the Neurological Sciences*, vol. 240, no. 1-2, pp. 59–64, 2006.

[29] A. Chiò, B. J. Traynor, F. Lombardo et al., "Prevalence of SOD1 mutations in the Italian ALS population," *Neurology*, vol. 70, no. 7, pp. 533–537, 2008.

[30] L. Corrado, R. Del Bo, B. Castellotti et al., "Mutations of FUS gene in sporadic amyotrophic lateral sclerosis," *Journal of Medical Genetics*, vol. 47, no. 3, pp. 190–194, 2010.

[31] J. Sreedharan, I. P. Blair, V. B. Tripathi et al., "TDP-43 mutations in familial and sporadic amyotrophic lateral sclerosis," *Science*, vol. 319, no. 5870, pp. 1668–1672, 2008.

[32] E. Pupillo, P. Messina, G. Logroscino et al., "Trauma and amyotrophic lateral sclerosis: a case-control study from a population-based registry," *European Journal of Neurology*, vol. 19, no. 12, pp. 1509–1517, 2012.

[33] S. Beretta, M. T. Carrì, E. Beghi, A. Chiò, and C. Ferrarese, "The sinister side of Italian soccer," *Lancet Neurology*, vol. 2, no. 11, pp. 656–657, 2003.

[34] M. R. Turner, C. Wotton, K. Talbot, and M. J. Goldacre, "Cardiovascular fitness as a risk factor for amyotrophic lateral sclerosis: indirect evidence from record linkage study," *Journal of Neurology, Neurosurgery & Psychiatry*, vol. 83, pp. 395–398, 2012.

[35] P. A. Dion, H. Daoud, and G. A. Rouleau, "Genetics of motor neuron disorders: new insights into pathogenic mechanisms," *Nature Reviews Genetics*, vol. 10, no. 11, pp. 769–782, 2009.

[36] T. Arai, M. Hasegawa, H. Akiyama et al., "TDP-43 is a component of ubiquitin-positive tau-negative inclusions in frontotemporal lobar degeneration and amyotrophic lateral sclerosis," *Biochemical and Biophysical Research Communications*, vol. 351, no. 3, pp. 602–611, 2006.

[37] M. Neumann, D. M. Sampathu, L. K. Kwong et al., "Ubiquitinated TDP-43 in frontotemporal lobar degeneration and amyotrophic lateral sclerosis," *Science*, vol. 314, no. 5796, pp. 130–133, 2006.

[38] C. Vance, B. Rogelj, T. Hortobágyi et al., "Mutations in FUS, an RNA processing protein, cause familial amyotrophic lateral sclerosis type 6," *Science*, vol. 323, no. 5918, pp. 1208–1211, 2009.

[39] Y. Yang, A. Hentati, H. X. Deng et al., "The gene encoding alsin, a protein with three guanine-nucleotide exchange factor domains, is mutated in a form of recessive amyotrophic lateral sclerosis," *Nature Genetics*, vol. 29, pp. 160–165, 2001.

[40] A. L. Nishimura, M. Mitne-Neto, H. C. A. Silva et al., "A mutation in the vesicle-trafficking protein VAPB causes late-onset spinal muscular atrophy and amyotrophic lateral sclerosis," *American Journal of Human Genetics*, vol. 75, no. 5, pp. 822–831, 2004.

[41] T. J. Kwiatkowski Jr., D. A. Bosco, A. L. LeClerc et al., "Mutations in the FUS/TLS gene on chromosome 16 cause familial amyotrophic lateral sclerosis," *Science*, vol. 323, no. 5918, pp. 1205–1208, 2009.

[42] H. Maruyama, H. Morino, H. Ito et al., "Mutations of optineurin in amyotrophic lateral sclerosis," *Nature*, vol. 465, no. 7295, pp. 223–226, 2010.

[43] H. X. Deng, W. Chen, S. T. Hong et al., "Mutations in UBQLN2 cause dominant X-linked juvenile and adult-onset ALS and ALS/dementia," *Nature*, vol. 477, pp. 211–215, 2011.

[44] M. DeJesus-Hernandez, I. R. Mackenzie, B. F. Boeve et al., "Expanded GGGGCC hexanucleotide repeat in noncoding region of C9ORF72 causes chromosome 9p-linked FTD and ALS," *Neuron*, vol. 72, no. 2, pp. 245–256, 2011.

[45] L. I. Bruijn, T. M. Miller, and D. W. Cleveland, "Unraveling the mechanisms involved in motor neuron degeneration in ALS," *Annual Review of Neuroscience*, vol. 27, pp. 723–749, 2004.

[46] H. D. Durham, J. Roy, L. Dong, and D. A. Figlewicz, "Aggregation of mutant Cu/Zn superoxide dismutase proteins in a culture model of ALS," *Journal of Neuropathology and Experimental Neurology*, vol. 56, no. 5, pp. 523–530, 1997.

[47] M. Watanabe, M. Dykes-Hoberg, V. Cizewski Culotta, D. L. Price, P. C. Wong, and J. D. Rothstein, "Histological evidence of protein aggregation in mutant SOD1 transgenic mice and in amyotrophic lateral sclerosis neural tissues," *Neurobiology of Disease*, vol. 8, no. 6, pp. 933–941, 2001.

[48] C. Soto, "Unfolding the role of protein misfolding in neurodegenerative diseases," *Nature Reviews Neuroscience*, vol. 4, no. 1, pp. 49–60, 2003.

[49] J. Wang, G. Xu, and D. R. Borchelt, "Mapping superoxide dismutase 1 domains of non-native interaction: roles of intra- and intermolecular disulfide bonding in aggregation," *Journal of Neurochemistry*, vol. 96, no. 5, pp. 1277–1288, 2006.

[50] B. S. Johnson, D. Snead, J. J. Lee, J. M. McCaffery, J. Shorter, and A. D. Gitler, "TDP-43 is intrinsically aggregation-prone, and amyotrophic lateral sclerosis-linked mutations accelerate aggregation and increase toxicity," *Journal of Biological Chemistry*, vol. 284, pp. 20329–20339, 2009.

[51] C. Vance, B. Rogelj, T. Hortobágyi et al., "Mutations in FUS, an RNA processing protein, cause familial amyotrophic lateral sclerosis type 6," *Science*, vol. 323, no. 5918, pp. 1208–1211, 2009.

[52] T. Arai, M. Hasegawa, H. Akiyama et al., "TDP-43 is a component of ubiquitin-positive tau-negative inclusions in frontotemporal lobar degeneration and amyotrophic lateral sclerosis," *Biochemical and Biophysical Research Communications*, vol. 351, no. 3, pp. 602–611, 2006.

[53] N. Shibata, A. Hirano, M. Kobayashi et al., "Intense superoxide dismutase-1 immunoreactivity in intracytoplasmic hyaline inclusions of familial amyotrophic lateral sclerosis with posterior column involvement," *Journal of Neuropathology and Experimental Neurology*, vol. 55, no. 4, pp. 481–490, 1996.

[54] J. S. Valentine, P. A. Doucette, and S. Z. Potter, "Copper-zinc superoxide dismutase and amyotrophic lateral sclerosis," *Annual Review of Biochemistry*, vol. 74, pp. 563–593, 2005.

[55] F. Arnesano, L. Banci, I. Bertini, M. Martinelli, Y. Furukawa, and T. V. O'Halloran, "The unusually stable quaternary structure of human Cu,Zn-superoxide dismutase 1 is controlled by both metal occupancy and disulfide status," *Journal of Biological Chemistry*, vol. 279, no. 46, pp. 47998–48003, 2004.

[56] C. Kayatekin, J. A. Zitzewitz, and C. R. Matthews, "Disulfide-Reduced ALS Variants of Cu, Zn Superoxide Dismutase Exhibit Increased Populations of Unfolded Species," *Journal of Molecular Biology*, vol. 398, no. 2, pp. 320–331, 2010.

[57] A. E. Svensson, O. Bilsel, C. Kayatekin, J. A. Adefusika, J. A. Zitzewitz, and C. Robert Matthews, "Metal-free ALS variants of dimeric human Cu,Zn-superoxide dismutase have enhanced populations of monomeric species," *PLoS ONE*, vol. 5, no. 4, Article ID e10064, 2010.

[58] M. Cozzolino, M. G. Pesaresi, V. Gerbino, J. Grosskreutz, and M. T. Carr?, "Amyotrophic lateral sclerosis: new insights into underlying molecular mechanisms and opportunities for therapeutic intervention," *Antioxidants & Redox Signaling*, vol. 17, no. 9, pp. 1277–1330, 2012.

[59] O. Spreux-Varoquaux, G. Bensimon, L. Lacomblez et al., "Glutamate levels in cerebrospinal fluid in amyotrophic lateral sclerosis: a reappraisal using a new HPLC method with coulometric detection in a large cohort of patients," *Journal of the Neurological Sciences*, vol. 193, no. 2, pp. 73–78, 2002.

[60] I. Puls, C. Jonnakuty, B. H. LaMonte et al., "Mutant dynactin in motor neuron disease," *Nature Genetics*, vol. 33, no. 4, pp. 455–456, 2003.

[61] J. F. Collard, F. Cote, and J. P. Julien, "Defective axonal transport in a transgenic mouse model of amyotrophic lateral sclerosis," *Nature*, vol. 375, no. 6526, pp. 61–64, 1995.

[62] J. Kong and Z. Xu, "Massive mitochondrial degeneration in motor neurons triggers the onset of amyotrophic lateral sclerosis in mice expressing a mutant SOD1," *Journal of Neuroscience*, vol. 18, no. 9, pp. 3241–3250, 1998.

[63] F. R. Wiedemann, K. Winkler, A. V. Kuznetsov et al., "Impairment of mitochondrial function in skeletal muscle of patients with amyotrophic lateral sclerosis," *Journal of the Neurological Sciences*, vol. 156, no. 1, pp. 65–72, 1998.

[64] A. Hirano, H. Donnenfeld, S. Sasaki, and I. Nakano, "Fine structural observations of neurofilamentous changes in amyotrophic lateral sclerosis," *Journal of Neuropathology and Experimental Neurology*, vol. 43, no. 5, pp. 461–470, 1984.

[65] J. D. Wood, T. P. Beaujeux, and P. J. Shaw, "Protein aggregation in motor neurone disorders," *Neuropathology and Applied Neurobiology*, vol. 29, no. 6, pp. 529–545, 2003.

[66] J. D. Atkin, M. A. Farg, A. K. Walker, C. McLean, D. Tomas, and M. K. Horne, "Endoplasmic reticulum stress and induction of the unfolded protein response in human sporadic amyotrophic lateral sclerosis," *Neurobiology of Disease*, vol. 30, no. 3, pp. 400–407, 2008.

[67] S. Chen, X. Zhang, L. Song, and W. Le, "Autophagy dysregulation in amyotrophic lateral sclerosis," *Brain Pathology*, vol. 22, no. 1, pp. 110–116, 2012.

[68] R. G. Cutler, W. A. Pedersen, S. Camandola, J. D. Rothstein, and M. P. Mattson, "Evidence that accumulation of ceramides and cholesterol esters mediates oxidative stress-induced death of motor neurons in amyotrophic lateral sclerosis," *Annals of Neurology*, vol. 52, no. 4, pp. 448–457, 2002.

[69] R. J. Ferrante, S. E. Browne, L. A. Shinobu et al., "Evidence of increased oxidative damage in both sporadic and familial amyotrophic lateral sclerosis," *Journal of Neurochemistry*, vol. 69, no. 5, pp. 2064–2074, 1997.

[70] M. Bogdanov, R. H. Brown, W. Matson et al., "Increased oxidative damage to DNA in ALS patients," *Free Radical Biology and Medicine*, vol. 29, no. 7, pp. 652–658, 2000.

[71] A. W. Girotti, "Lipid hydroperoxide generation, turnover, and effector action in biological systems," *Journal of Lipid Research*, vol. 39, no. 8, pp. 1529–1542, 1998.

[72] P. J. Shaw, P. G. Ince, G. Falkous, and D. Mantle, "Oxidative damage to protein in sporadic motor neuron disease spinal cord," *Annals of Neurology*, vol. 38, no. 4, pp. 691–695, 1995.

[73] D. Liu, J. Wen, J. Liu, and L. Li, "The roles of free radicals in amyotrophic lateral sclerosis: reactive oxygen species and elevated oxidation of protein, DNA, and membrane phospholipids," *FASEB Journal*, vol. 13, no. 15, pp. 2318–2328, 1999.

[74] B. J. Carter, P. Anklesaria, S. Choi, and J. F. Engelhardt, "Redox modifier genes and pathways in amyotrophic lateral sclerosis," *Antioxidants and Redox Signaling*, vol. 11, no. 7, pp. 1569–1586, 2009.

[75] H. F. Poon, K. Hensley, V. Thongboonkerd et al., "Redox proteomics analysis of oxidatively modified proteins in G93A-SOD1 transgenic mice-a model of familial amyotrophic lateral sclerosis," *Free Radical Biology and Medicine*, vol. 39, no. 4, pp. 453–462, 2005.

[76] J. J. Haddad, "Antioxidant and prooxidant mechanisms in the regulation of redox(y)-sensitive transcription factors," *Cellular Signalling*, vol. 14, no. 11, pp. 879–897, 2002.

[77] K. T. Turpaev, "Reactive oxygen species and regulation of gene expression," *Biochemistry*, vol. 67, no. 3, pp. 281–292, 2002.

[78] C. Iaccarino, M. E. Mura, S. Esposito et al., "Bcl2-A1 interacts with pro-caspase-3: implications for amyotrophic lateral sclerosis," *Neurobiology of Disease*, vol. 43, no. 3, pp. 642–650, 2011.

[79] C. Moreau, P. Gosset, J. Kluza et al., "Deregulation of the hypoxia inducible factor-1α pathway in monocytes from sporadic amyotrophic lateral sclerosis patients," *Neuroscience*, vol. 172, pp. 110–117, 2011.

[80] C. M. Karch, M. Prudencio, D. D. Winkler, P. J. Hart, and D. R. Borchelt, "Role of mutant SOD1 disulfide oxidation and aggregation in the pathogenesis of familial ALS," *Proceedings of the National Academy of Sciences of the United States of America*, vol. 106, no. 19, pp. 7774–7779, 2009.

[81] J. B. Proescher, M. Son, J. L. Elliott, and V. C. Culotta, "Biological effects of CCS in the absence of SOD1 enzyme activation: implications for disease in a mouse model for ALS," *Human Molecular Genetics*, vol. 17, no. 12, pp. 1728–1737, 2008.

[82] J. M. McCord and I. Fridovich, "Superoxide dismutase. An enzymic function for erythrocuprein (hemocuprein)," *Journal of Biological Chemistry*, vol. 244, no. 22, pp. 6049–6055, 1969.

[83] D. Sau, S. De Biasi, L. Vitellaro-Zuccarello et al., "Mutation of SOD1 in ALS: a gain of a loss of function," *Human Molecular Genetics*, vol. 16, no. 13, pp. 1604–1618, 2007.

[84] J. S. Beckman, M. Carson, C. D. Smith, and W. H. Koppenol, "ALS, SOD and peroxynitrite," *Nature*, vol. 364, no. 6438, p. 584, 1993.

[85] N. V. Blough and O. C. Zafiriou, "Reaction of superoxide with nitric oxide to form peroxonitrite in alkaline aqueous solution," *Inorganic Chemistry*, vol. 24, no. 22, pp. 3502–3504, 1985.

[86] M. F. Beal, R. J. Ferrante, S. E. Browne Jr., R. T. Matthews, N. W. Kowall, and R. H. Brown, "Increased 3-nitrotyrosine in both sporadic and familial amyotrophic lateral sclerosis," *Annals of Neurology*, vol. 42, no. 4, pp. 644–654, 1997.

[87] H. Tohgi, T. Abe, K. Yamazaki, T. Murata, E. Ishizaki, and C. Isobe, "Remarkable increase in cerebrospinal fluid 3-nitrotyrosine in patients with sporadic amyotrophic lateral sclerosis," *Annals of Neurology*, vol. 46, pp. 129–131, 1999.

[88] F. Casoni, M. Basso, T. Massignan et al., "Protein nitration in a mouse model of familial amyotrophic lateral sclerosis: possible multifunctional role in the pathogenesis," *Journal of Biological Chemistry*, vol. 280, no. 16, pp. 16295–16304, 2005.

[89] S. Guareschi, E. Cova, C. Cereda et al., "An over-oxidized form of superoxide dismutase found in sporadic amyotrophic lateral sclerosis with bulbar onset shares a toxic mechanism with mutant SOD1," *Proceedings of the National Academy of Sciences*, vol. 109, no. 13, pp. 5074–5079, 2012.

[90] R. W. Orrell, R. J. M. Lane, and M. Ross, "A systematic review of antioxidant treatment for amyotrophic lateral sclerosis/motor neuron disease," *Amyotrophic Lateral Sclerosis*, vol. 9, no. 4, pp. 195–211, 2008.

[91] S. A. Ezzi, M. Urushitani, and J. P. Julien, "Wild-type superoxide dismutase acquires binding and toxic properties of ALS-linked mutant forms through oxidation," *Journal of Neurochemistry*, vol. 102, no. 1, pp. 170–178, 2007.

[92] R. L. Redler, K. C. Wilcox, E. A. Proctor, L. Fee, M. Caplow, and N. V. Dokholyan, "Glutathionylation at Cys-111 induces dissociation of wild type and FALS mutant SOD1 dimers," *Biochemistry*, vol. 50, no. 32, pp. 7057–7066, 2011.

[93] K. Forsberg, P. A. Jonsson, P. M. Andersen et al., "Novel antibodies reveal inclusions containing non-native SOD1 in sporadic ALS patients," *PloS One*, vol. 5, no. 7, Article ID e11552, 2010.

[94] D. A. Bosco, G. Morfini, N. M. Karabacak et al., "Wild-type and mutant SOD1 share an aberrant conformation and a common pathogenic pathway in ALS," *Nature Neuroscience*, vol. 13, no. 11, pp. 1396–1403, 2010.

[95] A. C. Estévez, J. P. Crow, J. B. Sampson et al., "Induction of nitric oxide-dependent apoptosis in motor neurons by zinc- deficient superoxide dismutase," *Science*, vol. 286, no. 5449, pp. 2498–2500, 1999.

[96] Y. Furukawa, R. Fu, H. X. Deng, T. Siddique, and T. V. O'Halloran, "Disulfide cross-linked protein represents a significant fraction of ALS-associated Cu, Zn-superoxide dismutase aggregates in spinal cords of model mice," *Proceedings of the National Academy of Sciences of the United States of America*, vol. 103, no. 18, pp. 7148–7153, 2006.

[97] T. J. Cohen, A. W. Hwang, T. Unger, J. Q. Trojanowski, and V. M. Y. Lee, "Redox signalling directly regulates TDP-43 via cysteine oxidation and disulphide cross-linking," *The EMBO Journal*, vol. 31, no. 5, pp. 1241–1252, 2011.

[98] D. Dormann, R. Rodde, D. Edbauer et al., "ALS-associated fused in sarcoma (FUS) mutations disrupt transportin-mediated nuclear import," *EMBO Journal*, vol. 29, no. 16, pp. 2841–2857, 2010.

[99] S. P. Butcher and A. Hamberger, "In vivo studies on the extracellular, and veratrine-releasable, pools of endogenous amino acids in the rat striatum: effects of corticostriatal deafferentiation and kainic acid lesion," *Journal of Neurochemistry*, vol. 48, no. 3, pp. 713–721, 1987.

[100] I. Sen, A. Nalini, N. B. Joshi, and P. G. Joshi, "Cerebrospinal fluid from amyotrophic lateral sclerosis patients preferentially elevates intracellular calcium and toxicity in motor neurons via AMPA/kainate receptor," *Journal of the Neurological Sciences*, vol. 235, no. 1-2, pp. 45–54, 2005.

[101] A. Plaitakis and J. T. Caroscio, "Abnormal glutamate metabolism in amyotrophic lateral sclerosis," *Annals of Neurology*, vol. 22, no. 5, pp. 575–579, 1987.

[102] L. Van Den Bosch and W. Robberecht, "Different receptors mediate motor neuron death induced by short and long exposures to excitotoxicity," *Brain Research Bulletin*, vol. 53, no. 4, pp. 383–388, 2000.

[103] D. Trotti, "Neuronal and glial glutamate transporters possess an SH-based redox regulatory mechanism," *European Journal of Neuroscience*, vol. 9, no. 6, pp. 1236–1243, 1997.

[104] A. Plaitakis and E. Constantakakis, "Altered metabolism of excitatory amino acids, N-acetyl-aspartate and N- acetyl-aspartyl-glutamate in amyotrophic lateral sclerosis," *Brain Research Bulletin*, vol. 30, no. 3-4, pp. 381–386, 1993.

[105] J. D. Rothstein, L. J. Martin, and R. W. Kuncl, "Decreased glutamate transport by the brain and spinal cord in amyotrophic lateral sclerosis," *New England Journal of Medicine*, vol. 326, no. 22, pp. 1464–1468, 1992.

[106] J. D. Rothstein, M. Van Kammen, A. I. Levey, L. J. Martin, and R. W. Kuncl, "Selective loss of glial glutamate transporter GLT-1 amyotrophic lateral sclerosis," *Annals of Neurology*, vol. 38, no. 1, pp. 73–84, 1995.

[107] A. Volterra, D. Trotti, C. Tromba, S. Floridi, and G. Racagni, "Glutamate uptake inhibition by oxygen free radicals in rat cortical astrocytes," *Journal of Neuroscience*, vol. 14, no. 5, pp. 2924–2932, 1994.

[108] P. J. Shaw, "Glutamate, excitotoxicity and amyotrophic lateral sclerosis," *Journal of Neurology*, vol. 244, no. 2, pp. S3–S14, 1997.

[109] W. L. Miller, "Minireview: regulation of steroidogenesis by electron transfer," *Endocrinology*, vol. 146, no. 6, pp. 2544–2550, 2005.

[110] S. Jin, F. Zhou, F. Katirai, and P. L. Li, "Lipid raft redox signaling: molecular mechanisms in health and disease," *Antioxidants and Redox Signaling*, vol. 15, no. 4, pp. 1043–1083, 2011.

[111] W. A. Pedersen, W. Fu, J. N. Keller et al., "Protein modification by the lipid peroxidation product 4-hydroxynonenal in the spinal cords of amyotrophic lateral sclerosis patients," *Annals of Neurology*, vol. 44, no. 5, pp. 819–824, 1998.

[112] L. Dupuis, P. Corcia, A. Fergani et al., "Dyslipidemia is a protective factor in amyotrophic lateral sclerosis," *Neurology*, vol. 70, no. 13, pp. 1004–1009, 2008.

[113] L. Dupuis and J. P. Loeffler, "Neuromuscular junction destruction during amyotrophic lateral sclerosis: insights from transgenic models," *Current Opinion in Pharmacology*, vol. 9, no. 3, pp. 341–346, 2009.

[114] I. Choi, H. D. Song, S. Lee et al., "Direct observation of defects and increased ion permeability of a membrane induced by structurally disordered Cu/Zn-superoxide dismutase aggregates," *PloS One*, vol. 6, no. 12, pp. e28982–e28982, 2011.

[115] C. Taghibiglou, J. Lu, I. R. Mackenzie, Y. T. Wang, and N. R. Cashman, "Sterol regulatory element binding protein-1 (SREBP1) activation in motor neurons in excitotoxicity and amyotrophic lateral sclerosis (ALS): indip, a potential therapeutic peptide," *Biochemical and Biophysical Research Communications*, vol. 413, no. 2, pp. 159–163, 2011.

[116] E. Colman, A. Szarfman, J. Wyeth et al., "An evaluation of a data mining signal for amyotrophic lateral sclerosis and statins detected in FDA's spontaneous adverse event reporting system," *Pharmacoepidemiology and Drug Safety*, vol. 17, no. 11, pp. 1068–1076, 2008.

[117] I. R. Edwards, K. Star, and A. Kiuru, "Statins, neuromuscular degenerative disease and an amyotrophic lateral sclerosis-like syndrome: an analysis of individual case safety reports from vigibase," *Drug Safety*, vol. 30, no. 6, pp. 515–525, 2007.

[118] L. Zinman, R. Sadeghi, M. Gawel, D. Patton, and A. Kiss, "Are statin medications safe in patients with ALS?" *Amyotrophic Lateral Sclerosis*, vol. 9, no. 4, pp. 223–228, 2008.

[119] H. Toft Sørensen and T. L. Lash, "Statins and amyotrophic lateral sclerosis-the level of evidence for an association," *Journal of Internal Medicine*, vol. 266, no. 6, pp. 520–526, 2009.

[120] J. Zhai, A. L. Ström, R. Kilty et al., "Proteomic characterization of lipid raft proteins in amyotrophic lateral sclerosis mouse spinal cord," *FEBS Journal*, vol. 276, no. 12, pp. 3308–3323, 2009.

[121] M. F. Beal, "Aging, energy, and oxidative stress in neurodegenerative diseases," *Annals of Neurology*, vol. 38, no. 3, pp. 357–366, 1995.

[122] F. R. Wiedemann, G. Manfredi, C. Mawrin, M. Flint Beal, and E. A. Schon, "Mitochondrial DNA and respiratory chain function in spinal cords of ALS patients," *Journal of Neurochemistry*, vol. 80, no. 4, pp. 616–625, 2002.

[123] G. M. Borthwick, M. A. Johnson, P. G. Ince, P. J. Shaw, and D. M. Turnbull, "Mitochondrial enzyme activity in amyotrophic lateral sclerosis: implications for the role of mitochondria in neuronal cell death," *Annals of Neurology*, vol. 46, no. 5, pp. 787–790, 2001.

[124] P. M. Keeney and J. P. Bennett, "ALS spinal neurons show varied and reduced mtDNA gene copy numbers and increased mtDNA gene deletions," *Molecular Neurodegeneration*, vol. 5, no. 1, p. 21, 2010.

[125] M. B. Graeber, E. Grasbon-Frodl, U. V. Eitzen, and S. K. Kösel, "Neurodegeneration and aging: role of the second genome," *Journal of Neuroscience Research*, vol. 52, no. 1, pp. 1–6, 1998.

[126] K. C. Zimmermann, C. Bonzon, and D. R. Green, "The machinery of programmed cell death," *Pharmacology and Therapeutics*, vol. 92, no. 1, pp. 57–70, 2001.

[127] P. Nagley, G. C. Higgins, J. D. Atkin, and P. M. Beart, "Multifaceted deaths orchestrated by mitochondria in neurones," *Biochimica et Biophysica Acta*, vol. 1802, no. 1, pp. 167–185, 2010.

[128] C. Guégan, M. Vila, G. Rosoklija, A. P. Hays, and S. Przedborski, "Recruitment of the mitochondria-dependent apoptotic pathway in amyotrophic lateral sclerosis," *Journal of Neuroscience*, vol. 21, no. 17, pp. 6569–6576, 2001.

[129] L. J. Martin, Z. Liu, K. Chen et al., "Motor neuron degeneration in amyotrophic lateral sclerosis mutant superoxide dismutase-1 transgenic mice: mechanisms of mitochondriopathy and cell death," *Journal of Comparative Neurology*, vol. 500, no. 1, pp. 20–46, 2007.

[130] P. C. Wong, C. A. Pardo, D. R. Borchelt et al., "An adverse property of a familial ALS-linked SOD1 mutation causes motor neuron disease characterized by vacuolar degeneration of mitochondria," *Neuron*, vol. 14, no. 6, pp. 1105–1116, 1995.

[131] F. M. Menzies, M. R. Cookson, R. W. Taylor et al., "Mitochondrial dysfunction in a cell culture model of familial amyotrophic lateral sclerosis," *Brain*, vol. 125, no. 7, pp. 1522–1533, 2002.

[132] M. T. Carrì, A. Ferri, A. Battistoni et al., "Expression of a Cu,Zn superoxide dismutase typical of familial amyotrophic lateral sclerosis induces mitochondrial alteration and increase of cytosolic Ca2+ concentration in transfected neuroblastoma SH-SY5Y cells," *FEBS Letters*, vol. 414, no. 2, pp. 365–368, 1997.

[133] S. Sasaki and M. Iwata, "Ultrastructural study of synapses in the anterior horn neurons of patients with amyotrophic lateral sclerosis," *Neuroscience Letters*, vol. 204, no. 1-2, pp. 53–56, 1996.

[134] L. Siklós, J. Engelhardt, Y. Harati, R. G. Smith, F. Joó, and S. H. Appel, "Ultrastructural evidence for altered calcium in motor nerve terminals in amyotrophic lateral sclerosis," *Annals of Neurology*, vol. 39, no. 2, pp. 203–216, 1996.

[135] M. Cozzolino and M. T. Carrí, "Mitochondrial dysfunction in ALS," *Progress in Neurobiology*, vol. 97, no. 2, pp. 54–66, 2012.

[136] K. Y. Soo, J. D. Atkin, M. Farg, A. K. Walker, M. K. Horne, and P. Nagley, "Bim links ER stress and apoptosis in cells expressing mutant SOD1 associated with amyotrophic lateral sclerosis," *PloS One*, vol. 7, no. 4, Article ID e35413, 2012.

[137] K. Hong, Y. Li, W. Duan et al., "Full-length TDP-43 and its C-terminal fragments activate mitophagy in NSC34 cell line," *Neuroscience Letters*, vol. 530, no. 2, pp. 144–149, 2012.

[138] R. J. Braun and B. Westermann, "Mitochondrial dynamics in yeast cell death and aging," *Biochemical Society Transactions*, vol. 39, pp. 1520–1526, 2011.

[139] W. Duan, X. Li, J. Shi, Y. Guo, Z. Li, and C. Li, "Mutant TAR DNA-binding protein-43 induces oxidative injury in motor neuron-like cell," *Neuroscience*, vol. 169, no. 4, pp. 1621–1629, 2010.

[140] C. Jung, C. M. J. Higgins, and Z. Xu, "Mitochondrial electron transport chain complex dysfunction in a transgenic mouse model for amyotrophic lateral sclerosis," *Journal of Neurochemistry*, vol. 83, no. 3, pp. 535–545, 2002.

[141] A. Ferri, M. Cozzolino, C. Crosio et al., "Familial ALS-superoxide dismutases associate with mitochondria and shift their redox potentials," *Proceedings of the National Academy of Sciences of the United States of America*, vol. 103, no. 37, pp. 13860–13865, 2006.

[142] K. Aquilano, P. Vigilanza, G. Rotilio, and M. R. Ciriolo, "Mitochondrial damage due to SOD1 deficiency in SH-SY5Y neuroblastoma cells: a rationale for the redundancy of SOD1," *The FASEB Journal*, vol. 20, no. 10, pp. 1683–1685, 2006.

[143] E. M. O'Brien, R. Dirmeier, M. Engle, and R. O. Poyton, "Mitochondrial protein oxidation in yeast mutants lacking manganese- (MnSOD) or copper- and zinc-containing superoxide dismutase (CuZnSOD): evidence that mnsod and cuznsod have both unique and overlapping functions in protecting mitochondrial proteins from oxidative damage," *Journal of Biological Chemistry*, vol. 279, no. 50, pp. 51817–51827, 2004.

[144] S. Pickles and C. V. Velde, "Misfolded SOD1 and ALS: zeroing in on mitochondria," *Amyotrophic Lateral Sclerosis*, vol. 13, pp. 333–340, 2012.

[145] B. Bandy and A. J. Davison, "Mitochondrial mutations may increase oxidative stress: implications for carcinogenesis and aging?" *Free Radical Biology and Medicine*, vol. 8, no. 6, pp. 523–539, 1990.

[146] F. Zhang, A. L. Ström, K. Fukada, S. Lee, L. J. Hayward, and H. Zhu, "Interaction between familial Amyotrophic Lateral Sclerosis (ALS)-linked SOD1 mutants and the dynein complex," *Journal of Biological Chemistry*, vol. 282, no. 22, pp. 16691–16699, 2007.

[147] S. Sasaki and S. Maruyama, "Ultrastructutal study of skein-like inclusions in anterior horn neurons of patients with motor neuron disease," *Neuroscience Letters*, vol. 147, no. 2, pp. 121–124, 1992.

[148] D. A. Figlewicz, A. Krizus, M. G. Martinoli et al., "Variants of the heavy neurofilament subunit are associated with the development of amyotrophic lateral sclerosis," *Human Molecular Genetics*, vol. 3, no. 10, pp. 1757–1761, 1994.

[149] J. F. Collard, F. Cote, and J. P. Julien, "Defective axonal transport in a transgenic mouse model of amyotrophic lateral sclerosis," *Nature*, vol. 375, no. 6526, pp. 61–64, 1995.

[150] S. M. Chou, H. S. Wang, and K. Komai, "Colocalization of NOS and SOD1 in neurofilament accumulation within motor neurons of amyotrophic lateral sclerosis: an immunohistochemical study," *Journal of Chemical Neuroanatomy*, vol. 10, no. 3-4, pp. 249–258, 1996.

[151] H. Zhang, X. Kong, J. Kang et al., "Oxidative stress induces parallel autophagy and mitochondria dysfunction in human glioma U251 cells," *Toxicological Sciences*, vol. 110, no. 2, pp. 376–388, 2009.

[152] J. Lee, S. Giordano, and J. Zhang, "Autophagy, mitochondria and oxidative stress: cross-talk and redox signalling," *Biochemical Journal*, vol. 441, pp. 523–540, 2012.

[153] A. Li, X. Zhang, and W. Le, "Altered macroautophagy in the spinal cord of SOD1 mutant mice," *Autophagy*, vol. 4, no. 3, pp. 290–293, 2008.

[154] Y. Zhong, Q. J. Wang, X. Li et al., "Distinct regulation of autophagic activity by Atg14L and Rubicon associated with Beclin 1-phosphatidylinositol-3-kinase complex," *Nature Cell Biology*, vol. 11, no. 4, pp. 468–476, 2009.

[155] S. Sasaki, "Autophagy in spinal cord motor neurons in sporadic amyotrophic lateral sclerosis," *Journal of Neuropathology and Experimental Neurology*, vol. 70, no. 5, pp. 349–359, 2011.

[156] N. Morimoto, M. Nagai, Y. Ohta et al., "Increased autophagy in transgenic mice with a G93A mutant SOD1 gene," *Brain Research*, vol. 1167, no. 1, pp. 112–117, 2007.

[157] M. Schröder, "Endoplasmic reticulum stress responses," *Cellular and Molecular Life Sciences*, vol. 65, no. 6, pp. 862–894, 2008.

[158] J. D. Atkin, M. A. Farg, B. J. Turner et al., "Induction of the unfolded protein response in familial amyotrophic lateral sclerosis and association of protein-disulfide isomerase with superoxide dismutase 1," *Journal of Biological Chemistry*, vol. 281, no. 40, pp. 30152–30165, 2006.

[159] C. M. Haynes, E. A. Titus, and A. A. Cooper, "Degradation of misfolded proteins prevents ER-derived oxidative stress and cell death," *Molecular Cell*, vol. 15, no. 5, pp. 767–776, 2004.

[160] K. Kanekura, H. Suzuki, S. Aiso, and M. Matsuoka, "ER stress and unfolded protein response in amyotrophic lateral sclerosis," *Molecular Neurobiology*, vol. 39, no. 2, pp. 81–89, 2009.

[161] M. A. Farg, K. Y. Soo, A. K. Walker et al., "Mutant FUS induces endoplasmic reticulum stress in amyotrophic lateral sclerosis and interacts with protein disulfide-isomerase," *Neurobiology of Aging*, vol. 33, no. 12, pp. 2855–2868, 2012.

[162] E. V. Ilieva, V. Ayala, M. Jové et al., "Oxidative and endoplasmic reticulum stress interplay in sporadic amyotrophic lateral sclerosis," *Brain*, vol. 130, no. 12, pp. 3111–3123, 2007.

[163] J. D. Malhotra and R. J. Kaufman, "Endoplasmic reticulum stress and oxidative stress: a vicious cycle or a double-edged sword?" *Antioxidants and Redox Signaling*, vol. 9, no. 12, pp. 2277–2293, 2007.

[164] A. K. Walker and J. D. Atkin, "Mechanisms of neuroprotection by protein disulphide isomerase in amyotrophic lateral sclerosis," *Neurology Research International*, vol. 2011, Article ID 317340, 7 pages, 2011.

[165] R. B. Freedman, T. R. Hirst, and M. F. Tuite, "Protein disulphide isomerase: building bridges in protein folding," *Trends in Biochemical Sciences*, vol. 19, no. 8, pp. 331–336, 1994.

[166] C. I. Andreu, U. Woehlbier, M. Torres, and C. Hetz, "Protein disulfide isomerases in neurodegeneration: from disease mechanisms to biomedical applications," *FEBS Letters*, vol. 586, no. 18, pp. 2826–2834, 2012.

[167] J. J. Galligan and D. R. Petersen, "The human protein disulfide isomerase gene family," *Human Genomics*, vol. 6, no. 1, pp. 1–15, 2012.

[168] L. Ellgaard and L. W. Ruddock, "The human protein disulphide isomerase family: substrate interactions and functional properties," *EMBO Reports*, vol. 6, no. 1, pp. 28–32, 2005.

[169] B. Wilkinson and H. F. Gilbert, "Protein disulfide isomerase," *Biochimica et Biophysica Acta*, vol. 1699, no. 1-2, pp. 35–44, 2004.

[170] T. Tanaka, H. Nakamura, A. Nishiyama et al., "Redox regulation by thioredoxin superfamily; protection against oxidative stress and aging," *Free Radical Research*, vol. 33, no. 6, pp. 851–855, 2000.

[171] C. Turano, S. Coppari, F. Altieri, and A. Ferraro, "Proteins of the PDI family: unpredicted non-ER locations and functions," *Journal of Cellular Physiology*, vol. 193, no. 2, pp. 154–163, 2002.

[172] D. M. Ferrari and H. D. Söling, "The protein disulphide-isomerase family: unravelling a string of folds," *Biochemical Journal*, vol. 339, no. 1, pp. 1–10, 1999.

[173] G. Tian, S. Xiang, R. Noiva, W. J. Lennarz, and H. Schindelin, "The crystal structure of yeast protein disulfide isomerase suggests cooperativity between its active sites," *Cell*, vol. 124, no. 1, pp. 61–73, 2006.

[174] P. Klappa, L. W. Ruddock, N. J. Darby, and R. B. Freedman, "The b' domain provides the principal peptide-binding site of protein disulfide isomerase but all domains contribute to binding of misfolded proteins," *EMBO Journal*, vol. 17, no. 4, pp. 927–935, 1998.

[175] A. Pirneskoski, P. Klappa, M. Lobell et al., "Molecular characterization of the principal substrate binding site of the ubiquitous folding catalyst protein disulfide isomerase," *Journal of Biological Chemistry*, vol. 279, no. 11, pp. 10374–10381, 2004.

[176] G. Kozlov, P. Määttänen, D. Y. Thomas, and K. Gehring, "A structural overview of the PDI family of proteins," *FEBS Journal*, vol. 277, no. 19, pp. 3924–3936, 2010.

[177] Y. Dai and C. C. Wang, "A mutant truncated protein disulfide isomerase with no chaperone activity," *Journal of Biological Chemistry*, vol. 272, no. 44, pp. 27572–27576, 1997.

[178] C. E. Jessop, R. H. Watkins, J. J. Simmons, M. Tasab, and N. J. Bulleid, "Protein disulphide isomerase family members show distinct substrate specificity: P5 is targeted to BiP client proteins," *Journal of Cell Science*, vol. 122, no. 23, pp. 4287–4295, 2009.

[179] C. Appenzeller-Herzog, J. Riemer, E. Zito et al., "Disulphide production by Ero1α-PDI relay is rapid and effectively regulated," *EMBO Journal*, vol. 29, no. 19, pp. 3318–3329, 2010.

[180] F. Hatahet and L. W. Ruddock, "Protein disulfide isomerase: a critical evaluation of its function in disulfide bond formation," *Antioxidants and Redox Signaling*, vol. 11, no. 11, pp. 2807–2850, 2009.

[181] N. J. Bulleid and L. Ellgaard, "Multiple ways to make disulfides," *Trends in Biochemical Sciences*, 2011.

[182] S. Chakravarthi, C. E. Jessop, and N. J. Bulleid, "The role of glutathione in disulphide bond formation and endoplasmic-reticulum-generated oxidative stress," *EMBO Reports*, vol. 7, no. 3, pp. 271–275, 2006.

[183] J. Lundström and A. Holmgren, "Determination of the reduction-oxidation potential of the thioredoxin-like domains of protein disulfide-isomerase from the equilibrium with glutathione and thioredoxin," *Biochemistry*, vol. 32, no. 26, pp. 6649–6655, 1993.

[184] E. Gross, C. S. Sevier, N. Heldman et al., "Generating disulfides enzymatically: reaction products and electron acceptors of the endoplasmic reticulum thiol oxidase Ero1p," *Proceedings of the National Academy of Sciences of the United States of America*, vol. 103, no. 2, pp. 299–304, 2006.

[185] P. I. Merksamer, A. Trusina, and F. R. Papa, "Real-time redox measurements during endoplasmic reticulum stress reveal interlinked protein folding functions," *Cell*, vol. 135, no. 5, pp. 933–947, 2008.

[186] J. W. Cuozzo and C. A. Kaiser, "Competition between glutathione and protein thiols for disulphide-bond formation," *Nature Cell Biology*, vol. 1, no. 3, pp. 130–135, 1999.

[187] L. A. Rutkevich, M. F. Cohen-Doyle, U. Brockmeier, and D. B. Williams, "Functional relationship between protein disulfide isomerase family members during the oxidative folding of human secretory proteins," *Molecular Biology of the Cell*, vol. 21, no. 18, pp. 3093–3105, 2010.

[188] Y. Honjo, S. Kaneko, H. Ito et al., "Protein disulfide isomerase-immunopositive inclusions in patients with amyotrophic lateral sclerosis," *Amyotrophic Lateral Sclerosis*, vol. 12, no. 6, pp. 444–450, 2011.

[189] H. Tsuda, S. M. Han, Y. Yang et al., "The amyotrophic lateral sclerosis 8 protein VAPB is cleaved, secreted, and acts as a ligand for Eph receptors," *Cell*, vol. 133, no. 6, pp. 963–977, 2008.

[190] D. M. Townsend, Y. Manevich, H. Lin et al., "Nitrosative stress-induced S-glutathionylation of protein disulfide isomerase leads to activation of the unfolded protein response," *Cancer Research*, vol. 69, no. 19, pp. 7626–7634, 2009.

[191] T. Uehara, T. Nakamura, D. Yao et al., "S-Nitrosylated protein-disulphide isomerase links protein misfolding to neurodegeneration," *Nature*, vol. 441, no. 7092, pp. 513–517, 2006.

[192] X. Chen, C. Li, T. Guan et al., "S-nitrosylated protein disulphide isomerase contributes to mutant SOD1 aggregates in amyotrophic lateral sclerosis," *Journal of Neurochemistry*, vol. 124, no. 1, pp. 45–58, 2012.

[193] J. D. Rothstein, "Therapeutic horizons for amyotrophic lateral sclerosis," *Current Opinion in Neurobiology*, vol. 6, no. 5, pp. 679–687, 1996.

[194] D. W. Cleveland, "Neuronal growth and death: order and disorder in the axoplasm," *Cell*, vol. 84, no. 5, pp. 663–666, 1996.

7.2.4 Supplementary Figure 3

The results presented in the published manuscript: Walker, A. K., et al. (2013) "***ALS-associated TDP-43 induces endoplasmic reticulum stress, which drives cytoplasmic TDP-43 accumulation and stress granule formation"***. *PloS one* **8**: 1-12 the author performed all the experiments presented in figure 4, described in the Results section of the manuscript on page e81170 titled '**Over-expression of mutant TDP-43 induces ER stress to a greater extent than wild-type TDP-43**'.

OPEN ACCESS Freely available online

PLOS ONE

ALS-Associated TDP-43 Induces Endoplasmic Reticulum Stress, Which Drives Cytoplasmic TDP-43 Accumulation and Stress Granule Formation

Adam K. Walker[1,2¤], Kai Y. Soo[1], Vinod Sundaramoorthy[1], Sonam Parakh[1], Yi Ma[2], Manal A. Farg[1], Robyn H. Wallace[3], Peter J. Crouch[2,4], Bradley J. Turner[2], Malcolm K. Horne[2,5,6], Julie D. Atkin[1,2]*

1 Department of Biochemistry, La Trobe Institute for Molecular Science, La Trobe University, Bundoora, Victoria, Australia, **2** Florey Institute of Neuroscience and Mental Health, The University of Melbourne, Parkville, Victoria, Australia, **3** Queensland Brain Institute and School of Chemistry and Molecular Biosciences, The University of Queensland, Brisbane, Queensland, Australia, **4** Department of Pathology, The University of Melbourne, Parkville, Victoria, Australia, **5** Florey Department of Neuroscience and Mental Health, Faculty of Medicine, Dentistry & Health Sciences, The University of Melbourne, Parkville, Victoria, Australia, **6** Saint Vincent's Hospital, Fitzroy, Victoria, Australia

Abstract

In amyotrophic lateral sclerosis (ALS) and frontotemporal lobar degeneration, TAR DNA binding protein 43 (TDP-43) accumulates in the cytoplasm of affected neurons and glia, where it associates with stress granules (SGs) and forms large inclusions. SGs form in response to cellular stress, including endoplasmic reticulum (ER) stress, which is induced in both familial and sporadic forms of ALS. Here we demonstrate that pharmacological induction of ER stress causes TDP-43 to accumulate in the cytoplasm, where TDP-43 also associates with SGs. Furthermore, treatment with salubrinal, an inhibitor of dephosphorylation of eukaryotic initiation factor 2-α, a key modulator of ER stress, potentiates ER stress-mediated SG formation. Inclusions of C-terminal fragment TDP-43, reminiscent of disease-pathology, form in close association with ER and Golgi compartments, further indicating the involvement of ER dysfunction in TDP-43-associated disease. Consistent with this notion, over-expression of ALS-linked mutant TDP-43, and to a lesser extent wildtype TDP-43, triggers several ER stress pathways in neuroblastoma cells. Similarly, we found an interaction between the ER chaperone protein disulphide isomerase and TDP-43 in transfected cell lysates and in the spinal cords of mutant A315T TDP-43 transgenic mice. This study provides evidence for ER stress as a pathogenic pathway in TDP-43-mediated disease.

Citation: Walker AK, Soo KY, Sundaramoorthy V, Parakh S, Ma Y, et al. (2013) ALS-Associated TDP-43 Induces Endoplasmic Reticulum Stress, Which Drives Cytoplasmic TDP-43 Accumulation and Stress Granule Formation. PLoS ONE 8(11): e81170. doi:10.1371/journal.pone.0081170

Editor: Weidong Le, Institute of Health Science, China

Received February 21, 2013; **Accepted** October 9, 2013; **Published** November 29, 2013

Funding: This work was supported by the National Health and Medical Research Council of Australia (NHMRC, grants 454749, 1005651, 1006141, 1030513), www.nhmrc.gov.au, Amyotrophic Lateral Sclerosis Association, www.alsa.org, Bethlehem Griffiths Research Council, www.bethlehemgrf.com.au, a Henry H Roth Charitable Foundation Grant from the MND Research Institute of Australia, www.mndaust.asn.au/mndria, Australian Rotary Health, www.australianrotaryhealth.org.au, and the Brain Foundation, www.brainfoundation.org.au. AKW holds an NHMRC CJ Martin Biomedical Early Career Fellowship (1036835). The funders had no role in study design, data collection and analysis, decision to publish, or preparation of the manuscript.

Competing Interests: The authors have declared that no competing interests exist.

* E-mail: j.atkin@latrobe.edu.au

¤ Current address: Center for Neurodegenerative Disease Research, Department of Pathology and Laboratory Medicine, Perelman School of Medicine, University of Pennsylvania, Philadelphia, Pennsylvania, United States of America

Introduction

TAR DNA-binding protein 43 (TDP-43) is a protein constituent of pathologic cytoplasmic and intranuclear inclusions in neurons and glia of patients with sporadic and familial forms of amyotrophic lateral sclerosis (ALS) and frontotemporal lobar degeneration (FTLD) [1,2]. While predominantly a nuclear protein, a proportion of TDP-43 is cytoplasmic, even under normal conditions [3,4,5]. When nuclear localisation sequences of TDP-43 are genetically ablated, the protein accumulates in the cytoplasm and forms inclusions that are similar to those seen in disease [4,6]. Recently, it was shown that under cellular stress, TDP-43 accumulates in the cytoplasm and forms cytoplasmic stress granules (SGs) [7,8,9]. The sub-cellular location of the inclusions and the effects of TDP-43 inclusions on cellular physiology are not well known. Also, the relationship between SGs and inclusions remains controversial, although SGs could represent a precursor to TDP-43 inclusions [9,10].

SGs form rapidly in response to a variety of cellular insults and lead to translational repression of incorporated mRNAs [11]. SG assembly is usually initiated by the phosphorylation of eukaryotic initiation factor 2 alpha (eIF2α), which inhibits formation of the ternary complex ($eIF2/GTP/tRNA^{Met}$) required to initiate protein translation [12,13]. Although the specific stressors which direct TDP-43 to SGs *in vivo* remain unclear, conditions including endoplasmic reticulum (ER) stress, heat shock, oxidative stress, osmotic stress, and serum deprivation can all cause TDP-43-positive SG formation in certain cell types in cell culture systems [14]. Interestingly, different cell types display different levels of recruitment of TDP-43 to SGs in response to various stressors. For example, thapsigargin, which perturbs intracellular calcium stores and is widely used to induce ER stress, was previously shown to induce TDP-43 recruitment to SGs in HeLa cells but not in

Neuro2a cells [8,15]. Whether or not modulation of TDP-43 recruitment to SGs has an effect on disease-relevant processes, such as inclusion formation, remains debated [14]. However, alterations in TDP-43 levels alter SG dynamics, suggesting that SG changes could occur in disease [8].

ER stress and induction of the unfolded protein response (UPR) are central to ALS pathophysiology [16]. When the UPR is induced three distinct signalling pathways are activated, mediated by inositol requiring kinase 1 (IRE1), activating transcription factor 6 (ATF6), and protein-kinase-like endoplasmic reticulum kinase (PERK) [17,18,19]. IRE1 activation leads to the splicing of X-box binding protein 1 (XBP-1) mRNA within the nucleus to produce a functional transcription factor. When ATF6 is activated, it is transported to the cis-Golgi compartment and is cleaved to produce an active transcription factor. In addition, activation of PERK causes general translational repression by stimulating SG formation via phosphorylation of eIF2α. Other consequences of UPR induction include up-regulation of ER chaperones, such as protein disulphide isomerise (PDI) [20]. Although initially protective, if unresolved, the UPR triggers apoptosis by ER stress-specific cell death signals, including induction of C/EBP-homologous protein (CHOP) via the PERK and ATF6 pathways [21,22].

ER stress precedes the appearance of clinical features in ALS-linked mutant superoxide dismutase 1 (SOD1) transgenic rodents [23], and genetic manipulation of ER stress mediators modulates disease in these animals [24,25]. ER stress is present in sporadic and familial forms of ALS, including those cases caused by mutations in fused in sarcoma (FUS), which bears structural and functional similarities to TDP-43 [23,26,27]. Increased genetic susceptibility to ER stress has also been linked with ALS [28]. Although TDP-43 is C-terminally fragmented and hyper-phosphorylated in disease [1], the factors which trigger these changes remain poorly defined. However, ER stress also causes TDP-43 fragmentation in cell culture [15,29] and over-expression of TDP-43 causes changes in CHOP and XBP-1 signalling in cell culture and rat models of TDP-43-linked disease [30,31].

The chaperone protein disulphide isomerase (PDI) is induced by ER stress and is up-regulated in human sporadic ALS and in animal models of mutant SOD1-linked ALS [23,32,33]. PDI may protect against ER stress, inclusion formation and cell death associated with mutant SOD1 expression by modulating abnormal disulphide bond formation [27,34]. In addition, the cellular distribution of PDI in mutant SOD1 transgenic mice modifies disease processes [35] and PDI is a constituent of TDP-43-positive or FUS-positive inclusions found in motor neurons of ALS patients [26,36]. Cross-linking of TDP-43 via disulphide bonds alters its conformation and function [37], suggesting that PDI is a potential candidate for proteins that interact with TDP-43 and prevent TDP-43 misfolding.

In this study we examined whether ER stress could act as a stressor that leads to cytoplasmic accumulation of TDP-43 and subsequent incorporation of TDP-43 into SGs. Six different ALS-linked TDP-43 mutants were examined: A315T and M337V, which have been reported in multiple familial ALS pedigrees [38,39,40,41,42,43]; D169G, the only ALS-linked mutation identified that lies outside the C-terminal region [39]; and G294A, Q331K and N390D, which have been identified in sporadic ALS patients [39,40]. Pharmacological induction of ER stress in cell culture led to cytoplasmic accumulation of wildtype TDP-43 and all six TDP-43 mutants. Furthermore, ER stress caused the rapid incorporation of TDP-43 into cytoplasmic SGs. This process was enhanced by pharmacological treatment with salubrinal to inhibit the deactivation of eIF2α, a key upstream modulator of ER stress. We also demonstrate that C-terminal TDP-43 fragments form inclusions in close association with PDI and the ER/Golgi apparatus, suggesting that TDP-43 inclusion formation causes dysfunction of ER/Golgi components. Moreover, over-expression of mutant TDP-43, and to a lesser extent wildtype TDP-43, induced ER stress via several UPR pathways, including activation of XBP-1 and ATF6, thus linking ER stress to neurodegeneration. Finally we show up-regulation of PDI in the spinal cords of transgenic mutant A315T TDP-43 mice, and interaction of mutant TDP-43 with PDI, providing further evidence of an ER-associated protective response in TDP-43 proteinopathies.

Materials and Methods

DNA constructs

Site-directed mutagenesis was performed to remove the stop codon and insert a unique *Bam*HI restriction enzyme site into a pcDNA3.1(+) Myc-tagged human TDP-43-encoding construct [4]. The Myc-TDP-43 sequence was inserted between *Hind*III and *Bam*HI restriction sites in pmCherry.N1 (Clontech), to allow expression of human TDP-43 with a C-terminal mCherry tag. The subsequent wildtype Myc-TDP-43-mCherry construct was used as a template to produce six ALS-linked mutant TDP-43 expressing vectors (D169G, G294A, A315T, Q331K, M337V, N390D) by QuikChange site-directed mutagenesis (Stratagene) according to the manufacturer's instructions. The 218–414 TDP-43-mCherry construct was produced by cloning of a PCR product from a primer incorporating a unique *Hind*III restriction enzyme site immediately 5′ to the M218 codon of TDP-43 into a pCR2.1-TOPO vector (Invitrogen) with subsequent sub-cloning into pmCherry.N1 using *Hind*III and *Bam*HI restriction sites. EGFP-TDP-43 constructs were as described previously [7,44]. For the detection of ER stress, an ATF6-EGFP reporter construct (Addgene plasmid 32955) was used [45]. For co-immunoprecipitation experiments, a vector encoding PDI with a V5 epitope tag was used [46].

Cell culture

Mouse neuroblastoma Neuro2a (ATCC cell line CCL-131), human epithelial HeLa (ATCC cell line CCL-2) and human embryonic kidney HEK293T cell lines were maintained in high glucose DMEM (Gibco) with 10% heat-inactivated fetal calf serum (Gibco), 100 μg/mL penicillin and 100 μg/mL streptomycin. Cells were treated as indicated with thapsigargin (Sigma) to induce ER stress, MG132 (Sigma) to inhibit proteasomal function, cycloheximide (Sigma) as a general translation inhibitor, and arsenite (Sigma) as a standard oxidative stress inducer of SGs. For immunocytochemistry, cells were plated on poly-L-lysine-coated 12 mm glass coverslips. Cells were transfected with constructs using Lipofectamine2000 with PLUS reagent (Invitrogen) according to the manufacturer's protocol. Cell lysates were collected in TN buffer (50 mM Tris-HCl pH 7.5 and 150 mM NaCl) with 0.1% SDS, 1% protease inhibitor cocktail (Sigma) and 1% phosphatase inhibitor (Sigma) by incubation on ice for 10 min. The supernatant was cleared by centrifugation at 16,100 *g* for 10 min (the SDS-soluble fraction). Protein concentrations of cell and tissue lysates were determined using the BCA protein assay (Thermo Scientific) by comparison with bovine serum albumin (BSA) standards.

Immunocytochemistry and microscopy

Cells were fixed with 4% paraformaldehyde at room temperature for 15 min, permeabilised with 0.1% triton X-100 in PBS for

10 min and then blocked with blocking buffer (1% BSA in 0.03% triton X-100 in PBS) for 30 min at room temperature. Primary antibodies were diluted in blocking buffer and incubated overnight at 4°C. Primary antibodies were: mouse anti-PDI Ab2792 (Abcam), rabbit anti-TDP-43 10782 (Protein Tech Group), mouse anti-HuR 39-0600 (Invitrogen), rabbit anti-ERGIC53 E1031 (Sigma), rabbit anti-XBP-1 sc-7160 (Santa Cruz), mouse anti-GADD153/CHOP sc-7351 (Santa Cruz) and mouse anti-GM130 610823 (BD Transduction Labs). Cells were washed in PBS and then incubated with secondary antibody at 1:5000 in PBS for 1 h at room temperature. Secondary antibodies used were: goat-anti-rabbit IgG AlexaFluor® 488/594, goat anti-mouse IgG AlexaFluor® 647 or rabbit-anti-mouse IgG AlexaFluor® 488 (all from Molecular Probes). Nuclei were stained using TO-PRO®-3 Iodide stain (Invitrogen), Hoechst 33342 or DAPI diluted 1:2000-1:10000 in PBS for 10 min. Images were acquired with constant gain and offset settings where appropriate using an Olympus Fluoview 1000 inverted confocal laser-scanning microscope or an Olympus IX81 inverted fluorescence microscope with Olympus digital camera. For SG quantification, 40X images of at least five random fields of view taken at ½ radius of the coverslip were used for analysis from at least three independent experiments. Cells bearing two or more HuR-positive and/or TDP-43-positive non-nuclear foci of greater than ~1 μm in diameter were counted as cells containing SGs using ImageJ software. For detection of ER stress, 120 cells were counted in each group. An ATF6-GFP reporter construct was co-expressed with TDP-43 constructs and cells were immunostained for GM130 to visualise the Golgi apparatus. Cells in which ATF6 fluorescence co-localised with GM130 fluorescence, indicating translocation of ATF6 to the Golgi, were scored as having ER stress [45]. For detection of XBP-1 activation, cells were transfected with TDP-43 constructs and immunostained for XBP-1. Cells in which XBP-1 immunoreactivity was higher in the nucleus than the cytoplasm were scored as having ER stress, similar to previous studies [26,47]. Likewise, cells with nuclear immunoreactivity for CHOP were scored as having ER stress, as performed previously [27].

Transgenic mice

A315T TDP-43 transgenic mice were obtained from Jackson Laboratories and bred on a C57BL/6 background [48]. Experimental procedures and housing conditions for animals were approved by the University of Queensland and University of Melbourne Animal Ethics Committees. Spinal cords of three transgenic female mice at symptom onset (p92, p97 and p102) and age- and gender-matched non-transgenic littermate controls were analysed in triplicate by SDS-PAGE and immunoblotting. For immunohistochemistry, spinal cords of two male transgenic mice at p79 and p83 were analysed with matched non-transgenic littermates.

SDS-PAGE and immunoblotting

Protein samples were electrophoresed through SDS-polyacrylamide gels and transferred to nitrocellulose membranes. Membranes were blocked with 5% skim-milk in TBS or 3% BSA in TBS-T for 30 min then incubated with primary antibodies at 4°C for 12–16 h. Primary antibodies used were: mouse anti-FLAG M2 (Sigma), mouse anti-β-actin AC-15 (Sigma), mouse anti-TDP-43 2E2-D3 (Abnova), rabbit anti-PDI SPA-890 (Stressgen), mouse anti-V5 R960-25 (Invitrogen) and rabbit anti-red fluorescent protein (RFP; Affinity Bioreagents). Membranes were incubated with secondary antibodies for 1 h at room temperature. Secondary antibodies used were: HRP-conjugated goat anti-rabbit AB132P or goat anti-mouse AB326P at 1:10000 (both from Chemicon). Signals were detected using ECL reagent (Roche) with Biomax MR film (Kodak) or ChemiDoc imaging system (BioRad). Densitometry of immunoblots was performed using ImageJ software (NIH).

Immunoprecipitation

Cell lysates (1 mg protein) at 24 hr post-transfection were incubated with anti-PDI or anti-RFP antibody or irrelevant, isotype-matched control antibody (anti-HA, Sigma) and 100 μl 50% (wt/vol) protein A-Sepharose CL-4B (Amersham Biosciences) in TN buffer with 0.5% NP40 and incubated on a rotating wheel overnight at 4°C. Samples were centrifuged at 2000 *g* for 2 min, and Sepharose pellets were washed twice in TN buffer + NP40. For immunoblotting, immunoprecipitates were liberated by boiling in 4× SDS sample buffer with 20% β-mercaptoethanol.

Statistical analyses

Data are presented as mean ± standard error of the mean (SEM) from at least three independent experiments and were analysed by unpaired t-test or ANOVA followed by Bonferonni's post-test unless otherwise stated. $p<0.05$ was considered statistically significant.

Results

Sub-cellular location of wildtype and mutant TDP-43-mCherry proteins

Six TDP-43 mutations previously linked to ALS were chosen for investigation in this study: A315T, M337V, D169G, G294A, Q331K and N390D [38,39,40,41,42,43]. The cellular distribution of mCherry tagged proteins was analysed in Neuro2a cells using confocal microscopy. In contrast to the diffuse cytoplasmic staining of mCherry, transiently transfected TDP-43-mCherry constructs resulted in punctate fluorescence confined to, but dispersed throughout, the nucleus with exclusion from nucleoli (Fig. 1A) This distribution is similar to previous observations for endogenous TDP-43 [5,49,50] and confirms correct targeting of the fusion proteins (Fig. 1A).

There was moderate cytoplasmic fluorescence in approximately 10–20% of cells expressing either wildtype or mutant TDP-43-mCherry (Fig. 1C). The sub-cellular distribution of the wildtype and mutant proteins were similar and inclusions were not observed. Wildtype and mutant TDP-43-mCherry proteins (~70 kDa) were detected at levels similar to the endogenous protein with a transfection efficiency of approximate 50%, suggesting an approximate two-fold expression level of the fusion protein compared to endogenous in transfected cells (Fig. 1B).

ER stress causes redistribution of TDP-43 from the nucleus to the cytoplasm

ER stress was chronically induced in Neuro2a cells expressing TDP-43–mCherry by treating with 100 nM thapsigargin for 24 h. The cells were fixed 48 h after transfection, and examined by confocal fluorescence microscopy. Cytoplasmic TDP-43-mCherry was detected in approximately 50% of wildtype and mutant TDP-43 expressing cells treated with thapsigargin, compared with 10–20% of untreated cells (Fig. 1D). In comparison, cytoplasmic TDP-43-mCherry fluorescence was observed in almost all cells (95%) treated for 24 h with 10 μM MG132, a proteasome inhibitor [51] (Fig. 1E). Neither treatment caused cell death, and TDP-43-mCherry-positive inclusions were not observed in any of the conditions examined. Hence both ER stress and proteasome

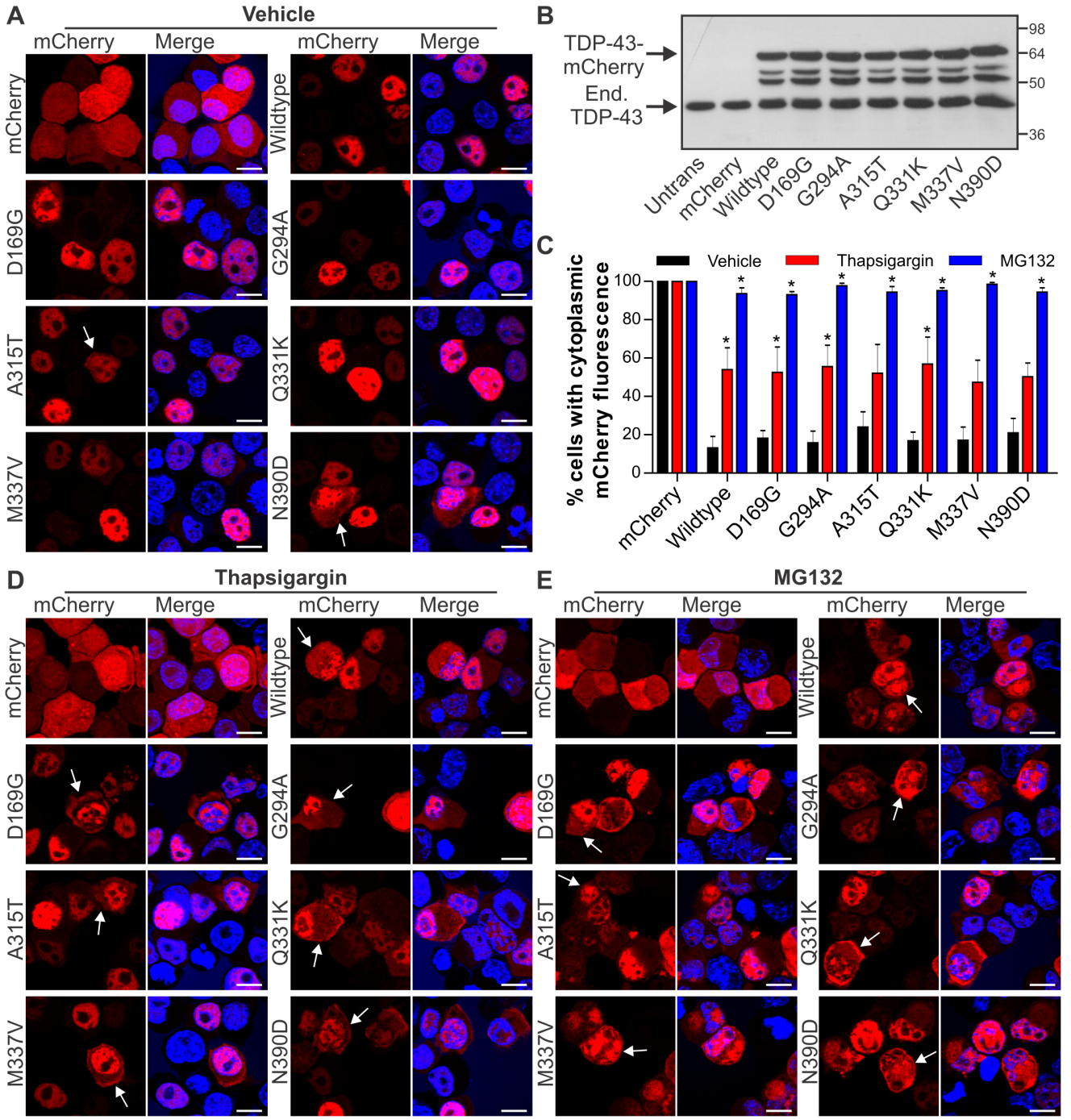

Figure 1. ER stress and proteasome inhibition cause redistribution of wildtype and ALS-linked mutant TDP-43. (**A**) Neuro2a cells were transfected with the construct indicated to the left of each series of panels (mCherry alone, wildtype TDP-43-mCherry, or mutant D169G, G294A, A315T, Q331K, M337V or N390D TDP-43-mCherry), and fixed at 48 h post-transfection. mCherry fluorescence is shown in the left panels, and Hoechst nuclei stain is shown in the merged right panels. Note the largely nuclear distribution of wildtype and mutant TDP-43-mCherry, but with low levels of non-nuclear mCherry fluorescence in some cells, indicated by arrows. (**B**) Immunoblot of cell lysates expressing mCherry alone or wildtype or mutant TDP-43-mCherry showing equal expression levels of all proteins, and levels of endogenous (End.) TDP-43. Approximate molecular weight markers are shown on the right. (**C**) Quantification of the effect of thapsigargin or MG132 treatment on the percentage of Neuro2a cells with cytoplasmic mCherry fluorescence. Results are expressed as mean ± SEM, $n=3$, *$p<0.05$ versus respective vehicle treated controls by two-way ANOVA with Bonferroni's post-test. (**D**) Neuro2a cells were transfected as in **A** and treated with 100 nM thapsigargin for 24 h prior to fixation. (**E**) Neuro2a cells were transfected as in **A** and treated with 10 μM MG132 for 24 h prior to fixation. Note the increased non-nuclear distribution of wildtype and mutant TDP-43-mCherry with both thapsigargin and MG132 treatment, indicated by arrows. All scale bars represent 10 μm.
doi:10.1371/journal.pone.0081170.g001

inhibition result in accumulation of both wildtype and mutant TDP-43 in the cytoplasm of cells without inclusion formation.

ER stress causes TDP-43-positive stress granule formation which is enhanced by salubrinal pre-treatment

SG formation was identified by immunoreactivity to antibodies against the SG component Hu-antigen R (HuR) [11] in HeLa cells, in which SGs can be readily visualised due to cell morphology. Cells were pre-treated with either salubrinal (50 μM) or cycloheximide (50 μg/mL) and then either ER stress (using thapsigargin) or oxidative stress (using arsenite) was acutely induced, with appropriate vehicle-treated controls in both pre-treatment and stress conditions. The purpose of salubrinal pre-treatment was to potentiate induction of the PERK-mediated ER stress pathway by inhibiting eIF2α dephosphorylation [52], whereas cycloheximide, which prevents SG formation by inhibiting translation, was used as a negative control.

Both TDP-43 and HuR were located primarily in the nucleus with no evident cytoplasmic puncta in the vast majority of vehicle treated cells regardless of pre-treatment with either vehicle control, 50 μM salubrinal or 50 μg/mL cycloheximide (Fig. 2A). Treatment with arsenite, which is a typical SG inducer, caused HuR-positive SG formation in 95–100% of vehicle or salubrinal pre-treated cells, which was completely inhibited by cycloheximide pre-treatment (Fig. 2B). However, TDP-43-positive SGs were rarely observed in arsenite-treated cells under these conditions (Fig. 2B, D), similar to previous findings in HEK293 cells [9]. Cytoplasmic puncta positive for TDP-43 but negative for HuR were rarely observed under any of the treatment conditions used. Salubrinal pre-treatment did not alter the percentage of cells bearing SGs or the percentage of TDP-43-positive SGs following arsenite-induced oxidative stress.

Next, the role of ER stress in SG assembly was investigated by acutely treating vehicle-, salubrinal- or cycloheximide-pre-treated cells with 10 μM thapsigargin for 1 h, which is consistent with conditions reported by others previously to induce SGs [53,54]. Approximately 20% of cells showed HuR-positive/TDP-43-negative SGs in both vehicle- or salubrinal-pre-treated conditions upon thapsigargin treatment, whereas SGs were not formed in thapsigargin treated cells pre-treated with cycloheximide (Fig. 2C, D). Additionally, thapsigargin treatment caused 20–30% of vehicle-pre-treated cells to form SGs positive for both HuR and TDP-43. Furthermore, salubrinal pre-treatment significantly increased the percentage of cells with HuR-positive/TDP-43-positive SGs to approximately 50%, but did not change the percentage of cells bearing HuR-positive/TDP-43-negative SGs, upon thapsigargin treatment (Fig. 2D). Overall, salubrinal pre-treatment increased the percentage of thapsigargin treated cells bearing HuR-positive SGs (with or without TDP-43) from ~40% in controls to ~75% (Fig. 2D).

These results demonstrate that ER stress is a potent inducer of TDP-43 recruitment to SGs, and that inhibiting eIF2α dephosphorylation with salubrinal specifically enhances the formation of TDP-43-positive SGs. Recruitment of TDP-43 to cytoplasmic SGs appeared to be specifically related to ER stress since treatment with arsenite to induce oxidative stress did not cause TDP-43 redistribution to SGs under the conditions used in these experiments.

C-terminal TDP-43 forms peri-nuclear inclusions that associate with markers of the ER-Golgi compartments

The sub-cellular positioning, relative to ER-Golgi proteins, of SGs formed by endogenous TDP-43 in thapsigargin-stressed was examined in HeLa cells, because their flat extended morphology lends itself to the examination of protein co-location using confocal microscopy. The TDP-43-positive SGs did not co-locate with PDI or markers of the ER or the Golgi apparatus (KDEL and ERGIC-53), implying that they form in the cytoplasm and outside of the ER-Golgi system (data not shown). We next produced a vector to allow expression of mCherry-tagged TDP-43 residues 218-414 (Fig. 3), since full-length wildtype or mutant TDP-43-mCherry did not form inclusions when expressed in several mouse or human cell lines (Fig. 1, Fig. 4 and data not shown). TDP-43 residues 218-414 correspond to the potentially pathogenic ~20 kDa caspase cleavage product previously shown to be a highly aggregate-prone species of TDP-43 [6,44,55].

Under basal conditions, the expression of 218–414 TDP-43-mCherry could not be detected by immunoblotting up to 72 h after transient transfection in Neuro2a cells, however diffuse cytoplasmic mCherry fluorescence was evident under confocal microscopy at very low levels in a small proportion of cells (Fig. 3A). In contrast, approximately 70% of cells treated with the proteasome inhibitor MG132 formed large juxta-nuclear inclusions that partially displaced the nucleus and were reminiscent of inclusions seen in human pathology (Fig. 3B). These data indicate that in cell culture, 218–414 TDP-43-mCherry is degraded rapidly by the proteasome, but that large inclusions form when the proteasome is inhibited.

Neuro2a or HeLa cells were transiently transfected with 218–414 TDP-43-mCherry, treated with MG132 and the sub-cellular location of 218–414 TDP-43-mCherry inclusions, relative to PDI and other proteins of the ER and Golgi apparatus was examined by immunocytochemistry. Small peri-nuclear inclusions accompanied by one or two larger juxta-nuclear inclusions were observed in most cells (Fig. 3C–E). These inclusions were surrounded by PDI, which is predominately found in the ER, consistent with a recent report describing the co-location of PDI with TDP-43 in sporadic ALS tissues (Fig. 3C) [36]. The relative locations of 218–414 TDP-43-mCherry inclusion and markers of the Golgi apparatus and ER-Golgi intermediate compartment (ERGIC, a distinct organelle which mediates trafficking between the ER and Golgi apparatus) was then examined. The large juxta-nuclear inclusions formed in close association with the cis-Golgi marker GM130 (Fig. 3D), often surrounding regions of GM130 immunoreactivity (Video S1). The 218–414 TDP-43-mCherry inclusions also showed partial co-location with the ERGIC marker, ERGIC-53 (Fig. 3E). Overall, these results indicate that 218–414 TDP-43 inclusions form adjacent to the nucleus and in close association with the Golgi and ERGIC when the proteasome is inhibited. The association between inclusions and TDP-43 pathology thus indicates possible disturbance of ER-Golgi transport function in ALS.

Over-expression of mutant TDP-43 induces ER stress to a greater extent than wildtype TDP-43

In the well-studied model of ALS induced by mutant forms of SOD1, ER stress and UPR induction precede inclusion formation [27,32,56]. Hence we asked whether wildtype and mutant TDP-43 can induce ER stress in cell culture. CHOP is a pro-apoptotic protein induced predominately via the PERK and ATF6 UPR pathways and its levels are a useful marker of UPR induction. We observed that at 18–24 h post-transfection, a greater proportion of Neuro2a cells demonstrated cytoplasmic rather than nuclear TDP-43, whereas after 24 h TDP-43 localised predominately in the nucleus. Hence we examined cells for induction of ER stress at 18 h post-transfection, CHOP levels in Neuro2a cells, measured by immunocytochemistry, were slightly but significantly greater in

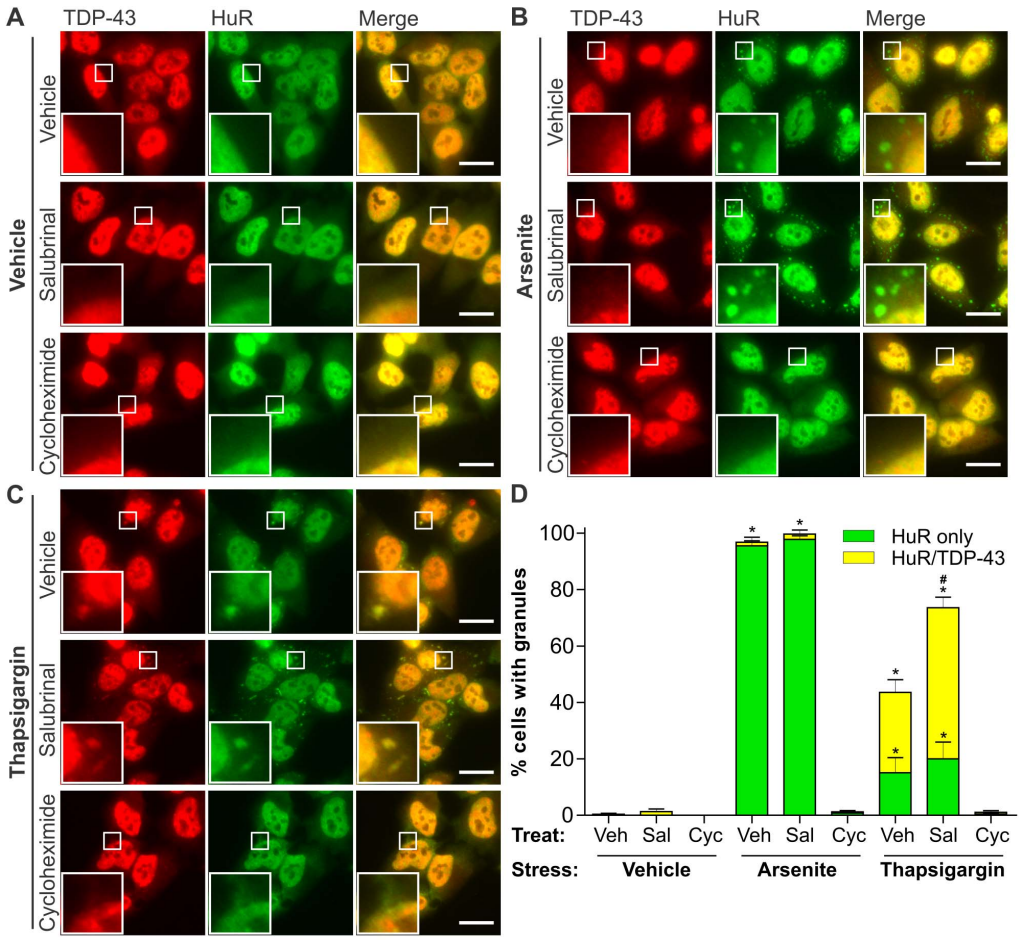

Figure 2. Formation of ER stress-induced TDP-43-positive stress granules is enhanced by salubrinal pre-treatment. HeLa cells were pre-treated for 2 h with either vehicle control, 50 μM salubrinal or 50 μg/mL cycloheximide and then stressed for an additional 1 h by treatment with vehicle control (**A**), 0.5 mM arsenite (**B**), or 10 μM thapsigargin (**C**) in the presence of the respective pre-treatment conditions. Cells were processed for immunocytochemistry using antibodies against TDP-43 (left panels) and HuR (middle panels). Merged images are shown on the right. Boxed regions in the main panels are shown magnified in the bottom left of each panel. (**D**) Quantification of the effect of aresenite or thapsigargin in the presence of salubrinal or cycloheximide on the formation of HuR-positive or HuR/TDP-43-positive cytoplasmic SGs. Results are expressed as mean ± SEM, $n = 3$, *$p < 0.05$ versus respective vehicle-treated controls, #$p < 0.05$ versus vehicle pre-treated/thapsigargin treated control, by two-way ANOVA followed by Bonferroni's post-test. All scale bars represent 20 μm.
doi:10.1371/journal.pone.0081170.g002

cells expressing wildtype TDP-43-mCherry compared to mCherry alone. Furthermore, CHOP levels in cells expressing two ALS-linked TDP-43 mutants, A315T or Q331K, were dramatically increased compared to both mCherry alone or wildtype TDP-43-mCherry (Fig. 4A). This was subsequently confirmed using EGFP-tagged TDP-43 Q331K and another ALS mutant, Q343R, showing increased CHOP activation in mutant expressing cells compared to control cells expressing EGFP alone or wildtype EGFP-TDP-43 (Fig. 4A–B).

Others have made the observation that CHOP, but no other UPR marker, is up-regulated following viral overexpression of wildtype TDP-43 in cell culture [31]. However, we examined additional markers of ER stress in Neuro2a cells using single-cell immunocytochemical analysis, which allows analysis of only transfected cells rather than analysis of the entire population as occurs using immunoblotting techniques [26,27,57,58]. IRE1 activation was measured by detection of nuclear XBP-1. Over-expression of wildtype TDP-43-mCherry slightly but significantly increased XBP-1 activation compared to mCherry expressing cells (Fig. 4C–D). Furthermore, XBP-1 activation was dramatically increased by expression of A315T or Q331K mutant TDP-43-mCherry compared to both mCherry alone or wildtype TDP-43-mCherry. Finally, over-expression of wildtype TDP-43-mCherry slightly increased activation of ATF6 compared to mCherry expressing cells, although this did not reach statistical significance. However, over-expression of Q331K mutant TDP-43-mCherry significantly increased activation of ATF6 (Fig. 4E–F). These data indicate that ALS-linked mutant TDP-43 proteins activate the major signalling pathways of ER stress. Furthermore, over-expression of wildtype TDP-43 also induces ER stress, but to a lesser extent than mutant TDP-43.

PDI co-immunoprecipitates with mutant TDP-43 and is up-regulated in transgenic A315T mutant TDP-43 mouse spinal cord

We showed that mutant TDP-43 induces ER stress and since abnormal TDP-43 disulphide bonding occurs in FTLD [37], we next examined the possibility that the ER disulphide-modulating chaperone PDI, which was previously implicated in mutant SOD1-linked and sporadic ALS [23,32], was also involved in

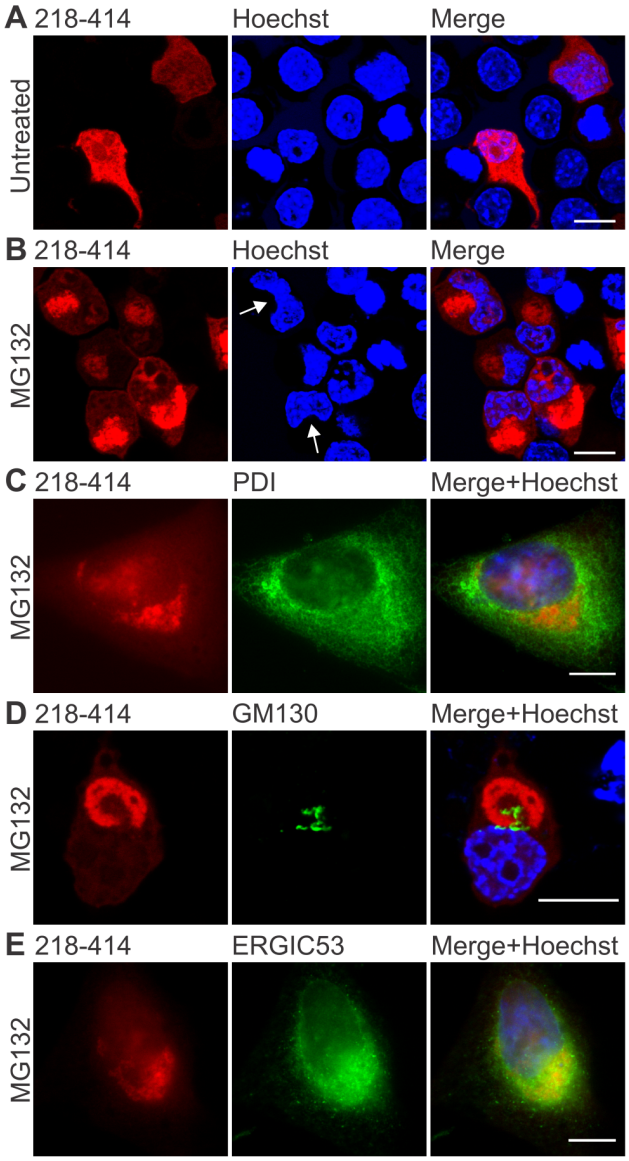

Figure 3. C-terminal 218–414 TDP-43 inclusions form in association with the Golgi and ER. (**A, B**) Expression of wildtype 218–414 TDP-43-mCherry in Neuro2a cells, with mCherry fluorescence (left images), Hoechst nuclei stain (middle images), and merged images (right). Panel **A** shows untreated cells, and panel **B** shows cells treated with 10 μM MG132 for 24 h. Arrows indicate nuclei showing distorted morphology, due to the presence of inclusions. Note that the mCherry fluorescence image shown in **A** was captured using increased gain and offset settings compared to that shown in **B** in order to allow detection. (**C**) MG132-treated HeLa cells expressing 218–414 TDP-43-mCherry (red, left image), with immunocytochemistry for PDI (green, middle image). (**D**) Neuro2a cells were transfected and treated as in **B** and processed for immunocytochemistry against GM130 (green, middle image). In MG132-treated HeLa cells expressing 218-414 TDP-43-mCherry (red, left image), immunocytochemistry is shown for (**E**) ERGIC53 (green, middle image). Merged images shown with Hoechst nuclei stain are on the right. All scale bars represent 10 μm.
doi:10.1371/journal.pone.0081170.g003

TDP-43-linked disease. Immunoprecipitation was used to examine interactions between PDI and TDP-43. Lysates from Neuro2a cells transfected with TDP-43-mCherry constructs were immunoprecipitated using an anti-PDI antibody, and immunoblot analysis revealed that mutant Q331K TDP-43, and to a lesser extent wildtype TDP-43, co-precipitated with PDI (Fig. 5A). Control reactions containing buffer only, untransfected cells or precipitation of Q331K TDP-43 cell lysates using an irrelevant, isotype-matched control antibody were negative, demonstrating a specific interaction between PDI and TDP-43. To confirm the interaction, we also performed co-immunoprecipitaion experiments using HEK293T cells co-transfected with TDP-43-mCherry and PDI-V5 encoding constructs using an anti-RFP antibody to bind the mCherry tag, followed by immunoblotting for V5, to detect over-expressed PDI-V5, and TDP-43, to confirm immunoprecipitation with the RFP antibody. PDI-V5 was markedly co-immunoprecipitated with mutant A315T and Q331K TDP-43-mCherry, and with wildtype TDP-43-mCherry and mCherry alone to a lesser extent (Fig. 5B). Control reactions containing buffer only, untransfected cells or precipitation of Q331K TDP-43 and PDI-V5 over-expressing cell lysates using an irrelevant, isotype-matched control antibody were negative (Fig. 5B).

The involvement of PDI in an *in vivo* model of TDP-43 proteinopathy was then examined using spinal cord tissues from transgenic A315T mutant TDP-43 mice [48]. By immunoblotting, PDI levels were modestly but significantly higher in A315T TDP-43 mouse spinal cords at disease onset (approximately p90–100) than in age, gender and litter-matched non-transgenic controls (Fig. 5C–D). When assessed by immunohistochemistry, PDI was more widely distributed in the spinal cord of transgenic A315T TDP-43 mice just prior to disease onset, compared to non-transgenic controls (Fig. 5E). PDI and TDP-43 were co-localised in a greater proportion of motor neurons in A315T TDP-43 mice than in non-transgenic controls (Fig 5F).

Discussion

In this study, we demonstrate that ER stress leads to accumulation of both wildtype and ALS-linked TDP-43 mutants in the cytoplasm and to incorporation of TDP-43 into cytoplasmic SGs, We also demonstrate that C-terminal TDP-43 inclusions, induced by proteasome inhibition, are closely associated with PDI and the ER-Golgi compartments, suggesting potential disturbances to these organelles in TDP-43-linked disease. Indeed, over-expression of wildtype TDP-43, and to an even greater extent ALS-linked mutant TDP-43, induced ER stress via multiple ER stress signalling pathways. Also, PDI, a chaperone induced during ER stress, interacted with TDP-43 and co-located with TDP-43 in the spinal cords of transgenic mutant A315T TDP-43 mice, consistent with the increasing evidence that alterations of PDI location and function are common features in ALS. These results suggest that ER stress is involved in modulating TDP-43 sub-cellular distribution, with potential implications for triggering pathology and neuronal death in TDP-43 proteinopathies (Fig. 6).

It is well established that ER stress is an upstream event in ALS and this study confirms that ALS-associated mutant TDP-43 joins the list of disease proteins that induce ER stress. ER stress is a feature of sporadic human ALS [23,27], in familial forms of ALS and FTLD, including those linked to FUS [26], vesicle-associated membrane protein-associated protein B (VAPB) [59] and valosin containing protein [60], and in mutant SOD1 animal and cell models [23,24,25,61]. As TDP-43 is the major pathological protein in most cases of ALS and FTLD, ER stress may be a trigger for TDP-43 dysfunction. This is supported by studies demonstrating fragmentation of TDP-43, another pathological feature of disease, following induction of ER stress in cell culture [15,29].

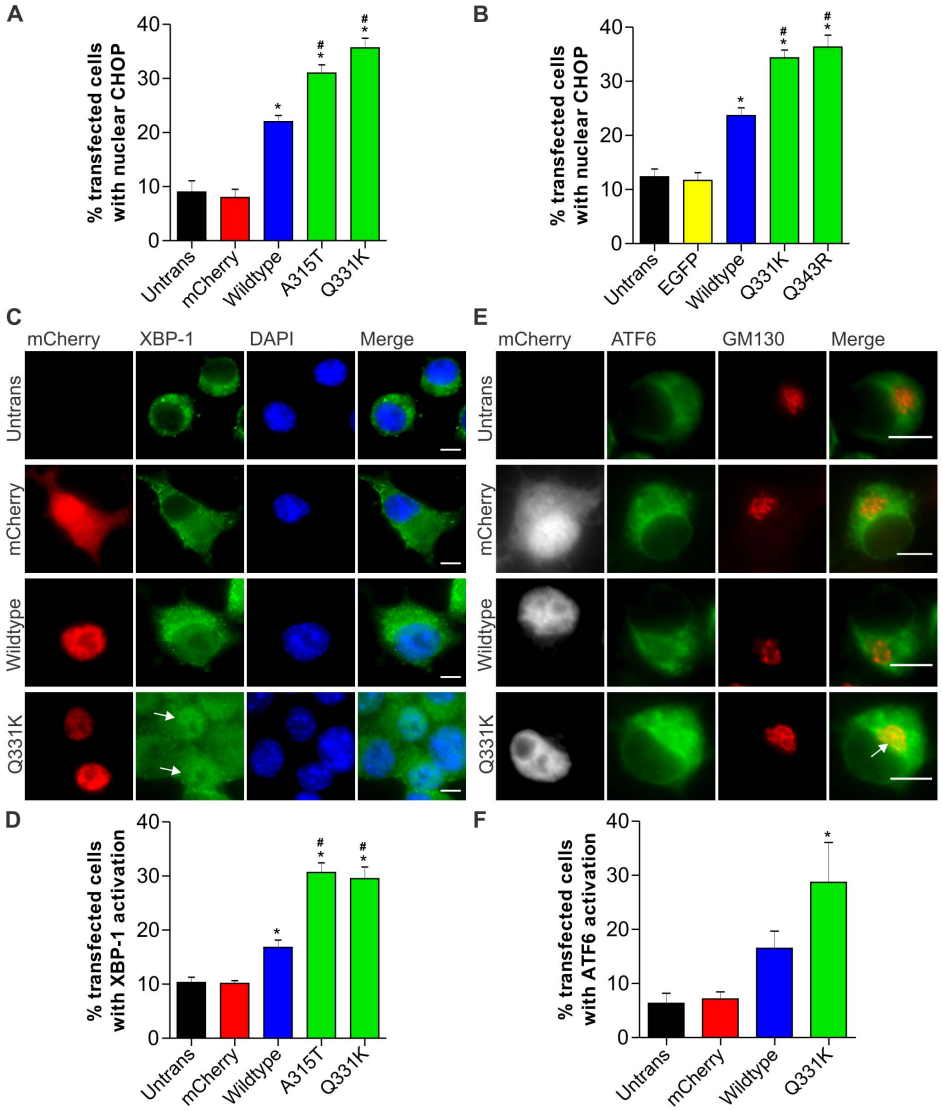

Figure 4. Wildtype and ALS-linked mutant TDP-43 proteins induce ER stress. (**A**) Increase in nuclear CHOP immunoreactivity in Neuro2a cells expressing wildtype and ALS mutant forms of TDP-43 linked with mCherry. (**B**) Increase in nuclear CHOP immunoreactivity in Neuro2a cells expressing wildtype and ALS mutant forms of TDP-43 linked with EGFP. (**C**) XBP-1 is activated in mutant TDP-43 Q331K cells, indicating induction of the IRE1 pathway of ER stress. Cells expressing TDP-43 mCherry (first column, red) are shown with XBP-1 (second column, green) and DAPI staining (third column, blue). Merge (fourth column) indicates overlays of the fluorescent images of XBP-1 and DAPI. Arrow indicates cells with increased nuclear XBP-1. Scale bars represent 5 μm. (**D**) Quantification of transfected cells with activation of XBP-1, as determined by an increase in nuclear XBP-1 immunoreactivity. (**E**) ATF6 translocates to the Golgi in mutant Q331K cells, indicating activation of the ATF6 pathway of ER stress. Neuro2a cells were co-transfected with mCherry constructs (first column, white) and ATF6-GFP (second column, green). Cells were fixed and immunostained for Golgi marker GM130 (third column, red). Merge (fourth column) indicates overlays of the fluorescent images of ATF6 and GM130. Arrow indicates co-localisation of ATF6 in the Golgi apparatus. Scale bars represent 10 μm. (**F**) Quantification of transfected cells with activation of ATF6, as determined by co-localisation of ATF6 with GM130. Data are represented as mean ± SEM; *$p<0.05$ versus mCherry or EGFP controls and #$p<0.05$ versus respective wildtype TDP-43 proteins, by one-way ANOVA with Tukey's post hoc test.
doi:10.1371/journal.pone.0081170.g004

We found that transfection with ALS-linked mutant TDP-43, and to a lesser extent wildtype TDP-43, increased ATF6 and XBP-1 activation and induced CHOP as markers of ER stress, at 18–24 h post-transfection. However at later time points the induction of ER stress was variable or not detected (data not shown). The reason for this is unclear but may be linked to accumulation of TDP-43 in the cytoplasm, which we found to vary considerably depending on time after transfection. This may explain the findings of a recent study which reported only up-regulation of CHOP, but not other markers of ER stress, in NSC-34 cells with viral over-expression of wildtype TDP-43 at 24–48 hr post-infection [31]. We recently found that cytoplasmic localisation of mutant FUS was required for ER stress induction, whereas cells with only nuclear FUS had undetectable levels of ER stress [26]. Hence it is possible that similar to FUS, ER stress is closely linked to, but precedes, accumulation of TDP-43 in the cytoplasm. Abnormal activation of XBP-1 has also been described in a rat model with over-expression of mutant TDP-43, in which neurons display an unexpected decrease in XBP-1 levels while microglia display increased XBP-1 [30]. Combined, these studies suggest a non-classical ER stress response in TDP-43-linked disease.

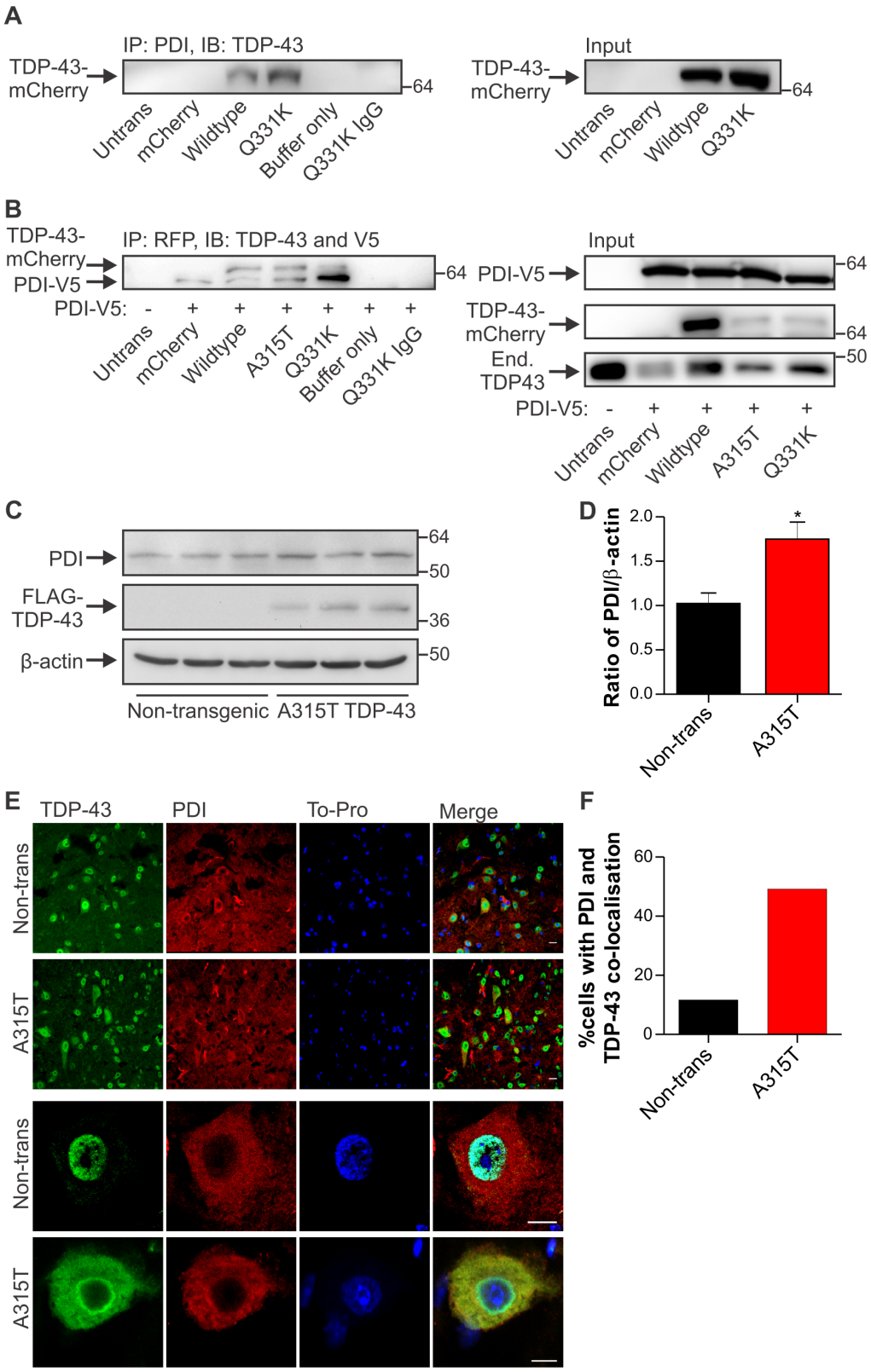

Figure 5. PDI co-precipitates with TDP-43 and is increased in mutant TDP-43 transgenic mouse spinal cords. (**A**) Co-immunoprecipitation of wildtype and mutant Q331K TDP-43-mCherry from Neuro2a cell lysates using an anti-PDI antibody followed by TDP-43 immunoblot. Control immunoprecipitations were performed using untransfected (Untrans) or mCherry expressing cell lysates, buffer only with coprecipitating antibodies or TDP-43 Q331K cell lysates using an irrelevant, isotype-matched control antibody (IgG). Input control (2%) shows expression of mCherry-TDP43 in wildtype and Q331K cell lysates. (**B**) Co-immunoprecipitation of PDI-V5 from wildtype and mutant A315T and Q331K TDP-43-mCherry from HEK293T cell lysates using an anti-RFP antibody to precipitate mCherry followed by TDP-43 and V5 immunoblot. Control

immunoprecipitations were performed using Untrans cell lysates or mCherry and PDI-V5 expressing cell lysates, buffer only with coprecipitating antibody or Q331K TDP-43 and PDI-V5 co-transfected cell lysates using an irrelevant, isotype-matched control antibody (IgG). Input control shows expression of PDI-V5, TDP-43-mCherry and endogenous (End.) TDP-43. Approximate molecular weight markers are shown on the right, and representative images are shown. (**C**) Proteins were extracted from spinal cords of three mutant A315T TDP-43 transgenic mice and three litter-matched non-transgenic controls, and immunoblotting was performed for PDI, FLAG-TDP-43 (detected using antibody against FLAG), and β-actin. (**D**) Quantification of PDI levels from immunoblots normalised to β-actin by densitometry. Data represent mean normalised values from three independent analyses and are shown as mean ± SEM. *$p<0.05$ versus non-transgenic controls by unpaired two-tailed t-test. (**E**) Immunohistochemistry for TDP-43 and PDI in non-transgenic and A315T mutant TDP-43 mouse spinal cords. Cells were immunostained for TDP-43 (first column, green), PDI (second column, red), and were stained using To-Pro to identify nuclei (third column, blue). Merged images (fourth column) are also shown. Increased co-localisation of PDI with TDP-43 is seen in A315T animals compared to non-transgenic controls (Non-trans). All scale bars represent 10 μm. (**F**) Quantification of the percentage of motor neurons in which PDI and TDP-43 were co-localised. A total of 60 cells per group were counted, and data represent mean values from two mice per group.
doi:10.1371/journal.pone.0081170.g005

We also interpret our findings as showing that ER stress is a key pathway in the formation of eIF2α-mediated SGs and the incorporation of TDP-43 into these SGs. Salubrinal, which inhibits dephosphorylation of eIF2α and potentiates the PERK pathway of ER stress, markedly increased TDP-43-positive SG formation following thapsigargin treatment. This argues that ER stress induces SGs via the eIF2α-mediated pathway. Indeed, ER stress activates PERK to inhibit protein translation, which is also the primary consequence of SG formation. The PERK arm of the UPR may be a defence against ALS because salubrinal is protective in a mutant $SOD1^{G93A}$ mouse model of ALS [61], and disease was accelerated in $SOD1^{G85R}$ mice with hemizygous deletion of PERK [25]. Interestingly, under basal conditions, prevention of eIF2α dephosphorylation alone is not sufficient to induce TDP-43 SG formation because the cellular stress of adding thapsagargin was required for SG formation and TDP-43 incorporation into SGs (Fig. 2). These results also show that ER stress is an important precursor to both SG formation and TDP-43 dysfunction in ALS. Previous findings showing ER stress-mediated cell death in mutant SOD1 models of ALS [24,57] suggest that ER stress could be similarly involved not only in SG formation and TDP-43 redistribution but also in neuron death in TDP-43-linked disease. Indeed, recent studies have shown a protective effect of salubrinal treatment in a *C. elegans* model of TDP-43 proteinopathy [62].

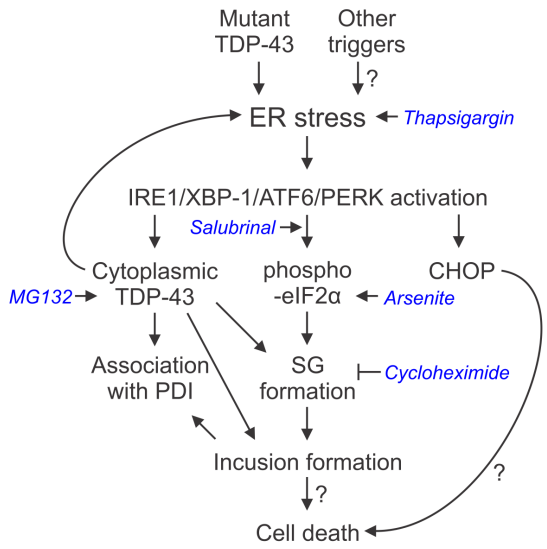

Figure 6. A model for the involvement of ER stress in TDP-43 proteinopathies. ER stress activation causes accumulation of cytoplasmic TDP-43, and induction of TDP-43-positive SGs, which could lead to inclusion formation and neuron death in disease. ER stress may also lead to cell death via apoptotic signalling involving the transcription factor CHOP, independent of SGs and inclusion formation. Additionally, TDP-43 shows increased association with the chaperone PDI in disease. Pharmacological agents used in this study are shown italicised in blue.
doi:10.1371/journal.pone.0081170.g006

It remains to be determined how different cellular stressors are able to differentially modulate TDP-43 redistribution into SGs. Previous studies have been conflicting in the effect of arsenite, a typical SG trigger, to form TDP-43 SGs. Some studies have indicated that arsenite does cause TDP-43 SG formation [8,63], while others have shown a lesser effect [9,37]. Our findings suggest that arsenite is not a strong inducer of TDP-43-positive SGs in HeLa cells under the conditions used here. Additionally, we show that salubrinal had no additive effect on the incorporation of TDP-43 into SGs following arsenite treatment, in contrast to the potentiation of TDP-43-positive SG formation with salubrinal treatment of cells under thapsigargin-induced ER stress. These results suggest differences in the mechanism of SG formation under different stress conditions, indicating potential differences in phosphorylation of eIF2α under different stress conditions, and highlighting the important role for ER stress in TDP-43 SG formation. Further investigation is warranted of the role of ER stress in TDP-43 accumulation and SG formation in neurons and *in vivo*.

We previously provided evidence that PDI can attenuate the effects of mutant SOD1 in cell models of ALS [27] and that PDI is up-regulated in sporadic human ALS spinal cord tissue [23]. Our findings here support other studies showing that PDI co-localisation with TDP-43-positive inclusions in sporadic ALS motor neurons [36], although the lack of full-length TDP-43 inclusions in our models makes direct comparison with human disease difficult. Thus TDP-43 can be added to the growing list of proteins linked to ALS that associate with PDI, including mutant SOD1 [32], FUS [26], and VAPB [64]. The co-immunoprecipitation of PDI with mutant TDP-43, and to a lesser extent wildtype TDP-43, in cell lysates implies that TDP-43 and PDI physically interact, suggesting that PDI is therefore in a position to protect against TDP-43 misfolding and aggregation. PDI is responsible for the isomerisation of protein disulphide bonds, forming native structures, and it is also a general protein chaperone. Cysteine oxidation and cross-linking of TDP-43 via disulphide bonds can alter conformations and function [37] and might induce aggregation of TDP-43 by a mechanism similar to that proposed for mutant SOD1 involving aberrant disulphide bonding [65]. Hence, it is tempting to speculate that the up-regulation of PDI is a cellular response to prevent further aggregation of abnormally disulphide bonded and misfolded TDP-43. Indeed, single nucleotide polymorphisms in the gene encoding PDI have recently been associated with risk of ALS, suggesting that PDI plays a role in protection against disease [66]. These findings align with previous results showing that enzymative inactivation of PDI in ALS patient spinal cords likely contributes to disease development [27],

suggesting multiple mechanisms for the involvement of PDI in ALS pathogenesis. However, further experiments are necessary to determine the mode of PDI interaction with ALS-associated proteins, including TDP-43, and the effect of PDI on TDP-43 misfolding. It should be noted that while typically regarded as being ER-resident, PDI is also present within the cell in a variety of additional locations, including in the cytoplasm and in the extracellular space [67]. PDI is redistributed from the ER to ER-derived cytoplasmic structures in a manner regulated by the reticulon protein family, and this redistribution is protective in mutant SOD1 mice [35] and modulates PDI function [68]. The location of C-terminal TDP-43 inclusions in close association with the ER, Golgi and ERGIC (Fig. 3) also suggests disturbance in the function of these organelles, and indeed our results, and those of others [69], suggest an increased cytoplasmic presence of PDI following ER stress induction. Further investigation of changes in the Golgi and ER components in animal models displaying TDP-43 inclusions and in ALS and FTLD patient tissues is warranted.

In conclusion, this study demonstrates that ER stress can be triggered by over-expression of wildtype TDP-43 and to an even greater extent ALS-linked mutant TDP-43, and that ER stress modulates TDP-43 sub-cellular distribution and SG formation, reminiscent of disease features. These findings imply that TDP-43 mutation carriers may be more susceptible to ER stress induction than other ALS patients. However, further experiments will be required, possibly comparing the effects of wildytpe and mutant TDP-43 in *in vivo* models, in order to conclusively identify differences in dysfunction of wildtype versus mutant TDP-43 with respect to ER stress in disease. Indeed, our results also indicate that ER stress is able to drive cytoplasmic relocation of wildtype TDP-43, suggesting that upstream cellular stress responses could drive TDP-43 pathology in sporadic ALS patients. It remains important to determine the upstream triggers of TDP-43-dysfunction in ALS, and to determine if modulation of ER stress responses can be used as a target for disease modifying therapies in TDP-43 proteinopathies.

Supporting Information

Video S1 Association of 218–414 TDP-43-mCherry inclusions with the Golgi apparatus. Neuro2a cells were transfected with the 218–414 TDP-43-mCherry construct, and treated with 10 μM MG132 for 24 h starting at 24 h post-transfection. Cells were processed for immunocytochemistry against GM130 (green) and serial z-stack images were taken at 0.50 μm intervals using confocal microscopy and post-processed using Olympus Fluoview v2.0 software. mCherry fluorescence is shown in red and nuclei (Hoechst dye) are shown in blue. Scale bar represents 10 μm.
(MOV)

Acknowledgments

We thank Dr Virginia Lee (University of Pennsylvania) for providing the myc-TDP-43 pcDNA construct, Dr Benjamin Wolozin (Boston University) and Dr Leonard Petrucelli (Mayo Clinic) for the EGFP-TDP-43 constructs, Dr Neil Bulleid (University of Glasgow) for the PDI-V5 construct, and Dr Ron Prywes (Columbia University) and Dr Jason Mackenzie (La Trobe University) for the ATF6-GFP construct.

Author Contributions

Conceived and designed the experiments: AKW KYS VS MKH JDA. Performed the experiments: AKW KYS VS SP YM MAF. Analyzed the data: AKW KYS VS SP JDA. Contributed reagents/materials/analysis tools: AKW KYS RHW PJC BJT MKH JDA. Wrote the paper: AKW MKH JDA.

References

1. Neumann M, Sampathu DM, Kwong LK, Truax AC, Micsenyi MC, et al. (2006) Ubiquitinated TDP-43 in frontotemporal lobar degeneration and amyotrophic lateral sclerosis. Science 314: 130–133.
2. Arai T, Hasegawa M, Akiyama H, Ikeda K, Nonaka T, et al. (2006) TDP-43 is a component of ubiquitin-positive tau-negative inclusions in frontotemporal lobar degeneration and amyotrophic lateral sclerosis. Biochem Biophys Res Commun 351: 602–611.
3. Buratti E, Dork T, Zuccato E, Pagani F, Romano M, et al. (2001) Nuclear factor TDP-43 and SR proteins promote in vitro and in vivo CFTR exon 9 skipping. Embo J 20: 1774–1784.
4. Winton MJ, Igaz LM, Wong MM, Kwong LK, Trojanowski JQ, et al. (2008) Disturbance of nuclear and cytoplasmic TAR DNA-binding protein (TDP-43) induces disease-like redistribution, sequestration, and aggregate formation. J Biol Chem 283: 13302–13309.
5. Wang IF, Reddy NM, Shen CK (2002) Higher order arrangement of the eukaryotic nuclear bodies. Proc Natl Acad Sci U S A 99: 13583–13588.
6. Nonaka T, Arai T, Buratti E, Baralle FE, Akiyama H, et al. (2009) Phosphorylated and ubiquitinated TDP-43 pathological inclusions in ALS and FTLD-U are recapitulated in SH-SY5Y cells. FEBS Lett 583: 394–400.
7. Liu-Yesucevitz L, Bilgutay A, Zhang YJ, Vanderweyde T, Citro A, et al. (2010) Tar DNA binding protein-43 (TDP-43) associates with stress granules: analysis of cultured cells and pathological brain tissue. PLoS ONE 5: e13250.
8. McDonald KK, Aulas A, Destroismaisons L, Pickles S, Beleac E, et al. (2011) TAR DNA-binding protein 43 (TDP-43) regulates stress granule dynamics via differential regulation of G3BP and TIA-1. Hum Mol Genet 20: 1400–1410.
9. Dewey CM, Cenik B, Sephton CF, Dries DR, Mayer P, 3rd, et al. (2011) TDP-43 is directed to stress granules by sorbitol, a novel physiological osmotic and oxidative stressor. Mol Cell Biol 31: 1098–1108.
10. Parker SJ, Meyerowitz J, James JL, Liddell JR, Crouch PJ, et al. (2012) Endogenous TDP-43 localized to stress granules can subsequently form protein aggregates. Neurochem Int 60: 415–424.
11. Anderson P, Kedersha N (2006) RNA granules. J Cell Biol 172: 803–808.
12. Kedersha NL, Gupta M, Li W, Miller I, Anderson P (1999) RNA-binding proteins TIA-1 and TIAR link the phosphorylation of eIF-2 alpha to the assembly of mammalian stress granules. J Cell Biol 147: 1431–1442.
13. Kedersha N, Anderson P (2009) Regulation of translation by stress granules and processing bodies. Prog Mol Biol Transl Sci 90: 155–185.
14. Dewey CM, Cenik B, Sephton CF, Johnson BA, Herz J, et al. (2012) TDP-43 aggregation in neurodegeneration: are stress granules the key? Brain Res 1462: 16–25.
15. Ayala V, Granado-Serrano AB, Cacabelos D, Naudi A, Ilieva EV, et al. (2011) Cell stress induces TDP-43 pathological changes associated with ERK1/2 dysfunction: implications in ALS. Acta Neuropathol 122: 259–270.
16. Walker AK, Atkin JD (2011) Stress signaling from the endoplasmic reticulum: A central player in the pathogenesis of amyotrophic lateral sclerosis. IUBMB life 63: 754–763.
17. Urano F, Wang X, Bertolotti A, Zhang Y, Chung P, et al. (2000) Coupling of stress in the ER to activation of JNK protein kinases by transmembrane protein kinase IRE1. Science 287: 664–666.
18. Haze K, Yoshida H, Yanagi H, Yura T, Mori K (1999) Mammalian transcription factor ATF6 is synthesized as a transmembrane protein and activated by proteolysis in response to endoplasmic reticulum stress. Mol Biol Cell 10: 3787–3799.
19. Harding HP, Zhang Y, Ron D (1999) Protein translation and folding are coupled by an endoplasmic-reticulum-resident kinase. Nature 397: 271–274.
20. Schroder M (2008) Endoplasmic reticulum stress responses. Cell Mol Life Sci 65: 862–894.
21. Ma Y, Brewer JW, Diehl JA, Hendershot LM (2002) Two distinct stress signaling pathways converge upon the CHOP promoter during the mammalian unfolded protein response. J Mol Biol 318: 1351–1365.
22. Schroder M, Kaufman RJ (2005) The mammalian unfolded protein response. Annu Rev Biochem 74: 739–789.
23. Atkin JD, Farg MA, Walker AK, McLean C, Tomas D, et al. (2008) Endoplasmic reticulum stress and induction of the unfolded protein response in human sporadic amyotrophic lateral sclerosis. Neurobiol Dis 30: 400–407.
24. Hetz C, Thielen P, Matus S, Nassif M, Court F, et al. (2009) XBP-1 deficiency in the nervous system protects against amyotrophic lateral sclerosis by increasing autophagy. Genes Dev 23: 2294–2306.
25. Wang L, Popko B, Roos RP (2011) The unfolded protein response in familial amyotrophic lateral sclerosis. Hum Mol Genet 20: 1008–1015.
26. Farg MA, Soo KY, Walker AK, Pham H, Orian J, et al. (2012) Mutant FUS induces endoplasmic reticulum stress in amyotrophic lateral sclerosis and interacts with protein disulfide-isomerase. Neurobiol Aging 33: 2855–2868.

27. Walker AK, Farg MA, Bye CR, McLean CA, Horne MK, et al. (2010) Protein disulphide isomerase protects against protein aggregation and is S-nitrosylated in amyotrophic lateral sclerosis. Brain 133: 105–116.
28. Liu Y, Lee SY, Neely E, Nandar W, Moyo M, et al. (2011) Mutant HFE H63D protein is associated with prolonged endoplasmic reticulum stress and increased neuronal vulnerability. J Biol Chem 286: 13161–13170.
29. Suzuki H, Lee K, Matsuoka M (2011) TDP-43-induced death is associated with altered regulation of BIM and Bcl-xL and attenuated by caspase-mediated TDP-43 cleavage. J Biol Chem 286: 13171–13183.
30. Tong J, Huang C, Bi F, Wu Q, Huang B, et al. (2012) XBP1 depletion precedes ubiquitin aggregation and Golgi fragmentation in TDP-43 transgenic rats. J Neurochem 123: 406–416.
31. Suzuki H, Matsuoka M (2012) TDP-43 toxicity is mediated by the unfolded protein response-unrelated induction of C/EBP homologous protein expression. J Neurosci Res 90: 641–647.
32. Atkin JD, Farg MA, Turner BJ, Tomas D, Lysaght JA, et al. (2006) Induction of the unfolded protein response in familial amyotrophic lateral sclerosis and association of protein-disulfide isomerase with superoxide dismutase 1. J Biol Chem 281: 30152–30165.
33. Ilieva EV, Ayala V, Jove M, Dalfo E, Cacabelos D, et al. (2007) Oxidative and endoplasmic reticulum stress interplay in sporadic amyotrophic lateral sclerosis. Brain 130: 3111–3123.
34. Wang J, Xu G, Borchelt DR (2006) Mapping superoxide dismutase 1 domains of non-native interaction: roles of intra- and intermolecular disulfide bonding in aggregation. J Neurochem 96: 1277–1288.
35. Yang YS, Harel NY, Strittmatter SM (2009) Reticulon-4A (Nogo-A) redistributes protein disulfide isomerase to protect mice from SOD1-dependent amyotrophic lateral sclerosis. J Neurosci 29: 13850–13859.
36. Honjo Y, Kaneko S, Ito H, Horibe T, Nagashima M, et al. (2011) Protein disulfide isomerase-immunopositive inclusions in patients with amyotrophic lateral sclerosis. Amyotroph Lateral Scler 12: 444–450.
37. Cohen TJ, Hwang AW, Unger T, Trojanowski JQ, Lee VM (2012) Redox signalling directly regulates TDP-43 via cysteine oxidation and disulphide cross-linking. Embo J 31: 1241–1252.
38. Gitcho MA, Baloh RH, Chakraverty S, Mayo K, Norton JB, et al. (2008) TDP-43 A315T mutation in familial motor neuron disease. Ann Neurol 63: 535–538.
39. Kabashi E, Valdmanis PN, Dion P, Spiegelman D, McConkey BJ, et al. (2008) TARDBP mutations in individuals with sporadic and familial amyotrophic lateral sclerosis. Nat Genet 40: 572–574.
40. Sreedharan J, Blair IP, Tripathi VB, Hu X, Vance C, et al. (2008) TDP-43 mutations in familial and sporadic amyotrophic lateral sclerosis. Science 319: 1668–1672.
41. Rutherford NJ, Zhang YJ, Baker M, Gass JM, Finch NA, et al. (2008) Novel mutations in TARDBP (TDP-43) in patients with familial amyotrophic lateral sclerosis. PLoS Genet 4: e1000193.
42. Corrado L, Ratti A, Gellera C, Buratti E, Castellotti B, et al. (2009) High frequency of TARDBP gene mutations in Italian patients with amyotrophic lateral sclerosis. Hum Mutat 30: 688–694.
43. Tamaoka A, Arai M, Itokawa M, Arai T, Hasegawa M, et al. (2010) TDP-43 M337V mutation in familial amyotrophic lateral sclerosis in Japan. Intern Med 49: 331–334.
44. Zhang YJ, Xu YF, Cook C, Gendron TF, Roettges P, et al. (2009) Aberrant cleavage of TDP-43 enhances aggregation and cellular toxicity. Proc Natl Acad Sci U S A 106: 7607–7612.
45. Chen X, Shen J, Prywes R (2002) The luminal domain of ATF6 senses endoplasmic reticulum (ER) stress and causes translocation of ATF6 from the ER to the Golgi. J Biol Chem 277: 13045–13052.
46. Jessop CE, Watkins RH, Simmons JJ, Tasab M, Bulleid NJ (2009) Protein disulphide isomerase family members show distinct substrate specificity: P5 is targeted to BiP client proteins. J Cell Sci 122: 4287–4295.
47. Balague O, Mozos A, Martinez D, Hernandez L, Colomo L, et al. (2009) Activation of the endoplasmic reticulum stress-associated transcription factor x box-binding protein-1 occurs in a subset of normal germinal-center B cells and in aggressive B-cell lymphomas with prognostic implications. Am J Pathol 174: 2337–2346.
48. Wegorzewska I, Bell S, Cairns NJ, Miller TM, Baloh RH (2009) TDP-43 mutant transgenic mice develop features of ALS and frontotemporal lobar degeneration. Proc Natl Acad Sci U S A 106: 18809–18814.
49. Ayala YM, Zago P, D'Ambrogio A, Xu YF, Petrucelli L, et al. (2008) Structural determinants of the cellular localization and shuttling of TDP-43. J Cell Sci 121: 3778–3785.
50. Fiesel FC, Voigt A, Weber SS, Van den Haute C, Waldenmaier A, et al. (2010) Knockdown of transactive response DNA-binding protein (TDP-43) downregulates histone deacetylase 6. Embo J 29: 209–221.
51. Lee DH, Goldberg AL (1998) Proteasome inhibitors: valuable new tools for cell biologists. Trends Cell Biol 8: 397–403.
52. Boyce M, Bryant KF, Jousse C, Long K, Harding HP, et al. (2005) A selective inhibitor of eIF2alpha dephosphorylation protects cells from ER stress. Science 307: 935–939.
53. Wehner KA, Schutz S, Sarnow P (2010) OGFOD1, a novel modulator of eukaryotic translation initiation factor 2alpha phosphorylation and the cellular response to stress. Mol Cell Biol 30: 2006–2016.
54. Arimoto K, Fukuda H, Imajoh-Ohmi S, Saito H, Takekawa M (2008) Formation of stress granules inhibits apoptosis by suppressing stress-responsive MAPK pathways. Nat Cell Biol 10: 1324–1332.
55. Zhang YJ, Xu YF, Dickey CA, Buratti E, Baralle F, et al. (2007) Progranulin mediates caspase-dependent cleavage of TAR DNA binding protein-43. J Neurosci 27: 10530–10534.
56. Oh YK, Shin KS, Yuan J, Kang SJ (2008) Superoxide dismutase 1 mutants related to amyotrophic lateral sclerosis induce endoplasmic stress in neuro2a cells. J Neurochem 104: 993–1005.
57. Soo KY, Atkin JD, Farg M, Walker AK, Horne MK, et al. (2012) Bim Links ER Stress and Apoptosis in Cells Expressing Mutant SOD1 Associated with Amyotrophic Lateral Sclerosis. PLoS ONE 7: e35413.
58. Farg MA, Soo KY, Warraich ST, Sundaramoorthy V, Blair IP, et al. (2013) Ataxin-2 interacts with FUS and intermediate-length polyglutamine expansions enhance FUS-related pathology in amyotrophic lateral sclerosis. Hum Mol Genet 22: 717–728.
59. Suzuki H, Kanekura K, Levine TP, Kohno K, Olkkonen VM, et al. (2009) ALS-linked P56S-VAPB, an aggregated loss-of-function mutant of VAPB, predisposes motor neurons to ER stress-related death by inducing aggregation of co-expressed wild-type VAPB. J Neurochem 108: 973–985.
60. Gitcho MA, Strider J, Carter D, Taylor-Reinwald L, Forman MS, et al. (2009) VCP mutations causing frontotemporal lobar degeneration disrupt localization of TDP-43 and induce cell death. J Biol Chem 284: 12384–12398.
61. Saxena S, Cabuy E, Caroni P (2009) A role for motoneuron subtype-selective ER stress in disease manifestations of FALS mice. Nat Neurosci 12: 627–636.
62. Vaccaro A, Patten SA, Aggad D, Julien C, Maios C, et al. (2013) Pharmacological reduction of ER stress protects against TDP-43 neuronal toxicity in vivo. Neurobiol Dis 55: 64–75.
63. Meyerowitz J, Parker SJ, Vella LJ, Ng D, Price KA, et al. (2011) C-Jun N-terminal kinase controls TDP-43 accumulation in stress granules induced by oxidative stress. Molecular neurodegeneration 6: 57.
64. Tsuda H, Han SM, Yang Y, Tong C, Lin YQ, et al. (2008) The amyotrophic lateral sclerosis 8 protein VAPB is cleaved, secreted, and acts as a ligand for Eph receptors. Cell 133: 963–977.
65. Furukawa Y, Fu R, Deng HX, Siddique T, O'Halloran TV (2006) Disulfide cross-linked protein represents a significant fraction of ALS-associated Cu, Zn-superoxide dismutase aggregates in spinal cords of model mice. Proc Natl Acad Sci U S A 103: 7148–7153.
66. Kwok CT, Morris AG, Frampton J, Smith B, Shaw CE, et al. (2013) Association studies indicate that protein disulfide isomerase is a risk factor in amyotrophic lateral sclerosis. Free Radic Biol Med 58: 81–86.
67. Turano C, Coppari S, Altieri F, Ferraro A (2002) Proteins of the PDI family: unpredicted non-ER locations and functions. J Cell Physiol 193: 154–163.
68. Bernardoni P, Fazi B, Costanzi A, Nardacci R, Montagna C, et al. (2013) Reticulon1-C modulates protein disulphide isomerase function. Cell death & disease 4: e581.
69. Tabata Y, Takano K, Ito T, Iinuma M, Yoshimoto T, et al. (2007) Vaticanol B, a resveratrol tetramer, regulates endoplasmic reticulum stress and inflammation. Am J Physiol Cell Physiol 293: C411–418.

7.2.5 Supplementary Figure 4

The result is presented in the published manuscript: Soo, K. Y., et al. (2015).”***Rab1-dependent ER–Golgi transport dysfunction is a common pathogenic mechanism in SOD1, TDP-43 and FUS-associated ALS***." *Acta neuropathologica*: 1-19 the author performed experiments presented in figure 1e, described in the Results section of the manuscript on page 4 under the section of ‘**ER-Golgi transport is inhibited in cells expressing proteins associated with ALS’.**

Acta Neuropathol (2015) 130:679–697
DOI 10.1007/s00401-015-1468-2

ORIGINAL PAPER

Rab1-dependent ER–Golgi transport dysfunction is a common pathogenic mechanism in SOD1, TDP-43 and FUS-associated ALS

Kai Y. Soo[1] · Mark Halloran[1,2] · Vinod Sundaramoorthy[1,2] · Sonam Parakh[1,2] · Reka P. Toth[2] · Katherine A. Southam[3] · Catriona A. McLean[4,5] · Peter Lock[1] · Anna King[6] · Manal A. Farg[1] · Julie D. Atkin[1,2]

Received: 16 December 2014 / Revised: 11 August 2015 / Accepted: 12 August 2015 / Published online: 23 August 2015

Abstract Several diverse proteins are linked genetically/pathologically to neurodegeneration in amyotrophic lateral sclerosis (ALS) including SOD1, TDP-43 and FUS. Using a variety of cellular and biochemical techniques, we demonstrate that ALS-associated mutant TDP-43, FUS and SOD1 inhibit protein transport between the endoplasmic reticulum (ER) and Golgi apparatus in neuronal cells. ER–Golgi transport was also inhibited in embryonic cortical and motor neurons obtained from a widely used animal model ($SOD1^{G93A}$ mice), validating this mechanism as an early event in disease. Each protein inhibited transport by distinct mechanisms, but each process was dependent on Rab1. Mutant TDP-43 and mutant FUS both inhibited the incorporation of secretory protein cargo into COPII vesicles as they bud from the ER, and inhibited transport from ER to the ER–Golgi intermediate (ERGIC) compartment. TDP-43 was detected on the cytoplasmic face of the ER membrane, whereas FUS was present within the ER, suggesting that transport is inhibited from the cytoplasm by mutant TDP-43, and from the ER by mutant FUS. In contrast, mutant SOD1 destabilised microtubules and inhibited transport from the ERGIC compartment to Golgi, but not from ER to ERGIC. Rab1 performs multiple roles in ER–Golgi transport, and over-expression of Rab1 restored ER–Golgi transport, and prevented ER stress, mSOD1 inclusion formation and induction of apoptosis, in cells expressing mutant TDP-43, FUS or SOD1. Rab1 also co-localised extensively with mutant TDP-43, FUS and SOD1 in neuronal cells, and Rab1 formed inclusions in motor neurons of spinal cords from sporadic ALS patients, which were positive for ubiquitinated TDP-43, implying that Rab1 is misfolded and dysfunctional in sporadic disease. These results demonstrate that ALS-mutant forms of TDP-43, FUS, and SOD1 all perturb protein transport in the early secretory pathway, between ER and Golgi compartments. These data also imply that restoring Rab1-mediated ER–Golgi transport is a novel therapeutic target in ALS.

Keywords TDP-43 · FUS · SOD1 · ER–Golgi transport · Amyotrophic lateral sclerosis

Electronic supplementary material The online version of this article (doi:10.1007/s00401-015-1468-2) contains supplementary material, which is available to authorized users.

✉ Julie D. Atkin
julie.atkin@mq.edu.au

1 Department of Biochemistry and Genetics, La Trobe Institute for Molecular Science, La Trobe University, Kingsbury Drive, Bundoora, VIC, Australia

2 Department of Biomedical Sciences, Faculty of Medicine and Health Science, Macquarie University, North Ryde, NSW, Australia

3 Menzies Research Institute Tasmania, University of Tasmania, Hobart, TAS, Australia

4 Department of Anatomical Pathology, Alfred Hospital, Prahran, VIC, Australia

5 Department of Medicine, Central Clinical School, Monash University, Clayton, VIC, Australia

6 Wicking Dementia Research and Education Centre, University of Tasmania, Hobart, TAS, Australia

Introduction

Amyotrophic lateral sclerosis (ALS) is a fatal neurodegenerative disorder characterised by degeneration and death of motor neurons. Multiple proteins are linked genetically to ALS, including superoxide dismutase 1

(SOD1) [55], TAR DNA binding protein (TDP-43) [68], and Fused in Sarcoma (FUS) [78]. TDP-43 and FUS are also associated with frontotemporal dementia and misfolded wildtype (WT) SOD1 is present in small granular aggregates in glia and motor neuron nuclei, although it has not been detected in the typical ubiquitinated TDP-43 pathological inclusions [13, 19, 20, 35]. Transgenic mice overexpressing mutant $SOD1^{G93A}$ develop features characteristic of ALS and are a widely used disease model. Many cellular defects have been implicated in the aetiology of ALS, including protein aggregation, endoplasmic reticulum (ER) stress, autophagy defects, RNA dysfunction and inhibition of axonal transport [54].

Efficient intracellular vesicle trafficking is essential for cellular survival. Proteins newly synthesised in the ER are packed into vesicles and transported to the Golgi apparatus via the ER–Golgi intermediate compartment (ERGIC) [37], and finally redistributed to their final destinations [15]. Hence ER–Golgi transport is a vital gateway to the endomembrane system. The ERGIC is a distinct organelle from the ER and cis-Golgi that concentrates and sorts protein cargo [1]. Functional ER–Golgi transport relies on coat protein complexes (COPs), that recruit cargo proteins [4], and deform the lipid bilayer of donor membranes into vesicles [43, 67]. COPII is essential for export from ER exit sites, and is composed of the GTPase Sar1 and two hetero-dimeric complexes, Sec23/Sec24 and Sec13/Sec31 [4, 38]. COPII vesicles move from the ER to ERGIC, and subsequently from ERGIC to Golgi. The latter, but not the former, step requires microtubules, comprised of tubulin [33]. Finally, COPII vesicles are docked via tethering factor p115 to receptor GM130, on the Golgi membrane.

Rab GTPases are master regulators of all intracellular vesicle trafficking events, and each Rab isoform has distinct target membranes [69]. Rab1 regulates ER–Golgi transport, including COPII vesicle budding, delivery, tethering, fusion to the Golgi [47, 56] and COPII function [63]. In yeast, the Rab1 homologue Ypt1 also mediates microtubule organisation and function, and loss of Ypt1 function results in microtubule defects [61]. Furthermore, Rab1/Ypt1 plays a central role in regulating the unfolded protein response (UPR), suggesting a regulatory mechanism linking vesicle trafficking to the UPR and ER homeostasis [75]. Inhibition of ER–Golgi transport also induces ER stress [48], providing a further link to the UPR.

Previously, we demonstrated that mutant TDP-43 (mTDP-43) [79] and mutant FUS (mFUS) [16] induce ER stress by an undefined mechanism. We also showed that mutant SOD1 (mSOD1) and aggregated WTSOD1 inhibit ER–Golgi transport, and consequently trigger ER stress from the cytoplasm, in cellular models of ALS [3, 72], although the molecular mechanisms involved remains unclear. Here, we demonstrate that mTDP-43, and mFUS also inhibit ER–Golgi transport. Furthermore, we also show that mTDP-43 and mFUS inhibit transport from the ER to ERGIC compartment, by preventing the incorporation of protein cargo into COPII vesicles. However, whilst mFUS was present within the ER, mTDP-43 was attached to the cytoplasmic face of the ER membrane, implying that mTDP-43 and mFUS inhibit transport by discreet mechanisms. In contrast, mSOD1 destabilised microtubules and inhibited transport from the ERGIC compartment to Golgi. Hence, these proteins each inhibit transport by different mechanisms. However, these processes are all Rab1-dependent, demonstrating that antagonism of Rab1 function is a common target shared by ALS-associated forms of SOD1, TDP-43 and FUS. Furthermore, overexpression of Rab1 restored ER–Golgi transport and reduced ER stress, mSOD1 inclusion formation and apoptosis in cells expressing mSOD1, mTDP-43 or mFUS, thus linking ER–Golgi transport inhibition to neurodegeneration. ER–Golgi transport was also inhibited in embryonic cortical and motor neurons obtained from $SOD1^{G93A}$ mice, thus validating this pathological mechanism in primary neurons and as a very early event in disease pathology. Moreover, Rab1 was also recruited to inclusions in spinal motor neurons displaying typical, ubiquitinated TDP-43 pathology in sporadic ALS (sALS) patients, thus implying that Rab1 misfolding and dysfunction is present in sporadic disease.

Materials and methods

Additional materials and methods can be found in Supplementary Materials.

VSVG assay to quantify ER–Golgi transport

Neuro2a cells were plated on 24-well plates with 13 mm coverslips. The following day, cells were co-transfected with TDP-43, FUS, or SOD1 and VSVG-tagged with fluorescent mCherry for indicated time points. Cells were incubated at 40 °C directly after transfection except in the case of the 72 h transfection experiments, where cells were first incubated at 37 °C for 48 h. The temperature was then shifted to 40 °C for a further 24 h after transfection to accumulate VSVG in the ER. Cycloheximide (Sigma, 01810, 20 μg/ml) was added and cells were shifted to the permissive temperature, 32 °C for 30 min. At each time interval, cells were washed with ice-cold PBS and fixed for immunocytochemistry as described. Twenty cells were scored in each experiment and all experiments were performed in triplicate. Image analysis was performed using Image J (http://rsbweb.nih.gov/ij/index.html): only single cells expressing both SOD1-EGFP/EGFP-TDP-43/HA-FUS and VSVG-mCherry were selected for analysis.

Plugins were used and the measuring areas were selected above a threshold against background staining. After analysis, the Mander's coefficient [36] in the range from 0 to 1.0 (representing 0–100 % overlapping pixels) was calculated to determine the degree of overlap between images. For Fig. 1e, the *x* axis values; 80, 40–80 and 40; refer to arbitrary units that represent the total pixel intensity quantified in each cells by using Image J. In each population, cells were separated into 3 categories, so a third of cells with the lowest pixel intensity were categorised as 'low', the next third was categorised as 'medium' and the remaining third were categorised as 'high' representing those cells with the greatest pixel intensities.

In vitro ER-budding assay

A modified in vitro assay [81] was used to analyse ER vesicle budding. Briefly, perforated Neuro2a cells co-transfected with VSVG-mCherry and SOD1, TDP-43 or FUS vectors were incubated with rat liver cytosol and an energy regenerating system (40 mM creatine phosphate, 0.2 mg/ml creatine phosphokinase and 1 mM ATP) at 32 °C for 30 min. Identical samples were incubated at 4 °C as a measure of non-specific ER fragmentation. The cells were removed by low speed centrifugation at 4000*g* for 1 min, followed by 15,000*g* for 1 min, and budded vesicles in the resulting supernatant were recovered by centrifugation at 100,000*g* for 1 h. The levels of VSVG cargo in the budded vesicle fractions were quantified using western blotting. The resulting quantities of budded vesicles were normalised to the levels of ERGIC53 from each sample.

Fluorescence protease protection assay

The fluorescence protease protection assay was performed as described previously [34]. Briefly, Neuro2a cells were transfected with the indicated plasmids 18 h before analysis. Cells were washed three times with KHM buffer (110 mM potassium acetate, 20 mM Hepes, 2 mM $MgCl_2$ in H_2O) for 1 min each wash. Digitonin (Sigma), at 55 % purity, was dissolved in H_2O by heating to 95–98° for 10 mg/ml stock. KHM buffer was removed and 1 ml of KHM buffer with 60 µM digitonin was added to cells. Fluorescence images were captured at regular intervals with ¼ s exposure; fluorescence exposure outside of this capture period was kept to a minimum to prevent photobleaching. Buffer was removed at 110 s after digitonin addition, and cells were washed briefly with KHM buffer. Proteinase-K (Qiagen, Victoria, Australia, stock 20 mg/ml) at 50 µg/ml in KHM buffer was added to cells. At 330 s, 1 % Triton-x-100 with proteinase-K in KHM buffer was added to the cells, and fluorescence images were captured at regular intervals using identical settings between samples.

Statistical analysis

All data are expressed as the mean ± standard error (SEM) and analysed for statistical significance by ANOVA followed by Tukey's post hoc test or 2-tailed student *t* test (GraphPad Prism, La Jolla, CA). The differences were considered significant at $p < 0.05$.

Results

ER–Golgi transport is inhibited in cells expressing proteins associated with ALS

Vesicular stomatitis virus glycoprotein-ts045 (VSVG) is a widely used marker for ER–Golgi trafficking. At 40 °C, VSVG reversibly misfolds and accumulates in the ER; traffic to the Golgi is restored at 32 °C [25]. To examine whether mTDP-43 and mFUS inhibit ER–Golgi transport, Neuro2a cells were co-transfected with mCherry-tagged VSVG and either EGFP-tagged WTTDP-43 or mTDP-43 (A315T/Q343R/Q331K) or HA-tagged WTFUS or mFUS (P525L/R524S/R522G/R521G) constructs at 40 °C. Localisation of VSVG with the ER (calnexin) or Golgi (GM130) was detected immunocytochemically and quantified using Mander's coefficient as previous [3]. In cells expressing WTTDP-43, EGFP, or untransfected cells, VSVG was efficiently transported to the Golgi, in contrast to mTDP-43 cells, where most VSVG remained in the ER (66, 61 and 47 %, respectively, $p < 0.0001$, Fig. 1a, b) and less transported to the Golgi (35, 42 and 48 %, respectively, $p < 0.0001$, Fig. 1b). Thus, three mTDP-43 proteins antagonise anterograde transport of VSVG from ER–Golgi. Immunoblotting revealed similar transfection efficiencies between EGFP, WTTDP-43 and mTDP-43 cells (Suppl. Fig. 1a), demonstrating that transport inhibition is independent of protein expression. Similarly, in cells expressing WTFUS or untransfected cells, VSVG was located predominantly in the Golgi (Suppl. Fig. 2a). In contrast, in cells expressing all four mFUS proteins, significantly less VSVG was transported from ER to Golgi (60 %, $p < 0.0001$ and $p < 0.05$ in R521G; Fig. 1c and Suppl. Fig. 2a). Again, similar transfection efficiencies were evident between WTFUS and mFUS (Suppl. Fig. 1b). Hence four ALS-associated mFUS proteins also inhibit ER–Golgi transport. Similarly, consistent with our previous studies in NSC-34 and SYSH5Y cells [3, 72], mSOD1 also inhibited transport of VSVG from ER to Golgi in Neuro2a cells (Fig. 1d), with similar transfection efficiencies (Suppl. Fig. 1c). The inhibition of ER–Golgi transport was not caused by non-specific over-expression of recombinant, mutant protein, because expression of mutant R311K Nck2 (Nck adaptor protein 2), a cytoplasmic adaptor protein [70]

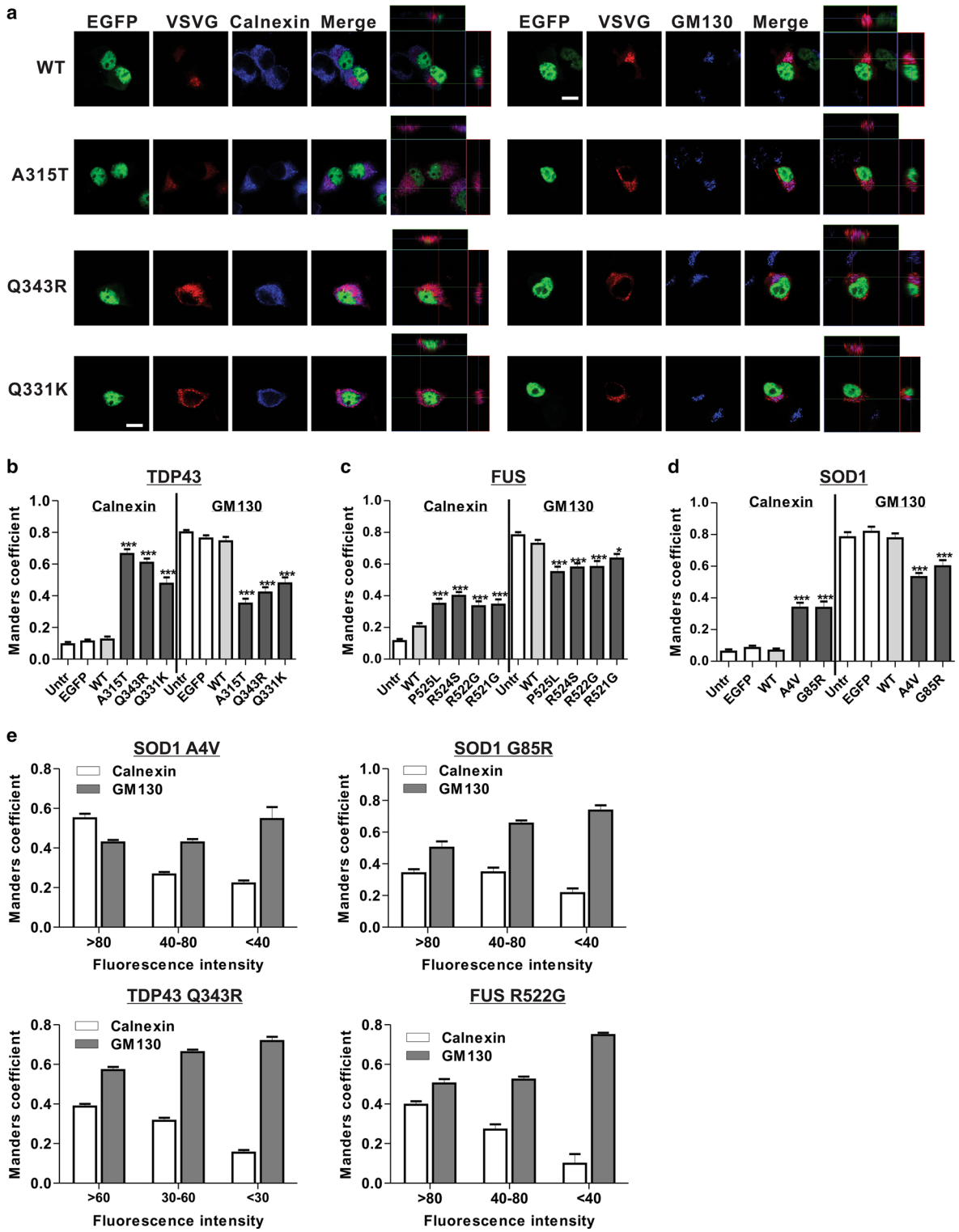

Fig. 1 ER–Golgi transport is inhibited in cells expressing mTDP-43, mFUS and mSOD1. **a** Representative fluorescence images and z-stack orthogonal views of cells expressing EGFP-tagged TDP-43 and VSVG-mCherry stained with markers of ER (calnexin) or cis-Golgi (GM130). The degrees of co-localisation of VSVG with calnexin or GM130 in cells expressing **b** TDP-43, **c** FUS, and **d** SOD1 were quantified using Mander's coefficient. **e** Cells expressing mSOD1 A4V or G85R (*top*), mTDP-43 Q343R (*bottom left*) or mFUS R522G (*bottom right*) were separated into intensity bins as shown on the *x* axis, and their Mander's coefficients (VSVG and calnexin or GM130) were plotted. Mean ± SEM, $n = 3$. $^{***}p < 0.001$, $^{*}p < 0.05$ difference with TDP-43 WT, EGFP vector alone or control untransfected cells (Untr). One-way ANOVA with Tukey's post hoc test

not previously linked to neurodegeneration, did not inhibit ER–Golgi transport (Suppl Fig. 2b).

To further confirm that mSOD1, mTDP-43 and mFUS specifically inhibit ER–Golgi transport, we purposefully classified individual cells according to three categories of fluorescence intensity and hence SOD1/TDP-43/FUS expression. The arbitrary values of low (~20) to high (~100) were calculated according to the pixel intensities, representing the levels of expression of SOD1, TDP-43 or FUS protein. Inhibition of transport correlated with protein expression level: cells with the highest expression of mSOD1 A4V, mSOD1 G85R, Q343R TDP-43 or R522G FUS inhibited ER–Golgi transport the greatest according to Mander's coefficient, and transport inhibition decreased with decreasing expression of mTDP-43 or mFUS (Fig. 1e). Hence the degree of transport inhibition correlates with protein expression level, confirming that ER–Golgi transport is inhibited specifically by mTDP-43, mFUS and mSOD1.

COPII vesicles are not transported to the Golgi in cells expressing mTDP-43, mFUS and mSOD1

VSVG depends on an over-expressed, non-physiological marker; hence we next sought to validate these findings using alternative approaches. We first examined bulk protein secretion in Neuro2a cells by quantifying the levels of total protein secreted into conditioned medium. Bulk protein secretion was less in cells expressing mTDP-43, mFUS or mSOD1 compared to control cells expressing WT proteins or EGFP alone (Suppl. Fig. 2c). Hence, consistent with the VSVG assay results, bulk protein secretion was inhibited in cells expressing mTDP-43, mFUS and mSOD1. However, defects in bulk protein secretion could also result from post-cis Golgi trafficking defects or dysfunction in other secretory processes. Thus, to provide further evidence for inhibition of ER–Golgi transport, we next examined COPII function in cells, which is easily visualised by dense clustering of COPII subunits adjacent to the perinuclear Golgi [23]. In untransfected cells, and cells expressing EGFP, WTSOD1, WTTDP-43 or WTFUS, COPII (Sec31) displayed the characteristic perinuclear pattern (Suppl. Fig. 3). In cells expressing mTDP-43, this pattern was lost, leaving a scattered peripheral pool of COPII (Suppl. Fig. 3a). Similar results were obtained in mFUS or mSOD1 cells (Suppl. Fig. 3b, c). Quantification revealed that perinuclear Sec31 was significantly decreased from 83–95 % in WTTDP-43, EGFP or untransfected cells, to 60 % in cells expressing mTDP-43 ($p < 0.001$, Suppl. Fig. 3d); from 82–93 % in WTFUS expressing or untransfected cells to 40–65 % in cells expressing mFUS ($p < 0.05$, Suppl. Fig. 3e); and from 75–95 % in WTSOD1, EGFP or untransfected cells to 45–47 % in cells expressing mSOD1 ($p < 0.01$, Suppl. Fig. 3f). These findings suggest that the organisation of COPII vesicles and the Golgi complex are abnormal in cells expressing mSOD1, mTDP-43 or mFUS, consistent with the presence of a block in ER–Golgi transport.

Secretory cargo and COPII are depleted from ER-derived vesicles in cells expressing mTDP-43 and mFUS

We next investigated possible mechanisms responsible for inhibition of ER–Golgi transport in ALS. We examined the first stage of transport, the incorporation of secretory cargo into COPII vesicles and budding from the ER, using an in vitro ER budding assay [49]. Sec23 is a marker of ER-budded vesicles and ERGIC is a marker of the ERGIC compartment that also localises on budded COPII vesicles. Budded vesicles were recovered and the VSVG content was analysed by quantitative western blotting (Fig. 2a, b, c). In untransfected cells and cells expressing EGFP or WTTDP-43, a similar proportion of VSVG was recovered in the budded vesicle fraction, similar to COPII (Sec23) (Fig. 2a, d). In contrast, in cells expressing Q343R TDP-43, VSVG was almost depleted (9-fold decrease, $p < 0.0001$, Fig. 2a, d). Immunoblotting revealed similar levels of ERGIC53 in all fractions, implying that vesicle number was consistent in all populations. However immunoblotting for COPII (Sec23), normalised to the levels of ERGIC53, revealed that COPII was also significantly depleted in Q343R TDP-43 vesicle fractions compared to WTTDP-43 and controls (1.4-fold decrease, $p < 0.001$, Fig. 2a, d). Similar results were obtained in cells expressing mFUS. A comparable proportion of VSVG was present in budded vesicles obtained from untransfected cells and cells expressing WTFUS. However, this proportion was significantly reduced in cells expressing R522G mFUS (2-fold, $p < 0.05$, Fig. 2b, e). COPII levels on the budded vesicles were also significantly decreased in cells expressing R522G FUS (1.25-fold, $p < 0.05$, Fig. 2b, e). Immunoblotting of total cell lysates confirmed that there were no differences in the overall expression of VSVG and COPII between cell populations (Suppl. Fig. 1d). Hence these data suggest that defects in incorporation of membrane-associated cargo into budding ER vesicles inhibit ER–Golgi transport in cells expressing mTDP-43 or mFUS.

In contrast, in cells expressing mSOD1, there were no significant differences in the proportion of VSVG or COPII associated with budded vesicles compared to untransfected cells or cells expressing EGFP or WTSOD1 (Fig. 2c, f). The expression levels of VSVG and COPII were also similar between the cell populations (Suppl. Fig. 1d), suggesting that secretory cargo incorporates normally into ER-derived vesicles in mSOD1 cells.

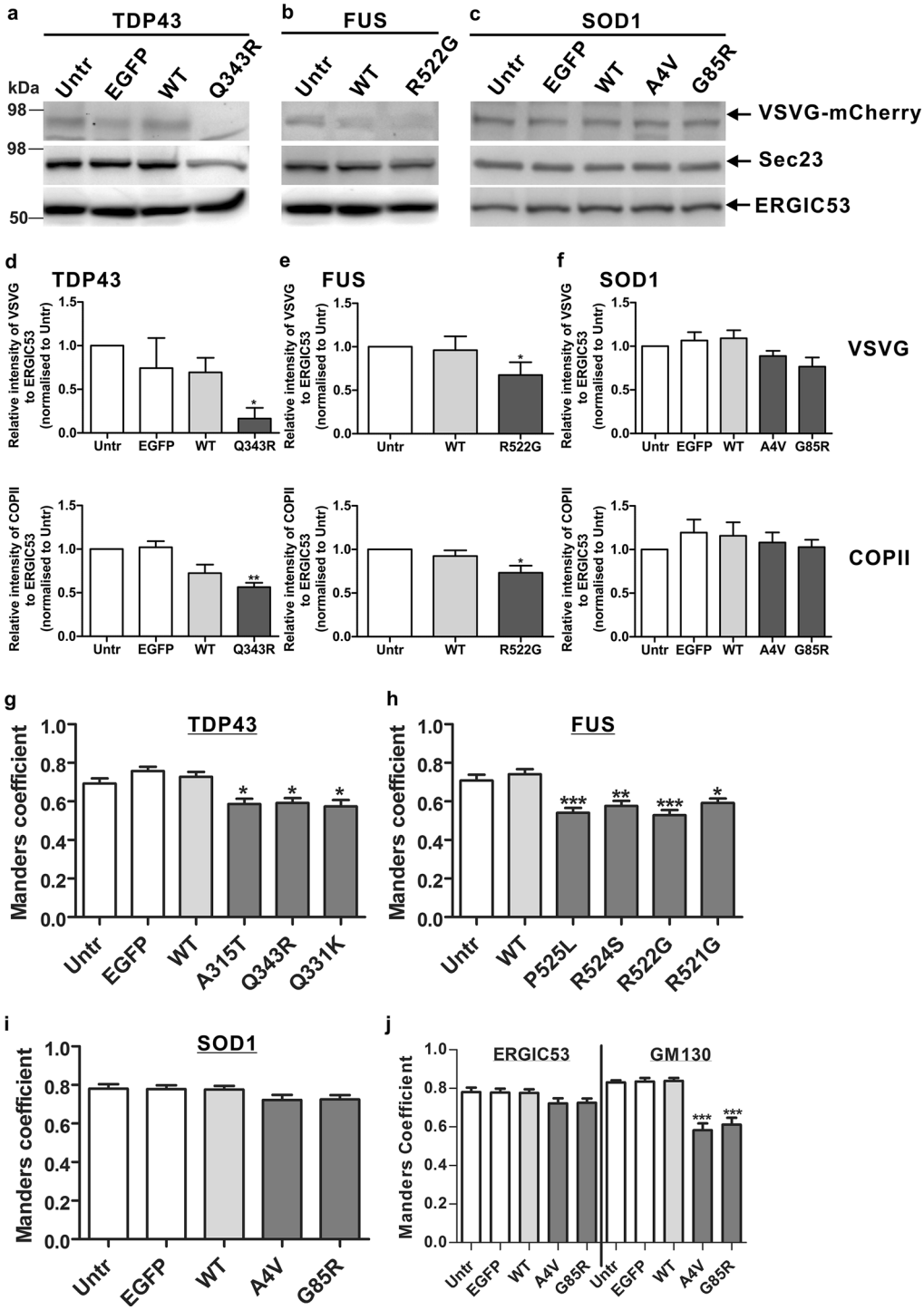

Fig. 2 mTDP-43 and mFUS have an inhibitory effect on ER vesicle budding, but not mSOD1. VSVG-mCherry was trapped in the ER and ER-vesicles budding was reconstituted in vitro in perforated cells expressing **a** EGFP-TDP-43, **b** HA-FUS or **c** SOD1-EGFP. Budded vesicles were collected and subjected to western blotting using anti-VSVG and anti-COPII (Sec23) antibodies. ERGIC53 was used for control of equivalent budded vesicles. Relative intensities of VSVG and COPII (Sec23) were quantified in cells expressing **d** EGFP-TDP-43, **e** HA-FUS or **f** SOD1-EGFP, first normalised to ERGIC53 intensity for the relevant lane, and then normalised again to the control untransfected cells (Untr). Mean ± SEM ($n = 3$). $^{**}p < 0.01$, $^{*}p < 0.05$ difference with untransfected cells. Cells expressing **g** EGFP-TDP-43, **h** HA-FUS or **i** SOD1-EGFP were treated as in Fig. 1 and immunostained with ERGIC53. The degrees of co-localisation of VSVG with ERGIC53 in cells were quantified using Mander's coefficient. **j** Cells expressing SOD1-EGFP were treated as in Fig. 1 and immunostained with ERGIC53 or cis-Golgi marker, GM130. The degrees of co-localisation of VSVG with ERGIC53 or GM130 in cells were quantified using Mander's coefficient. Mean ± SEM, $n = 3$. $^{***}p < 0.001$, $^{**}p < 0.01$, $^{*}p < 0.05$ difference with WT protein transfected cells. One-way ANOVA with Tukey's post hoc test

To verify that less secretory cargo incorporates into vesicles in cells expressing mTDP-43 or mFUS, we examined incorporation of VSVG into COPII vesicles by immunocytochemistry (Suppl. Fig. 4). Mander's coefficient between VSVG and ERGIC53 was similar in untransfected cells and cells expressing EGFP alone or WTTDP-43. However, significantly less VSVG co-localised with ERGIC53 in cells expressing mTDP-43 or mFUS compared to WTTDP-43, WTFUS or untransfected cells ($p < 0.05$, Fig. 2g, h and Suppl. Fig. 4a, b). Hence vesicular cargo does not incorporate normally into COPII vesicles in mTDP-43 or mFUS expressing cells. In contrast, there were no significant differences in Mander's coefficient between cells expressing mSOD1 and WTSOD1, EGFP or untransfected cells (Fig. 2i and Suppl. Fig. 4c); however, less VSVG co-localised with GM130 in cells expressing mSOD1 compared to WTSOD1 or untransfected cells (Fig. 2j). This provides further evidence that incorporation of secretory cargo into COPII vesicles, and their budding from the ER and transport to ERGIC, is normal in cells expressing mSOD1. Hence this implies that inhibition of ER–Golgi transport by mSOD1 is downstream of the ERGIC compartment.

TDP-43 and FUS are associated with the ER

The depletion of cargo after budding from the ER suggests dysfunction to the ER in mTDP-43 and mFUS expressing cells. Hence we next examined whether TDP-43 and FUS are present within the ER. Using immunocytochemistry and z-stack series confocal imaging, we demonstrated that mTDP-43 and mFUS partially co-localised with ER marker, calnexin, suggesting that at least a proportion of mTDP-43 and mFUS are localised in the ER (Fig. 3a). Calculation of Mander's coefficient also revealed increased co-localization between calnexin and mTDP-43 or mFUS, compared to WTTDP-43 or WTFUS (Fig. 3b, c), implying that the mutants associated more with the ER. Similarly, subcellular fractionation experiments demonstrated that endogeneous TDP-43 and FUS were present in the membrane fraction (containing the ER), as well as nuclear and cytoplasmic fractions, enriched in IRE1, Histone H3 and GAPDH, respectively (Fig. 3d). Both WT and mutant forms of TDP-43 and FUS were enriched in nuclear and membrane fractions but only slightly in the cytoplasmic fraction (Fig. 3d). To investigate this further, a fluorescence protease protection assay was performed, in which proteins contained within cellular membranes are protected from proteinase K after digitonin treatment [34] (Fig. 3e). In EGFP only expressing cells, the fluorescence disappeared following digitonin treatment, demonstrating that EGFP was expressed in the cytoplasm. In contrast, in cells expressing Dsred-tagged protein disulphide isomerase (PDI), a chaperone located in the ER of unstressed cells [82], the fluorescence was unchanged after extended proteinase K treatment (Fig. 3e). In cells expressing EGFP-TDP-43 (WT or Q343R), the fluorescence was retained after digitonin treatment, demonstrating that TDP-43 is associated with membranes, but it disappeared after addition of proteinase-K. Hence together with the calnexin immunocytochemistry results (Fig. 3a), these findings imply TDP-43 is present on the cytoplasmic face of the ER membrane. In contrast, in cells expressing GFP-FUS (WT or R521G), the fluorescence was retained after both digitonin and proteinase-K treatment (Fig. 3e). To confirm these findings, and to ascertain that the fluorescence was due to membrane bound protein, rather than misfolded cytosolic protein, Triton-x-100 was added as a final step. In cells expressing either WT or mFUS the fluorescence signal disappeared completely, similar to control cells expressing PDI-DsRed. Hence these data imply that both WT and mFUS are present within the ER lumen, similar to PDI (Fig. 3f).

mSOD1 inhibits COPII vesicular transport to the Golgi

We next examined possible mechanisms whereby mSOD1 inhibits transport. ER-derived vesicles bud and transport cargo normally to the ERGIC but not to the Golgi in mSOD1 expressing cells (Fig. 2j), suggesting that ERGIC–Golgi transport, a microtubule dependent step, rather than ER–ERGIC transport, a microtubule independent step, is inhibited in these cells. mSOD1, unlike WTSOD1, also binds aberrantly to tubulin [31, 83]. Together these data suggest that mSOD1 may disrupt microtubule function, thus disrupting ERGIC–Golgi transport. We, therefore, examined the stability of microtubules in cells expressing mSOD1 by quantitating the levels of acetylated tubulin: a post-translational modification that stabilises and regulates microtubule function [45]. Whilst the levels of acetylated tubulin were similar in untransfected cells and cells expressing EGFP or WTSOD1, significantly decreased levels were detected in cells expressing mSOD1 (Fig. 4a–c), revealing that fewer stable microtubules are present in mSOD1 cells. Both tubulin and acetylated tubulin also co-localised with mSOD1 inclusions (Fig. 4d, e). In control experiments, neither mTDP-43 nor mFUS inhibited tubulin acetylation, and one mutant mTDP-43, A315T, slightly increased the levels of acetylated tubulin (Suppl. Fig. 5a), suggesting that inhibition of tubulin acetylation is specific for mSOD1.

We next examined whether microtubule stabilising agents, Taxol or Epothilone D (EpoD), rescue ER–Golgi transport in cells expressing mSOD1. As expected, the levels of acetylated tubulin were increased in Taxol/EpoD treated cells, confirming that both compounds stabilise microtubules, and EpoD was more effective than Taxol

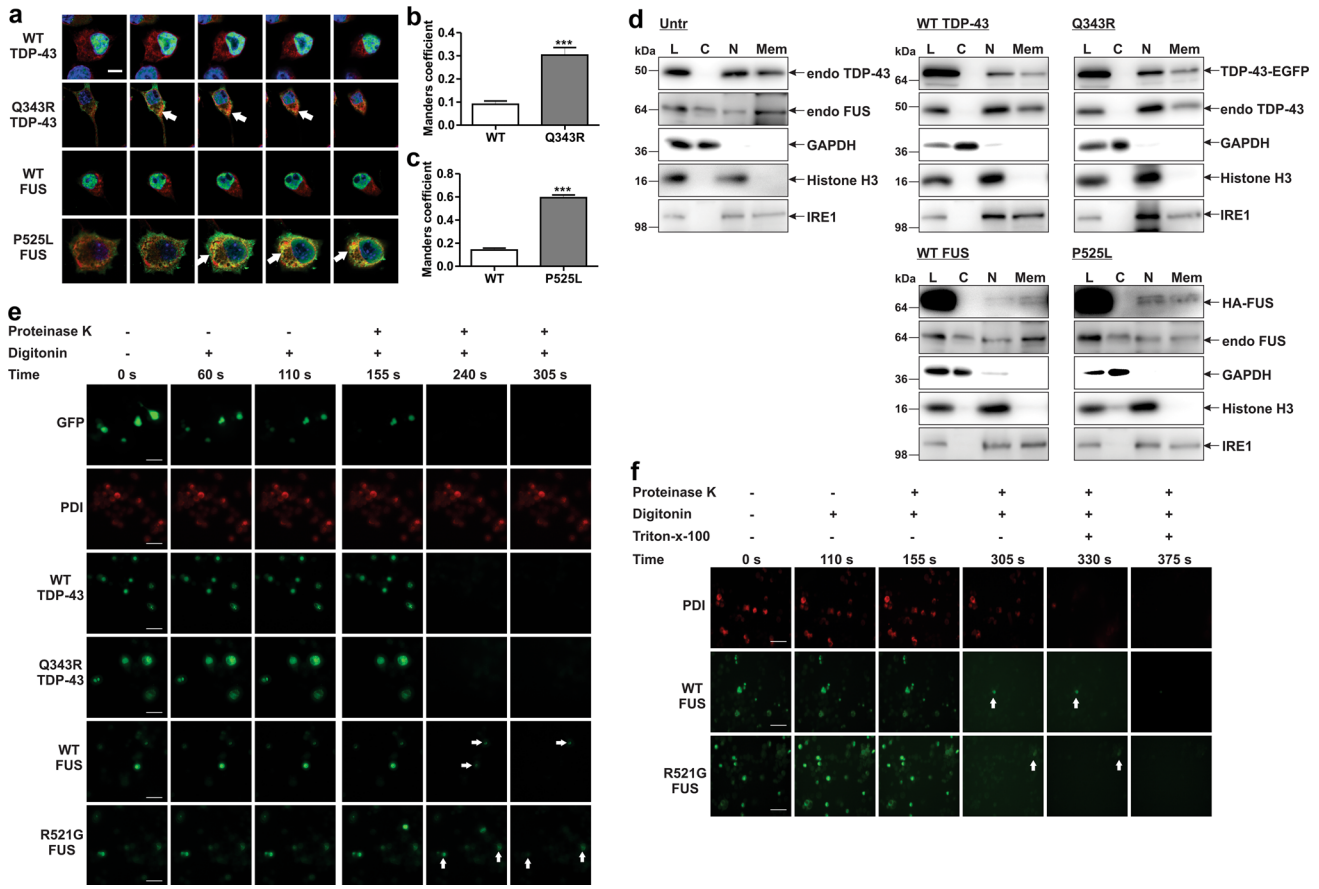

Fig. 3 TDP-43 is expressed on the ER membrane and FUS is located inside the ER. **a** Neuro2a cells expressing EGFP-TDP-43 (WT or Q343R, *green*) or HA-FUS (WT or P525L, *green*) were fixed and immunostained with anti-calnexin antibody (*red*). Nuclei were stained with Hoechst (*blue*). Z-series of merge images were shown. *Scale bar* 5 μm. *White arrows* indicate co-localization of calnexin with mTDP-43 or mFUS. Mander's coefficients of **b** TDP-43 or **c** FUS with calnexin were analysed. Mean ± SEM, $n = 3$. ***$p < 0.001$. One-way ANOVA with Tukey's post hoc test. **d** Subcellular fractionation of untransfected cells, cells expressing WTTDP-43, Q343R, WTFUS or P525L. Whole cell lysates (L), cytoplasmic (C), nuclear (N) and membrane (Mem) fractions from each sample were prepared, and western blotting for TDP-43, FUS, GAPDH, Histone H3 and IRE1 was performed. GADPH, Histone H3 and IRE1 were used as a marker of cytoplasm, nuclear and membrane, respectively. **e** Fluorescence protease protection assay demonstrated that TDP-43 is found on the ER membrane but FUS is found on the ER membrane and in the ER lumen. Neuro2a cells that expressed EGFP vector alone, PDI-dsred, EGFP-TDP-43 (WT or mutant) or GFP-FUS (WT or mutant) were subjected to the fluorescence protease protection assay. Individual images were taken before and after treatment with 60 μM digitonin and 50 μg/ml proteinase-K. **f** Fluorescence protease protection assay with 1 % Triton-x-100 treatment demonstrated that PDI and FUS (WT and mutant R521G) are present in the ER lumen. *White arrows* indicate the presence of FUS-GFP. *Scale bars* 50 μm

(Fig. 4f). Both compounds significantly increased ER–Golgi transport in cells expressing mSOD1 relative to control DMSO-treated cells (Fig. 4g). EpoD fully restored transport in both A4V and G85R cells, whereas Taxol fully restored transport in A4V, but only partially in G85R, expressing cells. In contrast, in control experiments, neither Taxol nor EpoD had any effect on the inhibition of VSVG transport from ER to Golgi, in cells expressing mTDP-43 or mFUS (Suppl. Fig. 5b). These findings reveal that stabilising microtubules rescues transport inhibition specifically in mSOD1 expressing cells. Furthermore, to provide further evidence that mutant SOD1 perturbs microtubule-based transport processes, we next examined the fusion of the autophagosome with the lysosome by co-expression with LC3 and LAMP1, as markers of each compartment, respectively. In cells expressing mSOD1 (A4V or G85R), significantly less CFP-LC3 co-localised with LAMP1-RFP, compared to in cells expressing WT or untransfected cells ($p < 0.01$, Suppl. Fig. 5c, d). Hence mSOD1 also inhibits autophagy-related trafficking, which is also microtubule-dependent. This was confirmed by treatment of mSOD1 expressing cells with EpoD, which restored the levels of autophagosome and lysosome fusion in cells expressing G85R to the levels found in control cells. For A4V, the levels were also increased but this was not statistically significant (Supp. Fig. 5e). These data, therefore, imply that unstable microtubules specifically impede ER–Golgi transport in cells expressing mSOD1.

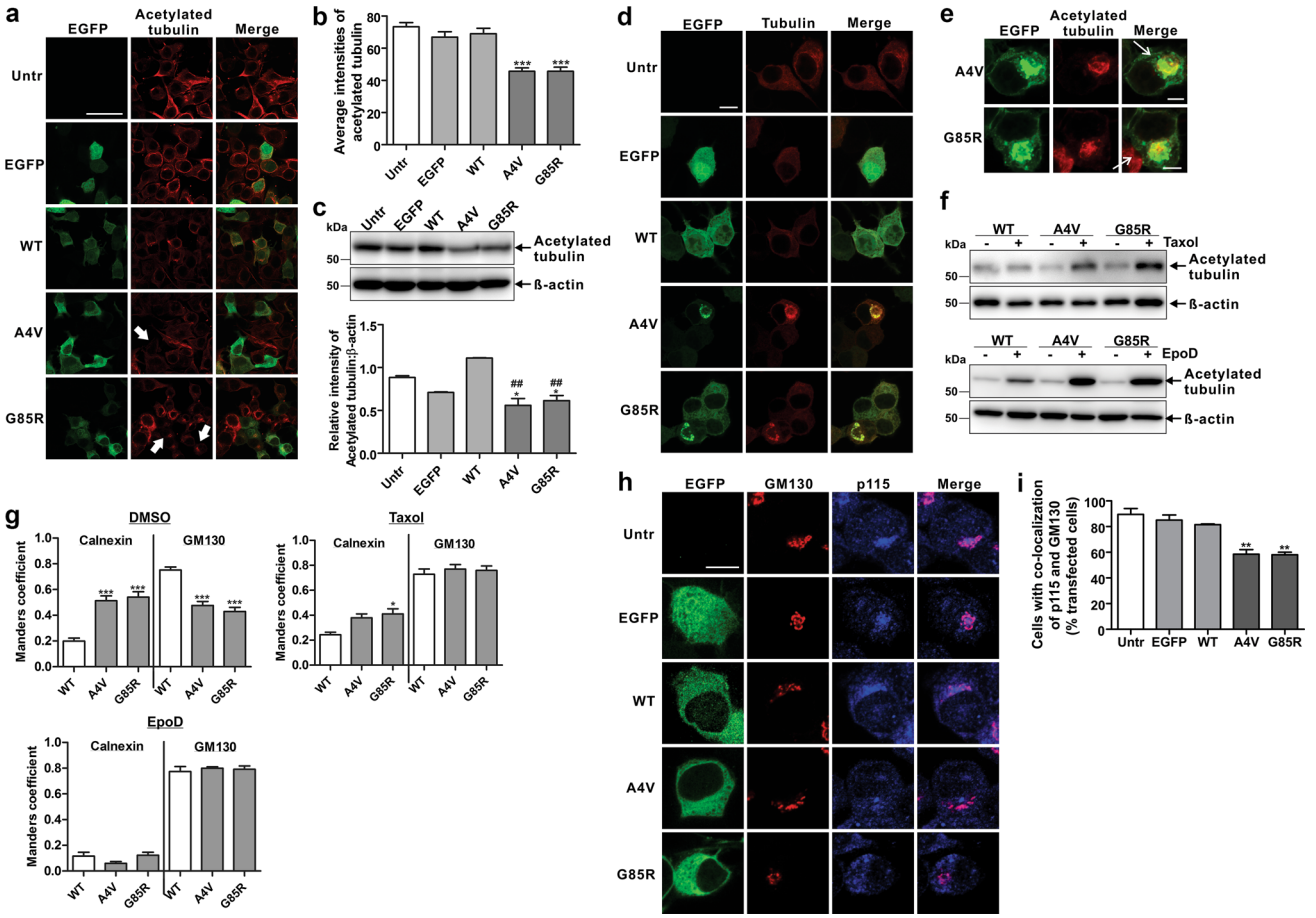

Fig. 4 COPII vesicles are unable to be transported to the Golgi complex in cells expressing mSOD1. **a** Neuro2a cells expressing SOD1-EGFP were fixed and immunostained with anti-acetylated tubulin antibodies. Merge images were shown. *Thick white arrows* indicate decreased fluorescence intensity of acetylated tubulin. **b** Quantified data for the average fluorescence intensities of acetylated tubulin in cells from **a**. **c** Immunoblotting of soluble cell lysates of untransfected (Untr), EGFP alone, WT or mSOD1 expressing cells. Blot was probed with anti-acetylated tubulin and anti-β-actin antibody was used for loading control. Graph represents the relative intensities of acetylated tubulin to β-actin. **d** Neuro2a cells co-expressing SOD1-EGFP (*green*) and tubulin-RFP (*red*) were fixed and visualised under confocal microscopy. Merge images were shown. **e** mSOD1 A4V or G85R transfected cells bearing inclusions were immunostained with anti-acetylated tubulin antibodies. Merge images were shown. *Thin white arrows* indicate co-localisation of mSOD1 inclusions and acetylated tubulin. **f** Immunoblotting of soluble cell lysates of cells expressing WT or mSOD1 upon Taxol and EpoD treatment. Blot was probed with anti-acetylated tubulin and anti-β-actin antibody was used for loading control. **g** Taxol or Epo D treated Neuro2a cells expressing WT or mSOD1 (A4V or G85R) were treated as in Fig. 1. The degrees of co-localisation of VSVG with calnexin or GM130 in cells were quantified using Mander's coefficient. **h** Neuro2a cells expressing SOD1-EGFP for fixed and immunostained with anti-p115 and anti-GM130 antibodies. Merge images of p115 and GM130 were shown. **i** Quantified data of SOD1-EGFP transfected cells with co-localisation of p115 and GM130. Mean ± SEM, $n = 3$. $^{***}p < 0.001$, $^{**}p < 0.01$, $^{*}p < 0.05$ difference with control untransfected cells (Untr), $^{\#\#}p < 0.001$ difference with WT transfected cells. One-way ANOVA with Tukey's post hoc test. *Scale bars* 10 μm

To confirm these findings, we also examined tethering of COPII vesicles to the cis-Golgi using immunocytochemistry for p115 and GM130, where co-localisation indicated efficient vesicular tethering. In cells expressing WTSOD1, EGFP or untransfected cells (Fig. 4h, i), p115 and GM130 were co-localised in 80–90 % of cells, suggesting that COPII vesicles tether efficiently to the Golgi. However, the proportion of cells with co-localised p115 and GM130 was significantly decreased (1.5-fold, $p < 0.01$) in mSOD1 expressing cells. Hence tethering of COPII vesicles to the Golgi is antagonised by mSOD1, consistent with the presence of less stable microtubules in these cells.

Overexpression of Rab1 rescues inhibition of ER–Golgi transport in cells expressing mTDP-43, mFUS or mSOD1

We next looked for possible molecular targets of mSOD1, mTDP-43 and mFUS. Most proteins involved in ER–Golgi transport perform narrow, highly specific functions. Hence, dysfunction in their activity would not explain the diverse

mechanisms of inhibition observed by mSOD1, mTDP-43 and mFUS. However, in contrast, Rab1 plays multiple roles in ER–Golgi transport, including vesicle budding, transport to the Golgi and microtubule stability. We, therefore, next investigated whether ALS-associated mutant proteins antagonise Rab1 function, and hence whether Rab1 over-expression could restore ER–Golgi trafficking. Rab1-tagged with FLAG or empty vector pCMV-FLAG as a control, was co-expressed in Neuro2a cells with EGFP-TDP-43, HA-FUS or SOD1-EGFP, and VSVG-mCherry. As expected, in cells co-expressing mTDP-43, mFUS or mSOD1 (with empty vector), more VSVG was retained within the ER and less was transported to the Golgi compared to controls (Fig. 5a–c). However, in cells co-expressing FLAG-Rab1, similar levels of VSVG were present in the Golgi in cells expressing mTDP-43, mFUS or mSOD1, as in controls expressing WT proteins, untransfected cells or EGFP alone (Fig. 5a–c). Immunoblotting using an anti-FLAG antibody confirmed that the expression levels of Rab1 were equivalent in cells expressing the ALS-mutants compared to controls (Suppl. Fig. 1e). Hence Rab1 rescues inhibition of ER–Golgi transport induced by mTDP-43, mFUS or mSOD1.

Overexpression of Rab1 rescues ER stress induced by mTDP-43, mFUS or mSOD1

We next examined whether overexpression of Rab1 can rescue ER stress in these cells, using activation of XBP1 as a marker of UPR induction [79]. XBP1 activation was significantly reduced in cells overexpressing Rab1 and mTDP-43, mFUS or mSOD1, compared to controls expressing empty vector (2-fold, $p < 0.05$), and it was restored to levels observed in cells expressing WT proteins, EGFP or untransfected cells (Fig. 5d). To rule out the possibility that the reduction of ER stress was due to restoration of Rab1 activity and not non-specific protein over-expression, two Rab1 mutants were examined; dominant negative Rab1S25N and constitutively active Rab1Q70L. Rab1S25N is maintained in an inactive GDP-bound state that cannot convert to its active GTP-bound form [42], whereas Rab1Q70L is constitutively active by remaining GTP-bound [18]. In contrast to WT Rab1, co-expression of Rab1S25N did not rescue ER stress in cells expressing mTDP-43, mFUS or mSOD1 (Fig. 5e). Furthermore, expression of GTP-bound Rab1Q70L decreased ER stress, indicated by XBP1 activation, induced by mTDP-43, mFUS or mSOD1 (2-fold, $p < 0.05$, Fig. 5f). To confirm the findings using XBP1, another marker of ER stress, nuclear immunoreactivity to CHOP [65], was examined in these cells, with similar findings (Suppl. Fig. 6). Hence the functional activity of Rab1 is protective against ER stress induced by mTDP-43, mFUS and mSOD1.

Fig. 5 Over-expression of Rab1 rescues ER–Golgi transport inhibition, ER stress, apoptosis and inclusion formation induced by mTDP-43, mFUS and mSOD1. Neuro2a cells co-expressing **a** EGFP-TDP-43, **b** HA-FUS or **c** SOD1-EGFP and empty pCMV-FLAG vector (CMV) (*top panels*) or FLAG-Rab1 (*bottom panels*) were also co-expressed VSVG, Mander's coefficients were quantified for transport of VSVG from ER to Golgi in transfected cells with/without Rab1 using calnexin and GM130. All other indications as in Fig. 1. Cells co-expressing TDP-43, FUS or SOD1 with **d** WTRab1, mutant Rab1 **e** S25N or **f** Q70L were fixed and immunostained with anti-XBP1 antibodies. Percentages of cells with XBP1 activation were quantified. Both inclusion formation and apoptotic nuclei were quantified for cells co-expressing SOD1 and **g** WT Rab1, mutant Rab1, **h** S25N or **i** Q70L. Mean ± SEM, $n = 3$. ***$p < 0.001$, **$p < 0.01$, *$p < 0.05$ difference with control untransfected cells (Untr). Unpaired student *t* test. Total 100 cells were scored from each group in each experiment. EGFP represents cells expressing EGFP vector alone

mSOD1 normally forms prominent inclusions in 15–18 % of cells and apoptosis in 10–15 % of cells [66]. Rab1 overexpression also significantly reduced the formation of inclusions (7–9 %, $p < 0.001$) and apoptosis ($p < 0.05$, 3-fold) in mSOD1 expressing cells (Fig. 5g). In control experiments, Rab1S25N did not affect mSOD1 inclusion formation and apoptosis (Fig. 5h), whereas Rab1Q70L further reduced mSOD1 inclusions (5–7 %, $p < 0.05$) and restored apoptosis to control levels (2.5 to 3-fold, $p < 0.0001$, Fig. 5i). These data thus link Rab1 functional activity to neurodegeneration and apoptosis in cells expressing mSOD1.

Rab1 is recruited to spinal motor neuron inclusions in patients with sALS and mis-localises in cells expressing ALS-associated SOD1, TDP-43 and FUS

We next examined the distribution of Rab1 in Neuro2a cells expressing TDP-43, FUS and SOD1 using immunocytochemistry. Rab1 was expressed diffusely in control cells and there was little co-localisation with WT TDP-43, FUS or SOD1. However, Rab1 co-localised extensively with mTDP-43 and mFUS (Fig. 6a, b). Analysis of Mander's coefficient revealed significantly increased co-localization of Rab1 with mTDP-43 and mFUS, compared to WT TDP-43 or FUS (Fig. 6c, d). Furthermore, Rab1 co-located with mSOD1 inclusions in approximately 20 % of cells (Fig. 6e) implying that mSOD1, mTDP-43 and mFUS alter the cellular distribution of Rab1. In contrast, other proteins involved in ER–Golgi transport, including COPII subunit Sec23 did not bind to mTDP-43 or mFUS (Suppl. Fig. 7). Hence together these data suggest that Rab1 is associated with pathogenic mechanisms involving mTDP-

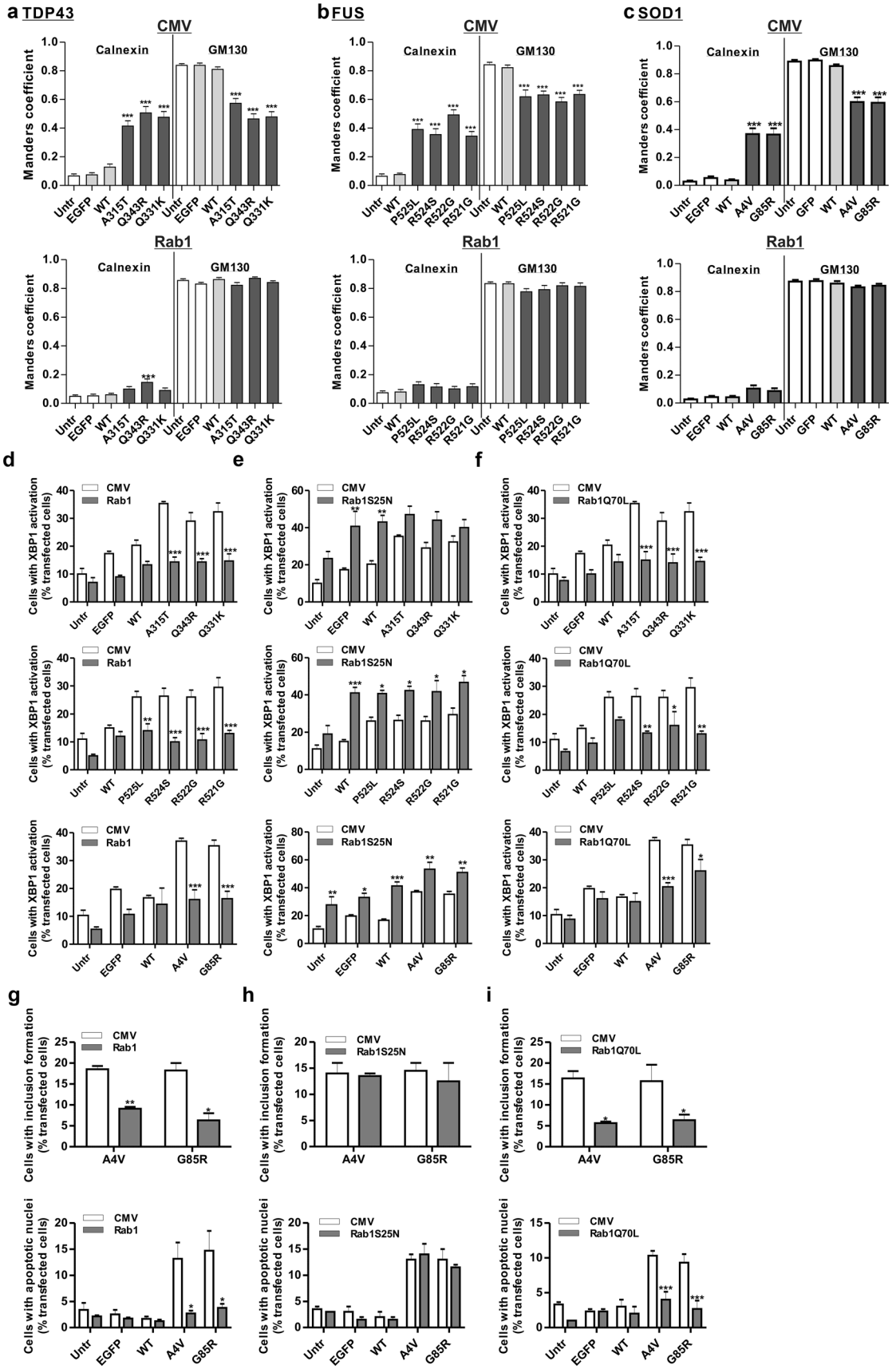
a TDP43
b FUS
c SOD1
CMV
Rab1
Calnexin
GM130
Manders coefficient
Untr
EGFP
WT
A315T
Q343R
Q331K
P525L
R524S
R522G
R521G
A4V
G85R
GFP
d
e
f
CMV
Rab1
Rab1S25N
Rab1Q70L
Cells with XBP1 activation (% transfected cells)
g
h
i
Cells with inclusion formation (% transfected cells)
Cells with apoptotic nuclei (% transfected cells)

43, mFUS and mSOD1. This was examined further in motor neurons of human spinal cord tissues from patients with sALS. For this analysis, large neurons located in the ventral horn region of spinal cord sections were identified as motor neurons (Suppl. Fig. 8a). Using immunohistochemistry, 80 % of motor neurons from sALS patients bore TDP-43 inclusions, all of which co-localised extensively with ubiquitin. Hence these motor neurons bear the typical ubiquitinated TDP-43 inclusions present in most cases of human ALS. Rab1 was expressed diffusely in control patients without neurological disease (Fig. 6f). However, in contrast, in an average of 50 % of sALS motor neurons, Rab1 formed prominent, inclusion-like structures (Fig. 6f, g). The presence of Rab1-positive inclusions in motor neurons was confirmed by performing immunohistochemistry using anti-Rab1 and anti-SMI32 antibodies (Suppl. Fig. 8b). Furthermore, approximately 40 % of the Rab1 inclusion-positive motor neurons co-localised with TDP-43 (Fig. 6f, h and Suppl. Fig. 8c). The Rab1-positive inclusions in sALS patients were intracytoplasmic punctate structures, some of which resembled Lewy-body-like or small Bunina body-like inclusions characteristic of ALS (Supp. Fig. 8d). In contrast, Rab1 was expressed diffusely in control motor neurons (Suppl. Fig. 8d). Hence, Rab1 is mis-localised and recruited into abnormal inclusions in motor neurons from sALS patients, thus implicating loss of Rab1 function in both sALS and familial ALS (fALS). Using immunoprecipitation, Rab1 also precipitated with phosphorylated TDP-43 in human sALS patient spinal cords (Suppl. Fig. 8e) and Rab1 and TDP-43 also co-precipitated more in cells expressing mTDP-43 (Suppl. Fig. 8f). Hence, Rab1 is mis-localised, recruited into abnormal inclusions and co-precipitates with pathological forms of TDP-43. This implies that a physical interaction exists between TDP-43 and Rab1, thus implicating loss of Rab1 function in both sALS and fALS.

ER–Golgi transport is inhibited in embryonic primary cortical and motor neurons from SOD1^{G93A} transgenic mice

Finally, we examined transgenic mice overexpressing SOD1^{G93A} for evidence of ER–Golgi transport inhibition in primary neurons. Primary embryonic cortical neurons and motor neurons isolated from SOD1^{G93A} and non-transgenic controls were transfected with VSVG-mCherry and ER–Golgi transport was quantified as above. In both cortical neurons (Fig. 7a, c) and motor neurons (Fig. 7b, d), ER–Golgi transport was inhibited in SOD1^{G93A} mice compared to controls ($\sim$2-fold, $p < 0.001$); more VSVG was retained in the ER and less transported to the Golgi. Hence these data provide further evidence that ER–Golgi transport is a pathogenic and early disease mechanism in ALS.

Discussion

Extensive evidence now implicates the failure of proteostasis as a trigger for neurodegeneration in ALS, and regulation of membrane trafficking is a key component of proteostasis. One third of all proteins transit through the ER–Golgi compartments destined for extracellular, transmembrane or other cellular locations [22]. ER–Golgi transport is, therefore, the most fundamental intracellular membrane trafficking system and it is a vital gateway to the endomembrane system. Disruption to ER–Golgi transport would therefore significantly impact on cellular function and viability. Here, we demonstrate that ALS-associated mSOD1, mTDP-43 and mFUS all inhibit ER–Golgi transport. We also detected inhibition of ER–Golgi transport in embryonic motor and cortical neurons obtained from SOD1^{G93A} mice, validating this process in primary neurons and as an early disease mechanism. Moreover, the presence of Rab1-positive inclusions in sALS patients implies that secretory protein transport may also be inhibited in sporadic disease. Furthermore, restoration of ER–Golgi transport by Rab1 in our study prevented inclusion formation and apoptosis, thus linking this mechanism to neuronal cell death and degeneration. Inhibition of cellular trafficking may therefore be an important component of proteostasis in ALS.

We found that each protein inhibited ER–Golgi transport by distinct processes, but each mechanism was dependent on Rab1 function. In cells expressing mTDP-43, COPII vesicles budded normally, but they were almost completely depleted of cargo. Similarly in mFUS expressing cells, the vesicles were also depleted of cargo, but to a lesser extent than mTDP-43. Previous studies have suggested that the eventual size of COPII vesicles depends on the cargo loaded into these vesicles [29]. In preliminary studies, we found that COPII vesicles were reduced in size in cells expressing mTDP-43 or mFUS, consistent with this property. However, further experiments are required to confirm these findings. The level of COPII but not ERGIC53 on these vesicles was also reduced compared to control cells, suggesting that smaller vesicle diameter correlates with less vesicular COPII, which would result in atypical vesicles. Both mTDP-43 and mFUS inhibited ER–ERGIC rather than ERGIC-Golgi transport, and we detected TDP-43 on the cytoplasmic face of the ER, whereas FUS was present within the ER lumen. Using Mander's coefficient, more mTDP-43 and mFUS co-

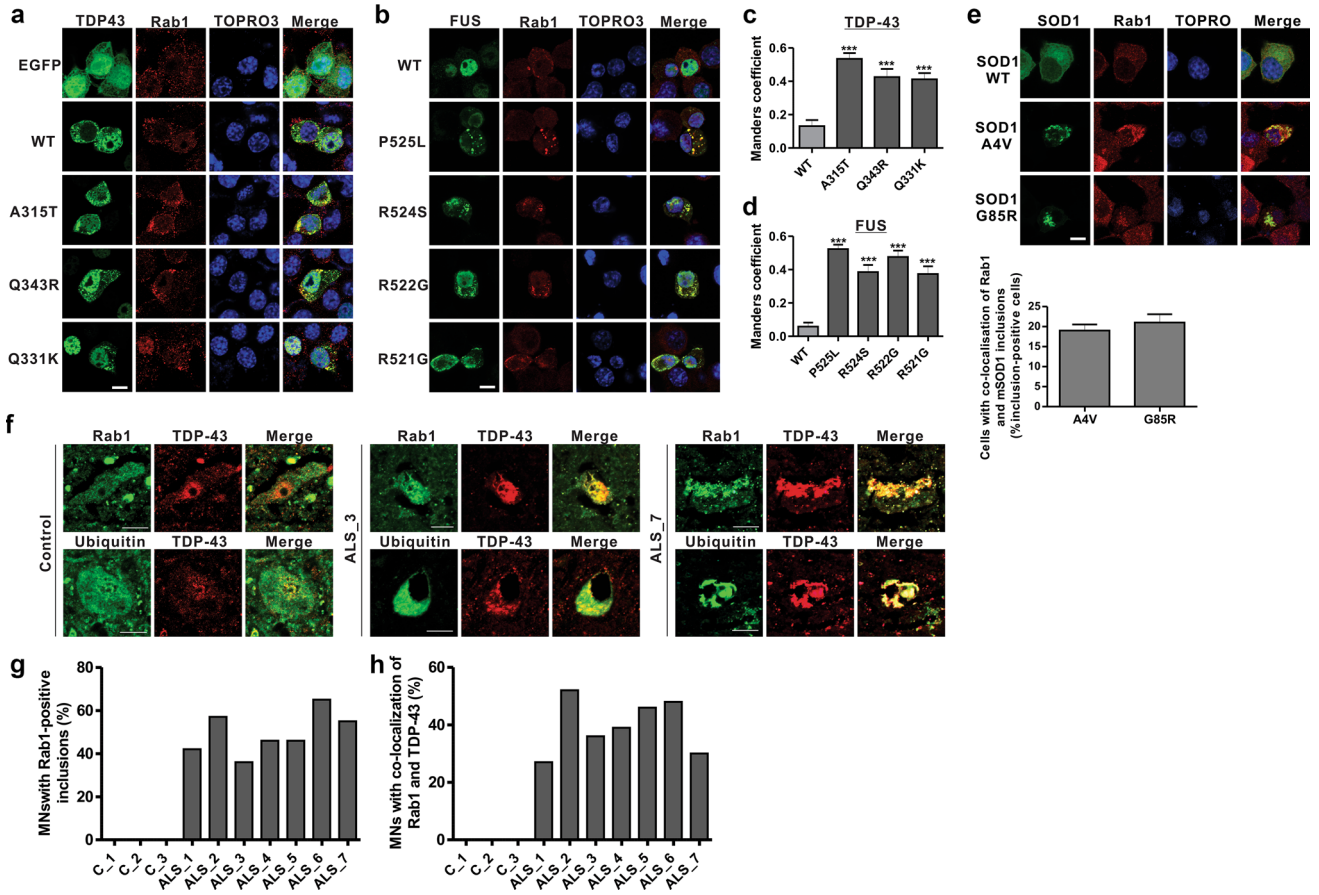

Fig. 6 Rab1 is mislocalised in cells expressing mTDP-43, mFUS and mSOD1 and forms inclusion-like structure in motor neurons from patients with sALS. Neuro2a cells expressing **a** EGFP-TDP-43 (WT or mutants) or EGFP vector alone; **b** HA-FUS (WT or mutants) were fixed and immunostained with anti-Rab1 antibodies. Representative images from each transfected cells were shown here. Nuclei were counter-stained with TOPRO-3 and merge images were shown. Mander's coefficients of co-localisation of Rab1 with **c** TDP-43 and **d** FUS were analysed. Mean ± SEM, $n = 3$. ***$p < 0.001$ difference with WT transfected cells. One-way ANOVA with Tukey's post hoc test. **e** SOD1-EGFP (WT or mutants) transfected cells were fixed and immunostained with anti-Rab1 antibodies. Representative images from each transfected cells were shown here. Nuclei were counter-stained with TOPRO-3 and merge images were shown. Graph represents percentage of inclusion-positive cells with co-localisation of Rab1 and mSOD1 inclusions. **f** Representative images of paraffin-fixed spinal cord sections from control individual and patients with sALS were dewaxed and immunostained with anti-Rab1, anti-TDP-43 and anti-ubiquitin antibodies. Images were fully reflective of the cells examined. **g** Graph represents percentage of motor neurons displayed Rab1 inclusions. **h** Graph represents percentage of Rab1-positive inclusion motor neurons with Rab1 and TDP-43 colocalization. Twenty to thirty motor neurons from each patient were scored. Merge images were shown. *Scale bars* 10 μm

localised with calnexin compared to WTTDP-43 or WTFUS. Hence, these data imply that mTDP-43 and mFUS inhibit ER–Golgi transport from either the cytoplasmic face of the ER or from within the ER lumen, respectively.

In contrast, in cells expressing mSOD1, COPII vesicles budded normally, were almost fully loaded with cargo, and were transported normally from ER to ERGIC. However, transport was inhibited between ERGIC and Golgi, and fewer acetylated microtubules were detected in mSOD1 expressing cells. Tubulin acetylation stabilises microtubules and promotes the recruitment of molecular motors kinesin-1 and cytoplasmic dynein [14, 53]. ERGIC–Golgi transport is a long-range, microtubule and dynein–dynactin-dependent step [1], in contrast to ER–ERGIC transport, which is short-range and microtubule independent. Our detection of inhibition of ERGIC–Golgi—but not ER–ERGIC—transport, and the loss of tethering of COPII vesicles to the Golgi in mSOD1 cells, is consistent with a microtubule-mediated defect. Previously, we could not detect SOD1 in the ER [3], similar to other groups [8, 41], suggesting that mSOD1 inhibits ER–Golgi transport from the cytoplasm. Dysfunction to microtubules would explain both inhibition of ER–Golgi transport and triggering of ER stress by cytoplasmic mSOD1. Consistent with our findings, previous studies have shown that tubulin and dynein both interact with mSOD1, and that mSOD1 modulates tubulin polymerisation [31, 83]. A recent study also

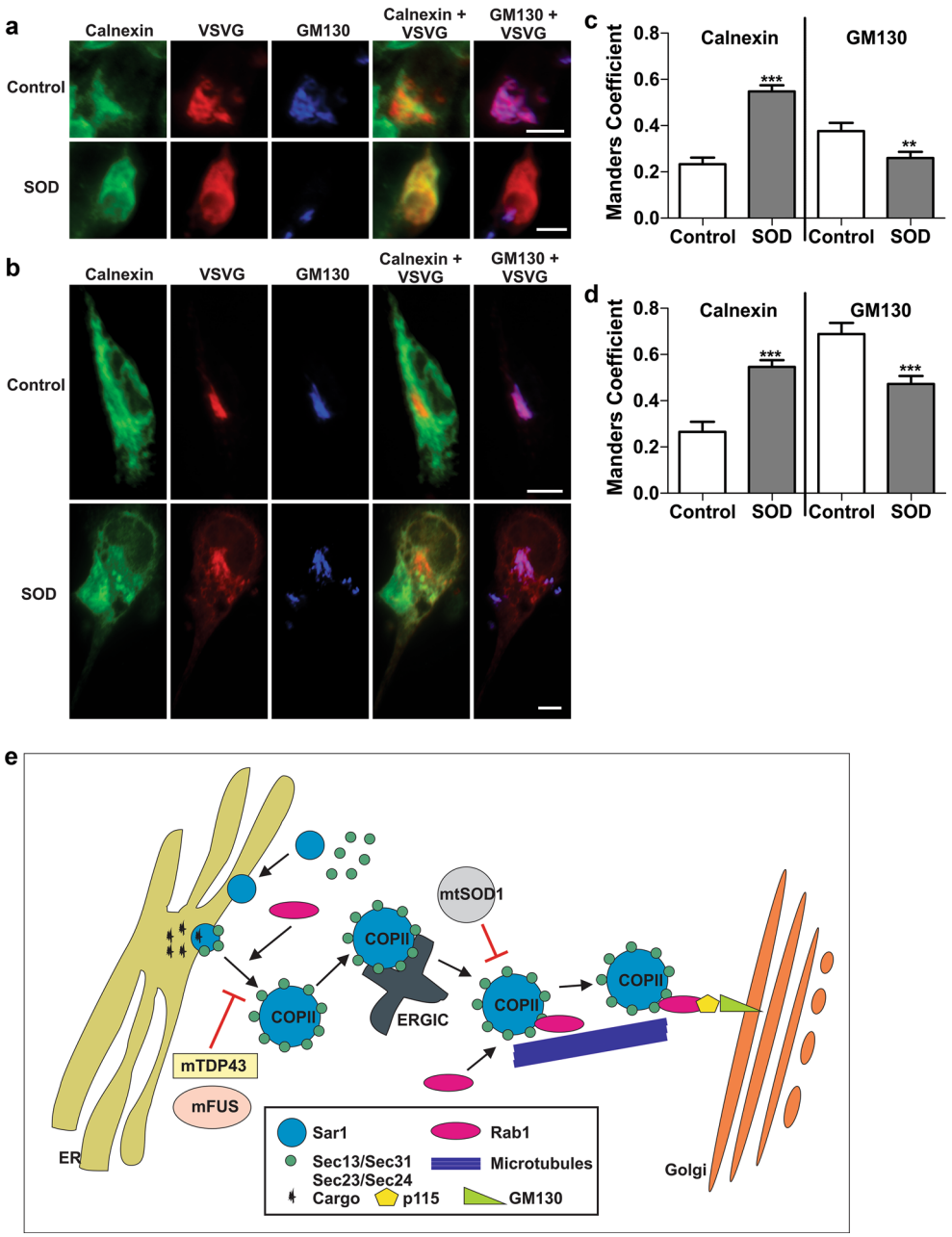

Fig. 7 ER–Golgi transport is inhibited in primary cortical neurons and motor neurons isolated from SOD1^{G93A} transgenic mice. Both **a** primary cortical neurons and **b** motor neurons are isolated from SOD1^{G93A} transgenic (SOD) or non-transgenic (control) mice at E13.5. Primary neurons were then transfected with VSVG-mCherry for 24 h and then fixed and immunostained with calnexin for ER (*green*) and GM130 for cis-Golgi (*blue*). Merge images were shown. *Scale bar* 10 μm. The degree of co-localisation of VSVG with calnexin or GM130 in primary **c** cortical neurons and **d** motor neurons was quantified using Mander's coefficient. Mean ± SEM, $n = 40$ cells. Total 4 mice were used in each group and 10 cells were scored from each mice. ***$p < 0.001$, **$p < 0.01$. Unpaired student t test. **e** Schematic diagram summarising how mTDP-43, mFUS and mSOD1 inhibit ER–Golgi transport. The primary response that ER–Golgi transport inhibited by mTDP-43 and mFUS is thought to be elicited by the depletion of Rab1 activity. One consequence is the cargo is unable to be sorted to COPII vesicles. In parallel, recruitment of COPII subunits to formation of vesicles could be antagonised. mSOD1 inhibits ER–Golgi transport could be resulting from a defect in the tethering process. This may be due to the interaction of mSOD1 with COPII vesicles or tubulin and dynein and thus leading to COPII vesicles are unable to be transported along microtubules to Golgi complex and thus decreasing the interaction of p115 with cis-Golgi marker, GM130

reported that mutations in the gene encoding tubulin Alpha 4A, a component of microtubules, (*TUBA4A*) cause 1 % of fALS cases [64]. Furthermore, these *TUBA4A* mutants destabilised the microtubule network, diminishing its re-polymerization capability [64]. Taken together, these data implicate microtubule dysfunction in ALS pathology.

Destabilisation of microtubules would impact on all microtubule-based processes, including axonal transport and autophagy-related trafficking, other mechanisms which are implicated in ALS [5, 32]. Indeed, we detected inhibition of autophagosome–lysosome fusion in cells expressing mSOD1, consistent with this notion. Rab1 is multi-tasking protein in ER–Golgi transport, mediating recruitment of cargo into COPII vesicles, regulation of COPII dynamics and function, transport between ER and ERGIC, and ERGIC and Golgi, recruitment of kinesin and dynein to microtubules, and microtubule organisation and function [27, 61, 63]. Previous studies have demonstrated that loss of Rab1 function prevents incorporation of secretory cargo into COPII vesicles [21] and leads to abnormal microtubules [61]. We observed that Rab1 overexpression rescued inhibition of ER–Golgi transport and ER stress triggered by mSOD1, mTDP-43 and mFUS, and apoptosis and inclusion formation triggered by mSOD1. However, the inactive mutant Rab1S25N did not rescue ER stress, and the constitutively active Rab1Q70L was more protective relative to WTRab1. This implies that the protective effects of Rab1 are driven specifically by its GTPase function, indicating that loss of Rab1 GTPase activity is associated with ER stress and neurodegeneration in ALS. These data, therefore, provide new evidence implying that restoring Rab1 function may be a novel therapeutic target in mSOD1, mTDP-43 and mFUS-associated ALS.

It should be noted that the studies using mSOD1 are less informative for the majority of ALS, because the TDP-43 pathology characteristic of most human ALS cases is not present in SOD1-associated ALS [20, 35]. FUS inclusions co-localise with TDP-43, p62 and ubiquitin and they are found in both FUS-associated fALS and also in some cases of sALS, but they are not associated with SOD1-fALS [13]. FUS also appears in TDP-43 inclusions in patients with TDP-43 mutations [13]. Since mSOD1 inclusions are distinct from both mTDP-43 and mFUS inclusions, in this study we focussed on recruitment of Rab1 to human motor neurons displaying the typical ubiquitinated TDP-43 inclusions found in most (97 %) ALS cases. Whilst Rab1 was distributed diffusely or punctate in control patients, it was recruited to these abnormal intracellular inclusions in sALS motor neurons. This implies that Rab1 is misfolded and loses its normal vesicular distribution in sALS, and hence is probably misfolded and non-functional in these patients. This suggests that similar pathological mechanisms are underway in sALS and fALS. In addition, previous studies have demonstrated that expression of Rab1 is upregulated in either lumbar spinal cords or blood from sALS patients [51, 57], providing further evidence that Rab1 is dysregulated in sALS. However, although glial pathology is implicated in both sALS and fALS [26, 46], in preliminary studies, Rab1 was not recruited to inclusions in either human astrocytes or microglial in sALS (data not shown). These data, therefore, imply that dysfunction to Rab1 is specific to motor neurons.

Inhibition of ER–Golgi transport is not specific to ALS. It has already been described in α-synuclein-associated Parkinson's disease [11]. However, whilst disease-associated A53T mutant α-synuclein delays ER–Golgi transport, WT α-synuclein also impairs transport [11], so trafficking inhibition is not specific for mutant α-synuclein. Furthermore, distinct mechanisms are involved: α-synuclein appears to antagonise SNARE function and inhibit SNARE complex assembly [73], thus inhibiting tethering and docking of transport vesicles with the Golgi [11]. Furthermore, α-synuclein was not observed in association with the ER in previous studies [11].

Similarly, in Huntington's disease post-Golgi cellular trafficking, rather than ER–Golgi trafficking, is inhibited by mutant huntingtin protein. This leads to less vesicular cargo leaving the trans-Golgi network, resulting in accumulation of protein in the Golgi, rather than the ER [12]. Whilst inhibition of post-Golgi transport in Huntington's disease could eventually perturb ER–Golgi transport [12], ER–Golgi trafficking defects are not the primary event and have not been previously demonstrated directly. Disruptions in ER and Golgi homeostasis are also associated with Alzheimer's and Prion diseases, but again involve distinct processes to ALS. Amyloid precursor protein has a signal peptide and hence it normally transits through the secretory pathway. However, whilst ER stress and Golgi fragmentation have been described previously in Alzheimer's disease, surprisingly a recent report described an increase in ER–Golgi transport, rather than decreased ER–Golgi transport, in cells in which β-amyloid accumulates [30], implying that different processes are underway in ALS and in Alzheimer's disease. Similarly, in prion-infected cells, VSVG is transported normally from ER to Golgi, but post-Golgi trafficking is significantly delayed. It is thought that prions may disturb post-Golgi trafficking of membrane proteins via accumulation in recycling endosomes [76]. Furthermore, Rab1 misfolding and recruitment to intracellular inclusions has not been described in patients with other neurodegenerative diseases. However, in our study, we found Rab1 recruitment to inclusions in sporadic patient motor neurons as well as in cells expressing mutant TDP-43, FUS or SOD1. Rab1 misfolding may, therefore, be a common process in ALS in contrast to other disorders. Hence whilst maintaining cellular proteostasis is fundamental in neurodegenerative conditions [24], there are clearly mechanisms specific to each disorder.

Maintaining proteostasis for post-mitotic cells presents specific challenges, and hence regulation of trafficking may be more critical for neurons than other cell types.

Furthermore, the ER in neurons is poorly characterised but it is much more extensive than in other cells [52], extending throughout the neuritic processes, where its functions are largely uncharacterised. The reason why motor neurons are selectively targeted in ALS remains to be clarified. However, motor neurons are characterised by very long axons, up to 1 m in length in an adult human, and efficient anterograde (and retrograde) transport is essential to transport essential proteins to and from the synapse from the soma, along the axon. In other types of neurons, this distance is much shorter than in motor neurons where the axons are extremely long relative to the size of the cell body. The relationship between transport between the ER–Golgi and along the axon is poorly understood but these two processes are closely linked [2, 52]. In preliminary studies we have observed that after VSVG traffics from ER to Golgi, it subsequently is transported along the axon. Hence if transport between ER and Golgi is inhibited, it is likely that axonal transport is also inhibited. Thus, perturbations in ER–Golgi transport in motor neurons with long axons may present serious challenges to cellular function. Hence the long axons may, therefore, impose much stricter trafficking requirements and confer selective vulnerability on the motor neuron.

Consistent with this notion, previous studies have demonstrated that the fast-fatigable (FF) and fast-resistant (FR) motor neuron axons are already affected at before clinical symptoms (p48–p50) and late presymptomatic (p80–p90) SOD1 mice, respectively, whereas axons of slow (S) motor neurons are much more resistant to neurodegeneration [50, 58]. Compared to S motor neurons, FF motor neuron are larger cells, with larger axonal diameters, and the velocity of axonal transport is greater [6], which may impart selective vulnerability to axonal transport dysfunction on FF cells. Interestingly, the FF motor neurons also are the first to develop ER stress [58], thus linking ER–Golgi transport, ER stress and axonal transport to specific vulnerability of motor neuron subtypes to neurodegeneration in ALS. FF motor neurons also fire at higher rates than S motor neurons [6], consistent with the greater requirement for proteins necessary for synaptic function, supplied from the cell body via efficient axonal transport [62]. A recent study also demonstrated that the molecular motor dynein, which mediates both ER–Golgi transport and retrograde axonal transport, is upregulated in more vulnerable motor neurons, such as hypoglossal and spinal motor neurons, compared to oculomotor neurons, which are less vulnerable in ALS [10]. Hence these studies, together with our findings, link inhibition of ER–Golgi transport, ER stress and axonal transport, to specific vulnerability of motor neuron subtypes to neurodegeneration in ALS.

Mutations in other genes causing ALS, including alsin, vesicle-associated protein, dynactin, CHMP2B, optineurin, and valosin-containing protein, encode other proteins implicated in intracellular trafficking. Furthermore, we demonstrated recently that the normal function of C9ORF72, which contains a non-coding repeat expansion mutation in fALS, is to regulate endocytosis and autophagy, but this is dysregulated in ALS patient tissues [17]. Several ER–Golgi transport proteins are implicated in other motor neuron disorders, including atlastin [7] and seipin [28]. Disruption in ER–Golgi trafficking has also been described in spontaneous mouse mutants with motor phenotypes, *pmn* [59] and *wobbler* [60]. In addition, mice with a deletion of Scy1, implicated in COPI-mediated Golgi–ER transport, display a motor neuron degenerative phenotype [44]. We also recently showed that ALS mutations in optineurin disrupt its normal association to myosin VI, which inhibits intracellular trafficking [71]. The optineurin–myosin VI association was also disrupted in sALS patients, linking these defects to sporadic disease [71]. These findings suggest that disturbances to intracellular trafficking may be fundamental in neuronal degeneration and maintenance of proteostasis.

ER–Golgi transport is functionally related to other cellular processes implicated in ALS; hence, transport inhibition would impact on other closely related events. ER stress and Golgi fragmentation result from dysfunction to ER–Golgi transport [40] and we previously demonstrated that inhibition of ER–Golgi transport preceded both events in cells expressing mSOD1, implying that ER stress and Golgi fragmentation are consequences not causes of ER–Golgi transport inhibition [3]. Previous reports described ER stress and Golgi fragmentation in early, preclinical disease stages (p30) in $SOD1^{G93A}$ mice [39, 58], prior to neuromuscular denervation and axon retraction [77]. Our finding that ER–Golgi transport is inhibited in embryonic motor neurons in $SOD1^{G93A}$ mice implies that this mechanism precedes ER stress and Golgi fragmentation in vivo, as in vitro [3]. Similarly, ER–Golgi transport and autophagy, a major degradation pathway for intracytosolic aggregate-prone protein, are also functionally linked. Rab1 regulates autophagy and ER/Golgi membranes are required for autophagosome formation [80]. Autophagy dysfunction is implicated in ALS and in degradation of mSOD1 and mTDP-43 [9], but the underlying mechanisms remain unclear. RNA dysfunction is now widely implicated in ALS and ER-derived vesicles are involved in RNA trafficking [74]. Furthermore, Ypt1 binds to HAC1 RNA and modulates the UPR [75]. This indicates that ER–Golgi trafficking and the UPR communicate via RNA interaction with Rab1. Whilst both ER–Golgi transport and axonal transport are also functionally linked and COPII is implicated in both processes [4, 38], we could not detect an interaction between mTDP-43 and mFUS and COPII (Suppl. Fig. 7). Hence despite our previous finding that

mSOD1 but not WTSOD1 interacts with COPII [3], COPII is not a common target of these proteins.

A schematic outlining possible mechanisms that inhibit ER–Golgi transport in ALS is presented in Fig. 7e. mTDP-43, mFUS and mSOD1 inhibit transport of ER-budded vesicles from ER to Golgi through antagonising Rab1 function, either via microtubule stability or COPII function. Modulation of disease processes common to multiple misfolded proteins in ALS has potential as a novel and effective therapeutic target: our data implicates Rab1 as a possible target. Description of the relationship between ER and Golgi transport to other pathogenic mechanisms is now warranted.

Acknowledgments We thank Professor Malcolm Horne and Professor Phillip Nagley for helpful discussions. Human patient and control lumbar region tissues were received from the Victorian Brain Bank Network, supported by University of Melbourne, Mental Health Research Institute of Victoria, and Victorian Forensic Institute of Medicine and funded by Neurosciences Australia and the National Health and Medical Research Council of Australia (NHMRC). This work was supported by NHMRC Project grants [# 1006141, 1030513 to JA], Bethlehem Griffiths Research Foundation, and Angie Cunningham Laugh to Cure MND grant [to JDA and KYS].

Compliance with ethical standards

Conflict of interest The authors declare no competing financial interests.

Ethical approval All procedures performed in studies involving human participants were in accordance with the ethical standards of the institutional and/or national research committee and with the 1964 Helsinki declaration and its later amendments or comparable ethical standards. All applicable international, national and/or institutional guidelines for the care and use of animals were followed. All procedures performed in studies involving animals were in accordance with the ethical standards of the institution or practice at which the studies were conducted.

References

1. Appenzeller-Herzog C, Hauri HP (2006) The ER-Golgi intermediate compartment (ERGIC): in search of its identity and function. J Cell Sci 119:2173–2183. doi:10.1242/jcs.03019
2. Aridor M, Fish KN (2009) Selective targeting of ER exit sites supports axon development. Traffic 10:1669–1684. doi:10.1111/j.1600-0854.2009.00974.x
3. Atkin JD, Farg MA, Soo KY, Walker AK, Halloran M, Turner BJ, Nagley P, Horne MK (2014) Mutant SOD1 inhibits ER-Golgi transport in amyotrophic lateral sclerosis. J Neurochem 129:190–204. doi:10.1111/jnc.12493
4. Barlowe C, Orci L, Yeung T, Hosobuchi M, Hamamoto S, Salama N, Rexach MF, Ravazzola M, Amherdt M, Schekman R (1994) COPII: a membrane coat formed by Sec proteins that drive vesicle budding from the endoplasmic reticulum. Cell 77:895–907
5. Bilsland LG, Sahai E, Kelly G, Golding M, Greensmith L, Schiavo G (2010) Deficits in axonal transport precede ALS symptoms in vivo. Proc Natl Acad Sci USA 107:20523–20528. doi:10.1073/pnas.1006869107
6. Borg J, Grimby L, Hannerz J (1979) Motor neuron firing range, axonal conduction velocity, and muscle fiber histochemistry in neuromuscular diseases. Muscle Nerve 2:423–430. doi:10.1002/mus.880020603
7. Botzolakis EJ, Zhao J, Gurba KN, Macdonald RL, Hedera P (2011) The effect of HSP-causing mutations in SPG3A and NIPA1 on the assembly, trafficking, and interaction between atlastin-1 and NIPA1. Mol Cell Neurosci 46:122–135. doi:10.1016/j.mcn.2010.08.012
8. Chang LY, Slot JW, Geuze HJ, Crapo JD (1988) Molecular immunocytochemistry of the CuZn superoxide dismutase in rat hepatocytes. J Cell Biol 107:2169–2179
9. Chen S, Zhang X, Song L, Le W (2012) Autophagy dysregulation in amyotrophic lateral sclerosis. Brain Pathol 22:110–116. doi:10.1111/j.1750-3639.2011.00546.x
10. Comley L, Allodi I, Nichterwitz S, Nizzardo M, Simone C, Corti S, Hedlund E (2015) Motor neurons with differential vulnerability to degeneration show distinct protein signatures in health and ALS. Neuroscience 291:216–229. doi:10.1016/j.neuroscience.2015.02.013
11. Cooper AA, Gitler AD, Cashikar A, Haynes CM, Hill KJ, Bhullar B, Liu K, Xu K, Strathearn KE, Liu F et al (2006) Alpha-synuclein blocks ER-Golgi traffic and Rab1 rescues neuron loss in Parkinson's models. Science 313:324–328. doi:10.1126/science.1129462
12. del Toro D, Canals JM, Gines S, Kojima M, Egea G, Alberch J (2006) Mutant huntingtin impairs the post-Golgi trafficking of brain-derived neurotrophic factor but not its Val66Met polymorphism. J Neurosci Off J Soc Neurosci 26:12748–12757. doi:10.1523/JNEUROSCI.3873-06.2006
13. Deng HX, Zhai H, Bigio EH, Yan J, Fecto F, Ajroud K, Mishra M, Ajroud-Driss S, Heller S, Sufit R et al (2010) FUS-immunoreactive inclusions are a common feature in sporadic and non-SOD1 familial amyotrophic lateral sclerosis. Ann Neurol 67:739–748. doi:10.1002/ana.22051
14. Dompierre JP, Godin JD, Charrin BC, Cordelieres FP, King SJ, Humbert S, Saudou F (2007) Histone deacetylase 6 inhibition compensates for the transport deficit in Huntington's disease by increasing tubulin acetylation. J Neurosci Off J Soc Neurosci 27:3571–3583. doi:10.1523/JNEUROSCI.0037-07.2007
15. Emr S, Glick BS, Linstedt AD, Lippincott-Schwartz J, Luini A, Malhotra V, Marsh BJ, Nakano A, Pfeffer SR, Rabouille C et al (2009) Journeys through the Golgi—taking stock in a new era. J Cell Biol 187:449–453. doi:10.1083/jcb.200909011
16. Farg MA, Soo KY, Walker AK, Pham H, Orian J, Horne MK, Warraich ST, Williams KL, Blair IP, Atkin JD (2012) Mutant FUS induces endoplasmic reticulum stress in amyotrophic lateral sclerosis and interacts with protein disulfide-isomerase. Neurobiol Aging. doi:10.1016/j.neurobiolaging.2012.02.009
17. Farg MA, Sundaramoorthy V, Sultana JM, Yang S, Atkinson RA, Levina V, Halloran MA, Gleeson P, Blair IP, Soo KY et al (2014) C9ORF72, implicated in amytrophic lateral sclerosis and frontotemporal dementia, regulates endosomal trafficking. Hum Mol Genet. doi:10.1093/hmg/ddu068
18. Filipeanu CM, Zhou F, Claycomb WC, Wu G (2004) Regulation of the cell surface expression and function of angiotensin II type 1 receptor by Rab1-mediated endoplasmic reticulum-to-Golgi transport in cardiac myocytes. J Biol Chem 279:41077–41084. doi:10.1074/jbc.M405988200
19. Forsberg K, Andersen PM, Marklund SL, Brannstrom T (2011) Glial nuclear aggregates of superoxide dismutase-1 are regularly present in patients with amyotrophic lateral sclerosis. Acta Neuropathol (Berl) 121:623–634. doi:10.1007/s00401-011-0805-3

20. Forsberg K, Jonsson PA, Andersen PM, Bergemalm D, Graffmo KS, Hultdin M, Jacobsson J, Rosquist R, Marklund SL, Brannstrom T (2010) Novel antibodies reveal inclusions containing non-native SOD1 in sporadic ALS patients. PLoS One 5:e11552. doi:10.1371/journal.pone.0011552
21. Garcia IA, Martinez HE, Alvarez C (2011) Rab1b regulates COPI and COPII dynamics in mammalian cells. Cell Logist 1:159–163. doi:10.4161/cl.1.4.18221
22. Ghaemmaghami S, Huh WK, Bower K, Howson RW, Belle A, Dephoure N, O'Shea EK, Weissman JS (2003) Global analysis of protein expression in yeast. Nature 425:737–741. doi:10.1038/nature02046
23. Haas AK, Yoshimura S, Stephens DJ, Preisinger C, Fuchs E, Barr FA (2007) Analysis of GTPase-activating proteins: Rab1 and Rab43 are key Rabs required to maintain a functional Golgi complex in human cells. J Cell Sci 120:2997–3010. doi:10.1242/jcs.014225
24. Hetz C, Mollereau B (2014) Disturbance of endoplasmic reticulum proteostasis in neurodegenerative diseases. Nat Rev Neurosci 15:233–249. doi:10.1038/nrn3689
25. Hirschberg K, Miller CM, Ellenberg J, Presley JF, Siggia ED, Phair RD, Lippincott-Schwartz J (1998) Kinetic analysis of secretory protein traffic and characterization of golgi to plasma membrane transport intermediates in living cells. J Cell Biol 143:1485–1503
26. Ilieva H, Polymenidou M, Cleveland DW (2009) Non-cell autonomous toxicity in neurodegenerative disorders: ALS and beyond. J Cell Biol 187:761–772
27. Ishida M, Ohbayashi N, Maruta Y, Ebata Y, Fukuda M (2012) Functional involvement of Rab1A in microtubule-dependent anterograde melanosome transport in melanocytes. J Cell Sci 125:5177–5187. doi:10.1242/jcs.109314
28. Ito D, Suzuki N (2007) Molecular pathogenesis of seipin/BSCL2-related motor neuron diseases. Ann Neurol 61:237–250. doi:10.1002/ana.21070
29. Jin L, Pahuja KB, Wickliffe KE, Gorur A, Baumgartel C, Schekman R, Rape M (2012) Ubiquitin-dependent regulation of COPII coat size and function. Nature 482:495–500. doi:10.1038/nature10822
30. Joshi G, Chi Y, Huang Z, Wang Y (2014) Abeta-induced Golgi fragmentation in Alzheimer's disease enhances Abeta production. Proc Natl Acad Sci USA 111:E1230–E1239. doi:10.1073/pnas.1320192111
31. Kabuta T, Kinugawa A, Tsuchiya Y, Kabuta C, Setsuie R, Tateno M, Araki T, Wada K (2009) Familial amyotrophic lateral sclerosis-linked mutant SOD1 aberrantly interacts with tubulin. Biochem Biophys Res Commun 387:121–126. doi:10.1016/j.bbrc.2009.06.138
32. Li L, Zhang X, Le W (2008) Altered macroautophagy in the spinal cord of SOD1 mutant mice. Autophagy 4:290–293
33. Lord C, Ferro-Novick S, Miller EA (2013) The highly conserved COPII coat complex sorts cargo from the endoplasmic reticulum and targets it to the golgi. Cold Spring Harb Perspect Biol 5(2), pii: a013367. doi:10.1101/cshperspect.a013367
34. Lorenz H, Hailey DW, Wunder C, Lippincott-Schwartz J (2006) The fluorescence protease protection (FPP) assay to determine protein localization and membrane topology. Nat Protoc 1:276–279. doi:10.1038/nprot.2006.42
35. Mackenzie IR, Bigio EH, Ince PG, Geser F, Neumann M, Cairns NJ, Kwong LK, Forman MS, Ravits J, Stewart H et al (2007) Pathological TDP-43 distinguishes sporadic amyotrophic lateral sclerosis from amyotrophic lateral sclerosis with SOD1 mutations. Ann Neurol 61:427–434. doi:10.1002/ana.21147
36. Manders EMM, Verbeek FJ, Atenm JA (1993) Measurement of co-localization of objects in dual-colour confocal images. J Microsc 169:375–382
37. Marie M, Sannerud R, Avsnes Dale H, Saraste J (2008) Take the 'A' train: on fast tracks to the cell surface. Cell Mol Life Sci CMLS 65:2859–2874. doi:10.1007/s00018-008-8355-0
38. Matsuoka K, Orci L, Amherdt M, Bednarek SY, Hamamoto S, Schekman R, Yeung T (1998) COPII-coated vesicle formation reconstituted with purified coat proteins and chemically defined liposomes. Cell 93:263–275
39. Mourelatos Z, Gonatas NK, Stieber A, Gurney ME, Dal Canto MC (1996) The Golgi apparatus of spinal cord motor neurons in transgenic mice expressing mutant Cu, Zn superoxide dismutase becomes fragmented in early, preclinical stages of the disease. Proc Natl Acad Sci USA 93:5472–5477
40. Nakagomi S, Barsoum MJ, Bossy-Wetzel E, Sutterlin C, Malhotra V, Lipton SA (2008) A Golgi fragmentation pathway in neurodegeneration. Neurobiol Dis 29:221–231. doi:10.1016/j.nbd.2007.08.015
41. Nishitoh H, Kadowaki H, Nagai A, Maruyama T, Yokota T, Fukutomi H, Noguchi T, Matsuzawa A, Takeda K, Ichijo H (2008) ALS-linked mutant SOD1 induces ER stress- and ASK1-dependent motor neuron death by targeting Derlin-1. Genes Dev 22:1451–1464
42. Nuoffer C, Davidson HW, Matteson J, Meinkoth J, Balch WE (1994) A GDP-bound of rab1 inhibits protein export from the endoplasmic reticulum and transport between Golgi compartments. J Cell Biol 125:225–237
43. Orci L, Palmer DJ, Ravazzola M, Perrelet A, Amherdt M, Rothman JE (1993) Budding from Golgi membranes requires the coatomer complex of non-clathrin coat proteins. Nature 362:648–652. doi:10.1038/362648a0
44. Pelletier S, Gingras S, Howell S, Vogel P, Ihle JN (2012) An early onset progressive motor neuron disorder in Scyl1-deficient mice is associated with mislocalization of TDP-43. J Neurosci Off J Soc Neurosci 32:16560–16573. doi:10.1523/JNEUROSCI.1787-12.2012
45. Perdiz D, Mackeh R, Pous C, Baillet A (2011) The ins and outs of tubulin acetylation: more than just a post-translational modification? Cell Signal 23:763–771. doi:10.1016/j.cellsig.2010.10.014
46. Philips T, Rothstein JD (2014) Glial cells in amyotrophic lateral sclerosis. Exp Neurol 262(Pt B):111–120. doi:10.1016/j.expneurol.2014.05.015
47. Plutner H, Cox AD, Pind S, Khosravi-Far R, Bourne JR, Schwaninger R, Der CJ, Balch WE (1991) Rab1b regulates vesicular transport between the endoplasmic reticulum and successive Golgi compartments. J Cell Biol 115:31–43
48. Preston AM, Gurisik E, Bartley C, Laybutt DR, Biden TJ (2009) Reduced endoplasmic reticulum (ER)-to-Golgi protein trafficking contributes to ER stress in lipotoxic mouse beta cells by promoting protein overload. Diabetologia 52:2369–2373. doi:10.1007/s00125-009-1506-5
49. Prosser DC, Tran D, Gougeon PY, Verly C, Ngsee JK (2008) FFAT rescues VAPA-mediated inhibition of ER-to-Golgi transport and VAPB-mediated ER aggregation. J Cell Sci 121:3052–3061. doi:10.1242/jcs.028696
50. Pun S, Santos AF, Saxena S, Xu L, Caroni P (2006) Selective vulnerability and pruning of phasic motoneuron axons in motoneuron disease alleviated by CNTF. Nat Neurosci 9:408–419. doi:10.1038/nn1653
51. Rabin SJ, Kim JM, Baughn M, Libby RT, Kim YJ, Fan Y, La Spada A, Stone B, Ravits J (2010) Sporadic ALS has compartment-specific aberrant exon splicing and altered cell-matrix adhesion biology. Hum Mol Genet 19:313–328. doi:10.1093/hmg/ddp498
52. Ramirez OA, Couve A (2011) The endoplasmic reticulum and protein trafficking in dendrites and axons. Trends Cell Biol 21:219–227. doi:10.1016/j.tcb.2010.12.003
53. Reed NA, Cai D, Blasius TL, Jih GT, Meyhofer E, Gaertig J, Verhey KJ (2006) Microtubule acetylation promotes kinesin-1

binding and transport. Curr Biol CB 16:2166–2172. doi:10.1016/j.cub.2006.09.014
54. Robberecht W, Philips T (2013) The changing scene of amyotrophic lateral sclerosis. Nat Rev Neurosci 14:248–264. doi:10.1038/nrn3430
55. Rosen DR, Siddique T, Patterson D, Figlewicz DA, Sapp P, Hentati A, Donaldson D, Goto J, O'Regan JO, Deng HX (1993) Mutation in Cu/Zn superoxide dismutase gene are associated with familial amyotrophic lateral sclerosis. Nature 362:59–62
56. Saraste J, Lahtinen U, Goud B (1995) Localization of the small GTP-binding protein rab1p to early compartments of the secretory pathway. J Cell Sci 108(Pt 4):1541–1552
57. Saris CG, Horvath S, van Vught PW, van Es MA, Blauw HM, Fuller TF, Langfelder P, DeYoung J, Wokke JH, Veldink JH et al (2009) Weighted gene co-expression network analysis of the peripheral blood from Amyotrophic Lateral Sclerosis patients. BMC Genom 10:405. doi:10.1186/1471-2164-10-405
58. Saxena S, Cabuy E, Caroni P (2009) A role for motoneuron subtype-selective ER stress in disease manifestations of FALS mice. Nat Neurosci 12:627–636
59. Schaefer MK, Schmalbruch H, Buhler E, Lopez C, Martin N, Guenet JL, Haase G (2007) Progressive motor neuronopathy: a critical role of the tubulin chaperone TBCE in axonal tubulin routing from the Golgi apparatus. J Neurosci Off J Soc Neurosci 27:8779–8789. doi:10.1523/JNEUROSCI.1599-07.2007
60. Schmitt-John T, Drepper C, Mussmann A, Hahn P, Kuhlmann M, Thiel C, Hafner M, Lengeling A, Heimann P, Jones JM et al (2005) Mutation of Vps54 causes motor neuron disease and defective spermiogenesis in the wobbler mouse. Nat Genet 37:1213–1215. doi:10.1038/ng1661
61. Schmitt HD, Wagner P, Pfaff E, Gallwitz D (1986) The ras-related YPT1 gene product in yeast: a GTP-binding protein that might be involved in microtubule organization. Cell 47:401–412
62. Shaw PJ, Eggett CJ (2000) Molecular factors underlying selective vulnerability of motor neurons to neurodegeneration in amyotrophic lateral sclerosis. J Neurol 247(Suppl 1):I17–I27
63. Slavin I, Garcia IA, Monetta P, Martinez H, Romero N, Alvarez C (2011) Role of Rab1b in COPII dynamics and function. Eur J Cell Biol 90:301–311. doi:10.1016/j.ejcb.2010.10.001
64. Smith BN, Ticozzi N, Fallini C, Gkazi AS, Topp S, Kenna KP, Scotter EL, Kost J, Keagle P, Miller JW et al (2014) Exome-wide rare variant analysis identifies TUBA4A mutations associated with familial ALS. Neuron 84:324–331. doi:10.1016/j.neuron.2014.09.027
65. Soo KY, Atkin JD, Farg M, Walker AK, Horne MK, Nagley P (2012) Bim links ER stress and apoptosis in cells expressing mutant SOD1 associated with amyotrophic lateral sclerosis. PLoS One 7:e35413. doi:10.1371/journal.pone.0035413
66. Soo KY, Atkin JD, Horne MK, Nagley P (2009) Recruitment of mitochondria into apoptotic signaling correlates with the presence of inclusions formed by amyotrophic lateral sclerosis-associated SOD1 mutations. J Neurochem 108:578–590
67. Spang A, Matsuoka K, Hamamoto S, Schekman R, Orci L (1998) Coatomer, Arf1p, and nucleotide are required to bud coat protein complex I-coated vesicles from large synthetic liposomes. Proc Natl Acad Sci USA 95:11199–11204
68. Sreedharan J, Blair IP, Tripathi VB, Hu X, Vance C, Rogelj B, Ackerley S, Durnall JC, Williams KL, Buratti E et al (2008) TDP-43 mutations in familial and sporadic amyotrophic lateral sclerosis. Science 319:1668–1672. doi:10.1126/science.1154584
69. Stenmark H (2009) Rab GTPases as coordinators of vesicle traffic. Nat Rev Mol Cell Biol 10:513–525. doi:10.1038/nrm2728
70. Stylli SS, Stacey TT, Verhagen AM, Xu SS, Pass I, Courtneidge SA, Lock P (2009) Nck adaptor proteins link Tks5 to invadopodia actin regulation and ECM degradation. J Cell Sci 122:2727–2740. doi:10.1242/jcs.046680
71. Sundaramoorthy V, Walker AK, Tan V, Fifita JA, McCann EP, Williams KL, Blair IP, Guillemin GJ, Farg MA, Atkin JD (2015) Defects in optineurin- and myosin VI-mediated cellular trafficking in amyotrophic lateral sclerosis. Hum Mol Genet. doi:10.1093/hmg/ddv126
72. Sundaramoorthy V, Walker AK, Yerbury J, Soo KY, Farg MA, Hoang V, Zeineddine R, Spencer D, Atkin JD (2013) Extracellular wildtype and mutant SOD1 induces ER-Golgi pathology characteristic of amyotrophic lateral sclerosis in neuronal cells. Cellular Mol Life Sci CMLS. doi:10.1007/s00018-013-1385-2
73. Thayanidhi N, Helm JR, Nycz DC, Bentley M, Liang Y, Hay JC (2010) Alpha-synuclein delays endoplasmic reticulum (ER)-to-Golgi transport in mammalian cells by antagonizing ER/Golgi SNAREs. Mol Biol Cell 21:1850–1863. doi:10.1091/mbc.E09-09-0801
74. Todd AG, Lin H, Ebert AD, Liu Y, Androphy EJ (2013) COPI transport complexes bind to specific RNAs in neuronal cells. Hum Mol Genet 22:729–736. doi:10.1093/hmg/dds480
75. Tsvetanova NG, Riordan DP, Brown PO (2012) The yeast Rab GTPase Ypt1 modulates unfolded protein response dynamics by regulating the stability of HAC1 RNA. PLoS Genet 8:e1002862. doi:10.1371/journal.pgen.1002862
76. Uchiyama K, Miyata H, Sakaguchi S (2013) Disturbed vesicular trafficking of membrane proteins in prion disease. Prion 7:447–451
77. van Dis V, Kuijpers M, Haasdijk ED, Teuling E, Oakes SA, Hoogenraad CC, Jaarsma D (2014) Golgi fragmentation precedes neuromuscular denervation and is associated with endosome abnormalities in SOD1-ALS mouse motor neurons. Acta Neuropathol Commun 2:38. doi:10.1186/2051-5960-2-38
78. Vance C, Rogeli B, Hortobagyi T, De Vos KJ, Nishimura AL, Sreedharan J, Hu X, Smith B, Ruddy D, Wright P et al (2009) Mutations in FUS, an RNA processing protein, cause familial amyotrophic lateral sclerosis type 6. Science 323:1208–1211
79. Walker AK, Soo KY, Sundaramoorthy V, Parakh S, Ma Y, Farg MA, Wallace RH, Crouch PJ, Turner BJ, Horne MK et al (2013) ALS-associated TDP-43 induces endoplasmic reticulum stress, which drives cytoplasmic TDP-43 accumulation and stress granule formation. PLoS One 8:e81170. doi:10.1371/journal.pone.0081170
80. Winslow AR, Chen CW, Corrochano S, Acevedo-Arozena A, Gordon DE, Peden AA, Lichtenberg M, Menzies FM, Ravikumar B, Imarisio S et al (2010) Alpha-synuclein impairs macroautophagy: implications for Parkinson's disease. J Cell Biol 190:1023–1037. doi:10.1083/jcb.201003122
81. Xu D, Hay JC (2004) Reconstitution of COPII vesicle fusion to generate a pre-Golgi intermediate compartment. J Cell Biol 167:997–1003. doi:10.1083/jcb.200408135
82. Yang YS, Harel NY, Strittmatter SM (2009) Reticulon-4A (Nogo-A) redistributes protein disulfide isomerase to protect mice from SOD1-dependent amyotrophic lateral sclerosis. J Neurosci Off J Soc Neurosci 29:13850–13859. doi:10.1523/JNEUROSCI.2312-09.2009
83. Zhang F, Strom AL, Fukada K, Lee S, Hayward LJ, Zhu H (2007) Interaction between familial amyotrophic lateral sclerosis (ALS)-linked SOD1 mutants and the dynein complex. J Biol Chem 282:16691–16699

7.2.6 Supplementary Figure 5

The author was part of the study Browne, E. C., et al. (2016). "***Efficacy of peptide nucleic acid and selected conjugates against specific cellular pathologies of amyotrophic lateral sclerosis***." Bioorganic & Medicinal Chemistry 24(7): 1520-1527. The author performed all the immunocytochemistry experiments described **on page 1523 (Figure 4), page 1524 (Figure 5)** of the manuscript. These studies demonstrated that administration of PNA1, 6-PNA1 and 7-PNA1 reduce mutant $SOD1^{A4V}$ inclusion formation and PNA1 and 6-PNA1 reduced ER stress in neuronal cells expressing mutant $SOD1^{A4V}$.

Bioorganic & Medicinal Chemistry 24 (2016) 1520–1527

Contents lists available at ScienceDirect

Bioorganic & Medicinal Chemistry

journal homepage: www.elsevier.com/locate/bmc

Efficacy of peptide nucleic acid and selected conjugates against specific cellular pathologies of amyotrophic lateral sclerosis

Elisse C. Browne [a], Sonam Parakh [b,d], Luke F. Duncan [a], Steven J. Langford [c], Julie D. Atkin [b,d], Belinda M. Abbott [a,*]

[a] Department of Chemistry and Physics, La Trobe Institute for Molecular Science, La Trobe University, Melbourne 3086, Australia
[b] Department of Biochemistry and Genetics, La Trobe Institute for Molecular Science, La Trobe University, Melbourne 3086, Australia
[c] School of Chemistry, Monash University, Clayton 3800, Australia
[d] Department of Biomedical Sciences, Faculty of Medicine and Health Science, Macquarie University, Sydney 2109, Australia

ARTICLE INFO

Article history:
Received 14 December 2015
Revised 9 February 2016
Accepted 17 February 2016
Available online 18 February 2016

Keywords:
Peptide nucleic acid
Amyotrophic lateral sclerosis
Vitamin conjugation

ABSTRACT

Cellular studies have been undertaken on a nonamer peptide nucleic acid (PNA) sequence, which binds to mRNA encoding superoxide dismutase 1, and a series of peptide nucleic acids conjugated to synthetic lipophilic vitamin analogs including a recently prepared menadione (vitamin K) analog. Reduction of both mutant superoxide dismutase 1 inclusion formation and endoplasmic reticulum stress, two of the key cellular pathological hallmarks in amyotrophic lateral sclerosis, by two of the prepared PNA oligomers is reported for the first time.

1. Introduction

Amyotrophic lateral sclerosis (ALS) is a fatal neurodegenerative disorder which affects the upper and lower motor neurons of the brain, brain stem and spinal cord.[1] It causes progressive muscle weakness, paralysis and death within 3–5 years of diagnosis and there is currently no effective treatment. Around 10% of ALS cases are familial (fALS), caused by genetic mutations. However, the majority of ALS (90%) is sporadic, with no previous family history.[2] Mutations in the superoxide dismutase 1 (SOD1) gene account for approximately 20% of familial ALS cases and the most common mutation in North America is A4V (alanine to valine).[3,4] SOD1 is a major cytosolic protein which catalyzes the reduction of harmful, free superoxide radicals into molecular oxygen and hydrogen peroxide.

The etiology of ALS remains unclear but the formation of intracellular ubiquitin-positive inclusions containing misfolded proteins is a characteristic pathological hallmark.[5] Misfolded SOD1 inclusions are present in both sporadic human[6] and familial ALS patients, as well as transgenic SOD1^{G93A} mice,[7] the most widely used animal disease model in preclinical studies. Stress in the endoplasmic reticulum (ER) is also recognized to be an important pathway to motor neuron death in ALS. ER stress is triggered when misfolded proteins accumulate within the ER. This triggers the unfolded protein response (UPR), a signaling pathway that aims to relieve the stress and thus restore homeostasis. However if ER stress is prolonged, apoptosis is triggered. The transition of UPR from cell survival to cell death is mediated by CCAAT-enhancer binding protein homologous protein (CHOP),[8] a transcription factor which translocates to the nucleus when activated. We and others previously demonstrated that ER stress is present in sporadic ALS patient tissues[9] as well as in cells expressing mutant SOD1 and transgenic SOD1^{G93A} mice.[10–14] Novel pharmacological agents that prevent the formation of misfolded mutant SOD1 inclusions and inhibit the activation of CHOP in cells expressing mutant SOD1, and hence the pro-apoptotic phase of UPR, would therefore have therapeutic application in ALS.

Antisense agents such as peptide nucleic acids (PNA) are short single stranded nucleic acid analogs designed to specifically bind to complementary messenger ribonucleic acid (mRNA) targets through Watson and Crick hydrogen bonding. As a result, these antisense agents can silence a particular gene of interest. PNA is a third generation oligonucleotide, which replaces the traditional phosphate backbone of RNA/DNA with a peptide backbone made up of repeating *N*-(2-aminoethyl)glycine units and the sugar moiety replaced with a methylene carbonyl linker where the nucleic bases are attached (Fig. 1).

The modified backbone of PNA gives rise to resistance to enzymatic degradation and leads to higher affinity binding, rates of

* Corresponding author.
E-mail address: b.abbott@latrobe.edu.au (B.M. Abbott).

http://dx.doi.org/10.1016/j.bmc.2016.02.022
0968-0896/

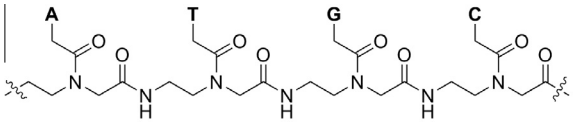

Figure 1. General structure of peptide nucleic acid (PNA) containing the four nucleobases of adenine (A), thymine (T), guanine (G) and cytosine (C).

association and subsequently an increase in duplex stability as there are no repulsive electrostatic interactions.[15] Additionally, the neutrality of the backbone significantly reduces the chance of undesired nonspecific interactions such as binding to cellular proteins.[16] PNA exhibits low toxicity in cells and is stable of a wide pH range, particularly toward the acidic end of the scale where DNA can be denatured.

The major limitation of PNA as an efficient antisense drug is its low phospholipid solubility due to the hydrophilic nature of the molecule, PNA does not readily cross cell membranes. Hydrophobic vitamins such as vitamin K and vitamin E are hypothesized as good candidates for conjugation to PNA. The main function of vitamin K is post-translational modification during the biosynthesis of vitamin K dependent proteins.[17] The synthetic form of this vitamin, vitamin K3 (menadione) has been found to readily cross the blood brain barrier as it is a small lipophilic molecule.[18] Despite its larger size, highly lipophilic vitamin E (tocopherol) has also been found to cross the blood brain barrier.[19] While the main task of this vitamin is as an antioxidant, vitamin E has also been shown to alleviate oxidative stress by promoting normal cell function.[20]

We have previously described the synthesis and conjugation of tocopherol (vitamin E) analogs to PNA for the investigation of effects on hybridization.[21] In this further study, we present the synthesis of a menadione (vitamin K) analog, its conjugation to the same nine nucleobase PNA oligomer and the subsequent hybridization results. In addition, this novel vitamin K conjugated oligomer, along with the previously synthesized three vitamin E derived conjugated PNA oligomers and the unconjugated PNA oligomer, were studied using cellular assays to determine their effects on the formation of mutant SOD1 inclusions and induction of on ER stress.

2. Results and discussion

2.1. Synthesis and thermodynamic studies of the menadione-PNA conjugate

The menadione analog was synthesized by the adaptation of the methods of Abell et al.[22] Commercially available menadione was directly brominated using molecular bromine in the presence of sodium acetate and glacial acetic acid to yield the brominated adduct **1**,[23] followed by reduction of the dione using potassium hydroxide and in situ methylation with dimethyl sulfate to give **2** in 45% yield over the two steps (Scheme 1). Alkylation of **2** using ethyl bromoacetate was achieved via a copper transmetalation reaction through a diaryl cuprate intermediate from treatment with *n*-butyllithium and copper bromide dimethyl sulfide. Increasing the number of equivalents of ethyl bromoacetate from 1.1 to 1.5 and extending the reaction time from 5 to 18 h resulted in an optimized yield of 55%, a considerable improvement over the previously reported 34% yield for this step.[22] Reduction of the ethyl ester **3** using lithium aluminum hydride proceeded in high yield to give the corresponding alcohol **4** which was succinylated using the anhydride to afford **5**. Ceric ammonium nitrate (CAN) was utilized to oxidatively deprotect the methoxy groups and restore the quinone functionality that is characteristic of the vitamin K family affording **6** in 84% yield.

Automated PNA synthesis was performed on PAL resin using standard protocols[24] and two PNA sequences were prepared as previously described: H-GCACGACTT-NH_2 (**PNA1**) and the complementary sequence H-AAGTCGTGC-NH_2 (**PNA2**).[21] Coupling of the menadione analog **6** to the growing oligomer of **PNA1** was then undertaken using the same automated synthetic protocols. Purification by reverse-phase high performance liquid chromatography (RP-HPLC) gave the desired menadione-PNA conjugated oligomer of **6-PNA1** (Fig. 2). Characterization was undertaken using MALDI-TOF mass spectrometry where *m*/*z* calculated for $C_{119}H_{150}N_{55}O_{33}$ requires $[M+H]^+$ 2734.069 and *m*/*z* of $[M+H]^+$ 2734.375 was found.

In order to determine the suitability of the conjugated menadione-PNA oligomer **6-PNA1**, the thermodynamics of hybridization to both the complementary PNA (**PNA2**) and DNA oligomers was undertaken to ensure conjugation did not impair hybridization (Tables 1 and 2). Two complementary methods were chosen for thermodynamic analysis of the duplexes, UV monitored melting curves (UVM)[25,26] and isothermal titration calorimetry (ITC).[27] Data for the control duplexes of **PNA1**/**PNA2** and **PNA1**/DNA was previously recorded[21] and is provided here to facilitate the comparison of the data obtained with the conjugated duplexes. The change in the thermodynamic differences between the two methods agree well with each other.

In the case for both conjugated duplexes, conjugation of the menadione analog does not appear to significantly affect the stability of the duplexes as reflected in the recorded thermal melting temperature (T_m). As expected, lower thermal stability and thus affinity was observed for the mixed duplexes of PNA and DNA oligomers.[28,29] However, the duplex binding affinity, which is related to the enthalpy change (ΔH°) is reduced in both of the conjugated duplexes to the same extent (approximately 73 kJ mol^{-1} on average). As a result of this, the free energy (ΔG°) is also reduced leading to less favorable duplex formation at 37 °C with the conjugated duplex despite no change in T_m. The reduction in ΔH° indicates that there is a weaker interaction between the two oligomers, most likely a result of steric bulk minimizing the interaction of the base pairs adjacent to the conjugate. However, the conformations of the base pairs or stacking patterns may also have an effect along with counter ion uptake and release and hydration factors may also have an effect. Despite the change in the enthalpy and free energy change for this duplex, the thermal melting temperature remains relatively unaffected overall.

2.2. PNA1, 6-PNA1 and 7-PNA1 inhibit the formation of mutant SOD1 inclusions in neuronal cell lines

We next examined the effect of the PNA compounds in cells expressing mutant SOD1 A4V. Mouse neuronal Neuro2a cells were transfected with a previously generated construct encoding SOD1 A4V,[30] tagged with Enhanced Green Fluorescent protein (EGFP) to aid in visualizing the expressed protein. We previously demonstrated that the presence of the EGFP tag does not affect the activity of the protein.[30] Cells were also treated 4 h post transfection either with dimethyl sulfoxide (DMSO) vehicle as a negative control, unconjugated PNA (**PNA1** or its complementary sequence **PNA2**), menadione-conjugate **6-PNA1** (Fig. 2), previously prepared vitamin E derived-conjugates **7- PNA1**, **8-PNA1** and **9-PNA1** (Fig. 3),[21] or (+/−)-*trans*-1,2-bis(2-mercaptoacetamido)cyclohexane (BMC), which we previously demonstrated significantly reduces the formation of mutant SOD1 A4V inclusions and reduced ER stress.[13]

Cells were transfected for 72 h and then examined by fluorescent microscopy with the percentage of cells bearing fluorescent green mutant SOD1 inclusions quantified. Untransfected cells (UTR) were included as a negative control to specifically determine

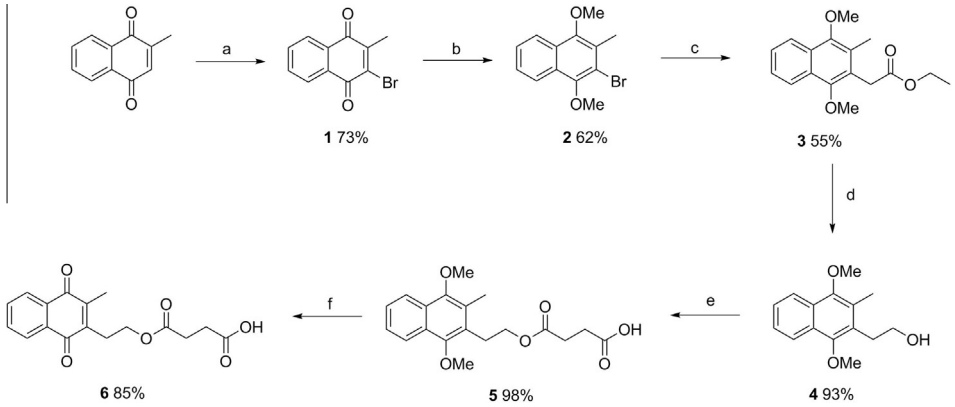

Scheme 1. Synthesis of a menadione analog. Reactions and conditions: (a) Br_2, sodium acetate, glacial acetic acid, 3 days; (b) tetrabutylammonium iodide, tetrahydrofuran/H_2O (3:1), 2.2 M $Na_2S_2O_4$(aq), 20 min then KOH, $(CH_3O)_2SO_2$, 12 h; (c) *n*-butyllithium in hexanes, diethyl ether, 0 °C, 30 min then CuBr·MeS, 2.5 h then $BrCH_2COOCH_2CH_3$, 0 °C, 2 h; (d) $LiAlH_4$, diethyl ether, 35 min; (e) triethylamine, succinic anhydride, 4-(dimethylamino)pyridine, CH_2Cl_2, 12 h; (f) CAN, CH_3CN/H_2O (3:2), 0 °C, 30 min then room temperature, 20 min.

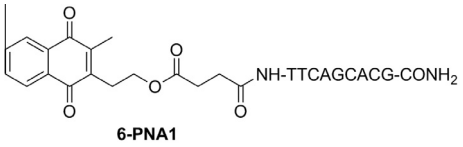

Figure 2. Conjugated menadione-PNA oligomer of **6-PNA1**.

the effects of transfection with mutant SOD1 and, as expected, rarely formed inclusions. However, in control DMSO only treated populations, 19% of transfected cells formed inclusions (Fig. 4A and B, additional low magnification images provided as Supplementary material) similar to our previous observations.[30] As in an earlier study, treatment with BMC significantly reduced the percentage of cells bearing inclusions to 14% compared to DMSO treated cells (p <0.05). Moreover, treatment of SOD1 A4V expressing cells with **6-PNA1** significantly decreased the percentage of cells bearing inclusions to 15% (p <0.05). Furthermore, treatment of cells with **PNA1** and **7-PNA1** significantly reduced the percentage of transfected cells bearing inclusions from 21% in DMSO treated cells to 11% (p <0.01) and 14% (p <0.05) respectively (Fig. 4A and C). There was a slight decrease in inclusion formation in cells treated with compounds **8-PNA1** (17%) and **9-PNA1** (16%), but this was not statistically significant. In contrast, treatment with the negative control PNA, **PNA2**, did not alter the percentage of cells bearing inclusions (20%) as expected. Hence this data indicates that compounds **PNA1**, **6-PNA1** and **7-PNA1** were all equally effective as BMC in preventing the formation of mutant SOD1 inclusions in neuronal cells, the characteristic pathological hallmark of ALS.

2.3. PNA1 and 6-PNA1 reduces ER stress in neuronal cells expressing mutant SOD1 A4V

Since **PNA1**, **6-PNA1** and **7-PNA1** reduced inclusion formation, we proceeded to investigate whether the PNA oligomers could inhibit ER stress induced by mutant SOD1 A4V. We examined the pro-apoptotic phase of UPR using nuclear immunoreactivity to CHOP, as previously described.[13] Neuro2a cells were transfected with the SOD1 A4V-EGFP construct and at 72 h post transfection, cells were fixed and immunocytochemistry for CHOP was performed. Activation of CHOP, indicated by immunoreactivity in the nucleus, was observed in 35% of transfected control cells that were treated with DMSO only (Fig. 5A and B, additional low magnification images provided as Supplementary material). However, in cells treated with **6-PNA1**, there was a significant reduction in the percentage of cells with nuclear immunoreactivity to CHOP compared to DMSO-treated cells (25%, p <0.001), demonstrating that **6-PNA1** is protective against ER stress induced by mutant SOD1 A4V. Similarly, BMC treatment was also protective against induction of UPR: the percentage of transfected cells with CHOP activation was significantly decreased in this cell population (30%, p <0.05).

PNA1 also significantly reduced CHOP activation, to only 26% transfected cells (p <0.05) compared to DMSO-treated cells (37%) (Fig. 5A and C). In contrast, treatment with the negative control PNA, **PNA2**, did not alter the percentage of cells with CHOP activation (40%) and hence ER stress. Treatment of cells with the remaining PNA oligomers (**7-PNA1**, **8-PNA1** and **9-PNA1**) significantly reduced the percentage of transfected cells with ER stress when compared with cells treated with **PNA2** (31%, all p <0.05). However this was not statistically significant when compared with cells treated with DMSO only. As expected, very few untransfected cells (UTR) displayed CHOP up-regulation. Hence these results reveal

Table 1
Thermodynamic data of duplex formation by UVM[a,b]

Duplex	T_m (°C)	$\Delta H°VH$ (kJ mol^{-1})	$\delta\Delta H$	$\Delta G°VH$ (kJ mol^{-1})[c]	$\delta\Delta G$[c]
PNA1/**PNA2**	64 (±1)	−202 (±6)		−14.1 (±1.7)	
6-PNA1/**PNA2**	66 (±1)	−123 (±5)	+79	−7.8 (±1.9)	+6.3
PNA1/DNA[d]	57 (±1)	−183 (±13)		−9.6 (±2.4)	
6-PNA1/DNA[d]	55 (±1)	−106 (±1)	+77	−6.6 (±0.5)	+3.0

[a] Values obtained are an average of a minimum of 3 experiments.
[b] Error corresponds to ±1 standard deviation.
[c] T = 310 K,
[d] DNA sequence used is 5′-AAGTCGTGC-3′.

Table 2
Thermodynamic data of duplex formation by ITC[a,b]

Duplex	$\Delta H°_b$ (kJ mol^{-1})	$\delta\Delta H$	$\Delta G°_b$ (kJ mol^{-1})[c]	$\delta\Delta G$[c]
PNA1/**PNA2**	−216 (±4)		−48.9 (±0.7)	
6-PNA1/**PNA2**	−143 (±3)	+73	−42.7 (±2.8)	+6.2
PNA1/DNA[d]	−169 (±1)		−48.4 (±3.2)	
6-PNA1/DNA[d]	−107 (±1)	+62	−41.8 (±0.5)	+6.6

[a] Values obtained are an average of a minimum of 3 experiments.
[b] Error corresponds to ±1 standard deviation.
[c] T = 310 K.
[d] DNA sequence used is 5′-AAGTCGTGC-3′.

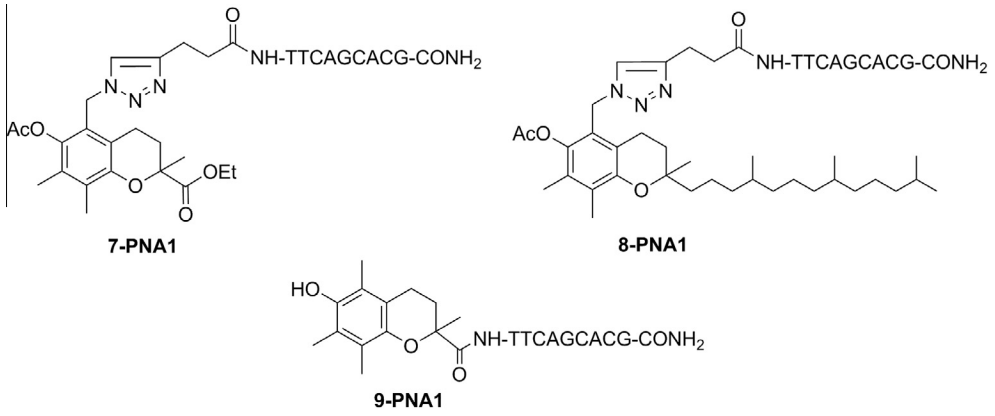

Figure 3. Conjugated vitamin E derived-PNA oligomers.[21]

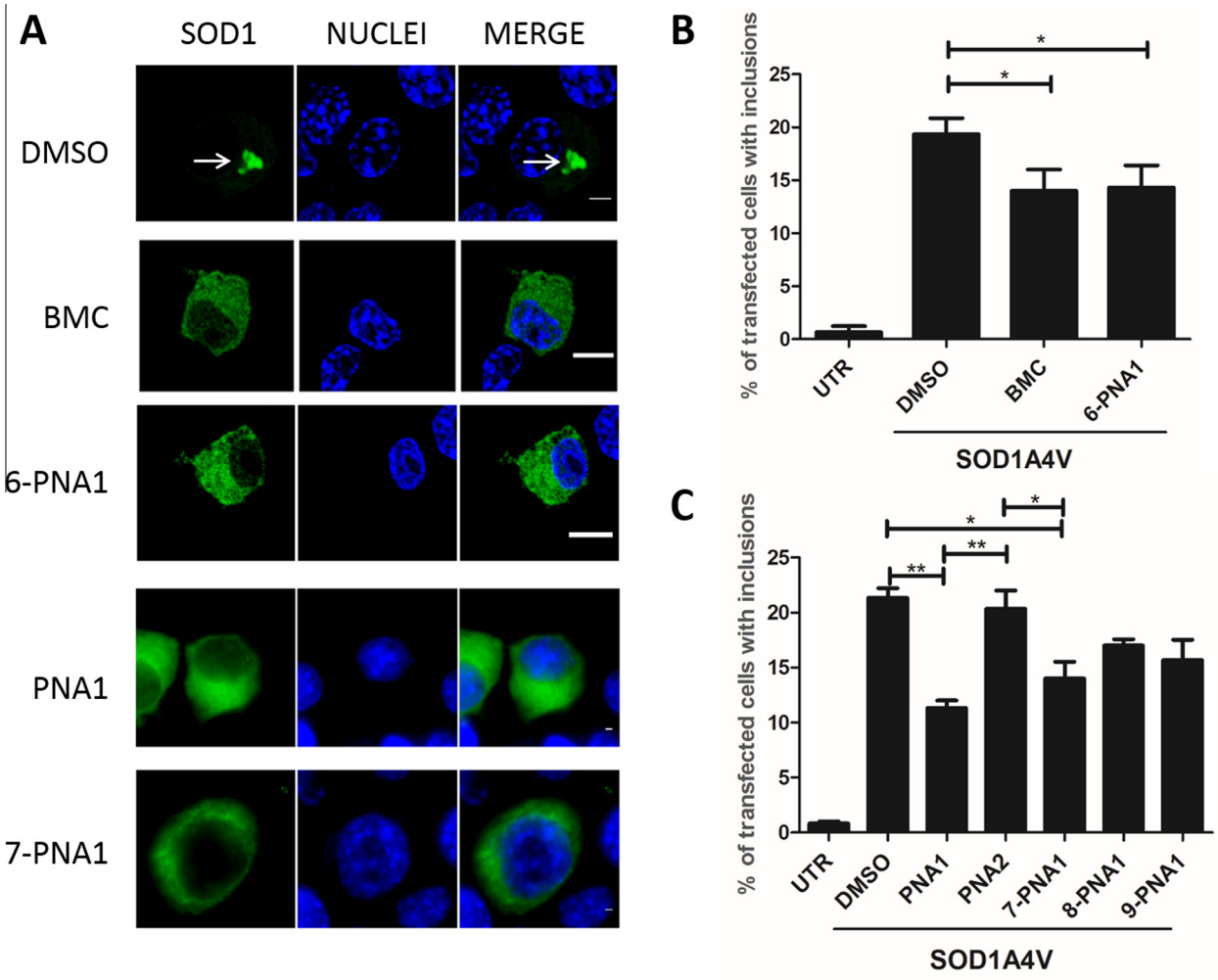

Figure 4. PNA1, **6-PNA1** and **7-PNA1** reduce mutant SOD1 A4V inclusion formation. Fewer mutant SOD1 A4V inclusions are formed in Neuro2a cells treated with PNA compared to cells only treated with DMSO. (A) Fluorescent microscopy images of mutant SOD1 A4V-EGFP expressing in Neuro2a cells at 72 h post transfection. White arrow indicates fluorescent green SOD1 inclusions, shown in first column. Nuclei are shown by Hoechst staining (blue, second column). Merge (third column) represents the combined images from first and second columns. Top panel indicates cells treated with DMSO alone, second panel, BMC treated cells and third panel, **6-PNA1** treated cells. The fourth and the fifth panels represent cells administered with **PNA1** and **7-PNA1**. Scale bar represents 10 μm. (B) Quantification of the percentage of cells bearing SOD1 A4V inclusions in BMC (positive control) and **6-PNA1** treated cells compared to DMSO-only treated cells. (C) Quantification of percentage of cells bearing SOD1 A4V inclusions in PNA treated cells compared to DMSO-only treated cells. In each cell population, 100 transfected cells were examined for the presence of fluorescent green inclusions. UTR represent control, untransfected cells. Data represented as Mean ± SD, $n = 3$, $^{*}p < .05$ $^{**}p < .01$ versus respective controls by one way ANOVA with Tukey's post hoc test.

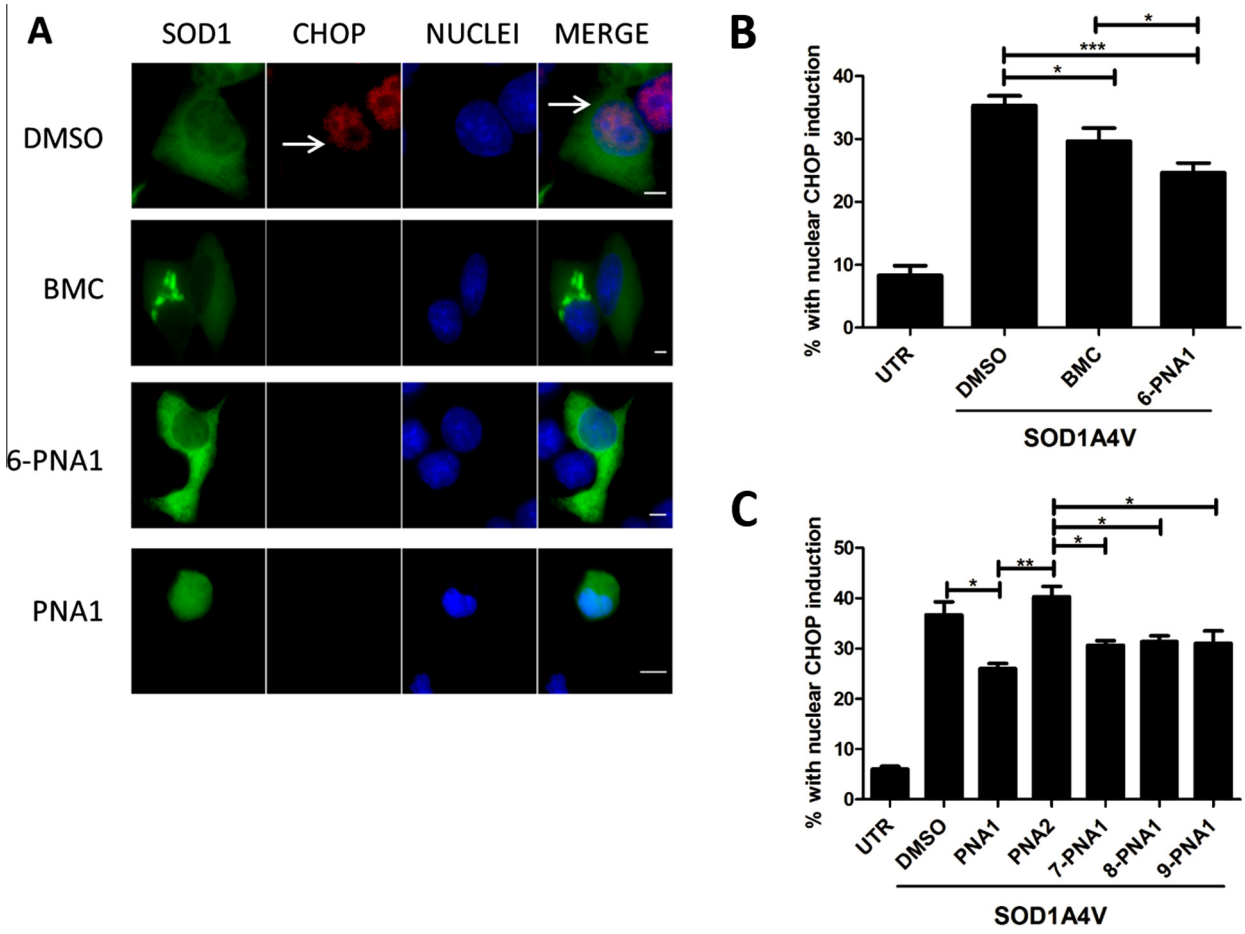

Figure 5. PNA1 and 6-PNA1 reduce activation of CHOP, and hence pro-apoptotic phases of UPR, in cells expressing mutant SOD1. Immunocytochemistry for CHOP was performed in Neuro2a cells expressing mutant SOD1 A4V at 72 h post transfection (A) Fluorescent microscopy images of mutant SOD1 A4V-EGFP transfected Neuro2a cells. White arrow indicates nuclear immunoreactivity to CHOP, indicating its activation, and hence induction of pro-apoptotic phases of UPR in these cells. Fluorescent mutant SOD1 A4V (green) is shown in the first column, immunofluorescence detection of CHOP (red) in the second column, nuclei are shown by Hoechst staining (blue) in the third column, and the fourth column represents merge image of all three. Top panel indicates cells treated with DMSO alone, second panel, BMC treated cells, third panel, **6-PNA1** treated cells, and the fourth panel represents cells administered with **PNA1**. Scale bar represents 10 μm. (B) Quantification of the percentage of cells with nuclear immunoreactivity to CHOP in BMC (positive control) and **6-PNA1** treated cells compared to DMSO-only treated cells. (C) Quantification of the percentage of cells with nuclear immunoreactivity to CHOP in **PNA1**, **7-PNA1**, and **9-PNA1** treated cells compared to either DMSO-only treated cells or negative control PNA (**PNA2**) treated cells. In each cell population, 100 transfected cells were examined for the presence of nuclear CHOP immunoreactivity. UTR represents control, untransfected cells. Data represented as Mean ± SD, $n = 3$, $^{*}p < .05$, $^{**}p < .01$, $^{***}p < .001$ versus respective controls by one way ANOVA with Tukey's post hoc test.

that the PNA compounds **PNA1** and **6-PNA1** were protective against the activation of CHOP, and hence induction of the pro-apoptotic phases of the UPR, in neuronal cells expressing mutant SOD1.

3. Conclusions

The synthesis of a menadione-PNA conjugate was carried out to facilitate thermodynamic studies by both UVM and ITC, which resulted in the formation of the expected duplex indicating thermodynamic stability. Cellular studies were then carried out on both unconjugated and conjugated PNA. We have shown for the first time that compounds containing the peptide nucleic acid sequence of H-GCACGACTT-NH_2 are effective against specific cellular signaling pathways, which complements earlier studies investigating the disease parameters in SOD1 mice but which did not look any further at the specific mechanisms involved. The synthesized PNA oligomers have demonstrated efficacy in reducing mutant SOD1 inclusion formation and ER stress, which are two key cellular pathological hallmarks in ALS, with the unconjugated **PNA1** and the menadione-conjugate **6-PNA1** found to be equally effective. While the conjugation of vitamin K did not strengthen the cellular effects over those observed by the unconjugated PNA, this work has shown that conjugation which is not detrimental to activity is possible and provides an important proof of concept in developing other conjugates. Further studies will be necessary to investigate any benefits vitamin K conjugation may have on the delivery of PNA in an animal model.

4. Experimental

4.1. Synthesis

NMR spectra were recorded on a Bruker Avance-300 Spectrophotometer (1H at 300.13 MHz and 13C at 75.47 MHz) or a Bruker Avance-400 spectrometer (1H at 400.13 MHz and 13C at 100.62 MHz). All PNA and PNA conjugates were analyzed by Matrix Assisted Desorption Ionization Time of Flight mass spectrometry (MALDI-TOF-MS) using an Ultraflex III instrument (Bruker Daltonics, Germany) and α-cyano-4-hydroxy cinnamic acid as the matrix. Electrospray ionization (ESI) mass spectrometry was carried out using an Esquire^{6000} ion trap mass spectrometer (Bruker Daltonics,

Germany). The samples were introduced at a flow rate of 4 μL/min and a mass range of 50 – 3000 *m*/*z* was recorded. A scan rate of 5500 *m*/*z*/*second* was used with the temperature set at 300 °C. The molecular ion peaks (*m*/*z*) were denoted $[M+H]^+$. TLC was performed using Merck Kieselgel 60 F_{254} plates. Drying and purification methods for solvents and reagents were followed by directions from Armarego and Chai.[31] Melting points were collected on hot stage Reichert 'Thermopan' apparatus. The DNA sequence used in the thermodynamic experiments was purchased from Sigma Aldrich.

4.1.1. 2-Methyl-3-bromo-1,4-napthoquinone 1

The synthesis of this compound was based on the method of Teeter et al.[23] Menadione (5.5 g, 31.94 mmol), glacial acetic acid (50 mL) and sodium acetate (11 g, 134.09 mmol) were heated in a conical flask until the suspension dissolved. To this, bromine (2 mL) was added and the flask was stoppered and placed in darkness for 3 days. Water (300 mL) was added and the resulting solid filtered, followed by recrystallisation from methanol to afford the brominated product **1** as bright yellow crystals (5.86 g, 73%), mp 150–152 °C (lit.[23] 151–152 °C). δ_H (300 MHz, $CDCl_3$): 8.15–8.09 (2H, m, Ar*H*), 7.76–7.69 (2H, m, Ar*H*), 2.38 (3H, s, ArCH_3). δ_C (75 MHz, $CDCl_3$): 181.9, 171.5, 148.5, 139.0, 134.1, 133.9, 131.6, 131.2, 127.5, 127.1, 17.9.

4.1.2. 2-Bromo-3-methyl-1,4-dimethoxynapthelene 2

The synthesis of this compound was adapted from the method of Abell et al.[22] To a stirred solution of **1** (1 g, 3.97 mmol), TBAI (176 mg, 0.48 mmol) in water (3.6 mL) and tetrahydrofuran (10.9 mL), a solution of sodium dithionite (4.16 g, 23.9 mmol) in water (10.9 mL) was added and the reaction stirred for 20 min. To this, a solution of potassium hydroxide (15.8 M, 5.8 mL) was added drop-wise and stirred for a further 5 min, at which time dimethylsulfate (4.5 mL, 47.8 mmol) was then added drop-wise and the reaction was stirred overnight. The product was extracted with CH_2Cl_2 (4 × 50 mL), dried with $MgSO_4$ and solvent removed in vacuo. The orange mass was recrystallized from methanol to afford **2** in 62% yield (2.78 g) as light orange crystals, mp 83–84 °C (lit.[22] 82–84 °C). δ_H (300 MHz, $CDCl_3$): 8.09–8.03 (2H, m, Ar*H*), 7.55–7.45 (2H, m, Ar*H*), 3.96 (3H, s, OCH_3), 3.87 (3H, s, OCH_3), 2.52 (3H, s, ArCH_3). δ_C (75 MHz, $CDCl_3$): 150.5, 149.8, 127.8, 127.6, 127.3, 126.5, 126.2, 122.4, 122.4, 117.2, 61.6, 61.3, 16.7.

4.1.3. Ethyl 2-(3-methyl-1,4-dimethoxynapthalen-2-yl)acetate 3

To a cooled solution of **2** (1.96 g, 6.97 mmol) in anhydrous ether (12 mL) under an atmosphere of argon, *n*-butyllithium (1.6 M in hexane, 5.0 mL, 8.02 mmol) was added drop-wise and stirred at 0 °C for 30 min. Copper bromide dimethyl sulfide complex (1.00 g, 4.88 mmol) was added and the solution stirred for 2.5 h. A chilled solution of ethyl bromoacetate (1.16 mL, 10.5 mmol) in ether (8 mL) was then added slowly and the reaction stirred at 0 °C for 2 h, at which time the reaction was warmed to room temperature and stirred for an additional 16 h. The reaction was quenched with 3 M HCl (15 mL) and the two layers were separated. The aqueous layer was extracted with ether (2 × 15 mL) and the combined organic extracts were washed with H_2O (30 mL), saturated aqueous $NaHCO_3$ (30 mL) and once more with H_2O (30 mL). The organic layer was dried with $MgSO_4$ and evaporated in vacuo. The crude orange oil was purified on silica by flash column chromatography, eluting with EtOAc/hexane (1:19) to yield **3** (1.10 g, 55%) as an orange oil. δ_H (300 MHz, $CDCl_3$): 8.06–8.04 (2H, m, Ar*H*), 7.49–7.46 (2H, m, Ar*H*), 4.19 (2H, q, *J* 7.2, OCH_2CH_3), 3.93 (2H, s, ArCH_2), 3.91 (3H, s, OCH_3), 3.86 (3H, s, OCH_3), 2.37 (3H, s, ArCH_3), 1.27 (3H, t, *J* 7.2, OCH$_2CH_3$). δ_C (75 MHz, $CDCl_3$): 171.7, 150.8, 150.1, 128.3, 127.1, 126.7, 126.0, 125.5, 124.1, 122.5, 122.3, 62.2, 61.4, 60.9, 33.1, 14.3, 12.7.

4.1.4. 2-(3-Methyl-1,4-dimethoxynapthelen-2-yl) ethanol 4

The synthesis of this compound was adapted from the method of Abell et al.[22] The ester **3** (873 mg, 3.03 mmol) was vigorously stirred in a solution of anhydrous ether (30 mL) under a bed of argon. To this, $LiAlH_4$ (288 mg, 7.57 mmol) was added and the reaction stirred for 35 min. The reaction was quenched using a saturated solution of aqueous NH_4Cl (10 mL), the two layers were separated and the aqueous layer was extracted with EtOAc (30 mL). The combined organic layers were washed with H_2O (15 mL) followed by brine (15 mL), dried with $MgSO_4$ and the solvent removed in vacuo. The resulting solid was purified on silica by flash column chromatography eluting with EtOAc/hexane (1:4) to afford **4** as an off white solid (692 mg, 93%), mp 68–70 °C (lit.[22] 66–69 °C). δ_H (300 MHz, $CDCl_3$): 8.01–7.99 (2H, m, Ar*H*), 7.46–7.43 (2H, m, Ar*H*), 3.89 (3H, s, OCH_3), 3.85 (3H, s, OCH_3), 3.83 (2H, t, *J* 7.2, CH_2CH_2OH), 3.11 (2H, t, *J* 6.9, ArCH_2CH_2), 2.78 (1H, s (b), *OH*), 2.41 (3H, s, ArCH_3). δ_C (75 MHz, $CDCl_3$): 150.6, 150.3, 127.9, 127.4, 127.0, 126.5, 125.8, 125.5, 122.2, 62.6, 62.0, 61.4, 18.5, 12.6.

4.1.5. 2-(3-Methyl-1,4-dimethoxynaphthalen-2-yl)ethyl hydrogen succinate 5

The synthesis of this compound was adapted from the method of Abell et al.[22] To a stirred solution of alcohol **4** (490 mg, 1.99 mmol) in CH_2Cl_2 (25 mL), a solution of TEA (400 μL, 2.88 mmol), succinic anhydride (420 mg, 4.18 mmol) and DMAP (22 mg, 0.18 mmol) in CH_2Cl_2 (15 mL) was added drop-wise and the reaction stirred overnight. The solvent was removed in vacuo and the resulting residue was dissolved in CH_2Cl_2 (30 mL) and washed with 10% HCl (20 mL) followed by H_2O (2 × 20 mL), dried with $MgSO_4$ and the solvent removed in vacuo to give **5** (680 mg, 98%) as a yellow oil. δ_H (300 MHz, $CDCl_3$): 8.06–7.99 (2H, m, Ar*H*), 7.46–7.44 (2H, m, Ar*H*), 4.28 (2H, t, *J* 7.5, OCH_2CH_2), 3.90 (3H, s, OCH_3), 3.85 (3H, s, *OCH*$_3$), 3.16 (2H, t, *J* 7.2, ArCH_2), 2.93 (1H, s, *OH*), 2.67–2.64 (4H, m, *CH*$_2$*CH*$_2$), 2.44 (3H, s, ArCH_3). δ_C (75 MHz, $CDCl_3$): 178.0, 172.2, 151.0, 150.2, 128.0, 127.1, 126.6, 126.2, 125.9, 125.5, 122.3, 122.2, 64.0, 62.2, 61.3, 28.9, 28.3, 26.7, 12.5.

4.1.6. 2-(3-Methyl-1,4-naphthoquinon-2-yl)ethyl hydrogen succinate 6

The synthesis of this compound was adapted from the method of Abell et al.[22] To a cooled solution of **5** (990 mg, 2.85 mmol), in a 2:1 solution of CH_3CN:H_2O (11 mL), a solution of ceric ammonium nitrate (3.92 g, 7.14 mmol) in 1:1 CH_3CN:H_2O (13 mL) was added drop-wise and the reaction stirred at 0 °C for 30 min, followed by 20 min at room temperature. The solution was diluted with H_2O (50 mL) and the bright yellow solution was extracted with CH_2Cl_2 (6 × 40 mL). The combined organic solution was washed with H_2O (50 mL), dried with $MgSO_4$ and the solvent removed in vacuo to afford **6** as a yellow-orange oil (762 mg, 84%). δ_H (400 MHz, $CDCl_3$): 8.08–8.04 (2H, m, Ar*H*), 7.71–7.67 (2H, m, Ar*H*), 4.28 (2H, t, *J* 6.6, OCH_2), 3.00 (2H, t, *J* 6.6, ArCH_2), 2.65–2.55 (4H, m, *CH*$_2$*CH*$_2$), 2.22 (3H, s, ArCH_3). δ_C (100 MHz, $CDCl_3$): 184.9, 184.3, 177.7, 172.0, 145.5, 142.6, 133.5, 133.5, 132.0, 131.9, 126.3, 63.0, 28.7, 26.7, 13.0.

4.2. PNA synthesis and characterization by UVM and ITC

4.2.1. Synthesis

Bhoc- and Fmoc-protected PNA monomers (A, C, G and T) and 2-aminoethoxy-2-ethoxyacetic acid (AEEA) were purchased from ASM Research Chemicals and were used without further purification. Automated synthesis was performed on an Expedite 8909 nucleic acid synthesizer, on a 2 μmol scale using Fmoc-PAL-PEG-PS resin (0.19 mmol/g) from Applied Biosystems, following the

standard protocols.[24] The synthetic procedure follows a deprotection and coupling strategy using solutions of 0.2 M PNA monomers in *N*-methylpyrrolidone for all monomers except for the C monomer (0.1 M) which was double coupled, deblocking solution (20% piperidine in DMF) then activation using a base solution (0.18 M HATU, 0.2 M DIPEA and 0.3 M 2,6-lutidine in DMF). Capping with 5% v/v acetic anhydride and 6% v/v 2,6-lutidine in DMF terminates incomplete sequences. Conjugates (0.2 M in DMF) were coupled to the PNA oligomer on resin following the same protocol. The PNA was cleaved from the resin using TFA/*m*-cresol (4:1) then precipitated and washed with ice cold ether and dried. The crude PNA was purified using a Phenomenex Jupiter C18 10 μm, 250 mm × 10 mm column, with gradient elution using water (Eluent A) and acetonitrile (Eluent B) with 0.1% TFA. The pure PNA fractions were collected, lyophilized and characterized by MALDI-TOF and ESI mass spectroscopy as appropriate.

4.2.2. Determination of solution concentration

All experiments were carried out in 10 mM sodium phosphate buffer (pH 7.0). The concentrations of both PNA and DNA strands were determined by UV absorption at a wavelength of 260 nm at 80 °C, using quartz cells with a 1 cm path length. The following extinction coefficients were used; εDNA:A = 15300 M^{-1} cm^{-1}, εDNA:G = 12220 M^{-1} cm^{-1}, εDNA:C = 7600 M^{-1} cm^{-1}, εDNA:T = 8700 M^{-1} cm^{-1}, εPNA:A = 13700 M^{-1} cm^{-1}, εPNA:G = 11700 M^{-1} cm^{-1}, εPNA:C = 6600 M^{-1} cm^{-1}, εPNAT = 8600 M^{-1} cm^{-1}.[24]

4.2.3. UV melting experiments

Melting curves were performed on a Varian Cary 100 Bio UV–Vis spectrophotometer with a Cary temperature controller. The duplexes formed during the ITC experiments were used directly to obtain the melting curves, as previously undertaken in the literature.[28] Samples were prepared by heating to 80 °C for 5 min, cooling to 20 °C over 20 min and holding at 20 °C for a further 20 min. The melting curves were measured at 260 nm, with the temperature increasing from 20 °C to 80 °C at a rate of 0.5 °C/min, with data collection occurring every 0.2 °C. Each duplex melting curve was performed in triplicate, at a minimum.

4.2.4. Determination of thermodynamic parameters via UVM

The melting temperature (T_m) is dependent upon α, which is the fraction of the single strand in a duplex state, as described by Marky and Breslaur[25] is shown by Eq. A below:

$$\alpha = \frac{A_s - A}{(A_s - A) + (A - A_d)} \quad \text{(A)}$$

where A is absorbance at a given T, and A_s and A_d are the absorbance from the single strand and the duplex respectively. The T_m of the duplex is determined where α = 0.5.

In order to calculate the van't Hoff enthalpy, the equilibrium constant (K) must be determined and expressed in terms of α for a non-complementary association, as shown in Eq. B, where CT is the total strand concentration and n is the number of strands associated with the complex.

$$K = \frac{\alpha}{(CT/n)^{n-1}(1-\alpha)^n} \quad \text{(B)}$$

Thus, the Gibbs free energy change can be determined (Eq. C) where a plot of ln (K) versus $1/T$ will determine both the enthalpy and entropy of the system (Eqs. D and E, respectively).

$$\Delta G_v H^\circ = -RT\ \ln(K) = \Delta H^\circ - T\Delta S^\circ \quad \text{(C)}$$

$$\Delta H_v H^\circ = \text{slope } (\ln(K) \text{ vs } 1/T)R \quad \text{(D)}$$

$$\Delta S_v H^\circ = \text{intercept } (\ln(K) \text{ vs } 1/T)R \quad \text{(E)}$$

4.2.5. Isothermal titration calorimetry

Calorimetric experiments were performed on a CSC 5300 Nano-ITC 111 instrument at 25 °C, where one of the oligomer strands (~0.1 mM, 100 μL) was titrated into 1.4 mL of the complementary strand (~5 μM). Each injection was 4 or 5 μL at 5 min intervals for a total of 25 injections. Stirrer speed was set to 250 rpm. Solutions were thoroughly degassed by sonification and absolute concentrations determined as outlined above. The reference cell was filled with degassed and deionized water. Isotherms were examined using the software NanoAnalyze v2.0, whereby the binding constant (K_b), intrinsic molar enthalpy change (ΔH_b°) and stoichiometry of binding (n) were determined by means of best fit (independent model) of the calorimetric data. The data was corrected by subtracting the heat of dilution from the experiment. Each duplex was titrated in triplicate, at a minimum.

4.3. Cellular biology

4.3.1. Constructs and cell lines

The mouse neuroblastoma Neuro-2a cell line (ATCC cell line CCL-131) was used for all transient transfections. The SOD1A4V-EGFP construct was as described previously.[30]

4.3.2. Cell culture and transfection

Neuro2a cells were maintained in Dulbecco modified Eagle's medium with 10% fetal calf serum, 100 mg/ml penicillin and 100 mg/ml streptomycin. Transfections were performed using Lipofectamine reagent 2000 (Invitrogen) according to the manufacturer's protocol. Cells transfected with SOD1A4V-EGFP were examined 72 h post-transfection by fluorescence microscopy and cells with prominent EGFP-positive inclusions were counted as a percentage of the total EGFP-positive, and hence transfected, cells. Treatment with PNA derivatives were added from a stock dissolved at 25 μM in DMSO. (+/−)-*trans*-1,2-bis(2-mercaptoacetamido)cyclohexane (BMC) (25 μM in DMSO) was also added to the transfected cell expressing SOD1 as a positive control, 4 h post transfection cells were analyzed for inclusion positive cells and ER stress as previously described.[13]

4.3.3. Immunofluorescence and microscopy

Cells were fixed with freshly prepared 4% (w/v) paraformaldehyde and incubated in the dark for 15 min. The cells were permeabilized with 0.2% (v/v) Triton-X in PBS for 5 min and blocked with 3% BSA in PBS for 30 min. After washing with 0.1% (v/v) Tween-20 in PBS, incubation with mouse anti-CHOP (1:50) (Abcam) antibody was performed in PBS at 4 °C overnight. The secondary antibody, AlexaFluor 568 conjugated rabbit anti-mouse IgG (1:250), was added for 1 h and incubated in the dark at room temperature. After washing, staining of nuclei was performed with Hoechst stain 33342 (Invitrogen) and mounted using fluorescent mounting media. The slides were observed under 100× magnification on an Olympus epifluorescent microscope. DAPI (nuclei), FITC (GFP fluorescence) filters were used for viewing and images taken using NIS-Elements BR 3.2 software.

4.3.4. Statistics

Cells transfected with SOD1-EGFP were counted (100 total) and the data was represented as Mean ± SD. Analyses were made using ANOVA followed by Tukey's post hoc test. (GraphPad Prism, San Diego, CA, USA). p-Values of 0.05 or less were considered significant. p <0.05*, p <0.01**, p <0.001***.

Acknowledgments

This work was supported by an Australian Research Council Discovery Project (DP0771578). E.C.B. is a recipient of an Aus-

tralian Postgraduate Award and LIMS Postgraduate Writing-Up Award. S.P. holds a La Trobe University Postgraduate Research Scholarship and a Macquarie University Postgraduate Research Scholarship.

Supplementary data

Supplementary data associated with this article can be found, in the online version, at http://dx.doi.org/10.1016/j.bmc.2016.02.022.

References and notes

1. Rosenfeld, J.; Strong, M. J. *Neurotherapeutics* **2015**, *12*, 317.
2. Rowland, L. P.; Shneider, N. A. *N. Engl. J. Med.* **2001**, *344*, 1688.
3. Rosen, D. R.; Siddique, T.; Patterson, D.; Figlewicz, D. A.; Sapp, P.; Hentati, A.; Donaldson, D.; Goto, J.; O'Regan, J. P.; Deng, H.-X.; Rahmani, Z.; Krizus, A.; McKenna-Yasek, D.; Cayabyab, A.; Gaston, S. M.; Berger, R.; Tanzi, R. E.; Halperin, J. J.; Herzfeldt, B.; Van den Bergh, R.; Hung, W.-Y.; Bird, T.; Deng, G.; Mulder, D. W.; Smyth, C.; Laing, N. G.; Soriano, E.; Pericak-Vance, M. A.; Haines, J.; Rouleau, G. A.; Gusella, J. S.; Horvitz, H. R.; Brown, R. H. *Nature* **1993**, *362*, 59.
4. Cudkowicz, M. E.; McKenna-Yasek, D.; Sapp, P. E.; Chin, W.; Geller, B.; Hayden, D. L.; Schoenfeld, D. A.; Hosler, B. A.; Horvitz, H. R.; Brown, R. H. *Ann. Neurol.* **1997**, *41*, 210.
5. Keerthana, S.; Kolandaivel, P. *J. Biomol. Struct. Dyn.* **2015**, *33*, 167.
6. Bosco, D. A.; Morfini, G.; Karabacak, N. M.; Song, Y.; Gros-Louis, F.; Pasinelli, P.; Goolsby, H.; Fontaine, B. A.; Lemay, N.; McKenna-Yasek, D.; Frosch, M. P.; Agar, J. N.; Julien, J. P.; Brady, S. T.; Brown, R. H., Jr. *Nat. Neurosci.* **2010**, *13*, 1396.
7. Brujin, L. I.; Houseweart, M. K.; Kato, S.; Anderson, K. L.; Anderson, S. D.; Ohama, E.; Reaume, A. G.; Scott, R. W.; Cleveland, D. W. *Science* **1998**, *281*, 1851.
8. Oyadomari, S.; Mori, M. *Cell Death Differ.* **2004**, *11*, 381.
9. Atkin, J. D.; Farg, M. A.; Walker, A. K.; McLean, C.; Tomas, D.; Horne, M. K. *Neurobiol. Dis.* **2008**, *30*, 400.
10. Atkin, J. D.; Farg, M. A.; Turner, B. J.; Tomas, D.; Lysaght, J. A.; Nunan, J.; Rembach, A.; Nagley, P.; Beart, P. M.; Cheema, S. S.; Horne, M. K. *J. Biol. Chem.* **2006**, *281*, 30152.
11. Saxena, S.; Cabuy, E.; Caroni, P. *Nat. Neurosci.* **2009**, *12*, 627.
12. Saxena, S.; Roselli, F.; Singh, K.; Leptien, K.; Julien, J. P.; Gros-Louis, F.; Caroni, P. *Neuron* **2013**, *80*, 80.
13. Walker, A. K.; Farg, M. A.; Bye, C. R.; McLean, C. A.; Horne, M. K.; Atkin, J. D. *Brain* **2010**, *133*, 105.
14. Atkin, J. D.; Farg, M. A.; Soo, K. Y.; Walker, A. K.; Halloran, M.; Turner, B. J.; Nagley, P.; Horne, M. K. *J. Neurochem.* **2014**, *129*, 190.
15. Dean, D. A. *Adv. Drug Delivery Rev.* **2000**, *44*, 81.
16. Hamilton, S. E.; Iyer, M.; Norton, J. C.; Corey, D. R. *Bioorg. Med. Chem. Lett.* **1996**, *6*, 2897.
17. Tsaioun, K. I. *Nutr. Rev.* **1999**, *57*, 231.
18. Thijssen, H. H. W.; Vervoort, L. M. T.; Schurgers, L. J.; Shearer, M. J. *Brit. J. Nutri.* **2006**, *95*, 260.
19. Gildea, B. D.; Casey, S.; MacNeill, J.; Perry-O'Keefe, H.; Sørensen, D.; Coull, J. M. *Tetrahedron Lett.* **1998**, *39*, 7255.
20. Manor, D.; Morley, S. *Vitamin E*; Academic Press: U.S.A., 2007. Vol. 76, pp 46–60.
21. Browne, E. C.; Langford, S. J.; Abbott, B. M. *Org. Biomol. Chem* **2013**, *11*, 6744.
22. Payne, R. J.; Daines, A. M.; Clark, B. M.; Abell, A. D. *Bioorg. Med. Chem.* **2004**, *12*, 5785.
23. Adams, R.; Geissman, T. A.; Baker, B. R.; Teeter, H. M. *J. Am. Chem. Soc.* **1941**, *63*, 528.
24. Braasch, D. A.; Corey, D. R. *Methods* **2001**, *23*, 97.
25. Marky, L. A.; Breslauer, K. J. *Biopolymers* **1987**, *26*, 1601.
26. Wartell, R. M.; Benight, A. S. *Phys. Rep.* **1985**, *126*, 67.
27. Ghai, R.; Falconer, R. K.; Collins, B. M. *J. Mol. Recognit.* **2011**, *25*, 32.
28. Chakrabarti, M. C.; Schwarz, F. P. *Nucleic Acids Res.* **1999**, *27*, 4801.
29. Jensen, K. K.; Orum, H.; Nielsen, P. E.; Nordén, B. *Biochemistry* **1997**, *36*, 5072.
30. Turner, B. J.; Atkin, J. D.; Farg, M. A.; Zang, D. W.; Rembach, A.; Lopes, E. C.; Patch, J. D.; Hill, A. F.; Cheema, S. S. *J. Neurosci.* **2005**, *25*, 108.
31. Armarego, W. L. F.; Chai, C. L. L. *Purification of Laboratory Chemicals*, 5th ed.; Elsevier, 2003.

7.2.7 Supplementary Figure 6

The manuscript "***ERp57 protects against toxicity induced by mutant SOD1 in ALS***" is ready to be submitted in the Journal "Neurobiology of Aging". The author performed all the experiments described in the manuscript except:

Result Section 4: Dr Vinod Sundaramoorthy kindly performed immunohistochemistry of human lumbar spinal cord sections of sporadic ALS patients and controls.

ERp57 protects against toxicity induced by mutant SOD1 in Amyotrophic Lateral Sclerosis

Sonam Parakh[1], Vinod Sundramoorthy[1], Damian Spencer[2] and Julie Atkin[1,2]

1 Department of Biomedical Sciences, Faculty of Medicine and Health Science,, Macquarie University, Sydney, Australia

2 Department of Biochemistry and Genetics, La Trobe Institute for Molecular Science, La Trobe University, Melbourne, Australia

Correspondence to: Julie Atkin,
Macquarie University | NSW | 2109
T +61 2 9850 2772 | F +61 2 9850 2701
E julie.atkin@mq.edu.au | **W** www.medicine.mq.edu.au

Abstract

Amyotrophic lateral sclerosis (ALS) is a rapidly progressing neurodegenerative disorder and mutations in superoxide dismutase 1 (SOD1) account for 20% of familial ALS cases. A characteristic pathological hallmark of ALS is the formation of intracellular misfolded protein inclusions, which in almost all ALS patients contain misfolded Tar-DNA binding protein 43 (TDP-43). Mutations in SOD1 also result in aggregation and the formation of misfolded SOD1 inclusions. The etiology of ALS remains unclear but endoplasmic reticulum (ER) stress and neuronal apoptosis are implicated. Protein disulphide isomerase (PDI) is an ER chaperone induced during ER stress which also possesses disulphide interchange activity, thus facilitating the formation of protein disulphide bonds misfolded proteins. PDI is the prototype of a family of more than 21 members, including ERp57, which is a related homologue of PDI that has been previously associated with glycosylated disulphide-bonded proteins. We previously demonstrated that over-expression of PDI is protective against mutant SOD1 inclusion formation, ER stress, and cell death in neuronal cell lines. However, PDI has also been associated with detrimental effects in some cases. In this study we demonstrate that over-expression of ERp57 is protective against mutant SOD1-induced aggregation, inclusion formation, ER stress and cell death in neuronal cells. ERp57 also co-localised with TDP-43-positive inclusions in lumbar spinal cords from sporadic ALS patients, suggesting it may also be protective against TDP-43 misfolding. These results reveal that

despite its preference for glycoproteins, ERp57 is protective against mutant SOD1 in ALS. Hence we conclude that other members of the PDI family are protective in ALS, thus implying that the PDI family has a broader therapeutic role in ALS than previously considered.

Introduction

Amyotrophic lateral sclerosis (ALS) is an adult-onset aggressive, neurodegenerative disorder characterised by degeneration of both upper motor neurons in the primary motor cortex and lower motor neurons in the brainstem and spinal cord [1]. Due to progressive denervation, in most cases death results within 3-5 years of diagnosis. Although 90% of cases lack an obvious genetic component (sporadic ALS, sALS), 10% of cases are inherited, and termed familial ALS (fALS) [2]. Amongst fALS cases, 20% are caused by mutations in the Superoxide dismutase1 (*SOD1*) gene [3].

SOD1 is a cytosolic, homodimeric protein which is responsible for catalysing free superoxide radicals [4]. The structure of SOD1 is stabilized by four cysteine residues present in each monomer, linked by disulphide bonds [5]. Mutant SOD1 has a highly destabilized structure, and it misfolds and forms reduced monomers, which are prone to aggregate [6]. Mutant SOD1 also induces endoplasmic reticulum (ER) stress *in vitro* [8] and cells forming mutant SOD1 inclusions develop ER stress and readily undergo apoptosis [8, 9]. ER stress is observed in early stages of disease in transgenic $SOD1^{G93A}$ mice, in cells expressing other mutant proteins linked to ALS, including the C9ORF72 repeat expansion that causes most cases of fALS [10], and is present in human sporadic lumbar spinal cords [11], indicating an important role in disease pathogenesis [12]. ER stress is induced when the load of misfolded protein within the ER increases, triggering a homeostatic mechanism called the unfolded protein response (UPR). This leads to the activation of protein-kinase-like endoplasmic reticulum kinase (PERK), inositol requiring kinase-1 (IRE-1) and transcription factor 6 (ATF6) [13]. Activation of IRE-1 results in the splicing of the transcription factor X-box binding protein 1 (XBP-1) messenger RNA to remove a stop codon and produce a functional transcriptional factor. If prolonged, the UPR leads to apoptosis, triggered by activation of CHOP which regulates the cellular transition from pro-survival to pro-apoptotic signalling during ER stress [12]. Activation of the UPR results in a decrease in general protein translation and induction of ER chaperones, including Protein disulphide isomerase (PDI) and Endoplasmic reticulum protein 57 (ERp57), which mediate the formation and rearrangement of protein disulphide bonds [14].

More than 21 members have been identified in the PDI family, which share an ER targeting sequence, a di-cysteine CXXC active site motif within a thioredoxin-like domain, which

responsible for the disulphide isomerase activity [15]. ERp57 is the second most abundant family member after PDI, which differs in its substrate specificity, as it acts preferentially on glycosylated proteins by associating non-covalently with chaperones calnexin and calreticulin [16]. ERp57 shares similar domain structure and sequence homology with PDI [17], consisting of two thioredoxin-like domains (*a* and *a'*) with active site sequences CGHC, and substrate binding, non-thioredoxin like domains *b* and *b'* [18]. However, PDI family members appear to have specific substrate binding activities, indicating there is some specificity in their activities.

ERp57 was previously found to be upregulated in spinal cords of transgenic $SOD1^{G93A}$ mice and of sporadic ALS patients, similar to PDI [12], indicating it may have a protective role in ALS. Consistent with this notion, proteomic screening in peripheral mononuclear cells from ALS patients, identified PDI and ERp57 as being possible ALS biomarkers due their significant up-regulation, and ERp57 was also implicated as a biomarker to monitor disease progression in clinical trials [19].

We previously established that over-expression of PDI is protective against inclusion formation, ER stress and apoptosis, in neuronal cells expressing mutant SOD1 A4V and G85R. However, it remains unclear if ERp57, or any other PDI family members, are also protective in cells expressing mutant SOD1, and also whether the chaperone or disulphide interchange activity is necessary for protection. We predicted that other family members would also be protective against mutant SOD1-induced neurodegeneration in neuronal cells. We examined whether ERp57 inhibit the formation of inclusions, induction ER stress, and toxicity, in neuronal cells expressing mutant SOD1. Catalytically inactive mutant protein was also examined to determine whether any protective effect was mediated by the chaperone or disulphide interchange activity of the PDI family members. Here, we demonstrate that ERp57 can abrogate the toxicity and misfolding induced by mutant SOD1, and this protection depended on the disulphide interchange activity. Hence the PDI family has a broader therapeutic role in ALS.

Results

i) ERp57 reduces mutant SOD1 inclusions in neuronal cell lines

Mutant SOD1 misfolds and forms cytoplasmic inclusions in neuronal cell lines, which are defined here as large protein aggregates visible under a light microscope [8]. NSC-34 cell lines were transfected with SOD1-EGFP and ERp57-V5 constructs. At 72 hr post transfection, cells were imaged using confocal fluorescence microscopy and the percentage of transfected cells (visualised by the presence of EGFP fluorescence) bearing mutant SOD1 inclusions was quantified (Figure 1A). Cells expressing GFP alone or wild-type SOD1 formed very few inclusions (<1%). Similar to previous observations, 17% of cells expressing mutant $SOD1^{A4V}$ formed inclusions [8]. However, when wild-type ERp57 was co-expressed with mutant $SOD1^{A4V,}$ this was significantly reduced to 10% (***p<.001). In contrast, co-expression of cysteine mutant ERp57 did not significantly alter the proportion of mutant $SOD1^{A4V}$ expressing cells bearing inclusions (14%, Figure 2B).

Furthermore, these observations were confirmed using mutant $SOD1^{G85R}$ in Neuro2a cells Supplementary figure 5A). Untransfected cells, cells expressing GFP alone or wild-type SOD1 formed very few inclusions (>1%), 16% of cells expressing mutant $SOD1^{G85R}$ formed inclusions. However, when wild-type ERp57 was co-expressed with mutant $SOD1^{A4V}$, this was significantly reduced to 10% (***p<.001). In contrast, co-expression of C24A_ERp57 did not significantly alter the proportion of mutant $SOD1^{G85R}$ expressing cells bearing inclusions (Supplementary figure 5B).

ii) ERp57 reduces ER stress induced by mutant SOD1 in neuronal cell lines

We previously demonstrated that mutant $SOD1^{A4V}$ induces ER stress which is associated with inclusion formation [8]. Next, we investigated whether ERp57 is also protective against ER stress induced by mutant $SOD1^{A4V}$ in neuronal cells. Using immunocytochemistry, two markers of ER stress were used to specifically examine only transfected cells. Nuclear immunoreactivity for XBP-1 was used to detect activation of the IRE-1 pathway, which is a marker of the early, prosurvival phase of UPR, and secondly, CHOP is a marker used to

examine ER stress induced *via* the PERK and ATF-6 pathway, during the pro-apoptotic phase of UPR.

NSC-34 cells co-expressing SOD1-EGFP and ERp57-V5 were immunostained using anti-XBP-1 antibodies, and at 72 hr post transfection, cells were examined individually for nuclear immunoreactivity to XBP-1, indicating UPR induction, using confocal microscopy (Figure 2A). Whereas few control cells demonstrated nuclear XBP-1 immunoreactivity (4% of untransfected cells and only 6% of EGFP only or wild-type SOD1 expressing cells), a significantly greater proportion of cells expressing mutant $SOD1^{A4V}$ 35% of cells expressed nuclear XBP-1. However, when mutant $SOD1^{A4V}$ expressing cells were co-transfected with wild-type ERp57, this proportion was significantly reduced to only 19% of transfected cells with nuclear XBP-1 immunoreactivity (**p<.01). Cysteine mutant ERp57 did not significantly reduce ER stress in cells expressing mutant $SOD1^{A4V}$ 29% of transfected cells displayed nuclear immunoreactivity to XBP-1 (Figure 2B).

Similarly in cells expressing mutant $SOD1^{G85R}$, few control cells demonstrated nuclear XBP-1 immunoreactivity (4% of untransfected cells, only 5% of cells expressing GFP and 7% of wild-type SOD1 expressing cells), a significantly greater proportion of cells expressing mutant $SOD1^{G85R}$ 25% of cells expressed nuclear XBP-1. However, when mutant $SOD1^{G85R}$ expressing cells were co-transfected with wild-type ERp57, this proportion was significantly reduced to only 9% of transfected cells with nuclear XBP-1 immunoreactivity (**p<.01). C24A_ERp57 did not significantly reduce ER stress in cells expressing mutant $SOD1^{G85R}$ 19% of transfected cells displayed nuclear immunoreactivity to XBP-1 (Supplementary Figure 6A, 6B).

Next, nuclear immunoreactivity to CHOP, indicating activation of pro-apoptotic UPR, was examined using confocal microscopy in NSC-34 cells expressing SOD1 and ERp57 at 72 hr post transfection (Figure 2C). Similar to the results obtained using XBP-1, only 2% of untransfected cells and cells expressing EGFP, and only 4% of cells expressing wild-type SOD1, displayed nuclear CHOP immunoreactivity. As expected, a much greater proportion of cells 56% expressing $SOD1^{A4V}$ displayed nuclear immunoreactivity to CHOP (Figure 2D), indicating activation of pro-apoptotic UPR. However, co-expression of wild-type ERp57 with mutant $SOD1^{A4V}$ led to a significant reduction in the proportion of cells with nuclear CHOP

immunoreactivity 40%, (**p<.01).In contrast, co-expression of cysteine mutant ERp57 with $SOD1^{A4V}$, did not significantly decrease the proportion of cells with nuclear immunoreactivity to CHOP 51%. Hence, as wild-type ERp57, but not cysteine mutant ERp57, reduced the proportion of cells with ER stress, as detected using two UPR markers, CHOP and XBP-1, these results imply that the disulphide interchange activity of ERp57 is protective against ER stress induced by mutant $SOD1^{A4V}$.

Similarly in cells expressing mutant $SOD1^{G85R}$, few control cells demonstrated nuclear CHOP immunoreactivity (2% of untransfected cells or GFP cells and 7% of wild-type SOD1 expressing cells), a significantly greater proportion of cells expressing mutant $SOD1^{G85R}$ 53% of cells expressed nuclear CHOP. However, when mutant $SOD1^{G85R}$ expressing cells were co-transfected with wild-type ERp57, this proportion was significantly reduced to only 35% of transfected cells with nuclear CHOP immunoreactivity (**p<.01). C24A_ERp57 did not significantly reduce ER stress in cells expressing mutant $SOD1^{G85R}$ 48% of transfected cells displayed nuclear immunoreactivity to CHOP (Supplementary Figure 6C, 6D).

iii) ERp57 reduces cell death in cells expressing $SOD1^{A4V}$ in neuronal cell lines

Mutant SOD1 triggers apoptosis of NSC-34 cells when expressed in cell culture [8]. Hence, we next investigated the effect of ERp57 on mutant SOD1 induced apoptosis in NSC-34 cells co-expressing SOD1-EGFP and ERp57-V5. Analysis of apoptosis was performed by quantification of apoptotic nuclei and caspase-3 activation, as in previous studies [8, 9]. Immunocytochemistry for cleaved caspase-3 and counter-staining for DAPI was performed at 72 hr post transfection (Figure 3A, 4A). Similar to previous findings, cells expressing diffuse SOD1 (i.e. no inclusions), either wild-type or mutant-A4V, displayed normal nuclear morphologies and little caspase-3 activation, indicating negligible levels of apoptotic cell death. In contrast, 28% of $SOD1^{A4V}$ expressing cells that bore inclusions contained fragmented nuclei, (Figure 3B), suggesting that apoptosis was underway. Similar results were obtained using caspase-3 immunocytochemistry: caspase-3 activation was observed in 24% of cells bearing mutant $SOD1^{A4V}$ inclusions. However, when wild-type ERp57 was co-expressed with mutant $SOD1^{A4V}$, significantly fewer cells were found to be undergoing apoptosis compared to cells expressing $SOD1^{A4V}$ alone. Quantification revealed that only 13% of these cells displayed condensed nuclei and only 18% demonstrated caspase-3

activation (***p<.001, Figure 3B). Hence, ERp57 is protective against apoptosis triggered by mutant SOD1. In contrast, co-expression of cysteine mutant ERp57 with $SOD1^{A4V}$ did not significantly decrease the proportion of cells with condensed nuclei or activated caspase-3. These results imply that the disulphide interchange activity of ERp57 is protective against apoptosis triggered by mutant$SOD1^{A4V}$.

Fragmented nuclei and nuclei without detectable DAPI were significantly more common (21%) in cells expressing $SOD1^{G85R}$ than in those expressing wild-type SOD1 (p<.001), consistent with previous observations. Co-expressing wild-type ERp57 with mutant $SOD1^{G85R}$ resulted in significantly fewer cells with apoptotic nuclei (15%, p<.001). Co-expressing C24A_ERp57 with mutant $SOD1^{G85R}$ did not reduce the proportion of cells with apoptotic nuclei 19% (Supplementary figure 7A, 7B).

iv) Endogenous ERp57 co-localises with mutant TDP-43 inclusions in sporadic ALS patients

Since ERp57 was protective in neuronal cells expressing mutant SOD1, we next investigated whether ERp57 was associated with intracellular inclusions in sporadic ALS patient tissues, which would imply that it is linked to protein misfolding in human ALS. Hence, we performed immunohistochemistry of human lumbar spinal cord sections of sporadic ALS patients and controls using anti-ERp57 and anti-TDP-43 antibodies. These experiments demonstrated that endogenous ERp57 co-localized strongly with TDP-43 inclusions in sporadic ALS spinal cord tissues, in contrast to control tissues, where the staining was diffuse (Figure 4A). Quantitative analysis of six ALS patient motor neurons revealed that 100% of TDP-43-immunopositive inclusions were also ERp57 immunoreactive. These data suggest that ERp57 is associated with TDP-43 misfolding, thus implying that ERp57 may have a broad protective role n ALS pathology.

Discussion

ERp57 is a multifunctional oxidoreductase and the closest known homologue of PDI. We previously demonstrated that PDI was protective against inclusion formation, ER stress, and apoptosis in cells expressing mutant SOD1. In this study we demonstrate that ERp57is also protective against mutant SOD1 aggregation, inclusion formation, ER stress and toxicity in neuronal cells. Previous studies have shown that the cells forming inclusions are selectively prone to apoptosis in contrast to cells that don't form inclusions [20]. Hence our study demonstrates that ERp57 is protective in ALS. Hence, there is clearly specificity in PDI family members in their protective activities in relation to ALS.

We also demonstrated that the disulphide interchange activity of ERp57 is essential for its protective function, thus providing some insight into the mechanism of protection in cells expressing mutant SOD1. Cysteine mutant ERp57 was not protective against mutant SOD1 inclusion formation, ER stress or apoptosis, suggesting that the protection is most likely modulated by disulphide bonding. Previous studies have demonstrated that mutations in SOD1 lead to conformational changes due to the formation of aberrant intermolecular disulphide bonds, thus inducing SOD1 aggregation and toxicity [21]. Since ERp57 facilitates the formation of the native disulphide bonds in proteins, its function could be further elucidated in ALS pathology. It could be hypothesized that ERp57 is refolding misfolded mutant SOD1 directly or alternatively that it reduces the misfolding of other target proteins *via* disulphide modulation, thus inhibiting ER stress and toxicity this way. It remains unclear how PDI itself is protective, whether this involves the disulphide interchange or chaperone activity. However, there is evidence that ERp57 is nitrated on tyrosine residues in $SOD1^{G93A}$ mice, thus implying a possible loss of the protective function during disease [22]. It could be speculated that although being protective ERp57 is non-functional due to post translational modifications. Hence, in ALS, the normal anti-aggregation properties of ERp57 could be inactivated, which may contribute to disease pathology. Similarly, aberrant cysteine residue modification by S-nitrosylation of PDI is present in ALS patient tissues suggesting that dysfunction of ER protein chaperones is linked to ALS [8]. Hence, replenishing ERp57 could be another way of protecting motor neurons against cellular stressors.

We did not directly demonstrate in this study that ERp57 and mutant SOD1 interact, but their co-localisation in neuronal cells and patient tissues, and the protective effect of ERp57

against mutant SOD1 misfolding, implies that they do. It remains to be determined in which subcellular compartment ERp57 and SOD1 would physically interact. ERp57localises in the nucleus, mitochondria and the cytosol as well as the ER?[23]. Previous studies have also speculated that mutant SOD1 is present in the ER [24], although this has been disputed in others [25, 26].

Further detailed investigation of the role of other PDI family members in ALS is warranted following the outcomes of this study. It is possible that different PDI family members prevent misfolding of specific substrates and that each misfolded protein engages specific family members. Alternatively, PDI family members may interact with their substrates in a cell-type specific manner. It is possible that PDI family members could compensate for each other's function. This would be another approach to understand the mechanism of protection of ERp57.

In summary, in this study we demonstrate that a novel PDI-like protein ERp57, is specifically protective against mutant SOD1 misfolding, ER stress, and toxicity. This study also suggests that other members of the PDI family may have specific protective roles against protein misfolding in ALS. Furthermore, we demonstrate that the disulphide activity of ERp57 is necessary for its protective function, hence this study sheds some light on possible ways to develop therapeutic targets against protein misfolding, the key pathology in ALS, and also the common pathology in neurodegenerative disorders. These findings will assist in further elucidating the role of ERp57 in protection against neurotoxicity and the mechanism by which PDI and ERp57 reduces SOD1 inclusions. Since death of motor neurons is the primary pathological event in ALS, the protective effect of ERp57 on neuronal apoptosis, suggests that it has potential as a novel therapeutic target.

Materials and Methods

Cell lines

Mouse motor neuron like NSC-34 cells were kindly provided by Professor Neil Cashman, University of Toronto. Mouse neuroblastoma Neuro-2a cell lines (ATCC cell line CCL-131) were maintained in Dulbecco's Modified Eagle Medium (DMEM) with 10% fetal calf serum, 100 ug/mL penicillin and 100 ug/mL streptomycin.

Constructs

Expression constructs for wild-type ERp57 and mutant ERp57in pcDNA3.1(+) were a generous gift from Dr Neil Bulleid, University of Glasgow, UK. Cysteine mutant ERp57 contained a replacement of cysteine residues at positions 60 and 490 with alanine, so that both CGHC active sites were mutated to CGHA. The SOD1-EGFP constructs were as described earlier [27].

Cell Culture and Transfection

NSC-34 cells and Neuro2a cells were maintained in Dulbecco's modified eagle medium (DMEM) with 10% fetal calf serum (FCS), incubated at 37°C with 5% CO_2. Transfections were performed using Lipofectamine reagent 2000 (Invitrogen) according to the manufacture's protocol. Cells were co-transfected with SOD1-EGFP constructs and ERp57-V5 constructs, and observed 72 hr post transfection using fluorescence microscopy.

Immunofluorescence and Microscopy

Cells were fixed with freshly prepared 4% (w/v) paraformaldehyde and incubated in the dark for 30 min. The cells were permeabilized with 0.1% (v/v) Triton-X in PBS for 5 min and blocked with 3% BSA in PBS for 30 min, followed by incubation with mouse anti-CHOP (1:50) (Santa Cruz), rabbit anti-XBP-1 (Santa Cruz) (1: 20), or cleaved anti-caspase-3 (1:100) (Cell signalling) antibodies in PBS at 4°C overnight. The secondary antibodies, AlexaFluor 568 conjugated rabbit anti-mouse IgG (1:250) or goat-anti-rabbit IgG AlexaFluor 568, were added for 1 hr and incubated in the dark at room temperature. After washing with PBS, staining of nuclei was performed using Hoechst stain 33342 (Invitrogen), and cells were mounted using fluorescent mounting media. DAPI (nuclei), FITC (GFP fluorescence) and TRITC (red fluorescence) filters were used for viewing the cells and images were taken using

an Olympus Fluoview 1000 laser scanning microscope. In dual-channel imaging, photomultiplier sensitivities and off sets were set to a level at which bleed through effects from one channel to another were negligible. Each experiment was performed four separate times. For detection of XBP-1 and CHOP activation, cells were co-transfected with SOD1-EGFP and ERp57-V5 constructs and immunocytochemistry using XBP-1 or CHOP antibodies respectively was performed. Cells in which immunoreactivity was detected in the nucleus compared to the cytoplasm were scored as positive, indicating induction of the UPR, as performed previously.

ERp57 and TDP-43 immunohistochemistry

Paraffin-embedded human lumbar spinal cord sections (14 µm) from non-neurological controls and ALS patients were obtained from the MND Research Tissue Bank of Victoria (details give in Table 1). The tissue sections were pre-heated at 65˚C for 15 minand then paraffin was removed by washing with xylene twice for 5 min and 2 min respectively, followed by washing with 100 % ethanol and 50 % ethanol for 5 min each. The sections were then washed with distilled water and soaked in PBS. Antigen retrieval was performed by boiling the sections in 10 mM sodium citrate buffer (pH 6) for 1 min. The sections were then incubated with blocking serum (3% goat serum, 0.3% triton x-100 in phosphate buffered saline (PBS)) for 30 min, followed by primary antibodies; rabbit anti-TDP43, 10782-2-AP-proteintech (1:50), mouse anti-ERp57, ab13506-abcam (1:100) prepared in blocking serum, overnight at 4˚C. The sections were then washed thrice with 0.1 % Tween 20 in PBS for 10 min each. Secondary AlexaFluor-488 or 594 conjugated anti-mouse or anti-rabbit antibodies (1:250, Molecular Probes) were added and incubated for 1 hr at room temperature. Finally, the sections were washed with 0.1 % Tween 20 in PBS and a coverslip was mounted with DAKO fluorescent mounting medium.

Table 1 Details of ALS patients and controls

Case	Gender	Age (years)	PMI (h)	Diagnosis
1	Female	88.6	6	Control
2	Male	84.6	68	Control
3	Male	84.8	59	ALS
4	Male	86.4	11	ALS

Human lumbar spinal cord segments (L3–L5) from 2 patients who died of respiratory failure caused by ALS were provided by the MND Research Tissue Bank of Victoria. Age = age at death, PMI = post-mortem interval.

Statistics

Cells co-expressing SOD1-EGFP and ERp57-V5 were examined (200 total) and the data was represented as Mean ± SD. Statistical analyses were made using ANOVA followed by Tukey's post hoc test (GraphPad Prism, San Diego, CA, USA). P-values of 0.05 or less were considered significant *$p<0.05$,**$p < 0.01$, ***$p<0.001$.

Figure legends

Figure 1 ERp57 is protective against inclusion formation induced by mutant $SOD1^{A4V}$ A) Immunofluorescence detection of EGFP positive inclusions present in NSC-34 cells expressing wild-type SOD1 (SOD1-WT) or SOD1A4V (green),when co-expressed with wild-type ERp57 (ERp57 wt) or C24A_ERp57 (red), examined by confocal microscopy. Nuclei are visualised by Hoechst staining (blue). Cells expressing wild-type SOD1 did not form inclusions (panel 1). Inclusion positive cells were present in cells expressing $SOD1^{A4V}$alone (panel 2) or co-expressing C24A_ERp57 (panel 4), represented by white arrows. In contrast, fewer cells formed inclusions in cells Over-expressing wild-type ERp57 with $SOD1^{A4V}$ (panel 3). Scale = 10 µm. B) Quantification of the percentage of transfected cells bearing inclusions in NSC-34 cells as represented in (A). Fewer cells formed inclusions when wild-type ERp57 was co-expressed with $SOD1^{A4V}$ (***p<.001) compared to cells co-expressing C24A_ERp57 or vector only. Data is shown as the mean + SD, n =4. C) Quantification of the percentage of Neuro2a cells bearing inclusions. Fewer cells formed inclusions when wild-type ERp57 was co-expressed with $SOD1^{A4V}$ (***p<.001) as compared to the C24A_ERp57 or vector only. Data is shown as the mean + SD, n =4.

Figure 2 ERp57 reduces ER stress in mutant $SOD1^{A4V}$ in neuronal cell lines.
A) Immunofluorescence detection of nuclear immunoreactivity to XBP-1 (centre) in $SOD1^{WT}$ and $SOD1^{A4V}$ cells co-expressing wild-type ERp57 or C24A_ERp57 transfected in cells determined by confocal microscopy, 72 hr post transfection. Untransfected cells (UTR) (panel 1) or cells expressing wild-type SOD1 (panel 2) showed few cells with XBP-1 activation. Cells transfected with $SOD1^{A4V}$ (panel 3) had nuclear XBP-1 induction as indicated with white arrows. Cells cotransfected with $SOD1^{A4V}$and wild-type ERp57 had few cells with nuclear XBP-1 (panel 4). Cells co-transfected with $SOD1^{A4V}$and C24A_ERp57 showed nuclear XBP-1 because of ER stress as indicated with white arrows (panel 5). Scale bar = 10 µm. B) Quantification of nuclear XBP-1 induction in NSC-34 cells when co-transfected with wild-type SOD1 and $SOD1^{A4V}$ with wild-type ERp57 or C24A_ERp57. 100 cells expressing XBP-1 in the nucleus were counted. The number of cells expressing XBP-1 decreased when wild-type ERp57 was transfected with $SOD1^{A4V}$ (**p<.01). Data represented as mean ±SD, n=4.

C) Immunofluorescence detection of nuclear CHOP immunoreactivity in wild-type SOD1 or $SOD1^{A4V}$ NSC-34 cells co-expressing wild-type ERp57 or C24A_ERp57, visualised by confocal microscopy. Few ells expressing GFP alone (pEGFP) (panel 1) or wild-type SOD1 (panel 2) displayed nuclear immunoreactivity to CHOP, indicating activation of the UPR. In contrast, nuclear reactivity to CHOP was more frequent in cells expressing $SOD1^{A4V}$ (panel 3), indicated by white arrows (middle and bottom panel). However, fewer cells co-expressing $SOD1^{A4V}$and wild-type ERp57 (panel 4) displayed nuclear CHOP immunoreactivity. Cells co-expressing $SOD1^{A4V}$ and C24A_ERp57 displayed more frequent nuclear immunoreactivity to CHOP, indicating the presence of ER stress (panel 5). Scale bar = 10 µm. D) Quantification of nuclear CHOP immunoreactivity in NSC-34 cells visualised in (A), co-expressing wild-type SOD1 or $SOD1^{A4V}$ with wild-type ERp57 or C24A_ERp57. For each population, 100 transfected cells expressing CHOP in the nucleus were counted. The percentage of $SOD1^{A4V}$cells expressing nuclear CHOP was significantly lower in cells co-expressing wild-type ERp57 compared to empty vector alone (**p<.01). There were also significantly fewer cells with CHOP activation when C24A_ERp57 wt was co-expressed with wild-type ERp57 and $SOD1^{A4V}$ (*p<.05).Data represented as mean ±SD, n=4.

Figure 3 ERp57 inhibits apoptotic cell death induced by mutant $SOD1^{A4V}$. A) NSC-34 cells were co-transfected with wild-type SOD1-WT or $SOD1^{A4V}$ (green panel) and wild-type ERp57 or C24A_ERp57 (red panel) for 72 hr. Nuclei are shown by Hoechst stain (blue). Arrow represents condensed or fragmented nuclei, indicating apoptosis is underway. Few cells expressing wild-type SOD1 (panel 1). However, cells expressing $SOD1^{A4V}$ (panel 2) displayed DAPI-stained condensed nuclei, indicating apoptosis, shown by white arrows (middle panel). Fewer cells co-expressing $SOD1^{A4V}$and wild-type ERp57 (panel 3) were undergoing apoptosis, whereas condensed or fragmented nuclei, indicated with white arrows, were much more common in cells expressing C24A_ERp57 (panel 4). Scale bar = 10 µm. Merge images in column 4 are overlays of the images of GFP fluorescence immunostained with cleaved caspase-3 (red), indicating activation of the enzyme DAPI (third column).
B) Quantification of apoptotic nuclei in cells in (A) expressing SOD1 and ERp57. Over-expression of wild-type ERp57 inhibits apoptotic cell death triggered by mutant SOD1. The number of transfected cells with apoptotic nuclei (condensed or fragmented) was counted (100 total cells). Over-expression of wild-type ERp57 with $SOD1^{A4V}$resulted in significantly fewer cells undergoing apoptosis, (***p<.001), n=4.

C) Caspase-3 activation, indicating apoptosis, in cells expressing $SOD1^{A4V}$ and ERp57. NSC-34 cells were co-transfected with wild-type SOD1 or $SOD1^{A4V}$ (green panel) and wild-type ERp57 or C24A_ERp57 (red panel) for 72 hr, followed by immunocytochemistry using anti-activated caspase-3 antibodies using confocal microscopy. Nuclei are shown by Hoechst stain (blue). Arrow represents caspase-3 activation, indicating apoptosis is underway. Merge images in column 4 are overlays of the images of GFP fluorescence immunostained with cleaved caspase-3 (red), Yellow arrows indicate presumed location of nuclei undetectable by DAPI staining, due to active apoptosis, under conditions used. Fewer cells expressing SOD1-WT (panel 1) displayed caspase-3 activation compared to cells expressing $SOD1^{A4V}$. Expression of $SOD1^{A4V}$ (panel 2) resulted in caspase-3 activation in 20% of cells, as indicated by white arrows (middle panel). Fewer cells co-transfected with $SOD1^{A4V}$and wild-type ERp57 (panel 3) displayed caspase-3 activation but apoptosis was more frequent in cells co-expressing with $SOD1^{A4V}$and ERp57, as indicated with white arrows (panel 4). Scale bar = 10 μm. D) Quantification of cells visualised in (C), immunostained for activated caspase-3. Results are expressed as mean ± SD, n=3. Over-expression of wild-type ERp57 with $SOD1^{A4V}$ significantly reduces apoptotic cell death compared to cells expressing empty vector only (***$p<.001$). However, there is no significant different in the percentage of $SOD1^{A4V}$cells with activated caspase-3 co-expressing C24A_ERp57 compared to $SOD1^{A4V}$with empty vector only.

Figure 4 ERp57 co-localises with TDP-43-positive inclusions in sporadic ALS patient lumbar spinal cords

A) Double immunohistochemistry of lumbar spinal cord sections of two patients with SALS and two control patients using antibodies against ERp57 and TDP-43. ERp57 was expressed diffusely in control patients (column 1) whereas ERp57 colocalizedwith 100% of TDP-43 inclusions in SALS motor neurons. Anti-ERp57 antibody immunostaining (green, first column), anti-TDP-43 antibody immunostaining (red, second column), merged of ERp57 and TDP-43 images shown in third column (yellow). ERp57 colocalises with TDP-43 inclusions in patient's sample (panel 2). Scale bar = 20 μm.

Supplementary Figures

Figure 5 ERp57 is protective against inclusion formation induced by mutant SOD1^{G85R}

A) Immunofluorescence detection of EGFP positive inclusions present in NSC-34 cells expressing wild-type SOD1 (SOD1-WT) or SOD1^{G85R} (green), when co-expressed with wild-type ERp57 (ERp57 wt) or C24A_ERp57 (red), examined by confocal microscopy. Nuclei are visualised by Hoechst staining (blue). Cells expressing wild-type SOD1 did not form inclusions (panel 1). Inclusion positive cells were present in cells expressing SOD1^{G85R} alone (panel 2) or co-expressing C24A_ERp57 (panel 4), represented by white arrows. In contrast, fewer cells formed inclusions in cells over-expressing wild-type ERp57 with SOD1^{G85R} (panel 3). Scale = 10 µm. Quantification of the percentage of transfected cells bearing inclusions in NSC-34 cells as represented in (A). Fewer cells formed inclusions when wild-type ERp57 was co-expressed with SOD1^{G85R} (***p<.001) compared to cells co-expressing C24A_ERp57 with vector only. Data is shown as the mean + SD, n =3.

Figure 6 ERp57 reduces ER stress induced by mutant SOD1^{G85R} in neuronal cell lines

A) Immunofluorescence detection of nuclear immunoreactivity to XBP-1 (centre) in SOD1^{WT} and SOD1^{G85R} cells co-expressing wild-type ERp57 or C24A_ERp57 transfected in cells determined by confocal microscopy, 72 hr post transfection. Untransfected cells (UTR) (panel 1) or cells expressing wild-typeSOD1 (panel 2) showed few cells with XBP-1 activation. Cells transfected with SOD1^{G85R} (panel 3) had nuclear XBP-1 induction as indicated with white arrows. Cells co-transfected with SOD1^{G85R} and wild-type ERp57 had few cells with nuclear XBP-1 (panel 4). Cells co-transfected with SOD1^{G85R} and C24A_ERp57 showed nuclear XBP-1 because of ER stress as indicated with white arrows (panel 5). Scale bar = 10 µm. B) Quantification of nuclear XBP-1 induction in NSC-34 cells when co-transfected with wild-type SOD1 and SOD1^{G85R} with wild-type ERp57 or C24A_ERp57. 100 cells expressing XBP-1 in the nucleus were counted. The number of cells expressing XBP-1 decreased when wild-type ERp57 was transfected with SOD1^{G85R} (**p<.01). Data represented as mean ±SD, n=3.

C) Immunofluorescence detection of nuclear CHOP immunoreactivity in wild-type SOD1 or SOD1^{G85R} NSC-34 cells co-expressing wild-type ERp57 or C24A_ERp57, visualised by confocal microscopy. Few ells expressing GFP alone (pEGFP) (panel 1) or wild-type SOD1

(panel 2) displayed nuclear immunoreactivity to CHOP, indicating activation of the UPR. In contrast, nuclear reactivity to CHOP was more frequent in cells expressing SOD1^{G85R} (panel 3), indicated by white arrows (middle and bottom panel). However, fewer cells co-expressing SOD1^{G85R} and wild-type ERp57 (panel 4) displayed nuclear CHOP immunoreactivity. Cells co-expressing SOD1^{G85R} and C24A_ERp57 displayed more frequent nuclear immunoreactivity to CHOP, indicating the presence of ER stress (panel 5). Scale bar = 10 µm.

D) Quantification of nuclear CHOP immunoreactivity in NSC-34 cells visualised in (A), co-expressing wild-type SOD1 or SOD1^{G85R} with wild-type ERp57 or C24A_ERp57. For each population, 100 transfected cells expressing CHOP in the nucleus were counted. The percentage of SOD1^{G85R} cells expressing nuclear CHOP was significantly lower in cells co-expressing wild-type ERp57 compared to empty vector alone ($p<.01$). There were also significantly fewer cells with CHOP activation between C24A_ERp57 co-expressed with SOD1^{A4V} and wild-type ERp57 and SOD1^{A4V} (**$p<.01$).Data represented as mean ±SD, n=4.

Figure 7 ERp57 inhibits apoptotic cell death induced by mutant SOD1^{G85R} A) NSC-34 cells were co-transfected with wild-type SOD1 or SOD1^{G85R} (green panel) and wild-type ERp57 or C24A_ERp57 (red panel) for 72 hr. Nuclei are shown by Hoechst stain (blue). Arrow represents condensed nuclei, indicating apoptosis is underway. Few cells expressing wild-type SOD1 (panel 1) were apoptotic. However, of cells expressing SOD1^{G85R} (panel 2) displayed DAPI-stained condensed nuclei, indicating apoptosis, shown by white arrows (middle panel). Fewer cells co-expressing SOD1^{G85R} and wild-type ERp57 (panel 3) were undergoing apoptosis, whereas condensed or fragmented nuclei, indicated with white arrows, were much more common in cells expressing C24A_ERp57 (panel 4). Scale bar = 10 µm. B) Quantification of apoptotic nuclei in cells in (A) expressing SOD1 and ERp57. Over-expression of wild-type ERp57 inhibits apoptotic cell death triggered by mutant SOD1^{G85R}. The number of transfected cells with apoptotic nuclei (condensed or fragmented) was counted (100 total cells). Over-expression of wild-type ERp57 with SOD1^{G85R} resulted in significantly fewer cells undergoing apoptosis, (***$p<.001$), n=3.

Acknowledgements

Tissues were received from the Victorian Brain Bank Network, supported by The Florey Institute of Neuroscience and Mental Health, The Alfred and the Victorian Forensic Institute of Medicine and funded in part by Australia's National Health & Medical Research Council and Parkinson's Victoria.

References

1. Turner, M.R. and M. Swash, *The expanding syndrome of amyotrophic lateral sclerosis: a clinical and molecular odyssey.* Journal of Neurology, Neurosurgery & Psychiatry, 2015: p. jnnp-2014-308946.
2. Rosenfeld, J. and M.J. Strong, *Challenges in the Understanding and Treatment of Amyotrophic Lateral Sclerosis/Motor Neuron Disease.* Neurotherapeutics, 2015: p. 1-9.
3. Rosen, D.R., et al., *Mutations in Cu/Zn superoxide dismutase gene are associated with familial amyotrophic lateral sclerosis.* Nature, 1993. **362**(6415): p. 59-62.
4. Bunton-Stasyshyn, R.K., et al., *SOD1 Function and Its Implications for Amyotrophic Lateral Sclerosis Pathology New and Renascent Themes.* The Neuroscientist, 2014: p. 1073858414561795.
5. Arnesano, F., et al., *The unusually stable quaternary structure of human Cu,Zn-superoxide dismutase 1 is controlled by both metal occupancy and disulfide status.* Journal of Biological Chemistry, 2004. **279**(46): p. 47998-8003.
6. Hough, M.A., et al., *Dimer destabilization in superoxide dismutase may result in disease-causing properties: Structures of motor neuron disease mutants.* Proceedings of the National Academy of Sciences of the United States of America, 2004. **101**(16): p. 5976-5981.
7. Forsberg, K., et al., *Novel antibodies reveal inclusions containing non-native SOD1 in sporadic ALS patients.* PloS one, 2010. **5**(7): p. e11552.
8. Walker, A.K., et al., *Protein disulphide isomerase protects against protein aggregation and is S-nitrosylated in amyotrophic lateral sclerosis.* Brain, 2010. **133**(1): p. 105-116.
9. Soo, K.Y., et al., *Recruitment of mitochondria into apoptotic signaling correlates with the presence of inclusions formed by amyotrophic lateral sclerosis-associated SOD1 mutations.* Journal of neurochemistry, 2009. **108**(3): p. 578-590.
10. Zhang, Y.-J., et al., *Aggregation-prone c9FTD/ALS poly (GA) RAN-translated proteins cause neurotoxicity by inducing ER stress.* Acta neuropathologica, 2014. **128**(4): p. 505-524.
11. Atkin, J.D., et al., *Endoplasmic reticulum stress and induction of the unfolded protein response in human sporadic amyotrophic lateral sclerosis.* Neurobiology of disease, 2008. **30**(3): p. 400-407.
12. Atkin, J.D., et al., *Induction of the unfolded protein response in familial amyotrophic lateral sclerosis and association of protein-disulfide isomerase with superoxide dismutase 1.* Journal of Biological Chemistry, 2006. **281**(40): p. 30152-65.
13. Hetz, C. and B. Mollereau, *Disturbance of endoplasmic reticulum proteostasis in neurodegenerative diseases.* Nature Reviews Neuroscience, 2014. **15**(4): p. 233-249.
14. Schroder, M., *Endoplasmic reticulum stress responses.* Cellular & Molecular Life Sciences, 2008. **65**(6): p. 862-94.
15. Kozlov, G., et al., *A structural overview of the PDI family of proteins.* FEBS journal, 2010. **277**(19): p. 3924-3936.
16. Jessop, C.E., et al., *ERp57 is essential for efficient folding of glycoproteins sharing common structural domains.* EMBO Journal, 2007. **26**(1): p. 28-40.
17. Maattanen, P., et al., *ERp57 and PDI: multifunctional protein disulfide isomerases with similar domain architectures but differing substrate-partner associations This paper is one of a selection of papers published in this Special Issue, entitled*

CSBMCB-Membrane Proteins in Health and Disease. Biochemistry and cell biology, 2006. **84**(6): p. 881-889.
18. Kozlov, G., et al., *Crystal structure of the bb' domains of the protein disulfide isomerase ERp57.* Structure, 2006. **14**(8): p. 1331-1339.
19. Nardo, G., et al., *Amyotrophic lateral sclerosis multiprotein biomarkers in peripheral blood mononuclear cells.* PloS one, 2011. **6**(10): p. e25545.
20. Soo, K.Y., et al., *Recruitment of mitochondria into apoptotic signaling correlates with the presence of inclusions formed by amyotrophic lateral sclerosis-associated SOD1 mutations.* Journal of Neurochemistry, 2009. **108**(3): p. 578-590.
21. Wang, J., G. Xu, and D.R. Borchelt, *Mapping superoxide dismutase 1 domains of non-native interaction: roles of intra-and intermolecular disulfide bonding in aggregation.* Journal of neurochemistry, 2006. **96**(5): p. 1277-1288.
22. Casoni, F., et al., *Protein Nitration in a Mouse Model of Familial Amyotrophic Lateral Sclerosis POSSIBLE MULTIFUNCTIONAL ROLE IN THE PATHOGENESIS.* Journal of Biological Chemistry, 2005. **280**(16): p. 16295-16304.
23. Turano, C., et al., *Proteins of the PDI family: unpredicted non-ER locations and functions.* Journal of cellular physiology, 2002. **193**(2): p. 154-163.
24. Urushitani, M., et al., *The endoplasmic reticulum-Golgi pathway is a target for translocation and aggregation of mutant superoxide dismutase linked to ALS.* The FASEB Journal, 2008. **22**(7): p. 2476-2487.
25. Nishitoh, H., et al., *ALS-linked mutant SOD1 induces ER stress-and ASK1-dependent motor neuron death by targeting Derlin-1.* Genes & development, 2008. **22**(11): p. 1451-1464.
26. Atkin, J.D., et al., *Mutant SOD1 inhibits ER-Golgi transport in amyotrophic lateral sclerosis.* Journal of neurochemistry, 2014. **129**(1): p. 190-204.
27. Turner, B.J., et al., *Impaired extracellular secretion of mutant superoxide dismutase 1 associates with neurotoxicity in familial amyotrophic lateral sclerosis.* The Journal of neuroscience, 2005. **25**(1): p. 108-117.

1A

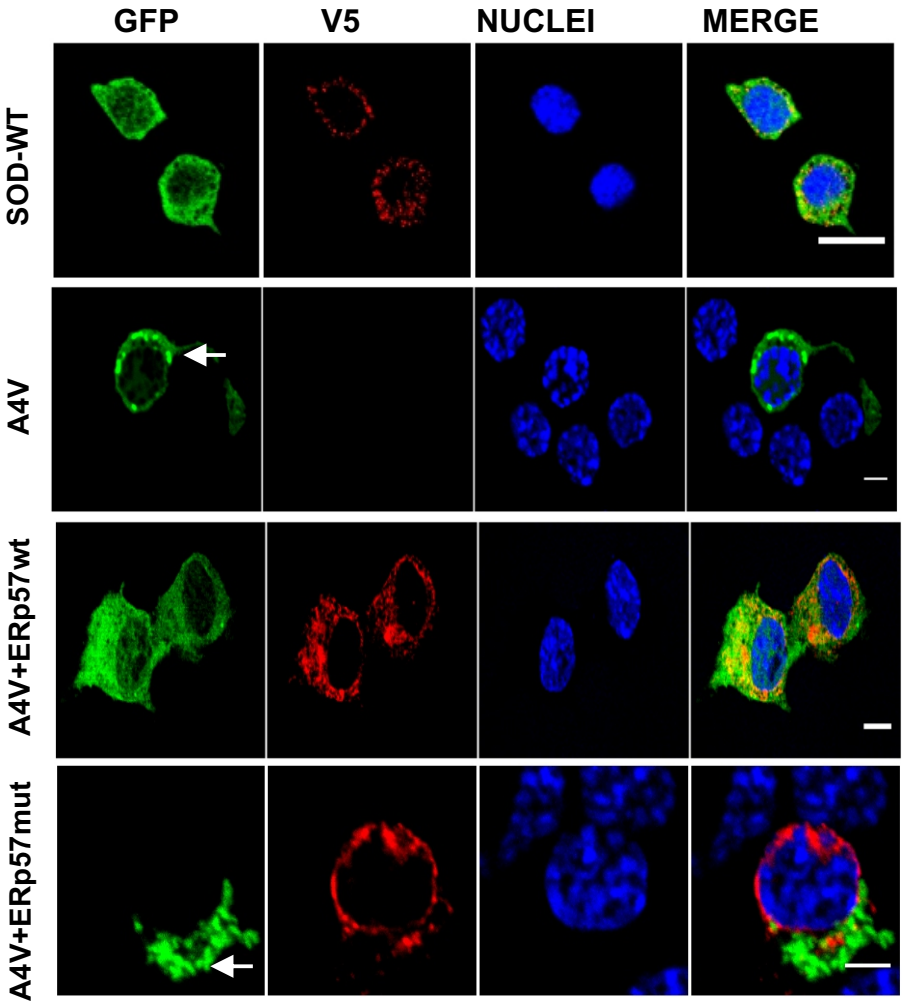
GFP
V5
NUCLEI
MERGE
SOD-WT
A4V
A4V+ERp57wt
A4V+ERp57mut

1B

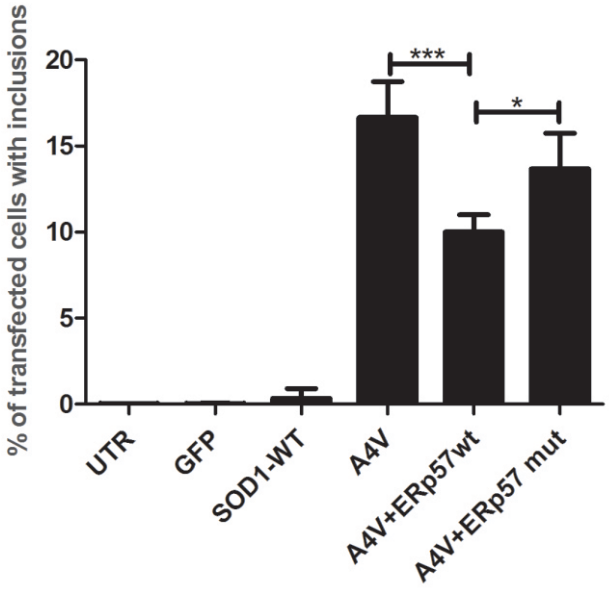
% of transfected cells with inclusions
20
15
10
5
0
***
*
UTR
GFP
SOD1-WT
A4V
A4V+ERp57wt
A4V+ERp57 mut

2A

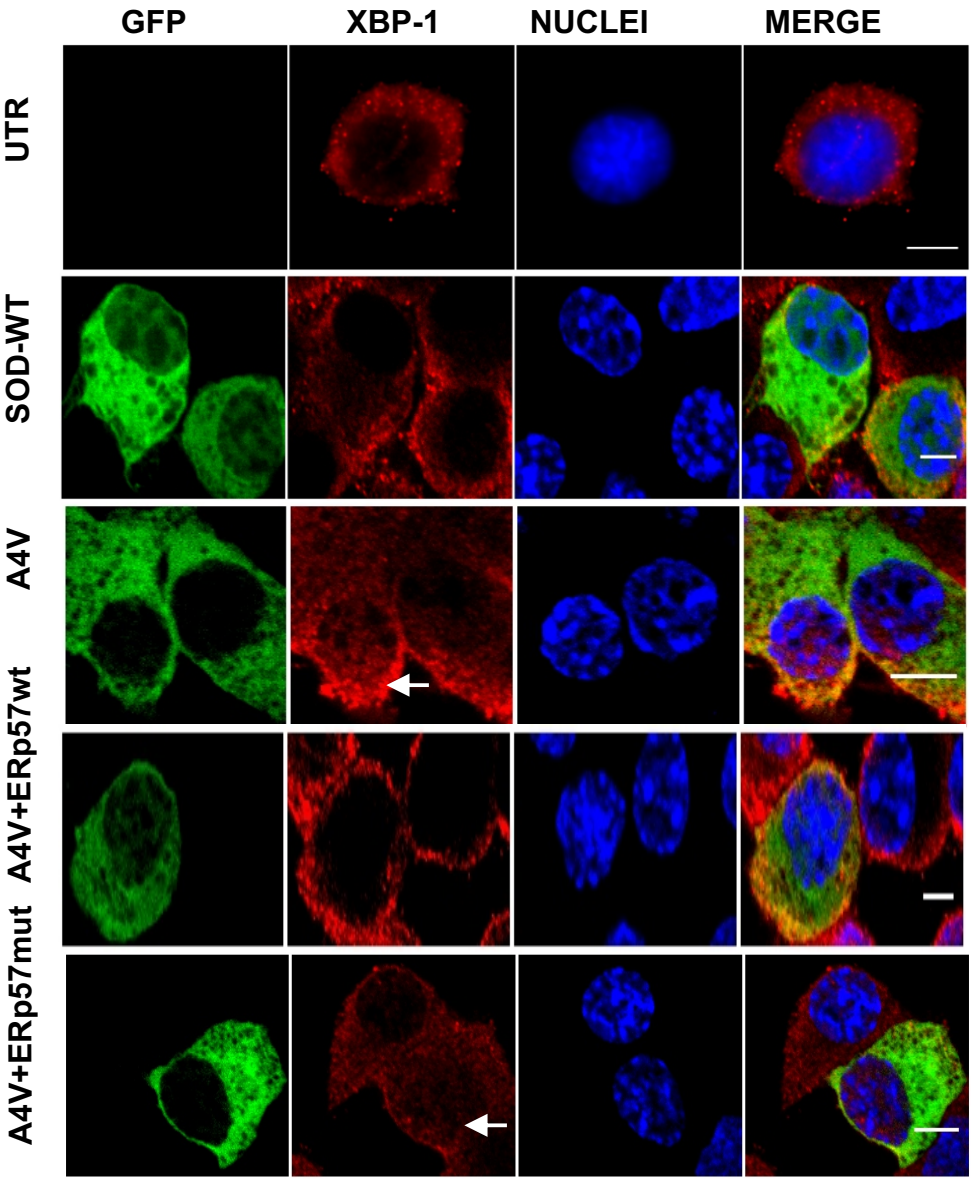
GFP
XBP-1
NUCLEI
MERGE
UTR
SOD-WT
A4V
A4V+ERp57wt
A4V+ERp57mut

2B

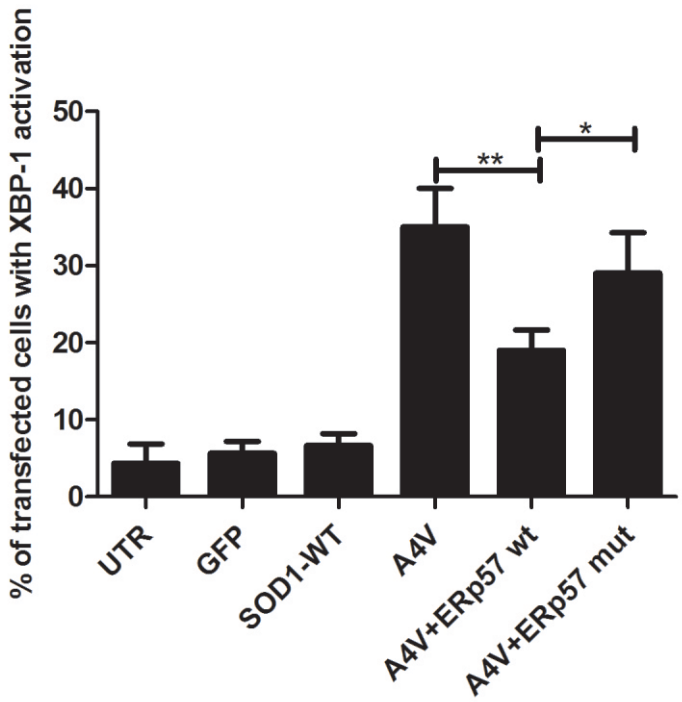
% of transfected cells with XBP-1 activation
50
40
30
20
10
0
**
*
UTR
GFP
SOD1-WT
A4V
A4V+ERp57 wt
A4V+ERp57 mut

2C

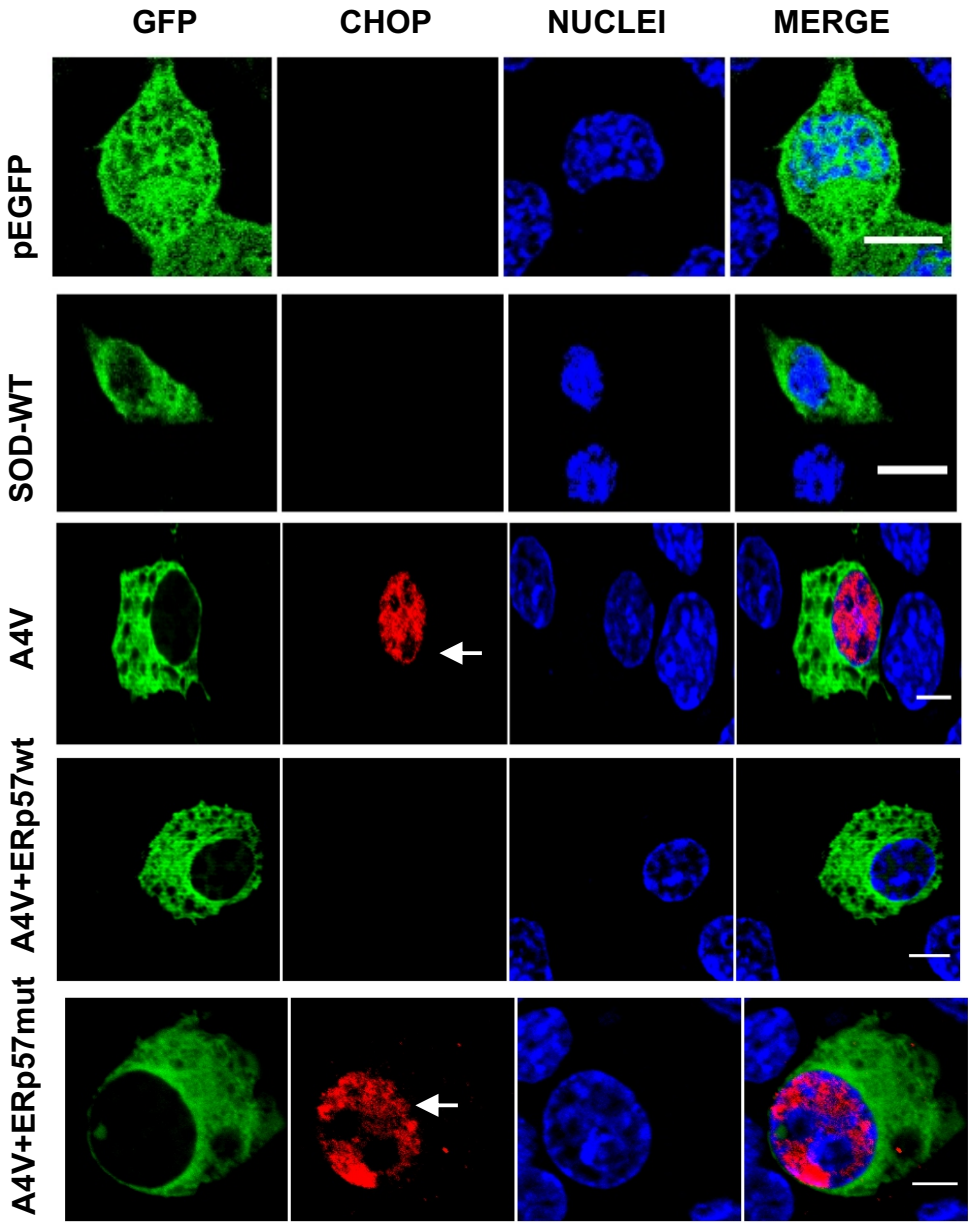
GFP
CHOP
NUCLEI
MERGE
pEGFP
SOD-WT
A4V
A4V+ERp57wt
A4V+ERp57mut

2D

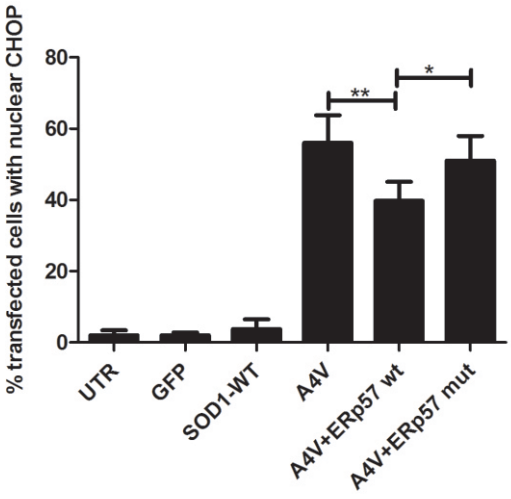
% transfected cells with nuclear CHOP
80
60
40
20
0
**
*
UTR
GFP
SOD1-WT
A4V
A4V+ERp57 wt
A4V+ERp57 mut

3A

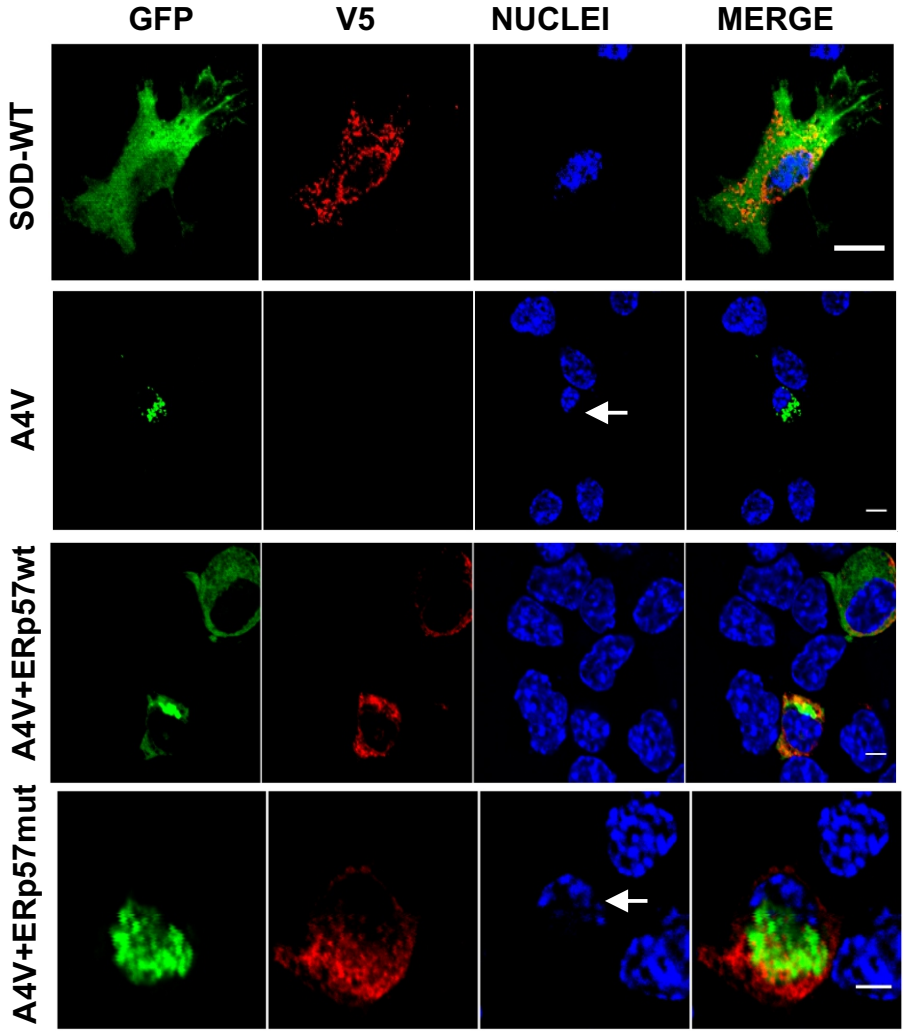
GFP
V5
NUCLEI
MERGE
SOD-WT
A4V
A4V+ERp57wt
A4V+ERp57mut

3B

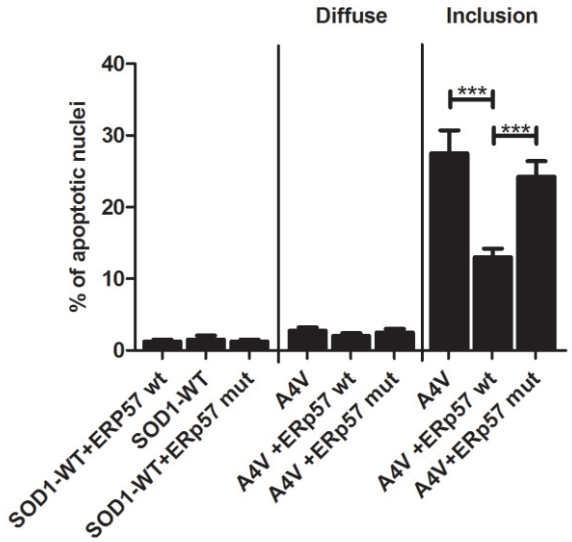
Diffuse
Inclusion
% of apoptotic nuclei
40
30
20
10
0
***
***
SOD1-WT+ERP57 wt
SOD1-WT
SOD1-WT+ERp57 mut
A4V
A4V +ERp57 wt
A4V +ERp57 mut
A4V
A4V +ERp57 wt
A4V+ERp57 mut

3C

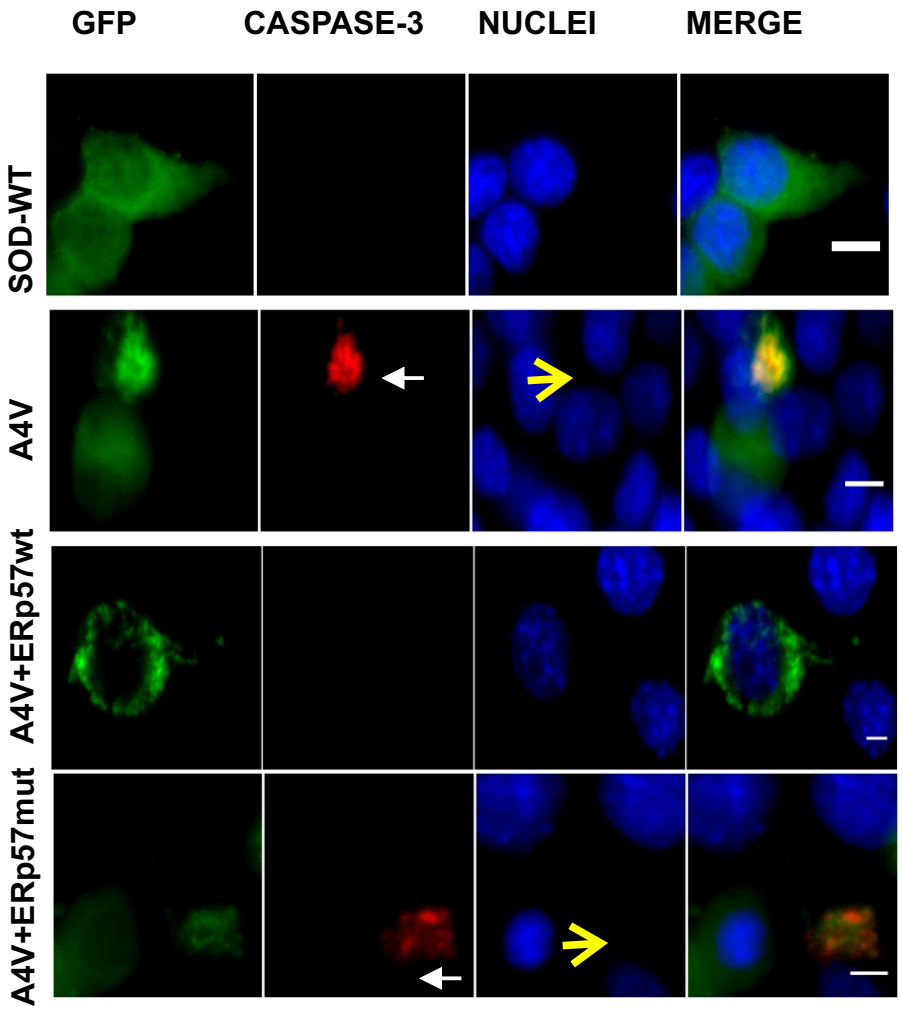
GFP
CASPASE-3
NUCLEI
MERGE
SOD-WT
A4V
A4V+ERp57wt
A4V+ERp57mut

3D

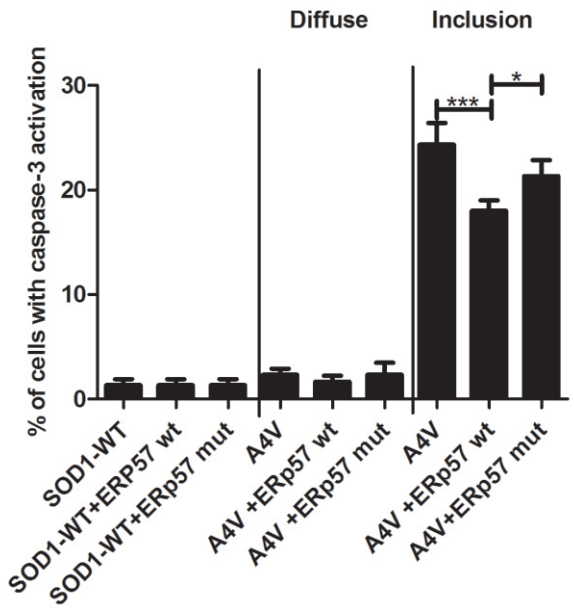
Diffuse
Inclusion
% of cells with caspase-3 activation
30
20
10
0
***
*
SOD1-WT
SOD1-WT+ERP57 wt
SOD1-WT+ERp57 mut
A4V
A4V +ERp57 wt
A4V +ERp57 mut
A4V
A4V +ERp57 wt
A4V+ERp57 mut

4A

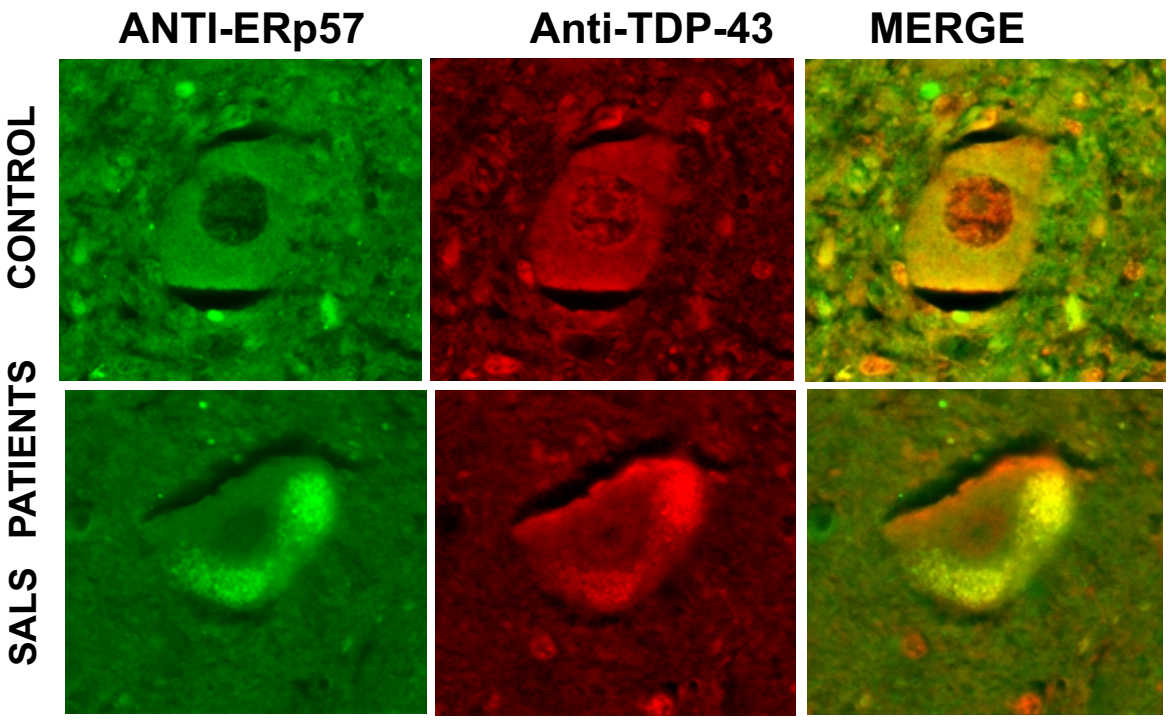

Supplementary data

5A

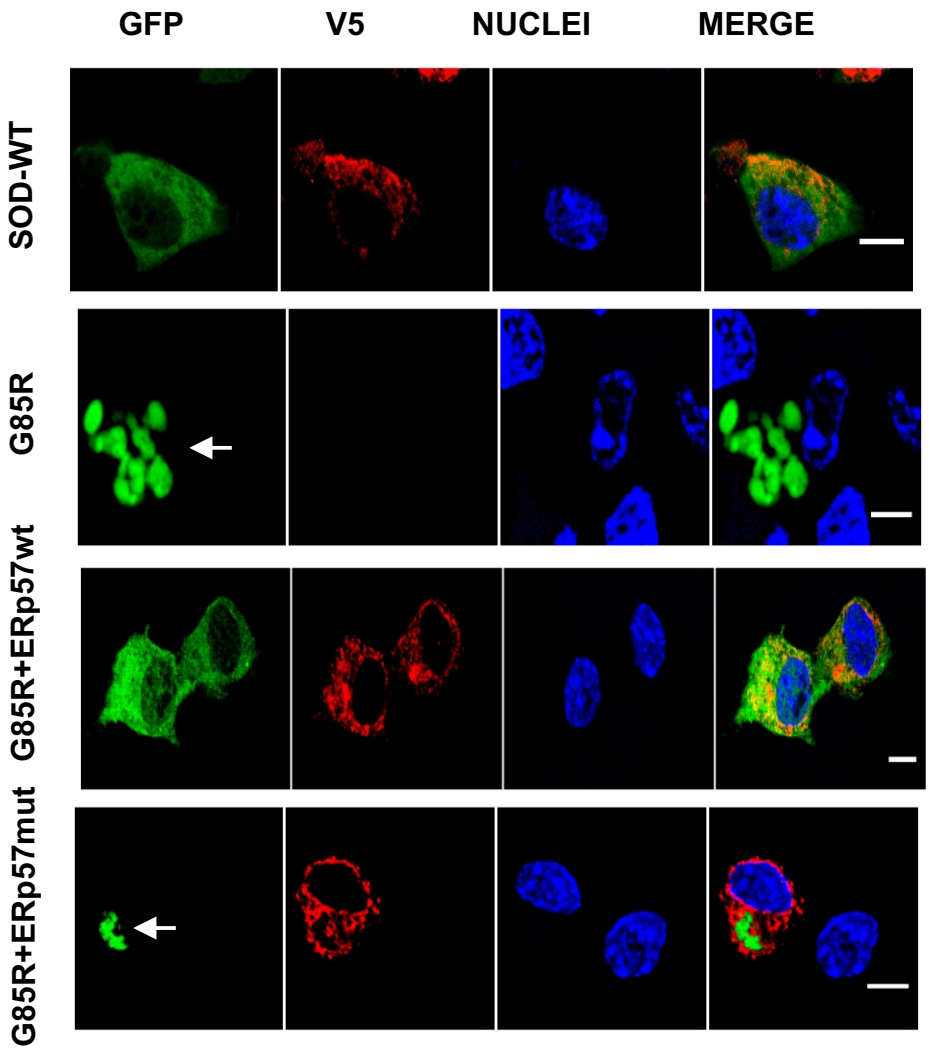

5B

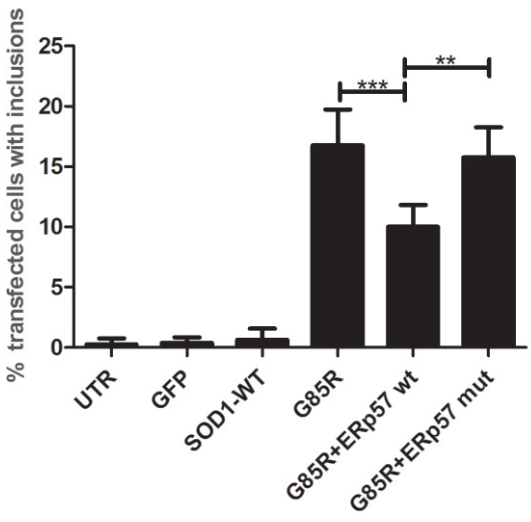

6A

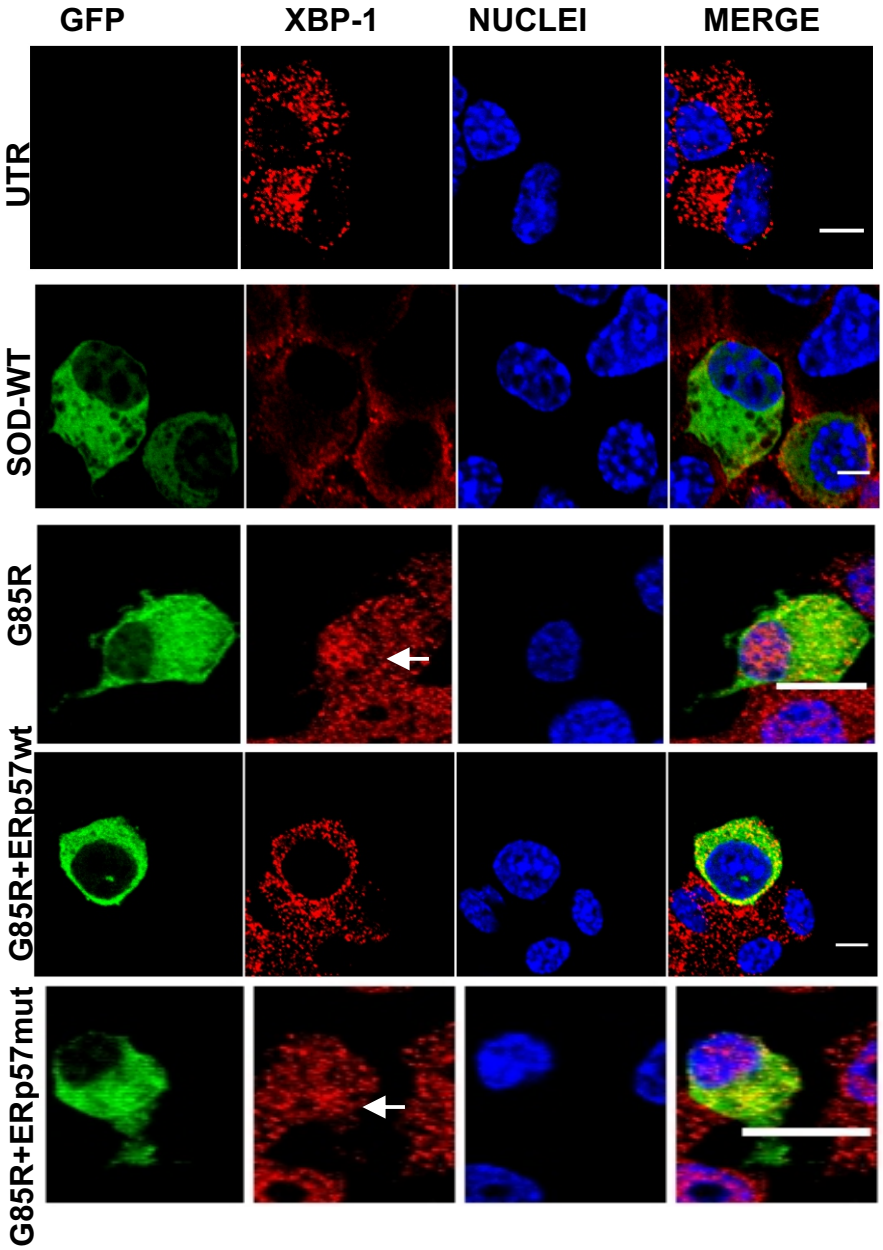
GFP
XBP-1
NUCLEI
MERGE
UTR
SOD-WT
G85R
G85R+ERp57wt
G85R+ERp57mut

6B

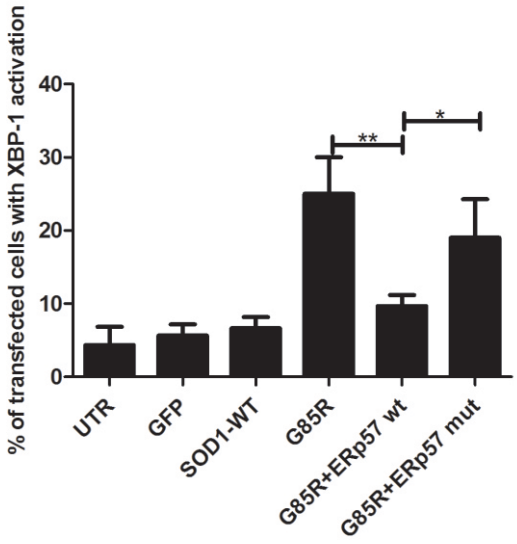
% of transfected cells with XBP-1 activation
40
30
20
10
0
**
*
UTR
GFP
SOD1-WT
G85R
G85R+ERp57 wt
G85R+ERp57 mut

6C

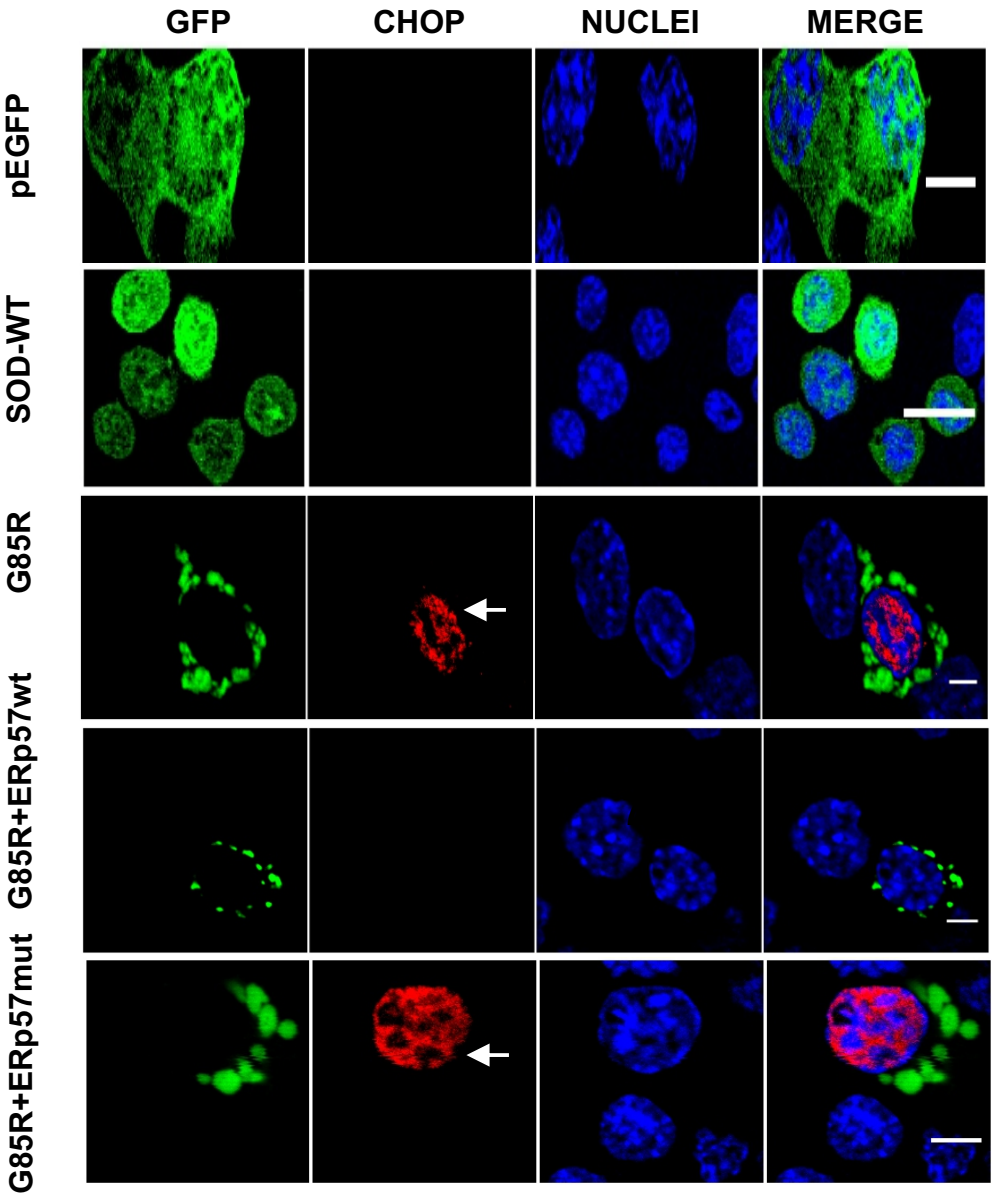
GFP
CHOP
NUCLEI
MERGE
pEGFP
SOD-WT
G85R
G85R+ERp57wt
G85R+ERp57mut

6D

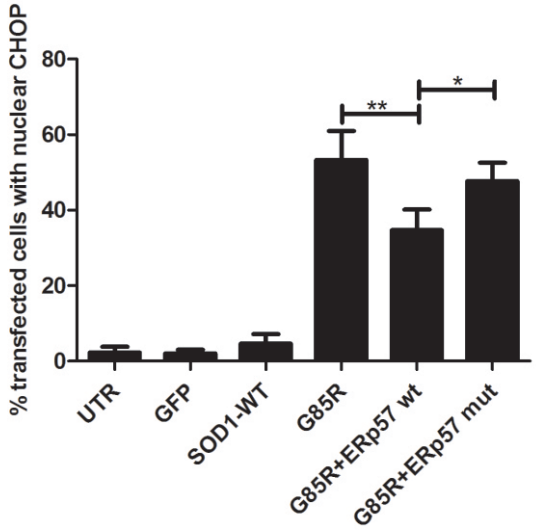
% transfected cells with nuclear CHOP
80
60
40
20
0
**
*
UTR
GFP
SOD1-WT
G85R
G85R+ERp57 wt
G85R+ERp57 mut

7A

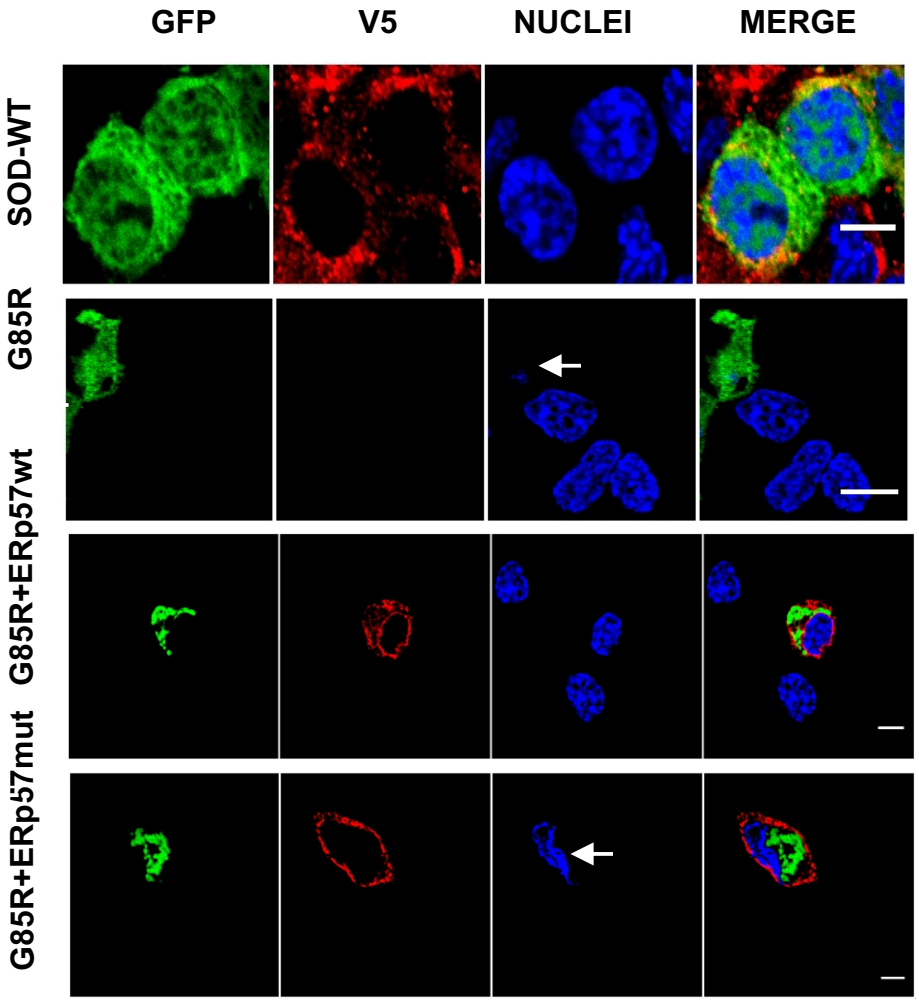
GFP
V5
NUCLEI
MERGE
SOD-WT
G85R
G85R+ERp57wt
G85R+ERp57mut

7B

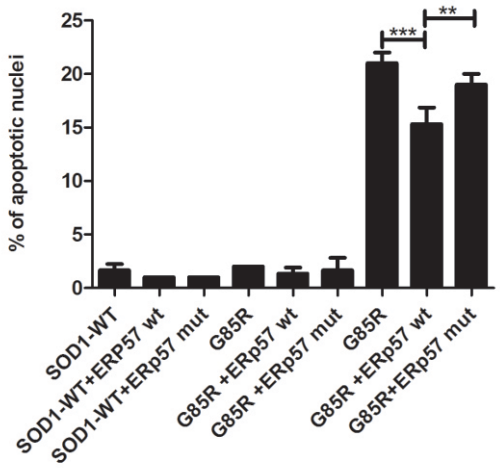
% of apoptotic nuclei
25
20
15
10
5
0
***
**
SOD1-WT
SOD1-WT+ERP57 wt
SOD1-WT+ERp57 mut
G85R
G85R +ERp57 wt
G85R +ERp57 mut
G85R
G85R +ERp57 wt
G85R+ERp57 mut

7.2.8 Supplementary Figure 7

The author was a part of the published review article: Halloran MA, Parakh S, Atkin JD (2013) "***The Role of S-nitrosylation and S-glutathionylation of Protein Disulphide Isomerase (PDI) in Protein Misfolding and Neurodegeneration***". International Journal of Cell Biology 797914:1-15.

Section 6 "**PDI family members**" on page 4 of the manuscript was contributed by the author.

Hindawi Publishing Corporation
International Journal of Cell Biology
Volume 2013, Article ID 797914, 15 pages
http://dx.doi.org/10.1155/2013/797914

Review Article

The Role of S-Nitrosylation and S-Glutathionylation of Protein Disulphide Isomerase in Protein Misfolding and Neurodegeneration

M. Halloran,[1] S. Parakh,[2] and J. D. Atkin[2]

[1] *Department of Neuroscience in the School of Psychological Science, La Trobe University, Bundoora, VIC 3086, Australia*
[2] *Department of Biochemistry, La Trobe University, Bundoora, VIC 3086, Australia*

Correspondence should be addressed to J. D. Atkin; j.atkin@latrobe.edu.au

Received 21 June 2013; Revised 19 August 2013; Accepted 2 September 2013

Academic Editor: Christian Appenzeller-Herzog

Neurodegenerative diseases involve the progressive loss of neurons, and a pathological hallmark is the presence of abnormal inclusions containing misfolded proteins. Although the precise molecular mechanisms triggering neurodegeneration remain unclear, endoplasmic reticulum (ER) stress, elevated oxidative and nitrosative stress, and protein misfolding are important features in pathogenesis. Protein disulphide isomerase (PDI) is the prototype of a family of molecular chaperones and foldases upregulated during ER stress that are increasingly implicated in neurodegenerative diseases. PDI catalyzes the rearrangement and formation of disulphide bonds, thus facilitating protein folding, and in neurodegeneration may act to ameliorate the burden of protein misfolding. However, an aberrant posttranslational modification of PDI, S-nitrosylation, inhibits its protective function in these conditions. S-nitrosylation is a redox-mediated modification that regulates protein function by covalent addition of nitric oxide- (NO-) containing groups to cysteine residues. Here, we discuss the evidence for abnormal S-nitrosylation of PDI (SNO-PDI) in neurodegeneration and how this may be linked to another aberrant modification of PDI, S-glutathionylation. Understanding the role of aberrant S-nitrosylation/S-glutathionylation of PDI in the pathogenesis of neurodegenerative diseases may provide insights into novel therapeutic interventions in the future.

1. Introduction

Neurodegenerative diseases share several common pathological characteristics, including the aberrant aggregation of misfolded proteins, leading to the formation of abnormal protein inclusions [1]. These diseases are also frequently classified as protein conformational disorders in which protein aggregation occurs due to the exposure of hydrophobic regions [2]. The most common neurodegenerative diseases include Alzheimer's disease (AD), Parkinson's disease (PD), amyotrophic lateral sclerosis (ALS), Creutzfeldt-Jakob disease (CJD), and Huntington's disease (HD). These diseases differ according to the specific group of neurons targeted and the type of misfolded proteins that aggregate. In AD, the accumulation of aggregated proteins occurs in cortical regions and involves both β-amyloid (βA), which forms extracellular amyloid plaques, and tau, which is hyperphosphorylated and forms intracellular neurofibrillary tangles (NFT) [3, 4]. PD involves the formation of Lewy bodies (LB) containing misfolded α-synuclein [5], and in HD aggregated Huntington protein with expanded polyglutamine repeats forms inclusions in the nucleus [6]. Similarly, in ALS, cytoplasmic inclusions contain copper/zinc (CuZn) superoxide dismutase 1 (SOD1) [7–9], TAR DNA binding protein 43 (TDP-43) [10–13], or fused in sarcoma/translated in liposarcoma (FUS/TLS) [14]. Recently, a hexanucleotide repeat expansion in an intronic region of the chromosome 9 open reading frame 72 (C9orf72) gene, encoding a gene of unknown function, was linked to the greatest proportion of familial ALS cases [15, 16]. For AD, PD, and ALS, 90–95% of cases arise sporadically, while the remainder are familial in nature. Genetic mutations in Amyloid Precursor Protein (APP), leads to increased accumulation of A-β and fibril formation [17–20], and Presenilin 1, 2 (PS 1, 2), which regulates APP processing via gamma

secretase [21–23], causes rare familial cases of AD [24]. Similarly, some forms of autosomal dominant familial PD is caused by α-synuclein mutations [25] leading to the aggregation of α-synuclein into insoluble fibrils, which are the primary components of LB [26], while mutations in PINK1, Parkin, and DJ-1 cause autosomal recessive PD cases [27]. However, in contrast to these conditions, HD is early onset and entirely genetic in nature.

The causal factors underlying the pathogenesis of sporadic neurodegenerative diseases remain poorly understood. However, due to the typical late onset of these disorders, neurodegeneration can be conceptualized as pathology that arises during the normal aging process, involving increases in oxidative stress and the production of free radicals which damage cells by decreasing antioxidant defenses. In AD, increased free radical accumulation and elevated levels of oxidative and nitrosative stress are associated with alterations in A-β metabolism [28, 29]. Meanwhile, in PD, nitrosative stress is associated with impairment of the mitochondrial respiratory chain, leading to energy deficiency and cell death [30]. In addition, oxidative and nitrosative stress are associated with endoplasmic reticulum (ER) stress, through the accumulation of misfolded proteins in the ER, and upregulation of molecular chaperones in the protein disulphide isomerase (PDI) family [31]. PDI possesses both general protein chaperone and disulphide interchange activity, thus facilitating the formation of native disulphide bonds in proteins. It also facilitates the degradation of these proteins via ER-associated degradation (ERAD), whereby irreparably misfolded proteins are targeted for retrotranslocation to the cytoplasm, where they undergo polyubiquitination and subsequent degradation by the proteasome [32–35]. There is now sufficient evidence that in conditions of elevated nitrosative stress, PDI undergoes an aberrant posttranslational modification known as S-nitrosylation, which inhibits its enzymatic activity [36]. Hence, in late onset neurodegenerative disease, there is a decrease in cellular defences and a corresponding increase in oxidative and nitrosative damage to lipids, proteins, DNA, and RNA [37, 38].

In this review, we will begin by examining the role of nitrosative stress, redox potential, and S-nitrosylation/S-glutathionylation of proteins linked to neurodegeneration. The structure and function of PDI family members will be discussed, and the importance of PDI in neurodegenerative disease will be highlighted. We will examine the evidence that PDI is aberrantly S-nitrosylated and discuss the functional significance of this modification in neurodegeneration. Finally, we speculate that PDI may also be S-glutathionylated in neurodegenerative disease.

2. Nitrosative Stress

Reactive nitrogen and oxygen species (RNS and ROS), primarily superoxide anion (O_2^-), hydrogen peroxide (H_2O_2), or nitric oxide (NO), are highly reactive molecules that normally function at low levels as mediators of intracellular signalling processes in mammalian cells [36, 39]. However, RNS and ROS can accumulate in cells under pathological conditions, triggering nitrosative or oxidative stress. This leads to numerous detrimental effects on cellular function including posttranslational modifications of proteins, lipid peroxidation, DNA, damage, and dysregulation of redox signalling [28, 37, 38, 40]. Nitrosative or oxidative stress results when there is an imbalance between the production of RNS/ROS and cellular antioxidant defence mechanisms such ascorbic acid, glutathione (GSH), or enzymes including superoxide dismutases, catalases, and glutathione peroxidases. GSH is a particularly important antioxidant as it is the most abundant cellular thiol-containing molecule; the ratio of reduced GSH to its oxidized form (GSSG) makes a major contribution to cellular redox potential and homeostasis [28, 29, 41]. However, the thiol/disulfide systems, which include GSH/GSSG, and plasma cysteine/cystine (Cys/CySS) pools are not necessarily in equilibrium and may respond differentially to specific stressors [42]. Nitrosative or oxidative stress may be induced by familial mutations, exogenous toxins (xenobiotics, pesticides), or via normal aging processes such as alterations in mitochondrial respiration [31, 43]. Neurons are particularly vulnerable to the effects of RNS/ROS due to a relative deficiency in antioxidant enzymes glutathione peroxidase (GPx) and catalase (Cat), compared to other cell types, and their higher metabolic demands which generate RNS/ROS from mitochondrial metabolism [38, 39, 43, 44].

RNS are derived primarily from O_2^- and NO, a small, diffusible inter- and intracellular messenger that normally mediates many intracellular signalling pathways [29, 31, 45, 46]. NO is generated by NO synthases (NOS) that use oxygen (O_2) and nicotinamide adenine dinucleotide phosphate (NADPH) oxidase to convert L-arginine to L-citrulline [47]. NOS is constitutively expressed in several isoforms in the central nervous system (CNS): endothelial NOS (eNOS), inducible NOS (iNOS), neuronal NOS (nNOS), and an isoform expressed in the inner mitochondrial membrane (mtNOS) [48–50]. The covalent addition of NO to a cysteine thiol or thiolate anion on specific proteins, to form an S-nitrosothiol (SNO) group, is a process termed "S-nitrosylation" [36, 51–56].

3. S-Nitrosylation

In recent years, S-nitrosylation has been increasingly implicated in many physiological and pathological conditions [36]. Under normal conditions, S-nitrosylation is a reversible posttranslational modification analogous to acetylation and phosphorylation that regulates protein activity [55, 57]. The SNO-group can be removed in these situations by denitrosylation enzymes, primarily S-glutathione reductase (GSNOR; alcohol dehydrogenase III) in conjunction with GSH and NADH as an electron donor [58, 59]. However, reduced oxidoreductase thioredoxin (TRX) [60, 61] can oxidize S-nitrosoglutathione (GSNO) to release GSH and NO [62, 63]. Recombinant human PDI can denitrosylate GSNO [64] and *in vitro* SOD1 can modify the stability of S-nitrosothiols by enhancing the decomposition of GSNO, resulting in production of NO [65], possibly by its reduced metal ions [66].

S-nitrosylation is both a reversible and irreversible process [67]. Under pathological conditions, S-nitrosylation of specific proteins is an abnormal, irreversible process and is linked to protein misfolding, ER stress, mitochondrial

dysfunction, synaptic degeneration, and cell death [36]. A well-recognized mechanism for NO production in neurodegenerative diseases is activation of N-methyl-D-Aspartate receptors (NMDAr) [68, 69]. Activation of NMDArs generates ROS and results in calcium (Ca^{2+}) influx into the cell [31, 70–72], which in turn activates nNOS to produce NO [50]. S-nitrosylation may also lead to NO-independent oxidation of proteins via ROS, producing reversible modifications in the form of intramolecular/mixed disulphide bonds. One of the proposed pathways for the further oxidation of cysteines is through the hydrolysis of sulfenic acid (SOH), which then may be susceptible to irreversible oxidation from accumulating ROS leading to stable sulfinic ($-SO_2H$) or sulfonic ($-SO_3H$) acid formation [73–75]. However, $-SO_2H$ can be reduced back to the free thiol group if the enzyme sulfiredoxin is induced and this can occur in neurons due to activation of NMDAr by increased synaptic activity [76]. In addition, S-nitrosylation can reversibly influence further posttranslation modifications of cysteine residues. When there are two proximal cysteine residues, S-nitrosylation of one of these can facilitate disulphide bond formation [77–79]. Under conditions of excessive nitrosative stress, however, S-nitrosylation inhibits the formation of disulphide bonds [67, 75]. Another pathological mechanism linked to S-nitrosylation has also been implicated in ALS. Cells expressing familial ALS mutants, SOD^{A4V} and SOD^{G37R}, have increased denitrosylation activity of GSNO in comparison to wild type (WT) SOD1 [80]. This deficiency in S-nitrosylation is especially elevated in mitochondria of mutant SOD1 cells [81].

Whilst most proteins contain multiple cysteine residues, the features underlying the specificity for S-nitrosylation are not fully defined, but appear to rely on tertiary rather than primary structure. Previous studies have suggested that the formation of S-nitrosylated proteins (SNO proteins) requires a cysteine flanked by a proximal acid-base motif, hydrophobic content, low pKa, and high exposure of sulfur atoms [67, 82]. However, a recent bioinformatics study predicted that the known SNO-Cys sites in proteins are more heterogenous than this, although the presence of a charged residue in close proximity to NO-Cys and another oppositely charged residue within a larger region was a common feature [82]. The stability of the resulting SNO-group depends upon the local environment of the cysteine residues, but studies of the dissociation energies of the S–N bond suggest that there is a wide variation, with this bond remaining stable theoretically from seconds to years [83, 84].

Up to one thousand SNO proteins have now been identified [85] including many proteins linked to neurodegenerative diseases [36, 77, 86–89]. For instance, S-nitrosylation of dynamin-related protein (Drp1) (SNO-Drp), found in postmortem brains of AD cases, is associated with β-A formation and subsequent activation of mitochondrial fission [77, 87]. In sporadic and familial PD, S-nitrosylated Parkin (SNO-Parkin) has reduced E3 ligase function, leading to proteasomal dysfunction [90]. Similarly, proteins involved in apoptosis (XIAP/Caspase 3, GAPDH-Siah), antioxidant activity (Prx2), the phosphatase pathway (PTEN), neuroinflammation (COX2), and autophagy (JNK1 and IKKβ) are also S-nitrosylated (for comprehensive review see [36]). Furthermore, SNO-proteins may alter cellular redox homeostasis through an interaction with GSH and therefore may influence other post-translational modifications, such as S-glutathionylation [36, 41]. Some proteins, such as NMDAr, are S-nitrosylated under both normal and pathological conditions [36]. S-nitrosylation/denitrosylation of NMDAr is important in physiological cellular signalling processes [52, 53, 91], but overactivation is associated with an increased production of SNO-proteins and neurodegeneration [31]. However, it should be noted that S-nitrosylation of NMDAr at Cys399 is protective by deactivation of the receptor, thus preventing glutamate excitotoxicity [53, 67, 78, 91].

4. S-Glutathionylation

S-glutathionylation is another posttranslational modification that has been implicated in the regulation of diverse proteins involved in energy metabolism, signalling pathways, Ca^{2+} homeostasis, antioxidant enzymatic activity, and protein folding [92] (for a comprehensive review see [41]). S-glutathionylation is induced by RNS/ROS and involves the formation of a disulfide between GSH and a cysteine residue [41]. As reduced GSH is the most abundant cellular thiol, it plays an important role in S-glutathionylation [41], although protein thiols represent a similar redox pool, and therefore may also be critical in providing antioxidant protection against oxidative stress [93]. S-nitrosylated cysteines can be converted to S-glutathionylated cysteines, supporting the premise that products of nitrosative stress induce S-glutathionylation [41]. However, the exact identity of the metabolites that act as proximal donors in this reaction remain to be elucidated [41] and it is unclear whether SNO proteins are intermediates for S-glutathionylation *in vivo*. Under oxidizing conditions, S-glutathionylation is reversible via the release of GSH from cysteine residues by thiol-disulphide oxidoreductase enzymes (TDOR). TDOR enzymes include TRX, which reduces intra- and intermolecular disulphide bonds, and glutaredoxin (GRX) which reduces protein-GSH bonds [94–96]. TRX and GRX catalyze the reduction of disulphide bonds and reactivate proteins that have undergone oxidation from sulfhydryl groups [95, 96]. Alterations in the ratio of GSH/GSSG and conditions that promote RNS/ROS production result in cysteine modifications that are precursors to the formation of mixed disulphides with GSH [95, 97, 98]. However, the role of S-glutathionylation during nitrosative and oxidative stress has not been completely defined. Glutathionylation at physiological levels may therefore represent a mechanism whereby cysteine residues faced with oxidation are protected from irreversible damage. The reduction of GSH-protein disulphide by GRX is essential in this process as it maintains the cellular availability of GSH and acts in concert with TRX to maintain the cellular thiol status [95].

S-glutathionylation has been implicated in neurodegeneration [95, 99–101]. The ratio of GSH/GSSG decreases in brains of aged rats [102], and accumulation of S-glutathionylated p53 in the inferior parietal lobule of AD patients

has also been reported [101]. In PD models, administration of the neurotoxin 1-methyl-4-phenyl-1,2,3,6-tetrahydropyridine (MPTP), which causes damage to dopaminergic neurons, caused an early decrease in the levels of GSH, inhibition of mitochondrial complex 1, and dopaminergic cell loss [103]. Furthermore, increases in GSH, GRX, and GSH reductase were detected in the brains of transgenic HD mice models (R6) [104, 105]. S-glutathionylation of SOD1 isolated from human erythrocytes at Cys111 promoted SOD1 monomer formation and subsequent aggregation [106]. Hence, alterations in S-glutathionylation and redox potential are important mediators of protein misfolding, and aberrant disulphide bond formation is implicated in this process.

5. ER Stress and Neurodegeneration

The major cellular location for protein disulphide bond formation is the ER. The highly oxidizing environment of this compartment (GSH : GSSG ratio~3 : 1) is necessary for formation of disulphide bonds and is in stark contrast to the reducing environment of the cytosol (GSH : GSSG ratio~100 : 1) [41, 92, 107]. The ER environment, therefore, is highly sensitive to changes in nitrosative and oxidative stress [31, 36].

ER stress is increasingly implicated as a pathogenic mechanism in neurodegenerative diseases [108–114]. ER stress occurs when misfolded proteins accumulate within the ER lumen, triggering the unfolded protein response (UPR) [115]. The UPR is a set of signalling pathways that initially aim to restore homeostasis by: (1) reducing protein synthesis and translocation, attenuating further accumulation of unfolded proteins in the ER, (2) activation of ER-resident chaperones including PDI to increase the protein folding capacity of the ER, and (3) induction of ERAD. The UPR activates three ER stress sensor proteins: inositol requiring kinase 1 (IRE1 α/β), double-stranded RNA-activated protein kinase-(PKR-) like ER kinase (PERK), and activating transcription factor 6 (ATF6), which transduce signals to the nucleus and cytosol [115, 116]. However, if homeostasis cannot be restored, apoptosis is triggered [115, 117]. Prolonged UPR activation linked to RNS or ROS triggers apoptosis through C/EBP homologous protein (CHOP), caspase 4, c-Jun, and c-Jun N-terminal kinase (JNK) [41, 118, 119].

PDI family members fulfil crucial roles in regulating ER stress by maintaining native protein conformation and facilitating protein degradation [120]. The remainder of this review will focus on the PDI family and the effect of S-nitrosylation/S-glutathionylation on PDI and its functional role in neurodegeneration.

6. PDI Family Members

There are currently 21 identified members of the PDI family [32, 120–125], which share several features in common; at least one domain with a TRX fold, the presence of a signal sequence, and ER localization due to the presence of an KDEL or other ER retention signal [32, 120, 126]. Whilst PDI family members contain a TRX domain, they essentially differ from TRX due to their higher redox potentials, substrate binding domains, and their ability to display both isomerase and chaperone activities, which renders them more efficient than TRX at forming/reforming disulphide bonds [127, 128]. Whilst PDI family members primarily mediate protein folding, other functions have also been ascribed to them, including regulation of Ca^{2+} homeostasis [129, 130] and ERAD, thus ameliorating protein misfolding within the ER [33–35].

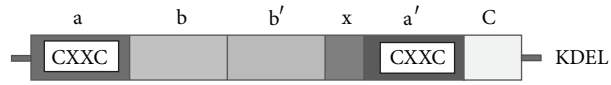

Figure 1: Domains of PDIA1. TRX-like domains representing catalytic active domains a a′. The b domain and b′ are catalytically inactive. The linker region is responsible for binding to the substrate. The C terminal is followed by an ER retrieval signal KDEL.

PDI disulphide-isomerase activity catalyzes the rearrangement of nonnative (incorrectly formed) disulphide bonds on nascent proteins, which would otherwise result in the formation of a misfolded structure. This activity is mediated through catalysis of thiol disulphide exchange (isomerization), whereby non-native disulphide bonds are initially reduced, and then oxidized to form the native structure [131–133]. Disulphide formation and stability are facilitated by the redox conditions of the ER [31]. Thus, active-site cysteines shift between two redox states: oxidation and the formation of disulphide bonds and reduction leading to the formation of thiols with free sulfhydryls [134]. In addition, PDI also has general chaperone activity which is independent of its disulphide interchange function [135–137]. This chaperone activity does not require its catalytic domains or active sites [138, 139].

PDI (PDIA1), the prototype of the PDI family, is a 55 kDa protein with two catalytically inactive TRX domains (b and b′), inserted between two TRX-like catalytic domains (a and a′), and an acidic C terminal domain with an ER-retention motif (KDEL). PDIA1 contains a CXXC catalytically active motif (Figure 1). All domains of PDI are required for efficient catalysis of disulphide bond formation and rearrangement [32, 120, 140]. The structure of yeast PDI has revealed that the binding of PDI to misfolded protein substrates is facilitated by two of the active cysteines positioned on opposite sides of the molecule [140, 141]. The noncatalytic b′ domain is situated on the base and is the major site for binding of substrates [141], although other domains also contribute to this process. The b-b combination of noncatalytic domains is present only in PDIA1, PDIA2 (PDIp), PDIA3 (ERp57), and PDIA4 (ERp72) family members [142–146]. PDIA1 has the broadest substrate specificity of the PDI family members examined to date [144].

PDIA2 is primarily expressed in pancreatic cells and dopaminergic neurons [146–148]. The domain structure of PDIA2 is similar to PDIA1, with a CXXC motif in the homologous a, a′ domains, intervening b, b′ domains, a x-linker region, and an N-terminal ER sequence [149]. PDIA2 also contains a KEEL motif at the C-terminus, an ER retention signal analogous to KDEL [150]. Similar to PDI, PDIA2 can

interact with protein substrates with and without cysteine residues [148, 151], suggesting that PDIA2 may act as a chaperone independent of catalyzing disulphide bond formation [147]. However, although its domain organization is similar to PDI, its physiological role remains unclear.

PDIA3 is the second most abundant soluble protein after PDIA1 found in the ER [120]. It contains a protein sequence homologous to PDIA1, with similarities in domain architecture but differences in substrate binding [152]. Whilst PDIA3 is an oxidoreductase with thiol-dependent reductase activity [153], it is different to the other PDI family members in that it acts primarily on glycosylated proteins by associating noncovalently with the lectin chaperones calnexin and calreticulin [154]. The catalytic properties differ from PDIA1 and the redox potential of PDIA3 is also lower than PDIA1 [155, 156]. PDIA3, like PDIA1, has two CXXC motifs at the conserved active sites and four similar TRX-like domains (a-b-b′-a′) [153, 156]. The C-terminus of PDIA3 has an ER retention signal with a sequence similar to that of PDIA1 [153] and a nuclear localisation signal near the C terminal with a high affinity for importin [128, 157, 158]. In addition, PDIA3 and PDIA1 differ in terms of substrate binding specificity due to differences in homology in their b′ domains. The binding domain of PDIA3 is enriched in lysine and arginine residues, so that PDIA3 binds to proteins containing negatively charged P domains, such as those found in calreticulin [142, 158]. The oxidative and catalytic property of PDIA3 and PDIA1 both rely on a charged glutamic acid and a pair of lysine residues found behind the active CXXC site [120].

Some PDI family members possess more than two CXXC active sites. PDIr, Erp46, and PDIA4, also known as Ca^{2+} binding protein (CaBP2) [159], all have three active sites [121, 160–163], and ERdJ5 contains four active sites [164]. PDIA4 is similar to PDIA1 in its catalytic domains but has lower sequence similarity in the other domains. It can also act as a substitute for PDIA3 in folding specific proteins, but it does not bind to glycoproteins [165]. Other PDI gene family members include DNAJC10, ERP27, ERP29 (ERP28), ERP44, PDIA5, PDIA6, PDILT, and TXNDC5 (for comprehensive review please refer to [125]). However, this review will focus on PDIA1, PDIA2, PDIA3, and PDIA4 as these are the only PDI family members to date that are reported to undergo S-nitrosylation.

7. The Presence of PDI in Non-ER Compartments

Whilst PDI family members are primarily considered to be ER-localized, they are also present in other cellular locations, including the nucleus, cytoplasm, cell surface, and extracellular space [128]. Few proteins linked to neurodegeneration are present in the ER, so it is possible that PDI plays an important role in these locations. In the ER, PDI must be maintained in a balance between its oxidized and reduced states to facilitate disulphide bond formation [166, 167]. However, in non-ER compartments, PDI family members have an increased ability to catalyze the reduction of disulphide bonds compared to the ER [168]. The mechanism of transit of PDI from the ER remains unknown, and because of the presence of the KDEL retention signal, observations of non-ER localized PDI have previously been questioned [128]. However, other primarily ER-localized proteins that possess a KDEL motif, such as calreticulin and binding immunoglobulin protein (BiP), are also secreted and located in the nucleus, cytoplasm and cell surface [169–176].

PDI in the cytosol has been postulated to act as a cofactor with insulin-degrading enzyme (IDE) during insulin metabolism, while acting in concert with reduced GSH to catalyze disulphide bond cleavage [177]. There is also evidence that PDI redistributes away from its ER location into the cytoplasm in pathological conditions. ER stress causes the redistribution of PDIA1 and PDIA3 from the ER to the cytosol [178], consistent with the notion that PDI in locations other than the ER is neuroprotective. Furthermore, one study demonstrated that overexpression of reticulon-4A (NOGO A) triggered the redistribution of PDI from the ER into vesicular-type structures localized in an undefined cellular compartment, both *in vitro* and *in vivo*, which occurred in the absence of the UPR [179]. Deletion of NOGO A, B from ALS mouse models, involving transgenic overexpression of mutant $SOD1^{G93A}$, led to earlier onset and increased disease progression, indicating that reticulons mediate PDI function and redistribution in neurodegeneration [179]. A more recent study, using human neuroblastoma SH-SY5Y cells overexpressing reticulon protein 1C (RTN-1C), demonstrated that redistribution of PDI away from the ER into vesicular structures led to a consequent increase in the enzymatic activity of PDI and a decrease in S-nitrosylation [180].

PDI has also been detected at the cell membrane, where a role in NO signalling has been described. S-nitrosylated extracellular proteins transfer NO to the cytosol via the reducing activity of cell surface PDI [181, 182]. During this process, cell-surface PDI also undergoes thiol modification [183]. Furthermore, PDIA3 interacts with prion proteins (PrP) at the cell surface and may play a key role in PrP accumulation [184]. In addition, PDIA1 and PDIA3 have been detected in the nucleus, where they are posited to anchor DNA loops to the nuclear matrix [128, 185, 186]. PDI-like activity has also been detected in mitochondria, although PDIA1 has not been identified in this compartment [187], and it is possible that Mia 40 contributes to this activity [188, 189].

PDIA1 and PDIA3 have also been detected at mitochondrial-associated ER membranes, where, remarkably, they may regulate apoptosis signalling [190]. The expression of polyglutamine expanded Huntington protein led to PDIA1 and PDIA3 accumulation in this location, where it triggered mitochondrial outer membrane permeabilization through activation of proapoptotic BCL-2 family members, triggering apoptosis [190]. Hence, whilst PDI functions protectively through its chaperone and isomerase activities [191], it can also trigger pro-apoptotic mechanisms [190]. While this process has not yet been fully defined, the novel proapoptotic function of PDI may represent a new link between protein misfolding and cell death.

8. Role of PDI in Neurodegeneration

There is now substantial evidence linking PDI family members to protein misfolding in neurodegeneration. PDIA1 is upregulated in AD brain tissues [192], PDIA3 forms a complex with calreticulin and A-β peptides in patients' CSF [193], and NFTs are immunopositive for PDI [194, 195]. Similarly, in cellular models of PD, treatment of dopaminergic neurons with 6-hydroxydopamine (6-OHDA) induces ER stress, oxidation, and aggregation of PDIA3 [196]. PDIA2 is upregulated in SH-SY5Y human neuroblastoma treated with either 1-methy-4-phenyl-pyridinium (MPP+) or proteasome inhibitor lactacystin while immunoreactivity to PDIA2 has also been detected in LB in postmortem brains of PD patients [146]. Furthermore, the a′ domain of PDIA1 inhibits α-synuclein fibril formation [197], and coexpression of PDIA1 decreased synphilin-1 positive LB formation in the cytoplasm [75]. PDIA1 was upregulated in the brains of Creutzfeldt-Jakob disease (CJD) patients [198], while PDIA1 and PDIA3 were upregulated in prion disease in scrapie infected rodents [199]. Pharmacological inhibition of PDIA3 using bacitracin increased the accumulation of aggregated PrP, also suggesting that PDI is not functional in prion disease [184]. Furthermore, upregulation of PDIA1 and PDIA3 was associated with mitochondrial dysfunction in cells expressing misfolded PrP [199]. The detection of mitochondrial apoptosis triggered by PDIA1 and PDIA3 in HD models [190] also highlights the intrinsic link between PDI upregulation and mitochondrial dysregulation in neurodegeneration [199].

There is also increasing evidence for an important role for PDI in ALS. PDIA1 is upregulated and is a component of TDP-43 and FUS-positive cytoplasmic inclusions in motor neurons of sporadic ALS patients [200, 201]. Additionally, PDIA1 is a risk factor for the development of ALS [202]. PDIA1 also colocalizes with mutant SOD1-positive inclusions in cell culture and transgenic SOD1 rodents [89, 203, 204]. Overexpression of PDIA1 decreases the formation of mutant SOD1 inclusions whereas knockdown of PDI using siRNA increases the proportion of inclusions [89]. Furthermore, a synthetic mimic of the PDIA1 active site; (±)-trans-1,2-bis (mercaptoacetamido)cyclohexane (BMC), is protective against mutant SOD1 aggregation in cell culture [89]. SOD1 contains four cysteine residues, and non-native disulphide bonds between Cys6 and Cys111 have been implicated in mutant SOD1 aggregation [205]. Conversely, upregulation of PDIA1 in microglia in $SOD1^{G93A}$ mice was associated with increased levels of NADPH oxidase (NOX), superoxide, and tumour necrosis factor-α. Pharmacological inhibition and knockdown of PDIA1 using siRNA decreased superoxide and NOX activation in microglia, therefore providing further evidence for a potential neurotoxic role of PDIA1 [206].

PDI is therefore upregulated during UPR activation and is part of a cellular protective mechanism that prevents protein misfolding and aggregation in neurodegeneration. PDI family members are especially vulnerable to oxidative and nitrosative-linked posttranslational modifications due to the highly oxidizing environment of the ER and the presence of cysteine residues in the PDI catalytic regions. Irreversible S-nitrosylation of PDI (SNO-PDI) may therefore ameliorate its protective function in neurodegenerative disorders and thus contribute to disease.

9. SNO-PDI and Neurodegeneration

PDI is S-nitrosylated by endogenous nNOS in both its TRX domains leading to a significant reduction in isomerase and chaperone activity [75]. Also, induction of SNO-PDI using NO donor S-nitrosocysteine (SNOC) completely abrogates the catalytic activity of PDI, resulting in neuronal cell death [207].

SNO-PDI has been detected in postmortem brain tissue of sporadic PD and AD patients [75] and lumbar spinal cord tissues of ALS patients and $SOD1^{G93A}$ mice [89]. This was linked to excessive production of NO or exposure to exogenous agents such as rotenone [75]. PDI was shown to be modified in the cysteine thiol groups in the C-terminal CXXC motif, leading to the accumulation of polyubiquitinated proteins and activation of the UPR [75]. SNO-PDI formation is associated with synphilin misfolding in PD [31] and mitochondrial mediated apoptosis in prion infection [199]. SNO-PDI is also found in cultured astrocytes after ischemia/reperfusion-induced iNOS production, leading to increases in ubiquitinated aggregates that colocalize with SOD1 [7].

One potential physiological mechanism of SNO-PDI production involves pathological hyperactivation of NMDAr [31] and inhibition of mitochondria leading to the generation of ROS, nNOS, and NO [31, 70, 71]. Exposure of cortical neurons to NMDA produces SNO-PDI, leading to an increase in polyubiquitinated proteins and apoptosis after 24 hrs of treatment. Furthermore, overexpression of WT PDI leads to a decrease in polyubiquitination and apoptosis, suggesting that PDI may provide protection against excitotoxicity from excessive stimulation of NMDA receptors [75]. Additionally, treatment with Rotenone, a mitochondrial complex inhibitor, produces elevated levels of SNO-PDI [75], suggesting that mitochondria are another source of NO or cytosolic nNOS [31]. NO disrupts Ca^{2+} homeostasis, potentially via S-nitrosylation of the ER Ca^{2+} channel ryanodine receptor, and induction of ER stress [57, 208]. ER-resident proteins are particularly vulnerable to S-nitrosylation and as such a positive feedback mechanism would create a scenario whereby excessive RNS/ROS increasingly deactivates protective ER-resident chaperones such as PDI, prolonging UPR activation, leading to increases in ROS/RNS generation eventually resulting in cell death [31]. ER dysfunction due to excessive oxidative/nitrosative stress may, thus, lead to the S-nitrosylation of PDI in neurodegenerative disease [31]. However, PDI family members PDIA1, PDIA3, and PDIA4 can be S-nitrosylated independently of UPR induction [209]. Alternatively, PDI located at the cell surface may also promote production of SNO proteins. It has been previously suggested that extracellular SNO proteins may transfer NO to the cytoplasm via the reducing activity of cell surface PDI [181, 182]. According to this theory, reduced NO may readily penetrate the plasma membrane, leading to SNO production [128] (Figure 2). Hence, the formation of SNO-PDI results in the abrogation of the normally protective isomerase/chaperone

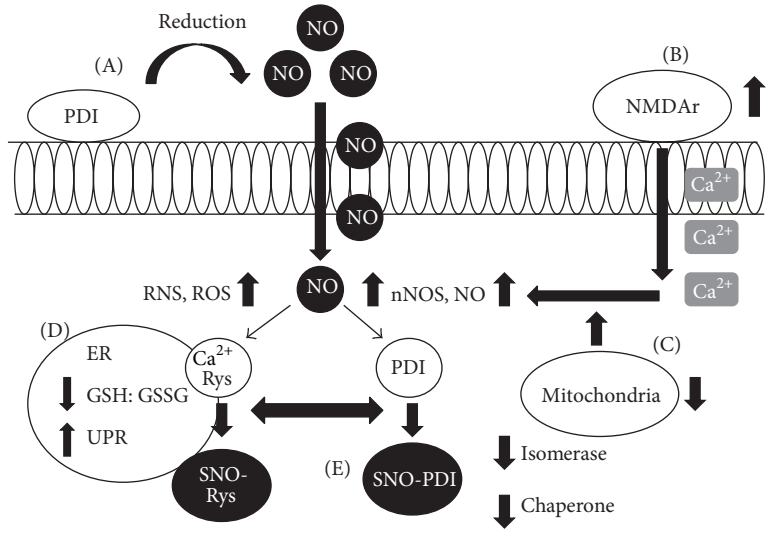

Figure 2: Cell surface PDI, NO, and SNO-PDI. (A) Cell surface PDI reduces NO from extracellular SNO proteins (SNO-P) and in the process undergoes thiol modification. (B) Hyperactivation of the NMDAr leads to an intracellular influx of Ca^{2+} ions (NMDAr may also undergo reversible S-nitrosylation to ameliorate excessive activity). (C) Inhibition of mitochondria contributes to an increase in intracellular NO which is potentially oxidized by O_2 leading to an increase in NO, nNOS, ROS, and RNS. (D) Increases in RNS/ROS alters the ER redox environment, and NO S-nitrosylates Ca^{2+} ryanodine (Ryn) receptor leading to a disruption in Ca^{2+} homeostasis. (E) ER-resident proteins such as PDI are vulnerable to S-nitrosylation, deactivating its isomerase and chaperone activity, leading to accumulation of misfolded proteins, ER stress, and UPR induction.

activity of PDI, which may contribute to protein misfolding and production of SNO proteins. This suggests that SNO-PDI may be a common pathological mechanism contributing to neurodegenerative diseases.

10. S-Glutathionylation and PDI

A link between S-glutathionylated PDI and neurodegenerative disease has not yet been established [210]. However, cysteine residues in the a and a′ domains of PDI make it a potential target for S-glutathionylation [211].

PDI has been shown to be S-glutathionylated at two of its four active cysteine sites (Cys53, Cys56 or Cys397, Cys400) [92]. S-glutathionylation was induced in these cells by treatment with anticancer agent O_2–[2,4-dinitro-5-(*N*-methyl-*N*-4-carboxyphenylamino) phenyl]1–(*N*,*N* dimethylamino)diazen-1-ium-1,2-diolate (PABA/NO), which led to a dose-dependent increase in intracellular NO [210], triggering UPR induction and cell death [92]. S-glutathionylation of PDI has been demonstrated in human leukemia (HL60) and ovarian cancer cells (SKOV3) inhibiting its isomerase function [205]. In addition, S-glutathionylation of PDI abrogates its chaperone activity and prevents binding to oestrogen receptor alpha (ERα) [212]. The PDI-ERα interaction may protect ERα from oxidation and ensure its native protein conformation [213]. However, aberrant S-glutathionylation of PDI leads to destabilisation of the receptor and dysregulatation of ERα signaling. This may subsequently mediate cell death via activation of the UPR and reduced ERα stability [212]. However, although PABA/NO treatment increased levels of intracellular NO, it did not lead to S-nitrosylation of PDI [210]. There are two pools of S-nitrosylated proteins, GSH stable and GSH labile proteins, with the latter pool being readily subject to conversion to S-glutathionylated products [41]. Therefore, the lack of SNO proteins after PABA/NO treatment may be due to conversion of SNO proteins to S-glutathionylated proteins [210] (Figure 3). This notion therefore provides a link between S-nitrosylation and S-glutathionylation, although the exact relationship between these modifications remains unknown [41].

S-glutathionylation of PDI was proposed to be an upstream signalling event triggering misfolded protein accumulation and UPR induction [210, 211]. As PDI may regulate redox potential at the cell surface [182, 214], it therefore may facilitate cell adhesion [215], antigen processing [216], and glioma cell invasion [217]. S-glutathionylation of cell surface proteins alters extracellular and intracellular redox homeostasis [210]. Hence, irreversible S-glutathionylation/S-nitrosylation of cell surface PDI could alter redox potential, leading to amelioration of the protective chaperone/isomerase functions of PDI. This mechanism may therefore contribute to the excessive production of SNO and S-glutathionylated proteins observed in neurodegenerative disease.

11. Conclusion

PDIs are a large family of chaperones and foldases which have complex yet still inadequately described functions with emerging roles in neurodegenerative diseases. Whilst S-nitrosylation plays a normal physiological role in signalling pathways, aberrant modification is triggered during

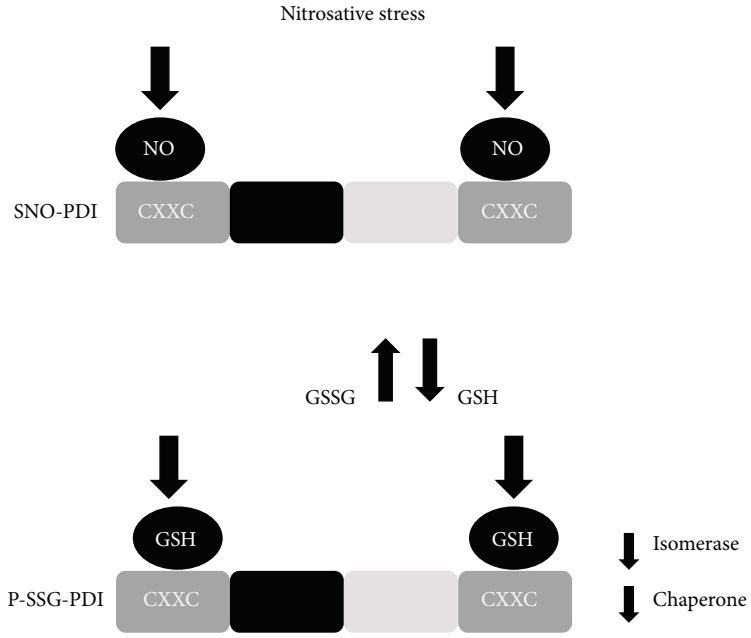

Figure 3: S-glutathionylation of PDI. Nitrosative stress from an exogenous agent (PABA/NO) increases intracellular NO and leads to the production of SNO-PDI. However, this may result in a decrease in GSSG/GSH ratio and increases in the free cellular pool of GSH. GSH then binds to the catalytic (a, a′) domains of PDI, resulting in S-glutathionylation (P-SSG) of its cysteine residues and attenuation of its protective isomerase and chaperone activity.

conditions of elevated nitrosative and oxidative stress. Accumulating evidence suggests that SNO-PDI plays a role in the pathogenesis of neurodegenerative diseases such as AD, PD, and ALS, and this may exacerbate neurodegeneration via a number of mechanisms. However, most of the available reports are correlative in nature and therefore more direct approaches examining the contribution of S-nitrosylation of PDI family members to neurodegeneration are warranted. S-nitrosylation is also linked to another previously described modification of PDI, S-glutathionylation, although the S-glutathionylation of PDI and its role in neurodegenerative diseases have not been elucidated. Whilst PDI family members are conventionally regarded as being ER localized, they are also present and catalytically active in several other cellular locations, which is likely to be particularly important in disease as few proteins associated with neurodegeneration are found in the ER. Finally, cell surface PDI, which reduces NO allowing it to pass through the plasma membrane, may lead to the production of SNO proteins and therefore also contribute to the pathogenesis of neurodegenerative diseases. The broad involvement of PDIs in human neurodegenerative diseases highlights the need for a better understanding of how they become inactivated by posttranslational modification, which is crucial to evaluate their use as possible targets for disease intervention.

References

[1] M. Takalo, A. Salminen, H. Soininen, M. Hiltunen, and A. Haapasalo, "Protein aggregation and degradation mechanisms in neurodegenerative diseases," *American Journal of Neurodegenerative Disease*, vol. 2, no. 1, pp. 1–14, 2013.

[2] C. Soto, "Unfolding the role of protein misfolding in neurodegenerative diseases," *Nature Reviews Neuroscience*, vol. 4, no. 1, pp. 49–60, 2003.

[3] G. G. Glenner and C. W. Wong, "Alzheimer's disease: initial report of the purification and characterization of a novel cerebrovascular amyloid protein. 1984," *Biochemical and Biophysical Research Communications*, vol. 425, no. 3, pp. 534–539, 2012.

[4] I. Grundke-Iqbal, K. Iqbal, Y. C. Tung, M. Quinlan, H. M. Wisniewski, and L. I. Binder, "Abnormal phosphorylation of the microtubule-associated protein τ (tau) in Alzheimer cytoskeletal pathology," *Proceedings of the National Academy of Sciences of the United States of America*, vol. 83, no. 13, pp. 44913–4917, 1986.

[5] M. G. Spillantini, M. L. Schmidt, V. M.-Y. Lee, J. Q. Trojanowski, R. Jakes, and M. Goedert, "α-synuclein in Lewy bodies," *Nature*, vol. 388, no. 6645, pp. 839–840, 1997.

[6] M. DiFiglia, E. Sapp, K. O. Chase et al., "Aggregation of huntingtin in neuronal intranuclear inclusions and dystrophic neurites in brain," *Science*, vol. 277, no. 5334, pp. 1990–1993, 1997.

[7] X. Chen, T. Guan, C. Li et al., "SOD1 aggregation in astrocytes following ischemia/reperfusion injury: a role of NO-mediated S-nitrosylation of protein disulfide isomerase (PDI)," *Journal of Neuroinflammation*, vol. 9, article 237, 2012.

[8] V. K. Mulligan, A. Kerman, R. C. Laister, P. R. Sharda, P. E. Arslan, and A. Chakrabartty, "Early steps in oxidation-induced SOD1 misfolding: implications for non-amyloid protein aggregation in familial ALS," *Journal of Molecular Biology*, vol. 421, no. 4-5, pp. 631–652, 2012.

[9] Y. Sheng, M. Chattopadhyay, J. Whitelegge, and J. S. Valentine, "SOD1 aggregation and ALS: role of metallation states and disulfide status," *Current Topics in Medicinal Chemistry*, vol. 12, no. 22, pp. 2560–2572, 2012.

[10] T. Arai, M. Hasegawa, H. Akiyama et al., "TDP-43 is a component of ubiquitin-positive tau-negative inclusions in frontotemporal lobar degeneration and amyotrophic lateral sclerosis," *Biochemical and Biophysical Research Communications*, vol. 351, no. 3, pp. 602–611, 2006.

[11] N. J. Cairns, M. Neumann, E. H. Bigio et al., "TDP-43 in familial and sporadic frontotemporal lobar degeneration with ubiquitin inclusions," *American Journal of Pathology*, vol. 171, no. 1, pp. 227–240, 2007.

[12] I. R. A. Mackenzie, E. H. Bigio, P. G. Ince et al., "Pathological TDP-43 distinguishes sporadic amyotrophic lateral sclerosis from amyotrophic lateral sclerosis with SOD1 mutations," *Annals of Neurology*, vol. 61, no. 5, pp. 427–434, 2007.

[13] M. Neumann, D. M. Sampathu, L. K. Kwong et al., "Ubiquitinated TDP-43 in frontotemporal lobar degeneration and amyotrophic lateral sclerosis," *Science*, vol. 314, no. 5796, pp. 130–133, 2006.

[14] H.-X. Deng, H. Zhai, E. H. Bigio et al., "FUS-immunoreactive inclusions are a common feature in sporadic and non-SOD1 familial amyotrophic lateral sclerosis," *Annals of Neurology*, vol. 67, no. 6, pp. 739–748, 2010.

[15] M. DeJesus-Hernandez, I. R. Mackenzie, B. F. Boeve et al., "Expanded GGGGCC hexanucleotide repeat in noncoding region of C9ORF72 causes chromosome 9p-linked FTD and ALS," *Neuron*, vol. 72, no. 2, pp. 245–256, 2011.

[16] A. E. Renton, E. Majounie, A. Waite et al., "A hexanucleotide repeat expansion in C9ORF72 is the cause of chromosome 9p21-linked ALS-FTD," *Neuron*, vol. 72, no. 2, pp. 257–268, 2011.

[17] S. Musardo, C. Saraceno, S. Pelucchi, and E. Marcello, "Trafficking in neurons: searching for new targets for Alzheimer's disease future therapies," *European Journal of Pharmacology*, 2013.

[18] A. Goate, M.-C. Chartier-Harlin, M. Mullan et al., "Segregation of a missense mutation in the amyloid precursor protein gene with familial Alzheimer's disease," *Nature*, vol. 349, no. 6311, pp. 704–706, 1991.

[19] J. Murrell, M. Farlow, B. Ghetti, and M. D. Benson, "A mutation in the amyloid precursor protein associated with hereditary Alzheimer's disease," *Science*, vol. 254, no. 5028, pp. 97–99, 1991.

[20] M.-C. Chartier-Harlin, F. Crawford, H. Houlden et al., "Early-onset Alzheimer's disease caused by mutations at codon 717 of the β-amyloid precursor protein gene," *Nature*, vol. 353, no. 6347, pp. 844–846, 1991.

[21] B. de Strooper, R. Vassar, and T. Golde, "The secretases: enzymes with therapeutic potential in Alzheimer disease," *Nature Reviews Neurology*, vol. 6, no. 2, pp. 99–107, 2010.

[22] D. J. Selkoe, "Alzheimer's disease: genes, proteins, and therapy," *Physiological Reviews*, vol. 81, no. 2, pp. 741–766, 2001.

[23] L. Wahlster, M. Arimon, N. Nasser-Ghodsi et al., "Presenilin-1 adopts pathogenic conformation in normal aging and in sporadic Alzheimer's disease," *Acta Neuropathologica*, vol. 125, no. 2, pp. 187–199, 2013.

[24] C. Cruchaga, S. Chakraverty, K. Mayo et al., "Rare variants in APP, PSEN1 and PSEN2 increase risk for AD in late-onset Alzheimer's disease families," *PLoS ONE*, vol. 7, no. 2, Article ID e31039, 2012.

[25] M. H. Polymeropoulos, C. Lavedan, E. Leroy et al., "Mutation in the α-synuclein gene identified in families with Parkinson's disease," *Science*, vol. 276, no. 5321, pp. 2045–2047, 1997.

[26] K. Arima, K. Uéda, N. Sunohara et al., "Immunoelectron-microscopic demonstration of NACP/α-synuclein-epitopes on the filamentous component of Lewy bodies in Parkinson's disease and in dementia with Lewy bodies," *Brain Research*, vol. 808, no. 1, pp. 93–100, 1998.

[27] V. Bonifati, "Autosomal recessive parkinsonism," *Parkinsonism and Related Disorders*, vol. 18, supplement 1, pp. S4–S6, 2012.

[28] I. Dalle-Donne, R. Rossi, R. Colombo, D. Giustarini, and A. Milzani, "Biomarkers of oxidative damage in human disease," *Clinical Chemistry*, vol. 52, no. 4, pp. 601–623, 2006.

[29] F. Mangialasche, M. C. Polidori, R. Monastero et al., "Biomarkers of oxidative and nitrosative damage in Alzheimer's disease and mild cognitive impairment," *Ageing Research Reviews*, vol. 8, no. 4, pp. 285–305, 2009.

[30] A. H. V. Schapira, J. M. Cooper, D. Dexter, J. B. Clark, P. Jenner, and C. D. Marsden, "Mitochondrial complex I deficiency in Parkinson's disease," *Journal of Neurochemistry*, vol. 54, no. 3, pp. 823–827, 1990.

[31] M. Benhar, M. T. Forrester, and J. S. Stamler, "Nitrosative stress in the ER: a new role for S-nitrosylation in neurodegenerative diseases," *ACS Chemical Biology*, vol. 1, no. 6, pp. 355–358, 2006.

[32] C. Appenzeller-Herzog and L. Ellgaard, "The human PDI family: versatility packed into a single fold," *Biochimica et Biophysica Acta*, vol. 1783, no. 4, pp. 535–548, 2008.

[33] P. Gillece, J. M. Luz, W. J. Lennarz, F. J. de la Cruz, and K. Römisch, "Export of a cysteine-free misfolded secretory protein from the endoplasmic reticulum for degradation requires interaction with protein disulfide isomerase," *Journal of Cell Biology*, vol. 147, no. 7, pp. 1443–1456, 1999.

[34] M. Molinari, C. Galli, V. Piccaluga, M. Pieren, and P. Paganetti, "Sequential assistance of molecular chaperones and transient formation of covalent complexes during protein degradation from the ER," *Journal of Cell Biology*, vol. 158, no. 2, pp. 247–257, 2002.

[35] B. Tsai, C. Rodighiero, W. I. Lencer, and T. A. Rapoport, "Protein disulfide isomerase acts as a redox-dependent chaperone to unfold cholera toxin," *Cell*, vol. 104, no. 6, pp. 937–948, 2001.

[36] T. Nakamura, S. Tu, M. W. Akhtar, C. R. Sunico, S. Okamoto, and S. A. Lipton, "Aberrant protein S-nitrosylation in neurodegenerative diseases," *Neuron*, vol. 78, no. 4, pp. 596–614, 2013.

[37] B. Chakravarti and D. N. Chakravarti, "Oxidative modification of proteins: age-related changes," *Gerontology*, vol. 53, no. 3, pp. 128–139, 2007.

[38] E. Mariani, M. C. Polidori, A. Cherubini, and P. Mecocci, "Oxidative stress in brain aging, neurodegenerative and vascular diseases: an overview," *Journal of Chromatography B*, vol. 827, no. 1, pp. 65–75, 2005.

[39] T. Finkel, "Signal transduction by reactive oxygen species," *Journal of Cell Biology*, vol. 194, no. 1, pp. 7–15, 2011.

[40] R. G. Cutler, W. A. Pedersen, S. Camandola, J. D. Rothstein, and M. P. Mattson, "Evidence that accumulation of ceramides and cholesterol esters mediates oxidative stress—induced death of motor neurons in amyotrophic lateral sclerosis," *Annals of Neurology*, vol. 52, no. 4, pp. 448–457, 2002.

[41] Y. Xiong, J. D. Uys, K. D. Tew, and D. M. Townsend, "S-glutathionylation: from molecular mechanisms to health outcomes," *Antioxidants and Redox Signaling*, vol. 15, no. 1, pp. 233–270, 2011.

[42] D. P. Jones, "Redefining oxidative stress," *Antioxidants and Redox Signaling*, vol. 8, no. 9-10, pp. 1865–1879, 2006.

[43] V. Calabrese, D. Boyd-Kimball, G. Scapagnini, and D. A. Butterfield, "Nitric oxide and cellular stress response in brain aging and neurodegenerative disorders: the role of vitagenes," *In Vivo*, vol. 18, no. 3, pp. 245–268, 2004.

[44] N. P. Kedar, "Can we prevent Parkinson's and Alzheimer's disease?" *Journal of Postgraduate Medicine*, vol. 49, no. 3, pp. 236–245, 2003.

[45] B. Chance, H. Sies, and A. Boveris, "Hydroperoxide metabolism in mammalian organs," *Physiological Reviews*, vol. 59, no. 3, pp. 527–605, 1979.

[46] J. Garthwaite and C. L. Boulton, "Nitric oxide signaling in the central nervous system," *Annual Review of Physiology*, vol. 57, pp. 683–706, 1995.

[47] D. S. Bredt, P. M. Hwang, C. E. Glatt, C. Lowenstein, R. R. Reed, and S. H. Snyder, "Cloned and expressed nitric oxide synthase structurally resembles cytochrome P-450 reductase," *Nature*, vol. 351, no. 6329, pp. 714–718, 1991.

[48] J. Bustamante, A. Czerniczyniec, and S. Lores-Arnaiz, "Brain nitric oxide synthases and mitochondrial function," *Frontiers in Bioscience*, vol. 12, no. 3, pp. 1034–1040, 2007.

[49] S. L. Elfering, T. M. Sarkela, and C. Giulivi, "Biochemistry of mitochondrial nitric-oxide synthase," *The Journal of Biological Chemistry*, vol. 277, no. 41, pp. 38079–38086, 2002.

[50] U. Forstermann, H. H. H. W. Schmidt, J. S. Pollock et al., "Isoforms of nitric oxide synthase. Characterization and purification from different cell types," *Biochemical Pharmacology*, vol. 42, no. 10, pp. 1849–1857, 1991.

[51] M.-C. Broillet, "S-nitrosylation of proteins," *Cellular and Molecular Life Sciences*, vol. 55, no. 8-9, pp. 1036–1042, 1999.

[52] S. Z. Lei, Z.-H. Pan, S. K. Aggarwal et al., "Effect of nitric oxide production on the redox modulatory site of the NMDA receptor-channel complex," *Neuron*, vol. 8, no. 6, pp. 1087–1099, 1992.

[53] S. A. Lipton, Y.-B. Choi, Z.-H. Pan et al., "A redox-based mechanism for the neuroprotective and neurodestructive effects of nitric oxide and related nitroso-compounds," *Nature*, vol. 364, no. 6438, pp. 626–632, 1993.

[54] N. Shahani and A. Sawa, "Protein S-nitrosylation: role for nitric oxide signaling in neuronal death," *Biochimica et Biophysica Acta*, vol. 1820, no. 6, pp. 736–742, 2012.

[55] J. S. Stamler, D. I. Simon, J. A. Osborne et al., "S-nitrosylation of proteins with nitric oxide: synthesis and characterization of biologically active compounds," *Proceedings of the National Academy of Sciences of the United States of America*, vol. 89, no. 1, pp. 444–448, 1992.

[56] J. S. Stamler, S. Lamas, and F. C. Fang, "Nitrosylation: the prototypic redox-based signaling mechanism," *Cell*, vol. 106, no. 6, pp. 675–683, 2001.

[57] T. Nakamura and S. A. Lipton, "S-nitrosylation of critical protein thiols mediates protein misfolding and mitochondrial dysfunction in neurodegenerative diseases," *Antioxidants and Redox Signaling*, vol. 14, no. 8, pp. 1479–1492, 2011.

[58] C. A. Staab, M. Hellgren, and J.-O. Höög, "Medium- and short-chain dehydrogenase/reductase gene and protein families: dual functions of alcohol dehydrogenase 3: implications with focus on formaldehyde dehydrogenase and S-nitrosoglutathione reductase activities," *Cellular and Molecular Life Sciences*, vol. 65, no. 24, pp. 3950–3960, 2008.

[59] L. Liu, A. Hausladen, M. Zeng, L. Que, J. Heitman, and J. S. Stamler, "A metabolic enzyme for S-nitrosothiol conserved from bacteria to humans," *Nature*, vol. 410, no. 6827, pp. 490–494, 2001.

[60] A. Holmgren, "Thioredoxin," *Annual Review of Biochemistry*, vol. 54, pp. 237–271, 1985.

[61] A. Holmgren, "Thioredoxin and glutaredoxin systems," *The Journal of Biological Chemistry*, vol. 264, no. 24, pp. 13963–13966, 1989.

[62] D. Nikitovic and A. Holmgren, "S-nitrosoglutathione is cleaved by the thioredoxin system with liberation of glutathione and redox regulating nitric oxide," *The Journal of Biological Chemistry*, vol. 271, no. 32, pp. 19180–19185, 1996.

[63] M. Benhar, M. T. Forrester, and J. S. Stamler, "Protein denitrosylation: enzymatic mechanisms and cellular functions," *Nature Reviews Molecular Cell Biology*, vol. 10, no. 10, pp. 721–732, 2009.

[64] I. Sliskovic, A. Raturi, and B. Mutus, "Characterization of the S-denitrosation activity of protein disulfide isomerase," *The Journal of Biological Chemistry*, vol. 280, no. 10, pp. 8733–8741, 2005.

[65] D. Jourd'heuil, F. S. Laroux, A. M. Miles, D. A. Wink, and M. B. Grisham, "Effect of superoxide dismutase on the stability of S-nitrosothiols," *Archives of Biochemistry and Biophysics*, vol. 361, no. 2, pp. 323–330, 1999.

[66] R. J. Singh, N. Hogg, J. Joseph, and B. Kalyanaraman, "Mechanism of nitric oxide release from S-nitrosothiols," *The Journal of Biological Chemistry*, vol. 271, no. 31, pp. 18596–18603, 1996.

[67] D. T. Hess, A. Matsumoto, S.-O. Kim, H. E. Marshall, and J. S. Stamler, "Protein S-nitrosylation: purview and parameters," *Nature Reviews Molecular Cell Biology*, vol. 6, no. 2, pp. 150–166, 2005.

[68] G. E. Hardingham and H. Bading, "Synaptic versus extrasynaptic NMDA receptor signalling: implications for neurodegenerative disorders," *Nature Reviews Neuroscience*, vol. 11, no. 10, pp. 682–696, 2010.

[69] L. V. Kalia, S. K. Kalia, and M. W. Salter, "NMDA receptors in clinical neurology: excitatory times ahead," *The Lancet Neurology*, vol. 7, no. 8, pp. 742–755, 2008.

[70] V. L. Dawson, T. M. Dawson, E. D. London, D. S. Bredt, and S. H. Snyder, "Nitric oxide mediates glutamate neurotoxicity in primary cortical cultures," *Proceedings of the National Academy of Sciences of the United States of America*, vol. 88, no. 14, pp. 6368–6371, 1991.

[71] V. L. Dawson and T. M. Dawson, "Nitric oxide neurotoxicity," *Journal of Chemical Neuroanatomy*, vol. 10, no. 3-4, pp. 179–190, 1996.

[72] C. Supnet and I. Bezprozvanny, "The dysregulation of intracellular calcium in Alzheimer disease," *Cell Calcium*, vol. 47, no. 2, pp. 183–189, 2010.

[73] Z. Gu, M. Kaul, B. Yan et al., "S-nitrosylation of matrix metalloproteinases: signaling pathway to neuronal cell death," *Science*, vol. 297, no. 5584, pp. 1186–1190, 2002.

[74] J. S. Stamler and A. Hausladen, "Oxidative modifications in nitrosative stress," *Nature Structural Biology*, vol. 5, no. 4, pp. 247–249, 1998.

[75] T. Uehara, T. Nakamura, D. Yao et al., "S-Nitrosylated protein-disulphide isomerase links protein misfolding to neurodegeneration," *Nature*, vol. 441, no. 7092, pp. 513–517, 2006.

[76] S. Papadia, F. X. Soriano, F. Léveillé et al., "Synaptic NMDA receptor activity boosts intrinsic antioxidant defenses," *Nature Neuroscience*, vol. 11, no. 4, pp. 476–487, 2008.

[77] D.-H. Cho, T. Nakamura, J. Fang et al., "β-amyloid-related mitochondrial fission and neuronal injury," *Science*, vol. 324, no. 5923, pp. 102–105, 2009.

[78] S. A. Lipton, Y.-B. Choi, H. Takahashi et al., "Cysteine regulation of protein function—as exemplified by NMDA-receptor modulation," *Trends in Neurosciences*, vol. 25, no. 9, pp. 474–480, 2002.

[79] J. S. Stamler, E. J. Toone, S. A. Lipton, and N. J. Sucher, "(S)NO signals: translocation, regulation, and a consensus motif," *Neuron*, vol. 18, no. 5, pp. 691–696, 1997.

[80] M. A. Johnson, T. L. Macdonald, J. B. Mannick, M. R. Conaway, and B. Gaston, "Accelerated S-nitrosothiol breakdown by amyotrophic lateral sclerosis mutant copper, zinc-superoxide dismutase," *The Journal of Biological Chemistry*, vol. 276, no. 43, pp. 39872–39878, 2001.

[81] C. M. Schonhoff, M. Matsuoka, H. Tummala et al., "S-nitrosothiol depletion in amyotrophic lateral sclerosis," *Proceedings of the National Academy of Sciences of the United States of America*, vol. 103, no. 7, pp. 2404–2409, 2006.

[82] S. M. Marino and V. N. Gladyshev, "Structural analysis of cysteine S-nitrosylation: a modified Aacid-based motif and the emerging role of trans-nitrosylation," *Journal of Molecular Biology*, vol. 395, no. 4, pp. 844–859, 2010.

[83] M. D. Bartberger, J. D. Mannion, S. C. Powell, J. S. Stamler, K. N. Houk, and E. J. Toone, "S-N dissociation energies of S-nitrosothiols: on the origins of nitrosothiol decomposition rates," *Journal of the American Chemical Society*, vol. 123, no. 36, pp. 8868–8869, 2001.

[84] J. S. Stamler and E. J. Toone, "The decomposition of thionitrites," *Current Opinion in Chemical Biology*, vol. 6, no. 6, pp. 779–785, 2002.

[85] D. Seth and J. S. Stamler, "The SNO-proteome: causation and classifications," *Current Opinion in Chemical Biology*, vol. 15, no. 1, pp. 129–136, 2011.

[86] K. K. K. Chung, T. M. Dawson, and V. L. Dawson, "Nitric oxide, S-nitrosylation and neurodegeneration," *Cellular and Molecular Biology*, vol. 51, no. 3, pp. 247–254, 2005.

[87] T. Nakamura, P. Cieplak, D.-H. Cho, A. Godzik, and S. A. Lipton, "S-Nitrosylation of Drp1 links excessive mitochondrial fission to neuronal injury in neurodegeneration," *Mitochondrion*, vol. 10, no. 5, pp. 573–578, 2010.

[88] A. H. K. Tsang, Y.-I. L. Lee, H. S. Ko et al., "S-nitrosylation of XIAP compromises neuronal survival in Parkinson's disease," *Proceedings of the National Academy of Sciences of the United States of America*, vol. 106, no. 12, pp. 4900–4905, 2009.

[89] A. K. Walker, M. A. Farg, C. R. Bye, C. A. McLean, M. K. Horne, and J. D. Atkin, "Protein disulphide isomerase protects against protein aggregation and is S-nitrosylated in amyotrophic lateral sclerosis," *Brain*, vol. 133, no. 1, pp. 105–116, 2010.

[90] D. Yao, Z. Gu, T. Nakamura et al., "Nitrosative stress linked to sporadic Parkinson's disease: S-nitrosylation of parkin regulates its E3 ubiquitin ligase activity," *Proceedings of the National Academy of Sciences of the United States of America*, vol. 101, no. 29, pp. 10810–10814, 2004.

[91] Y.-B. Choi, L. Tenneti, D. A. Le et al., "Molecular basis of NMDA receptor-coupled ion channel modulation by S-nitrosylation," *Nature Neuroscience*, vol. 3, no. 1, pp. 15–21, 2000.

[92] D. M. Townsend, "S-glutathionylation: indicator of cell stress and regulator of the unfolded protein response," *Molecular Interventions*, vol. 7, no. 6, pp. 313–324, 2008.

[93] R. E. Hansen, D. Roth, and J. R. Winther, "Quantifying the global cellular thiol-disulfide status," *Proceedings of the National Academy of Sciences of the United States of America*, vol. 106, no. 2, pp. 422–427, 2009.

[94] C. Jacob, I. Knight, and P. G. Winyard, "Aspects of the biological redox chemistry of cysteine: from simple redox responses to sophisticated signalling pathways," *Biological Chemistry*, vol. 387, no. 10-11, pp. 1385–1397, 2006.

[95] E. A. Sabens Liedhegner, X.-H. Gao, and J. J. Mieyal, "Mechanisms of altered redox regulation in neurodegenerative diseases-focus on S-glutathionylation," *Antioxidants and Redox Signaling*, vol. 16, no. 6, pp. 543–566, 2012.

[96] D. M. Ziegler, "Role of reversible oxidation-reduction of enzyme thiols-disulfides in metabolic regulation," *Annual Review of Biochemistry*, vol. 54, pp. 305–329, 1985.

[97] M. M. Gallogly and J. J. Mieyal, "Mechanisms of reversible protein glutathionylation in redox signaling and oxidative stress," *Current Opinion in Pharmacology*, vol. 7, no. 4, pp. 381–391, 2007.

[98] J. J. Mieyal, M. M. Gallogly, S. Qanungo, E. A. Sabens, and M. D. Shelton, "Molecular mechanisms and clinical implications of reversible protein S-glutathionylation," *Antioxidants and Redox Signaling*, vol. 10, no. 11, pp. 1941–1988, 2008.

[99] A. A. Brasil, A. Belati, S. C. Mannarino, A. D. Panek, E. C. A. Eleutherio, and M. D. Pereira, "The involvement of GSH in the activation of human Sod1 linked to FALS in chronologically aged yeast cells," *FEMS Yeast Research*, vol. 13, no. 5, pp. 433–440, 2013.

[100] B. Carletti, C. Passarelli, M. Sparaco et al., "Effect of protein glutathionylation on neuronal cytoskeleton: a potential link to neurodegeneration," *Neuroscience*, vol. 192, pp. 285–294, 2011.

[101] F. di Domenico, G. Cenini, R. Sultana et al., "Glutathionylation of the pro-apoptotic protein p53 in alzheimer's disease brain: implications for AD pathogenesis," *Neurochemical Research*, vol. 34, no. 4, pp. 727–733, 2009.

[102] Y. Zhu, P. M. Carvey, and Z. Ling, "Age-related changes in glutathione and glutathione-related enzymes in rat brain," *Brain Research*, vol. 1090, no. 1, pp. 35–44, 2006.

[103] J. Sian, D. T. Dexter, A. J. Lees et al., "Alterations in glutathione levels in Parkinson's disease and other neurodegenerative disorders affecting basal ganglia," *Annals of Neurology*, vol. 36, no. 3, pp. 348–355, 1994.

[104] Y. S. Choo, Z. Mao, G. V. Johnson, and M. Lesort, "Increased glutathione levels in cortical and striatal mitochondria of the R6/2 Huntington's disease mouse model," *Neuroscience Letters*, vol. 386, no. 1, pp. 63–68, 2005.

[105] J. H. Fox, D. S. Barber, B. Singh et al., "Cystamine increases L-cysteine levels in Huntington's disease transgenic mouse brain and in a PC12 model of polyglutamine aggregation," *Journal of Neurochemistry*, vol. 91, no. 2, pp. 413–422, 2004.

[106] K. C. Wilcox, L. Zhou, J. K. Jordon et al., "Modifications of superoxide dismutase (SOD1) in human erythrocytes: a possible role in amyotrophic lateral sclerosis," *The Journal of Biological Chemistry*, vol. 284, no. 20, pp. 13940–13947, 2009.

[107] C. Hwang, A. J. Sinskey, and H. F. Lodish, "Oxidized redox state of glutathione in the endoplasmic reticulum," *Science*, vol. 257, no. 5076, pp. 1496–1502, 1992.

[108] J. D. Atkin, M. A. Farg, A. K. Walker, C. McLean, D. Tomas, and M. K. Horne, "Endoplasmic reticulum stress and induction of the unfolded protein response in human sporadic amyotrophic lateral sclerosis," *Neurobiology of Disease*, vol. 30, no. 3, pp. 400–407, 2008.

[109] E. Colla, P. Coune, Y. Liu et al., "Endoplasmic reticulum stress is important for the manifestations of α-synucleinopathy in vivo," *Journal of Neuroscience*, vol. 32, no. 10, pp. 3306–3320, 2012.

[110] K. M. Doyle, D. Kennedy, A. M. Gorman, S. Gupta, S. J. M. Healy, and A. Samali, "Unfolded proteins and endoplasmic reticulum stress in neurodegenerative disorders," *Journal of Cellular and Molecular Medicine*, vol. 15, no. 10, pp. 2025–2039, 2011.

[111] H. A. Lashuel and H. Hirling, "Rescuing defective vesicular trafficking protects against alpha-synuclein toxicity in cellular and animal models of Parkinson's disease," *ACS Chemical Biology*, vol. 1, no. 7, pp. 420–424, 2006.

[112] R. J. S. Viana, A. F. Nunes, and C. M. P. Rodrigues, "Endoplasmic reticulum enrollment in Alzheimer's disease," *Molecular Neurobiology* , vol. 46, no. 2, pp. 522–534, 2012.

[113] R. Vidal, B. Caballero, A. Couve, and C. Hetz, "Converging pathways in the occurrence of endoplasmic reticulum (ER) stress in Huntington's disease," *Current Molecular Medicine*, vol. 11, no. 1, pp. 1–12, 2011.

[114] A. K. Walker and J. D. Atkin, "Stress signaling from the endoplasmic reticulum: a central player in the pathogenesis of amyotrophic lateral sclerosis," *IUBMB Life*, vol. 63, no. 9, pp. 754–763, 2011.

[115] D. Ron and P. Walter, "Signal integration in the endoplasmic reticulum unfolded protein response," *Nature Reviews Molecular Cell Biology*, vol. 8, no. 7, pp. 519–529, 2007.

[116] M. Schröder, "Endoplasmic reticulum stress responses," *Cellular and Molecular Life Sciences*, vol. 65, no. 6, pp. 862–894, 2007.

[117] H. Yoshida, "ER stress and diseases," *FEBS Journal*, vol. 274, no. 3, pp. 630–658, 2007.

[118] J. Hitomi, T. Katayama, Y. Eguchi et al., "Involvement of caspase-4 in endoplasmic reticulum stress-induced apoptosis and Aβ-induced cell death," *Journal of Cell Biology*, vol. 165, no. 3, pp. 347–356, 2004.

[119] F. Urano, X. Wang, A. Bertolotti et al., "Coupling of stress in the ER to activation of JNK protein kinases by transmembrane protein kinase IRE1," *Science*, vol. 287, no. 5453, pp. 664–666, 2000.

[120] L. Ellgaard and L. W. Ruddock, "The human protein disulphide isomerase family: substrate interactions and functional properties," *EMBO Reports*, vol. 6, no. 1, pp. 28–32, 2005.

[121] G. Kozlov, P. Määttänen, D. Y. Thomas, and K. Gehring, "A structural overview of the PDI family of proteins," *FEBS Journal*, vol. 277, no. 19, pp. 3924–3936, 2010.

[122] D. M. Ferrari and H.-D. Söling, "The protein disulphide-isomerase family: unravelling a string of folds," *Biochemical Journal*, vol. 339, no. 1, pp. 1–10, 1999.

[123] C. I. Andreu, U. Woehlbier, M. Torres, and C. Hetz, "Protein disulfide isomerases in neurodegeneration: from disease mechanisms to biomedical applications," *FEBS Letters*, vol. 586, no. 18, pp. 2826–2834, 2012.

[124] A. M. Benham, "The protein disulfide isomerase family: key players in health and disease," *Antioxidants and Redox Signaling*, vol. 16, no. 8, pp. 781–789, 2012.

[125] J. J. Galligan and D. R. Petersen, "The human protein disulfide isomerase gene family," *Human Genomics*, vol. 6, article 6, 2012.

[126] C. S. Sevier and C. A. Kaiser, "Conservation and diversity of the cellular disulfide bond formation pathways," *Antioxidants and Redox Signaling*, vol. 8, no. 5-6, pp. 797–811, 2006.

[127] H. C. Hawkins, E. C. Blackburn, and R. B. Freedman, "Comparison of the activities of protein disulphide-isomerase and thioredoxin in catalysing disulphide isomerization in a protein substrate," *Biochemical Journal*, vol. 275, no. 2, pp. 349–353, 1991.

[128] C. Turano, S. Coppari, F. Altieri, and A. Ferraro, "Proteins of the PDI family: unpredicted non-ER locations and functions," *Journal of Cellular Physiology*, vol. 193, no. 2, pp. 154–163, 2002.

[129] T. Higo, M. Hattori, T. Nakamura, T. Natsume, T. Michikawa, and K. Mikoshiba, "Subtype-specific and ER lumenal environment-dependent regulation of inositol 1,4,5-trisphosphate receptor type 1 by ERp44," *Cell*, vol. 120, no. 1, pp. 85–98, 2005.

[130] Y. Li and P. Camacho, "Ca^{2+}-dependent redox modulation of SERCA 2b by ERp57," *Journal of Cell Biology*, vol. 164, no. 1, pp. 35–46, 2004.

[131] A. Jansens, E. van Duijn, and I. Braakman, "Coordinated nonvectorial folding in a newly synthesized multidomain protein," *Science*, vol. 298, no. 5602, pp. 2401–2403, 2002.

[132] M. Schwaller, B. Wilkinson, and H. F. Gilbert, "Reduction-reoxidation cycles contribute to catalysis of disulfide isomerization by protein-disulfide isomerase," *The Journal of Biological Chemistry*, vol. 278, no. 9, pp. 7154–7159, 2003.

[133] K. W. Walker and H. F. Gilbert, "Scanning and escape during protein-disulfide isomerase-assisted protein folding," *The Journal of Biological Chemistry*, vol. 272, no. 14, pp. 8845–8848, 1997.

[134] M. M. Lyles and H. F. Gilbert, "Catalysis of the oxidative folding of ribonuclease A by protein disulfide isomerase: dependence of the rate on the composition of the redox buffer," *Biochemistry*, vol. 30, no. 3, pp. 613–619, 1991.

[135] M.-J. Gething and J. Sambrook, "Protein folding in the cell," *Nature*, vol. 355, no. 6355, pp. 33–45, 1992.

[136] R. J. Ellis and S. M. Hemmingsen, "Molecular chaperones: proteins essential for the biogenesis of some macromolecular structures," *Trends in Biochemical Sciences*, vol. 14, no. 8, pp. 339–342, 1989.

[137] A. Puig and H. F. Gilbert, "Protein disulfide isomerase exhibits chaperone and anti-chaperone activity in the oxidative refolding of lysozyme," *The Journal of Biological Chemistry*, vol. 269, no. 10, pp. 7764–7771, 1994.

[138] H. Quan, G. Fan, and C.-C. Wang, "Independence of the chaperone activity of protein disulfide isomerase from its thioredoxin-like active site," *The Journal of Biological Chemistry*, vol. 270, no. 29, pp. 17078–17080, 1995.

[139] Y. Dai and C.-C. Wang, "A mutant truncated protein disulfide isomerase with no chaperone activity," *The Journal of Biological Chemistry*, vol. 272, no. 44, pp. 27572–27576, 1997.

[140] G. Tian, S. Xiang, R. Noiva, W. J. Lennarz, and H. Schindelin, "The crystal structure of yeast protein disulfide isomerase suggests cooperativity between its active sites," *Cell*, vol. 124, no. 1, pp. 61–73, 2006.

[141] P. Klappa, L. W. Ruddock, N. J. Darby, and R. B. Freedman, "The b′ domain provides the principal peptide-binding site of protein disulfide isomerase but all domains contribute to binding of misfolded proteins," *EMBO Journal*, vol. 17, no. 4, pp. 927–935, 1998.

[142] G. Kozlov, P. Maattanen, J. D. Schrag et al., "Crystal structure of the bb′ domains of the protein disulfide isomerase ERp57," *Structure*, vol. 14, no. 8, pp. 1331–1339, 2006.

[143] G. Kozlov, P. Määttänen, J. D. Schrag et al., "Structure of the noncatalytic domains and global fold of the protein disulfide isomerase ERp72," *Structure*, vol. 17, no. 5, pp. 651–659, 2009.

[144] L. A. Rutkevich and D. B. Williams, "Participation of lectin chaperones and thiol oxidoreductases in protein folding within the endoplasmic reticulum," *Current Opinion in Cell Biology*, vol. 23, no. 2, pp. 157–166, 2011.

[145] G. Tian, F.-X. Kober, U. Lewandrowski, A. Sickmann, W. J. Lennarz, and H. Schindelin, "The catalytic activity of protein-disulfide isomerase requires a conformationally flexible molecule," *The Journal of Biological Chemistry*, vol. 283, no. 48, pp. 33630–33640, 2008.

[146] K. J. Conn, W. Gao, A. McKee et al., "Identification of the protein disulfide isomerase family member PDIp in experimental Parkinson's disease and Lewy body pathology," *Brain Research*, vol. 1022, no. 1-2, pp. 164–172, 2004.

[147] P. Klappa, T. Stromer, R. Zimmermann, L. W. Ruddock, and R. B. Freedman, "A pancreas-specific glycosylated protein disulphide-isomerase binds to misfolded proteins and peptides with an interaction inhibited by oestrogens," *European Journal of Biochemistry*, vol. 254, no. 1, pp. 63–69, 1998.

[148] J. Volkmer, S. Guth, W. Nastainczyk et al., "Pancreas specific protein disulfide isomerase, PDIp, is in transient contact with secretory proteins during late stages of translocation," *FEBS Letters*, vol. 406, no. 3, pp. 291–295, 1997.

[149] H. I. Alanen, K. E. H. Salo, M. Pekkala, H. M. Siekkinen, A. Pirneskoski, and L. W. Ruddock, "Defining the domain boundaries of the human protein disulfide isomerases," *Antioxidants and Redox Signaling*, vol. 5, no. 4, pp. 367–374, 2003.

[150] I. Raykhel, H. Alanen, K. Salo et al., "A molecular specificity code for the three mammalian KDEL receptors," *Journal of Cell Biology*, vol. 179, no. 6, pp. 1193–1204, 2007.

[151] P. Klappa, R. B. Freedman, and R. Zimmermann, "Protein disulphide isomerase and a lumenal cyclophilin-type peptidyl prolyl cis-trans isomerase are in transient contact with secretory proteins during late stages of translocation," *European Journal of Biochemistry*, vol. 232, no. 3, pp. 755–764, 1995.

[152] R. B. Freedman, T. R. Hirst, and M. F. Tuite, "Protein disulphide isomerase: building bridges in protein folding," *Trends in Biochemical Sciences*, vol. 19, no. 8, pp. 331–336, 1994.

[153] N. Hirano, F. Shibasaki, B. Sakai et al., "Molecular cloning of the human glucose-regulated protein ERp57/GRP58, a thiol-dependent reductase. Identification of its secretory form and inducible expression by the oncogenic transformation," *European Journal of Biochemistry*, vol. 234, no. 1, pp. 336–342, 1995.

[154] C. E. Jessop, S. Chakravarthi, N. Garbi, G. J. Hämmerling, S. Lovell, and N. J. Bulleid, "ERp57 is essential for efficient folding of glycoproteins sharing common structural domains," *EMBO Journal*, vol. 26, no. 1, pp. 28–40, 2007.

[155] M. Bourdi, D. Demady, J. L. Martin et al., "cDNA cloning and baculovirus expression of the human liver endoplasmic reticulum P58: characterization as a protein disulfide isomerase isoform, but not as a protease or a carnitine acyltransferase," *Archives of Biochemistry and Biophysics*, vol. 323, no. 2, pp. 397–403, 1995.

[156] E.-M. Frickel, P. Frei, M. Bouvier et al., "ERp57 is a multifunctional thiol-disulfide oxidoreductase," *The Journal of Biological Chemistry*, vol. 279, no. 18, pp. 18277–18287, 2004.

[157] C. Dingwall and R. A. Laskey, "Nuclear import: a tale of two sites," *Current Biology*, vol. 8, no. 25, pp. R922–R924, 1998.

[158] C. Turano, E. Gaucci, C. Grillo, and S. Chichiarelli, "ERp57/GRP58: a protein with multiple functions," *Cellular and Molecular Biology Letters*, vol. 16, no. 4, pp. 539–563, 2011.

[159] P. N. Van, K. Rupp, A. Lampen, and H.-D. Soling, "CaBP2 is a rat homolog of ERp72 with proteindisulfide isomerase activity," *European Journal of Biochemistry*, vol. 213, no. 2, pp. 789–795, 1993.

[160] P. Spee, J. Subjeck, and J. Neefjes, "Identification of novel peptide binding proteins in the endoplasmic reticulum: ERp72, calnexin, and grp170," *Biochemistry*, vol. 38, no. 32, pp. 10559–10566, 1999.

[161] I. E. Gulerez, G. Kozlov, A. Rosenauer, and K. Gehring, "Structure of the third catalytic domain of the protein disulfide isomerase ERp46," *Acta Crystallographica Section F*, vol. 68, no. 4, pp. 378–381, 2012.

[162] B. Knoblach, B. O. Keller, J. Groenendyk et al., "ERp19 and ERp46, new members of the thioredoxin family of endoplasmic reticulum proteins," *Molecular & Cellular Proteomics*, vol. 2, no. 10, pp. 1104–1119, 2003.

[163] T. Hayano and M. Kikuchi, "Molecular cloning of the cDNA encoding a novel protein disulfide isomerase-related protein (PDIR)," *FEBS Letters*, vol. 372, no. 2-3, pp. 210–214, 1995.

[164] P. M. Cunnea, A. Miranda-Vizuete, G. Bertoli et al., "ERdj5, an endoplasmic reticulum (ER)-resident protein containing DnaJ and thioredoxin domains, is expressed in secretory cells or following ER stress," *The Journal of Biological Chemistry*, vol. 278, no. 2, pp. 1059–1066, 2003.

[165] T. Soldà, N. Garbi, G. J. Hämmerling, and M. Molinari, "Consequences of ERp57 deletion on oxidative folding of obligate and facultative clients of the calnexin cycle," *The Journal of Biological Chemistry*, vol. 281, no. 10, pp. 6219–6226, 2006.

[166] A. Cabibbo, M. Pagani, M. Fabbri et al., "ERO1-L, a human protein that favors disulfide bond formation in the endoplasmic reticulum," *The Journal of Biological Chemistry*, vol. 275, no. 7, pp. 4827–4833, 2000.

[167] A. R. Frand and C. A. Kaiser, "Ero1p oxidizes protein disulfide isomerase in a pathway for disulfide bond formation in the endoplasmic reticulum," *Molecular Cell*, vol. 4, no. 4, pp. 469–477, 1999.

[168] J. Lundstrom and A. Holmgren, "Protein disulfide-isomerase is a substrate for thioredoxin reductase and has thioredoxin-like activity," *The Journal of Biological Chemistry*, vol. 265, no. 16, pp. 9114–9120, 1990.

[169] J. M. Holaska, B. E. Black, D. C. Love, J. A. Hanover, J. Leszyk, and B. M. Paschal, "Calreticulin is a receptor for nuclear export," *Journal of Cell Biology*, vol. 152, no. 1, pp. 127–140, 2001.

[170] S. Johnson, M. Michalak, M. Opas, and P. Eggleton, "The ins and outs of calreticulin: from the ER lumen to the extracellular space," *Trends in Cell Biology*, vol. 11, no. 3, pp. 122–129, 2001.

[171] H. L. Roderick, A. K. Campbell, and D. H. Llewellyn, "Nuclear localisation of calreticulin in vivo is enhanced by its interaction with glucocorticoid receptors," *FEBS Letters*, vol. 405, no. 2, pp. 181–185, 1997.

[172] K. Burns, B. Duggan, E. A. Atkinson et al., "Modulation of gene expression by calreticulin binding to the glucocorticoid receptor," *Nature*, vol. 367, no. 6462, pp. 476–480, 1994.

[173] S. Dedhar, "Novel functions for calreticulin: interaction with integrins and modulation of gene expression?" *Trends in Biochemical Sciences*, vol. 19, no. 7, pp. 269–271, 1994.

[174] S. A. Fraser, M. Michalak, W. H. Welch, and D. Hudig, "Calreticulin, a component of the endoplasmic reticulum and of cytotoxic lymphocyte granules, regulates perforin-mediated lysis in the hemolytic model system," *Biochemistry and Cell Biology*, vol. 76, no. 5, pp. 881–887, 1998.

[175] M. Michalak, E. F. Corbett, N. Mesaeli, K. Nakamura, and M. Opas, "Calreticulin: one protein, one gene, many functions," *Biochemical Journal*, vol. 344, no. 2, pp. 281–292, 1999.

[176] M. Ni, Y. Zhang, and A. S. Lee, "Beyond the endoplasmic reticulum: atypical GRP78 in cell viability, signalling and therapeutic targeting," *Biochemical Journal*, vol. 434, no. 2, pp. 181–188, 2011.

[177] V. J. Wroblewski, M. Masnyk, S. S. Khambatta, and G. W. Becker, "Mechanisms involved in degradation of human insulin by cytosolic fractions of human, monkey, and rat liver," *Diabetes*, vol. 41, no. 4, pp. 539–547, 1992.

[178] Y. Tabata, K. Takano, T. Ito et al., "Vaticanol B, a resveratrol tetramer, regulates endoplasmic reticulum stress and inflammation," *American Journal of Physiology: Cell Physiology*, vol. 293, no. 1, pp. C411–C418, 2007.

[179] Y. S. Yang, N. Y. Harel, and S. M. Strittmatter, "Reticulon-4A (Nogo-A) redistributes protein disulfide isomerase to protect mice from SOD1-dependent amyotrophic lateral sclerosis," *Journal of Neuroscience*, vol. 29, no. 44, pp. 13850–13859, 2009.

[180] P. Bernardoni, B. Fazi, A. Costanzi et al., "Reticulon1-C modulates protein disulphide isomerase function," *Cell Death & Disease*, vol. 4, article e581, 2013.

[181] N. Ramachandran, P. Root, X.-M. Jiang, P. J. Hogg, and B. Mutus, "Mechanism of transfer of NO from extracellular S-nitrosothiols into the cytosol by cell-surface protein disulfide isomerase," *Proceedings of the National Academy of Sciences of the United States of America*, vol. 98, no. 17, pp. 9539–9544, 2001.

[182] A. Zai, M. A. Rudd, A. W. Scribner, and J. Loscalzo, "Cell-surface protein disulfide isomerase catalyzes transnitrosation and regulates intracellular transfer of nitric oxide," *Journal of Clinical Investigation*, vol. 103, no. 3, pp. 393–399, 1999.

[183] C. M. Shah, S. E. Bell, I. C. Locke, H. S. Chowdrey, and M. P. Gordge, "Interactions between cell surface protein disulphide isomerase and S-nitrosoglutathione during nitric oxide delivery," *Nitric Oxide*, vol. 16, no. 1, pp. 135–142, 2007.

[184] J. C. Watts, H. Huo, Y. Bai et al., "Interactome analyses identify ties of PrP and its mammalian paralogs to oligomannosidic N-glycans and endoplasmic reticulum-derived chaperones," *PLoS Pathogens*, vol. 5, no. 10, Article ID e1000608, 2009.

[185] F. Altieri, B. Maras, M. Eufemi, A. Ferraro, and C. Turano, "Purification of a 57kDa nuclear matrix protein associated with thiol:protein-disulfide oxidoreductase and phospholipase C activities," *Biochemical and Biophysical Research Communications*, vol. 194, no. 3, pp. 992–1000, 1993.

[186] C. Gerner, K. Holzmann, M. Meissner, J. Gotzmann, R. Grimm, and G. Sauermann, "Reassembling proteins and chaperones in human nuclear matrix protein fractions," *Journal of Cellular Biochemistry*, vol. 74, no. 2, pp. 145–151, 1999.

[187] M. P. Rigobello, A. Donella-Deana, L. Cesaro, and A. Bindoli, "Isolation, purification, and characterization of a rat liver mitochondrial protein disulfide isomerase," *Free Radical Biology and Medicine*, vol. 28, no. 2, pp. 266–272, 2000.

[188] J. M. Müller, D. Milenkovic, B. Guiard, N. Pfanner, and A. Chacinska, "Precursor oxidation by Mia40 and Erv1 promotes vectorial transport of proteins into the mitochondrial intermembrane space," *Molecular Biology of the Cell*, vol. 19, no. 1, pp. 226–236, 2008.

[189] L. Wrobel, A. Trojanowska, M. E. Sztolsztener, and A. Chacinska, "Mitochondrial protein import: Mia40 facilitates Tim22 translocation into the inner membrane of mitochondria," *Molecular Biology of the Cell*, vol. 24, no. 5, pp. 543–554, 2013.

[190] B. G. Hoffstrom, A. Kaplan, R. Letso et al., "Inhibitors of protein disulfide isomerase suppress apoptosis induced by misfolded proteins," *Nature Chemical Biology*, vol. 6, no. 12, pp. 900–906, 2010.

[191] S. Tanaka, T. Uehara, and Y. Nomura, "Up-regulation of protein-disulfide isomerase in response to hypoxia/brain ischemia and its protective effect against apoptotic cell death," *The Journal of Biological Chemistry*, vol. 275, no. 14, pp. 10388–10393, 2000.

[192] J. H. Lee, S. M. Won, J. Suh et al., "Induction of the unfolded protein response and cell death pathway in Alzheimer's disease, but not in aged Tg2576 mice," *Experimental and Molecular Medicine*, vol. 42, no. 5, pp. 386–394, 2010.

[193] R. R. Erickson, L. M. Dunning, D. A. Olson et al., "In cerebrospinal fluid ER chaperones ERp57 and calreticulin bind β-amyloid," *Biochemical and Biophysical Research Communications*, vol. 332, no. 1, pp. 50–57, 2005.

[194] Y. Honjo, H. Ito, T. Horibe et al., "Derlin-1-immunopositive inclusions in patients with Alzheimer's disease," *Neuroreport*, vol. 23, no. 10, pp. 611–615, 2012.

[195] Y. Honjo, H. Ito, T. Horibe, R. Takahashi, and K. Kawakami, "Protein disulfide isomerase-immunopositive inclusions in patients with Alzheimer disease," *Brain Research*, vol. 1349, pp. 90–96, 2010.

[196] J. S. Kim-Han and K. L. O'Malley, "Cell stress induced by the parkinsonian mimetic, 6-hydroxydopamine, is concurrent with oxidation of the chaperone, ERp57, and aggresome formation," *Antioxidants and Redox Signaling*, vol. 9, no. 12, pp. 2255–2264, 2007.

[197] H. Cheng, L. Wang, and C.-C. Wang, "Domain a of protein disulfide isomerase plays key role in inhibiting α-synuclein fibril formation," *Cell Stress and Chaperones*, vol. 15, no. 4, pp. 415–421, 2010.

[198] B. C. Yoo, K. Krapfenbauer, N. Cairns, G. Belay, M. Bajo, and G. Lubec, "Overexpressed protein disulfide isomerase in brains of patients with sporadic Creutzfeldt-Jakob disease," *Neuroscience Letters*, vol. 334, no. 3, pp. 196–200, 2002.

[199] S. B. Wang, Q. Shi, Y. Xu et al., "Protein disulfide isomerase regulates endoplasmic reticulum stress and the apoptotic process during prion infection and PrP mutant-induced cytotoxicity," *PLoS ONE*, vol. 7, no. 6, article e38221, 2012.

[200] M. A. Farg, K. Y. Soo, A. K. Walker et al., "Mutant FUS induces endoplasmic reticulum stress in amyotrophic lateral sclerosis and interacts with protein disulfide-isomerase," *Neurobiology of Aging*, vol. 33, no. 12, pp. 2855–2868, 2012.

[201] Y. Honjo, S. Kaneko, H. Ito et al., "Protein disulfide isomerase-immunopositive inclusions in patients with amyotrophic lateral sclerosis," *Amyotrophic Lateral Sclerosis*, vol. 12, no. 6, pp. 444–450, 2011.

[202] C. T. Kwok, A. G. Morris, J. Frampton, B. Smith, C. E. Shaw, and J. de Belleroche, "Association studies indicate that protein disulfide isomerase is a risk factor in amyotrophic lateral sclerosis," *Free Radical Biology and Medicine*, vol. 58, pp. 81–86, 2013.

[203] J. D. Atkin, M. A. Farg, B. J. Turner et al., "Induction of the unfolded protein response in familial amyotrophic lateral sclerosis and association of protein-disulfide isomerase with superoxide dismutase 1," *The Journal of Biological Chemistry*, vol. 281, no. 40, pp. 30152–30165, 2006.

[204] E. V. Ilieva, V. Ayala, M. Jové et al., "Oxidative and endoplasmic reticulum stress interplay in sporadic amyotrophic lateral sclerosis," *Brain*, vol. 130, no. 12, pp. 3111–3123, 2007.

[205] J.-I. Niwa, S.-I. Yamada, S. Ishigaki et al., "Disulfide bond mediates aggregation, toxicity, and ubiquitylation of familial amyotrophic lateral sclerosis-linked mutant SOD1," *The Journal of Biological Chemistry*, vol. 282, no. 38, pp. 28087–28095, 2007.

[206] M. Jaronen, P. Vehviläinen, T. Malm et al., "Protein disulfide isomerase in ALS mouse glia links protein misfolding with NADPH oxidase-catalyzed superoxide production," *Human Molecular Genetics*, vol. 22, no. 4, pp. 646–655, 2012.

[207] T. Uehara, "Accumulation of misfolded protein through nitrosative stress linked to neurodegenerative disorders," *Antioxidants and Redox Signaling*, vol. 9, no. 5, pp. 597–601, 2007.

[208] L. Xu, J. P. Eu, G. Meissner, and J. S. Stamler, "Activation of the cardiac calcium release channel (Ryanodoine receptor) by poly-S-nitrosylation," *Science*, vol. 279, no. 5348, pp. 234–237, 1998.

[209] K. Ozawa, H. Tsumoto, W. Wei et al., "Proteomic analysis of the role of S-nitrosoglutathione reductase in lipopolysaccharide-challenged mice," *PROTEOMICS*, vol. 12, no. 12, pp. 2024–2035, 2012.

[210] D. M. Townsend, Y. Manevich, H. Lin et al., "Nitrosative stress-induced S-glutathionylation of protein disulfide isomerase leads to activation of the unfolded protein response," *Cancer Research*, vol. 69, no. 19, pp. 7626–7634, 2009.

[211] J. D. Uys, Y. Xiong, and D. M. Townsend, "Nitrosative stress-induced S-glutathionylation of protein disulfide isomerase," *Methods in Enzymology*, vol. 490, no. C, pp. 321–332, 2011.

[212] Y. Xiong, Y. Manevich, K. D. Tew, and D. M. Townsend, "S-glutathionylation of protein disulfide isomerase regulates estrogen receptor α stability and function," *International Journal of Cell Biology*, vol. 2012, Article ID 273549, 9 pages, 2012.

[213] J. R. Schultz-Norton, W. H. McDonald, J. R. Yates, and A. M. Nardulli, "Protein disulfide isomerase serves as a molecular chaperone to maintain estrogen receptor α structure and function," *Molecular Endocrinology*, vol. 20, no. 9, pp. 1982–1995, 2006.

[214] M. Tager, H. Kroning, U. Thiel, and S. Ansorge, "Membrane-bound proteindisulfide isomerase (PDI) is involved in regulation of surface expression of thiols and drug sensitivity of B-CLL cells," *Experimental Hematology*, vol. 25, no. 7, pp. 601–607, 1997.

[215] M. Swiatkowska, J. Szymański, G. Padula, and C. S. Cierniewski, "Interaction and functional association of protein disulfide isomerase with $\alpha v\beta 3$ integrin on endothelial cells," *FEBS Journal*, vol. 275, no. 8, pp. 1813–1823, 2008.

[216] B. Park, S. Lee, E. Kim et al., "Redox regulation facilitates optimal peptide selection by MHC class I during antigen processing," *Cell*, vol. 127, no. 2, pp. 369–382, 2006.

[217] D. Goplen, J. Wang, P. Ø. Enger et al., "Protein disulfide isomerase expression is related to the invasive properties of malignant glioma," *Cancer Research*, vol. 66, no. 20, pp. 9895–9902, 2006.

7.2.9 Supplementary Figure 8

The author was part of the study "***The unfolded protein response and the role of protein disulphide isomerase in neurodegeneration***" Frontiers in Cell and Developmental Biology 3:1-17

Section "**Recent developments in PDI function associated with neurodegeneration"** on **page 12** of the manuscript was contributed by the author.

frontiers in Cell and Developmental Biology

REVIEW
published: 08 January 2016
doi: 10.3389/fcell.2015.00080

The Unfolded Protein Response and the Role of Protein Disulfide Isomerase in Neurodegeneration

*Emma R. Perri[1], Colleen J. Thomas[2], Sonam Parakh[3], Damian M. Spencer[1] and Julie D. Atkin[1,3]**

[1] Department of Biochemistry and Genetics, La Trobe Institute for Molecular Science, La Trobe University, Melbourne, VIC, Australia, [2] Department of Physiology, Anatomy and Microbiology, School of Life Sciences, La Trobe University, Melbourne, VIC, Australia, [3] Department of Biomedical Sciences, Faculty of Medicine and Human Science, Macquarie University, Sydney, NSW, Australia

The maintenance and regulation of proteostasis is a critical function for post-mitotic neurons and its dysregulation is increasingly implicated in neurodegenerative diseases. Despite having different clinical manifestations, these disorders share similar pathology; an accumulation of misfolded proteins in neurons and subsequent disruption to cellular proteostasis. The endoplasmic reticulum (ER) is an important component of proteostasis, and when the accumulation of misfolded proteins occurs within the ER, this disturbs ER homeostasis, giving rise to ER stress. This triggers the unfolded protein response (UPR), distinct signaling pathways that whilst initially protective, are pro-apoptotic if ER stress is prolonged. ER stress is increasingly implicated in neurodegenerative diseases, and emerging evidence highlights the complexity of the UPR in these disorders, with both protective and detrimental components being described. Protein Disulfide Isomerase (PDI) is an ER chaperone induced during ER stress that is responsible for the formation of disulfide bonds in proteins. Whilst initially considered to be protective, recent studies have revealed unconventional roles for PDI in neurodegenerative diseases, distinct from its normal function in the UPR and the ER, although these mechanisms remain poorly defined. However, specific aspects of PDI function may offer the potential to be exploited therapeutically in the future. This review will focus on the evidence linking ER stress and the UPR to neurodegenerative diseases, with particular emphasis on the emerging functions ascribed to PDI in these conditions.

Keywords: endoplasmic reticulum stress (ER stress), unfolded protein response (UPR), protein disulfide isomerase (PDI), neurodegeneration, Alzheimer's disease (AD), Parkinson's disease (PD), amyotrophic lateral sclerosis (ALS), Huntington's disease (HD)

OPEN ACCESS

Edited by:
Bulent Mutus, University of Windsor, Canada

Reviewed by:
Carla Cirillo, KU Leuven, Belgium
Xin Qi, Case Western Reserve University School of Medicine, USA

****Correspondence:***
Julie D. Atkin
julie.atkin@mq.edu.au

Specialty section:
This article was submitted to Cellular Biochemistry, a section of the journal Frontiers in Cell and Developmental Biology

Received: *09 November 2015*
Accepted: *03 December 2015*
Published: *08 January 2016*

Citation:
Perri ER, Thomas CJ, Parakh S, Spencer DM and Atkin JD (2016) The Unfolded Protein Response and the Role of Protein Disulfide Isomerase in Neurodegeneration. Front. Cell Dev. Biol. 3:80. doi: 10.3389/fcell.2015.00080

INTRODUCTION

The endoplasmic reticulum (ER) is a fundamental cellular organelle responsible for the folding, post-translational modification, transportation, and quality control of newly synthesized proteins. The ER is therefore a key component of cellular protein homeostasis, or proteostasis, integrated mechanisms that control the regulation of protein trafficking, synthesis, folding, and degradation. The maintenance and regulation of proteostasis is a critical function for post-mitotic cells such as neurons and dysregulation of proteostasis is increasingly implicated in diseases that target neurons,

including neurodegenerative diseases. A pathological hallmark of these diseases is the accumulation of misfolded protein aggregates within affected neurons. Whilst neurodegenerative diseases differ in the proteins which misfold, and the sub-groups of neurons affected, abnormal protein misfolding is a common feature.

When the accumulation of misfolded or unfolded proteins occurs within the ER, this disturbs ER homeostasis, giving rise to ER stress. ER stress results in activation of the unfolded protein response (UPR) which aims to alleviate the stress. The UPR involves up-regulation of protein chaperones to promote protein folding, translational attenuation to reduce the load of proteins within the ER to prevent further accumulation of misfolded proteins, and up-regulation of ER-associated protein degradation (ERAD) and autophagy to promote degradation of misfolded proteins. Therefore, ER stress plays a pivotal role in cell survival by maintaining proteostasis. In circumstances of chronic or prolonged ER stress, however, the UPR becomes pro-apoptotic, therefore triggering cell death. ER stress is increasingly implicated as a key mechanism relevant to pathogenesis in neurodegenerative diseases, although differential effects are evident in different neurodegenerative conditions.

Chaperones promote the correct folding of proteins into their native conformations and hence are an important mechanism in proteostasis. One chaperone upregulated during the UPR is Protein Disulfide Isomerase (PDI), which is found primarily within the ER, but is also found in other cellular locations. PDI is the prototype of a family of proteins that possess two alternative functions; general chaperone activity and disulfide interchange activity; in which protein disulfide bonds are oxidized, reduced, or isomerized. As chaperones prevent protein misfolding, novel therapeutic strategies mimicking the functional activity of PDI may therefore be beneficial in disorders involving protein misfolding. Consistent with this notion, there is increasing evidence linking PDI to neurodegenerative diseases. Recent studies have revealed unconventional roles for PDI in these disorders, distinct from its normal function in the UPR and the ER, although these mechanisms remain poorly defined. This review will focus on the evidence linking ER stress and the UPR to neurodegenerative diseases, with particular emphasis on the role of PDI in these conditions.

NEURODEGENERATION

Neurodegenerative diseases have long been regarded as intangible mysteries of biomedical research and targeting these conditions therapeutically remains a major obstacle in medicine. Whilst these disorders are distinct in their clinical manifestations, they share a common pathological hallmark: the abnormal aggregation of misfolded proteins (Lindholm et al., 2006). Aggregation occurs when misfolded proteins expose hydrophobic regions that are normally hidden within the protein interior when folded in their native conformation. This exposure of normally buried regions promotes hydrophobic interactions with other proteins. Protein misfolding is triggered by genetic mutations in familial forms of disease, or by cellular conditions which cause wildtype proteins to misfold in sporadic forms of disease, although the latter processes remain poorly defined. The aggregation of misfolded proteins leads to the formation of prominent protein inclusions (Wolozin, 2012; **Figure 1**). The most prevalent neurodegenerative diseases include Alzheimer's disease (AD), Parkinson's disease (PD), amyotrophic lateral sclerosis (ALS), Huntington's disease (HD), and transmissible prion encephalopathies, such as Creutzfeldt-Jakob disease (CJD). These disorders differ in the proteins that misfold and the group of neurons which are affected (Soto, 2003; **Table 1**). An intriguing puzzle is why specific groups of neurons are selectively targeted in these conditions when the proteins that misfold are usually

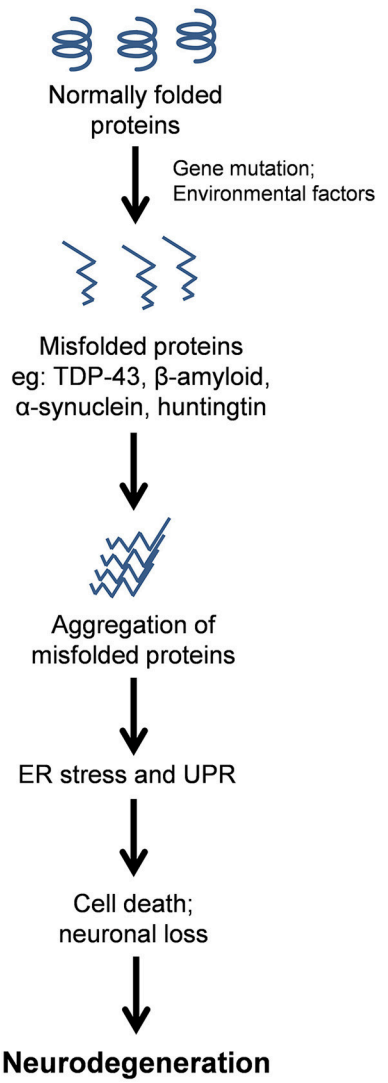

FIGURE 1 | Schematic representation of the protein pathology contribution to neurodegenerative disease via chronic Endoplasmic Reticulum (ER) stress. Misfolded proteins aggregate and form prominent inclusions as the characteristic pathological hallmark of these disorders. ER stress results from the accumulation of misfolded proteins within the ER, thus activating the Unfolded Protein Response (UPR), which if prolonged or unresolved, can result in neuronal cell death, and hence neurodegenerative disorders.

TABLE 1 | Genes and proteins implicated in common neurodegenerative diseases.

Neurodegenerative disease	Genes implicated in disease	Proteins encoded	References
Alzheimer's disease	APP	Amyloid precursor protein	Haass and Selkoe, 2007; Karran et al., 2011; Matus et al., 2011
	PSEN1	Presenilin-1	
	PSEN2	Presenilin-2	
	MAPT	Tau	
Parkinson's disease	SNCA	α-Synuclein	Chartier-Harlin et al., 2004; Schlehe et al., 2008; Volpicelli-Daley et al., 2011
	PARK2	Parkin	
	PINK1	PTEN-induced putative kinase 1	
	PARK7	DJ-1	
	UCH-L1	Ubiquitin carboxyl-terminal esterase L1	
	PARK8	LRRK2	
Amyotrophic lateral sclerosis	SOD1	Cu/Zn superoxide dismutase 1	Ferraiuolo et al., 2011; Turner et al., 2013; Leblond et al., 2014; Renton et al., 2014
	TARDBP	TAR DNA binding protein 43 (TDP-43)	
	FUS	Fused in sarcoma	
	C9orf72	Chromosome 9 open reading frame 72	
	ALS2	Alsin	
	SETX	Senataxin	
	VAPB	Vesicle-associated membrane protein-associated B	
	OPTN	Optineurin	
	VCP	Valosin-containing protein	
	UBQLN2	Ubiquilin 2	
	PFN1	Profilin 1	
	SQSTM1	Sequestosome 1	
	HnRNPA2B1/A1	Heterogenous nuclear ribonucleoprotein	
	TAF15	TATA box binding protein-associated factor	
Huntington's disease	HTT	Huntingtin	Carnemolla et al., 2009; Ross and Tabrizi, 2011
Creutzfeldt-Jakob disease	PRNP	PrP protein	Head and Ironside, 2012; Porter and Leemans, 2013

expressed ubiquitously in all cell types. At the biochemical level, however, these disorders share a common mechanism; formation of abnormal misfolded protein aggregates which lead to the protein inclusions characteristic of pathology in these disorders.

Alzheimer's Disease

AD is characterized by a progressive decline in memory, language, behavior, and cognitive function (Salminen et al., 2009). Neuronal degeneration in AD occurs in the cerebral cortex (in particular the frontal, temporal, and parietal lobes) and the hippocampus (Brundin et al., 2010; Fjell et al., 2014). Two types of misfolded protein inclusions are present in these tissues. Amyloid plaques are formed extracellularly by the aggregation of β-amyloid, which is produced by abnormal cleavage of amyloid precursor protein (APP), and neurofibrillary tangles, which are formed intracellularly in the cytoplasm by hyper-phosphorylation of the microtubule associated protein tau (Haass and Selkoe, 2007; Matus et al., 2011). Mutations that cause familial cases of AD occur in genes encoding APP, or the presenilin genes (PS1 and PS2) which encode proteins that comprise the secretase complex that regulates APP processing. These mutations alter the metabolism of β-amyloid, which either increase the total production of β-amyloid or reduce its rate of degradation. The increased levels of β-amyloid then lead to its oligomerization (Haass and Selkoe, 2007; Karran et al., 2011).

Parkinson's Disease

PD results from the degeneration of dopaminergic neurons primarily in the *substantia nigra pars compacta* in the midbrain (Matus et al., 2011). As a consequence, PD patients experience symptoms of motor dysfunction; tremors, bradykinesia (slowed movement), rigidity, loss of autonomic movement, and abnormal gait (Jankovic, 2008). The most widely studied gene linked to PD encodes α-synuclein, which causes rare autosomal dominant familial forms of disease (Chartier-Harlin et al., 2004). α-synuclein is found in both Lewy bodies and Lewy neurites, which are protein inclusion bodies found in the neuronal cytoplasm and processes, respectively (Volpicelli-Daley et al., 2011). Mutations in the genes encoding Parkin, PINK1, and DJ-1, LRRK2 and

UCH-L1 cause familial forms of PD, which arise through autosomal recessive inheritance (Schlehe et al., 2008).

Amyotrophic Lateral Sclerosis

ALS is characterized by the degeneration of upper motor neurons of the motor cortex and lower motor neurons of the brainstem and spinal cord (Kent-Braun et al., 1998). Patients typically experience symptoms of fatigue, muscle weakness and atrophy, followed by paralysis (Rothstein, 2009; Robberecht and Philips, 2013). There are numerous genes linked to ALS both genetically and/or pathologically (Leblond et al., 2014; Renton et al., 2014; **Table 1**). Protein inclusions in ALS form in the cytoplasm of degenerating motor neurons and depending on the patient, contain primarily [Cu/Zn] superoxide dismutase 1 (SOD1), TAR DNA binding protein 43 (TDP-43), fused in sarcoma (FUS), or by dipeptide repeat proteins produced by non-conventional repeat associated non-ATG translation, encoded by the Chromosome 9 open reading frame 72 repeat expansion (C9orf72) (Ferraiuolo et al., 2011; Turner et al., 2013; Leblond et al., 2014; Renton et al., 2014). Recent evidence has demonstrated that ALS is linked to closely to frontotemporal dementia (FTD) (Ling et al., 2013).

Huntington's Disease

Characterized by involuntary movements such as twitching and chorea (jerky movements of limbs), personality changes and dementia, HD is an autosomal dominant disease (Brundin et al., 2010). Mutations in the huntingtin (Htt) gene result from the expansion of a CAG repeat, which leads to an aberrantly long polyglutamine sequence in the huntingtin protein (Ross and Tabrizi, 2011). Huntingtin proteins with less than 35 polyglutamine repeats do not aggregate readily, however proteins with more than 40 repeats result in aggregation into inclusion bodies (Brundin et al., 2010). In general, longer lengths of polyglutamine repeats result in more rapid neurodegeneration and earlier disease onset than shorter repeats (Ross and Tabrizi, 2011). In contrast to the other neurodegenerative diseases in which most cases (85–90%) are sporadic, HD is entirely genetic in nature (Carnemolla et al., 2009).

Creutzfeldt-Jakob Disease and Other Prion Encephalopathies

Transmissible prion encephalopathies are neurodegenerative disorders in which proteins become infectious and protein misfolding propagates from one cell to another. These infectious proteins are termed prions (Makarava et al., 2012). The most common transmissible prion encephalopathy is CJD, in which patients experience memory loss, cognitive decline, personality changes, and psychosis (Porter and Leemans, 2013). The prion gene PRNP encodes cellular prion protein (PrP^{c}), which occurs naturally in both humans and animals. However, in CJD, the accumulation of abnormal prion protein, the scrapie isoform PrP^{Sc}, results, which is the major component of the purified infectious agent (Head and Ironside, 2012). PrP^{Sc} promotes refolding of natively folded PrP^{c} proteins into disease-associated misfolded PrP^{Sc} prions, resulting in insoluble protein inclusions in the brain and lympho-reticular tissues (Porter and Leemans, 2013). Not surprisingly, familial forms of CJD are caused by mutations in the PRNP gene (Head and Ironside, 2012).

Proteins misfold as part of normal cellular physiology, however normally, cells do not accumulate protein aggregates. Hence, what causes the formation of protein inclusions in neurodegeneration? A striking feature of neurodegenerative diseases is that they are late onset, and the probability of disease onset rises significantly with age. Therefore, pathology can be hypothesized to arise as a consequence of the normal aging process, whereby proteostasis becomes increasingly more difficult for cells to maintain as misfolded proteins continuously accumulate within the neuron. These mechanisms are not well understood, although decreases in chaperone activity or the efficiency of protein degradation processes over time may accelerate the accumulation of misfolded proteins (Nakamura and Lipton, 2011). Similarly, a decrease in antioxidant defenses during normal aging results in increases in the production of free radicals, therefore promoting oxidative stress (Halloran et al., 2013). Oxidative stress ultimately damages cells and is closely associated with ER stress (Lindholm et al., 2006; Kanekura et al., 2009). We describe below the increasingly complex relationship between the ER and protein misfolding in the context of age-related neurodegenerative disorders.

ER STRESS

The Endoplasmic Reticulum (ER) in Neurons

The ER is the largest membrane-bound organelle in the cell, and it possesses a diverse range of signaling and homeostatic functions. As well as the synthesis, folding/maturation, and trafficking of all secretory/transmembrane proteins, it also synthesizes lipids, plays a critical role in Ca^{2+} homeostasis, and is essential for compartmentalization of the nucleus and the structure of chromatin. Recently, novel ER functions have been described, including the regulation of mitochondrial function and the formation of autophagosomes, thus highlighting the importance of this organelle in cellular organization and proteostasis. The ER is well characterized in yeast and specialized secretory cells, but the ER in neurons is poorly studied in comparison. It is clear, however that the ER is much more extensive in neurons than in other cells, extending throughout the entire dendritic arbor and axon (Ramirez et al., 2011). There is evidence that multiple proteins are synthesized locally in both dendrites and axons (Lin and Holt, 2008; Yudin et al., 2008; Merianda et al., 2009). However, in these compartments, in particular within the axon, the ER remains largely uncharacterized.

Equipped with a variety of chaperones and folding enzymes, the ER maintains tight quality control measures to sustain its environment (Halperin et al., 2014). When nascent proteins enter the ER, the formation of disulfide bonds and other post-translational modifications facilitate correct protein folding. Disulfide bond formation is catalyzed by the PDI family of

proteins and is possible due to the oxidizing environment of the ER ($E^{\circ\prime} = -0.18\,V$; Woycechowsky and Raines, 2000; Wilkinson and Gilbert, 2004). These disulfide bonds ensure protein structural stability and promote assembly of multi-protein complexes (Woycechowsky and Raines, 2000). Correctly folded proteins are transported to the Golgi apparatus, where they are further sorted, modified and then packaged for secretion. The ER-Golgi route is an important cellular pathway; one third of all proteins transit the ER and Golgi compartments destined for transmembrane, ER or extracellular locations (Ghaemmaghami et al., 2003). Proteins which are unable to be correctly folded are directed to Endoplasmic Reticulum-Associated Degradation (ERAD), where misfolded proteins are transported to the cytosol for degradation by the proteasome, or by autophagy (Hetz and Mollereau, 2014).

The Unfolded Protein Response

The UPR is an adaptive mechanism designed to cope with protein folding alterations in the ER, and thus restore proteostasis (Walker, 2010). Under moderate misfolded protein accumulation, the UPR transduces information from the ER to the nucleus and cytosol and thereby inhibits protein translation, expands the ER membrane, recruits ER chaperones to aid in the correct folding of misfolded proteins, and promotes protein degradation in order to reduce the load of unfolded or misfolded proteins (Hetz, 2012). However, under conditions of chronic or irreversible ER stress, such as in disease states, the UPR shifts from being protective to pro-apoptotic, and multiple integrated apoptotic pathways can trigger cell death (**Figure 2**).

The UPR is mediated by three ER stress sensors; PKR-like endoplasmic reticulum kinase (PERK), inositol-requiring kinase 1 (IRE1), and activating transcription factor 6 (ATF6). These ER stress sensors are bound to the ER chaperone, BiP, under basal conditions, keeping them in an inactivated state. When ER stress arises, for example, there is an accumulation of misfolded proteins in the ER lumen, BiP dissociates from the ER stress sensors to preferentially bind the hydrophobic regions of the misfolded proteins, thus resulting in their activation (Rutkowski et al., 2006).

In one pathway, upon activation, PERK directly phosphorylates, and thus inhibits, the ubiquitous eukaryotic translation initiation factor 2α (eIF2α). As a consequence, there is a reduction in the entrance of newly synthesized proteins into the ER lumen, therefore reducing the load of ER protein-folding (Boyce et al., 2005). Phosphorylation of eIF2α also favors the selective translation of the mRNA encoding the transcription factor ATF4. ATF4 translocates to the nucleus where it induces the expression of ER chaperones, such as PDI, which increases refolding of misfolded proteins (Halperin et al., 2014). ATF4 also induces the expression of various genes involved in autophagy, antioxidant response, and amino acid biosynthesis and transport (Cao and Kaufman, 2012; Hetz and Mollereau, 2014).

A second pathway of the UPR is initiated by IRE1 which is activated upon its dimerization and auto-phosphorylation (Hetz, 2012). IRE1 degrades a subset of mRNAs which encode for ER-localized proteins by means of regulated IRE1 dependent decay (RIDD), thereby reducing protein synthesis in the ER (Cao and Kaufman, 2012). IRE1 also catalyses the splicing of the mRNA encoding transcription factor X-box binding protein 1 (XBP-1). This splicing removes a 26 base intron from XBP-1, resulting in a shift in the reading frame of its mRNA (Hetz and Mollereau, 2014). Spliced XBP-1 is a stable transcription factor

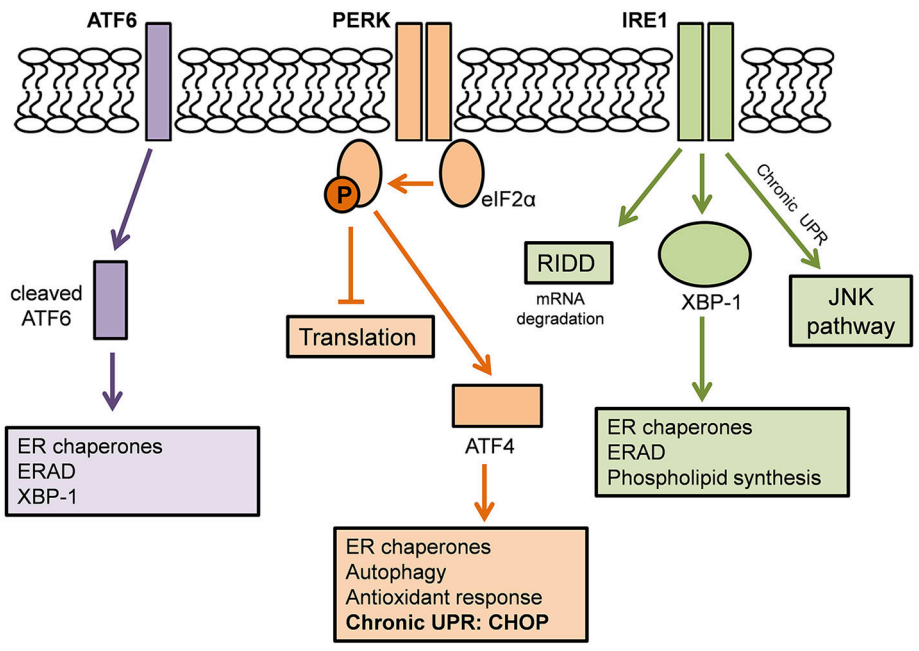

FIGURE 2 | The Unfolded Protein Response. Adapted from Hetz and Mollereau (2014). A schematic demonstrating the action of the three ER stress sensors on the Unfolded Protein Response.

which translocates to the nucleus to induce the upregulation of ER chaperones and proteins involved in the ER-associated degradation (ERAD) pathway. XBP-1 also controls phospholipid synthesis which is important for ER membrane expansion when the ER is under stress (Lee et al., 2003).

In a third pathway, upon UPR activation, ATF6 translocates from the ER membrane to the Golgi apparatus where it is cleaved by site-1 and site-2 proteases. The resulting cytosolic ATF6 fragment (ATF6f) translocates to the nucleus to induce gene expression of ER chaperones, ERAD components and XBP-1 (Schröder and Kaufman, 2005). Together, the ER stress sensors regulate the expression of a number of overlapping target genes, encoding for proteins which modulate adaptation to stress, thus promoting the survival of the cell.

Chronic Activation of the UPR

Under conditions of chronic or irreversible ER stress, such as those that occur in disease, there is a shift in the paradigm of the UPR from being pro-protective to pro-apoptotic. The UPR therefore induces apoptosis mediated by overlapping apoptotic signaling mechanisms (Ma and Hendershot, 2004). Sustained activation of the ER stress sensor PERK elicits a chain of transcriptional responses mediated by ATF4. ATF4 induces the upregulation of the transcription factor C/EBP-homologous protein (CHOP) and its target growth arrest and DNA damage-inducible 34 (GADD34). The promoter of CHOP contains the binding sites for several players of the UPR, including ATF4 and ATF6, and is a key mediator of ER stress induced apoptosis (Cao and Kaufman, 2012). CHOP can inhibit the expression of survival protein BCL-2 and simultaneously engage pro-apoptotic proteins such as Bcl2-interacting mediator of cell death (BIM) and p53 upregulated modulator of apoptosis (PUMA). The outcome is the activation of BAX- and BAK- dependent apoptosis at the mitochondria and the caspase cascade, which result in apoptosis of the cell (Soo et al., 2009; Hetz and Mollereau, 2014). Furthermore, CHOP induces ERO1α which causes oxidative stress by transferring electrons from PDI to O_2 to produce hydrogen peroxide. The activation of GADD34 results in the dephosphorylation of eIF2α, thus increasing protein synthesis and accentuating the ER and oxidative stress (Cao and Kaufman, 2012). IRE1 also plays a role in apoptosis of a cell through the recruitment of apoptosis signaling kinase (ASK1) which activates the c-Jun N-terminal kinase (JNK) pathway, which stimulates proinflammatory responses apoptotic pathways (Nishitoh et al., 2002), and also by direct interaction with BAX and BAK (Hetz et al., 2006). It is this apoptosis of cells which results in the degeneration of motor neurons characteristic of neurodegenerative diseases.

The UPR therefore constitutes a complex mechanism of integrated signaling pathways that responds to ER stress by either cellular adaptation, thus promoting the survival of the cell, or by triggering apoptosis. Similar to other aspects of neuronal ER biology, whilst the UPR is well-characterized in many cell types, its function in neurons is poorly understood (Wang and Kaufman, 2012) and the response of the UPR in the axonal and dendritic compartments remains uncharacterized. Similarly, it is unknown if the expression of UPR proteins is induced locally or somally in response to neuronal activity. Whilst mechanisms underlying the selective vulnerability of neurons to degeneration remain unknown, an interesting possibility is that the unique properties of the ER may contribute and render neurons particularly sensitive to ER stress. However, this possibility remains largely unexplored.

Protein Disulfide Isomerase

Structure and Expression of PDI

PDI is a 55kDa ER chaperone primarily localized in the ER (Ellgaard and Ruddock, 2005), however it has also been detected in the cytoplasm, nucleus and extracellularly in a biologically active state (Turano et al., 2002). PDI has four distinct domains within its structure; a, a', b, and b', with a highly acidic C-terminal extension and an x linker region (**Figure 3**). An ER-retention signal sequence (KDEL) lies at the C terminus (Hatahet and Ruddock, 2007). The a and a' domains are catalytic domains, similar to thioredoxin, which are separated by the two non-catalytic domains (b and b') (Hatahet and Ruddock, 2007), that only share 16.5% sequence identity (Xu et al., 2014). The catalytic domains contain an active site motif comprising two cysteine residues separated by glycine and histidine (Cys-Gly-His-Cys). The oxidoreductase activity of PDI relies on the thiol groups of these active site cysteines (Jessop et al., 2009). Each CGHC active site has a high disulfide reduction potential ($E^{\circ\prime} = -0.18$ V) and a low pK_a value ($pK_a = 6.7$) making it a competent oxidizing agent in the ER (Woycechowsky and Raines, 2000; Liu et al., 2013; **Figure 3**).

Functions of PDI

PDI has two major functions. Firstly, it is responsible for the oxidation (formation), reduction (break down) and isomerization (rearrangement) of protein disulfide bonds via disulfide interchange activity (illustrated in **Figure 4**). Secondly, PDI has general chaperone activity (Ferrari and Söling, 1999).

Disulfide interchange activity

The **a** and **a'** domains of PDI operate independently of one another, as disruption to one domain abolishes 50% of catalytic activity. However, disruption to the active site of both domains results in complete elimination of oxidoreductase activity (Xu et al., 2014). The redox state of the active site cysteine residues and the properties of its substrate determine whether PDI acts as an oxidase, reductase, or isomerase (Xu et al., 2014). In an oxidation reaction, whereby PDI mediates oxidative

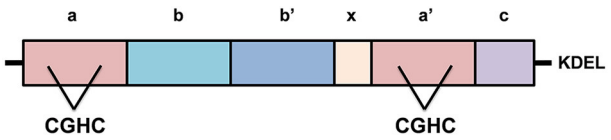

FIGURE 3 | The structure of Protein Disulfide Isomerase (PDI). PDI has four distinct domains, a, a', b, and b', as well as a linker region, "x", and its C-terminal extension with KDEL sequence. The catalytic domains, a and a', possess active sites containing the motif cysteine-glycine-histidine-cysteine (CGHC). KDEL, the ER retention signal sequence.

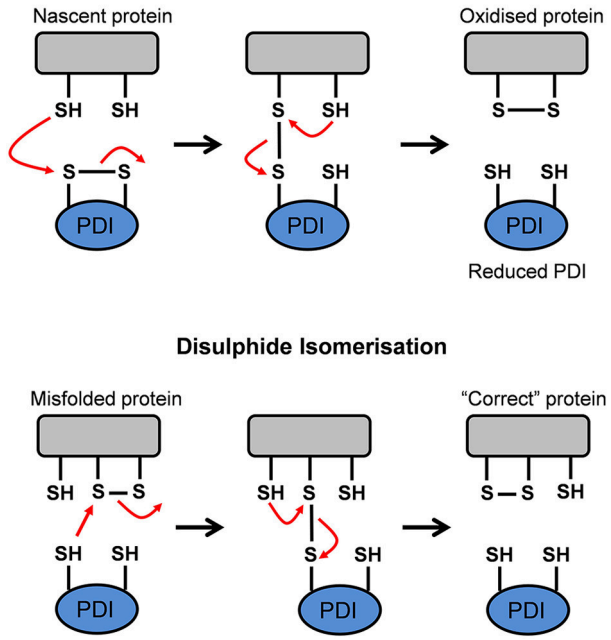

FIGURE 4 | Schematic representation of the disulfide interchange activity of Protein Disulfide Isomerase (PDI). PDI can form, break down, and rearrange disulfide bonds. This aids in promoting the formation of the native conformation in a misfolded or unfolded protein. Adapted from Forrester et al. (2006).

protein folding to form disulfide bonds in a nascent protein, the substrate dithiol is oxidized to a disulfide. The substrate's reduced cysteine thiols bind with the CGHC motif disulfide on PDI to form a PDI-protein complex. A second reduced thiol from the protein substrate interacts with the complex to produce an oxidized protein which is correctly folded and stabilized. Simultaneously, the active site disulfide in PDI is then reduced to the dithiol state (Forrester et al., 2006). When PDI is reduced after donating a disulfide bond to nascent proteins, it is subsequently reoxidized in the oxidizing environment of the ER. Alternatively, cellular regulators, such as endoplasmic reticulum oxidoreductin 1 (Ero1) interacts with, and reoxidises, the reduced PDI (Mezghrani et al., 2001; Medraño-Fernandez et al., 2014). Oxidative protein folding, however, is prone to error and incorrectly folded proteins can arise as part of normal physiology. Hence, non-native disulfide bonds need to be corrected via isomerization, or reduced to produce the native conformation (Wilkinson and Gilbert, 2004). In a reduction reaction, whereby PDI breaks down disulfide bonds in protein substrates, a substrate disulfide is reduced to the dithiol state, while an active site disulfide is formed in PDI. Reductants such as glutathione (GSH) and NADPH donate electrons to reduce the disulfide in PDI back to its dithiol state (Xu et al., 2014). When misfolded proteins form, isomerization of disulfide bonds is required to convert the disulfides to their native conformation. To facilitate isomerization, one of PDI's active sites must be in a reduced state (Medraño-Fernandez et al., 2014). Isomerization, or the rearrangement of disulfide bonds in a substrate protein, is initiated by the cysteine nearest the N-terminus at each PDI active site (CGHC). This cysteine binds a substrate disulfide which results in an intramolecular rearrangement within the substrate itself. Conversely, isomerization can be seen as repeated cycles of reduction and oxidation (Wilkinson and Gilbert, 2004). Ultimately, the impairment of PDI's activity can lead to the accumulation of misfolded proteins, resulting in ER stress and activation of the UPR (Forrester et al., 2006).

Chaperone function

Chaperone binding keeps proteins soluble and competent to fold in order to acquire their native structure (Kojer and Riemer, 2014). As a chaperone, PDI binds to misfolded proteins to prevent them from aggregating and targets misfolded proteins for degradation (Ma and Hendershot, 2004). Although all of the domains of PDI contribute to the binding of misfolded proteins, the **b'** domain comprises the principal substrate-binding site, utilizing hydrophobic interactions to exhibit high affinity and broad specificity (Xu et al., 2014).

S-Nitrosylation of PDI

Cellular redox states normally regulate cellular function and maintain homeostasis, but when redox homeostasis is disturbed, neurodegeneration can result. The ER is able to withstand mild insults of stress, however a build-up of reactive oxidative species (ROS) and reactive nitrogen species can result in oxidative and nitrosative stress in the ER (Halloran et al., 2013). Neurons are particularly vulnerable to redox dysregulation due to their large size and high oxygen consumption (Parakh et al., 2013). In addition, normal antioxidant defenses usually decline during the normal aging process and hence nitrosative and oxidative stress increases, thus rendering neurons susceptible to age-related degenerative conditions (Halloran et al., 2013). The excessive generation of nitric oxide (NO) has been implicated in AD, PD, and ALS (Forrester et al., 2006). In AD, elevated levels of oxidative and nitrosative stress are associated with alterations in amyloid-β metabolism (Mangialasche et al., 2009).

In conditions of elevated nitrosative stress, the active sites of PDI undergo an aberrant post-translational modification—S-nitrosylation—which prevents its normal enzymatic function (Forrester et al., 2006). Specifically, s-nitrosylation is the covalent addition of a nitric monoxide group to a cysteine thiol on PDI's active site, hence inhibiting its normal protective function, and resulting in the accumulation of misfolded proteins (Forrester et al., 2006). Uehara et al. (2006) demonstrated that PDI is s-nitrosylated in AD and PD patient brains, but not in that of healthy controls. Similarly, s-nitrosylated PDI levels in the lumbar spinal cords of ALS patients were approximately 5-fold greater compared to those of controls (Walker et al., 2010). S-nitrosylated PDI was also reported both in the brains of PrP^{Sc} infected rodents and in cell models of CJD bearing PrP^{Sc} misfolded proteins (Wang et al., 2012). Wu et al. (2014) investigated the effects of methamphetamine in cellular

models of PD on the basis that methamphetamine users pose a higher risk of developing neurodegenerative disorders. A significant increase in the levels of nitric oxide synthase (NOS), NO and α-synuclein 24 h after methamphetamine treatment was reported in these cells (Wu et al., 2014). These changes to the nitrosative state of the cells resulted in the augmented aggregation of α-synuclein and the s-nitrosylation of PDI, suggesting that PDI could be a potential target to prevent methamphetamine-induced neurodegeneration (Wu et al., 2014). Furthermore, S-nitrosylated PDI was detected following ischemia/reperfusion injury and the levels increased with the formation of mutant SOD1 aggregates in primary astrocytes (Chen et al., 2012). Similarly, S-NO PDI correlates with synphilin misfolding in Parkinson disease (Forrester et al., 2006). S-nitrosylation is also involved in the re-distribution of PDI away from the ER by reticulons which maintain the curvature of the ER (Bernardoni et al., 2013). The deletion of reticulon 4A is protective in mouse models of ALS (Yang et al., 2009).

PDI Family Members

The PDI family contains over 21 structurally-related members that constitutes a network of proteins which promote the oxidative folding of multi-disulfide proteins (Kojima et al., 2014; selected members are highlighted in **Figure 5**). All members contain two or more thioredoxin-like active sites and the majority of members in this family also act as chaperones (Turano et al., 2002). The most common active site motif amongst PDI family members is CGHC, which is present in PDI, ERp57, and ERp72 (**Figure 4**). ERp57 is the closest known homolog of PDI. It has the same domain structure as PDI, but it lacks the C-terminal acidic region (Frickel et al., 2004).

EVIDENCE FOR INDUCTION OF THE UPR IN NEURODEGENERATIVE DISEASES

There is increasing evidence that activation of the UPR is a feature of most neurodegenerative disorders. The most obvious association between ER stress and neurodegeneration is via chronic UPR activation during disease, thus triggering apoptosis and neuronal cell death. The up-regulation of UPR markers in disease-affected neurons has now been described in cellular and animal models of disease, as well as in post-mortem human tissues, for most of these disorders. The initial participation of the UPR in pathogenesis might be neuroprotective as has been proposed in recent studies, but sustained activation of the UPR may subsequently initiate or accelerate neurodegeneration. In some instances the misfolded proteins are present within the cytoplasm rather than the ER, and can trigger ER stress by indirect mechanisms, that nevertheless disrupt ER homeostasis (Nishitoh et al., 2008; Atkin et al., 2014). Together, these studies suggest that the UPR pathway may be a potential therapeutic target for neurodegenerative diseases. Recent developments in the use of human neurons derived from reprogrammed induced pluripotent stem cells (iPSCs) provide a useful tool to unravel pathological mechanisms in these disorders, and ER stress and activation of the UPR are increasingly implicated in these studies (**Table 2**).

Alzheimer's Disease

Whilst initial reports were contradictory, there is now convincing evidence for ER stress and UPR activation in AD, with recent studies suggesting that ER stress has a fundamental role in AD etiology. Hoozemans et al. (2005) demonstrated that the expression of ER chaperone, BiP, and the activated, phosphorylated form of UPR sensor PERK, were significantly increased in the temporal cortex and hippocampus in AD patients compared to controls. Furthermore, in a later study the same group reported upregulation of PERK, IRE1 and eIF2α in neurons of the hippocampus in AD patients; in particular, in neurons with granulovacuolar degeneration (Hoozemans et al., 2009). Evidence for pro-apoptotic UPR in AD was reported by Ghribi et al. (2004), when CHOP and JNK were up-regulated in animal disease models. Similarly, CHOP activation was detected in neuronal cells treated with Aβ (Chafekar et al., 2008). Lee and colleagues (2010a) detected increased levels of

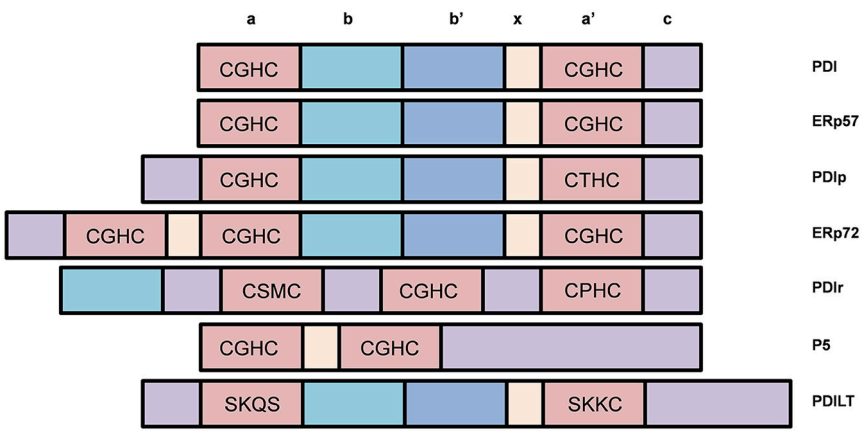

FIGURE 5 | Selected members of the Protein Disulfide Isomerase (PDI) family of chaperones and representation of their different domains. Most PDI family members possess disulfide interchange activity and many contain the CGHC motif similar to that of PDI.

TABLE 2 | Evidence for ER stress and the role of PDI in neurodegenerative diseases.

Neurodegenerative disease	Protein inclusions	Evidence for ER stress	Evidence for a role of PDI
Alzheimer's disease (AD)	β-Amyloid Tau	BiP, PERK, IRE1, and eIF2α upregulated in AD patients (Hoozemans et al., 2005, 2009). Cleaved caspases and JNK upregulated in AD patients (Ghribi et al., 2004; Lee et al., 2010a). CHOP upregulated in AD animal models and cell models treated with β-amyloid, and in AD patients (Ghribi et al., 2004; Chafekar et al., 2008; Lee et al., 2010a). IPSC-derived neurons and astrocytes from AD patients accumulate Aβ oligomers (Kondo et al., 2013).	PDI co-localizes with tau protein (Honjo et al., 2010). PDI levels increase 9.49 fold in tangle-bearing neurons in AD patients (Lee et al., 2010a). β-amyloid co-localizes with ERp57 (Erickson et al., 2005). Pharmacological activation of ERp57 reduces amyloid plaques and neurofibrillary tangles in brains, and improved object recognition memory in AD mouse models (Tohda et al., 2012).
Parkinson's disease (PD)	α-Synuclein	Upregulation of IRE1, PERK, eIF2α, and ATF4 in PD cell models (Ryu et al., 2002). Phosphorylated PERK and phosphorylated eIF2α detected in dopaminergic neurons of PD patients (Hoozemans et al., 2007). Co-localization of phosphorylated PERK and α-synuclein in dopaminergic neurons (Hoozemans et al., 2007). CHOP upregulation in dopaminergic neurons of mouse models and in cell models (Ryu et al., 2002; Holtz and O'Malley, 2003; Silva et al., 2005).	Upregulation of PDIA2 in PD cell models and post-mortem brain tissues of PD patients (Conn et al., 2004). PDIA2 immunoreactivity evident in Lewy Bodies (Conn et al., 2004). PDI upregulated in PD cell models (Ryu et al., 2002).
Amyotrophic lateral sclerosis (ALS)	SOD1 TDP-43 FUS C9orf72	UPR and CHOP induced prior to symptom onset in $SOD1^{G93A}$ mouse models (Atkin et al., 2006; Kikuchi et al., 2006; Saxena et al., 2009). PERK, IRE1 and ATF6 upregulated in post-mortem human spinal cord tissues (Atkin et al., 2008). Deletion of BIM, XBP-1, ASK1, Puma or ATF4 delays disease onset or extends survival in ALS mouse models (Kieran et al., 2007; Nishitoh et al., 2008; Hetz et al., 2009; Matus et al., 2013a,b). Pharmacological inhibition of eIF2α dephosphorylation extends survival of ALS mouse models (Boyce et al., 2005; Saxena et al., 2009).	PDI upregulated in $SOD1^{G93A}$ mouse models at presymptomatic, symptomatic and end stages of disease (Atkin et al., 2006, 2008). PDI co-localizes with inclusions in ALS mouse models, cell models and ALS patients (Atkin et al., 2006, 2008; Tsuda et al., 2008; Honjo et al., 2011; Farg et al., 2012; Walker et al., 2013). PDI and ERp57 upregulated in ALS patient and mouse model spinal cord tissues and patient CSF (Atkin et al., 2006, 2008). PDI over expression decreases mutant SOD1 inclusion formation, BiP and CHOP expression and PERK phosphorylation in ALS cell models (Walker et al., 2010). PDI knock down increases mutant SOD1 inclusion formation in ALS cell models (Walker et al., 2010).
Huntington's disease (HD)	Huntingtin	BiP and CHOP upregulated in post-mortem brains from HD patients and in HD cell models (Duennwald and Lindquist, 2008; Carnemolla et al., 2009). BIM upregulated in HD animal and cells models (García-Martínez et al., 2007; Kong et al., 2009; Leon et al., 2010). XBP-1 upregulated in striatum of HD patients (Vidal et al., 2012). XBP-1 knock down reduced neuron loss and mHtt levels, and improved motor performance in HD mouse models (Vidal et al., 2012).	Increased basal expression of PDI in HD cell models (Duennwald and Lindquist, 2008). PDI elevated in hippocampus of HD mouse models (Safren et al., 2014).
Creutzfeldt-Jakob disease (CJD)	Prion protein	Upregulation of caspase-12 in CJD cell models and post-mortem patient cortex tissues (Hetz et al., 2003). Upregulation of ERp57, Grp94 and BiP in HD cell models and patient cortex tissues (Hetz et al., 2003). Increased intracellular calcium release from the ER (Torres et al., 2010).	PDI overexpression in brains of CJD patients (Yoo et al., 2002). Increased expression of ERp57 (Hetz et al., 2005). ERp57 overexpression protects cells from PrP^{SC} toxicity and decreases rate of caspase-12 activation (Hetz et al., 2005).

cleaved caspase-12, cleaved caspase-3, cleaved caspase-4, and CHOP in the temporal cortex of AD patients. *In vitro* studies involving neuronal cells in culture exposed to Aβ oligomers, suggested that the ensuing activation of ER stress correlates with the induction of Tau phosphorylation, thus providing an interesting link between ER stress, Aβ-mediated neurotoxicity and Tau hyperphosphorylation (Resende et al., 2008; Ferreiro and Pereira, 2012). However, whilst UPR activation can induce Tau phosphorylation, Tau phosphorylation may not activate ER stress (Sakagami et al., 2013). Modulation of the UPR can also be protective in AD cellular and animal models. PERK knockdown in neuronal cells enhanced Aβ toxicity through reduced activation of eIF2α (Lee et al., 2010b). Furthermore, activating the eIF2α pathway with Salubrinal significantly reduced caspase-4 dependent apoptosis in Aβ treated neurons (Lee et al., 2010b). These results suggest that the PERK-eIF2α pathway may play a role in cell survival, rather than apoptosis during ER stress. Interestingly, pathological events described in AD, such as neurofibrillary tangles, neuroinflammation, altered calcium signaling, and excitotoxicity, were also recently linked to the occurrence of pathological ER stress (Cornejo and Hetz, 2013). Similarly, IPSC-derived neurons and astrocytes from APP-linked familial and sporadic AD patients accumulated Aβ oligomers, leading to ER and oxidative stress (Kondo et al., 2013). ER stress was recently shown to promote cholesterol synthesis and mitochondrial cholesterol trafficking in AD mouse models (Barbero-Camps et al., 2014). It has also been proposed that ER stress may interfere with the normal trafficking of APP through the normal secretory pathway, leading to the production of Aβ, and subsequent toxicity (Plácido et al., 2014).

Parkinson's Disease

There is compelling evidence that ER stress is linked to death of dopamine neurons in PD, although most of this has been obtained from cell culture studies. However, in the substantia nigra of PD patients, Hoozemans et al. (2007) demonstrated immunoreactivity for PERK and eIF2α in their phosphorylated, active forms in dopaminergic neurons. Moreover, phosphorylated PERK was co-localized with increased α-synuclein immunoreactivity in dopaminergic neurons, suggesting a close association between UPR activation and the aggregation of α-synuclein (Hoozemans et al., 2007). Ryu et al. (2002) demonstrated that IRE1 and PERK were up-regulated in cell culture models that mimic the selective dopaminergic neuron degeneration that occurs in PD, as well as downstream targets, eIF2α, ATF4 and CHOP. Holtz and O'Malley (2003) screened dopaminergic neuroblastoma MN9D cells exposed to either 6-OHDA or MPP^+ and noted that the most highly expressed transcript in both cases encodes for CHOP. Supporting this finding, Silva et al. (2005) demonstrated induction of CHOP in dopamine neurons of the substantia nigra in mouse models following intrastriatal injection of 6-OHDA (Silva et al., 2005). Similarly, overexpression of BiP or pharmacological modulation of the UPR in α-synuclein transgenic mice was protective (Colla et al., 2012; Gorbatyuk et al., 2012). More recently, cortical neurons generated from iPS cells of patients with α-synuclein mutations, identified ER stress as an early pathogenic phenotype (Chung et al., 2013). Interestingly, another recent study detected aberrant modification of ER stress sensors IRE1α and PERK by NO-mediated S-nitrosylation, in cell based models of PD. This resulted in loss of normal enzymatic function, leading to dysfunctional ER stress signaling and neuronal cell death Nakato et al. (2015). In contrast, other studies have demonstrated that some aspects of the UPR may be protective in PD. Overexpression of XBP-1 in MPP^+-induced cell models was protective by suppressing apoptosis in cells exposed to proteasome inhibitors (Sado et al., 2009). Similarly, transplanting neural stem cells into the right lateral ventricles of rodents with rotenone-induced PD resulted in higher rates of survival in XBP-1 transfected neural stem cells compared to non-transfected cells (Si et al., 2012). Additionally, dopamine levels in the substantia nigra were significantly increased, α-synuclein expression was decreased, and neurological symptoms were significantly improved, following the transplantation of XBP-1 transfected neural stem cells (Si et al., 2012). The results of these studies suggest that XBP-1 enhancement is a possible therapeutic strategy for PD.

Amyotrophic Lateral Sclerosis

Activation of the UPR is now well documented in cellular and animal models of ALS and in human patient tissues. Studies of transgenic mice expressing mutant $SOD1^{G93A}$, a widely used disease model, revealed that UPR sensors, chaperones and apoptotic effectors were up-regulated in lumbar spinal cords during disease (Atkin et al., 2006; Kikuchi et al., 2006). Furthermore, the UPR was induced 60 days prior to symptom onset, and was present initially in those subtypes of motor neurons that degenerate first in ALS, indicating an active role for ER stress in pathogenesis (Saxena et al., 2009). Whilst SOD1 mutations represent only 2% of all ALS, and may not accurately represent pathology in the more common forms of disease, similar findings were obtained in post-mortem human spinal cord tissues of sporadic ALS patients (Ilieva et al., 2007; Atkin et al., 2008; Ito et al., 2009), thus placing ER stress on a more generic pathophysiology for ALS. For example, PERK, IRE1, and ATF6 are all upregulated in post-mortem human spinal cord tissues (Atkin et al., 2008). More recently, ER stress has been detected in neuronal cells expressing ALS-associated mutants of FUS and TDP-43 (Farg et al., 2012; Walker et al., 2013) and in animal models based on TDP-43 (Walker et al., 2013). Similarly, the UPR is induced in cell culture by ALS-associated mutant VAPB (Suzuki et al., 2009) and hexanucleotide repeat expansions in C9ORF72 (Zhang et al., 2014). Several mechanisms have been proposed for induction of ER stress in ALS, including impairment of ERAD by binding to Derlin-1 (Nishitoh et al., 2008) or impairment of protein transport between the ER and Golgi apparatus (Sundaramoorthy et al., 2013; Atkin et al., 2014). These studies implicate triggering of ER stress from the cytoplasm rather than the ER, although mutant TDP-43 and mutant FUS were recently shown to be associated with the ER (Soo et al., 2015) The same study also demonstrated that overexpression of Rab1, an intracellular vesicle trafficking

regulator which plays a central role in UPR homeostasis, prevented ER stress in cells expressing mutant SOD1, TDP-43 and FUS. Furthermore, the presence of Rab1-positive inclusions in the motor neurons of human spinal cord tissues from sALS patients implies that Rab1 is misfolded and loses its normal vesicular distribution in sALS (Soo et al., 2015). Interestingly, Rab1 dysfunction has also been linked to PD (Cooper et al., 2006). In more recent studies, using reprogrammed IPS cells, ER stress was closely associated with the electrical excitability of motor neurons (Kiskinis et al., 2014), and that hyperexcitability may trigger ER stress (Wainger et al., 2014).

Several studies have demonstrated that modulation of the UPR genetically is protective in animal models of ALS. Deletion of BIM, XBP-1, ASK1, Puma or ATF4 either delays disease onset (Kieran et al., 2007; Matus et al., 2013a,b) or extends survival in transgenic mutant SOD1 mice (Nishitoh et al., 2008; Hetz et al., 2009). Similarly, pharmacological modulation of the UPR is protective in $SOD1^{G93A}$ mice (Saxena et al., 2009), and either *C.elegans* and zebrafish expressing mutant TDP-43 (Vaccaro et al., 2013). However, $SOD1^{G85R}$ mice with hemizygous deletion of PERK had a substantially accelerated disease onset and shortened lifespan compared to $SOD1^{G85R}$/$PERK^{+/+}$ controls (Wang et al., 2011), indicating that some aspects of UPR induction are protective against disease. Similarly, pharmacological inhibition of eIF2α dephosphorylation using salubrinal delays disease and extends survival of $SOD1^{G93A}$ mice (Boyce et al., 2005; Saxena et al., 2009) and decreased GADD34 slows disease progression and extends survival in this animal model (Wang et al., 2013). Together, these findings imply that PERK is a mediator of motor neuron survival in ALS, possibly by decreasing protein misfolding (Wang et al., 2011, 2013) or by inducing autophagy (Hetz et al., 2009). These results therefore highlight the opposing protective and pro-apoptotic properties of the UPR and suggest that selective targeting of specific components of the UPR could be beneficial in ALS.

Huntington's Disease

Evidence of induction of ER stress in human HD patients was provided by Carnemolla et al., where BiP and CHOP were up-regulated in post-mortem brains from HD patients (Carnemolla et al., 2009). Similarly, increased expression of XBP-1 was detected in the striatum of HD cases, although other markers (CHOP, ATF4, and GRP78) were not elevated (Vidal et al., 2012). ER stress is also detected early in HD mouse models and persists throughout the lifespan of these animals, similar to ALS rodent models (García-Martínez et al., 2007; Duennwald and Lindquist, 2008; Carnemolla et al., 2009). Duennwald and Lindquist (2008) demonstrated that in a striatal cell line derived from Htt knock-in mice, increased basal expression of UPR proteins BiP, CHOP and PDI was observed compared with control cells (Duennwald and Lindquist, 2008). The same study showed that toxic polyglutamine expansion repeats impaired ERAD and degradation pathways (Duennwald and Lindquist, 2008). This suggests that the polyglutamine repeat expansion of mutant Huntingtin compromises the proteasomal degradation of misfolded proteins in the ER, thus giving rise to ER stress. The induction of the pro-apoptotic protein BIM has also been linked to HD in both animal (García-Martínez et al., 2007) and cellular disease models (Kong et al., 2009; Leon et al., 2010). Additionally, caspase-12 and the JNK pathway were activated in cells expressing expanded polyglutamine aggregates. These data together suggest ER stress is linked to cell death in HD (Kouroku et al., 2002). ER stress has also been linked to motor phenotypes in HD. Silencing XBP-1 expression in mutant Htt (mHtt) transgenic mouse strain YAC128 reduced the loss of neurons in the striatum, decreased mHtt levels, and improved motor performance (Vidal et al., 2012). Conversely, ATF4 deficiency did not alter mHtt levels, highlighting the involvement of XBP-1 in HD pathogenesis (Vidal et al., 2012). Hence, whilst the XBP-1 pathway of the UPR is protective in PD, the opposite appears to be true in HD.

Creutzfeldt-Jakob Disease

Upregulation of caspase-12, ERp57, Grp94, and BiP was described by Hetz and colleagues in the cortex of post-mortem sporadic CJD and variant CJD patients compared to controls (Hetz et al., 2003). However, whether caspase-12 plays a role in neurodegeneration is controversial. Nevertheless, in neuronal cell cultures, PrP^{Sc} toxicity in CJD is associated with an increase in the release of intracellular calcium from the ER and the upregulation of ER chaperones, indicating a role for ER stress in prion diseases (Hetz et al., 2003; Torres et al., 2010). Similarly, prion replication and the expression of mutant PrP dysregulated ER calcium homeostasis, giving rise to ER stress in cell culture (Torres et al., 2010). Finally, another study showed that treatment of Neuro-2A cells with PrP^{Sc} resulted in the activation and upregulation of caspase-12 and significant upregulation of ER chaperones, ERp57, Grp94, and BiP (Hetz et al., 2003).

PDI IN NEURODEGENERATIVE DISEASES

As PDI can facilitate protein folding, it is not surprising that PDI is increasingly implicated in neurodegenerative diseases where protein misfolding is a key component (summarized in **Table 2**). PDI is often found co-localized with misfolded proteins in disease-affected tissues, implying a possible role for PDI in preventing protein misfolding (Atkin et al., 2006; Honjo et al., 2010, 2011; Farg et al., 2012; Walker et al., 2013). In some diseases, there is direct evidence that PDI prevents aggregation and associated-toxicity, thus raising the likelihood that PDI is a possible therapeutic target in neurodegeneration. Interestingly, a recent study provided evidence that PDI family member Erp57 can also mediate neurite outgrowth in neurons, thus adding further complexity to the functions of PDI in relation to neurodegeneration (Castillo et al., 2015). However, PDI is often S-nitrosylated in these disorders, which would prevent its normally protective function (Uehara et al., 2006).

PDI in Alzheimer's Disease

Honjo et al. (2010) identified neurofibrillary tangles in the brains of patients with AD in which PDI was co-localized with tau. The levels of PDI were also markedly increased (up to 9.5 fold) in neurofibrillary tangle-bearing neurons in AD brains compared with those of age-matched controls and immunohistochemistry

showed that PDI was primarily expressed in temporal cortex neurons in AD patients (Lee et al., 2010a). Immunoblotting studies of cerebrospinal fluid (CSF) from control patients indicated that a vast concentration of β-amyloid is normally bound to ERp57, forming a ERp57-β-amyloid complex (Erickson et al., 2005). This finding therefore implies that PDI family members normally prevent the aggregation of β-amyloid. Consistent with this notion, pharmacological activation of ERp57 using Disogenin significantly reduced amyloid plaques and neurofibrillary tangles in the cerebral cortex and hippocampus of a mouse model of AD, in which five familial AD human APP mutations were co-expressed (Tohda et al., 2012). Moreover, performance of object recognition memory was significantly improved in this mouse model, providing further evidence for a protective role for ERp57 (Tohda et al., 2012).

PDI in Parkinson's Disease

Conn et al. (2004) demonstrated an upregulation of PDI family member PDIA2 in SH-SY5Y human neuroblastoma cells exposed to MPP^+, but not other family members PDI, ERp57 and ERp72. Similarly, PDIA2 was upregulated in post-mortem brain tissues from PD patients and immunohistochemical studies demonstrated that PDIA2 immunoreactivity was evident in Lewy bodies of these patients (Conn et al., 2004). Unlike in SH-SY5Y cells, PDI is upregulated in PC12 cells exposed to MPP^+, rotenone and 6-Hydroxydopamine (Ryu et al., 2002).

PDI in Amyotrophic Lateral Sclerosis

PDI is upregulated in the spinal cords of $SOD1^{G93A}$ mouse models of ALS at presymptomatic (p60), symptomatic (p90), and end stages (p120) of disease, and in human patient spinal cords (Atkin et al., 2006, 2008). Similarly, ERp57 is upregulated in $SOD1^{G93A}$ mouse models at similar time points and in human patient tissues (Atkin et al., 2006). Furthermore, PDI associates with abnormal inclusions in $SOD1^{G93A}$ mouse models and neuronal cells in culture (Atkin et al., 2006), as well as in ALS patients (Atkin et al., 2008). PDI also co-localizes with inclusions formed by other ALS-linked proteins, TDP-43 (Honjo et al., 2011; Walker et al., 2013), FUS (Farg et al., 2012) and vesicle associated membrane protein (VAPB) (Tsuda et al., 2008), implying that PDI is linked to general protein misfolding in ALS. PDI over-expression decreased mutant SOD1 aggregation and inclusion formation in neuronal cells and decreased BiP and CHOP expression as well as PERK phosphorylation, in comparison to controls, indicating that PDI is also protective against ER stress (Walker et al., 2010). Furthermore, knock down of PDI increased the formation of mutant SOD1 inclusions (Walker et al., 2010). These data together suggest a protective role for PDI against abnormal protein aggregation and ER stress in ALS. This neuroprotection is further supported by the deletion of a PDI regulator, Reticulon-4A, which accelerates the degeneration of motor neurons in SOD1 mice models (Yang et al., 2009). Quantitative western blotting also revealed an upregulation of PDI in the CSF of ALS patients in comparison to controls (Atkin et al., 2008). This finding may explain why PDI is subsequently found in numerous cellular locations and secreted by various cell types, instead of being localized exclusively to the ER (Turano et al., 2002).

The profile of PDI in ALS has increased recently by the identification of PDI variants as a genetic risk factor for the disease. Kwok et al. (2013) reported that single nucleotide polymorphisms (SNPs) in the P4HB gene encoding PDI were associated with fALS and sALS. They reported significant genotypic associations for two SNPS, rs876016, and rs2070872, in fALS and significant allelic associations for rs876016 with both sporadic and familial forms, suggesting that these SNPs are risk factors for ALS (Kwok et al., 2013). Additionally, a more recent study by Yang and Guo (2015) examined these same two SNPs in sALS patients in the Chinese Han population. They demonstrated a significant association of these SNPs with sALS, implying that genetic variants in the P4HB gene may be a contributing factor for sporadic forms of ALS in the Chinese Han population. A further study by Gonzalez-Perez et al. (2015) identified 16 variants in PDI and ERp57, with 1-2% present in all fALS and 1% present in all sALS cases analyzed. This frequency is similar to that of other ALS-linked gene variants (Turner et al., 2013). Structural analysis of PDI variants predicted a change in the catalytic functioning of these proteins, and changes in the structure of ERp57 variants are thought to affect the calnexin-calreticulin cycle (Gonzalez-Perez et al., 2015).

PDI in Other Neurodegenerative Diseases

Upregulation of PDI is also implicated in HD and prion encephalopathies. Cells expressing polyglutamine expansion Htt repeats exhibited elevated PDI levels when compared to control cells expressing Htt with 25 repeats (Duennwald and Lindquist, 2008). Similarly, PDI was elevated in the hippocampus of transgenic mouse models of HD when compared to wildtype mice (Safren et al., 2014).

Yoo et al. (2002) observed an overexpression of PDI in the brains of CJD patients. Hetz et al. (2005) observed an upregulation of ERp57 in PrP^{sc} toxicity and also reported that ERp57 overexpression protected cells against PrP^{sc} toxicity and decreased the rate of caspase-12 activation (Hetz et al., 2005). Similarly, inhibition of ERp57 expression led to a significant increase in PrP^{sc} toxicity (Hetz et al., 2005). A study by Wang et al. (2012) evaluated the levels of some PDI family members in brain tissues of rodents infected with scrapie strain 263K. Western blot analysis revealed a significant upregulation in the expression of PDI, ERp57 and BiP, and a significant decrease in the levels of caspase-3. Increases in PDI and BiP were also observed in cells expressing PrP mutants, and furthermore, overexpression of PDI reduced ER stress and cytotoxicity in these cell models (Wang et al., 2012).

Recent Developments in PDI Function Associated with Neurodegeneration

Although PDI is generally associated with a protective effect in maintaining proteostasis, recent studies have suggested that in some circumstances, PDI activity can be detrimental and can even trigger apoptosis. This pro-apoptotic function of PDI is specifically associated with the presence of misfolded proteins:

expression of mutant huntingtin resulted in accumulation of PDI at ER-mitochondrial junctions and apoptotic cell death (Hoffstrom et al., 2010). Furthermore, inhibitors specifically targeting PDI reduced cellular toxicity induced by mutant Huntington (Hoffstrom et al., 2010). These data therefore point to a novel mechanism linking protein misfolding to apoptotic cell death induced by PDI. Other recent studies suggest that PDI can induce oxidative stress. PDI interacts with NADPH oxidase and overexpression of PDI leads to increased levels of ROS and apoptosis (Paes et al., 2011). Over-expression of PDI also appears to induce oxidative stress in microglial cells in $SOD1^{G93A}$ mice (Jaronen et al., 2013). The S-nitrosylation of PDI is also associated with potentially damaging consequences. Wang et al. (2012) found that S-NO PDI plays an essential role in the cytotoxicity induced by PDI. The opposing effects of PDI, both protective and harmful, were recently reviewed, and the reader is directed to this for further information (Parakh and Atkin, 2015).

CONCLUSION

ER stress has been widely studied in neurodegenerative diseases, and emerging evidence highlights the complexity of the UPR in these disorders, with both protective and detrimental components being described. Despite having different clinical manifestations, neurodegenerative diseases are similar in pathology; that is, an accumulation of misfolded proteins in neurons and subsequent disruption to cellular proteostasis. The PDI proteins are a large family of chaperones with complex functions which offer the potential to be exploited therapeutically in the future. However, the great complexity of the ER within neurons, particularly in the dendrite and axonal compartments, is only just becoming realized. Further studies in this area are warranted before the true contribution of the UPR and ER homeostasis to pathology can be appreciated.

AUTHOR CONTRIBUTIONS

EP wrote the manuscript with additional contributions and revisions from the other authors.

FUNDING

This work was supported by funding from the National Health and Medical Research Council of Australia (Project grants 1006141, 1030513, and 1086887) and the Motor Neurone Disease Research Institute of Australia, Angie Cunningham Laugh to Cure MND Grant. EP is supported by an Australian Postgraduate Award scholarship.

REFERENCES

Atkin, J. D., Farg, M. A., Soo, K. Y., Walker, A. K., Halloran, M., Turner, B. J., et al. (2014). Mutant SOD1 inhibits ER−Golgi transport in amyotrophic lateral sclerosis. *J. Neurochem.* 129, 190–204. doi: 10.1111/jnc.12493

Atkin, J. D., Farg, M. A., Turner, B. J., Tomas, D., Lysaght, J. A., Nunan, J., et al. (2006). Induction of the unfolded protein response in familial amyotrophic lateral sclerosis and association of protein-disulfide isomerase with superoxide dismutase 1. *J. Biol. Chem.* 281, 30152–30165. doi: 10.1074/jbc.M603393200

Atkin, J. D., Farg, M. A., Walker, A. K., McLean, C., Tomas, D., and Horne, M. K. (2008). Endoplasmic reticulum stress and induction of the unfolded protein response in human sporadic amyotrophic lateral sclerosis. *Neurobiol. Dis.* 30, 400–407. doi: 10.1016/j.nbd.2008.02.009

Barbero-Camps, E., Fernández, A., Baulies, A., Martinez, L., Fernández-Checa, J. C., and Colell, A. (2014). Endoplasmic reticulum stress mediates amyloid β neurotoxicity via mitochondrial cholesterol trafficking. *Am. J. Pathol.* 184, 2066–2081. doi: 10.1016/j.ajpath.2014.03.014

Bernardoni, P., Fazi, B., Costanzi, A., Nardacci, R., Montagna, C., Filomeni, G., et al. (2013). Reticulon1-C modulates protein disulphide isomerase function. *Cell Death Dis.* 4, e581. doi: 10.1038/cddis.2013.113

Boyce, M., Bryant, K. F., Jousse, C., Long, K., Harding, H. P., Scheuner, D., et al. (2005). A selective inhibitor of eIF2α dephosphorylation protects cells from ER stress. *Science* 307, 935–939. doi: 10.1126/science.1101902

Brundin, P., Melki, R., and Kopito, R. (2010). Prion-like transmission of protein aggregates in neurodegenerative diseases. *Nat. Rev. Mol. Cell Biol.* 11, 301–307. doi: 10.1038/nrm2873

Cao, S. S., and Kaufman, R. J. (2012). Unfolded protein response. *Curr. Biol.* 22, R622–R626. doi: 10.1016/j.cub.2012.07.004

Carnemolla, A., Fossale, E., Agostoni, E., Michelazzi, S., Calligaris, R., De Maso, L., et al. (2009). Rrs1 is involved in endoplasmic reticulum stress response in Huntington disease. *J. Biol. Chem.* 284, 18167–18173. doi: 10.1074/jbc.M109.018325

Castillo, V., Oñate, M., Woehlbier, U., Rozas, P., Andreu, C., Medinas, D., et al. (2015). Functional role of the disulfide isomerase ERp57 in axonal regeneration. *PLoS ONE* 10:e0136620. doi: 10.1371/journal.pone.0136620

Chafekar, S. M., Zwart, R., Veerhuis, R., Vanderstichele, H., Baas, F., and Scheper, W. (2008). Increased Aβ1-42 production sensitizes neuroblastoma cells for ER stress toxicity. *Curr. Alzheimer Res.* 5, 469–474. doi: 10.2174/156720508785908883

Chartier-Harlin, M.-C., Kachergus, J., Roumier, C., Mouroux, V., Douay, X., Lincoln, S., et al. (2004). α-synuclein locus duplication as a cause of familial Parkinson's disease. *Lancet* 364, 1167–1169. doi: 10.1016/S0140-6736(04)17103-1

Chen, X., Guan, T., Li, C., Shang, H., Cui, L., Li, X.-M., et al. (2012). SOD1 aggregation in astrocytes following ischemia/reperfusion injury: a role of NO-mediated S-nitrosylation of protein disulfide isomerase (PDI). *J. Neuroinflammation* 9:237. doi: 10.1186/1742-2094-9-237

Chung, C. Y., Khurana, V., Auluck, P. K., Tardiff, D. F., Mazzulli, J. R., Soldner, F., et al. (2013). Identification and rescue of α-synuclein toxicity in Parkinson patient–derived neurons. *Science* 342, 983–987. doi: 10.1126/science.1245296

Colla, E., Coune, P., Liu, Y., Pletnikova, O., Troncoso, J. C., Iwatsubo, T., et al. (2012). Endoplasmic reticulum stress is important for the manifestations of α-synucleinopathy *in vivo*. *J. Neurosci.* 32, 3306–3320. doi: 10.1523/JNEUROSCI.5367-11.2012

Conn, K. J., Gao, W., Mckee, A., Lan, M. S., Ullman, M. D., Eisenhauer, P. B., et al. (2004). Identification of the protein disulfide isomerase family member PDIp in experimental Parkinson's disease and Lewy body pathology. *Brain Res.* 1022, 164–172. doi: 10.1016/j.brainres.2004.07.026

Cooper, A. A., Gitler, A. D., Cashikar, A., Haynes, C. M., Hill, K. J., Bhullar, B., et al. (2006). α-Synuclein blocks ER-Golgi traffic and Rab1 rescues neuron loss in Parkinson's models. *Science* 313, 324–328. doi: 10.1126/science.1129462

Cornejo, V. H., and Hetz, C. (2013). The unfolded protein response in Alzheimer's disease. *Semin. Immunopathol.* 35, 277–292. doi: 10.1007/s00281-013-0373-9

Duennwald, M. L., and Lindquist, S. (2008). Impaired ERAD and ER stress are early and specific events in polyglutamine toxicity. *Genes Dev.* 22, 3308–3319. doi: 10.1101/gad.1673408

Ellgaard, L., and Ruddock, L. W. (2005). The human protein disulphide isomerase family: substrate interactions and functional properties. *EMBO Rep.* 6, 28–32. doi: 10.1038/sj.embor.7400311

Erickson, R. R., Dunning, L. M., Olson, D. A., Cohen, S. J., Davis, A. T., Wood, W. G., et al. (2005). In cerebrospinal fluid ER chaperones ERp57 and

calreticulin bind β-amyloid. *Biochem. Biophys. Res. Commun*. 332, 50–57. doi: 10.1016/j.bbrc.2005.04.090

Farg, M. A., Soo, K. Y., Walker, A. K., Pham, H., Orian, J., Horne, M. K., et al. (2012). Mutant FUS induces endoplasmic reticulum stress in amyotrophic lateral sclerosis and interacts with protein disulfide-isomerase. *Neurobiol. Aging* 33, 2855–2868. doi: 10.1016/j.neurobiolaging.2012.02.009

Ferraiuolo, L., Kirby, J., Grierson, A. J., Sendtner, M., and Shaw, P. J. (2011). Molecular pathways of motor neuron injury in amyotrophic lateral sclerosis. *Nat. Rev. Neurol.* 7, 616–630. doi: 10.1038/nrneurol.2011.152

Ferrari, D. M., and Söling, H. D. (1999). The protein disulphide-isomerase family: unravelling a string of folds. *Biochem. J.* 339(Pt 1), 1–10. doi: 10.1042/bj3390001

Ferreiro, E., and Pereira, C. M. F. (2012). Endoplasmic reticulum stress: a new playER in tauopathies. *J. Pathol.* 226, 687–692. doi: 10.1002/path.3977

Fjell, A. M., McEvoy, L., Holland, D., Dale, A. M., and Walhovd, K. B. (2014). What is normal in normal aging? Effects of aging, amyloid and Alzheimer's disease on the cerebral cortex and the hippocampus. *Prog. Neurobiol.* 117, 20–40. doi: 10.1016/j.pneurobio.2014.02.004

Forrester, M. T., Benhar, M., and Stamler, J. S. (2006). Nitrosative stress in the ER: a new role for S-Nitrosylation in neurodegenerative diseases. *ACS Chem. Biol.* 1, 355–358. doi: 10.1021/cb600244c

Frickel, E. M., Frei, P., Bouvier, M., Stafford, W. F., Helenius, A., Glockshuber, R., et al. (2004). ERp57 is a multifunctional thiol-disulfide oxidoreductase. *J. Biol. Chem.* 279, 18277–18287. doi: 10.1074/jbc.M314089200

García-Martínez, J. M., Pérez-Navarro, E., Xifró, X., Canals, J. M., Díaz-Hernández, M., Trioulier, Y., et al. (2007). BH3-only proteins Bid and BimEL are differentially involved in neuronal dysfunction in mouse models of Huntington's disease. *J. Neurosci. Res.* 85, 2756–2769. doi: 10.1002/jnr.21258

Ghaemmaghami, S., Huh, W. K., Bower, K., Howson, R. W., Belle, A., Dephoure, N., et al. (2003). Global analysis of protein expression in yeast. *Nature* 425, 737–741. doi: 10.1038/nature02046

Ghribi, O., Herman, M. M., Pramoonjago, P., Spaulding, N. K., and Savory, J. (2004). GDNF regulates the Aβ-induced endoplasmic reticulum stress response in rabbit hippocampus by inhibiting the activation of gadd 153 and the JNK and ERK kinases. *Neurobiol. Dis.* 16, 417–427. doi: 10.1016/j.nbd.2004.04.002

Gonzalez-Perez, P., Woehlbier, U., Chian, R.-J., Sapp, P., Rouleau, G. A., Leblond, C. S., et al. (2015). Identification of rare protein disulfide isomerase gene variants in amyotrophic lateral sclerosis patients. *Gene* 566, 158–165. doi: 10.1016/j.gene.2015.04.035

Gorbatyuk, M. S., Shabashvili, A., Chen, W., Meyers, C., Sullivan, L. F., Salganik, M., et al. (2012). Glucose regulated protein 78 diminishes α-synuclein neurotoxicity in a rat model of Parkinson disease. *Mol. Ther.* 20, 1327–1337. doi: 10.1038/mt.2012.28

Haass, C., and Selkoe, D. J. (2007). Soluble protein oligomers in neurodegeneration: lessons from the Alzheimer's amyloid [beta]-peptide. *Nat. Rev. Mol. Cell Biol.* 8, 101–112. doi: 10.1038/nrm2101

Halloran, M., Parakh, S., and Atkin, J. D. (2013). The role of s-nitrosylation and s-glutathionylation of protein disulphide isomerase in protein misfolding and neurodegeneration. *Int. J. Cell Biol.* 2013:797914. doi: 10.1155/2013/797914

Halperin, L., Jung, J., and Michalak, M. (2014). The many functions of the endoplasmic reticulum chaperones and folding enzymes. *IUBMB Life* 66, 318–326. doi: 10.1002/iub.1272

Hatahet, F., and Ruddock, L. W. (2007). Substrate recognition by the protein disulfide isomerases. *FEBS J.* 274, 5223–5234. doi: 10.1111/j.1742-4658.2007.06058.x

Head, M. W., and Ironside, J. W. (2012). Review: Creutzfeldt–Jakob disease: prion protein type, disease phenotype and agent strain. *Neuropathol. Appl. Neurobiol.* 38, 296–310. doi: 10.1111/j.1365-2990.2012.01265.x

Hetz, C. (2012). The unfolded protein response: controlling cell fate decisions under ER stress and beyond. *Nat. Rev. Mol. Cell Biol.* 13, 89–102. doi: 10.1038/nrm3270

Hetz, C., Bernasconi, P., Fisher, J., Lee, A.-H., Bassik, M. C., Antonsson, B., et al. (2006). Proapoptotic, B. A. X., and BAK modulate the unfolded protein response by a direct interaction with IRE1α. *Science* 312, 572–576. doi: 10.1126/science.1123480

Hetz, C., and Mollereau, B. (2014). Disturbance of endoplasmic reticulum proteostasis in neurodegenerative diseases. *Nat. Rev. Neurosci.* 15, 233–249. doi: 10.1038/nrn3689

Hetz, C., Russelakis-Carneiro, M., Kinsey, M., Castilla, J., and Soto, C. (2003). Caspase-12 and endoplasmic reticulum stress mediate neurotoxicity of pathological prion protein. *EMBO J.* 22, 5435–5445. doi: 10.1093/emboj/cdg537

Hetz, C., Russelakis-Carneiro, M., Wälchli, S., Carboni, S., Vial-Knecht, E., Maundrell, K., et al. (2005). The disulfide isomerase Grp58 is a protective factor against prion neurotoxicity. *J. Neurosci.* 25, 2793–2802. doi: 10.1523/JNEUROSCI.4090-04.2005

Hetz, C., Thielen, P., Matus, S., Nassif, M., Kiffin, R., Martinez, G., et al. (2009). XBP-1 deficiency in the nervous system protects against amyotrophic lateral sclerosis by increasing autophagy. *Genes Dev.* 23, 2294–2306. doi: 10.1101/gad.1830709

Hoffstrom, B. G., Kaplan, A., Letso, R., Schmid, R. S., Turmel, G. J., Lo, D. C., et al. (2010). Inhibitors of protein disulfide isomerase suppress apoptosis induced by misfolded proteins. *Nat. Chem. Biol.* 6, 900–906. doi: 10.1038/nchembio.467

Holtz, W. A., and O'Malley, K. L. (2003). Parkinsonian mimetics induce aspects of unfolded protein response in death of dopaminergic neurons. *J. Biol. Chem.* 278, 19367–19377. doi: 10.1074/jbc.M211821200

Honjo, Y., Ito, H., Horibe, T., Takahashi, R., and Kawakami, K. (2010). Protein disulfide isomerase-immunopositive inclusions in patients with Alzheimer disease. *Brain Res.* 1349, 90–96. doi: 10.1016/j.brainres.2010.06.016

Honjo, Y., Kaneko, S., Ito, H., Horibe, T., Nagashima, M., Nakamura, M., et al. (2011). Protein disulfide isomerase-immunopositive inclusions in patients with amyotrophic lateral sclerosis. *Amyotroph. Lateral Scler.* 12, 444–450. doi: 10.3109/17482968.2011.594055

Hoozemans, J. J. M., van Haastert, E. S., Eikelenboom, P., de Vos, R. A. I., Rozemuller, J. M., and Scheper, W. (2007). Activation of the unfolded protein response in Parkinson's disease. *Biochem. Biophys. Res. Commun.* 354, 707–711. doi: 10.1016/j.bbrc.2007.01.043

Hoozemans, J. J. M., van Haastert, E. S., Nijholt, D. A. T., Rozemuller, A. J. M., Eikelenboom, P., and Scheper, W. (2009). The unfolded protein response is activated in pretangle neurons in Alzheimer's Disease Hippocampus. *Am. J. Pathol.* 174, 1241–1251. doi: 10.2353/ajpath.2009.080814

Hoozemans, J. J. M., Veerhuis, R., van Haastert, E. S., Rozemuller, J. M., Baas, F., Eikelenboom, P., et al. (2005). The unfolded protein response is activated in Alzheimer's disease. *Acta Neuropathol.* 110, 165–172. doi: 10.1007/s00401-005-1038-0

Ilieva, E. V., Ayala, V., Jové, M., Dalfó, E., Cacabelos, D., Povedano, M., et al. (2007). Oxidative and endoplasmic reticulum stress interplay in sporadic amyotrophic lateral sclerosis. *Brain* 130, 3111–3123. doi: 10.1093/brain/awm190

Ito, Y., Yamada, M., Tanaka, H., Aida, K., Tsuruma, K., Shimazawa, M., et al. (2009). Involvement of CHOP, an ER-stress apoptotic mediator, in both human sporadic ALS and ALS model mice. *Neurobiol. Dis.* 36, 470–476. doi: 10.1016/j.nbd.2009.08.013

Jankovic, J. (2008). Parkinson's disease: clinical features and diagnosis. *J. Neurol. Neurosurg. Psychiatry* 79, 368–376. doi: 10.1136/jnnp.2007.131045

Jaronen, M., Vehviläinen, P., Malm, T., Keksa-Goldsteine, V., Pollari, E., Valonen, P., et al. (2013). Protein disulfide isomerase in ALS mouse glia links protein misfolding with NADPH oxidase-catalyzed superoxide production. *Hum. Mol. Genet.* 22, 646–655. doi: 10.1093/hmg/dds472

Jessop, C. E., Watkins, R. H., Simmons, J. J., Tasab, M., and Bulleid, N. J. (2009). Protein disulphide isomerase family members show distinct substrate specificity: P5 is targeted to BiP client proteins. *J. Cell Sci.* 122, 4287–4295. doi: 10.1242/jcs.059154

Kanekura, K., Suzuki, H., Aiso, S., and Matsuoka, M. (2009). ER stress and unfolded protein response in amyotrophic lateral sclerosis. *Mol. Neurobiol.* 39, 81–89. doi: 10.1007/s12035-009-8054-3

Karran, E., Mercken, M., and De Strooper, B. (2011). The amyloid cascade hypothesis for Alzheimer's disease: an appraisal for the development of therapeutics. *Nat. Rev. Drug Disc.* 10, 698–712. doi: 10.1038/nrd3505

Kent-Braun, J. A., Walker, C. H., Weiner, M. W., and Miller, R. G. (1998). Functional significance of upper and lower motor neuron impairment in amyotrophic lateral sclerosis. *Muscle Nerve* 21, 762–768.

Kieran, D., Woods, I., Villunger, A., Strasser, A., and Prehn, J. H. (2007). Deletion of the BH3-only protein puma protects motoneurons from ER stress-induced apoptosis and delays motoneuron loss in ALS mice. *Proc. Natl. Acad. Sci. U.S.A.* 104, 20606–20611. doi: 10.1073/pnas.0707906105

Kikuchi, H., Almer, G., Yamashita, S., Guégan, C., Nagai, M., Xu, Z., et al. (2006). Spinal cord endoplasmic reticulum stress associated with a microsomal accumulation of mutant superoxide dismutase-1 in an ALS model. *Proc. Natl. Acad. Sci. U.S.A.* 103, 6025–6030. doi: 10.1073/pnas.0509227103

Kiskinis, E., Sandoe, J., Williams, L. A., Boulting, G. L., Moccia, R., Wainger, B. J., et al. (2014). Pathways disrupted in human ALS motor neurons identified through genetic correction of mutant SOD1. *Cell Stem Cell* 14, 781–795. doi: 10.1016/j.stem.2014.03.004

Kojer, K., and Riemer, J. (2014). Balancing oxidative protein folding: the influences of reducing pathways on disulfide bond formation. *Biochim. Biophys. Acta* 1844, 1383–1390. doi: 10.1016/j.bbapap.2014.02.004

Kojima, R., Okumura, M., Masui, S., Kanemura, S., Inoue, M., Saiki, M., et al. (2014). Radically different thioredoxin domain arrangement of ERp46, an efficient disulfide bond introducer of the mammalian PDI family. *Structure* 22, 431–443. doi: 10.1016/j.str.2013.12.013

Kondo, T., Asai, M., Tsukita, K., Kutoku, Y., Ohsawa, Y., Sunada, Y., et al. (2013). Modeling Alzheimer's disease with iPSCs reveals stress phenotypes associated with intracellular Aβ and differential drug responsiveness. *Cell Stem Cell* 12, 487–496. doi: 10.1016/j.stem.2013.01.009

Kong, P.-J., Kil, M.-O., Lee, H., Kim, S.-S., Johnson, G. V., and Chun, W. (2009). Increased expression of Bim contributes to the potentiation of serum deprivation-induced apoptotic cell death in Huntington's disease knock-in striatal cell line. *Neurol. Res.* 31, 77–83. doi: 10.1179/174313208X331572

Kouroku, Y., Fujita, E., Jimbo, A., Kikuchi, T., Yamagata, T., Momoi, M. Y., et al. (2002). Polyglutamine aggregates stimulate ER stress signals and caspase-12 activation. *Hum. Mol. Genet.* 11, 1505–1515. doi: 10.1093/hmg/11.13.1505

Kwok, C. T., Morris, A. G., Frampton, J., Smith, B., Shaw, C. E., and de Belleroche, J. (2013). Association studies indicate that protein disulfide isomerase is a risk factor in amyotrophic lateral sclerosis. *Free Radic. Biol. Med.* 58, 81–86. doi: 10.1016/j.freeradbiomed.2013.01.001

Leblond, C. S., Kaneb, H. M., Dion, P. A., and Rouleau, G. A. (2014). Dissection of genetic factors associated with amyotrophic lateral sclerosis. *Exp. Neurol.* 262(Pt B), 91–101. doi: 10.1016/j.expneurol.2014.04.013

Lee, A.-H., Iwakoshi, N. N., and Glimcher, L. H. (2003). XBP-1 regulates a subset of endoplasmic reticulum resident chaperone genes in the unfolded protein response. *Mol. Cell. Biol.* 23, 7448–7459. doi: 10.1128/MCB.23.21.7448-7459.2003

Lee, J. H., Won, S. M., Suh, J., Son, S. J., Moon, G. J., Park, U.-J., et al. (2010a). Induction of the unfolded protein response and cell death pathway in Alzheimer's disease, but not in aged Tg2576 mice. *Exp. Mol. Med.* 42, 386–394. doi: 10.3858/emm.2010.42.5.040

Lee, K.-S., Lee, H. J., Kim, D. H., Noh, Y. H., Yu, K., Jung, H.-Y., et al. (2010b). Activation of PERK signaling attenuates Aβ-mediated ER stress. *PLoS ONE* 5:e10489. doi: 10.1371/journal.pone.0010489

Leon, R., Bhagavatula, N., Ulukpo, O., Mccollum, M., and Wei, J. (2010). BimEL as a possible molecular link between proteasome dysfunction and cell death induced by mutant huntingtin. *Eur. J. Neurosci.* 31, 1915–1925. doi: 10.1111/j.1460-9568.2010.07215.x

Lin, A. C., and Holt, C. E. (2008). Function and regulation of local axonal translation. *Curr. Opin. Neurobiol.* 18, 60–68. doi: 10.1016/j.conb.2008.05.004

Lindholm, D., Wootz, H., and Korhonen, L. (2006). ER stress and neurodegenerative diseases. *Cell Death Differ.* 13, 385–392. doi: 10.1038/sj.cdd.4401778

Ling, S.-C., Polymenidou, M., and Cleveland, D. W. (2013). Converging mechanisms in ALS and FTD: disrupted, RNA and protein homeostasis. *Neuron* 79, 416–438. doi: 10.1016/j.neuron.2013.07.033

Liu, H., Dong, X.-Y., and Sun, Y. (2013). Peptide disulfide RKCGCFF facilitates oxidative protein refolding by mimicking protein disulfide isomerase. *Biochem. Eng. J.* 79, 29–32. doi: 10.1016/j.bej.2013.06.010

Ma, Y., and Hendershot, L. M. (2004). ER chaperone functions during normal and stress conditions. *J. Chem. Neuroanat.* 28, 51–65. doi: 10.1016/j.jchemneu.2003.08.007

Makarava, N., Kovacs, G. G., Savtchenko, R., Alexeeva, I., Ostapchenko, V. G., Budka, H., et al. (2012). A new mechanism for transmissible prion diseases. *J. Neurosci.* 32, 7345–7355. doi: 10.1523/JNEUROSCI.6351-11.2012

Mangialasche, F., Polidori, M. C., Monastero, R., Ercolani, S., Camarda, C., Cecchetti, R., et al. (2009). Biomarkers of oxidative and nitrosative damage in Alzheimer's disease and mild cognitive impairment. *Ageing Res. Rev.* 8, 285–305. doi: 10.1016/j.arr.2009.04.002

Matus, S., Glimcher, L. H., and Hetz, C. (2011). Protein folding stress in neurodegenerative diseases: a glimpse into the ER. *Curr. Opin. Cell Biol.* 23, 239–252. doi: 10.1016/j.ceb.2011.01.003

Matus, S., Lopez, E., Valenzuela, V., Nassif, M., and Hetz, C. (2013a). Functional contribution of the transcription factor ATF4 to the pathogenesis of amyotrophic lateral sclerosis. *PLoS ONE* 8:e66672. doi: 10.1371/journal.pone.0066672

Matus, S., Valenzuela, V., Medinas, D. B., and Hetz, C. (2013b). ER dysfunction and protein folding stress in ALS. *Int. J. Cell Biol.* 2013:674751. doi: 10.1155/2013/674751

Medraño-Fernandez, I., Fagioli, C., Mezghrani, A., Otsu, M., and Sitia, R. (2014). Different redox sensitivity of endoplasmic reticulum associated degradation clients suggests a novel role for disulphide bonds in secretory proteins. *Biochem. Cell Biol.* 92, 113–118. doi: 10.1139/bcb-2013-0090

Merianda, T. T., Lin, A. C., Lam, J. S., Vuppalanchi, D., Willis, D. E., Karin, N., et al. (2009). A functional equivalent of endoplasmic reticulum and Golgi in axons for secretion of locally synthesized proteins. *Mol. Cell. Neurosci.* 40, 128–142. doi: 10.1016/j.mcn.2008.09.008

Mezghrani, A., Fassio, A., Benham, A., Simmen, T., Braakman, I., and Sitia, R. (2001). Manipulation of oxidative protein folding and PDI redox state in mammalian cells. *EMBO J.* 20, 6288–6296. doi: 10.1093/emboj/20.22.6288

Nakamura, T., and Lipton, S. A. (2011). S-nitrosylation of critical protein thiols mediates protein misfolding and mitochondrial dysfunction in neurodegenerative diseases. *Antioxid. Redox Signal.* 14, 1479–1492. doi: 10.1089/ars.2010.3570

Nakato, R., Ohkubo, Y., Konishi, A., Shibata, M., Kaneko, Y., Iwawaki, T., et al. (2015). Regulation of the unfolded protein response via S-nitrosylation of sensors of endoplasmic reticulum stress. *Sci. Rep.* 5:14812. doi: 10.1038/srep14812

Nishitoh, H., Kadowaki, H., Nagai, A., Maruyama, T., Yokota, T., Fukutomi, H., et al. (2008). ALS-linked mutant SOD1 induces ER stress-and ASK1-dependent motor neuron death by targeting Derlin-1. *Genes Dev.* 22, 1451–1464. doi: 10.1101/gad.1640108

Nishitoh, H., Matsuzawa, A., Tobiume, K., Saegusa, K., Takeda, K., Inoue, K., et al. (2002). ASK1 is essential for endoplasmic reticulum stress-induced neuronal cell death triggered by expanded polyglutamine repeats. *Genes Dev.* 16, 1345–1355. doi: 10.1101/gad.992302

Paes, A. M. D. A., Veríssimo-Filho, S., Guimarães, L. L., Silva, A. C. B., Takiuti, J. T., Santos, C. X., et al. (2011). Protein disulfide isomerase redox-dependent association with p47phox: evidence for an organizer role in leukocyte NADPH oxidase activation. *J. Leukoc. Biol.* 90, 799–810. doi: 10.1189/jlb.0610324

Parakh, S., and Atkin, J. D. (2015). Novel roles for protein disulphide isomerase in disease states: a double edged sword? *Front. Cell Dev. Biol.* 3:30. doi: 10.3389/fcell.2015.00030

Parakh, S., Spencer, D. M., Halloran, M. A., Soo, K. Y., and Atkin, J. D. (2013). Redox regulation in amyotrophic lateral sclerosis. *Oxid. Med. Cell. Longev.* 2013:408681. doi: 10.1155/2013/408681

Plácido, A., Pereira, C., Duarte, A., Candeias, E., Correia, S., Santos, R., et al. (2014). The role of endoplasmic reticulum in amyloid precursor protein processing and trafficking: implications for Alzheimer's disease. *Biochim. Biophys. Acta* 1842, 1444–1453. doi: 10.1016/j.bbadis.2014.05.003

Porter, M.-C., and Leemans, M. (2013). Creutzfeldt–Jakob disease. *CEACCP* 13, 119–124. doi: 10.1093/bjaceaccp/mkt002

Ramírez, O. A., Härtel, S., and Couve, A. (2011). Location matters: the endoplasmic reticulum and protein trafficking in dendrites. *Biol. Res.* 44, 17–23. doi: 10.4067/S0716-97602011000100003

Renton, A. E., Chiò, A., and Traynor, B. J. (2014). State of play in amyotrophic lateral sclerosis genetics. *Nat. Neurosci.* 17, 17–23. doi: 10.1038/nn.3584

Resende, R., Ferreiro, E., Pereira, C., and Oliveira, C. R. (2008). ER stress is involved in Aβ−induced GSK−3β activation and tau phosphorylation. *J. Neurosci. Res.* 86, 2091–2099. doi: 10.1002/jnr.21648

Robberecht, W., and Philips, T. (2013). The changing scene of amyotrophic lateral sclerosis. *Nat. Rev. Neurosci.* 14, 248–264. doi: 10.1038/nrn3430

Ross, C. A., and Tabrizi, S. J. (2011). Huntington's disease: from molecular pathogenesis to clinical treatment. *Lancet Neurol.* 10, 83–98. doi: 10.1016/S1474-4422(10)70245-3

Rothstein, J. D. (2009). Current hypotheses for the underlying biology of amyotrophic lateral sclerosis. *Ann. Neurol.* 65(Suppl 1.), S3–S9. doi: 10.1002/ana.21543

Rutkowski, D. T., Arnold, S. M., Miller, C. N., Wu, J., Li, J., Gunnison, K. M., et al. (2006). Adaptation to ER stress is mediated by differential stabilities of pro-survival and pro-apoptotic mRNAs and proteins. *PLoS Biol.* 4:e374. doi: 10.1371/journal.pbio.0040374

Ryu, E. J., Harding, H. P., Angelastro, J. M., Vitolo, O. V., Ron, D., and Greene, L. A. (2002). Endoplasmic reticulum stress and the unfolded protein response in cellular models of Parkinson's disease. *J. Neurosci.* 22, 10690–10698.

Sado, M., Yamasaki, Y., Iwanaga, T., Onaka, Y., Ibuki, T., Nishihara, S., et al. (2009). Protective effect against Parkinson's disease-related insults through the activation of XBP1. *Brain Res.* 1257, 16–24. doi: 10.1016/j.brainres.2008.11.104

Safren, N., Ayadi, A. E., Chang, L., Terrillion, C. E., Gould, T. D., Boehning, D. F., et al. (2014). Ubiquilin-1 overexpression increases the lifespan and delays accumulation of Huntingtin aggregates in the R6/2 mouse model of Huntington's disease. *PLoS ONE* 9:e87513. doi: 10.1371/journal.pone.0087513

Sakagami, Y., Kudo, T., Tanimukai, H., Kanayama, D., Omi, T., Horiguchi, K., et al. (2013). Involvement of endoplasmic reticulum stress in tauopathy. *Biochem. Biophys. Res. Commun.* 430, 500–504. doi: 10.1016/j.bbrc.2012.12.007

Salminen, A., Kauppinen, A., Suuronen, T., Kaarniranta, K., and Ojala, J. (2009). ER stress in Alzheimer's disease: a novel neuronal trigger for inflammation and Alzheimer's pathology. *J. Neuroinflammation* 6:41. doi: 10.1186/1742-2094-6-41

Saxena, S., Cabuy, E., and Caroni, P. (2009). A role for motoneuron subtype-selective ER stress in disease manifestations of FALS mice. *Nat. Neurosci.* 12, 627–636. doi: 10.1038/nn.2297

Schlehe, J. S., Lutz, A. K., Pilsl, A., Lämmermann, K., Grgur, K., Henn, I. H., et al. (2008). Aberrant folding of pathogenic parkin mutants: aggregation versus degradation. *J. Biol. Chem.* 283, 13771–13779. doi: 10.1074/jbc.M707494200

Schröder, M., and Kaufman, R. J. (2005). ER stress and the unfolded protein response. *Mutat. Res.* 569, 29–63. doi: 10.1016/j.mrfmmm.2004.06.056

Si, L., Xu, T., Wang, F., Liu, Q., and Cui, M. (2012). X-box-binding protein 1-modified neural stem cells for treatment of Parkinson's disease. *Neural Regen. Res.* 7, 736. doi: 10.3969/j.issn.1673-5374.2012.10.003

Silva, R. M., Ries, V., Oo, T. F., Yarygina, O., Jackson-Lewis, V., Ryu, E. J., et al. (2005). CHOP/GADD153 is a mediator of apoptotic death in substantia nigra dopamine neurons in an *in vivo* neurotoxin model of parkinsonism. *J. Neurochem.* 95, 974–986. doi: 10.1111/j.1471-4159.2005.03428.x

Soo, K. Y., Atkin, J. D., Horne, M. K., and Nagley, P. (2009). Recruitment of mitochondria into apoptotic signaling correlates with the presence of inclusions formed by amyotrophic lateral sclerosis—associated SOD1 mutations. *J. Neurochem.* 108, 578–590. doi: 10.1111/j.1471-4159.2008.05799.x

Soo, K. Y., Halloran, M., Sundaramoorthy, V., Parakh, S., Toth, R. P., Southam, K. A., et al. (2015). Rab1-dependent ER–Golgi transport dysfunction is a common pathogenic mechanism in SOD1, TDP-43 and FUS-associated ALS. *Acta Neuropathol.* 130, 679–697. doi: 10.1007/s00401-015-1468-2

Soto, C. (2003). Unfolding the role of protein misfolding in neurodegenerative diseases. *Nat. Rev. Neurosci.* 4, 49–60. doi: 10.1038/nrn1007

Sundaramoorthy, V., Walker, A., Yerbury, J., Soo, K., Farg, M., Hoang, V., et al. (2013). Extracellular wildtype and mutant SOD1 induces ER–Golgi pathology characteristic of amyotrophic lateral sclerosis in neuronal cells. *Cell. Mol. Life Sci.* 70, 4181–4195. doi: 10.1007/s00018-013-1385-2

Suzuki, H., Kanekura, K., Levine, T. P., Kohno, K., Olkkonen, V. M., Aiso, S., et al. (2009). ALS—linked P56S—VAPB, an aggregated loss—of—function mutant of VAPB, predisposes motor neurons to ER stress—related death by inducing aggregation of co—expressed wild—type VAPB. *J. Neurochem.* 108, 973–985. doi: 10.1111/j.1471-4159.2008.05857.x

Tohda, C., Urano, T., Umezaki, M., Nemere, I., and Kuboyama, T. (2012). Diosgenin is an exogenous activator of 1, 25D3-MARRS/Pdia3/ERp57 and improves Alzheimer's disease pathologies in 5XFAD mice. *Sci. Rep.* 2:535. doi: 10.1038/srep00535

Torres, M., Castillo, K., Armisén, R., Stutzin, A., Soto, C., and Hetz, C. (2010). Prion protein misfolding affects calcium homeostasis and sensitizes cells to endoplasmic reticulum stress. *PLoS ONE* 5:e15658. doi: 10.1371/journal.pone.0015658

Tsuda, H., Han, S. M., Yang, Y., Tong, C., Lin, Y. Q., Mohan, K., et al. (2008). The amyotrophic lateral sclerosis 8 protein VAPB is cleaved, secreted, and acts as a ligand for Eph receptors. *Cell* 133, 963–977. doi: 10.1016/j.cell.2008.04.039

Turano, C., Coppari, S., Altieri, F., and Ferraro, A. (2002). Proteins of the PDI family: unpredicted non-ER locations and functions. *J. Cell. Physiol.* 193, 154–163. doi: 10.1002/jcp.10172

Turner, M. R., Hardiman, O., Benatar, M., Brooks, B. R., Chio, A., de Carvalho, M., et al. (2013). Controversies and priorities in amyotrophic lateral sclerosis. *Lancet Neurol.* 12, 310–322. doi: 10.1016/S1474-4422(13)70036-X

Uehara, T., Nakamura, T., Yao, D., Shi, Z. Q., Gu, Z., Ma, Y., et al. (2006). S-nitrosylated protein-disulphide isomerase links protein misfolding to neurodegeneration. *Nature* 441, 513–517. doi: 10.1038/nature04782

Vaccaro, A., Patten, S. A., Aggad, D., Julien, C., Maios, C., Kabashi, E., et al. (2013). Pharmacological reduction of ER stress protects against TDP-43 neuronal toxicity *in vivo*. *Neurobiol. Dis.* 55, 64–75. doi: 10.1016/j.nbd.2013.03.015

Vidal, R. L., Figueroa, A., Court, F. A., Thielen, P., Molina, C., Wirth, C., et al. (2012). Targeting the UPR transcription factor XBP1 protects against Huntington's disease through the regulation of FoxO1 and autophagy. *Hum. Mol. Genet.* 21, 2245–2262. doi: 10.1093/hmg/dds040

Volpicelli-Daley, L. A., Luk, K. C., Patel, T. P., Tanik, S. A., Riddle, D. M., Stieber, A., et al. (2011). Exogenous α-Synuclein fibrils induce lewy body pathology leading to synaptic dysfunction and neuron death. *Neuron* 72, 57–71. doi: 10.1016/j.neuron.2011.08.033

Wainger, B. J., Kiskinis, E., Mellin, C., Wiskow, O., Han, S. S. W., Sandoe, J., et al. (2014). Intrinsic membrane hyperexcitability of amyotrophic lateral sclerosis patient-derived motor neurons. *Cell Rep.* 7, 1–11. doi: 10.1016/j.celrep.2014.03.019

Walker, A. K. (2010). Protein disulfide isomerase and the endoplasmic reticulum in amyotrophic lateral sclerosis. *J. Neurosci.* 30, 3865–3867. doi: 10.1523/JNEUROSCI.0408-10.2010

Walker, A. K., Farg, M. A., Bye, C. R., Mclean, C. A., Horne, M. K., and Atkin, J. D. (2010). Protein disulphide isomerase protects against protein aggregation and is S-nitrosylated in amyotrophic lateral sclerosis. *Brain* 133, 105–116. doi: 10.1093/brain/awp267

Walker, A. K., Soo, K. Y., Sundaramoorthy, V., Parakh, S., Ma, Y., Farg, M. A., et al. (2013). ALS-Associated TDP-43 Induces endoplasmic reticulum stress, which drives cytoplasmic TDP-43 accumulation and stress granule formation. *PLoS ONE* 8:e81170. doi: 10.1371/journal.pone.0081170

Wang, L., Popko, B., and Roos, R. P. (2011). The unfolded protein response in familial amyotrophic lateral sclerosis. *Hum. Mol. Genet.* 20, 1008–1015. doi: 10.1093/hmg/ddq546

Wang, L., Popko, B., and Roos, R. P. (2013). An enhanced integrated stress response ameliorates mutant SOD1-induced ALS. *Hum. Mol. Genet.* 23, 2629–2638. doi: 10.1093/hmg/ddt65

Wang, S.-B., Shi, Q., Xu, Y., Xie, W.-L., Zhang, J., Tian, C., et al. (2012). Protein disulfide isomerase regulates endoplasmic reticulum stress and the apoptotic process during prion infection and PrP mutant-induced cytotoxicity. *PLoS ONE* 7:e38221. doi: 10.1371/journal.pone.0038221

Wang, S., and Kaufman, R. J. (2012). The impact of the unfolded protein response on human disease. *J. Cell Biol.* 197, 857–867. doi: 10.1083/jcb.201110131

Wilkinson, B., and Gilbert, H. F. (2004). Protein disulfide isomerase. *Biochim. Biophys. Acta* 1699, 35–44. doi: 10.1016/S1570-9639(04)00063-9

Wolozin, B. (2012). Regulated protein aggregation: stress granules and neurodegeneration. *Mol. Neurodegener.* 7:56. doi: 10.1186/1750-1326-7-56

Woycechowsky, K. J., and Raines, R. T. (2000). Native disulfide bond formation in proteins. *Curr. Opin. Chem. Biol.* 4, 533–539. doi: 10.1016/S1367-5931(00)00128-9

Wu, X.-F., Wang, A.-F., Chen, L., Huang, E.-P., Xie, W.-B., Liu, C., et al. (2014). S-nitrosylating protein disulphide isomerase mediates α-synuclein aggregation caused by methamphetamine exposure in PC12 cells. *Toxicol. Lett.* 230, 19–27. doi: 10.1016/j.toxlet.2014.07.026

Xu, S., Sankar, S., and Neamati, N. (2014). Protein disulfide isomerase: a promising target for cancer therapy. *Drug Disc. Today* 19, 222–240. doi: 10.1016/j.drudis.2013.10.017

Yang, Y. S., Harel, N. Y., and Strittmatter, S., M. (2009). Reticulon-4A (Nogo-A) redistributes protein disulfide isomerase to protect mice from SOD1-dependent amyotrophic lateral sclerosis. *J. Neurosci.* 29, 13850–13859. doi: 10.1523/JNEUROSCI.2312-09.2009

Yang, Q., and Guo, Z.-B. (2015). Polymorphisms in protein disulfide isomerase are associated with sporadic amyotrophic lateral sclerosis in the Chinese Han population. *Int. J. Neurosci*. doi: 10.3109/00207454.2015.1050098. [Epub ahead of print].

Yoo, B. C., Krapfenbauer, K., Cairns, N., Belay, G., Bajo, M., and Lubec, G. (2002). Overexpressed protein disulfide isomerase in brains of patients with sporadic Creutzfeldt–Jakob disease. *Neurosci. Lett*. 334, 196–200. doi: 10.1016/S0304-3940(02)01071-6

Yudin, D., Hanz, S., Yoo, S., Iavnilovitch, E., Willis, D., Gradus, T., et al. (2008). Localized regulation of axonal RanGTPase controls retrograde injury signaling in peripheral nerve. *Neuron* 59, 241–252. doi: 10.1016/j.neuron.2008.05.029

Zhang, Y.-J., Jansen-West, K., Xu, Y.-F., Gendron, T. F., Bieniek, K. F., Lin, W.-L., et al. (2014). Aggregation-prone c9FTD/ALS poly (GA) RAN-translated proteins cause neurotoxicity by inducing ER stress. *Acta Neuropathol.* 128, 505–524. doi: 10.1007/s00401-014-1336-5

Conflict of Interest Statement: The authors declare that the research was conducted in the absence of any commercial or financial relationships that could be construed as a potential conflict of interest.

7.2.10 Ethics Applications

LA TROBE UNIVERSITY

Faculty of Science,
Technology & Engineering

T +61 3 9479 3698
F +61 3 947 2585
E k.collins@latrobe.edu.au

MEMORANDUM

TO: Dr J Atkin, Department of Biochemistry

FROM: Ms K. Collins, Secretary (Research Ethics), Faculty of Science, Technology and Engineering

SUBJECT: **MODIFICATION - Application FHEC10/R4 : New therapeutic approaches for ALS based on ER stress and induction of the UPR**

DATE: 3 April 2013

Thank you for submitting your modification request for ethics approval to the FHEC for the project referred to above. The FHEC has reviewed and approved the following modification/s which may commence now:

Request to extend the duration of the study from 1 March 2013 to 1 March 2015.

Please note that your request has been reviewed by a sub-committee of the UHEC to facilitate a decision before the next Committee meeting. This decision will require ratification by the UHEC and it reserves the right to alter conditions of approval or withdraw approval at that time. However, you may commence prior to ratification and you will be notified if the approval status of your project changes.

The following standard conditions apply to your project:

- **Limit of Approval.** Approval is limited strictly to the research proposal as submitted in your application while taking into account any additional conditions advised by the FHEC.
- **Variation to Project**. Any subsequent variations or modifications you wish to make to your project must be formally notified to the FHEC for approval in advance of these modifications being introduced into the project. This can be done using the appropriate form: Ethics – application for Modification to Project which is available on the Research Services website at http://www.latrobe.educ.au/research-services/ethics/HEC_human.htm. If the FHEC considers that the proposed changes are significant, you may be required to submit a new application form for approval of the revised project.
- **Adverse Events.** If any unforeseen or adverse events occur, including adverse effects on participants, during the course of the project which may affect the ethical acceptability of the project, the Chief Investigator must immediately notify the FHEC Secretary on telephone (03) 9479 3698. Any complaints about the project received by the researchers must also be referred immediately to the FHEC Secretary.
- **Withdrawal of Project**. If you decide to discontinue your research before its planned completion, you must advise the FHEC and clarify the circumstances.
- **Monitoring**. All projects are subject to monitoring at any time by the University Human Ethics Committee.
- **Annual Progress Reports**. You are required to submit a Progress Report annually (if your project continues for more than 12 months) and at the conclusion of your project. The form is

available on the Research Services website (see above address). Failure to submit a Progress Report will mean approval for this project will lapse.

- **Auditing**. An audit of the project may be conducted by members of the UHEC.
- **Final Report.** A Final Report (see above address) is required within six months of the completion of the project or by **31 December 2013.**

If you have any queries on the matters mentioned above or require any further clarification please contact me on telephone 9479 3698 or at email address k.collins@latrobe.edu.au.

Kaye Collins

MACQUARIE University ANIMAL RESEARCH AUTHORITY (ARA)

AEC Reference No.: 2015/013 **Date of Expiry:** 19 June 2016

Full Approval Duration: *19 June 2015 to 19 June 2018 (36 months)*

This ARA remains in force until the Date of Expiry (unless suspended, cancelled or surrendered) **and will only be renewed upon receipt of a satisfactory Progress Report before expiry (see Approval email for submission details).**

Principal Investigator:
Professor Roger Chung
School of Advanced Medicine
Macquarie University, NSW 2109
roger.chung@mq.edu.au
0402 808 958

Associate Investigators:
Vinod Sundaramoorthy 0430 198 649

In case of emergency, please contact:
the Principal Investigator / Associate Investigator named above
or Manager, CAF: 9850 7780 / 0428 861 163 and **Animal Welfare Officer**: 9850 7758 / 0439 497 383

The above-named are authorised by MACQUARIE UNIVERSITY ANIMAL ETHICS COMMITTEE to conduct the following research:

Title of the project: **Understanding mechanisms of neurodegeneration through the use of cultured neural cells**

Purpose: **4 - Research: Human or Animal Biology**

Aims: **To explore how expression of disease-causing mutations in specific genes causes impairment in intracellular processes, leading to neural dysfunction and death.**
To investigate how disease-causing gene mutations cause defects in protein balance, which may lead to abnormal protein function (specifically protein aggregation), and how these aggregated proteins may actually spread between neural cells to propagate spread of neurodegeneration to neighbouring cells.

Surgical Procedures category: 2 - Animal Unconscious without Recovery

All procedures must be performed as per the AEC-approved protocol, unless stated otherwise by the AEC and/or AWO.

Maximum numbers approved (for the Full Approval Duration):

Species	Strain	Age/Weight/Sex	Total	Supplier/Source
01 Mus	C57Bl6	Pregnant Females (embryonic day 14-17)	135	Animal Resources Centre, Perth or Australian BioResources
01 Mus	SOD1	Pregnant Females (embryonic day 14-17)	135	Australian BioResources
01 Mus	APP/PS1	Pregnant Females (embryonic day 14-17)	135	Australian BioResources, UNSW, UTAS
			TOTAL 405	

Location of research:

Location	*Full street address*
Central Animal Facility	Building F9A, Research Park Drive, Macquarie University, NSW 2109
School of Advanced Medicine	Level 1, F10A, 2 Technology Place, Macquarie University, NSW 2109

Amendments approved by the AEC since initial approval: N/A

Conditions of Approval: N/A

Being animal research carried out in accordance with the Code of Practice for a recognised research purpose and in connection with animals (other than exempt animals) that have been obtained from the holder of an animal suppliers license.

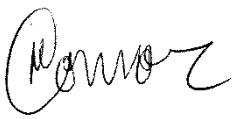

Professor Mark Connor (Chair, Animal Ethics Committee) **Approval Date: 18 June 2015**

ANIMAL ETHICS COMMITTEE
HOWARD FLOREY INSTITUTE

AEC APPLICATION FORM

***N.B.** If all sections of this form are not completed appropriately or there are major typographical errors, you risk AEC's consideration of this application being deferred to a later meeting.*

AEC Number: 09-005

Application for Approval of a project involving the use of animals by Staff of the Howard Florey Institute.

To: The Secretary
Animal Ethics Committee

I attach a proposal to use animals for the purpose specified on the attached sheets.

Project Title:

Brain infusion therapy for motor neuron disease

Date of this submission:	**Expected Date of Commencement**:	**Expected Expiry Date***:
23 January 2009	1 March 2009	1 March 2012

***** *Three years from approval unless otherwise requested.*

Principal Investigator/s *(please note PI's must be employees or official affiliates of HFI)*:

Dr Julie Atkin

Chairman's Comments:

09-005 Atkin
Brain infusion therapy for motor neuron disease
(Interviewed: Drs Tim Aumann, Bradley Turner and Mr Adam Walker)
Approved subject to the following:

1) The applicants were advised that it is the responsibility of the PIs to determine if OGTR approval is required and if so, no experimentation can commence until such approval is obtained.
2) Pages 3, and 13, species and reduction – embryos have to be counted from half gestation (E11 in this particular application) and be incorporated into the total number of animals.
3) Page 8 (F), scientific description – indicate the rationale for using male on aim 2, although this has been discussed at the interview.
4) Page 9, method of choice – add, cervical dislocation.
5) Page 11, maximum time under experimentation – replace "left until old age" with "allowed to survive in accordance with the SOP clinical monitoring."
6) Page 12, intervene to kill – add, animals will be killed if they lost more than 15% of their original body weight that was non-recoverable within one week.
7) Page 15, personnel – indicate the role, experience and training of Dr J Atkin and for all investigators and include experience using the SOD strain.

Date of Final Approval:	**Chairman**: